

---

**CDF STUDY REPORT**  
**COMET INTERCEPTOR**

**Assessment of Mission to Intercept a Long Period Comet or  
Interplanetary Object**

---



# CDF Study Report

## Comet Interceptor

### Assessment of Mission to Intercept a Long Period Comet or Interplanetary Object



This study is based on the ESA CDF Open Concurrent Design Tool (OCDT), which is a community software tool released under ESA licence. All rights reserved.

Further information and/or additional copies of the report can be requested from:

S. Bayon  
ESA/ESTEC/SCI-FMP  
Postbus 299  
2200 AG Noordwijk  
The Netherlands  
Tel: +31-(0)71-5655502  
Fax: +31-(0)71-5655985  
[Silvia.Bayon@esa.int](mailto:Silvia.Bayon@esa.int)

For further information on the Concurrent Design Facility please contact:

I. Roma  
ESA/ESTEC/TEC-SYE  
Postbus 299  
2200 AG Noordwijk  
The Netherlands  
Tel: +31-(0)71-5658453  
Fax: +31-(0)71-5656024  
[Ilaria.Roma@esa.int](mailto:Ilaria.Roma@esa.int)



#### FRONT COVER

Stylised image of a Long Period Comet being intercepted by the 3 elements of the Comet Interceptor Mission

## STUDY TEAM

This study was performed in the ESTEC Concurrent Design Facility (CDF) by the following interdisciplinary team:

TEAM LEADER			
AOGNC		POWER	
COMMUNICATIONS		PROGRAMMATICS/ AIV	
CONFIGURATION		CHEMICAL PROPULSION	
COST		ELECTRIC PROPULSION	
DATA HANDLING		RISK	
ENVIRONMENT		SOFTWARE	
GS&OPS		STRUCTURES	
MECHANISMS		SYSTEMS	
MISSION ANALYSIS		THERMAL	
PAYOUT/ DETECTORS			

Note: This study and the work detailed in this report builds on a previous CDF study, completed in early 2019. The authors of this report wish to acknowledge and thank the previous study team for their valuable contributions to the success of this study.

This Page Intentionally Blank

## TABLE OF CONTENTS

<b>1 INTRODUCTION .....</b>	<b>13</b>
1.1 Background .....	13
1.2 Objective.....	13
1.3 Scope .....	13
1.4 Important Remarks on Mission Baseline .....	15
1.5 Document Structure.....	15
<b>2 EXECUTIVE SUMMARY .....</b>	<b>17</b>
2.1 Study Flow.....	17
2.2 Requirements and Design Drivers.....	17
2.3 Mission and System Baselines .....	18
2.4 Option: Scanning Mirror Solution.....	23
2.5 Technical Conclusions.....	24
<b>3 MISSION OBJECTIVES .....</b>	<b>27</b>
<b>4 PAYLOAD .....</b>	<b>29</b>
4.1 Baseline Design – S/C A .....	29
4.1.1 CoCa .....	30
4.1.2 MIRMISS.....	32
4.1.3 DFP for S/C A.....	33
4.1.4 MANiaC.....	37
4.2 Baseline Design – Probe B2 (ESA) .....	39
4.2.1 DFP for probe B2 .....	39
4.2.2 EnVisS .....	40
4.2.3 OPIC .....	41
4.3 Baseline Design – Probe B1 (JAXA) .....	42
4.3.1 HI - Lyman- $\alpha$ Hydrogen Imager .....	43
4.3.2 PS - Plasma Suite .....	43
4.3.3 WAC – Wide Angle Camera.....	43
4.4 Payload Mechanisms and Interface Notes .....	44
4.4.1 Mechanisms .....	44
4.4.2 Sun Exclusion.....	44
4.4.3 Radiators/Thermal Dissipation.....	44
4.5 Pointing and Pointing Stability.....	44
4.6 Data Links (SpaceWire or other) .....	45
4.7 Synchronisation/Timing .....	45
4.8 Technology Needs .....	46
<b>5 MISSION ANALYSIS .....</b>	<b>47</b>
5.1 Requirements and Design Drivers.....	47
5.2 Assumptions and Trade-Offs .....	47
5.3 Preliminary Mission $\Delta v$ Budget.....	47

<b>5.4</b>	<b>From Launch to the Start of the Transfer .....</b>	<b>48</b>
5.4.1	Transfer to SEL2 .....	48
5.4.2	SEL2 Station-Keeping .....	49
<b>5.5</b>	<b>Generic Analysis of Heliocentric Transfer to the Comet .....</b>	<b>49</b>
<b>5.6</b>	<b>Transfer Strategies from SEL2.....</b>	<b>52</b>
5.6.1	Direct Transfer Strategy.....	52
5.6.2	Moon Swing-By Strategy.....	53
<b>5.7</b>	<b>Analysis of Reachable Targets.....</b>	<b>56</b>
5.7.1	$\Delta v$ and Transfer Time Maps .....	56
5.7.2	Reachable Area.....	58
<b>5.8</b>	<b>Probabilistic Reachability Analysis.....</b>	<b>62</b>
5.8.1	Approach .....	62
5.8.2	LPC Distribution .....	64
5.8.3	Mission Monte Carlo Simulations .....	65
5.8.4	Discussion .....	71
<b>5.9</b>	<b>Transfer Geometry .....</b>	<b>71</b>
5.9.1	Analysis of Manoeuvres .....	73
<b>5.10</b>	<b>Geometry of the Science Downlink Phase .....</b>	<b>75</b>
<b>5.11</b>	<b>Transfers to the Backup Targets .....</b>	<b>78</b>
5.11.1	Transfers to 73P .....	79
5.11.2	Transfers to 26P .....	87
5.11.3	Additional Backup Targets.....	89
<b>5.12</b>	<b>Options .....</b>	<b>91</b>
5.12.1	Use of SEP for Trajectory Corrections Towards SEL2 .....	91
5.12.2	Probabilistic Reachability Analysis with Chemical Propulsion .....	93
<b>6</b>	<b>ENVIRONMENT .....</b>	<b>95</b>
<b>6.1</b>	<b>Requirements and Design Drivers .....</b>	<b>95</b>
6.1.1	Design Drivers: Radiation Effects and Main Sources of Radiation Environment.....	95
6.1.2	Design Drivers: Dust Micro-Meteoroid Sources .....	96
<b>6.2</b>	<b>Assumptions and Trade-Offs .....</b>	<b>96</b>
<b>6.3</b>	<b>Baseline Design .....</b>	<b>96</b>
6.3.1	Radiation .....	96
6.3.2	Hypervelocity Impact Risk Assessment .....	102
<b>7</b>	<b>SYSTEMS.....</b>	<b>117</b>
<b>7.1</b>	<b>System Requirements and Design Drivers .....</b>	<b>117</b>
<b>7.2</b>	<b>System Assumptions and Trade-Offs .....</b>	<b>119</b>
7.2.1	S/C A.....	121
7.2.2	Probe B2 .....	136
<b>7.3</b>	<b>Mission System Architecture .....</b>	<b>148</b>
7.3.1	Mission Profile .....	148
7.3.2	System Modes .....	149
<b>7.4</b>	<b>System Baseline Design .....</b>	<b>150</b>
7.4.1	System Decomposition.....	150

7.4.2	Design Summary.....	150
7.4.3	Mass Budget.....	153
7.4.4	Equipment List.....	156
7.4.5	Power Budget .....	160
7.4.6	ΔV Budget.....	168
7.4.7	Payload Data Budget.....	169
7.5	System Options .....	170
7.5.1	S/C A .....	170
7.5.2	Probe B2 .....	172
7.6	Open Points .....	173
<b>8</b>	<b>CONFIGURATION.....</b>	<b>175</b>
8.1	Requirements and Design Drivers.....	175
8.2	Assumptions and Trade-Offs .....	175
8.3	Baseline Design .....	175
8.3.1	S/C A .....	178
8.3.2	Probe B1 .....	182
8.3.3	Probe B2 .....	182
8.4	Overall Dimensions.....	183
<b>9</b>	<b>STRUCTURES .....</b>	<b>187</b>
9.1	Requirements and Design Drivers.....	187
9.2	Assumptions and Trade-Offs .....	187
9.3	S/C A Structure Design Definition .....	188
9.3.1	Material Justification.....	190
9.4	Probe B2 Design Definition .....	191
9.4.1	Definition .....	191
9.4.2	Dimensioning Analysis Results .....	192
9.4.3	Mass Budget .....	193
<b>10</b>	<b>CHEMICAL PROPULSION .....</b>	<b>197</b>
10.1	Requirements and Design Drivers.....	197
10.2	Assumptions and Trade-Offs .....	197
10.3	List of Equipment.....	199
10.3.1	Hydrazine Tank D-358 .....	199
10.3.2	Thruster MONARC-5 .....	200
10.3.3	Latch Valve LPLV.....	201
10.3.4	Miscellaneous Equipment .....	201
<b>11</b>	<b>ELECTRIC PROPULSION .....</b>	<b>205</b>
11.1	Requirements and Design Drivers.....	205
11.2	Assumptions and Trade-Offs .....	205
11.3	Baseline Design .....	206
11.3.1	Propellant Budget .....	207
11.4	List of Equipment.....	208
11.5	Options .....	208

11.6 Open Issues .....	209
11.7 Technology Needs .....	210
<b>12 MECHANISMS.....</b>	<b>211</b>
12.1 Requirements and Design Drivers .....	211
12.1.1 Separation/Release Mechanisms.....	211
12.1.2 Antenna (Deployment and) Pointing Mechanism & HDRM on S/C A.....	212
12.1.3 SA Mechanism: HDRM and Hinges/Synchronization Device on S/C A ....	212
12.1.4 Solar Array Drive Mechanism (SADM) on S/C A.....	213
12.2 Assumptions and Trade-Offs .....	213
12.2.1 Separation/Release Mechanisms.....	213
12.2.2 Antenna Pointing Mechanisms and HDRM .....	215
12.2.3 Solar Array Mechanism: HDRM and Hinges/Synchronization Device .....	216
12.2.4 Solar Array Drive Mechanisms .....	217
12.3 Baseline Design .....	217
12.3.1 Separation/Release Mechanisms.....	217
12.3.2 Antenna Pointing Mechanisms and HDRM .....	219
12.3.3 Solar Array Mechanism: HDRM and Hinges/Synchronization Device .....	220
12.3.4 Solar Array Drive Mechanism.....	220
12.4 List of Equipment.....	221
12.4.1 Separation/Release Mechanisms.....	221
12.4.2 Antenna Pointing Mechanisms and HDRM .....	222
12.4.3 Solar Array Mechanism: HDRM and Hinges/Synchronization Device .....	222
12.4.4 Solar Array Drive Mechanism.....	223
12.5 Options .....	223
12.5.1 Electric Propulsion Pointing Mechanism (EPPM) .....	223
12.6 Technology Needs .....	225
<b>13 GUIDANCE, NAVIGATION AND CONTROL SYSTEM .....</b>	<b>227</b>
13.1 Requirements and Design Drivers .....	227
13.1.1 Design Drivers.....	227
13.2 Assumptions and Trade-Offs .....	228
13.2.1 Assumptions.....	228
13.2.2 Trade-Offs .....	229
13.3 Baseline Design .....	233
13.3.1 Separation Sequence .....	233
13.3.2 GNC Architecture .....	235
13.4 List of Equipment.....	238
13.4.1 Visual Navigation Camera .....	239
13.5 Options .....	239
13.6 Technology Needs .....	239
<b>14 ATTITUDE AND ORBIT CONTROL SYSTEM .....</b>	<b>241</b>
14.1 Requirements and Design Drivers .....	241
14.1.1 Design Drivers.....	242
14.2 Assumptions and Trade-Offs .....	243

14.2.1 Assumptions.....	243
14.2.2 Trade-Offs .....	245
14.3 Baseline Design .....	267
14.3.1 AOCS Modes .....	267
14.3.2 Attitude Control Propellant Budget.....	270
14.4 List of Equipment.....	271
14.4.1 Reaction Wheels.....	271
14.4.2 Star Tracker.....	272
14.4.3 Sun Sensors .....	272
14.4.4 Gyroscope.....	273
14.4.5 Navigation Camera .....	273
14.5 Options .....	273
14.6 Technology Needs .....	274
<b>15 POWER.....</b>	<b>277</b>
15.1 S/C A.....	277
15.1.1 Requirements and Design Drivers.....	277
15.1.2 Assumptions and Trade-Offs .....	277
15.1.3 Baseline Design .....	278
15.1.4 Technology Needs .....	282
15.2 Probe B1.....	283
15.3 Probe B2 .....	283
15.3.1 Requirements and Design Drivers.....	283
15.3.2 Assumptions and Trade-Offs .....	284
15.3.3 B2 Electrical Architecture .....	285
15.3.4 Baseline Design .....	288
15.3.5 Conclusions and follow up .....	289
15.3.6 Technology Needs .....	290
15.4 Budgets .....	290
15.4.1 Mass Budget .....	290
15.4.2 Power Budget .....	291
<b>16 TELECOMMUNICATIONS.....</b>	<b>293</b>
16.1 Requirements and Design Drivers.....	293
16.1.1 Design Drivers.....	295
16.2 Assumptions and Trade-Offs .....	295
16.2.1 TT&C Bandwidth Trade-Offs .....	298
16.2.2 TT&C Antenna Trade-Offs .....	299
16.2.3 TT&C RF Power Amplification Trade-Off .....	301
16.2.4 TT&C Addition of Ka-Band Downlink Trade-Off.....	302
16.2.5 ISL Trade-Offs.....	303
16.2.6 Probe B2 Magnetometer Boom and ISL.....	312
16.3 Baseline Design .....	313
16.3.1 Telecommunications Mass Budgets .....	314
16.3.2 Telecomms Power Budgets .....	315
16.3.3 Telecomms Link Budgets.....	316

16.4	List of Equipment.....	317
16.5	Options for S/C A TT&C.....	319
16.6	Options for ISL.....	319
16.7	Technology Needs .....	319
<b>17</b>	<b>DATA HANDLING.....</b>	<b>321</b>
17.1	Requirements and Design Drivers .....	321
17.2	Assumptions and Trade-Offs .....	321
17.3	Top level Design .....	322
17.4	List of Equipment.....	323
17.4.1	S/C A.....	323
17.4.2	Probe B2 .....	330
17.5	Technology Needs .....	335
<b>18</b>	<b>THERMAL .....</b>	<b>337</b>
18.1	Requirements and Design Drivers .....	337
18.1.1	TCS Requirements .....	337
18.1.2	TCS Design Drivers .....	340
18.2	Environment .....	341
18.3	Spacecraft Attitude.....	342
18.3.1	S/C A.....	342
18.3.2	Probe B2 .....	343
18.4	Unit Modes and Dissipations.....	343
18.4.1	S/C A.....	343
18.4.2	Probe B2 .....	345
18.5	Baseline Thermal Design .....	346
18.5.1	Thermal Control Design Approach.....	346
18.5.2	Unit Thermal Categories (thermal control and interface) .....	346
18.5.3	S/C A Thermal Architecture Principles .....	347
18.5.4	Probe B2 Thermal Control.....	350
18.6	Thermal Control Features .....	351
18.7	Radiator and Heater Power Sizing.....	351
18.7.1	S/C A.....	351
18.7.2	Probe B2 .....	354
18.8	List of Equipment.....	355
18.8.1	TCS Mass Budget .....	356
18.9	Technology Needs .....	358
<b>19</b>	<b>GROUND SEGMENT &amp; OPERATIONS .....</b>	<b>359</b>
19.1	Requirements and Design Drivers .....	359
19.2	Baseline Design Assumptions .....	359
19.2.1	Ground Segment Overview .....	359
19.3	Mission Phases - Operational Considerations and Assumptions .....	361
19.3.1	Development Phase.....	361
19.3.2	Launch and Early Orbit Phase (LEOP).....	361
19.3.3	Commissioning/Transfer Phase .....	363

19.3.4 L2 Waiting Phase .....	363
19.3.5 Interplanetary Transfer Phase .....	363
19.3.6 Approach Phase .....	364
19.3.7 Probes Release Phase .....	365
19.3.8 Comet Fly-By Phase .....	366
19.3.9 Post-Encounter Phases .....	366
19.3.10 Decommissioning and Disposal Phase .....	366
<b>19.4 Space and Ground Segment – Operational Considerations and Assumptions</b>	<b>367</b>
19.4.1 Space Segment .....	367
19.4.2 Ground Segment .....	368
<b>20 PROGRAMMATICS .....</b>	<b>371</b>
20.1 Requirements and Design Drivers .....	371
20.2 Assumptions and Trade-Offs .....	371
20.3 Technology Requirements .....	372
20.4 Model Philosophy .....	378
20.4.1 Equipment / Sub-System Level: .....	378
20.4.2 System Level: .....	378
20.5 Model Test Matrix .....	379
20.6 Ground Support Equipment .....	381
20.7 Development Approach .....	381
20.8 Schedule .....	381
20.9 Instruments and Payloads .....	385
20.10 Summary and Recommendations .....	385
<b>21 TECHNICAL RISK.....</b>	<b>387</b>
21.1 Reliability and Fault Management Requirements .....	387
21.2 Risk Management Process and Scope of Risk Assessment .....	388
21.2.1 Approach for Risk Identification and Risk Reduction (steps 2 and 3) .....	390
21.3 Risk Management Policy .....	392
21.3.1 Hazard Targets .....	392
21.3.2 Success Criteria .....	393
21.3.3 Severity and Likelihood Categorisations .....	394
21.3.4 Risk Index & Acceptance Policy .....	396
21.4 Risk Drivers .....	397
21.5 Top Risk Log (preliminary) .....	398
21.5.1 Risk Log General Conclusions .....	403
21.6 Risk Log Specific Conclusions and Recommendations .....	403
<b>22 SOFTWARE .....</b>	<b>405</b>
22.1 Requirements and Design Drivers .....	405
22.2 Assumptions and Trade-Offs .....	406
22.3 Baseline Design .....	406
22.3.1 S/C A General Architecture .....	406
22.3.2 Probes Communication .....	408
22.3.3 Probe B2 Functional Modes .....	409

22.3.4 Science Data Telemetry Storage and Downlink .....	409
22.4 Options .....	411
<b>23 COST .....</b>	<b>413</b>
<b>24 SCANNING MIRROR AND PERISCOPE OPTION .....</b>	<b>415</b>
24.1 Introduction .....	415
24.2 Definitions .....	415
24.3 Requirements and Design Drivers .....	415
24.4 Assumptions and Trade-Offs .....	415
24.5 Baseline Design .....	421
24.5.1 Design Summary .....	421
24.5.2 Mass Budget .....	423
24.5.3 Equipment List.....	425
24.5.4 Power Budget .....	427
24.5.5 Data Budget.....	434
24.5.6 ΔV Budget.....	434
24.6 Configuration .....	434
24.7 Mechanisms.....	436
24.7.1 Requirements and Design Drivers.....	436
24.7.2 Assumptions.....	437
24.7.3 Trade-Offs Overview .....	437
24.7.4 Scanning Mirror Design.....	438
24.7.5 Dichroic Beam Splitter .....	439
24.7.6 Periscope Design .....	440
24.7.7 List of Equipment.....	442
24.8 AOCS.....	443
24.8.1 Star Tracker Layout.....	443
24.8.2 Actuator Sizing .....	444
24.9 GNC .....	445
24.10 Telecommunications .....	446
24.10.1 Benefits on S/C A .....	446
24.10.2 Benefits for the ISL .....	446
24.11 System Conclusion .....	448
24.12 Technology Needs .....	450
<b>25 CONCLUSIONS.....</b>	<b>451</b>
25.1 Summary .....	451
25.2 Study Compliance Matrix.....	451
25.3 Major Findings .....	451
25.4 Areas for Further Investigation .....	453
<b>26 REFERENCES.....</b>	<b>455</b>
<b>27 ACRONYMS .....</b>	<b>461</b>
<b>A RISK LOG .....</b>	<b>471</b>

# 1 INTRODUCTION

## 1.1 Background

In July 2018, ESA issued to the science community a Call for a Fast (F) mission opportunity in ESA's Science Programme. After a two-phase review process the Comet Interceptor mission was selected by the SPC (in June 2019) for going into the study phase, starting with a Concurrent Design Facility (CDF) mission assessment study.

The Comet Interceptor spacecraft will be launched in 2028 towards the Sun-Earth L<sub>2</sub> (SEL<sub>2</sub>) Lagrange point on-board an Ariane 6.2 as co-passenger to the ARIEL M mission.

The mission aims to intercept a Long Period Comet (LPC) (with Dynamically New Comets, DNCs, representing the highest priority type of LPC) or an interstellar body in a fly-by scenario. The mission includes three elements, one main S/C (ESA) and two probes (one ESA and one JAXA) carried as payloads until the fly-by, at which point they are released to gather multi-point observations of the comet and its coma.

Requested by SCI-FM and funded by the DPTD basic activities, this second Comet Interceptor study carries on from the first Comet Interceptor study performed in the ESA CDF in early 2019. The second study was carried out by an interdisciplinary team of experts from ESA with the participation of JAXA and the mission proposer team in 6 sessions, starting with a kick-off on the 30<sup>th</sup> October 2019 and ending with an Internal Final Presentation on the 29<sup>th</sup> November 2019. Following the Internal Final Presentation, two additional Delta sessions related to a ‘scanning payload mirror’ option were carried out, with the final Delta session being held on the 11<sup>th</sup> December 2019.

## 1.2 Objective

The objectives of the study were to:

- Continue and develop further the Comet Interceptor mission, concluding on the mission feasibility, taking into account science and programmatic requirements;
- Consolidate the mission architecture including mission analysis and operational concepts;
- Elaborate the conceptual design of the S/C A (main S/C) and B<sub>2</sub> (ESA probe) following a “design-to-cost” approach and using as much as possible existing technology and/or platforms with the aim of confirming feasibility of the concept;
- Consolidate the definition of the schedule and programmatic approach, remaining compatible with the ARIEL mission schedule (dual launch scenario with DLS);
- Consolidate the mission cost assessment with a target of 150 M€ (total mission cost);
- Provide inputs to the RFI/ITT packages for the industrial procurements.

## 1.3 Scope

The study assessed a mission concept that requires a new approach in order to establish feasibility as the mission target could, in principle, be selected after the mission launch.

Even in those cases where the target is known before launch, it remains likely that the information is only available very late in the development process, and too late to allow significant changes to the design.

As such, the mission must be designed to allow as wide a degree of flexibility as possible in selecting potential targets, given their relative scarcity (see Chapter 5 Mission Analysis).

The Comet Interceptor mission proposes to park the main S/C (S/C A) in a Halo orbit around the SEL2 point after launch, wait for a target of opportunity, and then intercept this selected target. Feasibility is conditioned to a given targets-of-interest population and vice-versa, i.e. a given system design will constrain the population of reachable targets.

Comet Interceptor must also comply with the additional constraints derived from the status of co-passenger to the ARIEL mission, which is already at the end of Phase B1. Comet Interceptor must therefore minimise the impact on the ARIEL mission design and programmatic aspects.

The main areas of work in the study, in line with its objectives, for each domain of expertise, are given below:

- **Systems and Science team:** Consolidation of the reachable target population and the mission geometry envelope; consolidation of the science operational profile; breakdown of critical performance requirements and several system trade-offs; update of system budgets (delta-V, mass, power, data, etc.).
- **Payload, Science team and JAXA:** Consolidation of the Payload suite including main S/C and probes instruments; specification of the required instrument resources and operational constraints.
- **Mission Analysis:** Consolidation of the reachability probabilities for the given target population; assessment of backup opportunities; characterisation of downlink geometries for downlink of the science data after cometary flyby.
- **Environment:** Specification of the radiation, micrometeoroids and comet dust environments during the transfer and target encounter phases; assessment of mission risk due to hypervelocity impacts from dust particles.
- **Configuration/Structures:** Placement of all units and payloads within the spacecraft; definition of structural design; assessment of structural shielding concept required for micrometeoroid/dust environment.
- **Propulsion:** Optimisation of the different chemical and electrical propulsion designs identified in the previous study for the new system configuration and mission profiles.
- **Mechanisms:** Assessment of the state of technology and identification of candidates for all mechanisms, including those for probe separation and the antenna pointing/solar array drive mechanisms.
- **AOCS/GNC:** Assessment of relative navigation and control at target arrival, including target tracking capabilities and the impact on flyby altitudes for all spacecraft, and assessment of actuators required to meet slew and dust mitigation requirements.

- **Power:** Identification of critical drivers due to the variation of power demand and wide range of mission geometries during the different mission phases; trade-off for most efficient solution for energy provision of the probe B2.
- **Telecommunications:** Identification of the optimal architecture for communications to ground (using the main S/C as relay system for both probes after deployment during target fly-by).
- **Data Handling:** Identification of relevant technologies for the probes compatible with the mission needs.
- **Thermal:** Identification of critical drivers and restrictions due to the wide range of mission geometries during the different mission phases.
- **AIV:** Definition of the AIV strategy, and identification of cost and time reduction measures compatible with ARIEL mission schedule and AIV/T approach.
- **Ground Segment and Operations:** Identification of critical drivers and restrictions due to launch as co-passenger to ARIEL and operation of all three spacecraft during the short time duration fly-by; definition of the Ground Segment architecture.
- **Programmatic, Risk and Cost:** Consolidation of the mission implementation plan, identification and characterisation of mission risks and mitigation actions, and confirmation that cost estimation remains within provided ceiling.

## 1.4 Important Remarks on Mission Baseline

Due to time constraints, this CDF study investigated in more detail the most demanding scenario of the main S/C (S/C A) slewing during the fly-by (i.e. without the ‘scanning mirror’ for the CoCa instrument) and featuring electric propulsion, so as to establish its compatibility with the F-mission boundaries.

An option with a scanning mirror for the CoCa instrument has been addressed in the final stages of the study and was found advantageous at system level, as it seems to allow simplifying the S/C A design. This option is discussed in Chapter 24, Scanning Mirror and Periscope Option.

Following a preliminary assessment of the CDF results, a mission design based only on chemical propulsion and including the scanning mirror for CoCa is judged as providing acceptable science performance and as a better match to the strict programmatic boundaries of the F-mission; therefore, subject to further analysis and consolidation, this option was selected as the preferred baseline for the RFI issued to industry.

Nevertheless, the following report chapters (which detail a baseline including electrical propulsion and no scanning mirror) provide an important reference for the continuation of the study activities during Phase A/B for the majority of subsystems.

## 1.5 Document Structure

The layout of this report of the study results can be seen in the Table of Contents. The Executive Summary chapter provides an overview of the study; details of each domain addressed in the study are contained in specific chapters. The design option for the

---

scanning mirror for CoCa is detailed in Chapter 24, Scanning Mirror and Periscope Option.

Due to the different distribution requirements, and the fact that this version of the report is releasable to the public, the cost information has been excluded. The costing information is published in a separate document.

## 2 EXECUTIVE SUMMARY

### 2.1 Study Flow

In July 2018, ESA issued to the science community a Call for a Fast (F) mission opportunity in ESA's Science Programme. After a two-phase review process the Comet Interceptor mission was selected by the SPC (in June 2019) for going into the study phase, starting with a Concurrent Design Facility (CDF) mission assessment study.

The Comet Interceptor spacecraft will be launched in 2028 towards the Sun-Earth L<sub>2</sub> (SEL<sub>2</sub>) Lagrange point on-board an Ariane 6.2 as co-passenger to the ARIEL M mission.

The mission aims to intercept a Long Period Comet (LPC) (with Dynamically New Comets, DNCs, representing the highest priority type of LPC) or an interstellar body in a fly-by scenario. The mission includes three elements, one main S/C (ESA) and two probes (one ESA and one JAXA) carried as payloads until the fly-by, at which point they are released to gather multi-point observations of the comet and its coma.

Requested by SCI-FM and funded by the DPTD basic activities, this second Comet Interceptor study carries on from the first Comet Interceptor study performed in the ESA CDF in early 2019. The second study was carried out by an interdisciplinary team of experts from ESA with the participation of JAXA and the mission proposer team in 6 sessions, starting with a kick-off on the 30th October 2019 and ending with an Internal Final Presentation on the 29th November 2019. Following the Internal Final Presentation, two additional Delta sessions related to a 'scanning payload mirror' option were carried out, with the final Delta session being held on the 11th December 2019.

### 2.2 Requirements and Design Drivers

The main mission requirements and design drivers are the following:

- Shared, dual launch in 2028 with ARIEL (with a DLS) on-board Ariane 6.2 from Kourou
- Nominal mission lifetime up to 5 years with ~6 months of science operations
- Multi-element mission to support multi-point observations
  - One main S/C plus two probes (carried as payloads until the separation before the cometary flyby)
- Robust design due to unknown target (backup targets are identified)
  - Maximise reachable targets-of-interest population
  - Wide range of encounter conditions and Sun-Earth-Target geometries
- Very high fly-by relative velocity range (~10 to 70 km/s)
  - Target tracking capabilities
  - Micrometeoroid and dust environment

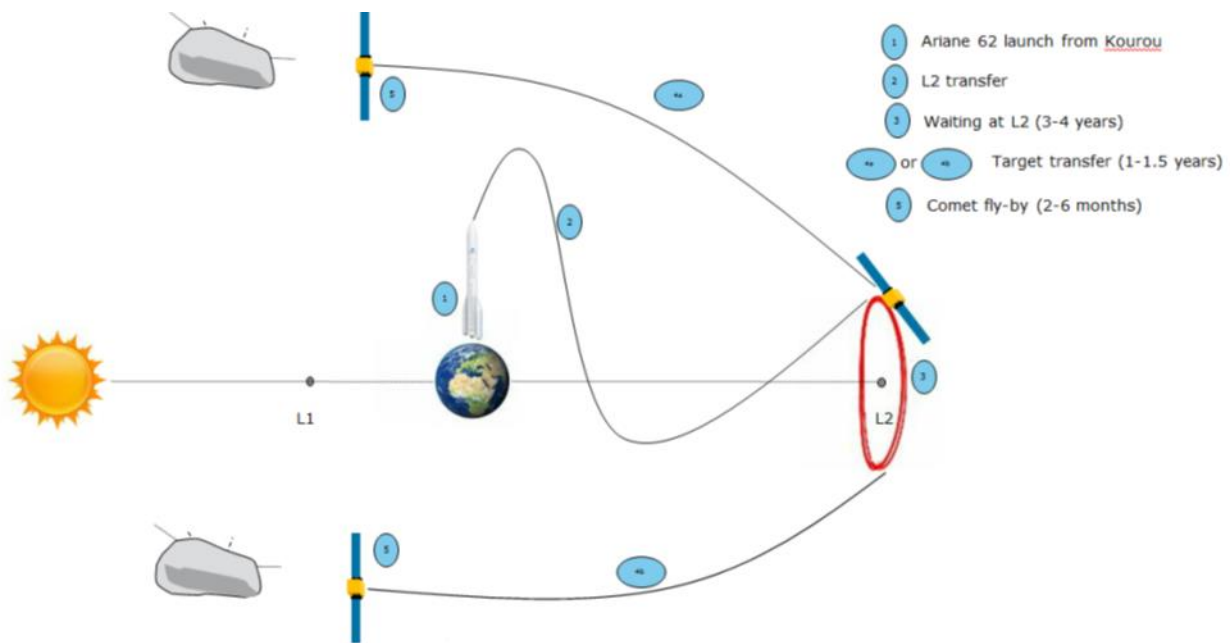
Some additional mission constraints were considered:

- All payload and platform units at least TRL 7 by Mission Adoption (Q4 2022)
- Programmatic compatibility with ARIEL mission schedule and AIV/T plan

- Maximum Cost at Completion (CaC) of 150 M€ (excluding launcher)
- Compliance to space debris mitigation requirements (ECSS standard).

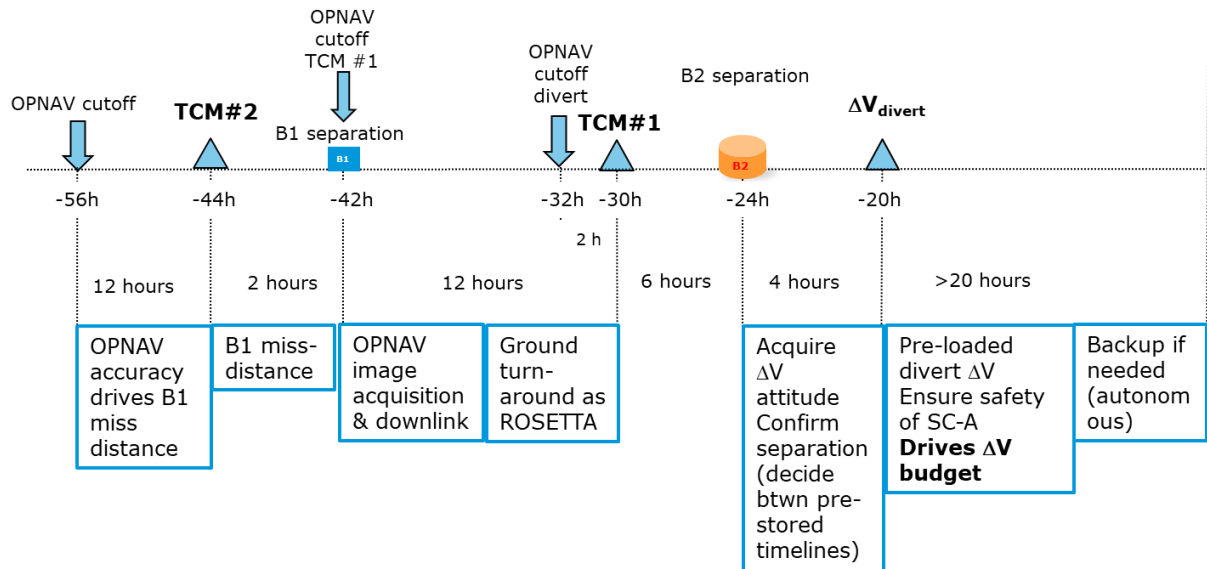
## 2.3 Mission and System Baselines

The Comet Interceptor mission is designed for a 5 years mission lifetime with up to 6 months of nominal science operations after encounter. Based on the overall mission concept, the mission timeline is highly dependent on finding a suitable target and the planned fly-by encounter. The main mission phases are schematically shown in Figure 2-1 below:



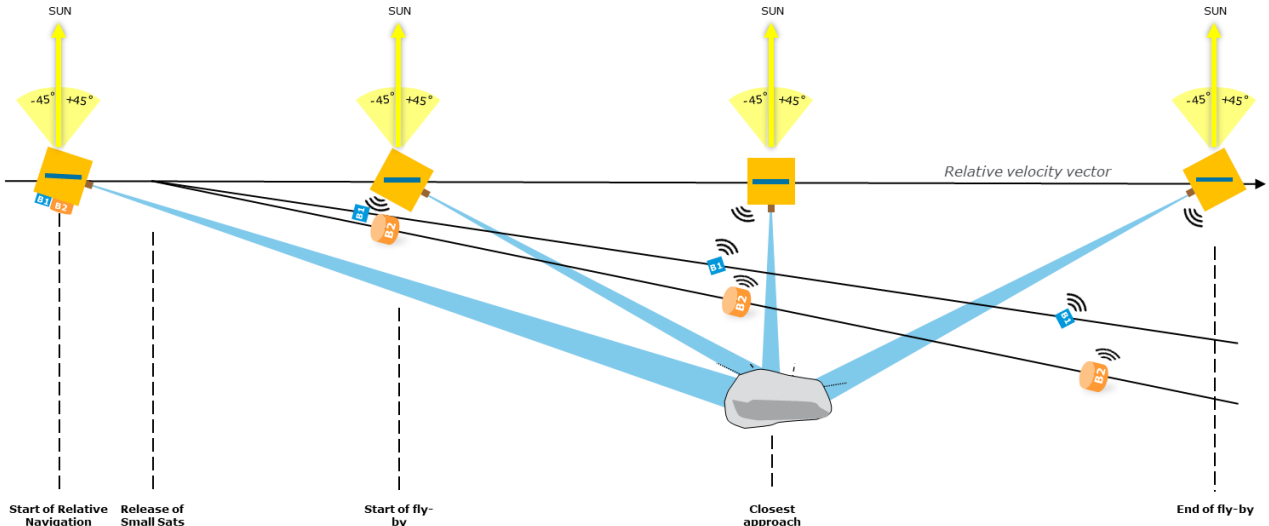
**Figure 2-1: Comet Interceptor Mission Profile**

The Fly-By phase is assumed to start 2-6 months before Closest Approach (CA) and is marked by the start of Relative Navigation to the Comet. Approximately 56 hours before S/C A reaches the closest approach, operations start becoming more active, and a more detailed timeline is presented (Figure 2-2) for this period (during which both probes are released and nominal science operations are performed).



**Figure 2-2: Comet Interceptor Fly-by Timeline (from -56 hours up to 0 hours – Closest Approach)**

The geometry of the spacecraft (S/C A) and the probes B1 and B2 with respect to the comet during the Fly-By Phase (with a focus on the closest approach) is presented in Figure 2-3.

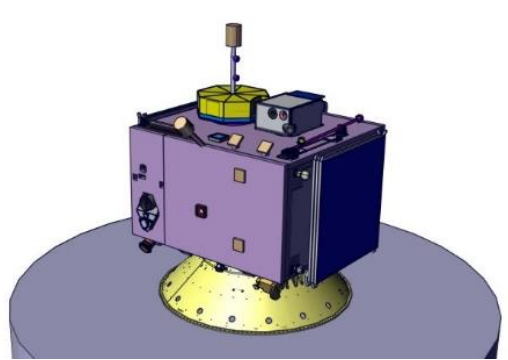
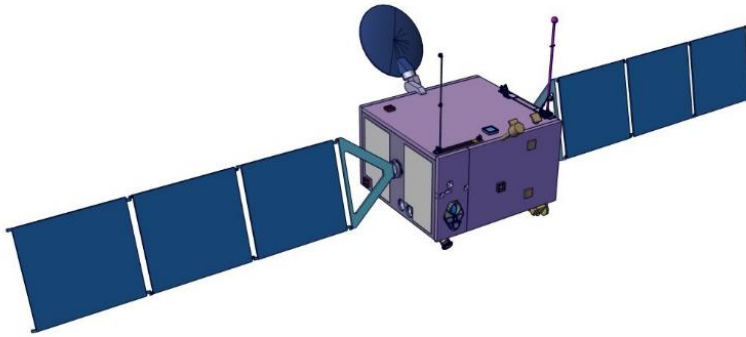


**Figure 2-3: Comet Interceptor Fly-by and Closest Approach Geometry**

The mission and system baseline summaries, including all elements – main S/C (S/C A) and both probes (B1 and B2) – are outlined in Table 2-1, Table 2-2, Table 2-3 and Table 2-4.

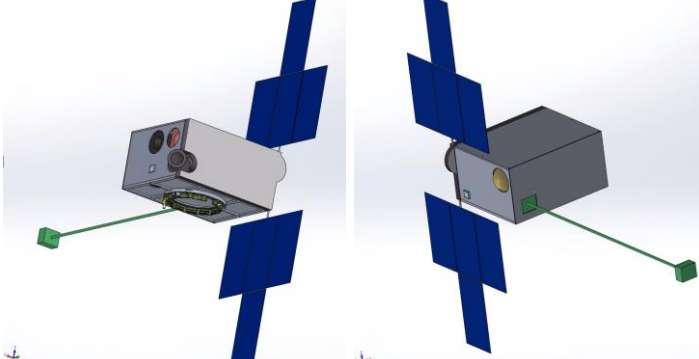
Comet Interceptor – Mission summary		
Lifetime	Nominal 5 years with maximum 6 months of Science Operations	
Launch	Launcher	Ariane 6.2
	Date	2028
	Configuration	Shared, dual launch with ARIEL mission
Orbit	Waiting phase	Halo orbit around SEL2 point
	Target transfer phase	Heliocentric trajectory close to Earth orbit
	Conditions at encounter	Heliocentric distances between 0.9 and 1.25 AU Solar phase angle range at encounter +/-45 deg Fly-by relative velocity at encounter ≤70 km/s
Overall system characteristics		
Mass	Dry mass	655 kg
	Wet mass	796 kg (incl. probes B1 and B2)
Dimensions	Stowed	1,974 mm x 2,073 mm x 1,976 mm
	Deployed	9,768 mm x 2,999 mm x 2,484 mm
Delta-V	Chemical propulsion	110 m/s
	Electric propulsion	1522.5 m/s

**Table 2-1: Mission summary**

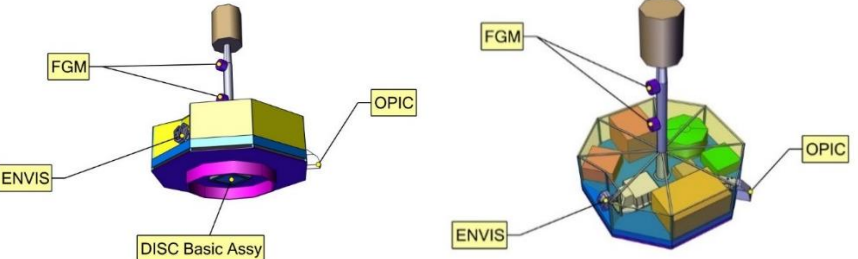
Main S/C (S/C A, ESA) – System baseline summary	
Configuration stowed	
Configuration deployed	
Mass	Dry Mass (w/ margin)      655kg

	Wet Mass	796 kg (incl. probes B1 and B2)
Dimensions	Stowed	1,974 mm x 2,073 mm x 1,976 mm
	Deployed	9,768 mm x 2,999 mm x 2,484 mm
Instruments	CoCa, DFP, MANiac (with rotating mechanism) and MIRMISS	
AOCS	6x Sun sensors 2x Star trackers (STR) 2x Inertial Measurement Unit (IMU) 2x Navcam 4x 4 Nms / 0.215 Nm Reaction Wheels (RW)	
Communications	1x 0.9 m diameter steerable X-band High Gain Antenna (HGA) 2x X-band Low Gain Antenna (LGA) 2x X-band Deep Space Transponder (DST) 2x S-band Inter-Satellite Link (ISL) transceivers 6x S-band ISL Low Gain Antenna (LGA)	
Data Handling	1x On-Board Computer (OBC) 1x Remote Interface Unit (RIU)	
Power	2x 3 m <sup>2</sup> solar arrays 1x Power Conversion and Distribution Unit (PCDU): MPPT for 28V non-regulated bus 1x 512 Wh Secondary Battery	
Chemical Propulsion	Monopropellant (Hydrazine) blow-down system 4(+4)x 5N thrusters 2x 33 L Hydrazine tank (usable)	
Electrical Propulsion	1x PPS-1350 Hall effect thruster 2x 32 L Xenon tank (usable)	
Thermal	Radiators, SLI and MLI, heat pipes, heaters and thermistors	
Structures	Aluminium skin and honeycomb core central shear, side, baseplate and top panels Varying thicknesses of Al and honeycomb depending on the panel's shielding necessity. Primary micrometeroid shielding on 3 panels.	
Mechanisms	1x Launcher separation mechanism 1x B1 linear-separation mechanism 1x B2 linear-separation mechanism 1x 2 degrees of freedom Antenna Pointing Mechanism (APM) 2x Solar Array Driving Mechanism (SADM) 8x Solar panel Hold Down and Release Mechanism (HDRM)	

**Table 2-2: S/C A: system baseline summary**

Probe B1 (JAXA) – System baseline summary	
Configuration	
Mass estimation	30 kg (including separation mechanism on B1 and A)
Dimensions	Stowed 576 mm x 426 mm x 300 mm
	Deployed 1616 mm x 1489 mm x 534 mm
Instruments	HI, PS, WAC, Ion Mass Spectrometer & Deployable Magnetometer

**Table 2-3: Probe B1: system baseline summary**

Probe B2 (ESA) – System baseline summary	
Configuration	
Mass estimation	40 kg (including separation mechanism on B2)
Dimensions	851 mm x 600 mm x 600 mm
Payload	DFP, EnVisS, FGM and OPIC
AOCS	1x momentum wheel
Communications	1x S-band Inter-Satellite Link (ISL) 1x S-band toroidal antenna
Data Handling	1x On-board Computer (OBC)
Power	1x 1546 Wh Primary Battery 1x Power Distribution Unit (PDU)
Thermal	Radiators, SLI and MLI, paints, heaters and thermistors
Structures	Aluminium baseplate stiffened with Aluminium ribs and side walls MLI tent & Communication antenna support structure
Mechanisms	1x B2 linear-separation mechanism

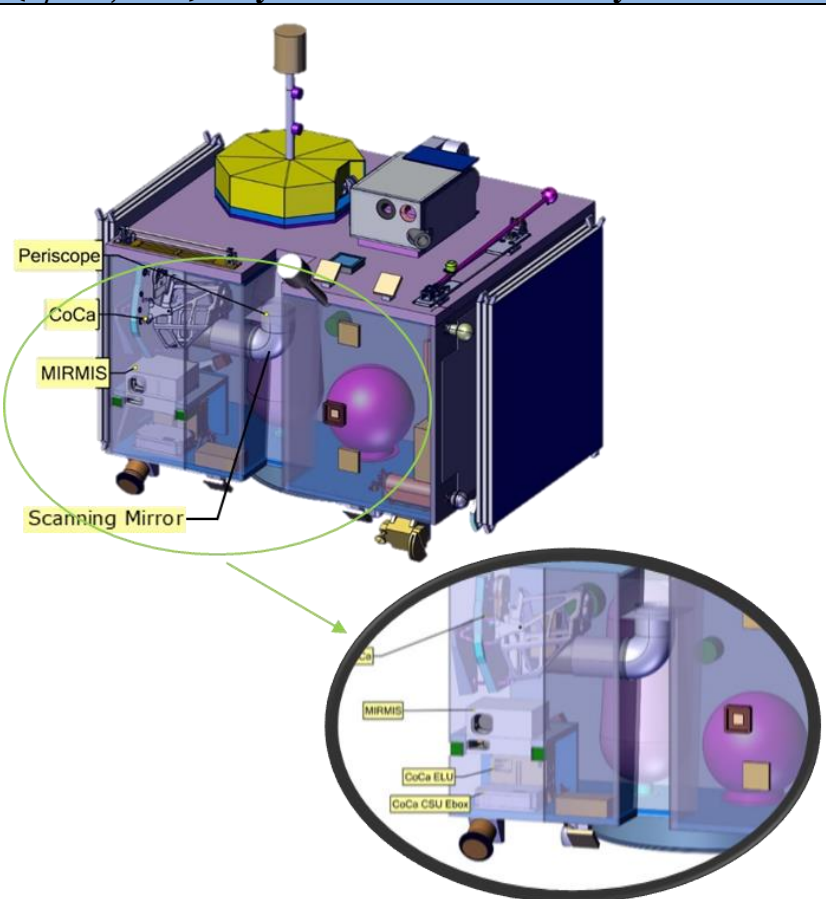
**Table 2-4: Probe B2: system baseline summary**

## 2.4 Option: Scanning Mirror Solution

Two post-IFP delta-sessions were held in order to assess a system concept, whereby the S/C A maintains a constant orientation during the fly-by, and only the relevant payload(s) are rotated to observe the comet. This was investigated in order to determine if such an approach would be more mass efficient (smaller reaction wheels, less shielding) and/or less risky or costly.

Note that only a delta-assessment from the original baseline (slewing) concept was performed.

The summary of this option is shown in Table 2-5 below:

Main S/C (S/C A, ESA) – System baseline summary		
Configuration stowed		
Mass	Dry Mass (w/ margin)	604 kg
	Wet Mass	738 kg (incl. probes B1 and B2)
Dimensions	Stowed	1,974 mm x 2,073 mm x 1,976 mm
	Deployed	9,768 mm x 2,999 mm x 2,484 mm
Instruments	CoCa, DFP, MANiac (no rotation mechanism) and MIRMISS	

AOCS	6x Sun sensors (SS) 2x Star trackers (STR) 2x Inertial Measurement Unit (IMU) 2x Navcam 4x 4 Nms / 0.095 Nm Reaction Wheels (RW)
Communications	1x 0.9 m diameter steerable X-band High Gain Antenna (HGA) 2x X-band Low Gain Antenna (LGA) 2x X-band Deep Space Transponder (DST) 2x S-band Inter-Satellite Link (ISL) transceivers 2x S-band ISL Low Gain Antenna (LGA)
Data Handling	1x On-Board Computer (OBC) 1x Remote Interface Unit (RIU)
Power	2x 3 m <sup>2</sup> solar arrays 1x Power Conversion and Distribution Unit (PCDU): MPPT for 28V non-regulated bus 1x 512 Wh Secondary Battery
Chemical Propulsion	Monopropellant (Hydrazine) blow-down system 4(+4)x 5N thrusters 2x 33 L Hydrazine tank (usable)
Electrical Propulsion	1x PPS-1350 Hall effect thruster 2x 32 L Xenon tank (usable)
Thermal	Radiators, SLI and MLI, heat pipes, paints, heaters and thermistors
Structures	Aluminium skin and honeycomb core central shear, side, baseplate and top panels. Varying thicknesses of Al and honeycomb depending on the panel's shielding necessity. Primary micrometeoroid shielding on 1 panel.
Mechanisms	1x Launcher-separation mechanism 1x B1 linear-separation mechanism 1x B2 linear-separation mechanism 1x 2 degrees of freedom Antenna Pointing Mechanism (APM) 8x Solar panel Hold Down and Release Mechanism (HDRM) 1x Scanning Mirror Assembly (Mirror, Baffle, Drive, Bearings, Ebox) 1x Periscope

**Table 2-5: S/C A summary – Scanning Mirror and Periscope Option**

## 2.5 Technical Conclusions

The Comet Interceptor 2 study was undertaken in order to consolidate and further the work of the previous Comet Interceptor CDF study. While some important open issues still could not be closed during the second study (discussed further below), no technical showstoppers were identified for the mission. Nonetheless, it is clear that the mission remains challenging within the programmatic constraints (particularly regarding launch mass and cost). Furthermore, the risks posed by the cometary dust environment will require particular focus in the coming phases.

The main open issues and areas of concern to be studied in follow up activities are:

- There remain significant open issues in the **modelling of the cometary dust environment**, particularly for large particles. As these large particles are the ones most impacting mission risk, dedicated work is recommended on closing these uncertainties as soon as possible.
- A concept involving a scanning mirror for the CoCa instrument has been addressed in the final stages of the study and was found advantageous at system level, as it seems to allow simplifying the S/C A design. However, further work is needed in order to consolidate the concept.
- In addition, only a simple assessment could be performed for the system option of removing the electric propulsion system to reduce the mission cost. A detailed assessment should be performed in later work.
- For the baselined system option including the electric propulsion, the use of an EP thruster gimbal to save AOCS propellant mass (to correct for misalignments) should be traded against the mass due to misalignment. However the mass savings (ca. 12 kg for the gimbal compared to ca. 26 kg for the AOCS propellant) may not be sufficient to justify the additional cost.
- The probe B2 power architecture baselined a case that used only a primary battery as power source, in order to limit the mass, cost and complexity. The power experts highlighted at the end of the study potential new developments that could alleviate some of these concerns, however their impact could not be assessed within the available time. These should be re-assessed, to determine if they can increase the available science time and robustness with a reasonable system-level impact.
- The placement of the FGM instrument on the probe B2 poses challenges, due to its need to be placed on the anti-ram face, which also houses the ISL antenna. An initial assessment showed that the FGM interferes with the gain pattern of the ISL antenna. A solution was proposed to place the ISL antenna on top of the FGM boom, however the full impacts of this and a concrete design proposal could not be made in the time available.

This Page Intentionally Blank

### 3 MISSION OBJECTIVES

Comet Interceptor is a mission aiming to explore a comet entering the Solar System for the first time in order to:

- Assess the bulk shape of the nucleus and the morphology of its surface at a scale comparable to the best images returned by previous comet flyby missions, and those returned by *New Horizons* of Kuiper Belt Objects
- Determine the bulk composition of the nucleus' surface
- Investigate activity in a fresh comet
- Assess the molecular composition of the coma simultaneously at multiple locations and the isotopic composition along one path
- Identify parent and daughter neutral and ion species and assess their relationship in the coma
- Characterise the dust in the coma
- Assess the structure of boundaries and regions in the plasma environment of a comet
- Assess the energy, mass and momentum transfer in the cometary environment, through the coma and across boundaries
- Assess how plasma and dust interact in various regions of the coma.

To this aim, the mission architecture consists of three spacecraft: the main S/C (or S/C A) and two probes (denoted as B1 and B2). All three spacecraft carry science instruments, as detailed in Chapter 4. The multiple viewing positions offered by this configuration will greatly increase the 3D information provided on the target and its jets/coma.

The ultimate science objective of the mission is to understand the diversity of comets by characterising a Long Period Comet (LPC), which would broaden our understanding of comet morphology, composition, and plasma environment. Such a comet would offer a unique viewpoint along the evolutionary path of comets from their formation to migration into the inner Solar System.

To achieve its goals and increase the probability of finding an interesting target, this mission takes full advantage of the designated launch configuration, i.e. dual launch with ARIEL to SEL2. The Comet Interceptor spacecraft waits orbiting around SEL2 (2-3 years, depending on the target and selection criteria) until the target discovery.

The likelihood of an early detection will soon be greatly increased by the Large Synoptic Survey Telescope (LSST), which will increase the distance at which LPCs are discovered inbound. Comets are expected to be found at  $\sim$ 20 AU, giving warning times of  $> 5$  years. Therefore, the target may actually be known before launch (but not before the design has to be frozen).

Although unlikely to occur, this mission also considers the possibility that an interstellar target (highly hyperbolic orbit) could be discovered and reached. The ‘Oumuamua study (Seligman & Laughlin 2018) showed that the expectation would be for the LSST to find one accessible target in  $\sim$ 10 years. Therefore, a non-negligible chance exists of

discovering a suitable target within the waiting period in SEL2. The science payload complement is optimised for the scenario of visiting a LPC but would still be useful for the case of an interstellar target.

In order to assess the feasibility of such a mission concept before going out to industry, SCI-FM requested an internal CDF study. In fact, two CDF studies were carried out to analyse different launch configurations (e.g. stacked launch versus dual launch featuring a dual launch structure (DLS)) and different payload compliments.

The main objectives of the CDF studies could be summarised as:

- Assessing the feasibility of the Comet Interception mission concept taking into account the science goals but considering the F-mission call programmatic requirements as well as the compatibility with the ARIEL mission interface requirements
- Consolidating the mission architecture, including mission analysis and operational concepts in order to derive requirements
- Consolidating the conceptual design of the two European spacecraft (S/C A and probe B2) by applying a “design-to-cost” approach (e.g. using existing technology and/or platforms as much as possible) in order to derive requirements
- Deriving interface requirements for the JAXA-provided B1 probe
- Defining the schedule and programmatic approach remaining compatible with the Ariel mission schedule
- Assessing the mission cost and associated risks, with a target of 150 MEuro (excluding the launcher).

The outputs of the CDF study were set to form the basis for the RFI and ITT processes to be issued to industry in 2020. In addition, the FEM produced during the study may be used by Arianespace to run a preliminary Coupled Load Analysis (CLA) and derive the loads applicable to the upper passenger on top of the DLS, in this case the Comet Interceptor spacecraft.

## 4 PAYLOAD

The Model Payload for the Comet Interceptor mission comprises instruments on the S/C A (ESA), probe B2 (ESA), and the probe B1 (JAXA). The payload that is presented here was used to size the mission, in particular with respect to power, mass, data rate, volume and accommodation.

To size the communications sub-system, the data rates and volumes of the instruments had to be derived. This was achieved using an observation timeline, established for the time of “Closest Approach (CA)” (see Systems chapter 7.3.1). The time shortly before and after the Closest Approach (CA) to the comet is the scientifically most valuable time of this mission. It is therefore critical to be able to downlink data from the probes to the main S/C in real-time before the CA, in case communication is not possible after the CA (e.g. due to failure of one of the probes). The data rates and data volume were also used to assess the feasibility of the data downlink for this period of time.

### 4.1 Baseline Design – S/C A

In this section the instruments for S/C A are described. Their details are listed in Table 4-1, including their mass (incl. 20% equipment maturity margin), average power consumption, physical size, FoV, and data volume.

Instrument	Mass [kg]	Power [W]	Length [mm]	Width [mm]	Height [mm]	Diam. [mm]	FoV	Data volume [Gb]
<b>CoCa Camera Support</b>	8.22	14.40	530	450	350	-	$0.69^\circ \times 0.92^\circ$	128.00
<b>CoCa Electronics Unit</b>	2.52	-	176	236	117	-	-	-
<b>CoCa Proximity Electronics Unit</b>	1.02	-	70	240	160	-	-	-
<b>CoCa Radiator</b>	0.21	-	-	-	-	-	-	-
<b>CoCa harness + therm. insulation</b>	0.82	-	-	-	-	-	-	-
<b>DFP COMetary Plasma Light Instrument boom 1</b>	0.36	-	1063	20	20	-	-	-
<b>DFP COMPLIMENT+FGM +boom 2</b>	2.04	-	1200	200	200	-	-	-
<b>DFP COMetary Plasma Light Instrument probe</b>	-	-	-	40	-	40	-	-
<b>DFP E-Box</b>	5.93	20.16	252	216	158	-	-	6.79
<b>DFP Dust Impact Sensor and Counter</b>	0.42	-	121	116	46	-	-	-
<b>DFP Low Energy Electron Spectrometer 1</b>	0.96	-	-	-	114	130	$0-70^\circ \times 360^\circ$	-
<b>DFP Solar wind and Cometary Ions and Energetic Neutral Atoms-ENA sensor</b>	1.08	-	140	200	180	-	$150^\circ \times 15^\circ$	-

Instrument	Mass [kg]	Power [W]	Length [mm]	Width [mm]	Height [mm]	Diam. [mm]	FoV	Data volume [Gb]
<b>DFP Solar wind and Cometary Ions and Energetic Neutral Atoms-Ion sensor</b>	-	-	-	-	-	-	close to 2 Pi	-
<b>MANiaC Sensor Head Unit</b>	1.08	21.60	120	400	130	-	-	-
<b>MANiaC Neutral Density Gauge</b>	0.24	3.60	80	80	120	-	-	-
<b>MANiaC Electronics Unit</b>	4.20	2.4	176	236	197	-	-	5.60
<b>MANiaC harness+rotat. mechanism</b>	1.02	-	-	-	-	-	-	-
<b>A MIRMISS Thermal InfraRed Imager</b>	6.72	9.00	213	253	170	-	9° x 9°	1.01
<b>A MIRMISS Near InfraRed Sensor</b>	-	-	-	-	-	-	6.7° x 5.4°	3.36
<b>A MIRMISS Mid-InfraRed Sensor 1</b>	-	-	-	-	-	-	1° (circular)	0.15
<b>A MIRMISS Mid-InfraRed Sensor 2</b>	-	-	-	-	-	-	-	-
<b>A MIRMISS Radiator</b>	0.21	-	-	-	-	-	-	-
<b>Sum</b>	<b>37.07</b>	<b>71.16</b>						

**Table 4-1: Payload for S/C A**

Details of the instruments are listed in the following sub-sections.

#### 4.1.1 CoCa

The Comet Camera CoCa is designed for colour imaging of the target's surface at a resolution sufficient to determine its structure and homogeneity. It is based on the CaSSIS instrument from the ExoMars Trace Gas Orbiter (TGO) and is a spare from this instrument. However, some changes will need to be implemented for CoCa, e.g. a filter mechanism.

CoCa (see Figure 4-1) consists of two main units: the camera support unit (CSU) and the electronics unit (ELU).

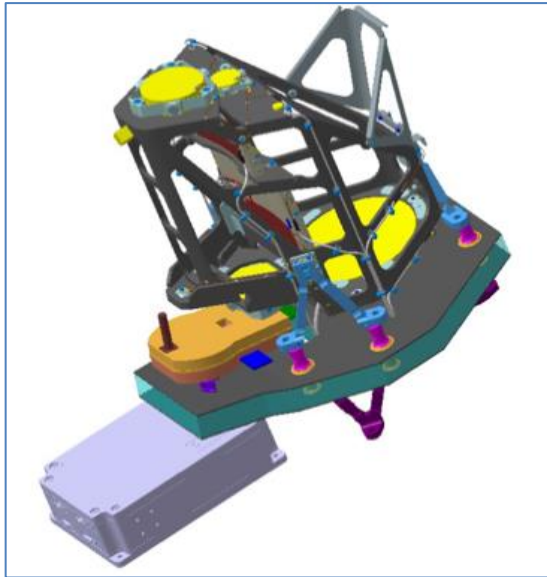


**Figure 4-1: CoCa CAD image with CSU and ELU.**

A fact sheet for CoCa is given in Table 4-2:

Accommodation	Body-mounted on S/C A, pointed in the line of sight of the comet
IFoV	8 µrad/px
FoV	0.69° × 0.92°
Pointing direction/accuracy	Nucleus <0.1° from detector centre
Exposure times	220 µs (fly-by) to 15 min (identification)
Minimum framing rate	<1 fps
Filters	475 nm ( $\Delta\lambda=150$ nm) BLU 675 nm ( $\Delta\lambda=100$ nm) ORG 775 nm ( $\Delta\lambda=100$ nm) RED 900 nm ( $\Delta\lambda=150$ nm) NIR
Mass	12.81 kg (incl. 20% margin, harness, thermal insulation, radiator)
Power	14.40 W (on; incl. 20% margin); 25 W (peak)
Volume	CSU: 530 × 450 × 350 mm <sup>3</sup> ; ELU: 176 × 236 × 117 mm <sup>3</sup>
Data volume for the flyby	128 Gb

**Table 4-2: CoCa fact sheet**

**Environment requirements:** The same EMC requirements as for ExoMars TGO shall be applied (e.g. in-rush current tests shall be carried out according to ECSS-E-ST-20-07C, etc).

**Accommodation requirements:** The telescope shall point at the comet. The Sun must be kept >40° from the boresight during science and >10° from the boresight during safe modes.

**Data rate/volume:** The data volume is ca. 128 Gb for the entire mission.

#### 4.1.2 MIRMISS

The Modular Infrared Molecules and Ices Sensor (MIRMISS), is the hyper and multispectral imaging system for S/C A. It covers the spectral range 0.9 to  $\sim 25 \mu\text{m}$  and will map the ice and mineral composition of the target nucleus and coma and the surface temperature of the nucleus.

Measurements of the spatial distribution of ices, minerals and surface temperatures are essential to define the formation, evolution, and structure of the CI target nucleus and coma. Mapping of compositional diversity could indicate whether the nucleus is a rubble-pile object with different evolutionary histories, or a uniform body formed as a single process.

The spectral imaging will enable to assign compositional information to various geological structures imaged by MIRMISS itself, or at higher resolution by CoCa. It will also provide spatial context to the measurements made by the instruments on probes B1 and B2.

Thermal maps will provide information on surface roughness, porosity and sub-surface temperature structure that are not resolvable with CoCa.

The MIRMISS spectral range is covered by four channels (see Figure 4-2):

- MIRMISS NIR - hyperspectral camera 0.9 to  $1.7 \mu\text{m}$  (TBC)
- MIRMISS MIR 1 and 2 - dual channel single-point spectrometer  
 $\sim 2.5 - 4.0 - 7.0 \mu\text{m}$  (TBC)
- MIRMISS TIRI – Multispectral Thermal Imager  $\sim 6 - 25 \mu\text{m}$

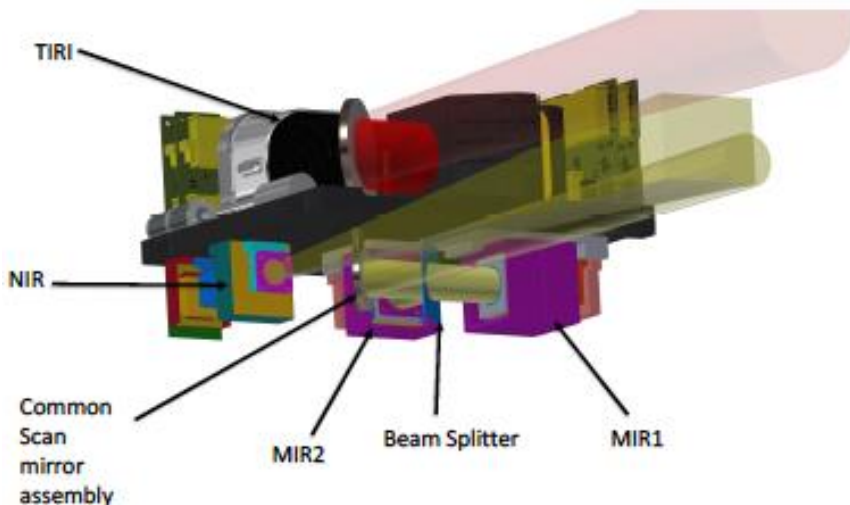


**Figure 4-2: MIRMISS layout showing the four channels in the “Double decker” configuration**

The NIR spectral imager has been successfully demonstrated in Low Earth Orbit (LEO) on board the Reaktor Hello World CubeSat. It needs to be assessed how this heritage can be applied for the Comet Interceptor mission.

**Environment requirements:** Currently not identified.

**Accommodation requirements:**

MIRMISS shall be pointing at the comet during flyby with a tolerance of ~1 mrad. Spectroscopic mapping is performed by scanning the cometary nucleus / coma. All channels are boresighted and their FoVs aligned. The pointing accuracy shall be within ±30mrad to guarantee that the nucleus is in the MIRMISS-TIRI field of view.

Sun intrusion is tolerable for short exposures (<1 second), while TIRI employs a mirror, which shall be parked in the sun-safe position for launch.

During operation, the thermal control of all channels requires that they are not exposed directly to warm surfaces (e.g., solar panels, radiators) or direct sunlight.

**Data rate/volume:**

- Depends on available downlink budget. The baseline is 4.5 Gb with margin including calibration frames.
- MIRMISS has its own data storage. It can be sized from 8 Gb to 128 Gb. It is foreseen to buffer all data within the instrument during observations.

#### 4.1.3 DFP for S/C A

The Dust Field and Plasma (DFP) package is a combined experiment dedicated to the in situ, multi-point study of the multi-phased ionized and dusty environment in the coma of the target LPC and of its interaction with the surrounding space environment and the Sun.

The DFP will measure magnetic field, the electric field, plasma parameters (density, temperature, speed), the distribution functions of electrons, ions and energetic neutrals, spacecraft potential and the cometary (nm size) dust impact.

The DFP comprises five sensors on S/C A and central electronics.

The DFP sensors on S/C A are:

##### 4.1.3.1 COMPLIMENT

The COMetary Plasma Light InstrUMENT is a combined plasma and E-field instrument including a double Langmuir Probe and a Mutual Impedance experiment, with electric field measurement capabilities. Its heritage is based on a subpart of the JUICE/RPWI package and Rosetta RPC-MIP and RPC-LAP. COMPLIMENT runs simultaneously in “Langmuir” mode and “Mutual Impedance Probe” mode aiming to monitor the cold plasma (ion and electron density plus electron temperature), the integrated EUV flux and the S/C potential.

Note that this instrument consists of sensors mounted on **two booms**. One is completely dedicated to the COMPLIMENT instrument and the other boom is also carrying one flux-gate magnetometer and a combined Langmuir Probe and FGM (see Section 4.1.3.3 and Figure 4-3).

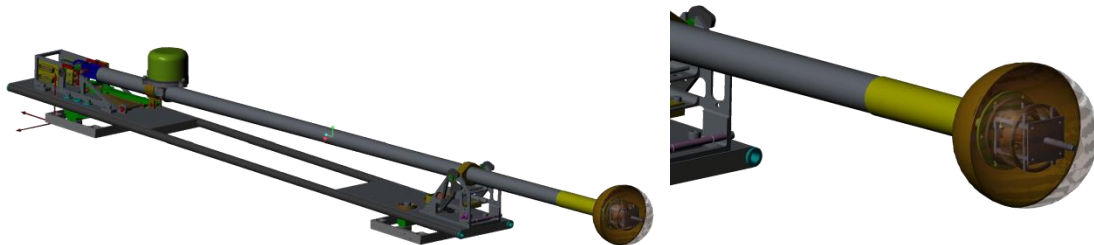


**Figure 4-3: Left: Combined COMPLIMENT and FGM boom; Right: model of combined Langmuir Probe and FGM sensor**

#### 4.1.3.2 DISC

DISC is an impact sensor, comprised of a 0.5 mm thin Al square diaphragm with a sensitive area of 100 cm<sup>2</sup> to measure the incident grain momentum. This instrument is based on the Rosetta GIADA payload subsystem.

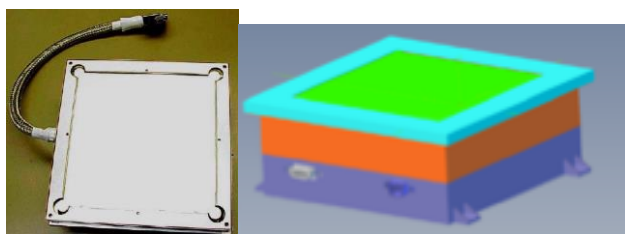


**Figure 4-4: DISC prototype and CAD drawing**

#### 4.1.3.3 FGM

The DFP/FGM provides high accuracy and high-time resolution measurements of the magnetic field magnitude and direction. It consists of one 3-axis fluxgate sensor and one combined Langmuir Probe and FGM sensor, mounted on a deployable boom. The inboard sensor monitors magnetic disturbance signals. Both sensors use one electronics board each, incorporated into the common electronics box.

The single magnetometer is the same design as the SOSMAG on board GEO-KOMPSAT-2A. Some customization with regards to integration of the electronics into a common box needs to take place in the first development phases.

The combined Langmuir Probe and FGM sensor is a new development.

#### 4.1.3.4 LEES

The DFP/LEES sensor (Low-Energy Electron Spectrometer) will measure the properties of negatively charged particles in the solar wind and in the vicinity of the comet: electrons, photoelectrons, and negative ions. In particular, photoelectrons will provide unique measurements in order to check the magnetic connectivity of the spacecraft with the comet. LEES will also provide unique measurements on the ionization sources of the coma.

LEES is a top-hat type electrostatic analyser (see Figure 4-5) with a FoV deflector system to allow electrostatic deflection of incoming electrons by up to 70°.

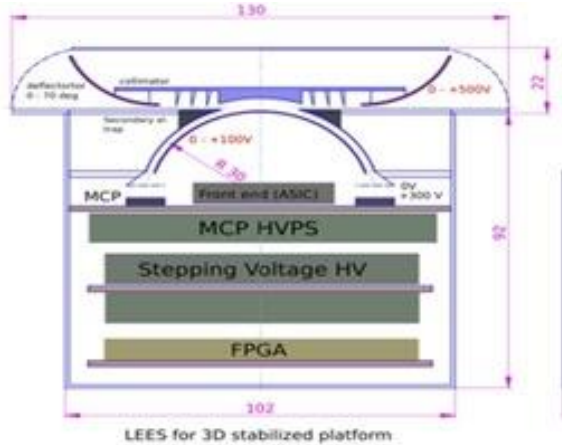


**Figure 4-5: LEES drawing**

The design of the LEES sensor is similar to that of the miniature spectrometer ELS for the ASPERA-3/4 for ESA MEX and VEX.

#### 4.1.3.5 SCIENA

The DFP Solar wind and Cometary Ions and Energetic Neutral Atoms (SCIENA) instrument measures energetic particles of solar wind and cometary origin, both with and without charge. SCIENA (see Figure 4-6) consists of a main body with electronics and two sensor-heads, one for ions (Ion) and one for Energetic Neutral Atoms (ENA). Their respective fields of view are:  $150^\circ \times 15^\circ$  for ENA and close to  $2\pi$  for Ion.

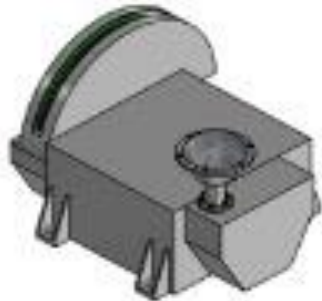


**Figure 4-6: SCIENA drawing with Ion and ENA sensors**

The **Ion** observational capabilities allow for direct detection of solar wind and cometary ions, providing energy, direction and a rough mass estimate.

The **ENA** measurement capability allows studying the direct interaction of the solar wind with the neutral atmosphere, providing a continuous monitoring of the dynamic pressure of the solar wind, an estimate of the position of the regions of strongest interaction between the solar wind and the coma as well as the coupling between the coma and the cometary ions.

This instrument has heritage from SWIM on Chandrayan, MIPA on Bepi-Colombo.

#### 4.1.3.6 E-box:

The central electronics of the DFP are accommodated in one unit and consists of the Box, Dust Analyzer & Processing Unit (DAPU), a single DC-DC power converter (DCDC)

for all elements, Langmuir Probe board, HF and MP boards, FGM board and DISC board.

### **Environment requirements for DFP:**

#### ***LEES:***

- EMC: Conductive spacecraft 5V (TBC) drop between 2 points. DC magnetic, 200 nT (TBC) at 1 m for 1 eV electron measurements.
- Contamination: Particulate: ISO 7 clean room.
- AIT/AIV requirements: Nitrogen purge.

#### **Accommodation requirements:**

**DISC:** DISC shall be mounted on the S/C face orthogonal to the S/C ram direction and exposed to the dust flux. The sensor is not sensitive to Sun exposure, but thermal stability should be provided (TBD). No baffle is needed. The sensor can be mounted directly on the external surface of the S/C or just behind a small square aperture. The sensor is not sensitive to the spin of the probe B2.

#### **COMPLIMENT:**

- Avoid spacecraft wake as much as possible.
- Maximise distance between probes by mounting them at the tips of the booms and mount the booms on opposite sides of the spacecraft.
- Constant probe illumination is preferable. Having any one probe constantly in the shadow shall be avoided.
- Free line-of-sight between probes is preferable.
- The sensors should be accommodated on the S/C as far away as possible from electro-magnetic disturbances (i.e. reaction wheels, solar panels, cameras etc.).

**FGM:** The sensors should be placed as far away as possible from magnetic disturbances (i.e. reaction wheels, solar panels, cameras etc). FGM should be in constant illumination (Sun-lit) during the Closest Approach.

**SCIENA:** This instrument shall be placed at one edge of the S/C with a 45° angle to the edge. There shall be an overlap of the SCIENA FoVs and the one of CoCa. The thruster plumes shall be avoided to minimise contamination of the instrument.

**LEES:** It shall be mounted on a side of the S/C with an unobscured FoV. The instrument shall also be angled by 45°, as SCIENA.

An illustration of the draft locations of the SCIENA and LEES instruments, also with respect to the location of CoCa, is given in Figure 4-7.

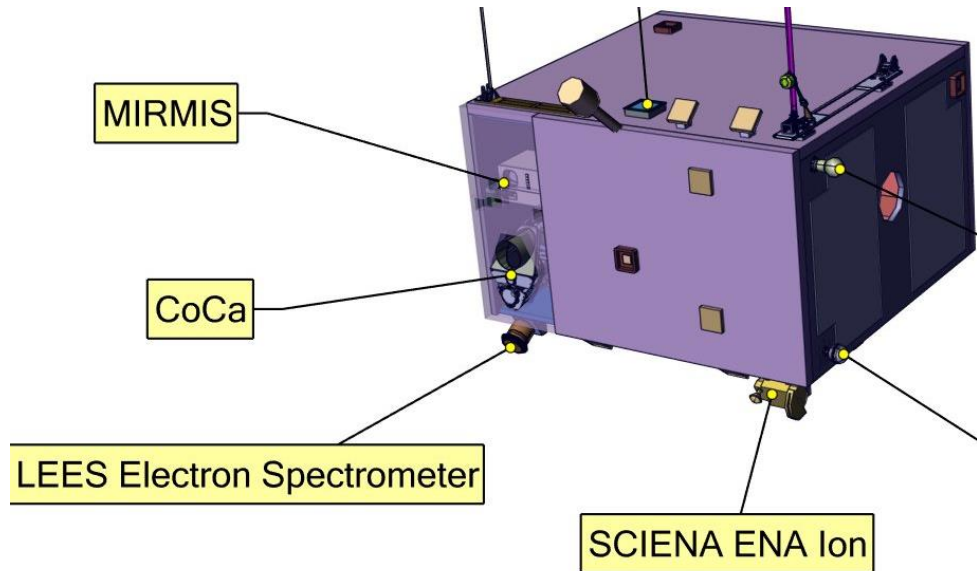


**Figure 4-7: LEES and SCIENA accommodation on S/C A; the relative location of CoCa and other instruments is also shown**

**Data rate/volume:** The combined data volume of the DFP is 6.78 Gb.

#### 4.1.4 MANiaC

MANiaC is a mass spectrometer based on the time-of flight principle, which will measure in situ volatiles' total and relative abundances in the coma.

The design is based on the NGMS instrument for Roskosmos's Luna Resurs and on Rosetta ROSINA-RTOF. The instrument consists of two main elements:

- An (ion) source/antechamber, based on the JUICE PEP Neutral Ion Mass Spectrometer (NIM).
- A neutral density gauge, based on the Rosetta ROSINA-Cometary Pressure Sensor (COPS)

In addition, MANiaC comprises an electronics box containing three boards, and a DPU with an instrument internal processor and all software, incl. compression algorithm.

Note that this instrument was moved from the spinning probe B2 to the 3-axis stabilised S/C A and therefore, to maximise the particle flow, a rotation mechanism shall be implemented to point the inlets in the flow of particles during the Closest Approach.

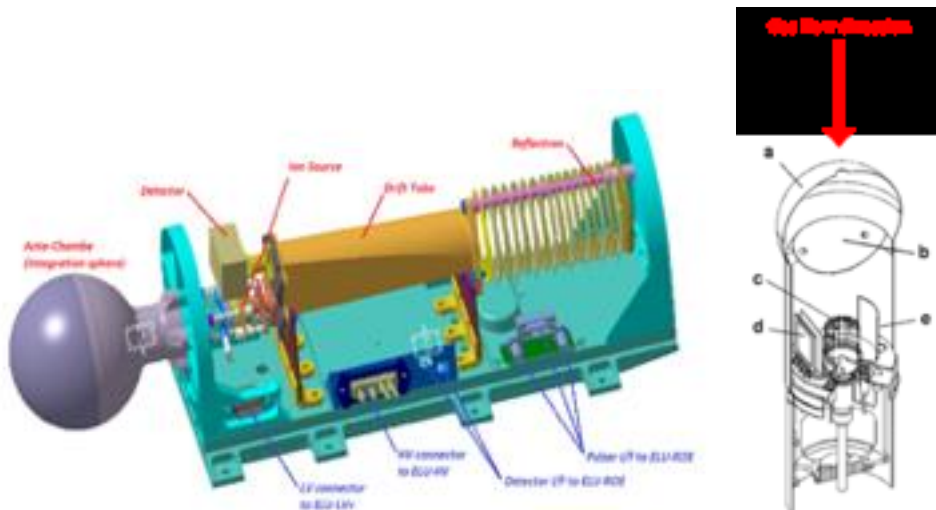


**Figure 4-8: MANiaC SHU top view (left) and NGD schematic (right)**

**Environment requirements:** Currently not identified.

**Accommodation requirements:**

MANiaC and the pressure sensor should be placed such that the disturbance of the gas the spacecraft is passing through is minimised. E.g. the reflection of volatiles on S/C body etc shall be minimised. The MANiaC antechamber and pressure sensor should be separated by ca. 20 – 30 cm to avoid mutual disturbance of the gas flow but still allow cross-correlation of the gas parameters.

The antechamber of MANiaC and the pressure sensor should be protruding from the spacecraft. The inlet hole in the antechamber can be made in any orientation perpendicular to the main axis and has to point in the ram direction at Closest Approach.

**The following shall be considered for MANiaC:**

- Antechamber inlets (for both the MANiaC MS and MANiaC NDG) have to track, within 10°, the direction of motion of S/C A w.r.t. the target. 10° ensures maximum ram pressure in the gauge even if the gas motion is perpendicular to the S/C motion at closest approach (CA). E.g. cometary gas moving at 1 km/s perpendicular to 10 km/s flyby velocity leads to an aberration angle of  $\text{atan}(1/10)=5.7^\circ$ . Together with a pointing uncertainty of 10° the influx into the chamber is still >95% of the maximum ( $\cos(15.7\text{deg})=0.96$ ).
- If no scanning platform for the camera(s) is used: A built-in motor mechanism may rotate both antechambers to counter the slew of the S/C (~180° required). The rotation of the antechambers is limited to a single plane. Hence the axes of rotation of the two antechambers have to be parallel to the slew axis of the spacecraft.
- The axes of rotation of the antechamber of the Mass Spectrometer (MS) is parallel to the long axis of the instrument. Same alignment for the NDG.
- The NDG antechamber may protrude the MS antechamber to avoid “shadowing” of the latter (or vice versa).

- MS and NDG should be placed within 40 cm from each other which corresponds to approximately 2-3 times the protruding size of the gauges which limits mutual interference while being located close enough to allow for cross-calibration.
- Minimise S/C structure in the FoV (nominally  $2\pi$ , but modified by the cosine w.r.t to the inlet alignment) throughout the  $180^\circ$  slew to reduce S/C background contribution and scattering of cometary volatiles on S/C surfaces before reaching the inlets. Particularly critical for the centre of the FoV and the time around closest approach.

**Data rate/volume:** MANIaC foresees a data rate of 160 kbps and a data volume of 5.6 Gb in total.

## 4.2 Baseline Design – Probe B2 (ESA)

In this section the instruments for probe B2 (ESA) are described. Their budgets are listed in Table 4-3, together with their mass (incl. 20% equipment maturity margin), average power consumption, physical size, FoV, data rate. Their heritage from previous instruments and missions is listed in the text further down.

Instrument	Mass [kg]	Power [W]	Length [mm]	Width [mm]	Height [mm]	Diam. [mm]	FoV	Data volume [Gb]
<b>B2 DFP Dust Impact Sensor and Counter</b>	0.42		121	116	46	-	-	-
<b>B2 DFP E-Box</b>	2.69	8.40	102	252	164	-	-	0.32
<b>B2 DFP FGM boom</b>	0.65		200	30	30		-	-
<b>B2 DFP FGM_sensor 1</b>	0.16	0.90	-	-	40	50	-	-
<b>B2 DFP FGM_sensor 2</b>	0.16	0.90	-	-	40	50	-	-
<b>B2 Entire Visible Sky</b>	1.20	8.40	128	194	134	-	$180^\circ \times 45^\circ$	4.32
<b>B2 Optical Imager for Comets</b>	0.42		74	145	51	-	$18^\circ.3 \times 18^\circ.3$	3.43
<b>Sums</b>	<b>5.69</b>	<b>18.6</b>						

**Table 4-3: Payload for probe B2**

Details of the instruments are listed in the following sub-sections.

### 4.2.1 DFP for probe B2

The DFP for probe B2 is comprised of the FGM and DISC instruments.

#### FGM:

A dedicated FGM boom is foreseen to accommodate the two FGM sensors. The exact location of this boom is yet to be defined, as the probe communications antenna needs to be accommodated close by. This issue needs to be further investigated, and is discussed in more detail in Chapter 16.2.6.



**Figure 4-9: Probe B2 FGM sensor schematic**

#### DISC:

Impact sensor; 0.5 mm thin Al square diaphragm with a sensitive area of 100 cm<sup>2</sup> to measure the incident grain momentum. This instrument is based on the Rosetta GIADA payload subsystem.

All requirements and recommendations are the same as for the corresponding instruments on S/C A (see Section 4.1.3).

**Data rate/volume:** The data volume for the entire fly-by is 0.32 Gb, with a variable data rate.

#### 4.2.2 EnVisS

EnVisS is a multispectral and polarimetric imager with a FoV that will cover as much as possible of the visible sky, mapping the distribution of neutral and ionized gas coma species, as well as the brightness and polarimetric properties of light scattered and reflected by dust particles. The “three-polaroid” observing technique provides simultaneous observations of the intensity, degree of linear polarization, and angle of polarization, and has been used successfully on other missions such as SOHO and STEREO. EnVisS employs rotational push-frame imaging, an adaptation of the traditionally linear scanning equivalent, instead using the probe rotation to scan the surroundings.

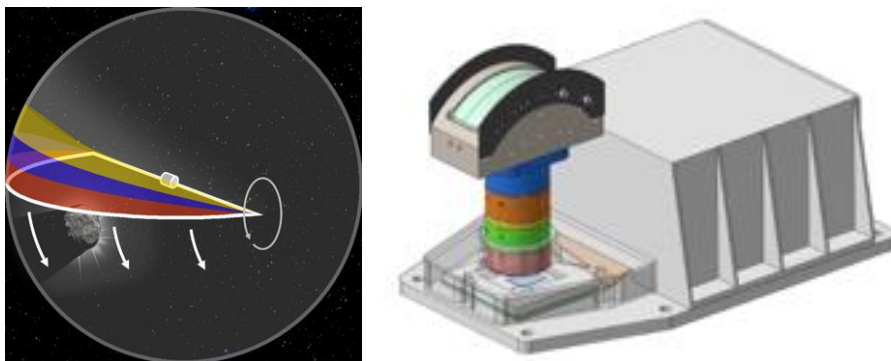


**Figure 4-10: EnVisS' image scanning principle, right: CAD drawing of EnVisS**

The EnVisS' image scanning uses the probe spin to allow the camera's 180° FoV (white) to image the entire sky. Coloured strips represent multiple scan lines (see Figure 4-10).

**Environment requirements:** As the instrument will be working in the visible wavelength range, standard cleanliness level should be sufficient. Currently no other requirements are identified.

**Accommodation requirements:** There will be a baffle to minimise Sun intrusion, but there will be a fraction of each spacecraft spin when the Sun will be impinging directly on the optics and detector. This is not expected to be a problem for the optics and baffles since B2 will be rotating quite rapidly.

**Data rate/volume:** The data volume for the entire fly-by is 4.32 Gb, with a variable data rate.

#### 4.2.3 OPIC

The OPIC goal is mapping of the target and its dust jets at visible and near-infrared wavelengths. The camera will be a broadband monochrome imager covering the wavelength range 400 – 800 nm with a FoV of  $18.3^\circ \times 18.3^\circ$ .

Note that OPIC originally consisted of a visual and near infra-red (NIR) channel. The NIR channel was moved to S/C A and is now part of the MIRMISS instrument.

OPIC will be pointed out of the side of the probe, i.e. perpendicular to the flight direction, behind the dust shield for protection, and a fixed,  $45^\circ$  flat mirror periscope exposed to the dust flow will direct the FoV towards the flight direction. Immediately before closest approach, once the nucleus is no longer expected to be in the forward direction as seen by probe B2, the mirror will be flipped aside. This will be realized via a one-time failsafe mechanism. The instrument will point sideways, unobscured, seeing the nucleus once per probe rotation from relatively close range.

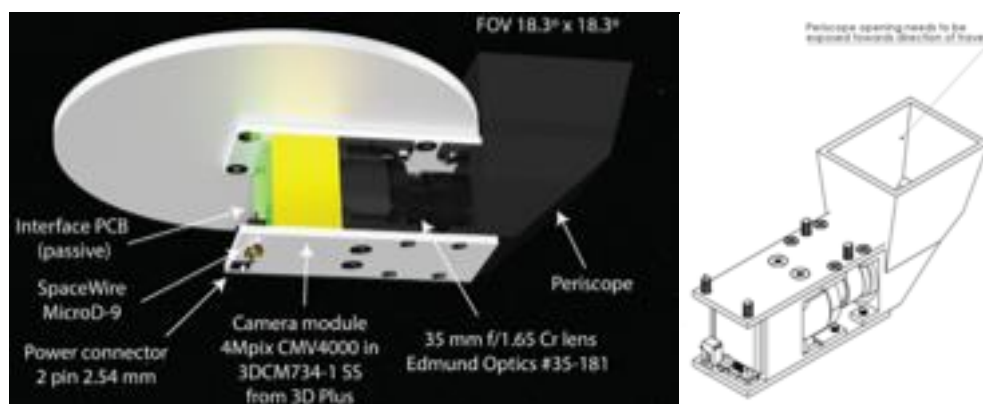


**Figure 4-11: OPIC instrument concept (left); drawing showing the “periscope” (right).**

#### Heritage:

The current design of the camera is based on a space-qualified 3D-Plus' FPA 4Mpx CMOS 3DCM73x sensor, as used in VTT's visible range hyper-spectral camera on the Aalto-1 nano-satellite.

**Environment requirements:** Currently not identified.

**Accommodation requirements:**

**FoV:** The current requirement is ca. 20°, but this will need another trade-off between a narrower field of view with provides better imaging results and better pointing capability.

**Orientation:** The camera needs to point at the comet, which is realized with a periscope (see above), e.g. the camera points to the side of the probe, and the 45° mirror turns the FoV towards the comet.

**Sun exclusion angle:** The current estimate is 45° (TBC).

**Data rate/volume:** For OPIC, the data rate ranges were identified as follows:

**Minimum:** 1 image from further out (with coma) and 1 image at the closest approach (with as much nucleus revealed as possible). Assuming lossy compression and 8-bit depth, the resulting data volume would be 2.5 Mbytes for 2048 × 2048.

**Optimum:** At least 8 images: 20 Mb

**Ideal:** One image per rotation; the production rate depends on the rotation rate and flyby speed.

**Data rate/volume:** The data volume is 3.43 Gb for the mission.

### 4.3 Baseline Design – Probe B1 (JAXA)

The instruments for probe B1 will be provided by JAXA and are briefly described below. The budgets for the instruments of probe B1 (JAXA) are listed in Table 4-4, together with their mass (incl. 20% equipment maturity margin), average power consumption, data rate, and notes. Some more information on these instruments is listed in the text further down, but this payload was not analysed in detail in this CDF study.

Instrument	Mass [kg]	Mass elements [kg]	Power [W]	Data rate [kb/s]	Notes
<b>HI:</b> Lyman- α Hydrogen imager	2.20	-	3.00	0.07	Volume: 3U; Temp: Ops: -20 to +50°C; Storage: -30 to +60°C
<b>PS:</b> Plasma Suite	10.50	-			Volume: 8U; Temp.: Ops: -20 to +45°C; Storage: -30 to +70°C
<b>MAG + boom:</b> Magnetometer		4.5	3.00		
<b>ICA:</b> Ion Composition Analyzer		6.0	8.00		
<b>WAC:</b> Wide Angle Camera	1.00	-	5.00		Volume: 1U; FoV: 30°-60°; Temp.: Ops: -20 to +50°C; Storage: -30 to +60°C
<b>Total</b>	<b>12.70</b>		<b>19.00</b>		

**Table 4-4: Payload for probe B1 (JAXA)**

Details of the instruments, as presented in the proposal, are listed in the following subsections.

#### 4.3.1 HI - Lyman- $\alpha$ Hydrogen Imager

The Lyman- $\alpha$  Hydrogen imager will provide data to further the understanding of the evolution of a DNC or another new object to the inner solar system, and material transport to the inner solar system. This instrument is composed of a telescope, a bandpass filter for H Lyman- $\alpha$ , and an MCP detector to obtain the image of hydrogen Lyman- $\alpha$  emission around the target.

**Heritage** is the PROCYON/LAICA, which is almost identical to this instrument.

**Alignment requirement:** Alignment with visible telescope on S/C A pre-release, with accuracy of  $<0.5^\circ$  (TBD;  $1^\circ$  for worst case).

**Data rate/volume:** Data rate: 32kB/frame, 1 frame/hour resulting in 0.07 kbps.

#### 4.3.2 PS - Plasma Suite

The Plasma Suite will observe the local plasma environment of the solar wind and coma. It consists of a conventional fluxgate magnetometer (**MAG**) based on the instrumentation heritage of ERG/MGF and BepiColombo/MGF-I, and an ion composition analyser (**ICA**) based on Kaguya/IMA and BepiColombo/MSA. MAG will measure the magnetic field from DC to 100s of Hz. ICA will measure ions in the energy range of 10 eV to 20 keV/q, with composition analyses using time-of-flight techniques.

**Accommodation:** Tip of a boom (MAG). Without significant FoV interference (ICA)

##### Environment Requirements:

**EMC requirements:** Probe background B-field stability at MAG sensor should be  $<0.5$  nT. S/C surface should be conductive and grounded to primary power source return, in order to avoid the substantial deflection of low-energy plasmas.

**Other requirements:** Continuous gaseous nitrogen (GN<sub>2</sub>) purge until a few hours pre-launch.

**Data rate/volume:** Data rate: 514 kbps (MAG~2kbps + ICA~512kbps); nominal plan is to be stored in a data recorder (>1Gb) of B1 bus and reproduced post-flyby, while 128 kbps (TBD) communication with S/C A is also considered.

#### 4.3.3 WAC – Wide Angle Camera

The WAC will provide data to support aims to uncover the shape of the nucleus by obtaining images of it from locations distant from, and non-colinear with, S/C A. The FoV is 30-60°, which enables continuous imaging for >1-2 sec at fly-by. Probe B1, which is planned to traverse the coma out of the S/C A – probe B2 – cometary nucleus plane, enables the capture of several images at out-of-plane positions. The target spatial resolution is  $<100\text{-}200$  m/pix. The Wide Angle Camera is composed of one component including optics, a detector, and electronics, and is connected to the probe B1 electronics by two wire harnesses for telemetry/command and power.

**Heritage:** Design of WAC is based on Hayabusa2/(DCAM, MINERVA/WAC, or ONC-W)

**Data rate/volume:** The data volume is 20MB for the entire fly-by.

## 4.4 Payload Mechanisms and Interface Notes

### 4.4.1 Mechanisms

The following main mechanisms were identified during the CDF study:

- CoCa: Filter-wheel (4+ filters) mechanism; low TRL
- MIRMISS-TIRI: scan/calibration between target and Black Body
- MANIAC: Motor free, one-time fail-safe mechanism to cut off the antechamber and possibly rotation mechanism (for the baseline mission case, of a slewing S/C A during the flyby)
- Booms of COMPLIMENT/DFP and FGM/DFP (TBC)
- Scanning Mirror for CoCa and MIRMISS (TBC): scanning mirror protected by a periscope to track the comet at encounter without slewing the S/C (for the mission option, discussed in Chapter 24, of a non-slewing S/C during the flyby).

### 4.4.2 Sun Exclusion

Information for S/C A and B2:

- **CoCa:** The Sun must be kept  $>40^\circ$  from the boresight and  $>10^\circ$  from the boresight during emergency/safe mode (especially important if no periscope is used).
- **EnVisS:** It needs to see the Sun once in a while to determine the exact spin period of the spacecraft to aid full-sky image reconstruction. No maximum time is given, but a "pulse" is mentioned.
- **MANIAC, MIRMISS, OPIC:** Currently no requirement for Sun exclusion

### 4.4.3 Radiators/Thermal Dissipation

CoCa and MIRMISS will need heat dissipation and therefore radiators foreseen for them. The EnVisS radiator is TBC.

The thermal range requirements of all instruments are given in the thermal section Table 18-2: S/C A: Op. and Non-Op. Design Temperature Limits

## 4.5 Pointing and Pointing Stability

- CoCa; Pointing requirement: APE  $<0.1^\circ$
- DFP: no pointing requirements
  - S/C attitude reconstruction is required with few degrees' precision and sensors location on S/C depend on pre-defined pointing
  - DFP/DISC pointing will be defined by the accommodation with sensitive surface orthogonal to the ram direction
- MANIAC: no pointing requirements, only orientation of inlet of the ante-chamber is important, but this will be handled by MANIAC internally
- MIRMISS:

- Pointing requirement:  $\pm 30$  mrad; guarantees that the nucleus is in the TIRI module FoV
- Alignment requirement:  $\pm 1$  mrad; co-aligned with CoCa
- MIRMISS modules (TITI, NIR, MIR1,2) will be co-aligned internally.
- EnVisS: no pointing requirements; instrument needs to be placed almost perpendicular to the spin axis of probe B2
- OPIC: no pointing requirements; the instrument shall be aligned with the probe B2 spin axis.

## 4.6 Data Links (SpaceWire or other)

All payloads baselined SpaceWire for the data link to the spacecraft DHS, except for MIRMISS. The MIRMISS team is still trading off between a serial link using RS-422, RS-485 or LVDS and possibly SpaceWire or CAN (using 11-bit or 29-bit identifier).

For Phase 0, SpaceWire was baselined for all instruments to keep the interfaces simple and uniform. The MIRMISS team has confirmed their willingness to decide on SpaceWire.

Data links in detail:

- **CoCa:** Main and redundant SpaceWire (SpW) communications to the DPM for data
- **DFP-A:** SpaceWire at 10 MHz, using CCSDS/PUS protocol
- **MANiAC:** The data link for the scientific data needs to be a fast one (e.g. SpaceWire).
- **MIRMISS:** Can accept a serial link using RS-422, RS-485 or LVDS. The other options available are SpaceWire or CAN (using 11-bit or 29-bit identifier).
- **DFP-B:** SpaceWire at 10 MHz, using CCSDS/PUS protocol
- **EnVisS:** SpaceWire is assumed
- **OPIC:** SpaceWire is assumed.

## 4.7 Synchronisation/Timing

Payloads with timing or synchronisation requirements (also between those on different spacecraft) are listed here below:

- **EnVisS:** They will use an FPGA to maintain the instrument clock. They need to detect the Sun image in the camera data stream to form the synchronisation pulse.
- **DFP/FGM (on S/C A):** They have an interface between FGM and the DPU which consists of a serial link, a synchronization signal and a power supply. Not clear if this applies to DFP/FGM on probe B2 as well.
- **MIRMISS:** Synchronisation is mentioned in the context of time stamps, but no details are given.
- **CoCa, MANiAC, OPIC:** No mention of synchronisation or timing.

## 4.8 Technology Needs

There are several Technology Development Activities needed for the Comet Interceptor Payload. These are handled through dedicated activities and not listed here.

## 5 MISSION ANALYSIS

### 5.1 Requirements and Design Drivers

SubSystem Requirements		
Req. ID	Statement	Parent ID
MA-010	<p>The Comet Interceptor main S/C shall be able to perform trajectory correction manoeuvres early after launch (~1-2 days).</p> <p><i>Justification: in order to correct the initial errors in perigee velocity (launcher dispersion + fixed launch program) as currently envisaged for ARIEL (RD[1]) such as to achieve the correct transfer orbit towards SEL2.</i></p>	

### 5.2 Assumptions and Trade-Offs

Assumptions	
1	Transfers are computed departing exactly from SEL2. The impact of departing from an orbit around SEL2 is not considered at this stage.
2	Transfer to the comet can take as much as 4 years (i.e. of the 5 years lifetime, 1 year as a minimum is considered for transfer to SEL2 and waiting phase).
3	The study region for the comet interception is the Sun-centred annulus with radius in the range [0.7,1.3] AU. <i>Note that this defines the region for analysis only, the system design envelope considers only the range [0.9, 1.25] AU.<sup>1</sup></i>
4	No constraint is applied to the direction or distance to the Sun of the transfer manoeuvres.
5	No constraint is applied to the transfers in terms of minimum and maximum distance to the Sun. <i>Note that this defines the region for analysis only, as for Assumption 3.</i>
6	No constraint is applied to the transfers as a result of the geometry at comet interception (relative velocity, phase angle, Sun illumination, etc). <i>Note that this defines the region for analysis only, the system design envelope places constraints on all these.<sup>1</sup></i>
7	Navigation of a Moon swing-by with SEP is considered feasible for a minimum altitude above 5000 km.

### 5.3 Preliminary Mission Δv Budget

A preliminary ΔV budget was proposed at the beginning of the study based on the mission design for the ARIEL mission (RD[1]) and experience with previous and current missions to the SEL2 libration point. The budget is summarised in Table 5-1 and covers

<sup>1</sup> See the Systems chapter for more information.

the mission phases from launch until the end of the transfer to the comet, though only an indication for the transfer Delta-V is given. The manoeuvres during the comet flyby have been addressed in the GNC analysis and are not given here. Note that margins are not used in these values provided by the Mission Analysis team. Applicable margins are applied at system level following the margin philosophy of the CDF studies.

Manoeuvre	Day	$\Delta v$ (m/s)	Comments
TCM#1 deterministic part	1-2	15	Recommended with chemical propulsion (CP) (see 5.4.1)
TCM#1, TCM#2 & TCM#3 stochastic	#1: 1-2 #2: 5 #3: 20	40	Recommended with CP (see 5.4.1)
Orbit insertion	~30	0	Note: 15 m/s was recommended at the beginning of the study to allow flexibility in the orbit around SEL2. The current value assumes launch into the same transfer orbit towards SEL2 and injection into a similar SEL2 orbit as for ARIEL.
Station Keeping at SEL2 parking orbit	Parking phase	5 m/s per year	Conservative value for CP or electric propulsion (EP)
Transfer to the comet	-	Variable	Drives the reachability of comets and needs to be decided at system level. Current assumed values: 1.5 km/s for EP, 425 or 700 m/s for CP
Moon flyby navigation	-	25	Optional when using Moon flyby strategy, and can be taken out of the transfer Delta-V.

**Table 5-1: Preliminary  $\Delta v$  budget, excluding operations during comet flyby**

## 5.4 From Launch to the Start of the Transfer

### 5.4.1 Transfer to SEL2

The spacecraft will be injected into a SEL2 transfer trajectory together with ARIEL. In general, a free transfer is assumed, i.e. a trajectory that will allow reaching an orbit around SEL2 without any insertion manoeuvre. Two types of free transfers exist: slow (100-120 days) and fast (30 days), both corresponding to local minima of the transfer  $\Delta v$ . A deterministic manoeuvre is usually needed after separation, to correct the apogee altitude, since the launcher uses a fixed launch program with a given apogee. This first manoeuvre can be performed together with the TCM to correct launcher dispersion.

Because of the time criticality of the first correction manoeuvres, such manoeuvres are assumed implemented with CP (see 5.12.1).

#### 5.4.2 SEL2 Station-Keeping

The intrinsic unstable nature of SEL2 requires periodic station-keeping manoeuvres for any orbit around that point. The dynamics time scales of the Sun-Earth system are, nevertheless, sufficiently slow; if the unstable component is triggered, the time to escape is usually around 60-90 days, allowing an ample window for recovery.

The frequency of station-keeping (SK) may be selected following operational constraints and mission budgets. One manoeuvre per month (28 days) allows for a beneficial 4-weeks operational cycle and a sufficiently low  $\Delta v$  budget. The frequency can be reduced, up to 3-4 months, at the expense of the  $\Delta v$  budget.

A full SK analysis was not performed within the CDF study. Given the peculiar nature of the mission, the SK schedule can be tuned in order to satisfy operational constraints and reduce complexity. It is also remarked that the actual SK budget will depend on the reached operational orbit around SEL2; a budget of 5 m/s per year is representative of several SEL2 orbits and is suggested as baseline.

The SK manoeuvre direction will, in general, try to compensate the unstable component of the SEL2 orbit. If thrust direction constraints are to be enforced, the SK manoeuvres can be constrained to only one hemisphere by biasing the SEL2 trajectory. This bias doubles the SK allocated  $\Delta v$  (RD[1]).

### 5.5 Generic Analysis of Heliocentric Transfer to the Comet

One of the main tasks of Mission Analysis during the study has been to characterise the reachable comet targets in terms of the required Delta-V and transfer time. This requires a global approach that despite simplifying the problem still gives a good approximation of the previous parameters.

For energetic reasons it is easy to understand that the transfer from the SEL2 region to the comet must remain in the ecliptic plane. Even a small inclination change of 1-degree requires the spacecraft to provide a  $\Delta v$  over 500 m/s. Thus the comet has to be intercepted at one of the crossings of the comet's orbit with the ecliptic plane, that is at the ascending or descending node.

The geometry of the problem is fully defined by the following two parameters, as in Figure 5-1:

- $R_c$  – Radius at encounter = Radius of comet at ascending/descending node with the Ecliptic
- $\theta$  - Phase angle of Earth at encounter, measured as Comet-Sun-Earth angle.

Given the random distribution of target comets (LPCs), these two geometry parameters are also random, so the encounter might occur in general for any  $R_c$  and any phase angle  $\theta$  within [-180, 180] deg. In the following analysis we will assume  $R_c$  within [0.7, 1.3] AU.

Notice that the phase angle  $\theta$  is measured positive counter-clockwise from the comet to Earth. This angle has an opposite sign to the phase angle of the comet encounter in the Sun-Earth rotating frame that will be illustrated in many of the projections of the transfers in the following results.

For a given  $R_c$  the  $\Delta v$ -optimal transfer from Earth makes use of the well-known Hohmann transfer orbit illustrated in Figure 5-1. The corresponding  $\Delta v$  departure manoeuvre at Earth (or escape velocity) is tangential and the transfer time can be obtained with

$$\Delta v^H = v_E \left( \sqrt{\frac{2R_c}{1+R_c}} - 1 \right), \quad \Delta t^H = 0.5 \left( \frac{1+R_c}{2} \right)^{3/2}$$

where  $v_E$  is the circular velocity of Earth ( $\sim 29.8$  km/s),  $R_c$  must be given in AU and  $\Delta t$  is obtained in years. These formulas lead to  $\Delta v$  of 2.8 km/s and 1.9 km/s for 0.7 and 1.3 AU respectively. Thus the required  $\Delta v$  grows very quickly when  $R_c$  deviates from the Earth radius, especially for  $R_c < 1$  AU, and it can already be anticipated that it will be difficult to reach comets at the limits of the considered  $R_c$  region. The transfer time for the same 2  $R_c$  values corresponds to 143 days and 225 days, roughly half year  $\pm 40$  days.

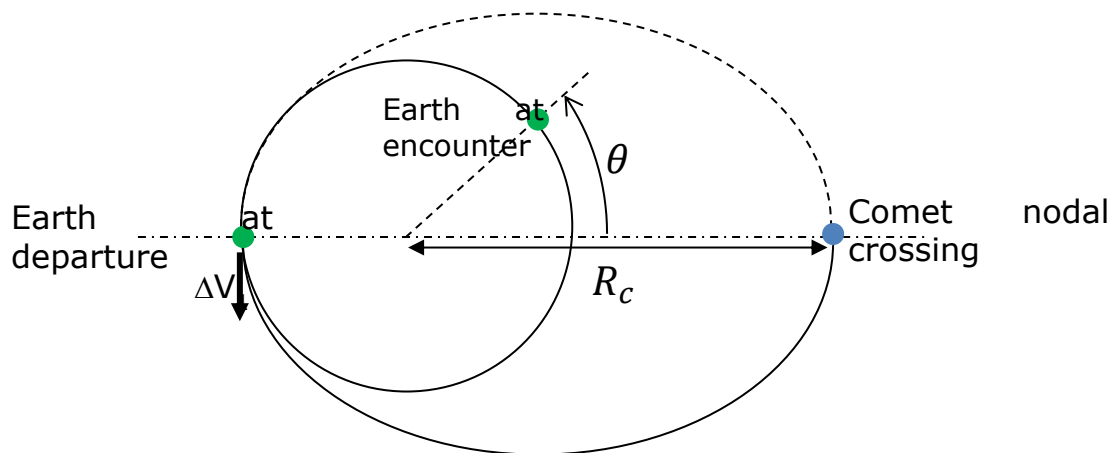


**Figure 5-1: Earth-Comet Transfer Geometry (Hohmann transfer)**

For given  $R_c$ , the Hohmann transfer leads to a fixed phase angle  $\theta$  which is the difference of the angle travelled by Earth and the 180 deg travelled by the spacecraft. If  $R_c > 1$  AU the spacecraft drifts behind Earth, as its angular velocity is smaller, and  $\theta$  is positive. Contrarily for  $R_c < 1$  AU the spacecraft drifts ahead of Earth leading to negative  $\theta$ . For  $R_c = 1.3$  AU the corresponding  $\theta$  is roughly 42 deg, while for  $R_c = 0.7$  AU  $\theta$  takes a value of -39 deg.

Additional intermediate orbits can be introduced in order to reach larger  $\theta$  values. If  $\Delta t^H$  is the transfer time and  $\theta^H$  the phase angle corresponding to the (half-revolution) Hohmann transfer for a given  $R_c$ , and the transfer takes  $n$  additional orbits, the total transfer time and phase angle can be obtained by:  $\Delta t = (2n + 1)\Delta t^H$ ,  $\theta = (2n+1)\theta^H$ . Thus, taking  $R_c = 1.3$  AU as an example, the 0.5 revolutions Hohmann transfer requires 225 days for phase angle 42 deg, the 1.5 revolutions transfer requires 675 days for 126 deg, and the 2.5 revolutions transfer 900 days for 210 deg.

If the  $\Delta v$  of the Hohmann manoeuvre is split in 2 burns applied at the same point, the intermediate orbit can be used as a “phasing” orbit to adjust  $\theta$  to any value in between

$[(2n-1)\theta^H, (2n+1)\theta^H]$  at no  $\Delta v$  cost. The transfer time takes then a value in the range  $[(2n-1)\Delta t^H, (2n+1)\Delta t^H]$ . Thus for the above example, with 1.5 revolutions transfer using 2 burns any phase angle between 42 deg and 126 deg can be obtained with a transfer duration between 225 days and 675 days.

Therefore, provided that the resulting transfer times are compatible with the mission, the previous “extended 2-burns” Hohmann strategy provides flexibility to reach different values of  $\theta$  for given  $R_c$ . For  $R_c > 1$  the reachable values of  $\theta$  are above  $\theta^H$  (positive). For  $R_c < 1$  the reachable values of  $\theta$  are below  $\theta^H$  (negative).

Other  $\theta$  values remain harder to achieve. For  $R_c > 1$  and a negative target value of  $\theta$  it is either necessary to first reduce the orbit period (by reducing the perihelion) to make first Earth drift behind the spacecraft before a Hohmann-like half revolution, or to use a larger number of intermediate phasing orbits such as to let Earth drift ahead more than half revolution to come up from -180 deg. The first option results in spending more  $\Delta v$  than the Homann strategy, and the second option while not penalising the  $\Delta v$  may result in much longer transfer times unpractical for the mission. Exactly the opposite occurs for  $R_c < 1$  and positive target  $\theta$ .

In a general case, a 2-manoeuvres strategy is expected to be flexible enough to solve the transfer for given  $R_c$  and  $\theta$  targets. The size and timing of the two manoeuvres can be subject to constrained optimization, and the Pareto-optimal solutions in terms of  $\Delta v$  and transfer time can be obtained. This allows to trade the benefit of additional transfer time for the propulsion requirement.

Typically in such a Pareto-front we would expect to see sudden improvement in the  $\Delta v$  when the transfer time increases such that an extra revolution can be used. This is illustrated in Figure 5-2, that shows the intermediate results of a heuristic global optimization process – Differential Evolution (DE) computes thousands of possible transfers. The dotted line has been manually added to represent the Pareto-front. The studied case corresponds to  $R_c = 1.1$  AU and  $\theta = -150$  deg, for which a Hohmann transfer would require 0.7 km/s and 196 days (0.54 years), but lead instead to  $\theta^H = 13.7$  deg. Adjusting the phasing just with intermediate orbits would require 8.5 revolutions and an almost 9-year transfer. The figure allows identifying transfer solutions with 1.5, 2.5 and 3.5 revolutions that require decreasing  $\Delta v$ , though still much higher than  $\Delta v^H$ . Also worth noticing, for integer number of revolutions it is much harder to complete the transfer in terms of  $\Delta v$ .

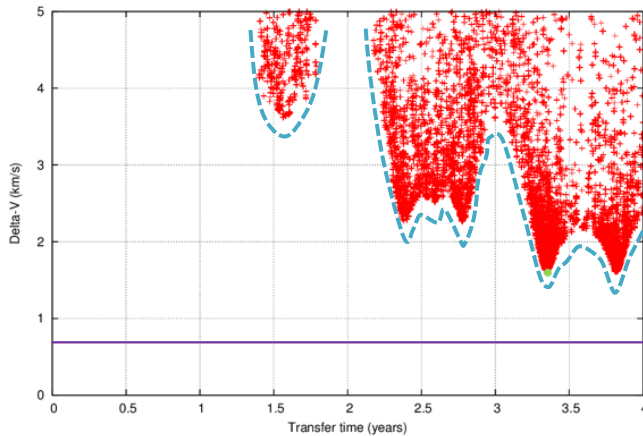


**Figure 5-2: Illustration of  $\Delta v$  – transfer time Pareto-front for a given comet target  
 $(R_c=1.1 \text{ AU}, \theta=-150 \text{ deg})$**

## 5.6 Transfer Strategies from SEL2

Two strategies have been regarded for the transfer from the parking orbit around SEL2 to the comet flyby. The first is a direct transfer manoeuvring from SEL2, and the second makes use of a gravity assist with the Moon.

### 5.6.1 Direct Transfer Strategy

This strategy considers that the spacecraft performs an impulsive manoeuvre to leave from the parking orbit around SEL2 and a second impulsive manoeuvre at a given time on the way to the comet intercept.

To compute the size of the first manoeuvre, the actual radius (1.01 AU) and inertial velocity of SEL2 ( $\sim 30.1 \text{ km/s}$ ) need to be considered. The difference of  $\Delta v^H$  between departure from Earth and departure from SEL2 is given in Figure 5-3 as a function of the target  $R_c$ . For  $R_c <= 1 \text{ AU}$  a 0.5 km/s penalty has to be paid, while for  $R_c >= 1.08 \text{ AU}$  a similar 0.5 km/s saving is obtained. For the intermediate range between 1 AU and 1.08 AU the penalty is gradually converted into the saving.

However it is worth pointing out that it is in this intermediate range where the differences between this simplified 2-body dynamics model (Sun gravity only) with the 3-body dynamics (including Sun and Earth gravity) might become more apparent. Thus the real direction and size of the first manoeuvre to leave SEL2 might differ from the ones predicted with the 2-body dynamics. This needs to be accounted for with margins.

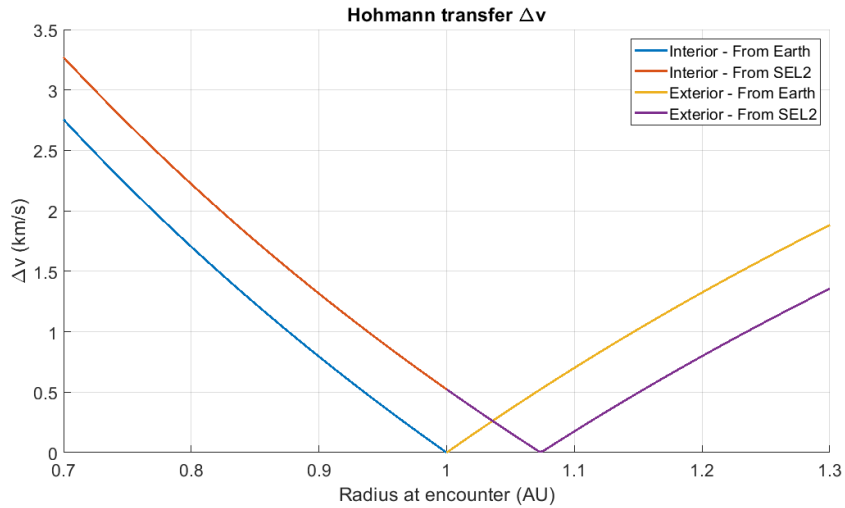


**Figure 5-3: Hohmann transfer  $\Delta v$  difference for Earth and SEL2 departure**

### 5.6.2 Moon Swing-By Strategy

The Moon swing-by strategy was devised to reduce the overall  $\Delta v$  budget, in particular for the targets with negative phase angle at encounter ( $\theta < 0$ ), as it results in efficiency in reducing the heliocentric energy to obtain the necessary phasing trajectory.

- From a three-body dynamics perspective, the strategy is employing the SEL2 manifold to go in the Earth's direction, and then employs the Moon to change the manifold shape and obtain a deviation in the outgoing leg.
- From a two-body heliocentric perspective, the Moon swing-by can be interpreted as a free deviation of the outgoing asymptote, thus modifying the state at the Earth sphere of influence (SOI) exit.

The strategy can be further refined introducing a manoeuvre at the SOI, to modify the  $v_\infty$  vector, and a deep-space manoeuvre (DSM) which assists in achieving the correct phasing.

#### 5.6.2.1 Background

The SEL2 manifold goes towards the Earth with a fixed shape, and a virtually free manoeuvre is needed for the injection (a significant  $\Delta v$  at SEL2 would fall into the category of impulsive transfers).

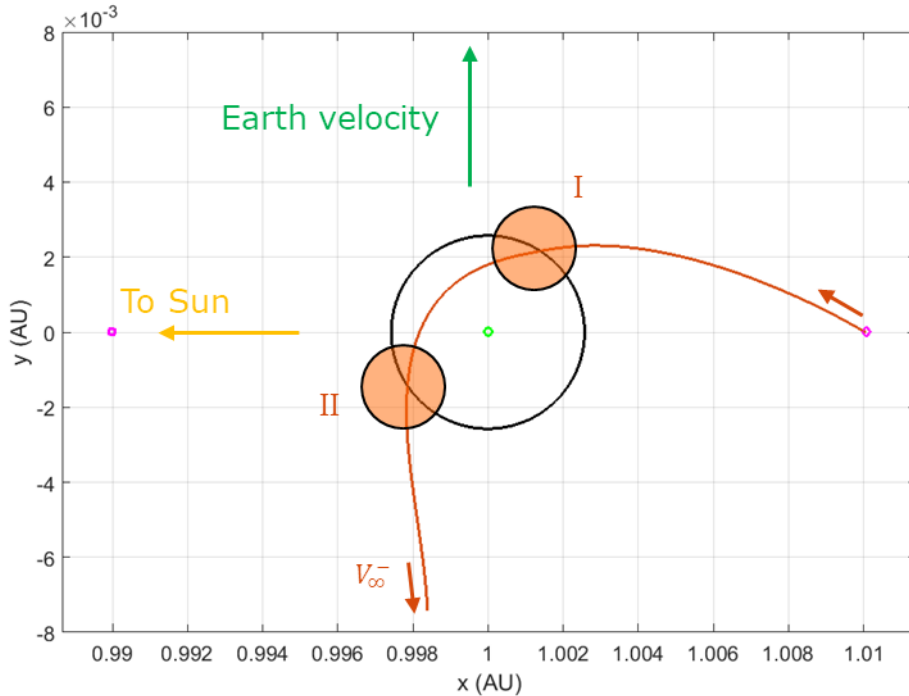


**Figure 5-4: SEL2 manifold with Moon orbit encounters**

Figure 5-4 depicts the shape of this manifold, highlighting the two possible encounters with the orbit of the Moon:

- I. The first encounter is effective to change the perigee of the subsequent Earth passage, and can modify the outgoing asymptote in anti-tangential direction
- II. The second encounter can be employed to modify the outgoing asymptote and obtain a radial escape, thus obtaining a quasi-resonant (up to 1:1 resonance) heliocentric orbit.

For the purposes of the present study, only the first Moon encounter is effective, as it's needed to reduce the heliocentric energy.

### 5.6.2.2 Global analysis

In order to obtain a general-purpose analysis of the Moon swing-by strategy, it is useful to investigate the Earth-centric  $v_\infty$  magnitude and direction obtained after the swing-by, at Earth SOI. This can be treated as an Earth-escaping asymptote from the heliocentric point of view, and used for analysis of the reachable targets.

Figure 5-5 depicts the results of the Moon swing-by analysis. By using the Moon swing-by altitude as a variable, the corresponding  $v_\infty$  magnitude and inertial direction are obtained, and can be used as parameters for the comet transfer analysis. A cubic fit was employed to speed up the calculations inside the transfer optimization process.

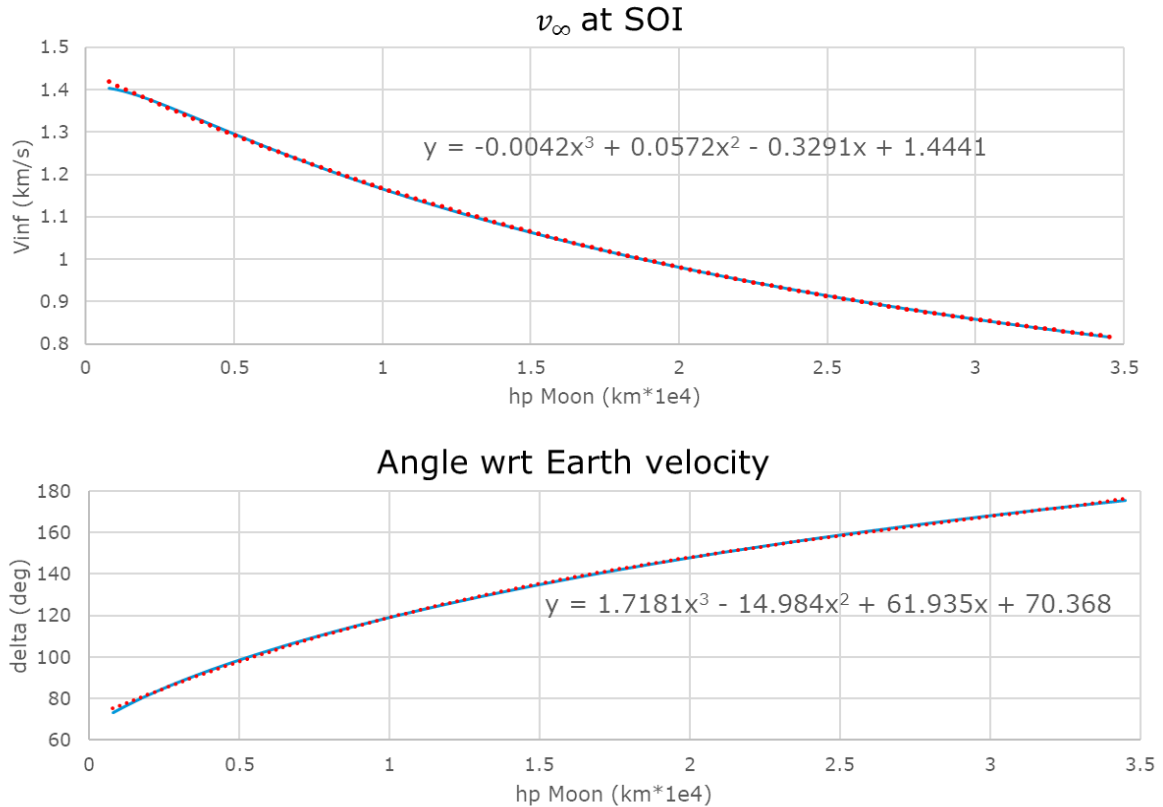


**Figure 5-5: Altitude- $v_\infty$  plots for Moon swing-by analysis**

### 5.6.2.3 Operational aspects

The Moon swing-by allows to save  $\Delta v$ , but introduces an additional complexity to the transfer problem. A full operations analysis was not performed within the CDF; it is suggested to take into account a 25 m/s allocation to navigate the Moon swing-by (targeting and clean-up).

The transfer from SEL2 to Moon encounter takes approximately 4 months, due to the manifold dynamics. This increases the total time of flight and must be considered, at the advantage of having a quasi-free transfer.

### 5.6.2.4 Eclipses

When performing the Moon swing-by strategy, eclipses due to the Moon are possible in the transfer arc.

- Long, infrequent eclipses can take place when the S/C is moving radially towards the Earth-Moon system, if the Moon is passing in the S/C-Sun line. These eclipses may be avoided using an out of plane motion, not considered in this study;
- A ~1 hour eclipse will take place some hours prior to the swing-by, due to the geometry of the encounter. This eclipse cannot be avoided, and its exact beginning and duration are dictated by the swing-by altitude and approach geometry.

## 5.7 Analysis of Reachable Targets

Considering the 2 strategies above and working in the simplified 2-body dynamics model (Sun gravity only) with impulsive manoeuvres, a global analysis of the transfers has been carried out to characterise the reachable comet targets in terms of the required  $\Delta v$  and transfer time.

### 5.7.1 $\Delta v$ and Transfer Time Maps

The approach for a given  $R_c$  and  $\theta$  is to perform a series of global optimizations using the Differential Evolution (DE) algorithm for increasing values of the transfer angle, i.e. the angle travelled by the spacecraft in the ecliptic plane from departure to comet interception. By increasing this angle in integer number of revolutions, the different optimal solutions in the  $\Delta v$ - $\Delta t$  Pareto front can be explored. If the mission limits the available  $\Delta v$  and/or  $\Delta t$ , those transfers that are feasible under such constraints can be identified.

The optimization algorithm uses following optimization variables: true anomaly of Earth at departure, size and direction of departure manoeuvre, and true anomaly travelled to second manoeuvre. In the case of the Moon swing-by strategy, the altitude of the swing-by also needs to be optimised (within the range [5000, 35000] km), while the departure manoeuvre is added to the Earth escape velocity vector achieved after the Moon swing-by at such altitude. Given the values for all the previous parameters it is possible to compute the location and time of the second manoeuvre, and the time required for the transfer to the comet intercept to satisfy the desired  $\theta$  target. The second arc of the transfer trajectory is computed by using a solver of the Lambert problem (i.e. orbit connecting two position vectors in a given transfer time).

This optimization algorithm has been used to sweep the entire  $R_c$ - $\theta$  domain for  $R_c \in [0.7, 1.3]$  AU at 0.02 AU steps and  $\theta \in [-180, 180]$  deg at 5 deg steps in order to obtain maps of the results. For each map computation  $31^*73=2263$  DE global optimizations are run.

The results are provided in Figure 5-6 and Figure 5-7, each figure showing 4 plots for different numbers of heliocentric revolutions of the transfer with the left map representing  $\Delta v$  and the right map representing  $\Delta t$ . Notice that the yellow region indicates  $\Delta v > 3$  km/s. From these result it is observed that:

- Direct transfers favour  $R_c > 1$  AU and  $\theta > 0$  (first  $R_c$ - $\theta$  quadrant) and Moon swing-by transfers favour  $R_c < 1$  AU and  $\theta < 0$  (third  $R_c$ - $\theta$  quadrant). Thus the strategies are complementary and can be combined to reach more targets for the same  $\Delta v$  and transfer time. There is a large region as well where transfer is possible with both strategies.
- Transfers requiring near-zero  $\Delta v$  (black region) exist for both strategies and are more common with the Moon swingby.
- For the same  $\Delta v$ , longer transfers will allow reaching more targets.
- Given more than 2 revolutions for the heliocentric transfer it is possible to cover almost entirely the studied domain with  $\Delta v \leq 3$  km/s and  $\Delta t \leq 4$  years.

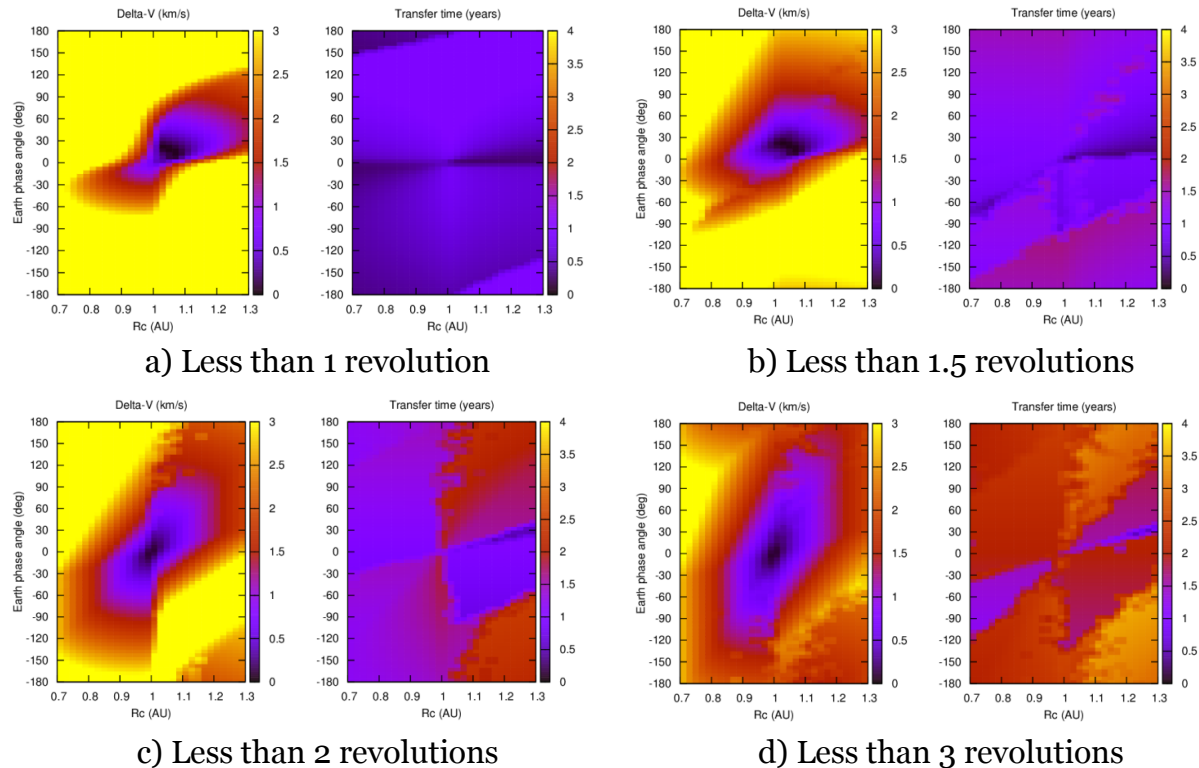


**Figure 5-6:  $\Delta v$  and  $\Delta t$  maps as function of  $R_c-\theta$  - Direct Transfer Strategy**

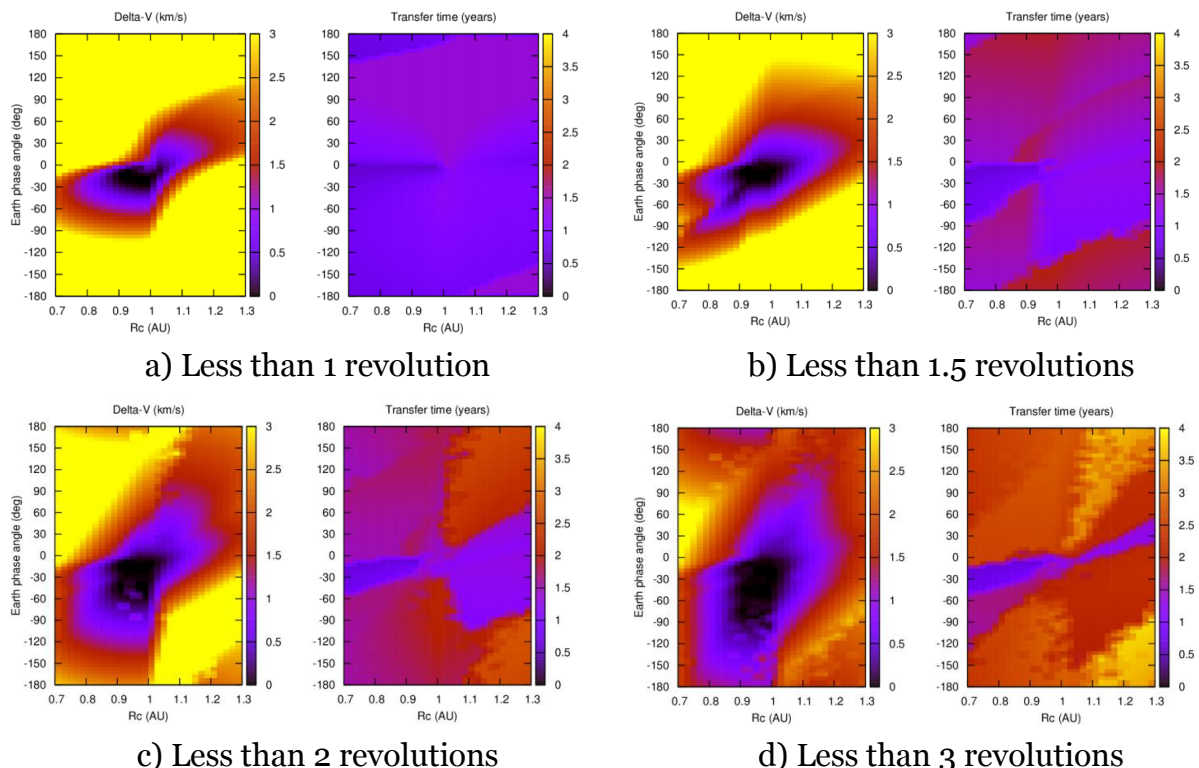


**Figure 5-7:  $\Delta v$  and  $\Delta t$  maps as function of  $R_c-\theta$  - Moon Swingby Strategy**

### 5.7.2 Reachable Area

From the previous results, the next step is to understand the targets in the  $R_c\text{-}\theta$  domain that can be reached for given limits of  $\Delta v$  and total transfer time. Given these limits the results from the previous maps can be explored to identify feasible transfers for any of the points in the map. This process has been performed parametrically to analyse the sensitivity to  $\Delta v$  and  $\Delta t$ .

In addition, to account for uncertainties in the transfer computations, due to simplified model for dynamics and/or manoeuvres, margins have been included as in Table 5-2.

Propulsion	SEP	CP
$\Delta v$ margin	+15%	+5%
$\Delta t$ margin	+10%	0%
Moon swing by - Time from SEL2 to Earth escape	135 days	135 days
Moon swingby - Navigation $\Delta v$	25 m/s	25 m/s

**Table 5-2: Margins and assumptions for reachable area analysis.**

Results of the reachable area are presented in polar plots to show the real physical dimensions of the area. Figure 5-8 and Figure 5-9 give the results for CP and SEP, respectively, whereas for CP a smaller range of  $\Delta v$  is analysed and for SEP up to 3 km/s are covered. Colours in the plots represent the strategy that allows to reach a given target (either direct transfer, Moon swing-by or both strategies).

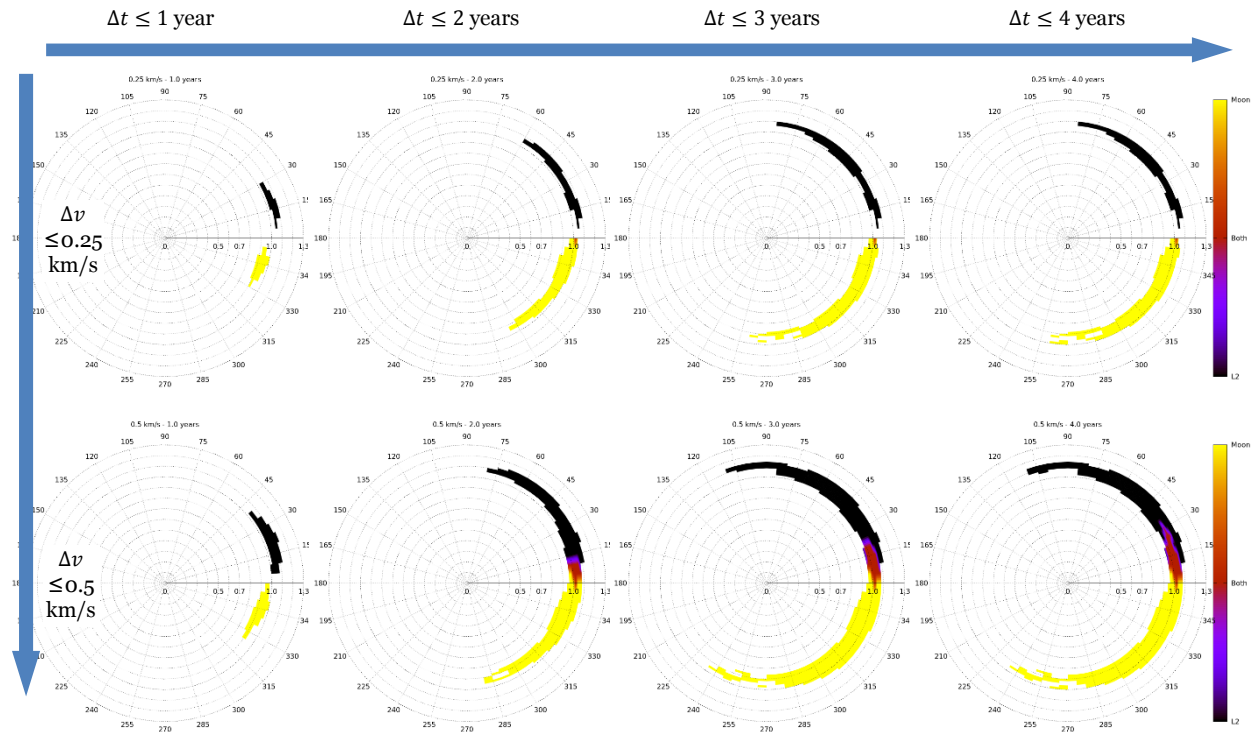


**Figure 5-8: Reachable heliocentric area for CP mission as function of  $\Delta v$  and  $\Delta t$**

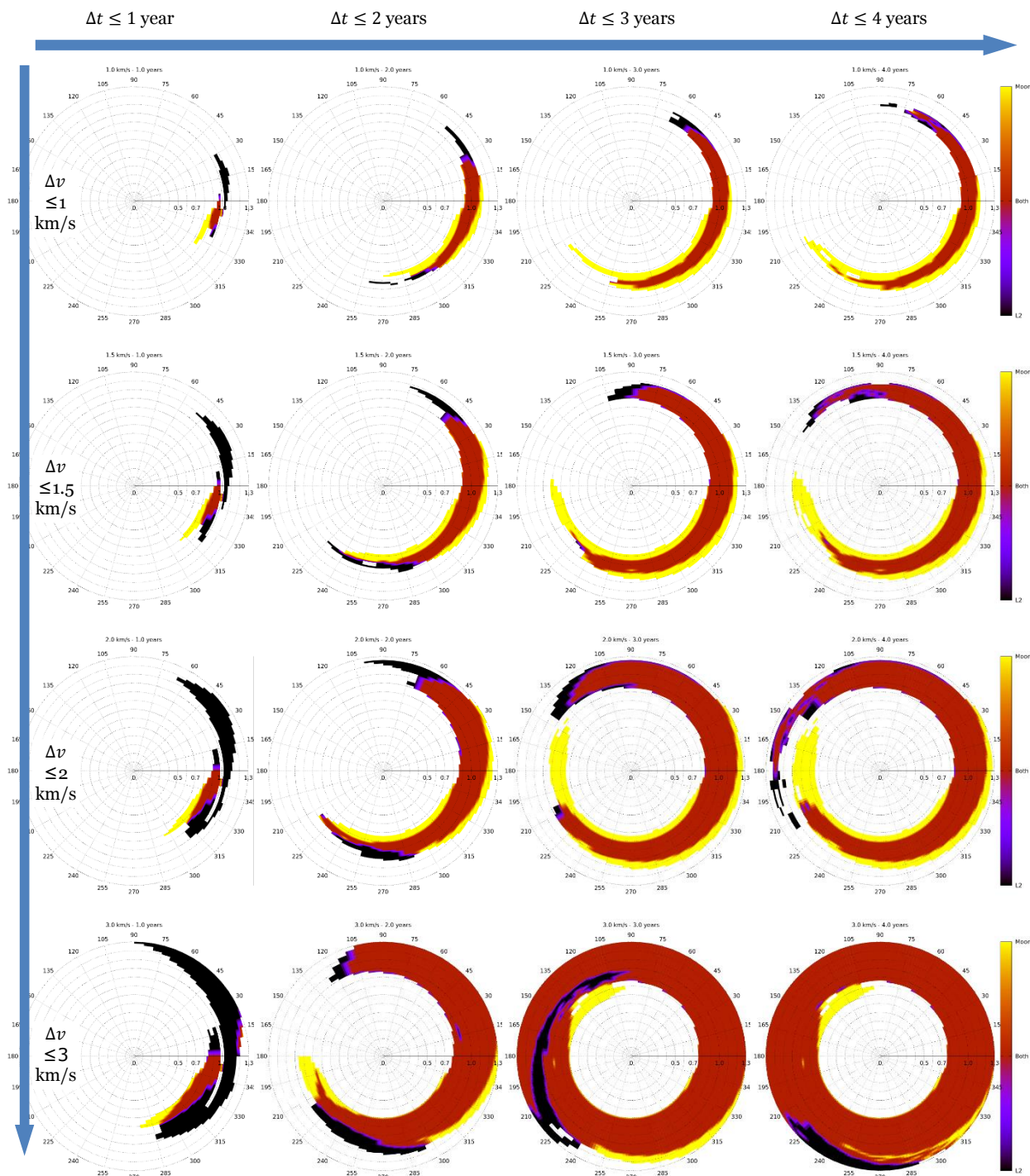


**Figure 5-9: Reachable heliocentric area for SEP mission as function of  $\Delta v$  and  $\Delta t$**

As a measure of the performance of a given design that limits  $\Delta v$  and  $\Delta t$  it is proposed to use the Normalized Reachable Area (NRA), which is defined as the area of the region of reachable targets divided by the area of the circle with radius 1 AU ( $=\pi \text{ AU}^2$ ). The normalization removes the  $\pi$  factor leading to more human-friendly values. In addition it is not needed to specify the area units.

When looking at reference areas to make comparisons, additional advantages of the NRA arise. The annulus for  $R_c \in [1-x, 1+x]$  AU has a normalized area of  $4x$ , e.g. for  $R_c \in [0.8, 1.2]$  the normalized area is 0.8. Thus the normalized area of the entire  $R_c - \theta$  domain explored in the study ( $R_c \in [0.7, 1.3]$ ) is 1.2. In addition, the annulus for  $R_c \in [0.9, 1.2]$  has a normalized area of 0.63.

The NRA for all the different cases has been computed and is presented in Figure 5-10 for a SEP mission. In general it is observed that the NRA is increased by about 100%, i.e. approximately doubles its value, when 2 years instead of 1 year are allowed for the transfer from SEL2. This is also the case when 3 years are considered instead of 2 years. However, increasing the transfer time to 4 years provides only an additional small improvement over 3 years.

Also in general the Direct Transfer and the Moon swing-by strategies alone lead to similar NRA, except for the 1-year transfer case that penalizes in excess the Moon swing-by strategy. Combining both strategies generally increases the NRA by about 25-50%.

A likely case for the spacecraft  $\Delta v$  capability is 1.5 km/s. Looking at up to 3-year transfer the NRA for direct transfer or Moon swingby alone is about 0.4, while both strategies together arrive at 0.62, thus almost equal to the  $R_c \in [0.9, 1.2]$  region or half the  $R_c \in [0.7, 1.3]$ . Sensitivity to  $\Delta v$  change of 0.5 km/s above or below shows almost a linear behaviour, as the change increases or reduces the NRA by about 50%, respectively.

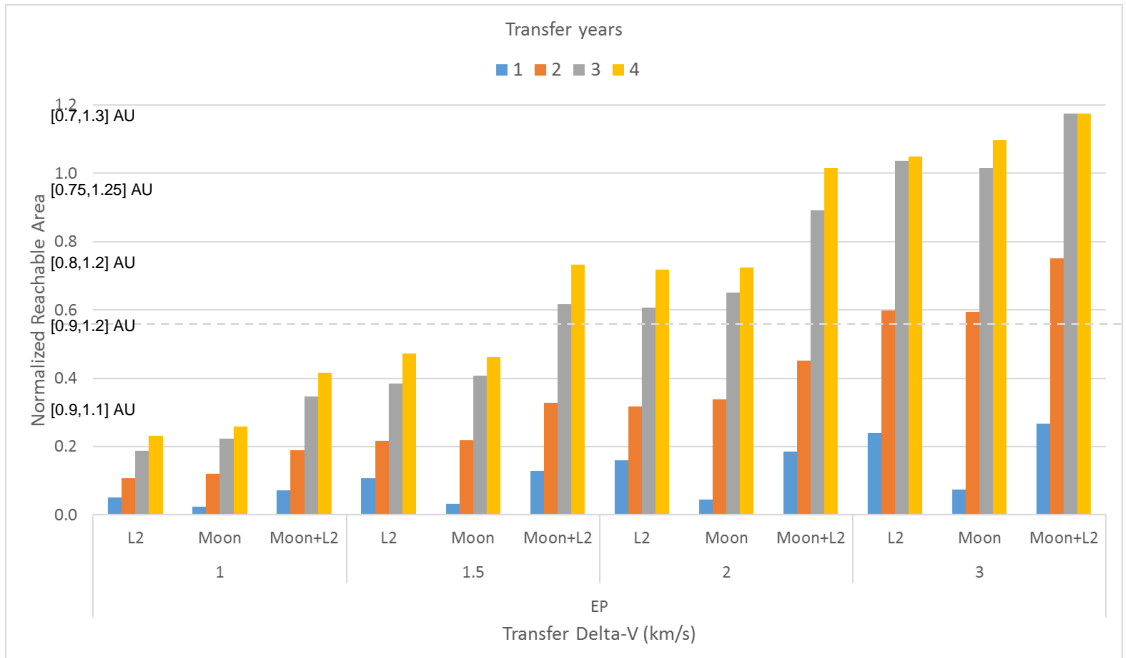


**Figure 5-10: NRA for SEP mission as function of  $\Delta v$  and  $\Delta t$**

Figure 5-11 shows the results corresponding to a CP mission. A transfer  $\Delta v$  of 1 km/s is explored, although this is considered very challenging for the spacecraft design, as the CP propellant would reduce dramatically the mass available for the payload and the platform dry mass.

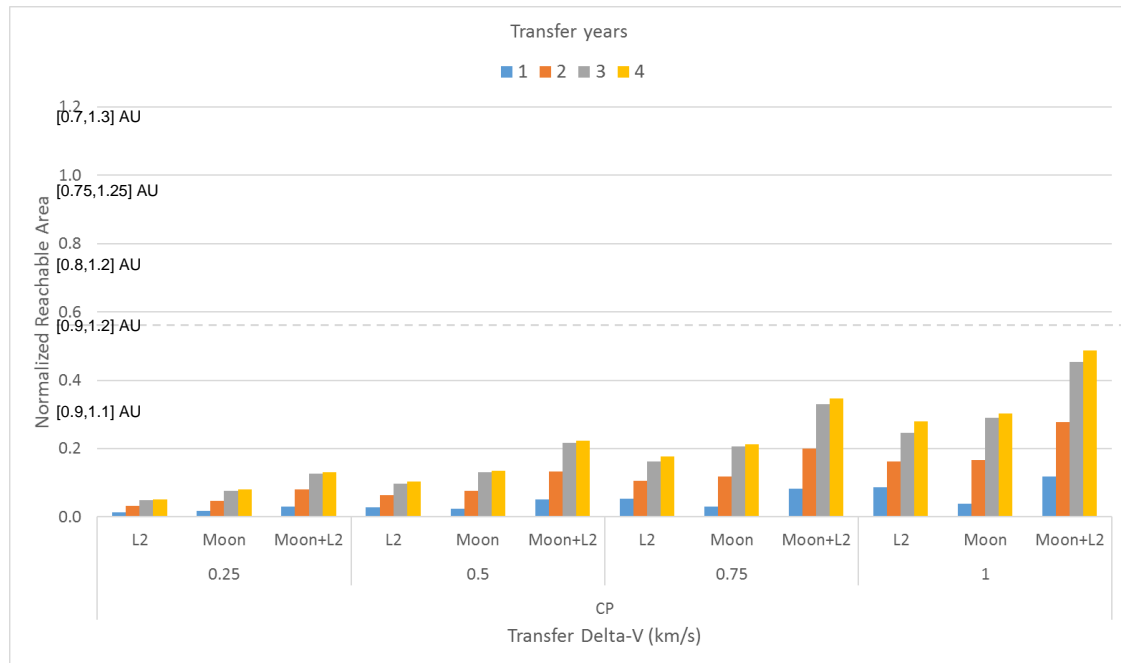


**Figure 5-11: NRA for CP mission as function of  $\Delta v$  and  $\Delta t$**

## 5.8 Probabilistic Reachability Analysis

The probability of having a reachable LPC/DNC target under given mission constraints was assessed and used as a tool to identify, together with the system team, limits to critical design parameters. To this end a mission simulator, simulating individual missions, was set up and used for a Monte-Carlo analysis assessing the probability of a mission having a LPC/DNC target. Note that this analysis refers exclusively to a LPC/DNC target, while a separate study has been performed to assess the reachability of backup targets out of the known periodic comets.

The mission duration stated in this section refers to the time between launch and arrival at a comet and does not account for post encounter activities.

### 5.8.1 Approach

A distribution of LPCs with perihelion less than two AU was provided and used for generating random LPCs (see RD[3] and RD[4]). Therefore, empirical cumulative distribution functions for the argument of perihelion, eccentricity and inclination were obtained from the available dataset. The longitude of the ascending node, argument of perihelion and epoch of perihelion were assumed to be uniformly distributed. Additionally, each LPC was randomly selected to be a DNC with a probability of 40%. While it is difficult to determine if a discovered LPC is actually a DNC this measure provides an estimate on the probability of having a DNC as a target.

A set of 140,000 LPCs with perihelia between January 1<sup>st</sup> 2027 and January 1<sup>st</sup> 2037 was generated and used for the further study. Additionally, each comet was assigned with a random detection distance following the distribution in Figure 5-12, which is taken from figure 4.3.1 of the Phase-2 proposal (see RD[2]). The detection time is then calculated with the known orbital parameters. If the detection distance is below the comet's perihelion the detection time is set to the time of perihelion and if the detection distance is higher than the aphelion the comet is set to be known. This detection model does not account for surface properties and possible correlations between orbital parameters and detection distance.

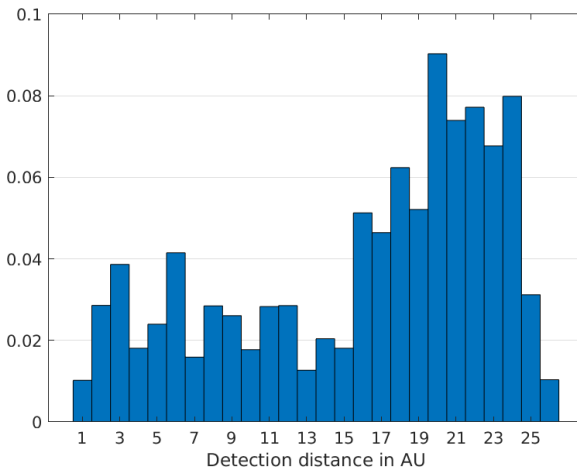


**Figure 5-12: Histogram of LPC detection distance (from RD[2]).**

Encounter parameters are calculated assuming simplified 2-body dynamics with the Sun as the central body. Encounters are assumed to be at the comet's nodes when passing the Ecliptic. For each comet the time of passing the nodes, the heliocentric distance of the nodes  $R_c$  and the Comet-Sun-Earth angle  $\Theta$  at the nodes is calculated. Assuming a spacecraft on a circular orbit with radius  $R_c$  the following parameters are calculated:

- The relative velocity between spacecraft and comet
- Solar-Phase angle (angle between relative velocity and comet-Sun vector)

While the spacecraft is likely not on a circular orbit during encounter the assumption provides a good estimate, especially considering the high encounter velocities of the comets. Additionally, the  $\Delta V$  and transfer time to the comet are interpolated from the  $\Delta V$  transfer time maps (see section 5.7.1). Only comets with  $0.7 \text{ AU} < R_c < 1.3 \text{ AU}$  are considered reachable and available in the maps. The margins described in Table 5-2 are applied to the interpolated values. Both the direct and the moon-flyby strategy were considered.

General statistics of the LPC distributions will be presented in the next section and the results of the Monte-Carlo analysis in the subsequent section.

### 5.8.2 LPC Distribution

A general analysis of the distribution of LPCs was conducted. Figure 5-13 shows the cumulative distribution of the time between detection and perihelion in years. More than half of the targets are detected more than 5 years before perihelion and approximately 25% of the targets are detected only within three years before perihelion. The perihelion is not necessarily close to the passing of the nodes, however, analysis showed that the median difference between perihelion and the node is around 120 days. Therefore, the time between detection and perihelion provides a first estimate on the time between detection and encounter. Considering a transfer time of three and more years and the necessary minimum time between detection of the comet and earliest possible departure, a significant number of comets are not reachable due to insufficient time after detection.

The implemented method for obtaining the detection time does not account for the comet's magnitude or a correlation between the detection distance and orbital parameters.

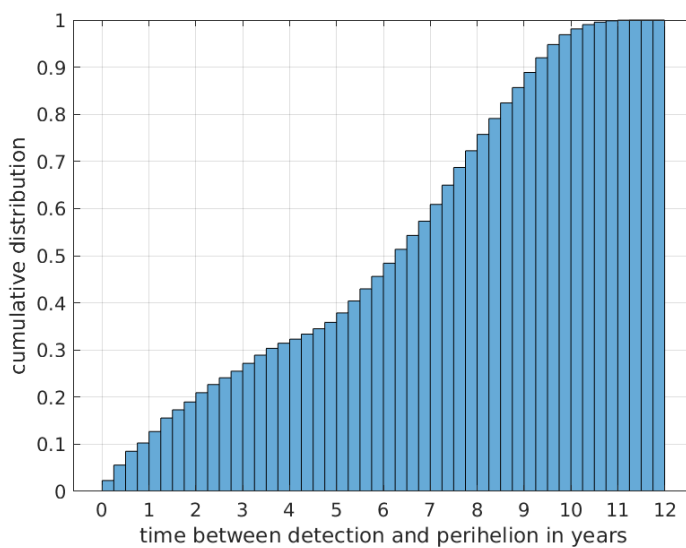


**Figure 5-13: Cumulative density function of detection time before perihelion**

Figure 5-14 shows the distribution of various encounter parameters for the population of reachable LPCs ( $0.7 < R_c < 1.3$  AU). The relative velocity can reach values up to 80 km/s and the median is at 54 km/s. The solar phase angle is symmetrically distributed around 90 degrees. Due to the taken assumptions the solar phase angle directly includes the information whether the encounter is on the inbound or on the outbound leg of the comet's orbit. For angles less than 90 degrees the encounter is on the inbound leg and for values greater than 90 degrees on the outbound leg. Due to the symmetrical distribution, constraining the encounters to only inbound ones would simply halve the number of possible targets. The heliocentric distance at encounter is shifted towards values greater than one AU and the Comet-Sun-Earth angle is also shifted to positive values. This corresponds to encounters trailing the Earth's orbit. The distance from Earth at encounter peaks at around 0.25 AU and decreases gradually to the maximum value of 2.3 AU.

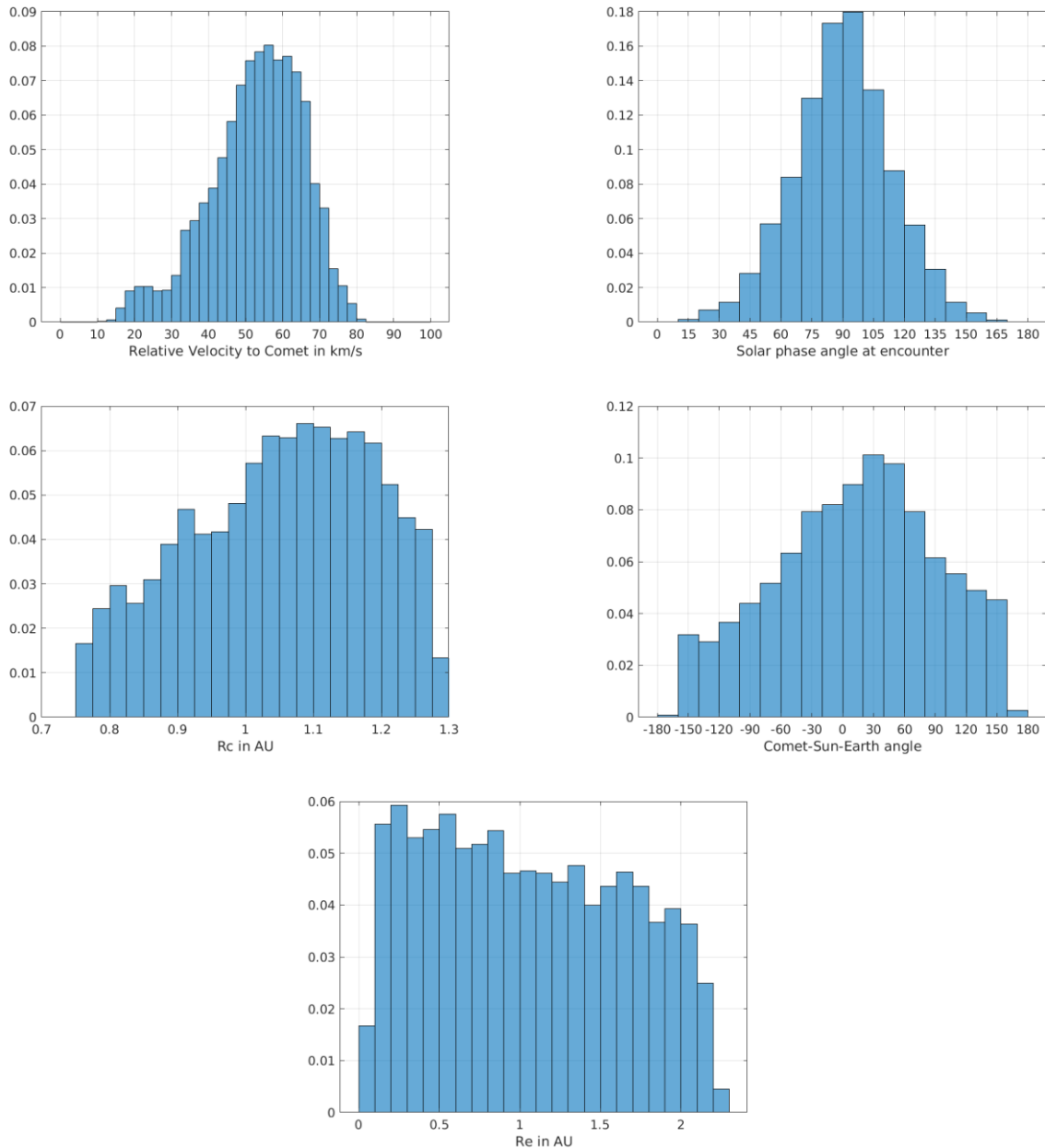


**Figure 5-14: Encounter parameter distributions**

### 5.8.3 Mission Monte Carlo Simulations

The following section describes the Monte-Carlo simulations. For each simulated mission a set of LPCs is drawn from the population. For the 10 year dataset and with an expected rate of 7 LPCs/year this corresponds to 70 comets per mission. Then the comets are filtered by applying mission constraints and checking for reachable targets. The available constraints are:

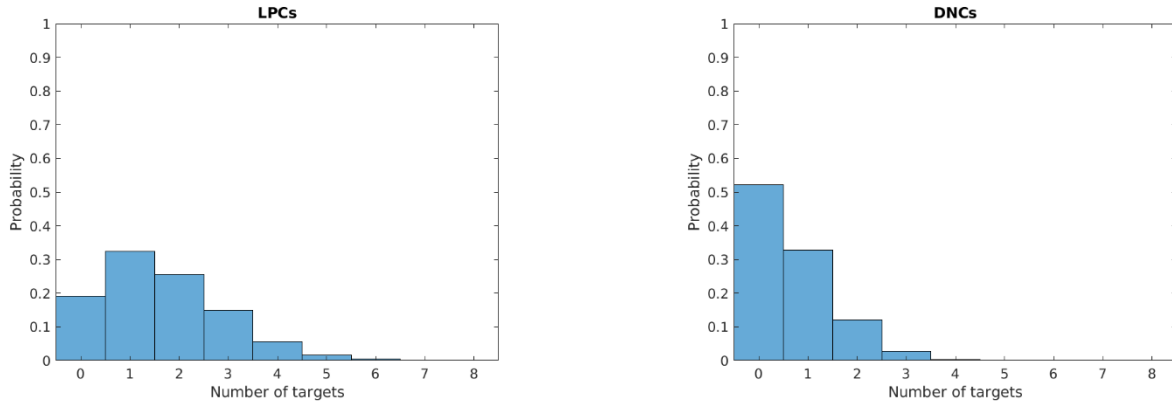
- The mission duration  $\Delta t_{\text{Mission}}$  (the encounter and departure must be within the given interval, which is assumed from launch to comet flyby)

- The maximum  $\Delta V_{\max}$  (maximum  $\Delta V$  for the transfer from SEL2 to the comet; not considering initial  $\Delta V$  to reach L2)
- The maximum transfer time to the comet  $\Delta t_{\text{transfer\_max}}$
- The minimum time between detection of a comet and earliest departure  $\Delta t_{\text{detection\_departure}}$  (set to 180 days)
- The latest target selection date, where the comet must be known before  $t_{\text{latest\_selection}}$  (set to 3 years after launch)
- The relative velocity between comet and spacecraft at encounter  $V_{\text{encounter}}$
- The Solar phase angle at encounter (angle between  $V_{\text{encounter}}$  and Comet-Sun vector)
- The heliocentric distance at encounter  $R_c \in [0.7, 1.3]$
- The distance from Earth at encounter  $R_e \in [0, 2.3]$
- The Comet-Sun-Earth angle  $\Theta$
- The Sun-Earth-Comet angle, used to avoid encounters in solar conjunctions; must be greater than 5 degrees for inferior and 10 degrees for superior conjunctions.

For each simulated mission the aforementioned constraints are applied. The number of comets that fulfil the constraints are then counted as valid targets for the mission. Repeating this process provides an estimate for the probability of having at least one valid target. Figure 5-15 shows two histograms providing the probability of  $n$  targets for an exemplary mission using the baseline constraints as specified in Table 5-3. Both the probability of a LPC and a DNC target are depicted. The bar for 0 targets directly provides the probability of having no LPC/DNC target. For the LPCs the probability of having no target is approximately 19% and the probability of having one target 32%. In 49% of the simulations there was more than one possible LPC target during a mission, though only one can eventually be visited. The probability for the DNC targets was directly obtained from the simulation by defining an LPC as a DNC with a 40% probability. It is also possible to calculate the probability of having no DNC target  $p_{0\_DNC}$  if the probability of  $n$  LPC targets  $p_{n\_LPC}$  and the probability of a LPC being a DNC  $p_{DNC}$  is known. It is given by:

$$p_{0\_DNC} = \sum_{n=0}^N p_{n\_LPC} * (1 - p_{DNC})^n$$

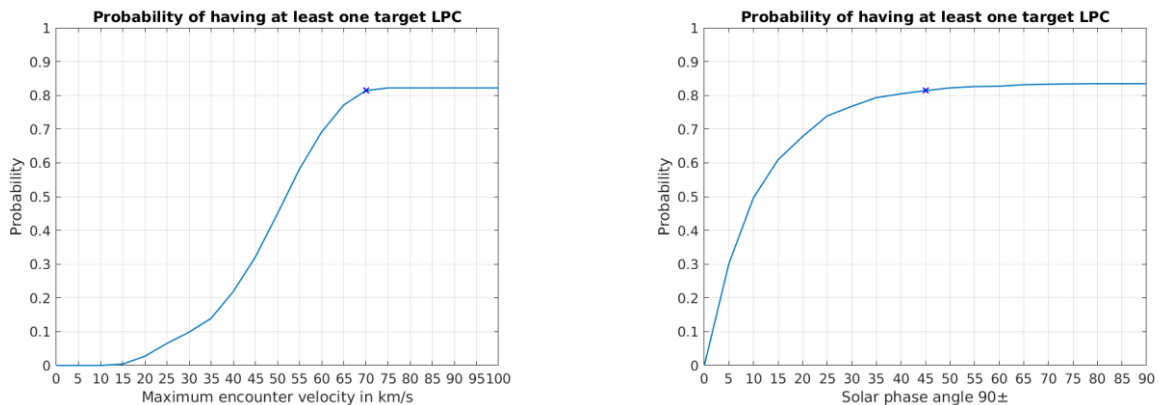
It is seen that the ratio of DNCs/LPCs has a significant influence on the result. In the present analysis a value of 0.4 was used for this quantity.



**Figure 5-15: Probability of n targets**

A sensitivity analysis on the impact of single constraints on the probability of having a target was performed. Figure 5-16 shows the results of this analysis for the encounter velocity, the solar phase angle and the heliocentric distance of the encounter. The figures were generated by varying the respective variable while keeping the others at the baseline setting, which is given in Table 5-3. Repeated Monte Carlo simulations with varied constraints were conducted and the probability of at least one target sampled. The blue cross marks the baseline value for the given parameter. The maximum relative encounter velocity was varied in 5 km/s steps from 0 to 100. The solar phase angle interval was varied in 5 degrees steps from  $90 \pm 0$  to  $90 \pm 90$  degrees. The heliocentric distance at encounter was studied for intervals with lower limit fixed at 0.9 AU and upper limit varied in 0.05 AU steps, e.g. the value 1 AU in the x-axis represents the interval [0.9, 1.0] AU. The results of the analysis led to the following system design constraints:

- $V_{\text{encounter}} < 70 \text{ km/s}$
- Solar phase angle at encounter  $\varepsilon [45, 135]$
- the heliocentric distance at encounter  $R_c \varepsilon [0.9, 1.25]$



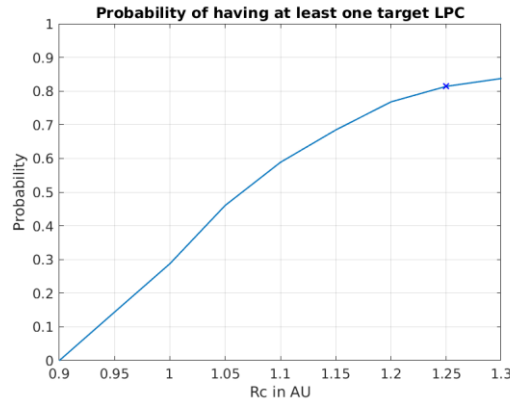


**Figure 5-16: Sensitivity of target probability to single parameters**

Table 5-3 summarises the results from the target reachability analysis. The detection model reduces the probability of having a LPC target from 95% to 91%. Adding the system constraints the probability decreases to 81%. The probability of having a DNC target in this configuration is approximately 50%. If instead of both the direct and the Moon swing-by strategy only direct transfers to the target are allowed the probability of having a target decreases by approximately 10% (see last row in table).

Case	LPCs	DNCs
$\Delta V < 1.5 \text{ km/s}$ 5y – Comets assumed to be known	95%	71%
$\Delta V < 1.5 \text{ km/s}$ 5y – Using detection model	91%	61%
$\Delta V < 1.5 \text{ km/s}$ 5y – Detection + System constraints: $\Delta t_{\text{detection\_departure}} = 180\text{d}$ , $t_{\text{latest\_selection}} = \text{launch} + 3\text{y}$ , $V_{\text{encounter}} < 70 \text{ km/s}$ , Solar Phase Angle $\in [45, 135]$ , $Rc \in [0.9, 1.25]$ , conjunction avoidance	81%	48%
<b>Baseline</b>		
$\Delta V < 1.5 \text{ km/s}$ 5y – Detection + System constraints: $\Delta t_{\text{detection\_departure}} = 180\text{d}$ , $t_{\text{latest\_selection}} = \text{launch} + 3\text{y}$ , $V_{\text{encounter}} < 70 \text{ km/s}$ , Solar Phase Angle $\in [45, 135]$ , $Rc \in [0.9, 1.25]$ , conjunction avoidance; <b>Only direct transfers</b>	71%	39%

**Table 5-3: Probability of having at least one target LPC/DNC**

A further analysis on the influence of  $\Delta V$  and mission duration on the probability of having a target was conducted. Figure 5-17 shows the results from this analysis. The blue cross marks the baseline scenario with a 5 y mission and a  $\Delta V$  of 1.5 km/s. The figures were generated with the baseline mission constraints, provided in the previous table. Changing the limits affects the shape of the curves. By increasing  $\Delta V$  or the mission duration the probability of having at least one target is increased. Additionally, increasing the mission duration and decreasing the  $\Delta V$  is possible while keeping the same probability. Increasing the mission duration from 5 to 6 years while keeping the same probability for having a DNC target, allows a  $\Delta V$  reduction from 1.5 km/s to approximately 1.2 km/s. If instead of the probability the  $\Delta V$  is kept constant increasing the mission duration by one year increases the probability of having at least one DNC

target by the same order as increasing the  $\Delta V$  from 1.5 km/s to 2 km/s in the 5 year mission.

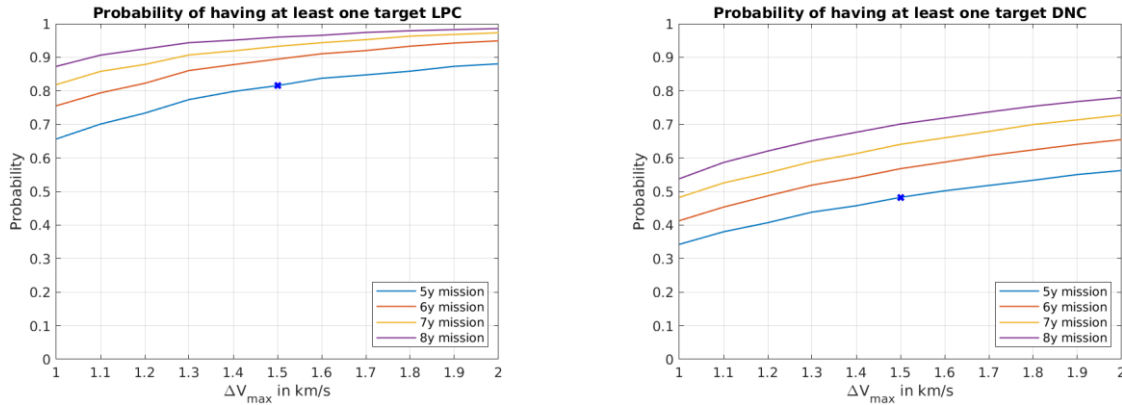


**Figure 5-17: Influence of mission duration &  $\Delta V$  on mission success (EP)**

### 5.8.3.1 LPC rate sensitivity

The influence of the rate of expected LPCs with  $q < 2$  AU per year on the probability of having at least one target was studied. Therefore, the number of comets per year was varied in between 5 and 9. The same mission constraints as in the baseline were applied (see Table 5-3). The results of the analysis are found in Table 5-4. As expected increasing the rate of LPCs increases the probability of having at least one LPC target.

N LPCs/year	5	6	7	8	9
LPC	69%	76%	<b>81%</b>	85%	88%
DNC	38%	43%	<b>48%</b>	53%	58%

**Table 5-4: Probability of having at least one target for different rates of LPCs**

### 5.8.3.2 Transfer time

The transfer time from SEL2 to the target was left free for the analysis. The cumulative density function of this parameter for simulated missions is shown in Figure 5-18. The data was normalized to missions having at least one valid target. If multiple targets were available two different target selection strategies were applied. The first favouring the shortest possible transfer and the second favouring the longest possible one. It is seen that for both strategies most transfers are shorter than three years. This can be in parts explained with maps used for interpolation, which provide transfer times of up to four years. But the determining factor is probably the mission duration of five years. For transfers taking three years, the encounter must be within the last two years of a mission, reducing the probability for such an event. The target selection significantly influences the required transfer time. If the shortest transfer is selected more than 50% of the missions with a target have transfer times of less than one year.

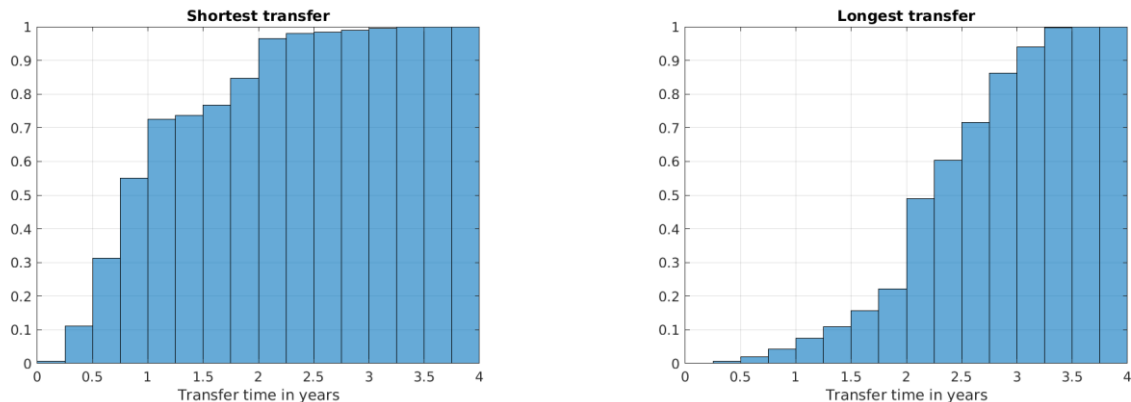


**Figure 5-18: Distribution of transfer times from SEL2 to target**

### 5.8.3.3 Post-Encounter Earth distance

A further analysis on the post-encounter distance from Earth was conducted. With the given interval of the heliocentric distance  $R_c \in [0.9, 1.25]$  the possible Earth distance at encounter  $R_e \in [0, 2.25]$ . However, depending on the encounter geometry the distance will evolve differently in the months after the encounter. Especially, for encounters with  $\Theta > 0^\circ$  &  $R_c > 1$  AU the distance is expected to increase after the encounter, since the encounter position is trailing behind Earth.

Figure 5-19 shows the distribution of the mean Earth distance within 6 months after encounter. The left figure shows the distributions for all reachable LPC targets. The right figure shows a distribution for individual missions. In each mission with at least one LPC target one was selected according to a given criterion. The criteria are:

- Minimum mean distance from Earth 180 days after encounter
- Minimum transfer time to the target.

The selection of the target if multiple are available has a significant influence on the post encounter distance. Selecting the shortest transfer, 50% of the missions have mean post encounter distances from Earth smaller than 0.99 AU. Favouring the shortest post encounter distance, 50% of the missions have a mean post encounter distance less than 0.78 AU. If necessary, this can be part of the target selection process. With both methods the maximum mean distance in the 6 months after encounter is approximately 2 AU.

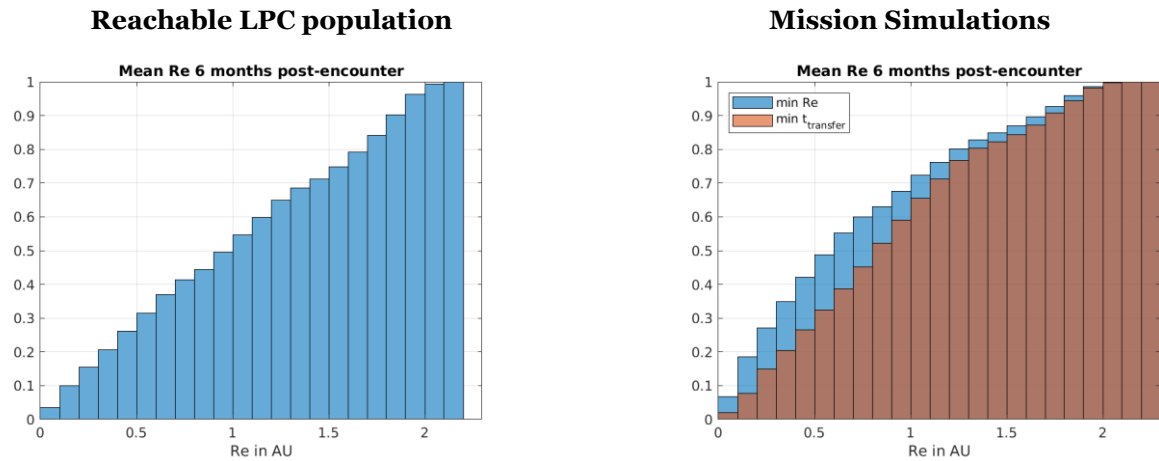


**Figure 5-19: Mean post encounter Earth distance**

#### 5.8.4 Discussion

The conducted analysis showed that by imposing necessary mission constraints the probability of having at least one LPC/DNC target during a mission significantly drops. The results are sensitive to the underlying distribution of LPCs, the detection model and the ratio of DNCs/LPCs. The reachability of a backup target can be ensured by selecting corresponding mission constraints. The available backup targets identified in this study are reported in the next section.

#### 5.9 Transfer Geometry

This section studies the geometry of the transfer trajectories to reach the different targets as function of  $R_c$  and  $\Theta$ . The results are based on 2-body dynamics model considering only the Sun gravity. This model is representative enough for the transfer in terms of the drift with respect to Earth to reach the target.

Four values of  $R_c$  have been investigated from 0.9 AU to 1.2 AU at 0.1 AU, as well as  $\Theta$  covering the range  $[-150, 150]$  deg in 30 deg steps. For each target a feasible trajectory has been selected that requires a Delta-V below 1.5 km/s (-10% margin) and that minimises the transfer duration. Both strategies, direct transfer from SEL2 and Moon flyby, are considered.

The XY projection of the transfers in the Sun-Earth rotating frame is shown in Figure 5-20. A marker shows the location of the DSM, which tends to be either at perihelion or at aphelion. For  $R_c=1$  AU all targets are reached drifting from Earth in the direction towards the target. However, for other values of  $R_c$  some of the targets need to be reached by drifting on the opposite direction and passing behind the Sun. This is the case of 0.9 AU and  $\Theta=150$  deg (behind Earth), which is reached drifting ahead of Earth. The opposite is even clearer for targets above 1 AU and  $\Theta$  from -150 to -90 deg, which are reached via long trailing orbits.

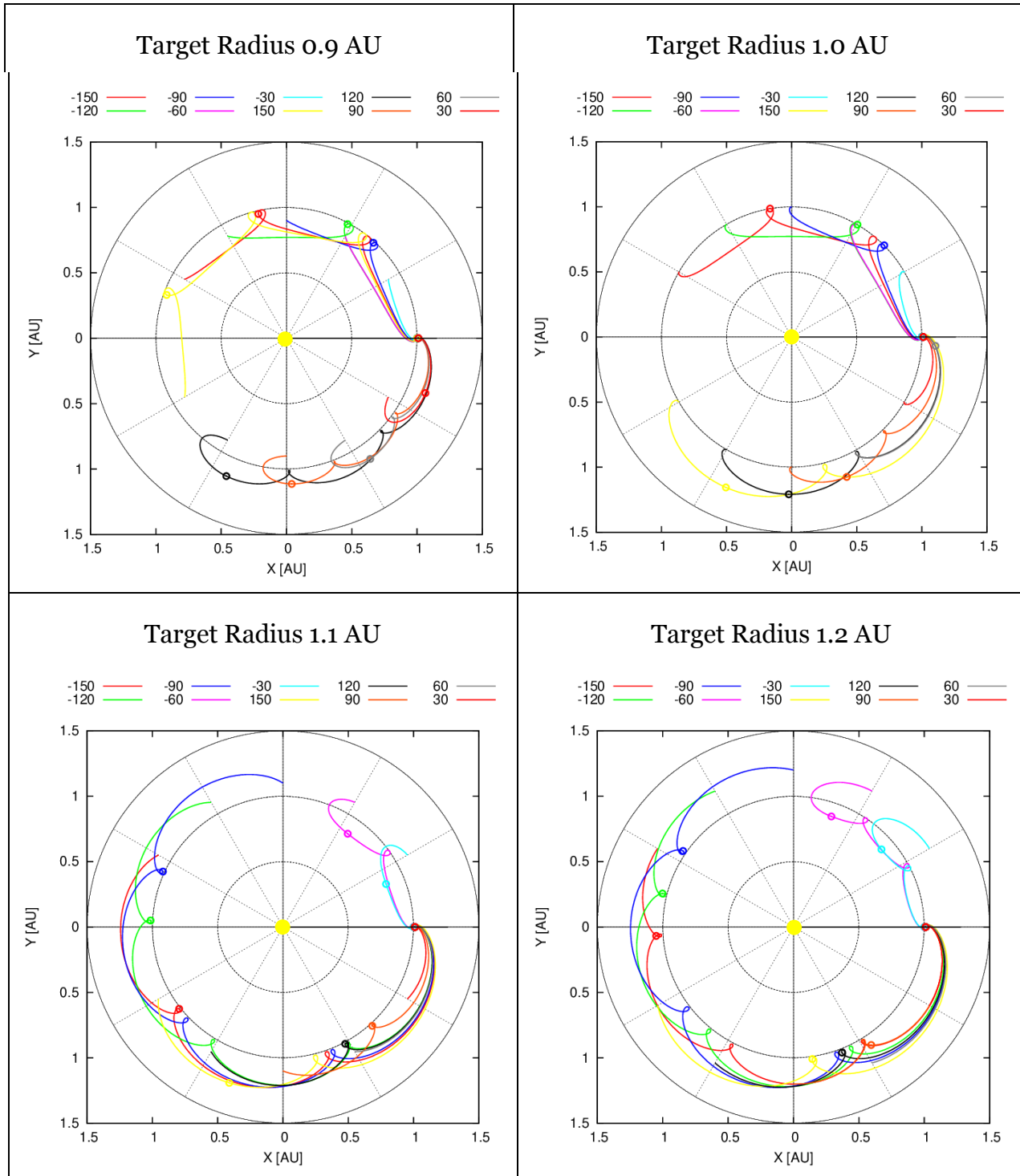


**Figure 5-20: Transfer trajectories in Sun-Earth rotating frame**

The duration of the transfer orbit as function of  $R_c$  and  $\Theta$  is given by Figure 5-21. The plot shows separately markers for both strategies, direct from SEL2 and Moon swing-by, out of which the shortest is selected. For  $|\Theta| \leq 75$  deg transfers of less than an orbital revolution are generally possible, with transfer durations between 0.5 and 1.25 years.

Out of this interval transfers require more than one revolution with duration between 1.5 and 2.5 years.

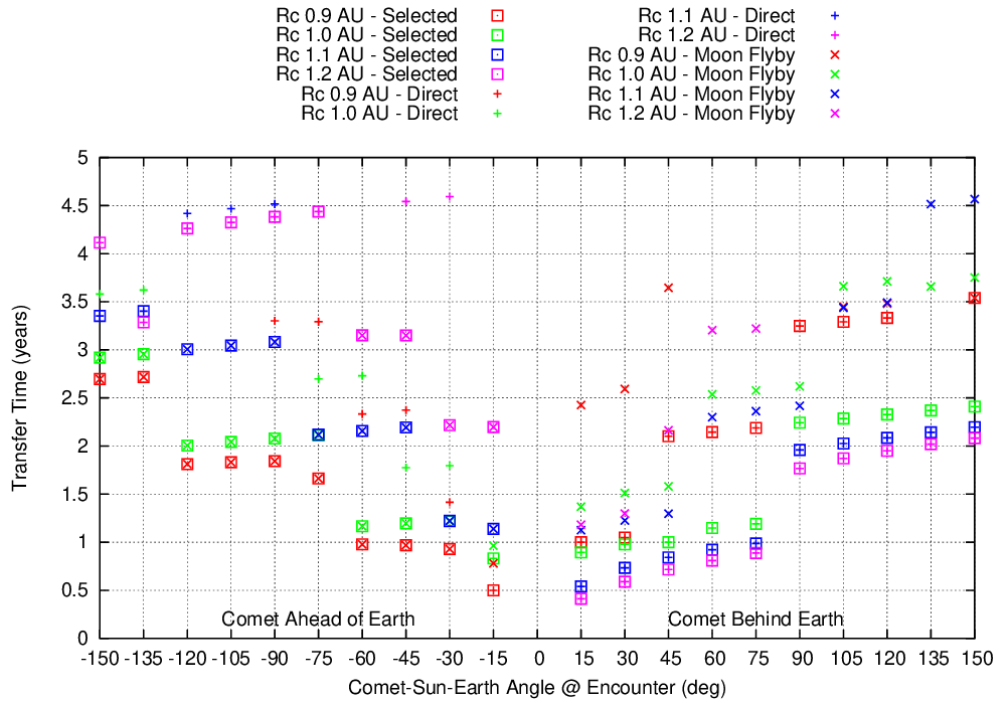


**Figure 5-21: Selected transfer durations**

### 5.9.1 Analysis of Manoeuvres

The same 2-body dynamics model is used to analyse the distance to the Sun and the direction of the manoeuvres in terms of the Sun aspect angle. This model gives an approximation for the 2 impulsive manoeuvres. It is expected that the size and direction of the second burn, i.e. the intermediate DSM, implemented with EP will be similar to the impulsive one. For the first burn, the model totally fails to describe accurately the long EP burn that is needed to leave SEL2, which will require a quite complex structure. However, it can be used to understand the direction of the first burn at the Earth SOI after the Moon flyby strategy.

The distance to the Sun of the first burn can be considered close to 1 AU. For the second burn it depends on the target as it is shown in Figure 5-22. It is worth mentioning that while for most of the cases the manoeuvre is close to 1 AU from the Sun, in some cases it is needed to perform this manoeuvre at aphelion up to 1.25 AU or perihelion down to 0.85 AU.

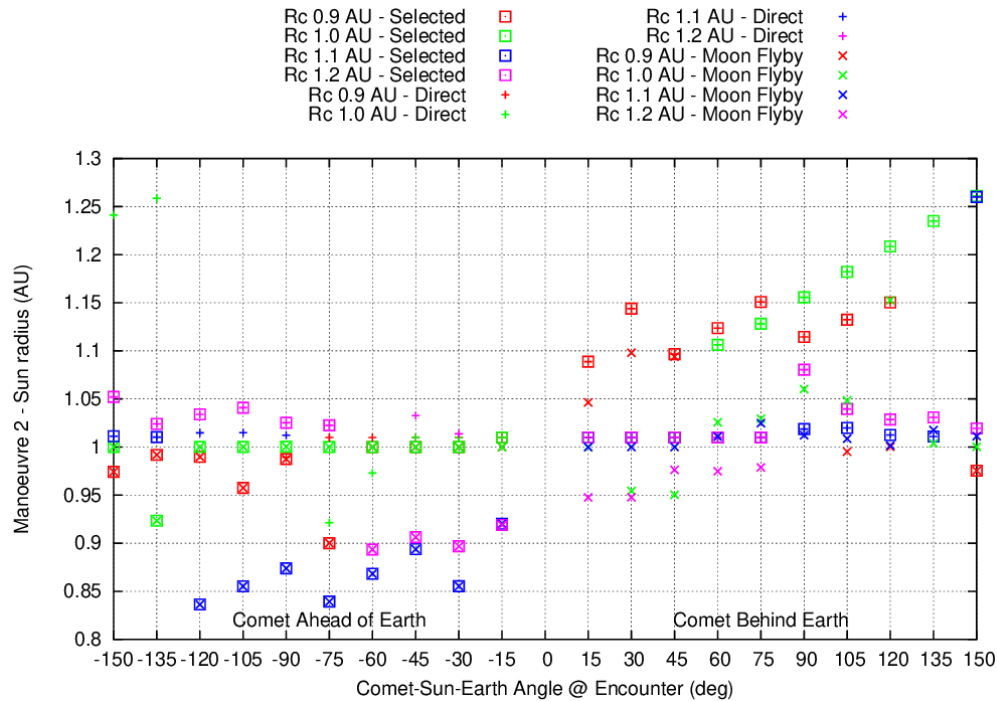


**Figure 5-22: Distance to Sun at second burn / intermediate DSM**

Figure 5-23 shows the Sun aspect angle of both manoeuvres, indicating a range of  $\pm 45$  deg around Sun aspect angle of 90 deg. Optimal manoeuvres tend to be in the tangential direction, thus both plots show that the Sun aspect angle does not deviate more than 30 deg with respect to the normal to the Sun. Exception to this is found only for transfers going to 1 AU and low  $\Theta$  for which the optimizer converged to a 1 burn solution, though the Delta-V of this burn is split in 2.

As mentioned above the results for the first burn and direct from SEL2 are not to be trusted, and actually optimal transfers have been found that require significant thrusting in the anti-radial direction at the start of the transfer, i.e. transfers leaving in the  $-X$  direction of the Sun-Earth rotating frame. In order to avoid this anti-radial thrusting, a mitigation measure can be using the equivalent transfer with Moon flyby, or using less-efficient transfer leaving SEL2 in the  $-Y$  direction, incurring a small Delta-V and transfer time penalty.

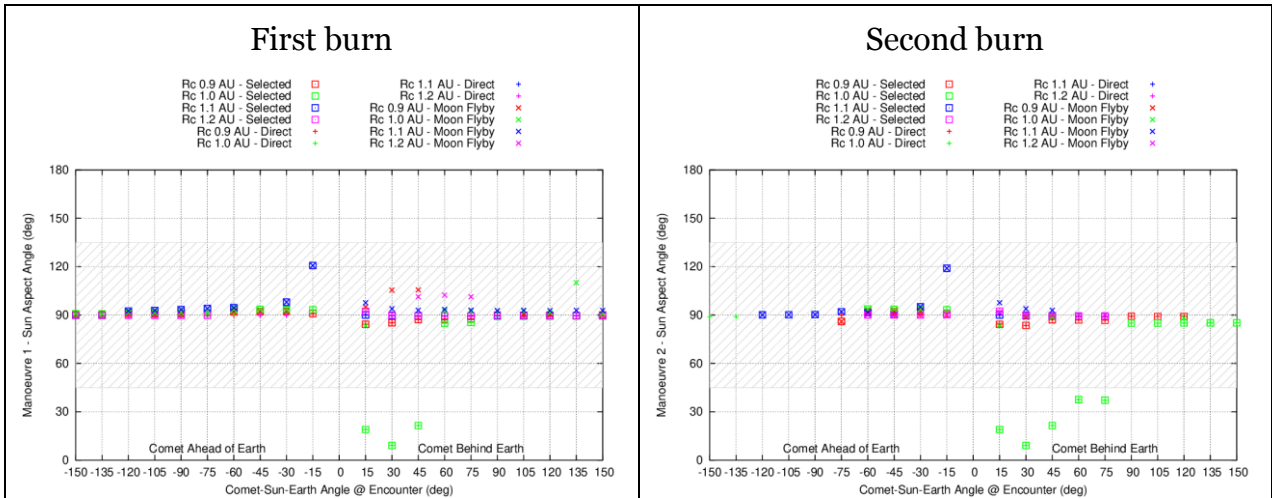


**Figure 5-23: Sun aspect angle of manoeuvres**

## 5.10 Geometry of the Science Downlink Phase

During this phase of the mission spacecraft A will downlink the science data acquired during the comet flyby. Nominally this phase is assumed to extend for 180 days following the comet flyby. The evolution of the distance to Earth during this phase drives the downlink capability. As indicative figure of merit the average Earth distance ( $R_E$ ) over the 180-day downlink period is used. In reality, the data bit rate varies with  $1/R_E^2$ , such that a better indication could be provided by averaging this quantity. In the practice it has been observed just a small difference between both methods for most of the cases relevant for Comet Interceptor.

Reference transfer trajectories in the 2-body dynamics model have been analysed for several values of the radius  $R_c$  and Comet-Sun-Earth angle  $\Theta$  (30 deg steps) at the comet encounter. The trajectories are compatible with an overall EP Delta-V of 1.5 km/s (-10% margin) and have been selected favouring the shortest transfer time. A period of 540 days after the comet flyby is investigated in order to understand the possible benefit of delaying the start of the data downlink a maximum of approximately 1 year.

Figure 5-24 shows the projection of the post-encounter trajectories onto the XY-plane of the Sun-Earth rotating frame (left) and the evolution of the distance to Earth. The radius at encounter is 1 AU. The distance plot shows markers to indicate the average  $R_E$  for the first 180 days after the flyby, and for the alternative period delayed by 1 year. The figures clearly show that the spacecraft will always be drifting away from Earth, so that there is no benefit by delaying the start of the science data downlink.

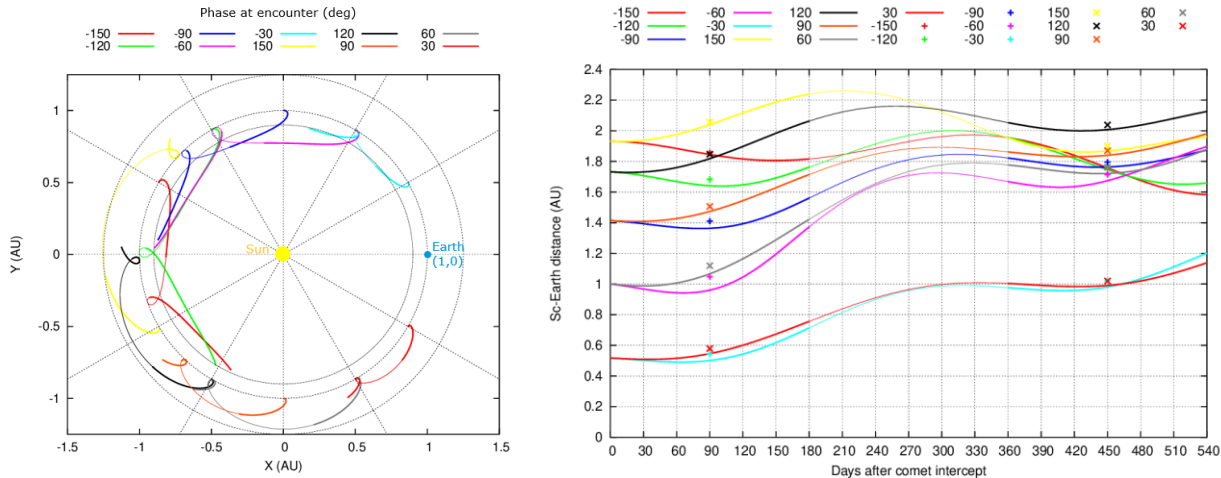


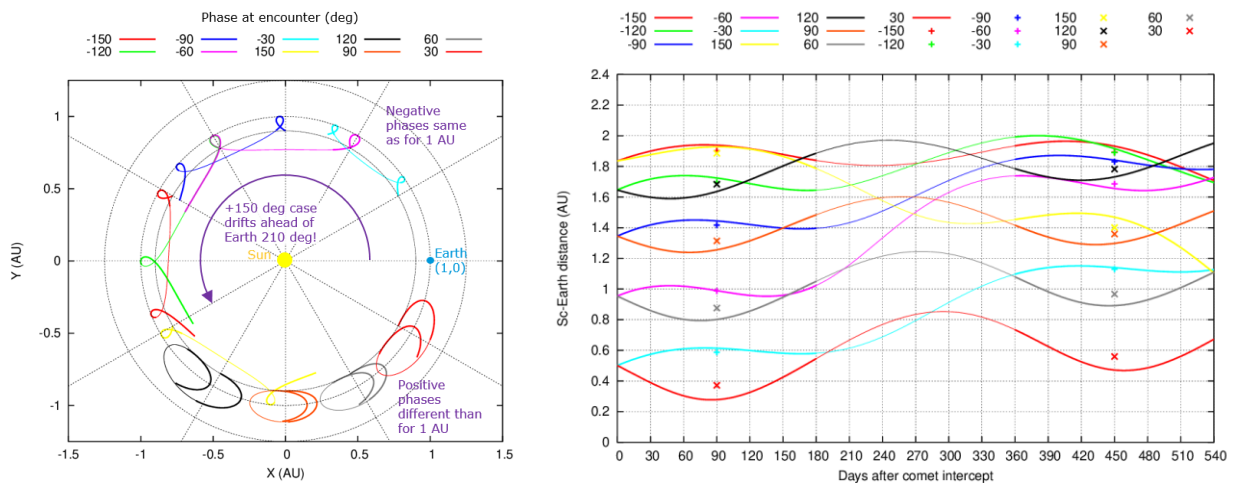
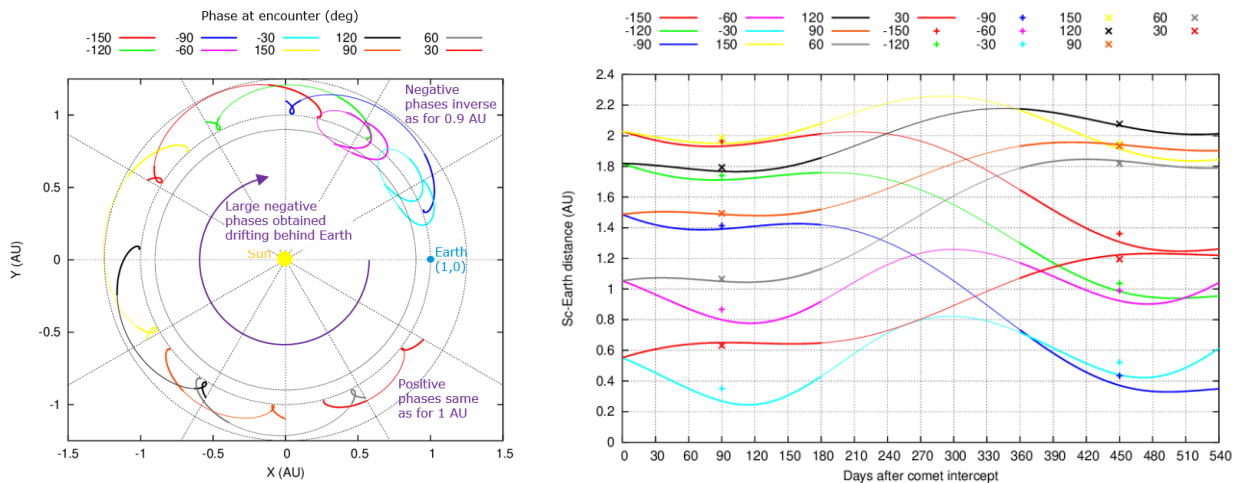
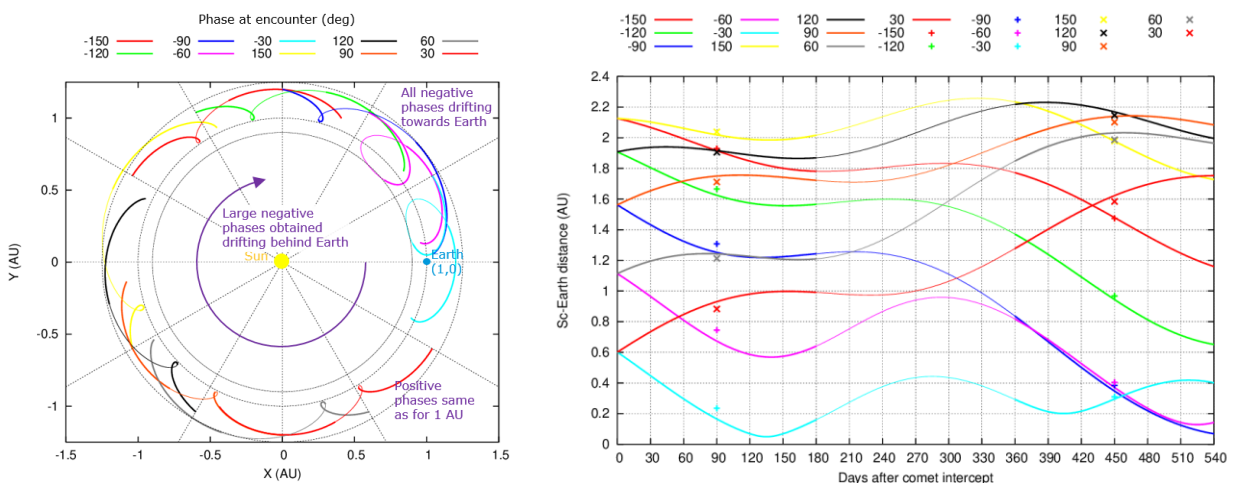
**Figure 5-24: Post encounter trajectory and evolution of Earth distance -  $R_c=1$  AU**

Looking at the same figures for  $R_c=0.9$  AU (Figure 5-25) it is observed that it is more efficient to reach large positive  $\Theta$  (behind Earth) by going all the way from the other side of the Sun drifting actually ahead of Earth. The opposite is observed for  $R_c$  higher than 1 AU, as large negative  $\Theta$  (ahead of Earth) are achieved by drifting behind Earth (Figure 5-26 and Figure 5-27). For such cases, which in the first 180 post-encounter days are far away from Earth, there could be a benefit by delaying the downlink phase, however because the transfer times are long (3 to 4.5 years) the mission duration constraint might be a limiting factor.<sup>2</sup>

When going to encounter at 1.2 AU a different family of trajectories appear to target moderately  $\Theta$  angles (ahead of Earth up to about -60 deg). These targets are reached by lowering the perihelion to induce a drift ahead of Earth and then a DSM that raises the aphelion, such that the drift is reverted. After the flyby the spacecraft will be getting closer to Earth, which is beneficial for the data downlink already in the first 180 post-encounter days.

In conclusion delaying the science downlink phase is not found promising for the mission.

<sup>2</sup> In addition, system reliability and cost for the extended pre-downlink phase mission would need to be considered.

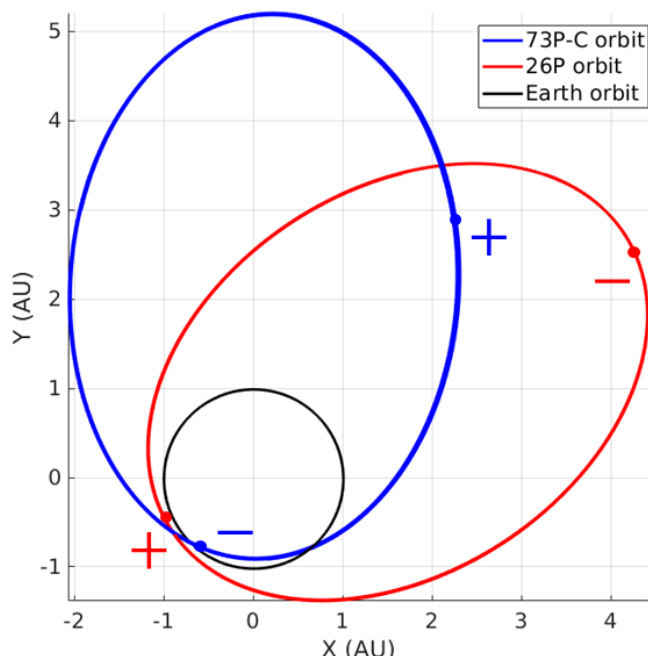

**Figure 5-25: Post encounter trajectory and evolution of Earth distance -  $R_c=0.9$  AU**

**Figure 5-26: Post encounter trajectory and evolution of Earth distance -  $R_c=1.1$  AU**

**Figure 5-27: Post encounter trajectory and evolution of Earth distance -  $R_c=1.2$  AU**

## 5.11 Transfers to the Backup Targets

Two backup targets have been identified by the proposal team: the comet 73P/Schwassmann–Wachmann and the comet 26P/Grigg–Skjellerup. These targets can be reached if, during the nominal mission lifetime, no reachable LPC is identified. Table 5-5 summarises the relevant data for the backup targets analysis.

	<b>73P</b>	<b>26P</b>
Inclination (deg)	6.2	22.4
Period (years)	5.35	5.23
Perihelion (AU)	0.92	1.08
Distance at node (AU)	1.01	1.08
Earth phase at node (deg)	-35.5	47.7

**Table 5-5: Backup targets relevant data**



**Figure 5-28: Backup targets orbits (ecliptic plane projections)**

Figure 5-28 depicts the heliocentric orbits of 73P and 26P, highlighting the ascending (+) and descending (-) nodes. Table 5-6 reports the dates of the nodes within the mission timeline.

Note that the energetically efficient nodes, i.e. the nodes closer to the Earth orbits, are the descending node for 73P and the ascending node for 26P, highlighted in Table 5-6. Furthermore, due to the 5-years mission duration constraint, only the descending node of 73P is strictly feasible, whereas the second ascending node of 26P would require a 6 year transfer if the 2028 launch constraint is enforced. The first ascending node of 26P is too early for a realistic transfer design launching in 2028.

73P	26P
2028 DEC 27 (+)	2029 MAR 17 (+)
2033 APR 05 (-)	2031 SEP 20 (-)
2034 MAY 02 (+)	2034 JUN 10 (+)

**Table 5-6: Backup targets node dates**

Since the backup targets are known, and well-defined boundary conditions are available, the transfers to such targets have been analysed in greater detail, underlining the diversity of possible transfers with different models and options.

All transfers are depicted in the Sun-Earth rotating frame, to underline the characteristics of the three-body dynamics.

### 5.11.1 Transfers to 73P

#### 5.11.1.1 Single-impulse transfers

Single-impulse transfers are the most straightforward, and preliminary results can also be obtained with a two-body model. Due to the peculiar dynamics of SEL2, nevertheless, a three-body model (Sun-Earth-SC) is needed to fully grasp the variety of options that are available, and to obtain a realistic  $\Delta v$  budget. In particular, the Earth gravity significantly affects the  $\Delta v$  obtained with a two-body model.

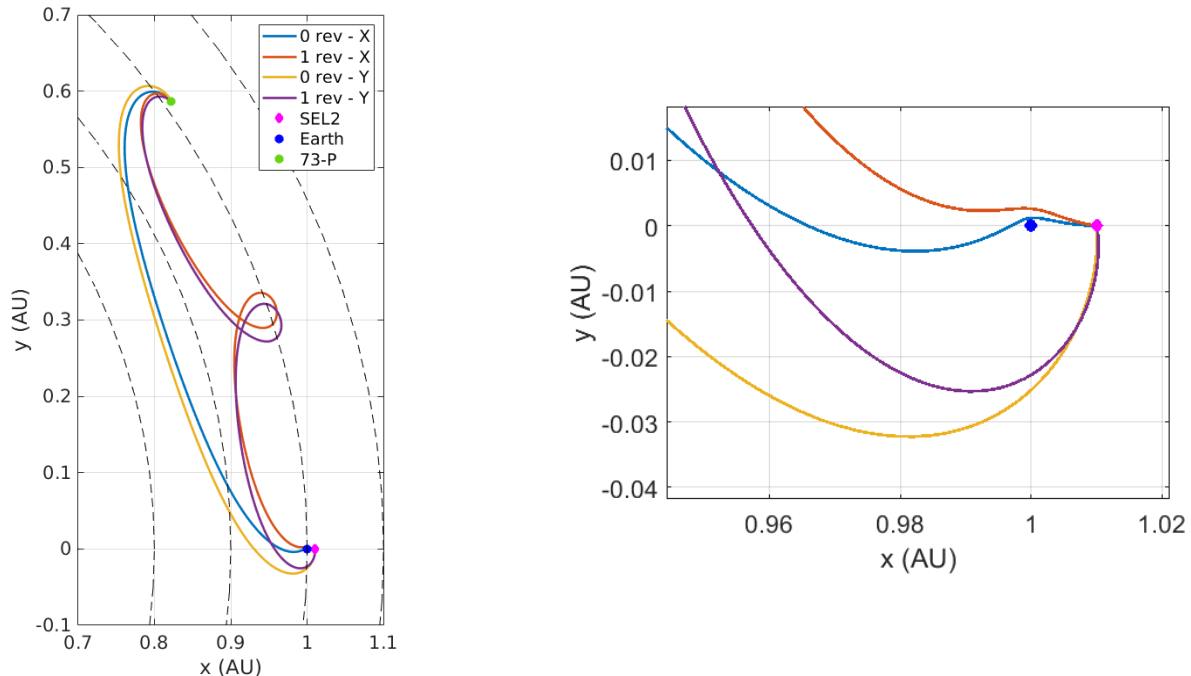


**Figure 5-29: Single-impulse transfers to 73P (Sun-Earth rotating frame)<sup>3</sup>**

<sup>3</sup> Note that 0-revolution transfers are reported for completeness despite going lower than the 0.9 AU thermal design limit. 1-revolution transfers are the baseline for compatibility with the spacecraft design and the lower  $\Delta V$ .

As depicted in Figure 5-29, two types of transfers are identified, labelled according to the prominent direction of the manoeuvre:

- *X*-type transfers are obtained with a mostly radial burn, towards the Earth. The passage in proximity of the Earth allows to exploit its gravity to reduce time of flight and  $\Delta v$ .
- *Y*-type transfers are obtained with a mostly tangential burn, and are more similar to a two-body phasing trajectory.

Both transfer types exist for different values of heliocentric revolutions. Table 5-7 and Table 5-8 report, respectively, the budgets for the different transfer types including the minimum Earth distance. The angle  $\phi$  indicates the manoeuvre direction with respect to the Sun-Earth line.

	$\Delta v$ (km/s)	$\phi$ (deg)	TOF (days)	$r_E$ min (km)	$r_s$ min (AU)
0 rev	1.79	179	303	177,000	0.86
1 rev	1.31	172	657	387,000	0.93

**Table 5-7: *X*-type single-impulse transfers to 73P**

	$\Delta v$ (km/s)	$\phi$ (deg)	TOF (days)	$r_E$ min (km)	$r_s$ min (AU)
0 rev	1.87	-87	332	>SOI	0.86
1 rev	1.35	-82	675	>SOI	0.92

**Table 5-8: *Y*-type single-impulse transfers to 73P**

Times of flight and trajectory shapes are similar for both *X*- and *Y*-type transfer. The difference lies in the Earth passage, which allows the *X*-type to save a little time and  $\Delta v$ . Operational and system constraints may drive the transfer type selection, e.g. to avoid thrusting in the Sun direction or to avoid possible eclipses. For *Y*-type transfers, the minimum Earth distance is not significant, being larger than Earth's SOI (~900,000 km).

### 5.11.1.2 Two-impulse transfers

Introducing a second impulse helps in reducing the  $\Delta v$  for some targets. The second impulse can be a Deep Space Manoeuvre (DSM) or a powered gravity assist. Other possible types of two-impulse transfers have not been considered within the CDF study. The Moon swing-by strategy, described in detail in section 5.11.1.3, is a particular sub-class of the two-impulse transfers.

It is noted that, for 73P, two impulses are not needed for *Y*-type transfers; indeed, the optimal *Y*-type solution is the single-impulse transfer.

The *X*-type transfers need the addition of a DSM to adjust the phasing and reach the target; this DSM is roughly at the perihelion of the transfer orbit. The transfer with Earth gravity assist is obtained only for the 0 revolution case, as it's not effective for the 1 revolution case due to the different geometry of the escape arc, which does not pass close to the Earth.

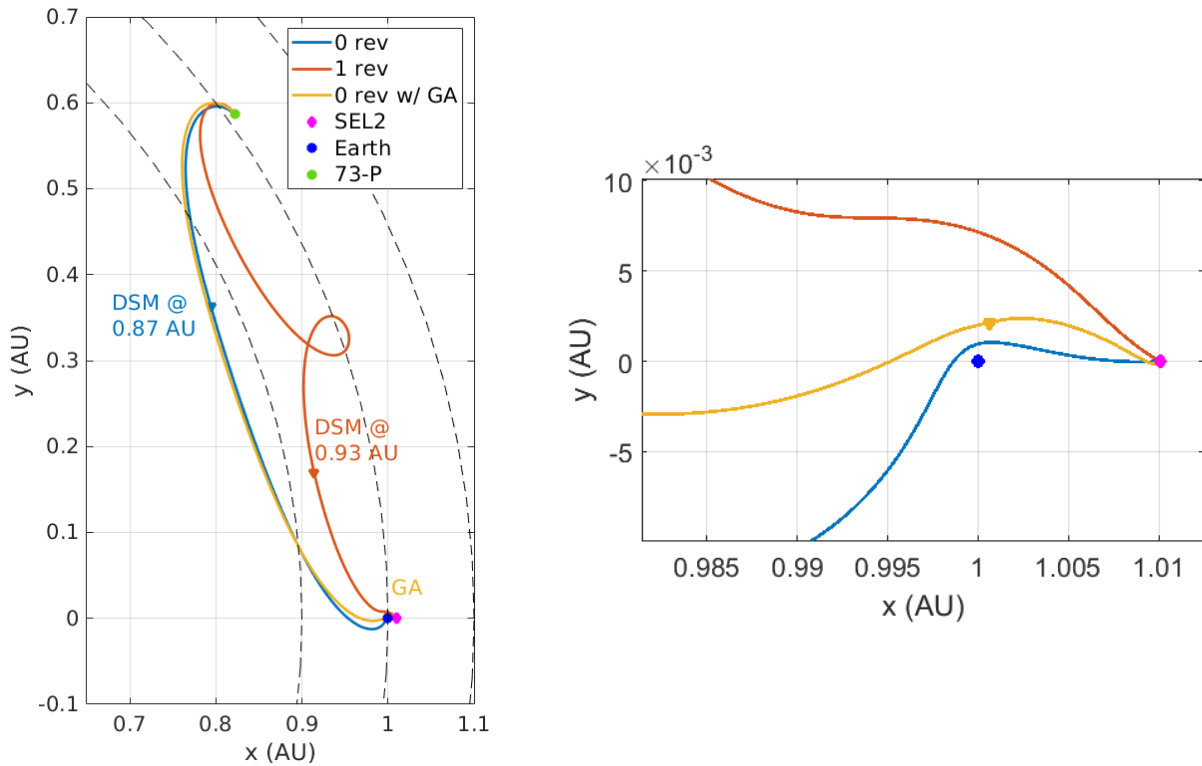


**Figure 5-30: Two-impulse transfers to 73P (Sun-Earth rotating frame)<sup>4</sup>**

	X-type		w/ EGA
	0 rev	1 rev	1 rev
<b><math>\Delta v</math> 1 (km/s)</b>	1.24	0.56	0.028
<b><math>\phi</math> 1 (deg)</b>	183	151	-130
<b>ToF 1 (days)</b>	192	232	83
<b><math>\Delta v</math> 2 (km/s)</b>	0.12	0.18	0.96
<b><math>\phi</math> 2 (deg)</b>	116	100	-184
<b>ToF 2 (days)</b>	138	532	296
<b><math>\Delta v</math> tot (km/s)</b>	1.36	0.74	0.99
<b>TOF tot (days)</b>	329	764	379
<b><math>r_E</math> min (km)</b>	129,000	950,000	324,000
<b><math>r_s</math> min (AU)</b>	0.87	0.93	0.86

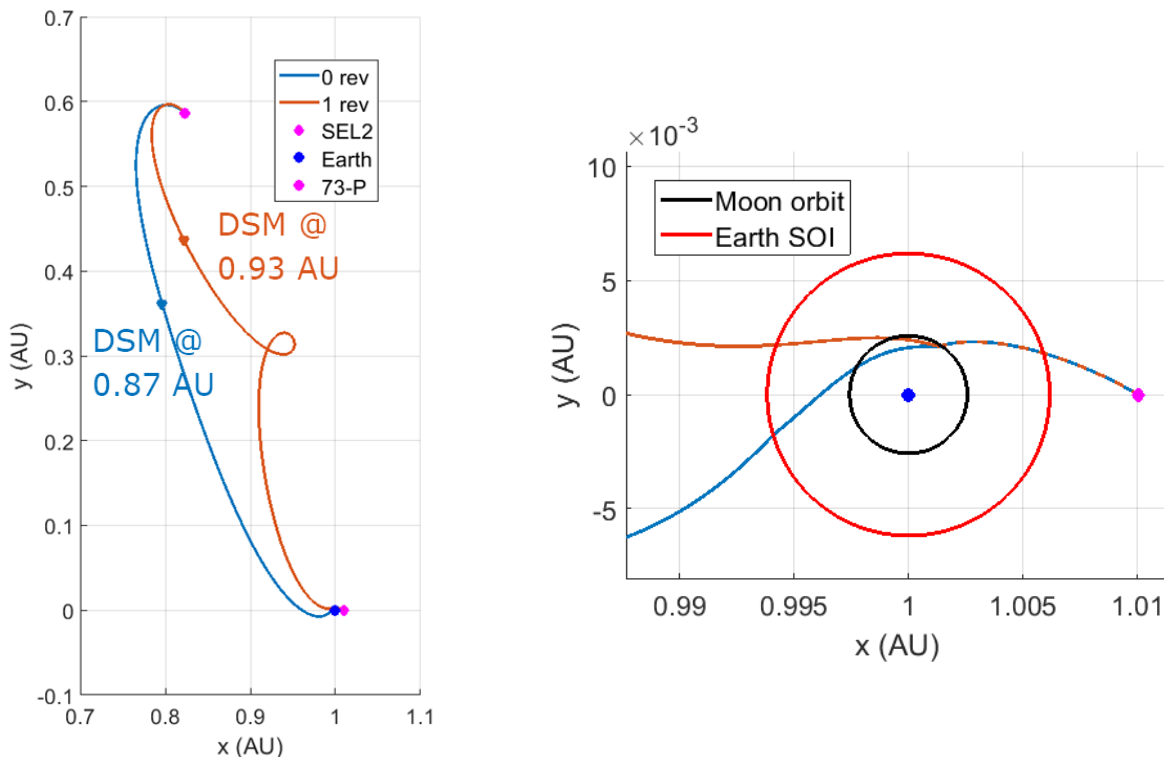
**Table 5-9: Two-impulse transfers to 73P: X-type and with powered EGA**

<sup>4</sup> Note that 0-revolution transfers are reported for completeness despite going lower than the 0.9 AU thermal design limit. 1-revolution transfers are the baseline for compatibility with the spacecraft design and the lower  $\Delta V$ .

### 5.11.1.3 Transfers with Moon swing-by

The overall Moon swing-by transfer strategy is described in section 5.6.2. It derives from the  $X$ -type transfers, and employs the Moon gravity to deviate the outgoing asymptote; a DSM then adjusts the phasing, as in the two-impulse strategy. A manoeuvre at the Earth SOI can be added to modify the  $v_\infty$  vector. The minimum altitude considered for the Moon swing-by is 5,000 km; a navigation budget of 25 m/s can be assumed to operate such kind of swing-by.

It is noted that quasi-free opportunities exist for more than 1 revolution transfers.



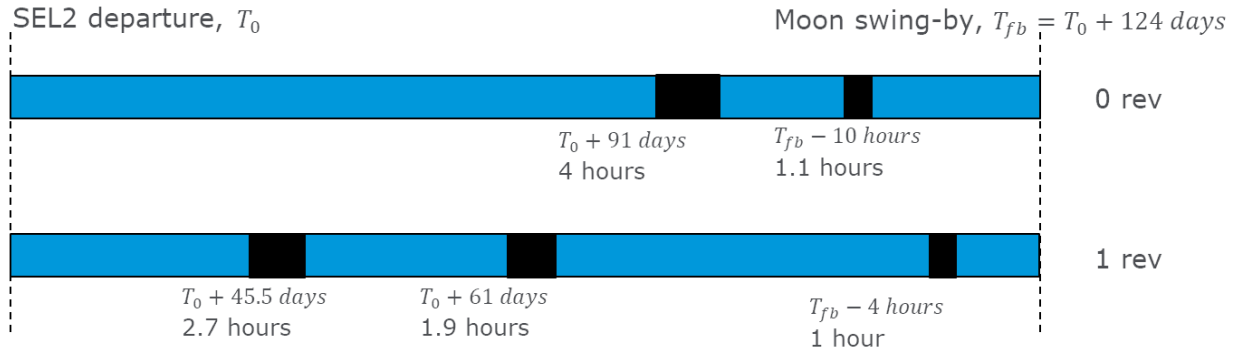
**Figure 5-31: Moon swing-by transfers to 73P<sup>5</sup>**

Figure 5-31 depicts the transfers to 73P with the Moon swing-by strategy. The transfer parameters are summarised in Table 5-10. Additionally, Figure 5-32 report a timeline (not to scale) of the eclipses prior to the swing-by.

	$h_{\text{Moon}}$ (km)	$r_E$ min (km)	SOI $\Delta v$ (m/s)	T to DSM (days)	DSM (m/s)	$\Delta v$ tot (m/s)	TOF tot (days)
0 rev	16,000	303,000	294	306	133	427	445
1 rev	5,500	350,000	0	610	53	53	779

**Table 5-10: Moon swing-by transfers to 73P**

<sup>5</sup> Note that 0-revolution transfers are reported for completeness despite going lower than the 0.9 AU thermal design limit. 1-revolution transfer is the baseline for compatibility with the spacecraft design and the lower  $\Delta V$ .



**Figure 5-32: Eclipses for Moon swing-by transfer to 73P**

#### 5.11.1.4 Summary of impulsive transfers

A summary of the options and relative parameters for 73P transfers is presented in Table 5-11 and Table 5-12, for the 0 and 1 revolutions cases respectively. Figure 5-33 shows a synoptic summary of the transfer options.

	<b>1 imp - Y</b>	<b>1 imp - X</b>	<b>2 imp - X</b>	<b>2 imp - EGA</b>	<b>2 imp - LGA</b>
$\Delta v$ (km/s)	1.87	1.79	1.36	0.99	0.43
TOF (days)	332	303	329	379	445
$r_E$ min (km)	>SOI	177,000	129,000	324,000	303,000
Departure	2032-May-08	2032-Jun-06	2032-May-11	2032-Mar-22	2032-Jan-16

**Table 5-11: Transfers to 73P, 0 revolutions**

	<b>1 imp - Y</b>	<b>1 imp - X</b>	<b>2 imp - X</b>	<b>2 imp - EGA</b>	<b>2 imp - LGA</b>
$\Delta v$ (km/s)	1.35	1.31	0.74	-	0.053
TOF (days)	675	657	764	-	779
$r_E$ min (km)	>SOI	387,000	950,000	-	350,000
Departure	2031-May-31	2031-Jun-18	2031-Mar-03	-	2031-Feb-16

**Table 5-12: Transfers to 73P, 1 revolution**

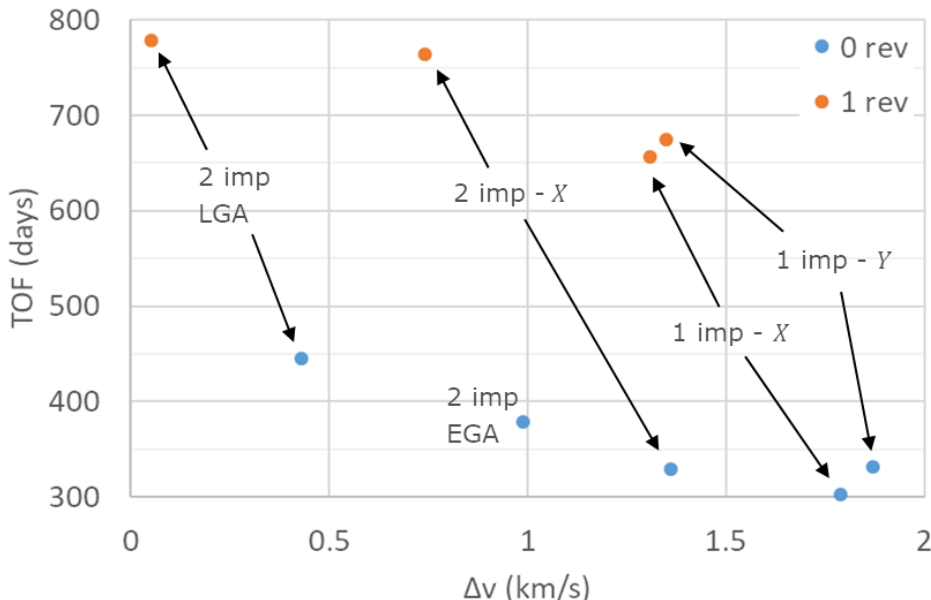


**Figure 5-33: Summary of transfers to 73P**

### 5.11.1.5 Low-thrust transfers

Detailed low-thrust trajectories have been analysed for the backup target 73P, being the most significant trajectory, where the non-linear three-body effects are more prominent. In principle, a low-thrust trajectory can be estimated by taking the impulsive burn  $\Delta v$ , and computing the needed burn time, checking its compatibility with the transfer time.

Gravity losses can occur when the burn is performed away from its optimal location, due to the finite amount of time necessary; nevertheless, in the complex three-body dynamics this phenomenon might yield a reduction of the  $\Delta v$ , as the manoeuvre is actually being performed more and more in a favourable location. This is observed in particular for the SEL2 burns of the X-type transfers: as the burn is carried out, the spacecraft is moving towards the Earth, and the burn becomes more and more efficient in changing the energy, exploiting the Earth gravitational field.

For this reason, single-impulse low-thrust transfers may limit the optimiser to find minimum  $\Delta v$  trajectories. Within the CDF, only two-arc transfers were considered for low-thrust trajectories; it is advised, for future studies, to relax the constraint on the number of powered arcs, to maximise the favourable exploitation of the three-body dynamics.

Figure 5-34 depicts the two-arc low-thrust transfers to 73P. The detail in Earth proximity shows the reason of the counter-intuitive behaviour of  $\Delta v$  vs.  $T/m$  ratio: starting from SEL2, the spacecraft thrusts while getting closer to the Earth and increasing its velocity, thus the energy change is performed more efficiently. Table 5-13 and Table 5-14 report the details of the different burn and coasting arcs. Note that the problem was formulated in a simplified form for the purpose of the CDF; a full optimisation of the low-thrust trajectory shall be performed if a refined analysis is needed.

<b><u>0.05</u></b> <b>mN/kg</b>	<b>Arc 1</b>			<b>Arc 2</b>			<b><math>\Delta v</math></b> <b>(m/s)</b>	<b>TOF</b> <b>(days)</b>
	$\Delta v$ (m/s)	$T_{burn}$ (d)	$T_{coast}$ (d)	$\Delta v$ (m/s)	$T_{burn}$ (d)	$T_{coast}$ (d)		
<b>0 rev</b>	821	187	106	215	48	111	1036	453
<b>1 rev</b>	373	86	173	187	43	496	560	797

**Table 5-13: X-type, two-arc low-thrust transfer to 73P,  $T/m = 0.05$  mN/kg**

<b><u>0.10</u></b> <b>mN/kg</b>	<b>Arc 1</b>			<b>Arc 2</b>			<b><math>\Delta v</math></b> <b>(m/s)</b>	<b>TOF</b> <b>(days)</b>
	$\Delta v$ (m/s)	$T_{burn}$ (d)	$T_{coast}$ (d)	$\Delta v$ (m/s)	$T_{burn}$ (d)	$T_{coast}$ (d)		
<b>0 rev</b>	819	93	144	166	19	128	985	384
<b>1 rev</b>	495	57	170	181	20	528	676	775

**Table 5-14: X-type, two-arc low-thrust transfer to 73P,  $T/m = 0.10$  mN/kg**

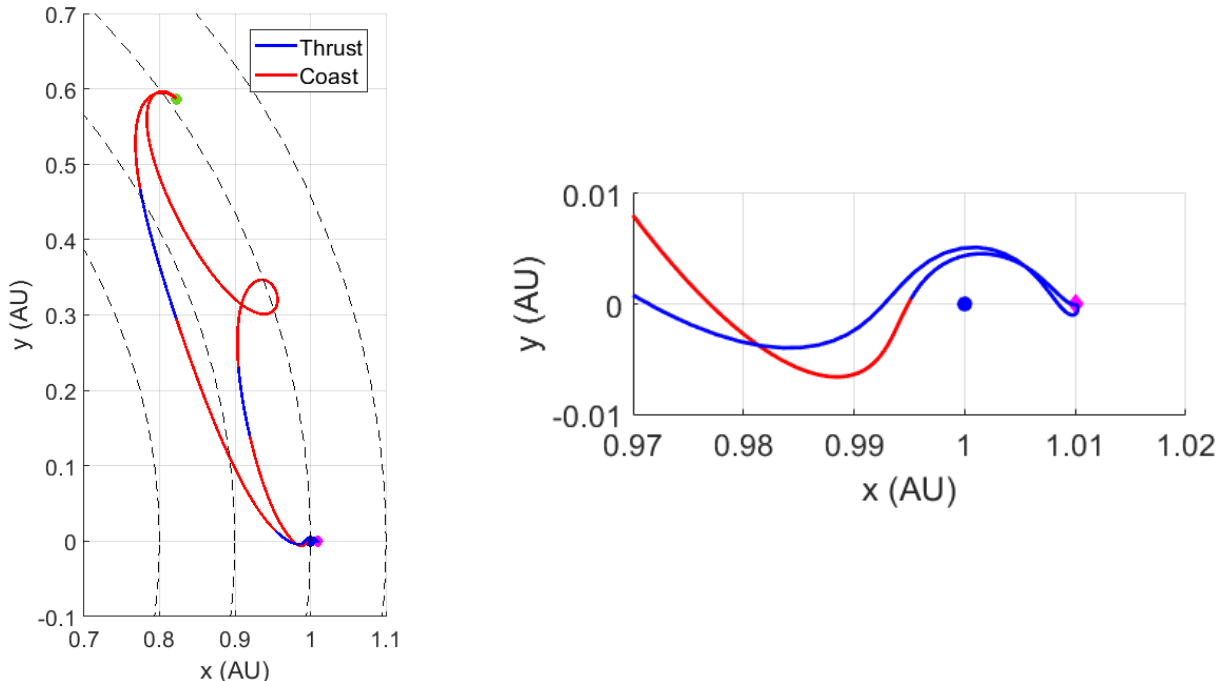


**Figure 5-34: Two-arc low-thrust trajectories to 73P (Sun-Earth rotating frame)<sup>6</sup>**

Figure 5-35 depicts the thrust angle, for different values of  $T/m$  ratio. This angle is computed between the thrust direction and the Sun direction, such that a  $90^\circ$  angle means that the thrust is circumferential.

The thrust direction during the first burn follows an irregular pattern: first, the thrust is nearly radial, in order to inject into the Earth-bound manifold, and then it follows the local velocity vector, exploiting the passage close to the Earth. Not that, as the  $T/m$  ratio

<sup>6</sup> Note that 0-revolution transfers are reported for completeness despite going lower than the 0.9 AU thermal design limit. 1-revolution transfer is the baseline.

decreases, the initial thrust profile manifests a steep variation, since the thrust need to be radial in average, but distributed along a longer arc.

During the second burn, the thrust is always tangent to the local velocity vector, in average.

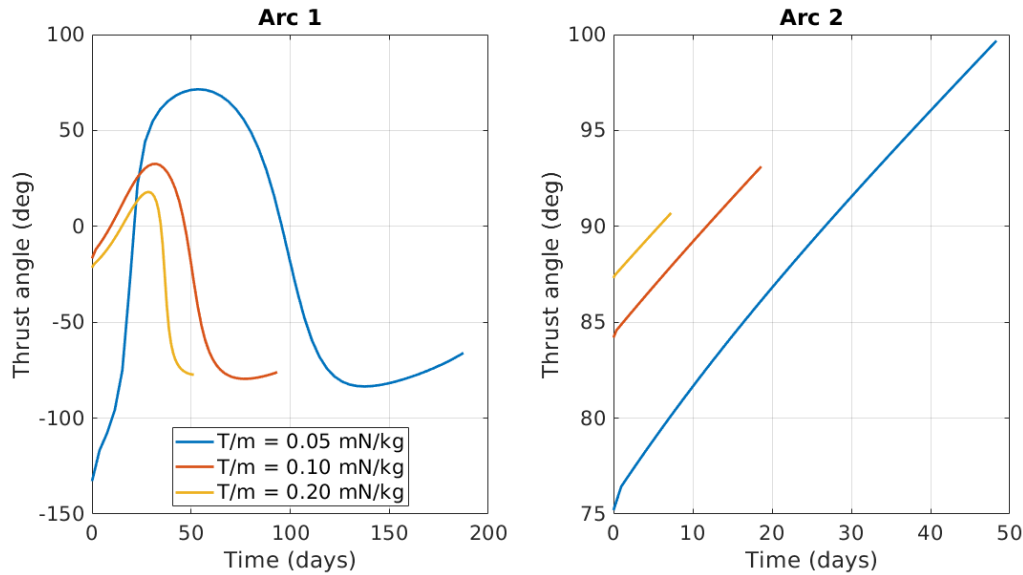


**Figure 5-35: Thrust angles wrt radial direction**

#### 5.11.1.6 Geometry at encounter

The encounter geometry for 73P is depicted in Figure 5-36. The spacecraft velocity at encounter is nearly contained in the normal-to-Sun plane, as the heliocentric orbit is nearly circular. Table 5-15 reports the encounter angles and relative velocity for the two transfer cases.

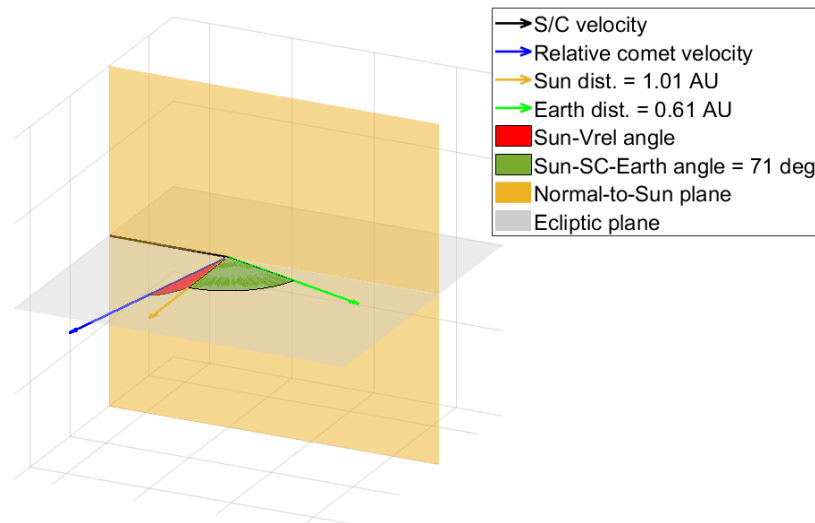


**Figure 5-36: 73P encounter geometry**

	$V_{rel}$ (km/s)	Sun – $V_{rel}$ angle (deg)	Sun – $V$ angle (deg)
0 rev	14.2	43	91
1 rev	13.6	42	90

**Table 5-15: 73P encounter features**

### 5.11.2 Transfers to 26P

The comet 26P crosses the ecliptic in a favourable position, where cheap transfers naturally exist thanks to the SEL2 dynamics. Only the single-impulse transfers were analysed for this target, as the  $\Delta v$  budget is significantly lower than 73P's and refined transfer strategies are not necessary.

#### 5.11.2.1 Single-impulse transfers

Y-type transfers for 26P require a lower  $\Delta v$ , because the intercept point is further away than SEL2. The inertial motion of SEL2 thus plays in favour of the transfer, and the tangential impulse needed to escape is reduced. This is also noted computing the two-body Hohmann transfer from SEL2 and from Earth.

The SEL2 manifold yields a quasi-free 1 revolution X-type transfer to 26P. This is due to the particularly favourable location of the 26P encounter, and should be considered a special case. Being the SEL2 manifold shape fixed, such kind of transfers can exist only for a limited set of targets that match the particular location condition.

Figure 5-37 depicts the single-impulse transfers to 26P. Table 5-16 and Table 5-17 report the transfer parameters. Note that minimum Earth distance is larger than SEL2 distance ( $\sim 0.01$  AU), and thus than Earth's SOI.

	$\Delta v$ (km/s)	$\phi$ (deg)	TOF (days)	$r_E$ min (km)
1 rev	0.015	-39	744	>SEL2

**Table 5-16: X-type single-impulse transfer to 26P**

	$\Delta v$ (km/s)	$\phi$ (deg)	TOF (days)	$r_E$ min (km)
0 rev	0.73	78	329	>SEL2
1 rev	0.14	61	665	>SEL2

**Table 5-17: Y-type single-impulse transfers to 26P**

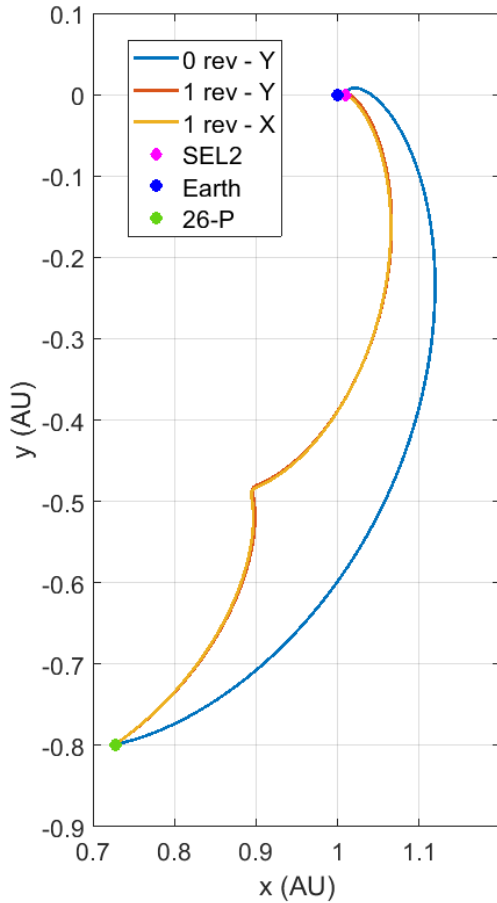


**Figure 5-37: Single-impulse transfers to 26P (Sun-Earth rotating frame)**

#### 5.11.2.2 Summary of impulsive transfers

Although less options have been considered for 26P, Table 5-18 and Table 5-19 report a summary of the analysed transfers, in analogy with 73P transfer summary. An asterisk, \*, indicates transfers that were not investigated.

	<b>1 imp - Y</b>	<b>1 imp - X</b>	<b>2 imp - X</b>	<b>2 imp - EGA</b>	<b>2 imp - LGA</b>
$\Delta v$ (km/s)	0.73	-	*	*	*
TOF (days)	329	-	*	*	*
$r_E$ min (km)	>SEL2	-	*	*	*
Departure	2033-Jul-16	-	*	*	*

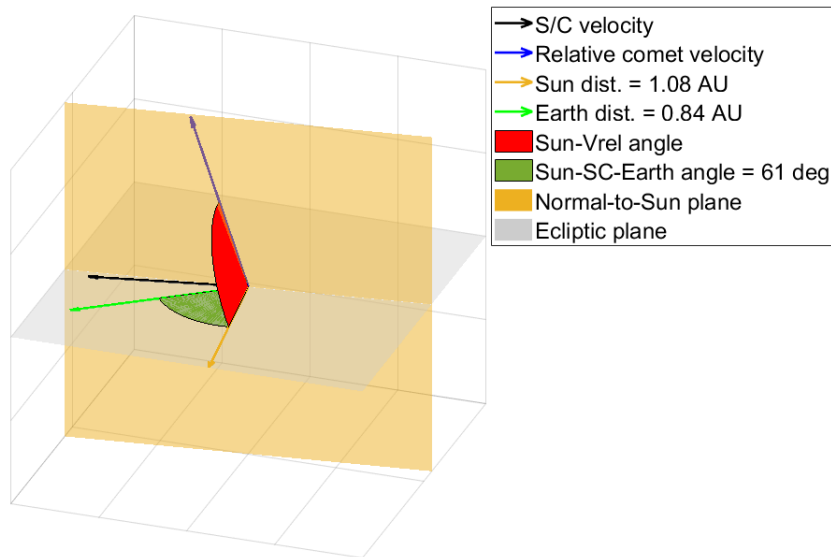
**Table 5-18: Transfers to 26P, 0 revolutions**

	<b>1 imp - Y</b>	<b>1 imp - X</b>	<b>2 imp - X</b>	<b>2 imp - EGA</b>	<b>2 imp - LGA</b>
$\Delta v$ (km/s)	0.14	0.015	*	*	*
TOF (days)	665	774	*	*	*
$r_E$ min (km)	>SEL2	>SEL2	*	*	*
Departure	2032-Aug-14	2032-Apr-27	*	*	*

**Table 5-19: Transfers to 26P, 1 revolution**

### 5.11.2.3 Geometry at encounter

Figure 5-38 depicts the encounter geometry for 26P. The encounter features are reported in Table 5-20.


**Figure 5-38: 26P encounter geometry**

	$V_{rel}$ (km/s)	Sun – $V_{rel}$ angle (deg)	Sun – $V$ angle (deg)
0 rev	14.9	96	86
1 rev	15.0	90	89

**Table 5-20: 26P encounter features**

### 5.11.3 Additional Backup Targets

To ensure availability of backup targets for the mission an extended search for backup targets was conducted. The science team provided a list with 67 interesting targets. Updated ephemeris for these targets were retrieved for January 1<sup>st</sup> 2028 and 2033 from JPL's HORIZONS system. These comets were fed into the mission simulator described in Section 5.8.3 and targets with valid encounter parameters identified. For these

targets optimal impulsive transfers with 0 and 1 revolution and  $\Delta V < 1.5$  km/s were calculated. This process reduced the initial list of 67 comets to 11 comets with feasible encounters between September 2031 and September 2037. Figure 5-39 provides a Gantt chart of the backup targets showing the start of the transfer and the encounter. In average every 9-12 months a backup target, which can be reached in 1-2 years is available. This list was again provided to the science team for further assessment. Note that the list is not necessarily complete. For this analysis only targets that are reachable with a direct transfer and with short transfer times were considered. More targets might become available if longer transfers are allowed. However, for the backup target short transfers are favoured, as they maximise the waiting time in SEL2.

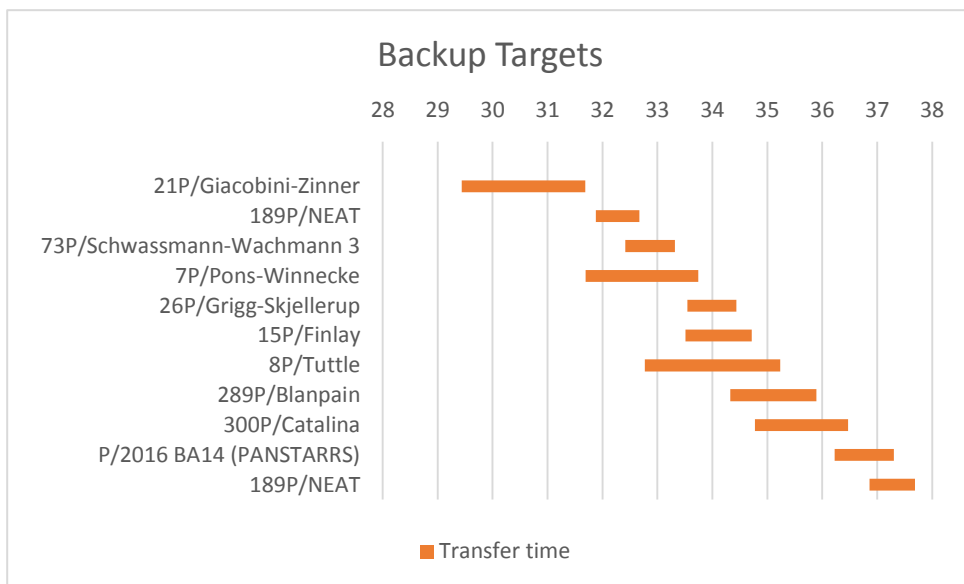


**Figure 5-39: Gantt chart of backup targets**

Table 5-21 summarises the encounter features of the additional backup targets. The values were obtained with the simplified model of the spacecraft moving on a circular orbit (see section 5.8). The values provided in the above sections for 73P and 26P (see sections 5.11.1 and 5.11.2) were obtained with the actual state of the spacecraft at encounter and are generally more accurate than the values in Table 5-21. The simplified model for 73P provides a solar phase angle at encounter of 41 degrees, whereas the refined model provides values of 42 and 43 degrees (see Table 5-15). For the encounter features of 26P this effect is even more apparent. The more the Sun spacecraft velocity angle deviates from 90 degrees the stronger the deviation of the solar phase angle between the simplified model and the refined one. According to the simplified model 73P and 300P violate the  $90 \pm 45$  degrees constraint of the solar phase angle. However, considering the more refined model of 73P this value gets closer to the limit of 45 degrees.

Comet	Encounter Date	Departure date	$\Delta V$ (km/s)	$\theta$ (deg)	Rc (AU)	Re (AU)	Solar Phase Angle * (deg)	$V_{\text{encounter}}^* \text{ km/s}$
21P/Giacobini-Zinner	07/09/31	09/06/29	1.220	-29.2	1.07	0.53	97	16
189P/NEAT	01/09/32	16/11/31	1.220	58.4	1.21	1.10	74	20
<b>73P/Schwassmann-Wachmann 3</b>	05/04/33	11/05/32	1.360	-35.3	1.00	0.61	41	13
7P/Pons-Winnecke	28/09/33	09/09/31	1.465	93.3	1.13	1.55	95	13
<b>26P/Grigg-Skjellerup</b>	10/06/34	16/07/33	0.730	48.1	1.08	0.86	88	15
15P/Finlay	18/09/34	04/07/33	0.570	-18.0	1.01	0.32	109	15
8P/Tuttle	26/03/35	07/10/32	0.910	96.5	1.08	1.55	75	11
289P/Blanpain	23/11/35	28/04/34	0.979	-7.3	0.97	0.13	74	33
300P/Catalina	19/06/36	10/10/34	0.878	-6.4	0.93	0.14	33	10
P/2016 BA14 (PANSTARRS)	20/04/37	23/03/36	0.244	30.7	1.02	0.54	99	14
189P/NEAT	08/09/37	10/11/36	1.309	64.8	1.21	1.20	74	14

**Table 5-21: Encounter features of additional backup targets. \*values are obtained from a simplified model with the spacecraft on a circular orbit**

## 5.12 Options

### 5.12.1 Use of SEP for Trajectory Corrections Towards SEL2

The feasibility of a full SEP spacecraft that performs the necessary trajectory corrections on the way to SEL2 was analysed during the study. The reference for this analysis is the ARIEL mission design (RD[1]).

For ARIEL, 3 trajectory corrections, TCM-#1, -#2 & -#3 will be performed with the on-board CP system on days 1-2, 5 and 20, respectively. The objective of these manoeuvres is to correct the initial errors in perigee velocity coming from the stochastic launcher dispersion ( $\sim 4$  m/s) and the deterministic fixed launch program ( $\sim 1.5$  m/s). In addition, following manoeuvres must correct the residual error left after the previous manoeuvre. For Ariel TCM#1 is allocated  $\sim 45$  m/s, while TCM-#2 & -#3 are allocated about 1-2 m/s each.

The  $\Delta v$  required for the correction of the perigee velocity errors grows with time at a rate  $\sim \sqrt{t}$ , as show in Figure 5-40. Thus the correction manoeuvres have to be implemented as fast as possible or otherwise they will suffer a large penalty in  $\Delta v$  size, e.g. in 2 days the amplification factor is about 9 fold. Hence the criticality of TCM#1 and the need to implement it within the 1<sup>st</sup> day after separation (although for the allocation 2 days are assumed).

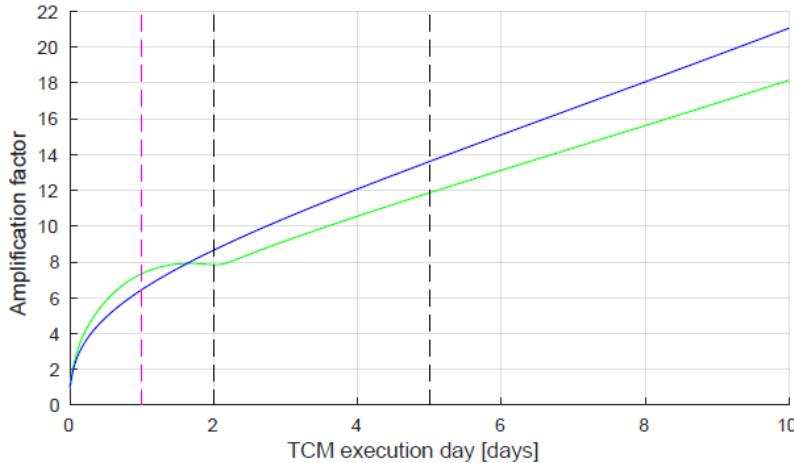


**Figure 5-40: Amplification factor of  $\Delta v$  of TCM as function of time (From RD[1])**

When considering a SEP system to implement these corrections, several concerns arise. First is the time required to commission and get operationally ready the SEP system. For complex missions like Bepi-Colombo this phase took several weeks, though the mission did not have a requirement of very early thrust in the trajectory. Commissioning of simpler SEP systems should be shorter, probably in the order of days, but it is still deemed unrealistic that the first operation of the SEP can be as fast as for CP.

Second is the duration of the SEP burns that can easily take many days, especially for the first correction, when the transfer to SEL2 has to be finalised in about 30 days.

Third is the negative impact that missed thrust (unplanned outages due to safe modes) will have in the capability of the SEP to correct the initial velocity errors.

Mission analysis looked at 2 sample cases to illustrate the problem:

- a) TCM#1 starting 2 days after separation with 0.05 mN/kg (i.e. initial thrust 40 mN for 800 kg spacecraft)

A 45 m/s correction (same as ARIEL needs at day 2 for an 8.3 amplification factor) would require 10 days continuous thrusting. During the thrusting time the amplification factor keeps acting and grows up to a value of 24, with an average over the thrusting period of ~16. Thus the SEP would need to keep operating for at least an extra 10 days. This scenario renders infeasible as the thrust to mass ratio is not high enough to correct the initial errors in a reasonable time.

- b) TCM#1 starting 2 days after separation with 0.2 mN/kg (i.e. initial thrust 160 mN for 800 kg spacecraft)

The same initial 45 m/s burn for TCM#1 requires 2.6 days. In the burn period the amplification factor goes from 8.3 at 2 days to 13 at 4.6 days, so about 11 in average, which means that the actual correction requires 60 m/s. This  $\Delta v$  size can be achieved in 3.5 days, a period during which the average amplification factor is 11.2. Thus it is possible to see that this case should converge to a thrust arc of less than 4 days and a total correction  $\Delta v$  of 65 m/s.

Therefore the conclusion is that feasibility of trajectory corrections during the transfer to SEL2 is very challenging, and requires an early operation of the SEP engine(s), that puts pressure on this sub-system and on the operational procedures for its commissioning, and a large thrust-to-mass ratio that would also require oversizing the SEP system. The recommendation is to perform the post-separation TCMs on the way to SEL2 with CP.

### 5.12.2 Probabilistic Reachability Analysis with Chemical Propulsion

An additional analysis considering chemical propulsion for the transfer to the target was conducted. The same baseline configuration as for the electric propulsion was used, except for the reference  $\Delta V$ . Two scenarios with  $\Delta V = 425$  m/s and  $\Delta V = 700$  m/s were taken for reference. Note that the values at  $\Delta V_{\max} = 1$  km/s are different from Figure 5-17. This is due to the different margins for chemical and electric propulsion (see Table 5-2).

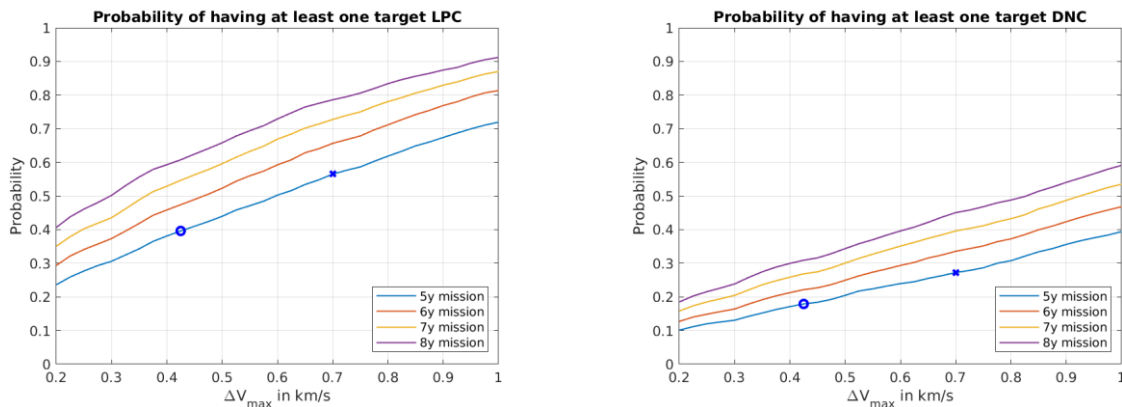


Figure 5-41: Influence of mission duration &  $\Delta V$  on mission success (CP)

This Page Intentionally Blank

## 6 ENVIRONMENT

### 6.1 Requirements and Design Drivers

The main drivers of the Comet Interceptor mission space environment have been identified as radiation, micrometeoroids and cometary dust.

Radiation is a combination of solar particle events and galactic cosmic rays impinging on the spacecraft and leading to long-term/cumulative degradation of e.g. materials and components and also to single event effects that can occur anytime during the mission. Since the spacecraft will quickly leave the Earth's radiation belts during the transfer to L2 and spend the whole mission close to 1 AU, the radiation environment is considered to be similar to any mission outside the magnetosphere and around 1 AU (e.g. lunar missions, or L1, L2, L4 and L5).

Microparticles and cometary dust are impinging frequently on the spacecraft. This leads to a risk for failures/damages on the spacecraft and also to attitude disturbances. Compared to Earth orbiting missions, especially LEO, the microparticle environment is considered to be less severe due to the absence of man-made debris. However, in addition to the standard micro-meteoroid environment described and predicted by models in RD[5], this mission will encounter the local dust and gas environment generated by the visited comet. Therefore, impacts on the spacecraft will occur and potentially lead to damage.

Additional environmental aspects, as for example surface and internal charging, have not been addressed yet but might cause failure.

The radiation environment for the nominal and extended mission duration has been assessed within the SPENVIS framework. The work performed within this CDF study focusses on the radiation and cometary environment. The presented work is based on RD[5] for the radiation part.

#### 6.1.1 Design Drivers: Radiation Effects and Main Sources of Radiation Environment

In general, the energetic particle environment consists of geo-magnetically trapped charged particles, solar protons and galactic cosmic rays. It is the penetrating particles that pose the main problems, which include upsets to electronics, payload interference, degradation and damage to components, materials and solar cells. The main components of the radiation environment are:

##### 6.1.1.1 The Radiation Belts

These encircle the Earth and contain electrons and protons that are trapped in the geo-magnetic field. An inner relatively stable belt contains mostly protons with energies up to several hundred MeVs. An outer highly dynamic belt consists primarily of energetic electrons with energies up to a few MeVs. The MEO orbit is particularly severe with respect to radiation since it is located at the heart of the outer electron belt. In this case, since the mission will quickly leave the Earth magnetosphere and never cross it again, even in the Lunar fly-by transfer, the total effect of the trapped protons and electrons will be minimal with regards to the other sources.

### 6.1.1.2 Solar Particle Events

Events of strongly enhanced fluxes of primarily protons originate from the Sun, usually with a duration in the order of a couple of days. These events occur randomly and mainly during periods of solar maximum (~7 years of the 11 year solar cycle). The events are also accompanied by enhanced fluxes of heavy ions. The geo-magnetic field can provide an element of shielding from these particles in equatorial zones at lower altitudes.

### 6.1.1.3 Galactic Cosmic Rays

A continuous flux of very high energy particle radiation is received from outside the heliosphere. Although the flux is very low, they include heavy ions capable of causing intense ionisation as they pass through matter. Although their contribution to the total dose is insignificant, they are important when analysing single event effects. The geo-magnetic field can provide an element of shielding of these particles in equatorial zones at lower altitudes.

## 6.1.2 Design Drivers: Dust Micro-Meteoroid Sources

**Cometary dust environment:** the release rate of dust from the cometary surface is primarily caused by ice sublimation, driven by the distance from the Sun, with peak rates in excess of 10000kg/s for long period comets. In comparison, interstellar objects such as ‘Oumuamua have negligible activity. Due to the cometary activity and the high mission fly-by velocity, the local cometary dust environment becomes a major risk and thus design driver. It is anticipated that dedicated dust shielding will be necessary.

## 6.2 Assumptions and Trade-Offs

Since the CDF study focussed on the interception orbit of the comet, the transfer to the L<sub>2</sub> waiting point has been simplified to a parabolic escape from the Earth orbit, reflecting the small amount of time that the spacecraft will spend in the radiation belts. The rest of the mission lifetime is simplified to 3 years in interplanetary space at 1 AU (average between 0.9 and 1 AU) and 2 years at 0.9 AU, as this is considered conservative for solar particle radiation.

Assumptions	
1	Spacecraft located in interplanetary space at 1 AU over 3 years and 0.9 AU over 2 years
2	Mission lifetime is 5 years.
3	Spacecraft Geometry: available from CAD model

## 6.3 Baseline Design

### 6.3.1 Radiation

Due to the absence of geomagnetically trapped particles, the cumulative radiation effects are dominated by solar protons and Galactic Cosmic Rays. These environments are modelled here by the ESP-PSYCHIC model (ion range Hydrogen to Uranium with 90% confidence level) and the ISO 15390 model (ion range Hydrogen to Uranium from the 1996 solar minimum data), respectively.

### 6.3.1.1 Total Ionising Dose (TID)

The obtained TID dose-depth curve produced by the SHIELDOSE-2 model, for a Silicon target at the centre of an aluminium sphere is provided in Figure 6-1, and Table 6-1 for the nominal 5 yr lifetime, shown for segment 1 (3 years at 1 AU) and segment 2 (2 years at 0.9 AU).

EEE parts with about 10 krad(Si) TID sensitivity would require a shielding of about 9 mm of aluminium equivalent. This already includes the required margin factor of 2 between the expected dose level and the target sensitivity.

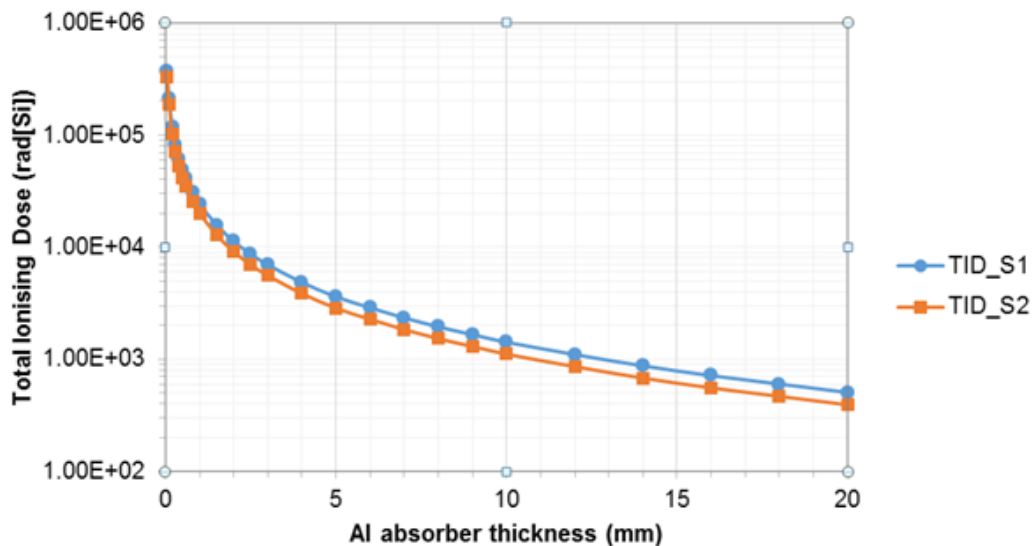


**Figure 6-1: Total Ionising Dose - depth curve for Segment 1 (S1) and Segment 2 (S2)**

Al absorber thickness		Total Ionising dose (for S1)	Total Ionising dose (for S2)
(mm)	(g.cm <sup>-2</sup> )	(rad[Si])	(rad[Si])
0.05	0.014	3.71E+05	3.29E+05
0.1	0.027	2.12E+05	1.87E+05
0.2	0.054	1.18E+05	1.02E+05
0.3	0.081	8.21E+04	7.02E+04
0.4	0.108	6.20E+04	5.25E+04
0.5	0.135	4.97E+04	4.18E+04
0.6	0.162	4.18E+04	3.49E+04
0.8	0.216	3.10E+04	2.57E+04
1	0.27	2.43E+04	2.01E+04
1.5	0.405	1.57E+04	1.28E+04
2	0.54	1.13E+04	9.10E+03

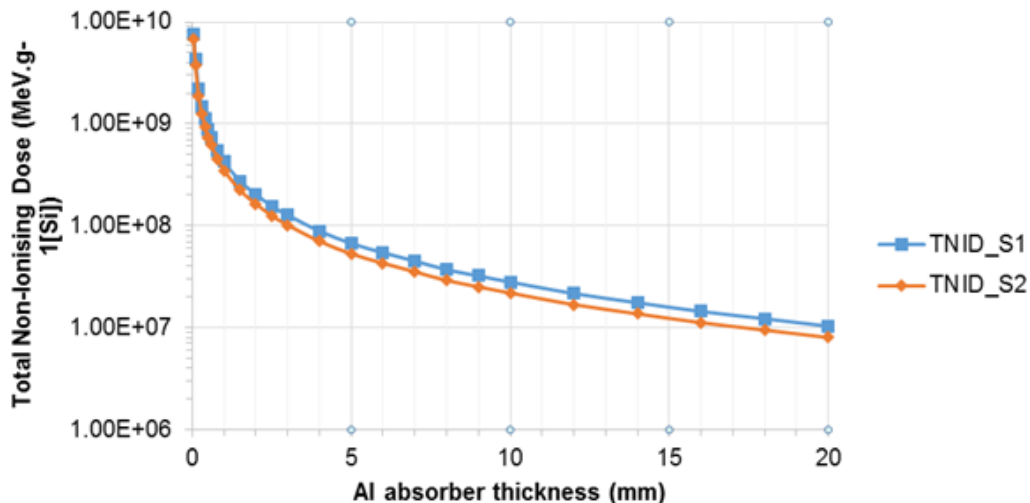
Al absorber thickness		Total Ionising dose (for S1)	Total Ionising dose (for S2)
(mm)	(g.cm <sup>-2</sup> )	(rad[Si])	(rad[Si])
2.5	0.675	8.68E+03	6.98E+03
3	0.81	6.97E+03	5.58E+03
4	1.08	4.86E+03	3.86E+03
5	1.35	3.61E+03	2.86E+03
6	1.62	2.88E+03	2.27E+03
7	1.89	2.34E+03	1.84E+03
8	2.16	1.94E+03	1.53E+03
9	2.43	1.66E+03	1.30E+03
10	2.7	1.42E+03	1.11E+03
12	3.24	1.10E+03	8.60E+02
14	3.78	8.73E+02	6.80E+02
16	4.32	7.15E+02	5.55E+02
18	4.86	6.01E+02	4.67E+02
20	5.4	5.065E+02	3.93E+02

**Table 6-1: Total Ionising Dose - depth data**

### 6.3.1.2 Total Non-ionising Dose (TNID)

The obtained TNID dose-depth curve is produced by the JPL Si model and provided for the nominal 5 yr lifetime in Figure 6-2 and Table 6-2, split in segment 1 and segment 2.

Sensitive parts with about 1E8 MeV/g(Si) of TNID sensitivity require a shielding of about 10 mm of aluminium equivalent. This already includes the required margin factor of 2 between the expected dose level and the target sensitivity.


**Figure 6-2: Total Non-Ionising Dose - depth curve**

Al absorber thickness (mm)	Total Non-Ionising dose (for S1) (MeV/g[Si])	Total Non-Ionising dose (for S2) (MeV/g[Si])
0.05	7.55E+09	6.69E+09
0.1	4.24E+09	3.75E+09
0.2	2.18E+09	1.89E+09
0.3	1.46E+09	1.25E+09
0.4	1.11E+09	9.45E+08
0.5	8.79E+08	7.41E+08
0.6	7.39E+08	6.18E+08
0.8	5.45E+08	4.52E+08
1	4.25E+08	3.50E+08
1.5	2.75E+08	2.23E+08
2	2.04E+08	1.65E+08
2.5	1.56E+08	1.26E+08
3	1.27E+08	1.02E+08
4	8.88E+07	7.05E+07
5	6.73E+07	5.32E+07
6	5.46E+07	4.30E+07
7	4.51E+07	3.54E+07
8	3.72E+07	2.91E+07
9	3.23E+07	2.52E+07
10	2.81E+07	2.20E+07
12	2.17E+07	1.69E+07
14	1.76E+07	1.37E+07
16	1.45E+07	1.12E+07
18	1.23E+07	9.51E+06
20	1.04E+07	8.04E+06

**Table 6-2: Total Non-Ionising Dose - depth data**

### 6.3.1.3 Solar cell degradation

The impingement of charged particles on the solar cells leads to their performance degradation over the mission lifetime. This depends on the mission environment and lifetime, the cell type, the cover glass thickness and the back-shielding by the panel. Due to the absence of trapped particles solar cell degradation is not expected to be a limiting factor for the mission.

Since AZUR AG30 is the most recent solar cell model implemented in the EQ-FLUX and MC-SCREAM models (respectively used to model the 1MeV equivalent electron flux and the solar cell power degradation), only results for this solar cell type are provided here.

The equivalent 1 MeV electron fluence is provided in Figure 6-3 and Table 6-4. The data of the degradation is shown in Table 6-4.

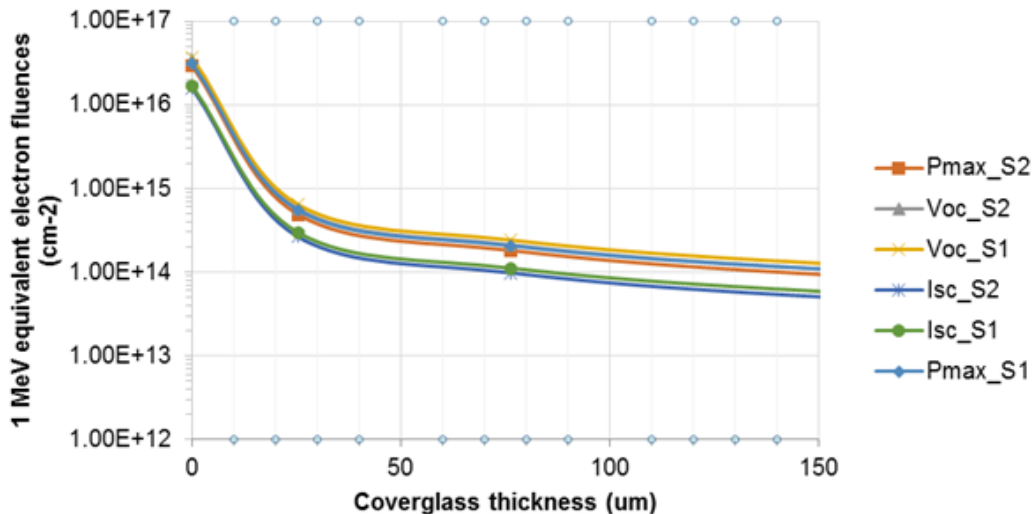


**Figure 6-3: AZUR 3G30 equivalent 1 MeV electron fluence as function of cover glass thickness**

Coverglass thickness	Solar protons (for S1)			Solar protons (for S2)		
	micron	Pmax [W]	Voc [V]	Isc [A]	Pmax [W]	Voc [V]
<b>0</b>	3.12E+16	2.93E+16	3.42E+16	1.58E+16	3.65E+16	1.69E+16
<b>25.4</b>	5.48E+14	4.87E+14	5.69E+14	2.63E+14	6.40E+14	2.96E+14
<b>76.2</b>	2.07E+14	1.81E+14	2.12E+14	9.78E+13	2.41E+14	1.12E+14
<b>152.4</b>	1.08E+14	9.25E+13	1.08E+14	5.00E+13	1.26E+14	5.81E+13
<b>304.8</b>	5.20E+13	4.38E+13	5.11E+13	2.36E+13	6.08E+13	2.81E+13
<b>508</b>	3.09E+13	2.56E+13	2.99E+13	1.38E+13	3.61E+13	1.67E+13
<b>762</b>	2.04E+13	1.67E+13	1.95E+13	9.02E+12	2.38E+13	1.10E+13
<b>1524</b>	8.74E+12	7.00E+12	8.17E+12	3.78E+12	1.02E+13	4.72E+12

**Table 6-3: AZUR 3G30 equivalent 1MeV electron fluence**

'Thickness' [cm]	'Density' [g/cm <sup>3</sup> ]	'Parameters'	'Efficiency' (S1) [%]	'Efficiency' (S2) [%]
1.00E-03	5.31E+00	'Ipmax'	99.66	99.61
1.00E-03	5.31E+00	'Isc'	99.76	99.73
1.00E-03	5.31E+00	'Pmax'	97.42	97.1
1.00E-03	5.31E+00	'Voc'	96.06	95.79
1.00E-03	5.31E+00	'Vpmax'	94.64	94.34

**Table 6-4: AZUR 3G3o remaining efficiency in solar cell parameters**

#### 6.3.1.4 Single Event Effects (SEE)

Complementary to the previously discussed cumulative dose effects, also single event effects (SEEs) are relevant. They can be differentiated between short-term and long-term SEEs. The former can be seen as introduced by the peak fluxes along the mission trajectory, leading to non-destructive failures such as e.g. reboots, bit upsets or sensor background. The latter is related to the fluence of particles over the mission duration and thus quantifies the impact of destructive effects such as e.g. latch-ups, burn-outs and memory errors.

Additional to the solar particles also Galactic Cosmic Rays (GCRs) contribute significantly to SEEs. The ISO 15390 model for the ion range hydrogen to uranium and for solar minimum (worst-case) has been applied. Note that for targets with low Linear Energy Transfer threshold also indirect ionization by protons becomes relevant.

##### 6.3.1.4.1 Long-term SEEs

The obtained LET fluence spectrum for a 1 g.cm<sup>-2</sup> equivalent Al shielding is provided in Figure 6-4 for the 5 yr mission lifetime. Note that these levels are comparable to GEO environments. Therefore, it is expected that equipment designed for GEO should be suitable for usage in this mission. However, the actual rates of respective errors highly depend on the LET threshold and the sensitive area/volume of the component but also on the overall accommodation in /shielding by the spacecraft.

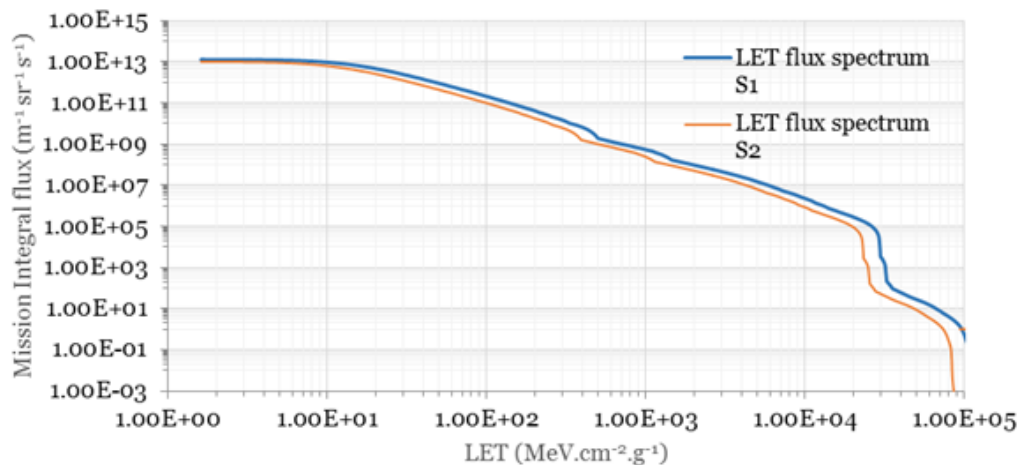


**Figure 6-4: LET flux spectrum for a 1 g.cm<sup>-2</sup> equivalent Al shielding**

#### 6.3.1.4.2 Short-term SEEs

The obtained LET flux spectra for the worst week average over the mission lifetime, as depicted in Figure 6-5, has been determined with the CREME-96 model for the ion range hydrogen to uranium. This spectrum is similar for GEO and polar missions and thus no significant design impacts are anticipated here.

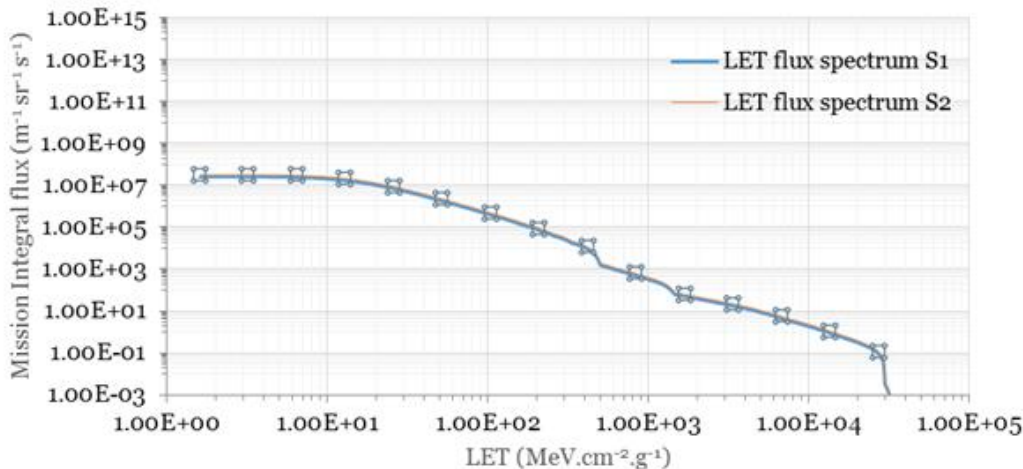


**Figure 6-5: LET flux spectrum for a 1 g.cm<sup>-2</sup> equivalent Al shielding**

#### 6.3.2 Hypervelocity Impact Risk Assessment

##### 6.3.2.1 Interceptor trajectory and geometry considerations

As dust production from a cometary surface is not homogeneous and correlates with illumination in active phases, an encounter trajectory avoiding closest approach in direct view of the comet subsolar area might be beneficial. Generally, the spacecraft/dust shield attitude would need to be adjusted as a function of comet phase angle.

In addition, the B1 & B2 probes released on orbits at closer altitudes from the cometary surface encounter a higher level of risk due to the cometary flux scaling up.

##### 6.3.2.2 Cometary environment model(s)

Physical models of (inner) cometary comas based on gas dynamic approaches have been developed by Crifo and Rodionov RD[6]. Those employ a combination of fluid and direct simulation Monte-Carlo (DSMC) approaches to solve for the moments of the gas and dust distributions in the cometary coma.

Such models include gas (water and CO and photo-dissociated products) and dust production terms (usually due to dusty ice sublimation or CO diffusion or a combination of both), and are solving spatial and temporal distributions of emitted cometary constituent in the gas and solid phases from the comet nucleus up to  $\sim 10^5$  km. An example output of such a model is provided in Figure 6-6 below, illustrating dust density and velocity distribution in an axial symmetric model resulting from CO diffusion for 67P and the associated velocity distributions, in the inner coma (40x40km) space.

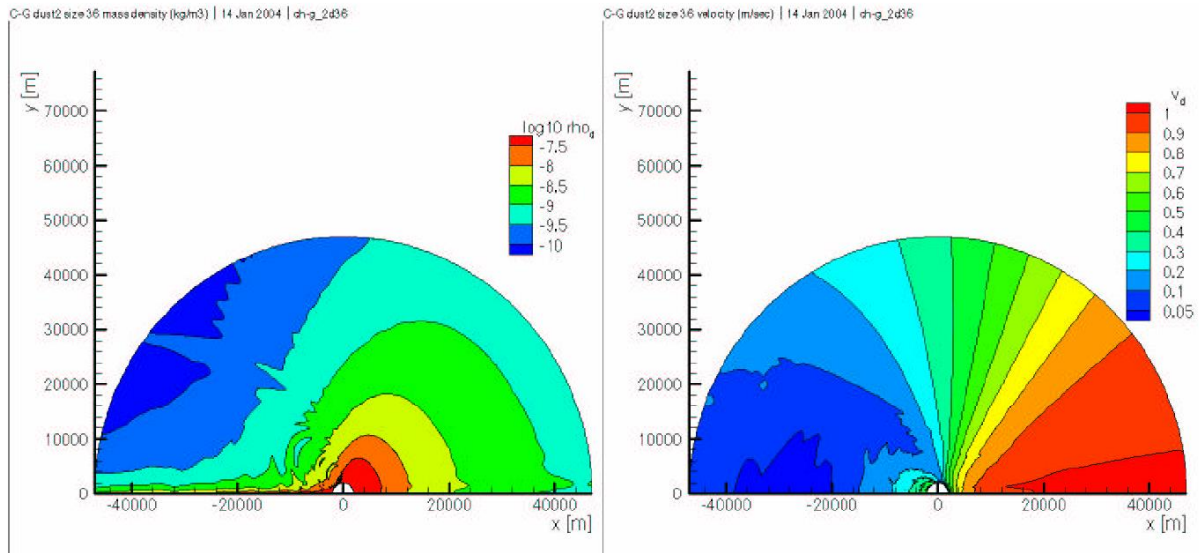


**Figure 6-6: illustration of density (left panel) and velocity (right panel) distribution of dust in a comet inner coma (RD[6]), accounting for illumination angle**

The sizes of the emitted dust grains typically range from submicron to a few meters. The grains are accelerated within a few nuclear radii from the surface, until the expanding gas becomes too diluted to exert a significant drag force. The terminal speeds reached by the dust are size dependent, ranging from about the speed of the gas for the smallest particles to a few m/s for the largest ones. Once out of the acceleration zone the dominating forces are radiation pressure and solar gravitation.

**The cometary dust grains velocities are negligible compared with Comet Interceptor encounter velocity.**

In the course of Rosetta mission preparation, an ESA engineering model was developed to evaluate the action of cometary gas and dust on the Rosetta spacecraft when crossing the inner coma RD[7]. This model was constrained with optical observations of 46P/Wirtanen, further developed to account for heliocentric distance dependence and non-homogeneous surface activity due to sun light distribution RD[8], and enhanced to allow for a better analysis of spectral observation of the coma by Rosetta instruments RD[9]. The model main properties are summarised below:

- The cometary nucleus is assumed to be spherical
- The activity distribution is axis – symmetric with respect to the comet-Sun line or radially symmetric (for analytical estimates of the density as function of distance)
- The main gas species densities, velocities and temperature, as well as number density and velocity of dust particles of different mass classes are computed
- Mass classes range from  $10^{-20}$  to  $10^4$  kg
- Dust grains have same mass and radius per class
- Grains spherical shape is assumed, and  $1000\text{kg/m}^3$  density
- The gas flow is assumed not to be influenced by dust

- The main species production rates ( $\text{H}_2\text{O}$  and  $\text{CO}$ ) are prescribed, with water sublimation depending on the angle between the surface normal and the Sun comet axis and are integrated in order to match observations (P/Wirtanen).
- The cometary activity (Sun distance dependent) drives gas / dust production rate
- The dust activity is described by the dust/gas mass ratio: dust mass is dominated by large grains, depending on maximum liftable dust mass, which depends on activity. The number of dust particles leaving the surface is computed based on the dust/ gas ratio.
- The dust dynamic in the coma is computed subject to drag force and gravitational acceleration
- Mass distribution** is constrained by the total mass released from the surface (dust/mass ratio), described by a cumulative mass distribution (number of particles  $N$  having a mass greater than a given mass) – binned over [ $10^{-20}$  to  $10^4 \text{kg}$ ] mass interval, as shown in Table 6-5 below.

$i$	Mass interval $\log([\text{kg}])$	$m_{d,i}$ [kg]	$s_i$ [m]	Abundance $p_i$	Mass fraction $\xi_i$
1	[-20,-19]	3.51E-20	2.03E-08	4.51E-01	2.38E-08
2	[-19,-18]	3.50E-19	4.37E-08	2.48E-01	1.31E-07
3	[-18,-17]	3.50E-18	9.42E-08	1.37E-01	7.21E-07
4	[-17,-16]	3.49E-17	2.03E-07	7.62E-02	4.00E-06
5	[-16,-15]	3.45E-16	4.35E-07	4.33E-02	2.25E-05
6	[-15,-14]	3.36E-15	9.29E-07	2.50E-02	1.26E-04
7	[-14,-13]	3.17E-14	1.96E-06	1.31E-02	6.27E-04
8	[-13,-12]	2.94E-13	4.13E-06	4.89E-03	2.16E-03
9	[-12,-11]	2.78E-12	8.72E-06	1.13E-03	4.71E-03
10	[-11,-10]	2.71E-11	1.86E-05	1.83E-04	7.46E-03
11	[-10,-9]	2.68E-10	4.00E-05	2.53E-05	1.02E-02
12	[-9,-8]	2.67E-09	8.61E-05	3.28E-06	1.32E-02
13	[-8,-7]	2.67E-08	1.85E-04	4.17E-07	1.67E-02
14	[-7,-6]	2.67E-07	3.99E-04	5.26E-08	2.11E-02
15	[-6,-5]	2.67E-06	8.60E-04	6.63E-09	2.66E-02
16	[-5,-4]	2.67E-05	1.85E-03	8.35E-10	3.35E-02
17	[-4,-3]	2.67E-04	3.99E-03	1.05E-10	4.21E-02
18	[-3,-2]	2.67E-03	8.60E-03	1.32E-11	5.30E-02
19	[-2,-1]	2.67E-02	1.85E-02	1.67E-12	6.68E-02
20	[-1,0]	2.67E-01	3.99E-02	2.10E-13	8.40E-02
21	[0,1]	2.67E+00	8.60E-02	2.64E-14	1.06E-01
22	[1,2]	2.67E+01	1.85E-01	3.32E-15	1.33E-01
23	[2,3]	2.67E+02	3.99E-01	4.18E-16	1.68E-01
24	[3,4]	2.67E+03	8.60E-01	5.27E-17	2.11E-01

**Table 6-5: Cometary dust mass distribution assumed in RD[7] to RD[9]**

- The mass distribution does not depend on the heliocentric distance and on the surface location.

For timing reasons, the ESA cometary environment model was not used in this study, however an adapted version could be considered for further cometary environment assessment.

A simplified parametric model of dust production as function of distance based on RD[10] is used to derive fluxes as a function of cometary activity. The cometary dust is emitted from a spherical nucleus and its parameters within the surrounding shells are computed. The shells are evenly distributed from closest approach to 50000km from the cometary nucleus in 10km steps. The intersection volumes between each shell and the spacecraft cross-sectional area moving through the shell are computed. The mass and number fluxes of the cometary dust within the respective shells are computed. Such a model, being fully spherical, does not account for the spatial variability of the emitted flux from the cometary surface and from that point of view can be considered as conservative. The mass distribution of dust assumed is given in Table 6-6.

mass	N per m-3	M fraction	radius (for 1000 kg/m3)
1.00E+02	1.00E-11	45.365781%	0.2879412
1.00E+01	8.80E-11	39.921888%	0.1336505
1.00E+00	2.20E-10	9.980472%	0.062035
1.00E-01	6.90E-10	3.130239%	0.0287941
1.00E-02	9.90E-10	0.449121%	0.013365
1.00E-03	7.20E-10	0.032663%	0.0062035
1.00E-04	1.00E-08	0.045366%	0.0028794
1.00E-05	1.00E-07	0.045366%	0.0013365
1.00E-06	6.90E-06	0.313024%	0.0006204
1.00E-07	1.20E-04	0.544389%	0.0002879
1.00E-08	2.40E-04	0.108878%	0.0001337
1.00E-09	8.78E-04	0.039836%	6.204E-05
1.00E-10	3.21E-03	0.014575%	2.879E-05
1.00E-11	1.18E-02	0.005333%	1.337E-05
1.00E-12	4.30E-02	0.001951%	6.204E-06
1.00E-13	1.57E-01	0.000714%	2.879E-06
1.00E-14	5.76E-01	0.000261%	1.337E-06
1.00E-15	2.11E+00	0.000096%	6.204E-07
1.00E-16	7.71E+00	0.000035%	2.879E-07
1.00E-17	2.82E+01	0.000013%	1.337E-07

**Table 6-6: Cometary dust mass distribution from RD[11] and RD[12]**

A cube-shaped spacecraft with 1 m length, depth and width is assumed crossing all shells, and rotating so that face A faces the comet, see Figure 6-7. Face A, face B and face

C are facing in ram direction consecutively and their angles to the ram direction are computed. As the cometary dust grains velocities are negligible compared to the Comet Interceptor encounter velocity, the cometary dust parameters on the spacecraft coming from the ram direction are computed for the different faces A, B and C, while the flux of other directions is neglected. This allows providing an estimate of the local cometary dust flux on the spacecraft faces, as well as integrated fluxes for each face along the spacecraft trajectory. Note that **the spherical model does not account for drag and radiation pressure forces**.

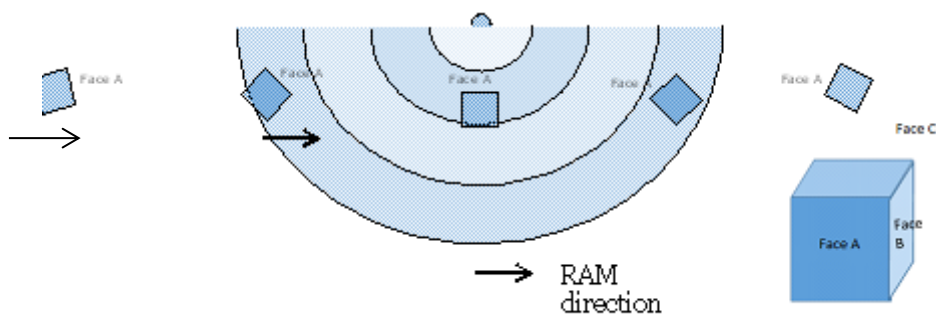


**Figure 6-7: Spacecraft A fly-by geometry, showing assumed shells for flux calculations**

The simplified model has been benchmarked against published Giotto's data collected during its encounter with Comet Halley. This represents the best observational evidence for an active long period comet encountered with a relative velocity close to 70km/s, which corresponds to the upper limit of the relative velocity range assumed for Comet Interceptor.

The impact of dust particles on the GIOTTO spacecraft is recorded from 287,000 km pre encounter to 202,000 km post encounter, with a closest encounter of around 600 km to Halley. Piezo-electric systems with thin film capacitors and impact charge systems were used for the mass sensitive detectors allowing a mass distribution larger than from approximately  $10^{-19}$  kg to be determined. For the mass distribution analysis, data from the GIOTTO DIDSY sensor and the GIOTTO PIA sensor were combined. The GIOTTO DIDSY Sensor has different subsystems with varying effective area, geometric area and sensor configuration. The DIDSY instrument normally cycles through modes including DID 2 and DID 3 sensor. For DID 2 or 3 the limiting mass is  $4 \times 10^{-12}$  kg and for DID 2 and 3 is  $1 \times 10^{-10}$  kg. The PIA sensor has three different channels with limiting masses of  $10^{-19}$  kg,  $10^{-17}$  kg and  $10^{-15}$  kg.

The total dust production from Halley (4 km radius of the nucleus) is calculated using the surface emission rate per square meter and the upper mass limit, which suggests a total dust production of 3300 kg/s for masses until 1 g and a total dust production of around 33000 kg/s for an upper mass limit of 1 kg. Values within this range are used for comparison and benchmarking of the Comet Interceptor model.

Based on the simplified spherical model an activity of 3300kg/s allows to obtain a cumulated encountered mass up to 25mg for masses up to 1g, and a total mass of 2.1g

for the whole mass range. Those values can be compared with published values of respectively 37mg and 1.9g.

To match the measured cumulated mass of 37mg reported, an activity of 4600 kg/s needs to be assumed, while the effective 200mg consistent with S/C attitude observations (integrated for masses up to 1g) would actually correspond to 33000kg/s. However, in this case as demonstrated later in Figure 6-13 the total integrated mass would exceed by orders of magnitude the total mass of 1.9g estimated from the combination of the measured particles and intercepted mass determined from the attitude perturbations of Giotto during encounter. Hence it is not possible to use a cometary activity parameter to provide a consistent description of Giotto's observations. The emitted mass distribution can be tuned further (at a later stage), however limitations in terms of forces ruling grain dynamics, emission spatial in-homogeneities and actual Giotto's instruments viewing factor during the flyby cannot be included at this point.

Based on those assumptions and limitations, it is demonstrated that a cometary activity of 3300kg/s is representative of the total mass accumulation observed - however it is based on a modelled mass distribution strongly favouring low masses.

The total fluence encountered is compatible with an activity assumption closer to 30000kg/s, while assuming such activity the total mass encountered is then significantly in excess of the observed one (factor of 3 to 4).

#### 6.3.2.2.1 Model biases and equivalent cometary activity

The computed cumulated fluence per mass bin depends in a large extend on the assumed mass distribution of particles present in the coma which relies in our case on previous work carried out based on Rosetta observations RD[11], RD[12], a fairly significant uncertainty being associated to it. Such distribution is shown on Figure 6-8 below.

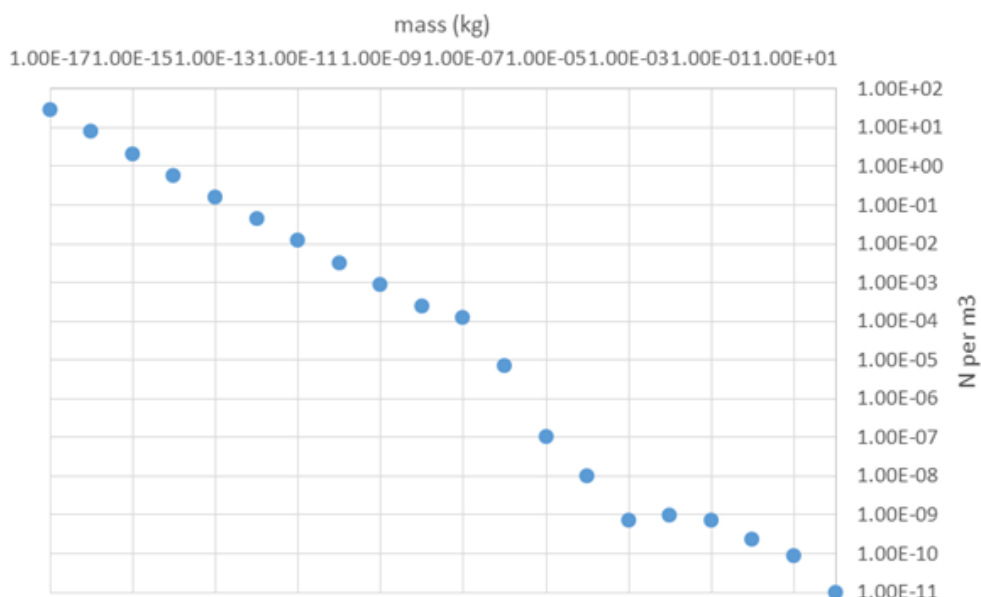


**Figure 6-8: Number of particles per m<sup>3</sup> for each mass bin based on RD[11], RD[12]**

Besides, mass flux distributions derived from Giotto data in a mass range up to  $10^{-8}$  kg have been published. Such fluxes measured by Giotto instruments during a short period (integration time not known) at 912km from the nucleus combined with scaled fluxes values from a cometary coma model of 67P (ref.) (3300kg/s, 68km/s relative velocity) for larger masses (using a mass index of -3), are presented in Figure 6-9. At first order, the modelled cometary flux (orange dots) is found to be in reasonable qualitative agreement with the published data. In fact the model exceeds the measured cumulated fluxes for masses below  $10^{-15}$  kg (which is consistent with the absence of radiation pressure forces).

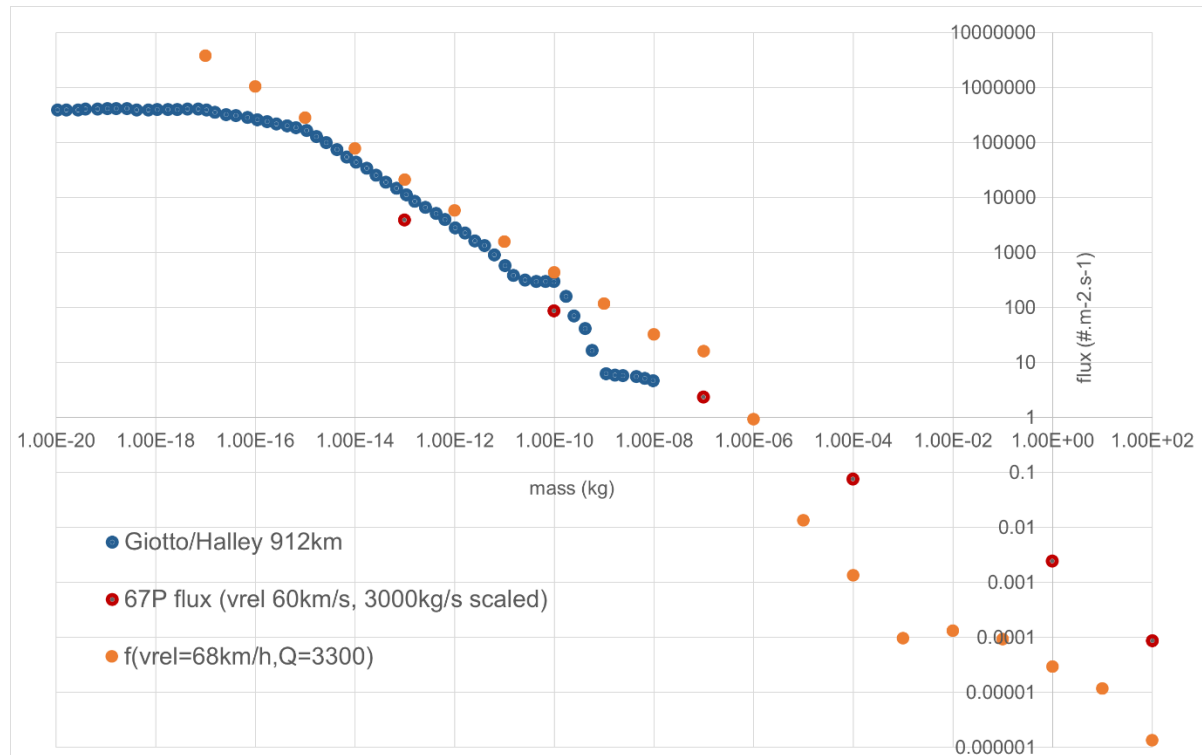


**Figure 6-9 Flux per mass bin shown for different cometary activities for a at closest approach**

Towards large masses a crossing point is suggested at mass 1 mg above which the computed flux becomes smaller than the reference values relying on Giotto data and 67P modelled data. Hence along our model assumption cometary fluxes are underestimated by one order of magnitude or more for masses typically above 10 mg (note: mass range not directly accessible to Giotto instruments).

**Considering that masses larger than 5-10 mg are threshold masses for dust impact along Comet Interceptor trajectory (in the sense that the encounter rate becomes lower than 1 for masses > 10mg) the discrepancy observed for large masses does not affect significantly our conclusion.**

**However, the model underestimates the encounter rate for masses larger than  $\sim 10$ mg. The probability of encounter for large masses, while low, would not be zero, and especially for particles in the range  $\sim 100$ mg, still**

**significant as suggested by the 67P based model and Giotto's reported observations.**

Another point of comparison is provided in terms of mass distribution of cumulated fluences (integrated fluences for masses  $> m$ ) plotted on Figure 6-10 against Giotto cumulated fluences (grey triangles): similarly, the modelled fluences start to underestimate Giotto fluences for masses above typically  $\sim 1\text{-}10\text{mg}$ .

Note that the Giotto fluences have been fitted to the following function:

$$\log \varphi(m) = k(\log(m) - \log(m_c)) + k'|\log(m) - \log(m_c)|^p + c$$

With  $k = -0.854$  ( $m < m_c$ ),  $k = -0.5$  ( $m > m_c$ ),  $k' = 0.239$  ( $m < m_c$ ),  $k' = 0$  ( $m > m_c$ ),  $p = 1.450$ ,

$C = 5.903 = \log \varphi(m_c)$  ( $m < m_c$ ),  $c = 4.345 = \log \varphi(m_c)$  ( $m > m_c$ )

$M_c = 4 \times 10^{-13} \text{ kg}$  and  $m_l = 1 \times 10^{-8} \text{ kg}$ .

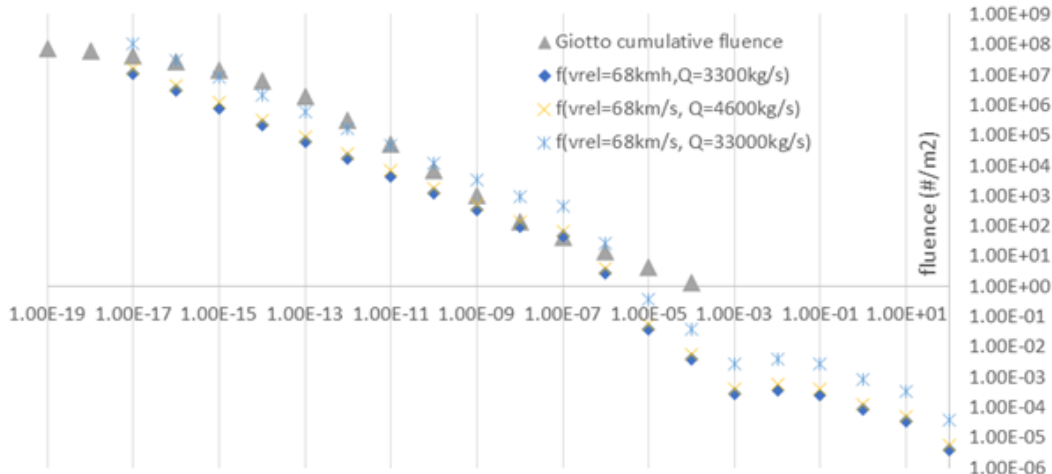


**Figure 6-10: Comparison of cumulated fluences of Giotto's data with modelled fluences for modelled activities of 33000 kg/s, 4600 kg/s, and 3300 kg/s**

In Figure 6-10 Giotto's data (grey triangles) account for masses fluxes accumulated by the dust instruments for masses below 1 g and fluxes inferred from Giotto's attitude perturbations, which results in total encountered mass of 1.9g, possibly including particles of several 100 mg. While modelled fluences compatible with the integrated mass encountered below 1 g (resp. 3300kg/s and 4600kg/s) fail to reach the reconstructed fluence except between masses  $10^{-9}$  to  $10^{-7}$  kg, an activity level of 33000 kg/s compares well with the reconstructed fluence up to  $\sim 10\text{mg}$ .

For larger masses the model seems to underestimate the actual fluences at those masses. This can result from a mass distribution with a larger mass index than that actually occurring at Halley during Giotto's encounter for large masses. However there are only 2 data points stemming from the data analysis at 10mg and 100mg. One has to keep in mind that a direct comparison of such mass fluences distributions is somewhat entailed with large uncertainties, since strongly biased by unknowns such as the actual

flyby geometry, emission in-homogeneities, actual instruments viewing geometry, time integration schemes and averaging effects present in the data. Hence better than order of magnitude agreement is possibly unlikely. Further and again, a slightly better mass distribution assumption and time integration window used to reconstruct the cumulated fluence from Giotto's data can be approximated with some further analysis which was not possible in the frame of this CDF study.

Last but not least, in order to obtain a total cumulated fluence compatible with Giotto's Particle Impact Analyser medium sensitivity channel observations (fluence at mass  $10^{-17}\text{kg}$ ), a cometary activity of close to  $Q \sim 30000\text{kg/s}$  needs to be assumed, while an activity of  $3300\text{kg/s}$  provides a good match with PIA-3 channel (fluence at mass  $10^{-15}\text{kg}$ ) as demonstrated on Figure 6-11.

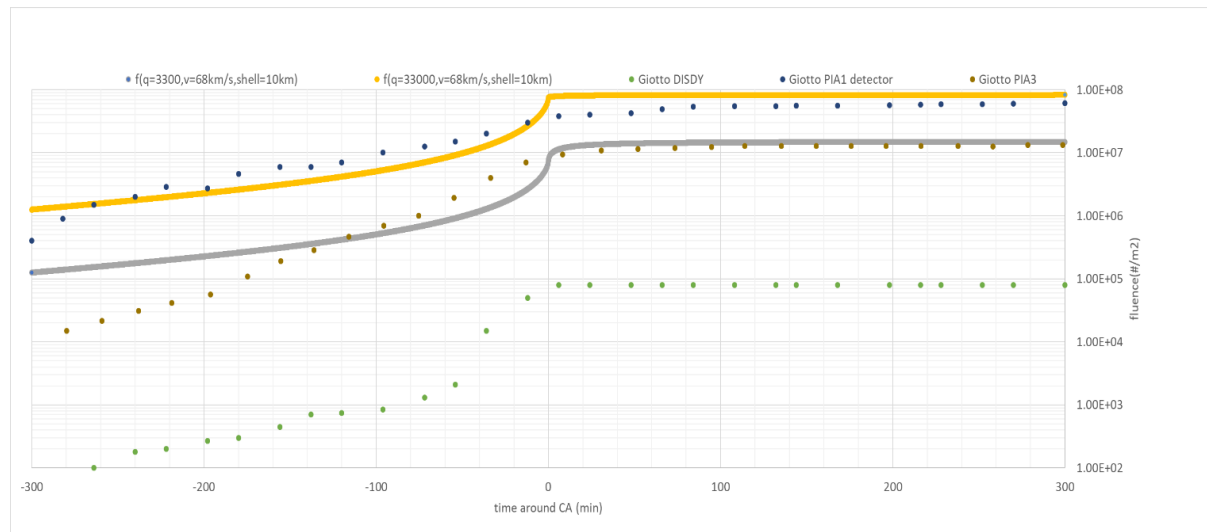


**Figure 6-11: Cumulated fluences over time for different activities for comparison**

The DIDSY fluence is smaller than the PIA fluence as the DIDSY sensor is sensitive to larger masses.

#### 6.3.2.2.2 Mass threshold for impact risk assessment

For system sizing the critical quantity is the cumulated number of particles encountered along the trajectory per mass bin. Figure 6-12 below gathers cumulated numbers for closest approach distances relevant for a 1m radius spacecraft hence an equivalent  $3.14\text{m}^2$  surface area, assuming a  $33000\text{kg/s}$  activity and a  $68\text{km/s}$  fly by velocity.

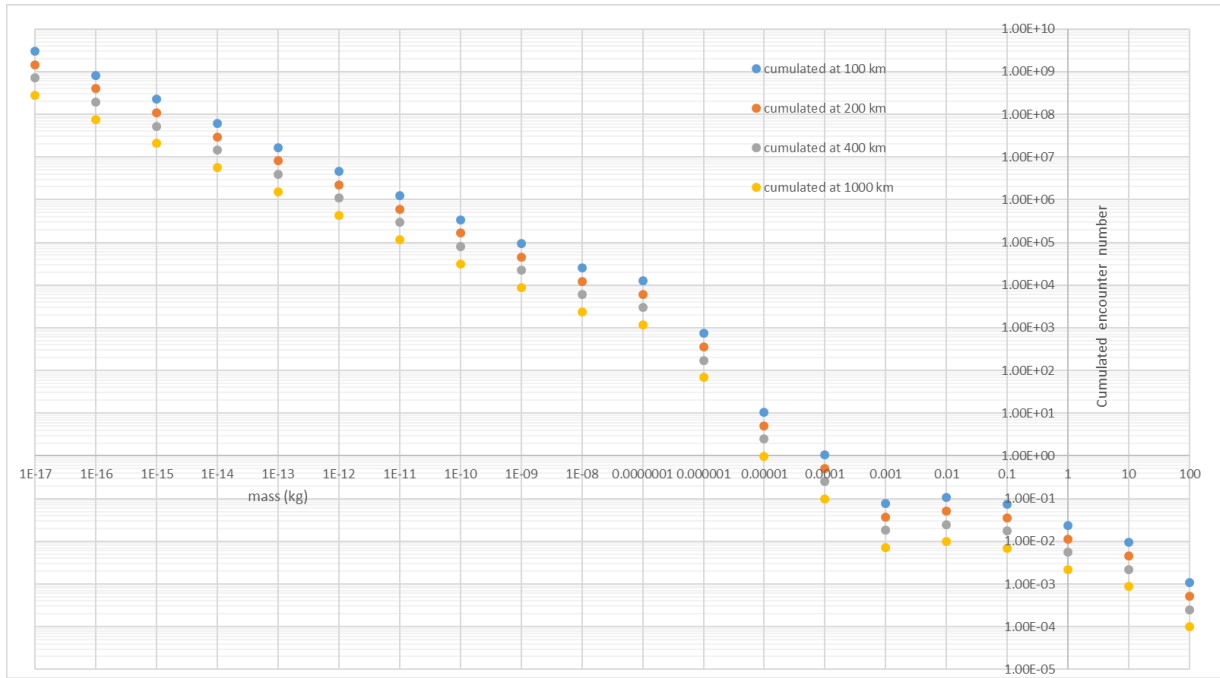


**Figure 6-12: cumulated particles per mass bin along the whole trajectory for a fly by velocity of 68 km/s and a cometary activity of 33000 kg/s for varying closest encounters to the comet, 100 km, 200 km, 400 km and 1000 km, assuming a 1m S/C radius.**

Such numbers demonstrates that for a  $r=1\text{m}$  radius spacecraft the chances to encounter at least one particle along the trajectory occurs for masses below typically 10mg (resp. 5mg) at 1000km closest approach, and 100mg (resp. 10mg) at 100km closest approach. This is indeed conservative within the assumptions of a spherical model and the comparatively smaller surface areas of S/C A and probe B2.

To get a more representative picture the total cumulated fluence ( $\#/ \text{m}^2$ ) per mass bin along the trajectory of Comet Interceptor S/C A with an equivalent cross-sectional area (assumed  $2.2\text{m}^2$ ), at 1000km closest approach (CA) was computed, and is plotted in Figure 6-13, using a 33000kg/s activity assumption.

**S/C A** can be assumed to encounter at least 1 particle for particle masses below **10mg** (CA = 1000km).

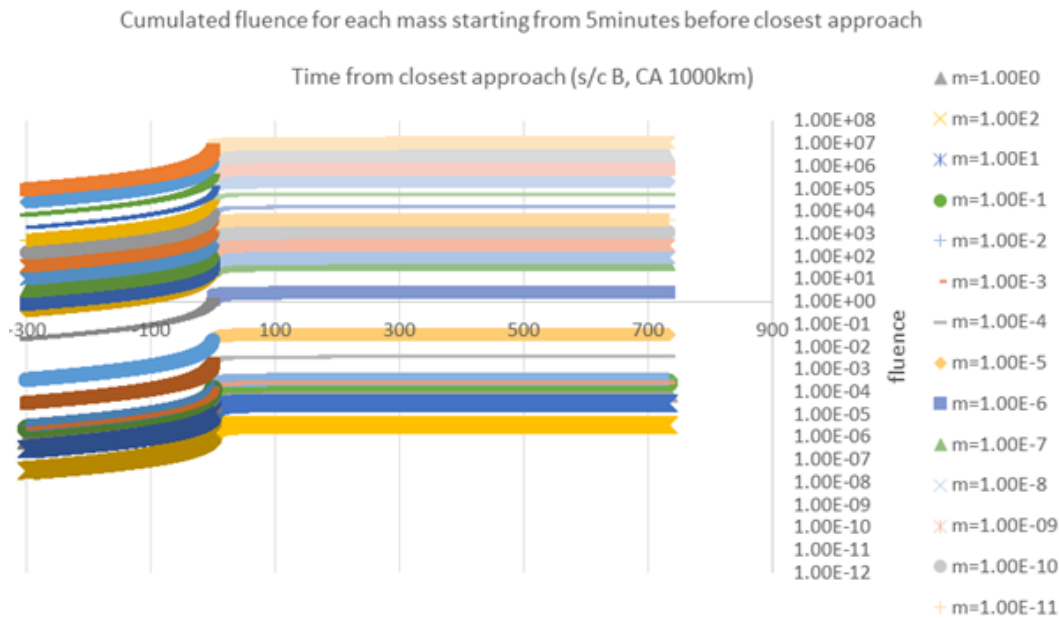


**Figure 6-13 : cumulated fluence per mass bin for equivalent S/C A cross-sectional area ( $2.2\text{m}^2$ ) computed from the simplified environment model. Note: “S/C B” in the plot title should be “S/C A”.**

#### 6.3.2.2.3 Conclusions:

1. For a model representative of total cumulated fluences at low masses in a worst case Giotto’s scenario, a cometary activity of  $Q \sim 3000\text{kg/s}$  shall be assumed. This activity is physically wrong given the number of assumptions and lack of physics in the simplified cometary model, however has the advantage of producing comparable number fluences per mass bin – but with an overestimated cumulated mass by a factor 3 to 4.
2. The computed total mass encountered is consistent with Giotto’s total mass of 1.9g assuming a cometary activity of  $3300\text{kg/s}$ , but the total cumulated fluence per mass distribution is underestimated. This is again because the mass distribution is strongly biased towards small masses. A mass distribution stemming from Giotto’s encounter data could help reduce those inconsistencies. This aspect is not trivial and cannot be addressed in the current time frame.
3. For a more accurate cumulated encounter number determination, the mass distribution should be adjusted significantly. However, we have relied on our bracketing of Giotto’s data in terms of both cumulated fluences and cumulated masses encountered. Based on that approach the cumulated encounter number computed demonstrates that S/C A can be assumed to encounter at least 1 particle for particle masses below  $10\text{mg}$  (CA =  $1000\text{km}$ ).
4. Note that a scaling of this analysis for the probe B2 is provided in the Systems chapter, see Section 0.

### 6.3.2.3 Impact risk assessment for S/C A

The fluxes calculated for face A, B, C on the S/C A are used to derive the risk of a failure due to hypervelocity impact on the spacecraft. The risk on critical components is the driver for the shielding of the S/C A. The risk is calculated for a closest distance of 1000 km and a cometary activity of 3000 kg/s using the SRL triple wall ballistic limit equation valid for a double honeycomb structure, see Figure 6-14. The critical units and respective failure rates and risks are identified in Table 6-7 Critical Units dimensions on the spacecraft faces A, B and C; BLE shielding configurations (triple wall equation). Note that the three walls are defined by the equipment wall thickness (rear wall), the equivalent thickness of the two inner facesheets of the double honeycomb structure as bumper and the thickness of the outermost honeycomb facesheet (outer bumper).

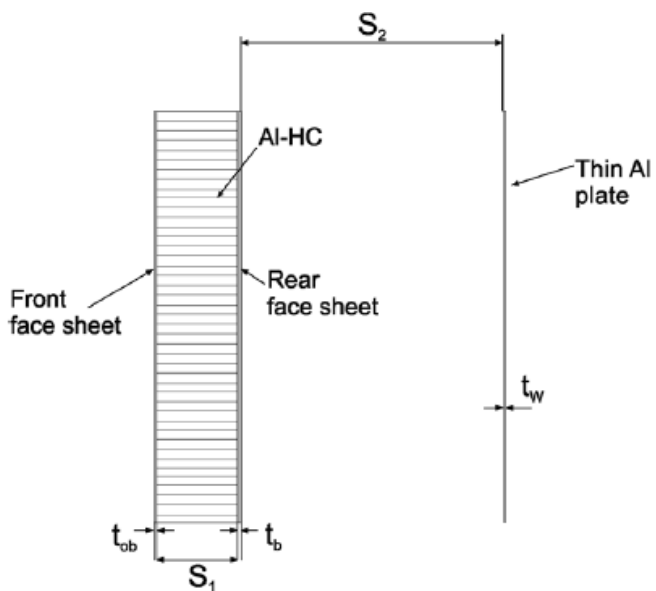


Fig. 4. Principle set-up for application of the SRL BLE.

**Figure 6-14: Example of triple wall equation**

Unit	surface-area-of-unit-in-A-B-C-directions			BLE-shielding-configurations						MATLAB-script-results				Anticipated-risk					
	SAB	SB	SC	BLE	t <sub>rear-wall</sub>	S2	t <sub>b</sub>	S1	t <sub>ob</sub>	[cm]	[cm]	[cm]	[cm]	Nfail-A	Nfail-B	Nfail-C	Nfail-total	risk	
EP-tank1	[m <sup>2</sup> ]	[m <sup>2</sup> ]	[m <sup>2</sup> ]	SRL-triple/-3	0.2	10/20/10	0.2	5	0.03	0.046	0.013	0.046	6.99E-03	0.70%	6.99E-03	0.70%	6.99E-03	99.30%	
EP-tank2	0.0000	0.071	0.132	SRL-triple/-3	0.2	10/20/10	0.2	5	0.03	0.046	0.013	0.046	6.99E-03	0.70%	6.99E-03	0.70%	6.99E-03	99.30%	
CP-tank1	0.126	0.0000	SRL-triple/-3	0.2	10/20/10	0.2	5	0.03	0.046	0.013	0.046	7.41E-03	0.74%	7.41E-03	0.74%	7.41E-03	99.25%		
CP-tank2	0.0000	0.126	0.126	SRL-triple/-3	0.2	10/20/10	0.2	5	0.03	0.046	0.013	0.046	7.41E-03	0.74%	7.41E-03	0.74%	7.41E-03	99.25%	
batteries	0.033	0.066	0.0000	SRL-triple/-3	0.2	20/10/0	0.2	5	0.03	0.045	0.011	0.045	0.011	3.33E-03	0.33%	3.33E-03	0.33%	3.33E-03	99.67%
RFDN	0.0000	0.030	0.040	SRL-triple/-3	0.2	10	0.2	5	0.03	0.046	0.045	0.046	3.19E-03	0.37%	3.19E-03	0.37%	3.19E-03	99.63%	
OBCr	0.0000	0.050	0.059	SRL-triple/-3	0.2	20/5/5	0.2	5	0.03	0.011	0.28	0.17	2.41E-02	2.35%	2.41E-02	2.35%	2.41E-02	97.65%	
RIU	0.0000	0.078	0.0000	SRL-triple/-3	0.2	20	0.2	5	0.03	0.012	0.015	0.012	1.17E-03	0.12%	1.17E-03	0.12%	1.17E-03	99.88%	
PCDU	0.077	0.106	0.0000	SRL-triple/-3	0.2	20	0.2	5	0.03	0.011	0.013	0.011	2.22E-03	0.22%	2.22E-03	0.22%	2.22E-03	99.75%	
PPU	0.0000	0.074	0.036	SRL-triple/-3	0.2	20	0.2	5	0.03	0.011	0.013	0.011	1.36E-03	0.14%	1.36E-03	0.14%	1.36E-03	99.85%	
BPRU	0.0000	0.050	0.038	SRL-triple/-3	0.2	10	0.2	5	0.03	0.046	0.045	0.046	4.03E-03	0.40%	4.03E-03	0.40%	4.03E-03	99.60%	
DSt	0	0.050	0.050	SRL-triple/-3	0.2	10	0.2	5	0.03	0.046	0.045	0.046	4.55E-03	0.45%	4.55E-03	0.45%	4.55E-03	99.55%	
TWT	0.024	0.027	0	SRL-triple/-3	0.2	10	0.2	5	0.03	0.046	0.045	0.046	2.30E-03	0.23%	2.30E-03	0.23%	2.30E-03	99.77%	
TWT-EP/C	0.013	0.024	0	SRL-triple/-3	0.2	10	0.2	5	0.03	0.046	0.045	0.046	1.68E-03	0.17%	1.68E-03	0.17%	1.68E-03	99.83%	
SADM	0.042	0.042	0.042	SRL-triple/-3	0.2	20	0.2	5	0.03	0.011	0.013	0.011	1.46E-03	0.15%	1.46E-03	0.15%	1.46E-03	99.85%	
antennae	external-shielding-and-failure-mode-unclear																		
APM	external-shielding-and-failure-mode-unclear assumed-to-be-not-located-on-surfaces-ABCs																		
EP-thuster	assumed-to-be-not-located-on-surfaces-ABCs																		
	%	%	%							%	%	%	%	%	%	%	7.10%		

The results of the risk analysis are shown in Table 6-7. The risk per unit is of the order of 1%, with the highest risk obtained for the OBC. This is mainly due to the proximity of the unit to the structural panels and the related reduction of efficiency of multi wall shielding. The total risk for a failure in any unit due to meteoroid impacts is about 7%. This is understood to be comparably high. Lower results are anticipated once more sophisticated and detailed assessments are performed, in particular a 3D ray-tracing analysis.

Note that there are several effects that are understood to potentially strongly affect the findings presented here:

1. The applied Ballistic Limit Equation (BLE) might not be representative of the actual spacecraft configuration and the failure mechanism. Depending on the actual spacecraft design appropriate damage equations may need to be applied.
2. The assumed shielding configuration and failure scenario, penetration of a 2 mm thick Al wall may be too conservative. Actual spacecraft design and relevant failure mechanism have to be reviewed.
3. The comparison relies on the fact that the spacecraft configuration does not vary during the mission. It might be that instruments as cameras are covered during transfer to the comet and only opened in the local environment.
4. For the tanks additional shielding is considered. Leading to about 1 kg of shielding mass per tank. Without this additional shield the risk per tank is above 10% and driving the risk for losing the mission.

In addition, the risk associated to the released probes have not been included in this assessment.

For the instruments an estimation of the particle fluence on the aperture has been performed. For this, the particle fluence as function of mass and simulation step has been derived, see Figure 6-15. Note that here the fluence per individual time and mass bin is indicated and also the cumulative fluence, which is understood here are the integral over time and over higher mass bins. The time to closest approach and the corresponding angle between surface normal and velocity vector are indicated in Figure 6-16.

To derive from the flux the number of particles on the instrument aperture the maximum incidence angle per instrument to impact the first surface has been estimated as indicated in Table 6-8. The angles roughly correspond to trajectory steps 39-41 and about 30 seconds to point of closest approach. Once the minimum particle mass causing a failure has been identified the corresponding failure rate can be determined. Assuming that a microgram particle causes a failure leads to an estimated risk of about 1 % / m<sup>2</sup>.

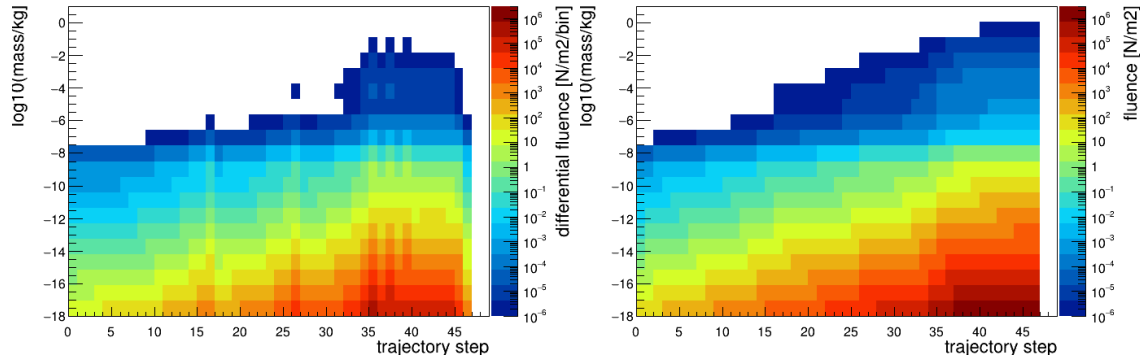


**Figure 6-15: The differential fluence per bin (left) and the cumulative fluence (right) of dust particles along the simulation**

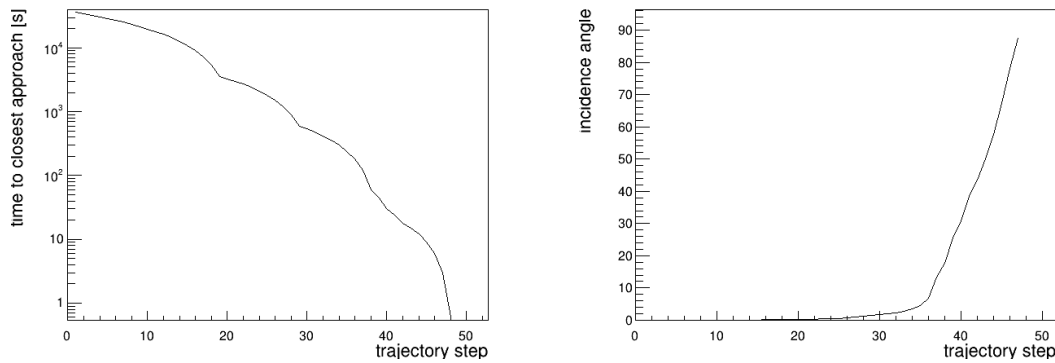


**Figure 6-16: The time to closest approach (left) and angle between surface normal and velocity vector (right) per time step**

Instrument	First surface diam [mm]	Distance [mm]	External cutout diam [mm]	Angle [deg]
CoCa	135	330	135	22.2
Mirmis 1	40	110	40	20.0
Mirmis 2	70	110	70	32.5
Mirmis 3	18	165	80	16.5

**Table 6-8: Assumed instrument aperture geometry and derived maximum angle of incidence to hit the first surface**

## 7 SYSTEMS

### 7.1 System Requirements and Design Drivers

The mission requirements for Comet Interceptor are listed in Table 7-1.

Mission Requirements		
Req. ID	Statement	Req. Comments
MIS-010	The mission shall intercept a Long Period Comet (LPC) or an interstellar body in a fly-by scenario.	See science requirements for more details
MIS-020	The mission shall include one main S/C (ESA) (hereafter S/C A) and two probes (one JAXA and one ESA) (namely probes B1 and B2, respectively) in order to gather multi-point observations of the comet and its coma.	
MIS-030	The mission shall embark the instruments as specified in the relevant Instrument Interface Description Documents (and summarised in Chapter 4).	
MIS-040	The mission shall allow parking the spacecraft in a Halo orbit around the SEL2 point after launch, wait for a target of opportunity, and then intercept it.	Ability to find a suitable target comet
MIS-050	The mission shall allow a fly-by to backup target comets 73P/Schwassmann–Wachmann (TBC) and 26P/Grigg–Skjellerup (TBC) within the nominal mission lifetime.	Ability to find a suitable backup comet in case no other suitable target is found
MIS-060	The mission shall be compatible with a launch together with the ARIEL mission/spacecraft.	Mission constraint for a shared launch with ARIEL
MIS-070	The nominal mission lifetime shall be maximum 5 years (TBC).	F-class mission constraint
MIS-080	The mission shall be compatible with ESA's F-mission budget Cost to Completion (CaC) not exceeding 150 M€.	F-class mission constraint

**Table 7-1: Comet Interceptor Mission Requirements**

The mission requirements imply the following major design drivers:

**MIS-010, MIS-020 and MIS-030** severely drive the mission profile, transfer to the comet and the fly-by geometry. The probability to reach a suitable target within the mission timeframe as a function of the mission capabilities is considered a major design driver with the ultimate objective to limit the mission trade space. Moreover, due to the

unknown environment for the target object, a robust S/C A configuration is deemed necessary.

**MIS-040** drives the design of the S/C A in terms of the delta-V capability for the transfer from L2 to the target object.

**MIS-050** restricts the waiting time in L2 for finding a suitable target; if no suitable target is found, the identified backup target objects selected would allow fulfilling the mission objectives.

**MIS-060** drives the programmatic schedule in order for the compatibility with a shared launch with ARIEL to be met.

**MIS-070** and **MIS-080** immediately call for components/unit/equipment to be as far as possible available in order to avoid development costs and minimise the mass in order to reduce the launch costs.

The system requirements for Comet Interceptor are listed in Table 7-2:

System Requirements		
Req. ID	Statement	Parent ID
SYS-010	The Comet Interceptor S/C shall contain one main S/C (S/C A - ESA) and two probes (B2 - ESA and B1 - JAXA).	MIS-020
SYS-020	The Comet Interceptor S/C shall be launched by the Ariane 62 launcher from Kourou (Guiana Space Centre).	MIS-060
SYS-030	The Comet Interceptor S/C shall be launched in 2028.	MIS-080
SYS-040	The Comet Interceptor S/C nominal lifetime shall be maximum 5 years (TBC).	MIS-070
SYS-050	The Comet Interceptor S/C shall embark the instruments as specified in the relevant Instrument Interface Description Documents (and summarised in Chapter 4).	MIS-030
SYS-060	The Comet Interceptor S/C A post flyby phase duration shall be maximum 6 months.	MIS-020, MIS-070
SYS-070	All Comet Interceptor S/C equipment shall be TRL 6 by Mission Selection (Q1 2020) and TRL 7 by Mission Adoption (Q4 2022).	MIS-060
SYS-080	The Comet Interceptor S/C A shall provide the mechanical, thermal and electrical interfaces for both probes B1 and B2.	MIS-020
SYS-090	The S/C A, B1 and B2 configurations shall ensure unobstructed fields of view for the instruments for observation purposes and for the communication antennas.	MIS-020
SYS-100	The S/C A shall carry the probes (B1 and B2) from integration up to their separation before the flyby.	MIS-020
SYS-101	The mission shall allow a release of the probe B2 at least 24 hours (TBC) before the closest approach.	MIS-020
SYS-102	The mission shall allow a flyby altitude for the probe B2 of between 100 m to 400 m (TBC).	MIS-020
SYS-103	The mission shall allow a release of the probe B1 at least 48	MIS-020

	hours (TBC) before the closest approach.	
SYS-104	The mission shall allow a flyby altitude for the probe B1 of between 100 m to 400 m (TBC).	MIS-020
SYS-110	The instruments on B1 and B2 shall be used only after separation of the spacecraft from S/C A.	MIS-020, MIS-030
SYS-120	Check-out operation activities of the scientific instruments and the rest of equipment on-board the probes B1 and B2 shall be possible before their separation from S/C A.	MIS-020, MIS-030
SYS-130	The probe B2 shall be designed considering a design-to-cost approach.	MIS-080
SYS-140	The probe B2 shall be designed for a 24h (TBC) lifetime.	MIS-020, MIS-030, MIS-080
SYS-150	The probe B2 shall be spin-stabilised.	MIS-020, MIS-030

**Table 7-2: Comet Interceptor System Requirements**

## 7.2 System Assumptions and Trade-Offs

The following system assumptions are considered for the purpose of the CDF Study:

Assumptions	
1	A target maximum wet mass of 650 kg (excluding adapter) in order to be compatible with the use of a dual launch with ARIEL and the Dual Launch Structure (DLS).
2	Commissioning within 3 months from launch.
3	Decommissioning phase duration less than 2 weeks.
4	Maximum relative velocity at encounter of 70km/s.
5	The range of heliocentric distances between 0.9AU and 1.25AU.
6	Solar phase angle range at encounter +/-45deg.
7	S/C A closest approach to target at 1000 km.
8	Probes B1 and B2 closest approach are expected to target below 400 km. The exact distances are to be decided in later phases.

**Table 7-3: Comet Interceptor System Assumptions**

Table 7-4 lists the system trade-offs which have been performed during the study. More details for each of the listed trade-off are given in the sections below.

Spacecraft	Trade-off
S/C A	Configuration trade-off in order to investigate possible accommodation options for the payloads, thrusters, communication antennae, probes B1 and B2
	Fly-by geometry and probes release strategy
	Dust particle size and required shielding

Spacecraft	Trade-off
	AOCS architecture for dust particle impact recovery and RCS thrusters placement
	HGA antenna placement and required mechanisms
	Solar Array size with respect to the operating point of the Electric Propulsion thruster
Probe B2	Dust particle size and required shielding
	AOCS architecture and release mechanism
	Power architecture
	Placement of the FGM boom with respect to the ISL antenna

**Table 7-4: System trade-offs**

An analysis regarding target reachability was performed at the beginning of the Comet Interceptor CDF Study. More details regarding the analysis of reachable targets is provided in the Mission Analysis chapter (Section 5).

The S/C will intercept the comet at its node, i.e. when the comet crosses the Ecliptic plane, as shown in Figure 7-1 below. The intercept region is defined by:

- The range of allowed heliocentric distances of the encounter
- The phase angle of Earth at encounter

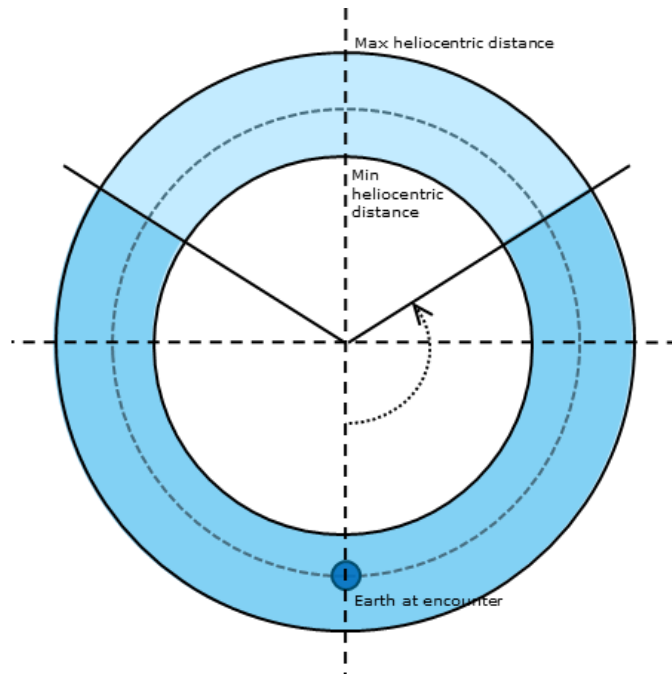


**Figure 7-1: Intercept region for Comet Interceptor**

The intercept region and the encounter conditions drive the mission design. A first level assessment was performed during the study in order to understand the impact of these parameters and conditions to the design of various sub-systems:

Intercept region parameters	Design drivers
Min. and max. heliocentric distance	Thermal subsystem design (hot/cold case)
	Communications distance during transfer and for the science data downlink
	Power subsystem design (for all S/C)
Earth-Sun-comet angle	Delta-V and trajectory
	Communication during and after encounter
	S/C Configuration

**Table 7-5: Intercept region parameters and design drivers**

Encounter condition parameters	Design drivers
Max relative velocity	Tracking strategy: AOCS and configuration
	Navigation & separation strategy: GNC and OPS
	Dust shielding needs (& nutation control for B2)
Solar phase angle	Thermal aspects: configuration & tracking
	B2 design: power, thermal

**Table 7-6: Encounter condition parameters and design drivers**

A sensitivity analysis on the impact of single constraints on the probability of having a target was performed during the study, as defined in the relevant Mission Analysis chapter. In addition, a sensitivity analysis was performed in order to estimate the probability of reaching a LPC when the encounter velocity, the solar phase angle and the heliocentric distance of the encounter are all taken into account. The analysis led to the following system design constraints, chosen to achieve the best balance of the design drivers reported in Table 7-6, while still maintaining a high (81%) probability of reaching a LPC:

- Relative velocity at encounter:  $\leq 70$  km/s
- Solar phase angle at encounter:  $+/- 45\text{deg}$
- Heliocentric distance at encounter range: 0.9 to 1.25AU

## 7.2.1 S/C A

### 7.2.1.1 Configuration Trade-off

#### Assumptions

The following working assumptions were done for the configuration trade-off:

<b>Assumptions</b>	
1	Electric propulsion thruster placed in the $-Z$ axis, together with the launcher I/F.
2	Two deployable solar arrays in the $+/- Y$ axes.

<b>Assumptions</b>	
3	Release of the probes B1 and B2 should not drastically change the CoM for S/C A.
4	Payload instruments preferably placed on the same face.
5	NavCam should be pointing parallel to CoCa.
6	Star Tracker optical head pointed away from the Sun.

**Table 7-7: Configuration Trade-off Assumptions**

### **Rationale**

The objective of exploring the configuration trade space was to narrow down the possible options and derive high level placement constraints for various elements for the driving mission phases (e.g. high relative velocity fly-by at the comet). Additionally, other constraints impacting configuration from LEOP, L2 transfer, waiting at L2, transfer to the comet were identified and taken into account for the overall configuration trade-off.

### **Options**

36 options were initially identified and traded-off against the criteria described in the paragraph below. 6 options were down selected as most promising and further discussed in order for a baseline to be selected. The driving elements identified were:

- Pointing and position of the HGA
- B1 & B2 accommodation and release
- RCS thrusters placement.

### **Criteria**

The options identified for the Configuration trade-off have been traded-off against the criteria listed in Table 7-8.

<b>Sub-System/ Topic</b>	<b>Criteria</b>	<b>Weighting</b>
<b>Communications</b>	HGA can always point to Earth during EPS thrusting	3
	HGA can always point to Earth during RCS thrusting (during LEOP and L2 transfer)	0
	HGA can always point to Earth during flyby	3
<b>AOCS/Propulsion</b>	Significant change in CoG around EPS thrust axis after release of probes	3
<b>Payloads + NavCam</b>	Payloads + NavCam always pointing at target during communications during flyby	2
	Payloads + NavCam always pointing at target during RCS manoeuvres during flyby	0
	Payloads pointing at comet during flyby as long as communication is not on	5
	Payloads + NavCam always pointing at target during probe release during flyby	0
<b>Plumes</b>	Avoidance of RCS plume impingement on optical	3

Sub-System/ Topic	Criteria	Weighting
	payloads	
<b>Dust</b>	Critical external bus units (e.g. solar arrays, HGA, tanks) protected from dust during flyby	5
	Payload units protected from dust during flyby	4
<b>Thermal (Probe)</b>	Probes in shadow during transfer to comet	2
	Probes in shadow during flyby (before release)	2
<b>Structures/Config</b>	Mass imbalance during launch	1
	Space for accommodation on all external surfaces	5
<b>Sun avoidance</b>	Payloads avoiding sun during EPS thrusting (incl. radial thrust)	5
	Payloads avoiding sun during RCS thrusting (any direction)	3
	Payloads on probes avoiding Sun during flyby communications	5
	Payloads on probes avoiding Sun nominal science during flyby pre-release	5
	Payloads on probes avoiding Sun during RCS thrusting	1
	Payloads on probes avoiding Sun during EP thrusting	5

**Table 7-8: Configuration Trade-off Criteria**

#### **Rationale for Final selection**

The baseline configuration selected for S/C A takes into account the following placement for the major configuration units, as shown in Figure 7-2 below:

- Solar Arrays on +/- Y
- Electric Thruster on -Z
- Radiators/cold face +/- Y
- High Gain Antenna stowed on -X and pointing towards +Z
- B1 & B2 on +Z
- Optical Payloads on +X
- Reaction Control Thrusters on -Z

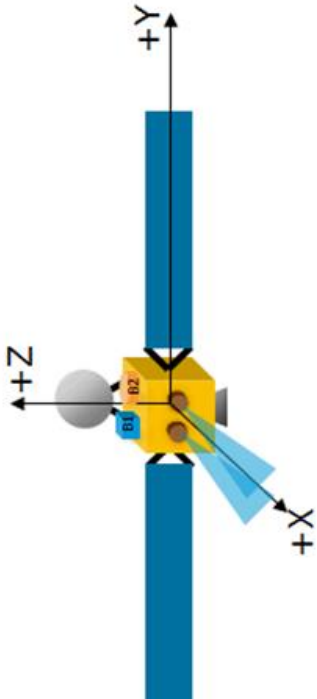


**Figure 7-2: S/C A Baseline Configuration Schematics**

### 7.2.1.2 Fly-by Geometry

#### Assumptions

Two release cases for probes B1 and B2 were investigated during the CDF study. For probe B2, the assumption was made that the release strategy has to allow for it to spin along its relative velocity axis. Hence, the two release cases:

- Release B2 in the RAM direction of S/C A
- Release B2 in the anti-RAM direction of S/C A

However, the relative geometry at the closest encounter is also important and it is a key driver for the ISL link. Therefore, for each of the above release case, three options were traded-off for the release direction:

- All three S/C in parallel
- B1 and B2 with closest encounter before S/C A
- B1 and B2 with closest encounter after S/C A.

#### Options

The results of the trade-off are reported in Table 7-9 below:

Weighting		Probe flybys...						Notes	
		Anti-ram...			Ram...				
		before S/C A	parallel to S/C A	after S/C A		parallel to S/C A	after S/C A		
Ram face same as interfacing panel to S/C A	2		5			1		Lower weighting assumes that similar strengthening of the panel opposite to the interfacing panel is possible, but would incur a non-negligible mass penalty.	
Delta-v to achieve S/C flyby geometry	1		3			3		Low weighting assumes that the delta-V impact for the manoeuvres is able to be easily accommodated on S/C A.	
ISL mass/performance/power on B2	2		3			3		Current understanding is that there is no gain in flying before/after S/C A, as the benefits in antenna aspect angles are offset by increases in range. Indeed, the considered cases with delays perform worse due to the higher ranges.	
ISL antenna placing on B2	3		5			5		Assumes that ISL antenna is not possible on B2 face with separation mechanism (possibly not valid assumption)	
FGM placement on B2	3		5			1		Assumes that FGM placement is not possible on interfacing face to S/C A, and that FGM must be placed into anti-ram (i.e. wake) direction. Also assumes that if B2 is before or parallel to S/C A, then a toroidal antenna will be used on the anti-ram face which makes accommodating the FGM difficult.	
OPIC calibration before	1		1			5		From OPIC IDD: "If OPIC can be powered on before A and B2 separation, precise	

separation								on-board calibration can be done by observing background stars before B2 spacecraft separates from the A spacecraft in order to constrain the point spread function and to calibrate photometrically. No additional calibration is intended." OPIC points in RAM direction.
<b>SCORES:</b>		<b>50</b>			<b>34</b>			

**Table 7-9: Flyby Geometry Trade-off**

### Rationale for Final selection

The above system assessment highlights the fact that the preferred release geometry for the probes is in the anti-RAM direction, with a flyby parallel to S/C A. Schematically, the approach is shown in Figure 7-3 below:

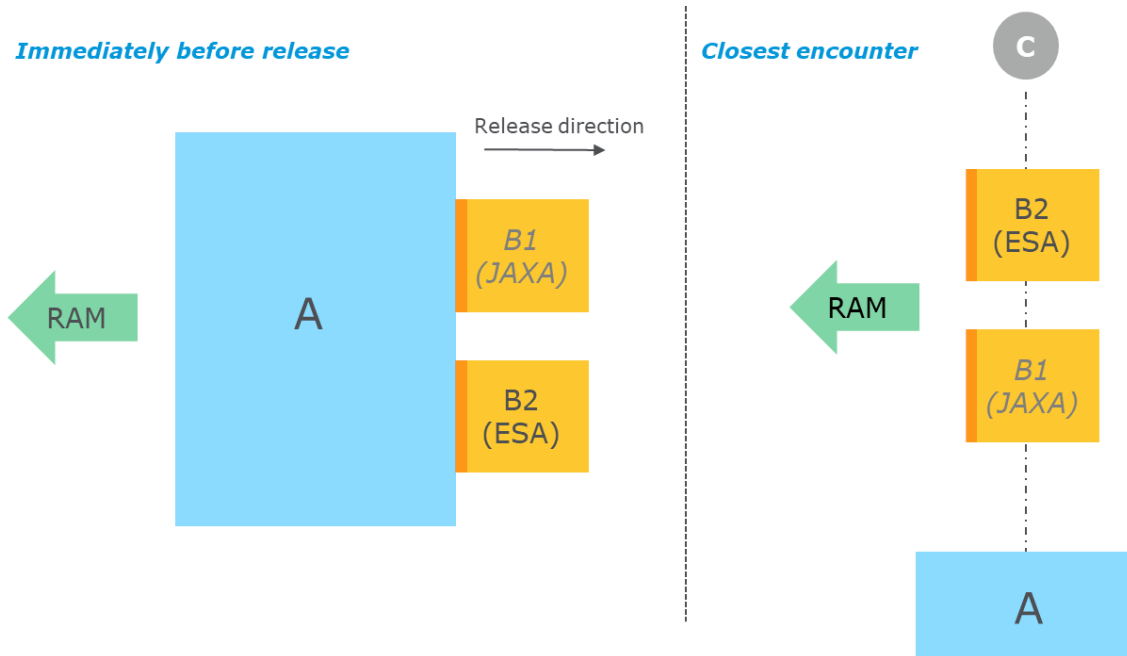


**Figure 7-3: Proposed Release Geometry for B1 and B2**

### 7.2.1.3 Dust particle size and shielding

#### Assumptions

The following assumptions were made for the dust particle sizing and required shielding estimation:

Assumptions	
1	The cross-sectional area of S/C A towards the oncoming flow is assumed as a circle with radius of 1 m (i.e. area of $3.14 \text{ m}^2$ ). Note that the true value should be closer to the range $1.6 - 2.3 \text{ m}^2$ given the final design, but this conservative assumption was taken early on for the system sizing and thus includes margin.
2	Spherical grains density of $1000 \text{ kg/m}^3$
3	Probe B2 radius = $0.3 \text{ m}$
4	S/C A Closest Approach (CA) altitude = $1000 \text{ km}$
5	Probe B2 CA altitude range = $[100, 200, 400] \text{ km}$

**Table 7-10: Assumptions for the dust particle sizing and shielding analysis**

#### Rationale

By definition of the Comet Interceptor mission, the spacecraft will encounter dust particles of various sizes and masses. The spacecraft shall be robust to the encounter of a uniform impact profile of small size particles with high encounter probabilities as well as a single impact of a larger particle with a very low impact probability. Protection from single impact particles requires shielding (to avoid penetration and damages) as well as adequate attitude control capabilities to maintain (or come back to) the nominal attitude of the spacecraft. Those perturbations might result in a range of risks from the degradation of the mission performances to the loss of the spacecraft. Depending on the baseline particle to be protected from and the level of risk to be accepted, the impact of the protection design on the spacecraft (e.g. mass, power, cost) must be considered.

The dust particle simulations discussed in Chapter 6 provide the cumulated number of particle impacts, depending on the particle mass, during the fly-by of the comet. With relevant margins, they were used to estimate the sizes and probabilities of the largest particles that might reasonably be encountered during the fly-by. The probability per particle mass category is dependent on the closest approach distances: 100, 200, 400 & 1000 km were considered and are assessed below.

#### Simulations & Results

Figure 7-4 shows the expected number of impacts per particle mass bin, considering the following assumptions:

- Number of dust particle swept by a spacecraft along the fly-by trajectory
- $R = 1 \text{ m}$  radius spacecraft (as above, the actual cross-sectional area is expected to be in the range  $1.6 - 2.3 \text{ m}^2$ ).
- Spherical grains density of  $1000 \text{ kg/m}^3$

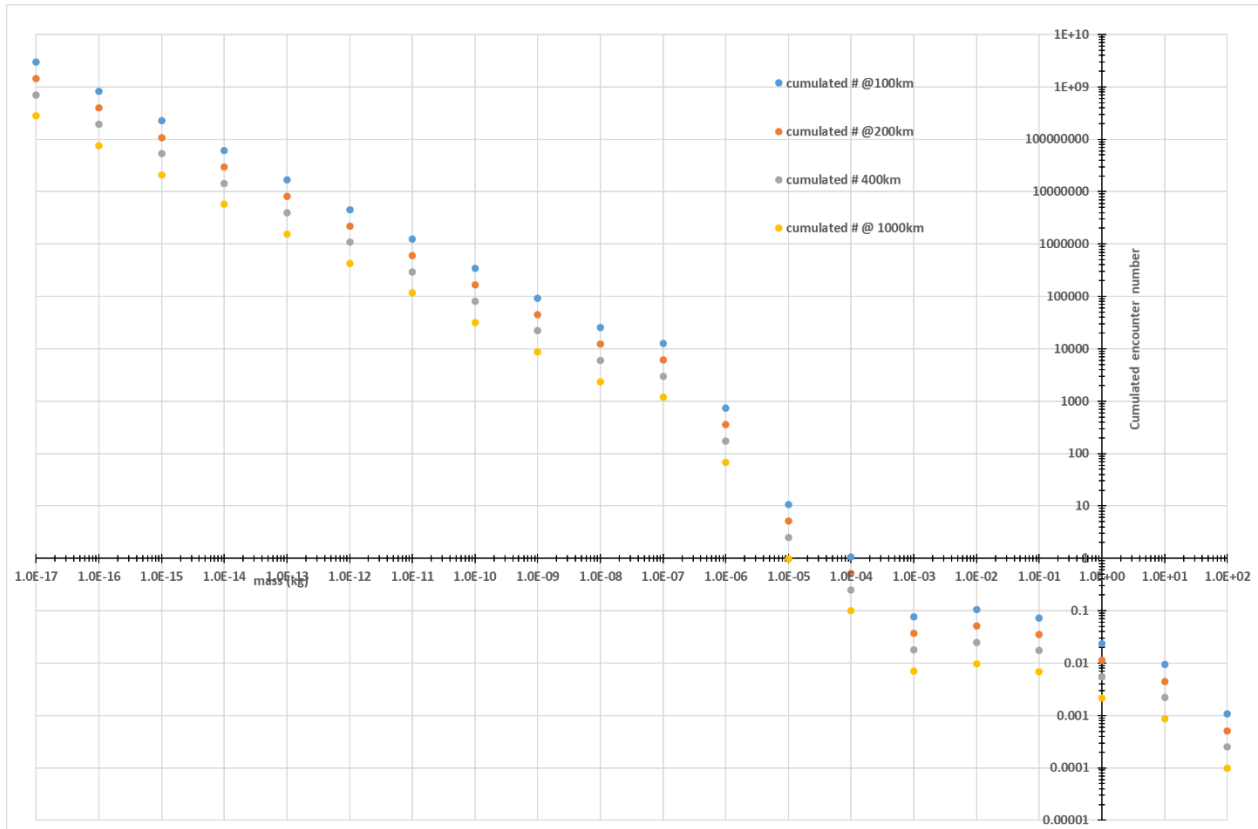


**Figure 7-4: Cumulated number of impact depending on the mass of the dust particle**

This simulation, made originally for S/C A, can be adapted for probe B2. Knowing that the B2 radius is 0.3 m, it is deduced that its area is 9% of the  $R = 1$  m reference case. Moreover, B2 experiences only half of the fly-by, as its minimum requirement is to survive up to CA only. Based on this, the results for S/C A (at 1000 km), and probe B2 (at 100, 200 and 400 km) are shown in Figure 7-5.

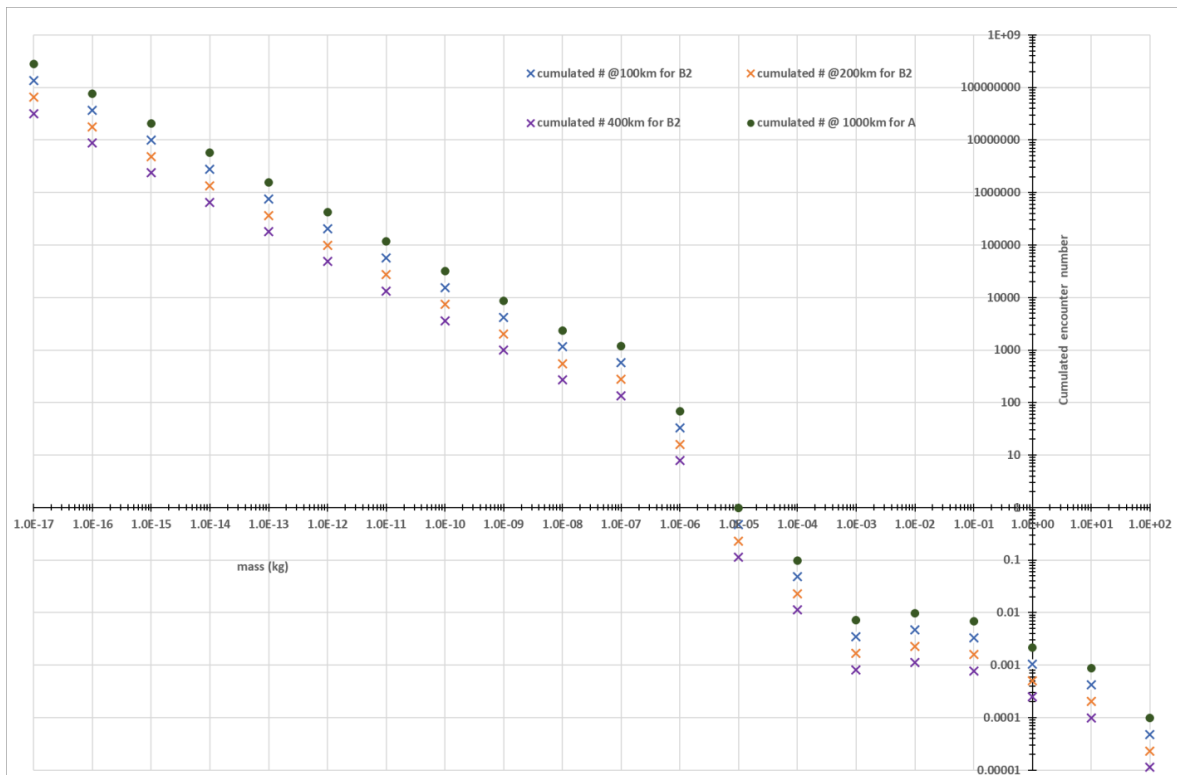


**Figure 7-5: Cumulated number of dust impacts as a function of particle mass for S/C A and probe B2**

The results of the simulation is summarised in Table 7-11 & Table 7-12, for S/C A and probe B2 respectively, showing the resulting impact probabilities for particles of different mass.

For S/C A at 1000 km:

		Resulting probability for a fixed particle mass		
CA distance	10 mg		1000 mg	
	100 mg	1000 mg	1000 mg	1000 mg
<b>1000 km</b>	98.9 %	9.9 %	0.7 %	0.07 %

**Table 7-11: Probability of impact/dust particle mass for S/C A**

For probe B2 at 100, 200 & 400 km:

		Resulting probability for a fixed particle mass		
CA distance	10 mg		1000 mg	
	100 mg	1000 mg	1000 mg	1000 mg
<b>100 km</b>	47.99 %	4.8 %	0.35 %	0.035 %
<b>200 km</b>	23.11 %	2.31 %	0.17 %	0.017 %
<b>400 km</b>	11.33 %	1.13 %	0.08 %	0.008 %

**Table 7-12 : Probability of impact/dust particle mass for probe B2**

### Rationale for final selection

For S/C A, it can be seen that the probability of hitting a 10 mg particle is around 100% and for 100 mg, it is approximately 10%. As such, the system should be compatible with impacts up to at least 100 mg, and indeed may have to endure several particles with masses on the order of 10 mg. Both the structural shielding and AOCS have been designed accordingly.

For probe/C B2, the probability goes from 47% to 12% from 100 km to 400 km, demonstrating that a CA at higher distance is safer (although impacting the science return). However even in the case of a 400 km flyby for B2, the probability of a 10 mg impact is far from being negligible, and as such the structures and AOCS were designed to cope with this. The likelihood of a 100 mg impact is also non-negligible, however the system level impacts were considered too high (in terms of mass and power for the AOCS) to afford full resilience against such particles. As such, a 100 mg particle may well lead to the loss of B2.

It shall be noted here, as discussed in the Environment chapter, that there is still considerable uncertainty for the dust modelling, particularly for larger particles. As such, the sizing case for shielding and AOCS should be reconsidered in later phases, pending updates in the dust modelling.

#### **7.2.1.4 HGA Antenna placement and mechanisms**

##### **Assumptions**

The following assumptions were made for the placement of the HGA antenna and its driving mechanisms:

<b>Assumptions</b>	
1	The S/C A attitude at the beginning and end of the fly-by (from when Relative Navigation starts until probe separation) is the most constraining due to simultaneous TT&C and the use of NavCam.
2	The HGA shall be pointed to Earth for all possible flyby geometries (e.g. heliocentric distance and solar phase angle, as defined in Table 7-3)
3	TT&C during the minutes around closest approach is assumed as not required
4	Dust profile is symmetrical for before and after closest encounter

**Table 7-13: HGA Antenna Placement Assumptions**

##### **Rationale**

Given the large array of comet encounter geometries that results from the range of heliocentric distances ( $0.9 \text{ AU} < R_c < 1.25 \text{ AU}$ ), and phase angles of Earth at encounter  $\theta$  ( $0 < \theta < 360^\circ$ ), there is no singular direction for the relative position of the Earth from S/C A at the encounter. This means that the spacecraft must be able to provide the High Gain Antenna (HGA) with a pointing freedom close to 360 degrees on the ecliptic plane. In addition, during the 2 months prior to the fly-by, it can be expected that the direction of the sun vector may vary +/- 45 degrees with respect to the normal vector of the spacecraft face that would nominally point directly into the sun, assuming that the NavCam is pointing along the relative velocity vector (i.e. pointing directly at the comet).

Providing the range of pointing required for communications to Earth can be achieved in two ways. One option would rely on slewing the spacecraft to point the HGA (which is either fixed or has a small rotation range) to Earth. However such a degree of operational freedom is challenging, as communications to Earth are required during the long EP thrusting arcs, as well as during the relative navigation to the comet nucleus and science activities, when the NavCam and instruments are pointing towards the comet. In these instances, the spacecraft attitude is strictly constrained. Note that particularly during the final months preceding the fly-by (e.g. from approximately 2 months before closest approach), the communications passes will likely be long and frequent, making such a solution unfavourable.

Instead, a pointing mechanism was selected to provide the necessary degrees of freedom given the operating constraints.

An evaluation of several options for an HGA structure/mechanism with variable levels of complexity was performed, in order to understand what would be the necessary pointing freedom required given the potential variance in encounter geometries. The assessment concluded the in order to minimise the required spacecraft slewing during the pre-fly-by phase, the antenna would be required to have a DoF of 270 degrees. Based on this, various options were evaluated.

### Options

Several design options were assessed, offering different levels of independence from the spacecraft attitude (thus requiring more or less slewing of the spacecraft).

The first option considered a fixed podium with a capability of providing an HGA FoV higher than 180 degrees. However, for the 0.9m diameter HGA, and the desired rotation DoF of 270 degrees, the analysis showed that the podium would have to be at least 1.4m high, not accounting for potential interference of the B1 and B2 probes attached to the +Z face prior to release.

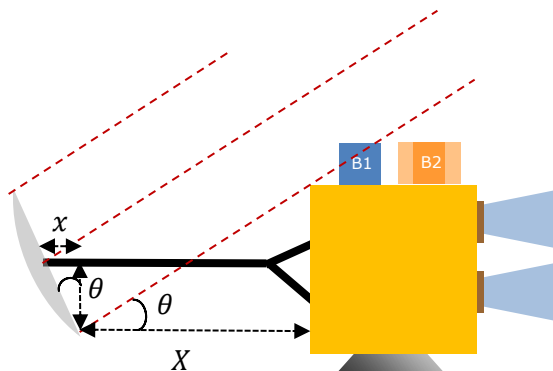


**Figure 7-6: HGA option 1 - Small mechanical pivot arm (1 DoF)**

For the second option a mechanical pivot arm with a HGA FoV of 270 degrees is considered. This option allows for the best decoupling between the spacecraft attitude and the antenna pointing requirements, not requiring any manoeuvres on the spacecraft side that could lead to losing the comet from the NavCam field of view (for some interception geometries, only a roll around the spacecraft-comet vector is required).

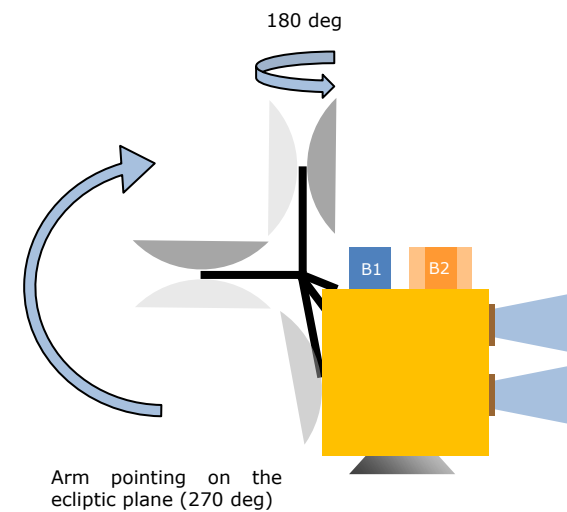


**Figure 7-7: HGA option 2 - Small mechanical pivot arm (2 DoF)**

Option 3 considers a small fixed podium with a capability of a HGA rotation of maximum 180 degrees. This reduced range allows for a reduction of the podium height, but requires the spacecraft to perform slews while losing the comet from the NavCam FoV.

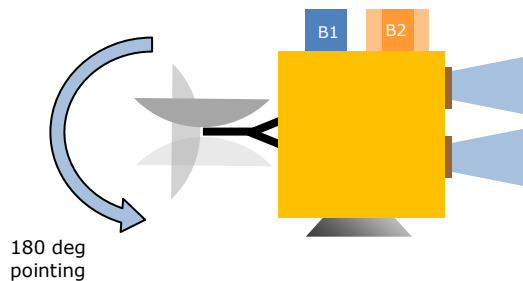


**Figure 7-8: HGA option 3 - Pivot on top of podium (1 DoF)**

Option 4 is considered to be the least complex regarding the Antenna Pointing Mechanism (APM) design, assuming a one-time deployable arm, which gives a fixed relative pointing of the HGA with respect to the spacecraft. This would require that the HGA pointing requires the spacecraft to perform slews for pointing, which has an impact on operations, relative navigation and performing science observations (as discussed above).

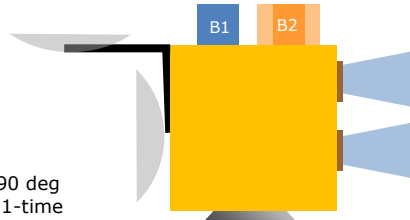


**Figure 7-9: HGA option 4 - One-time deployable arm (0 DoF)**

### Criteria

The criteria considered for this assessment are described in Table 7-14. They are presented in the decreasing order of importance assumed for the assessment.

Criteria
1 Minimization of slewing during 2 months before fly-by (when NavCam is in use)
2 Minimization of operational complexity
4 Minimization of mechanism mass
3 Minimization of mechanism cost

**Table 7-14: Criteria considered High Gain Antenna (HGA) placement and mechanisms**

### Rationale for Final selection

As the criteria with the highest weights are the ones regarding the minimisation of the required slewing and of the operational complexity, the major driver for the chosen design was to ensure HGA pointing was as independent as possible from the S/C attitude. The mass and cost penalty of going for a more complex mechanism solution is offset by the fact that risk is reduced in the relative navigation phase, while science data is maximised.

As such, Option 2 is baselined, to keep operational complexity low. This results in the HGA being stowed on the -X face (opposite to the Field of View of the optical instruments). There is still the possibility to attach the arm to the -X/+Z edge or the -X/-Z edge. The -X/-Z option is considered to avoid impingement from the electric propulsion thruster or reaction control thruster plumes.

- Stowed on -X, arm on -X/+Z



- Stowed on -X, arm on -X/-Z



**Figure 7-10: Pointing capability of the proposed HGA pointing mechanism in each of the two placement options (-X/+Z edge and -X/-Z edge)**

This option results in the attitude described in Figure 7-11 for the S/C during the fly-by. The only additional requirement on the S/C attitude coming for ensuring permanent TT&C before and after closest approach is a 180 degree roll around the S/C-comet axis during this stage. This means that in theory there would be no constraints in the geometry requiring for the S/C to point away from the comet at any time (other than the closest approach phase) to perform TT&C. It should be noted that for the duration of the closest approach, communications to Earth are assumed as not required.

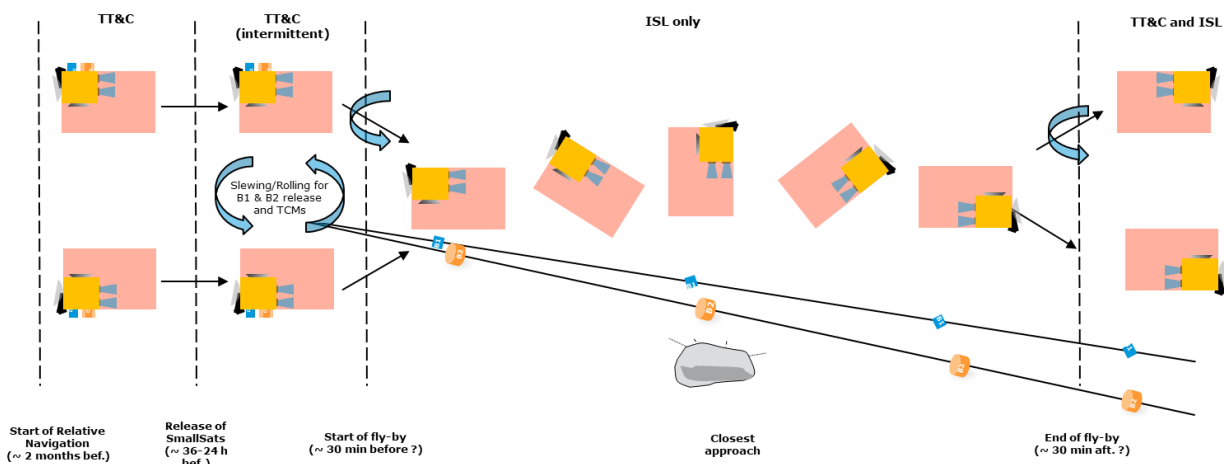


**Figure 7-11: Attitude profile during pre-fly-by, closest approach and post-fly-by**

### 7.2.1.5 Solar Array Size / Operating point of the EP thruster

#### Assumptions

The following assumptions are made for the trade-off regarding the solar array sizing with respect to the operating point for the EP thruster:

Assumptions	
1	The required EP propellant mass was computed based on a total spacecraft mass during EP thrusting as: the sum of the S/C dry mass, the CP propellant mass used during “Fly-by”, and half of the CP propellant mass used for “AOCS during Mission”
2	Solar array specific mass: 4.91 kg/sqm
3	Solar cell performance (@ 1AU) 231.18 W/sqm
4	Sizing heliocentric distance: 1 AU
5	PCDU, Harness, LCL losses taken into account (7% in total)
6	Thruster performance (Isp vs. Power) as per the baselined thruster assumption (similar to the thruster flown on SMART-1 – see Electric Propulsion Chapter for details)
7	No impacts on potential structural reinforcement for higher SA mass was taken into account

**Table 7-15: Assumptions for the Solar Array/EP Operating point sizing assessment**

### **Rationale and Options**

From the S/C power budget (Section 7.4.4), the most demanding mode is the Electric Propulsion Thrusting Mode. This is mainly due to the fact that the EP thruster consumes a significant amount of power (801 W operation point baselined, but power could go up to 1500 W). However, while increasing the power available to the EP thruster (changing its operation point) results in a higher specific impulse (Isp) and thus lower propellant mass, the larger power demand drives the sizing of the solar array (SA), which in turn increases the overall S/C mass.

Therefore, the SA sizing is directly related to the power made available for EP thruster during the EPTH mode. As such, a coupled assessment was performed to trade-off between a higher operating point for the thruster (and therefore higher power and thus solar array mass) or operating with lower thruster efficiency (lower power, and therefore lower solar array mass, but higher propellant mass).

### **Rationale for Final selection**

Based on a simple assessment at system level, Figure 7-12 shows the dependency between the mass of the combined EP propellant + SA mass against the SA area (calculated by varying the EP thruster operating points).

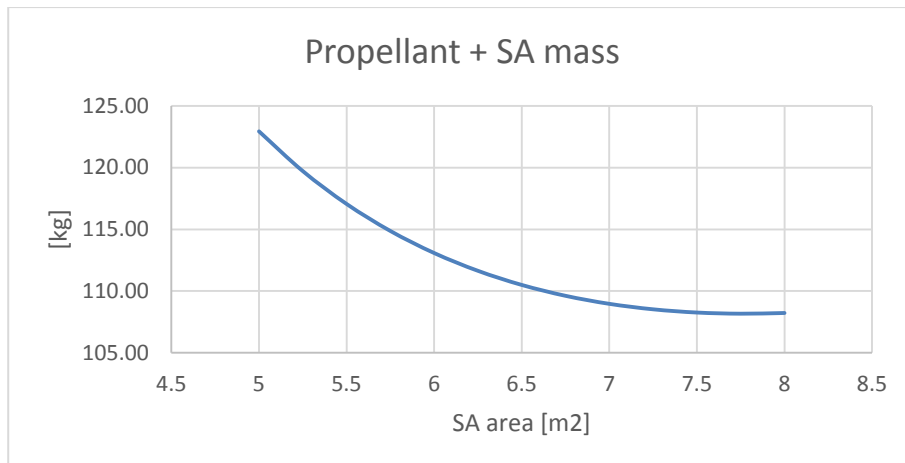


**Figure 7-12: EP propellant + SA mass vs. SA area for various EP thruster operating points**

The analysis shows that the resulting EP propellant plus SA mass is significantly higher for SA areas lower than 6 m<sup>2</sup> (1 m<sup>2</sup> decrease results in an approximate 10 kg increase in mass), leading to higher overall mass. In the range between 6 m<sup>2</sup> and 8 m<sup>2</sup>, the potential for mass savings is only in the range of around 5 kg.

From a Systems perspective, based on this sensitivity assessment, the sizing of the Power Subsystem (Chapter 15) based on the system level power budget, the SA area considered is 6 m<sup>2</sup> for the baseline.

### 7.2.2 Probe B2

#### 7.2.2.1 AOCS architecture (and S/C release mechanism)

##### Assumptions

The following assumptions are made for the trade-off for the AOCS architecture:

Assumptions	
1	Target payload pointing error less than 20 degrees during fly-by
2	No active attitude control
3	Platform spin rate of 6-15 rpm (Payload requirement)
4	Gyroscopic stability covers the uniform small particles dust field
5	Maximum moment arm = 0.03 m

**Table 7-16: Assumptions for AOCS architecture of probe B2**

##### Rationale:

The instruments on probe B2 require that the spin axis on B2 does not deviate by more than 20 degrees from the target vector. The initial target vector will be determined at the release of B2 and shall be almost parallel to the velocity vector of S/C A at B2 separation, as B2 is released in ram/anti-ram direction of S/C A. Moreover, considering the configuration and design of EnVisS, a platform spin rate of 6-15rpm is required.

In order to maintain the B2 pointing error lower than 20 degrees during fly-by in a design-to-cost approach, utilising passive and simple means (such as the inherent gyroscopic stability of B2 and an appropriate mass balancing) is necessary. These solutions can likely cover the effects of the uniform small dust particle impacts; however, they cannot provide robustness to larger single particle impacts (e.g. the 10 mg and 100 mg impacts discussed in Section 7.2.1.3 above).<sup>7</sup>

In combination with a trade-off performed by the AOCS team, a trade-off on potential solutions was also performed at system level in order to evaluate the wider system level issues of the various options.

### **Options:**

The first option ensures robustness of the design to all dust particle impacts up to 100 mg, due to including a momentum wheel of 16 Nms. It is thus the safest option. The principle of the momentum wheel solution is to spin it prior to the B2 release, using the power supply from S/C A. By reducing the power on the wheel, after release, a spin on the platform at the desired rate can be reached. However, power is needed to counter the friction torques, and maintain a steady spin. The impact of this solution for B2 in terms of mass and power would translate into 5kg additional mass as well as the 8W power consumption of the wheel at steady state. Moreover, a translational release mechanism is needed, a clampband with pushers, which adds 1 kg to B2.

The second option is very similar to the first option, the only difference between the two being the momentum capacity of the wheel, which is now reduced to 4 Nms. The impact on B2 for this solution implies a saving of 2.3 kg compared to option 2, at the cost of non-robustness to 100 mg particle for any fly-by velocities greater than 18 km/s. Moreover, the steady state power consumption is the same as the 16 Nms wheel presented above.

The third option is driven by the desire to keep B2 as simple as possible. Therefore, no additional AOCS equipment is required, and the spin required by the P/L as well as for gyroscopic stability is provided entirely by the spin-up release mechanism from S/C A. The mechanism is able to provide a spin rate of 15 rpm (equivalent to approx. 2 Nms) which ensures survivability of the B2 when exposed to the uniform dust environment but is considered not robust to 100 mg impacts. It is the cheapest, lightest and least power demanding option but implies additional risks on B2 mission. However, the spin-up release mechanism needs to be adapted based on heritage from other missions (e.g. Beagle).

The last option is embarking an active attitude control system. Additional equipment is needed for this design solution, e.g. cold gas thrusters as well as a gyro or star tracker. This solution has a cost and a mass impact for B2, which is considered particularly challenging when applying a design to cost approach for B2. Moreover, the placement of the thrusters is particularly constraining in terms of volume and plume impingement constraints for the P/L. Similarly to the other two concepts here above, a clampband with pushers is needed, which adds 1 kg to B2.

<sup>7</sup> As demonstrated in the AOCS chapter, Section 14.2.2.7.

All the considerations taken into account for each solution in the trade-off are summarised in Table 7-17.

		Momentum wheels			Active attitude control
Criteria		16Nms	4 Nms	No wheel	
<b>Mass on B2</b>		5kg	2.7kg	0 kg	Cold gas thrusters: 2-10kg Gyro: 1.5kg or Star Tracker: 0.35-1.5kg
<b>Science impact</b>		Potential issues from power on the momentum wheel could (worst case) cause EMC effects with the instruments, or general added micro vibrations from the wheels.			Potential plume impingement on the instruments during firing and additional micro-vibrations
<b>Mechanism</b>		3 kg on S/C A 1 kg on B2	3 kg on S/C A 1 kg on B2	3 kg on S/C A 1 kg on B2	3 kg on S/C A 1 kg on B2
<b>Mechanism simplicity</b>		Clampband with pushers	Clampband with pushers	Spin-up and release	Clampband with pushers
<b>TOTAL MASS on B2</b>		6 kg	3.7 kg	1 kg	Depends on solution
<b>Cost</b>		Average	Average	Good	Most expensive
<b>Power</b>		~8 W	~8 W	0 W	10-40W
<b>Dust robustness to particles of.... (nominally at 70 km/s)</b>	<b>10mg</b>	Yes	Yes	Robust only up to 35 km/s	Yes
	<b>100mg</b>	Yes	Sufficient for 100mg impact only up to 18 km/s	No	Yes

Table 7-17: Characteristics table of the B2 AOCS trade-off solutions

#### Rationale for final selection:

The active attitude control solution is robust to all dust particle scenarios up to 100 mg but impacts the mass, power, cost, complexity and P/L due to plume contamination for B2. This design option does not suit the design philosophy stated for B2. Therefore, this option is discarded. Probe B2 is envisioned to be a simple, low complexity, low redundancy and low cost probe with a short lifetime (24h). Furthermore, based on the dust impact probability assessment, the baseline mass of dust particle to be protected from is considered to be 10 mg (see Section 7.2.1.3). Hence, the 16 Nms momentum wheel (assuring robustness to 100 mg) would require oversizing B2. Considering the limited mass and power budget available for B2, the development overhead of the spin-up release mechanism and the need of robustness to all 10 mg particles, *the 4 Nms momentum wheel is the baseline for the B2*.

### 7.2.2.2 Power architecture

#### Assumptions

The following assumptions are made for the trade-off for the power architecture:

Assumptions	
1	Probe B2 has a lifetime of 24h (duration from the release of B2 to CA)
2	Platform spin rate of 6-15 rpm (Payload requirement)
3	PCDU mass = 0.4 kg, PDU mass = 0.2 kg
4	Primary Battery effective energy density = 214 Wh/kg ( <i>refers to an approximation of the energy available to the bus after losses, packing factors, DoD limits, etc</i> ) <sup>8</sup>
5	Secondary Battery effective energy density = 86 Wh/kg ( <i>refers to an approximation of the energy available to the bus after losses, packing factors, DoD limits, etc</i> ) <sup>9</sup>
6	Mass density of the solar array = 5 kg/m <sup>2</sup>
7	Effective solar array power density after 5 years in space = 216.7 W/m <sup>2</sup>
8	Peak power consumption considered for the analysis = 60.7 W (including system margin of 20%, for the breakdown per subsystem see Table 7-19 below)
9	External side wall area of B2 = 0.08 m <sup>2</sup>
10	A worst-case solar offset angle of 45 deg is used for all solar power cases

**Table 7-18: Assumptions for Power architecture**

#### Rationale

Probe B2 is a probe with a limited lifetime of ~24h (TBC). Power is required for the bus avionics, the inter-satellite link, the instruments and for the momentum wheel (discussed in Section 7.2.2.1 above). To power the spacecraft for 24 hours, several power subsystem design options with different reliability, complexity and cost are proposed, to cover all possible sources of energy generation, storage and distribution.

#### Options

Various power subsystem design options were proposed and traded-off at system level:

##### Concept A: Solar arrays + Secondary battery + PCDU.

Concept A relies on solar energy for the generation of power. The solar panels are placed on the side panels of probe B2, which would need to be added to the current design<sup>10</sup>. A secondary battery is used to store the energy produced by the solar panels, in times of surplus power generation. The secondary battery is fully charged by S/C A prior to B2 release.

##### Concept B: Solar arrays + Primary battery + Secondary battery + PCDU.

Concept B relies on solar energy for the generation of power, complemented by the energy stored in the primary battery. The solar panels are placed on the side panels of

<sup>8</sup> Note that 309 Wh/kg was used in an earlier trade-off, as discussed in the trade-off below.

<sup>9</sup> Note that 160 Wh/kg was used in an earlier trade-off, as discussed in the trade-off below.

<sup>10</sup> As there are no load-bearing side walls in the current design capable of mounting solar cells.

probe B2, which (as for Concept A) would need to be added to the current design. A secondary battery is used to store any energy surplus produced by the solar panels, and can be used to cover the peak powers of e.g. payload operations and communications. The secondary battery is fully charged by S/C A prior to B2 release.

For this option, the primary battery is designed to cover the energy shortfall not covered by the power generation of the solar panels nor by the initial state of charge of the secondary battery before release.

The sizing of the secondary battery here could be considered arbitrary, particularly for a case where the load is considered constant (e.g. constant payload and communications). As such, a sizing case was defined to cover a failure case, namely the loss of the primary battery. In this instance, the secondary battery was sized to allow a low (ca. 20 %) duty cycling of the payload and communications in the event of primary battery failure.

#### Concept C: Primary battery + PDU.

Concept C relies on a non-rechargeable battery with an energy capacity equal to the energy needs of the full B2 mission. It is important to properly evaluate the loads of each unit of B2, the margins and to take into account the inherent degradation losses of the primary battery before arrival at the comet.

#### Concept D: Solar arrays + Primary battery + PCDU.

Concept D is similar to Concept B as it also relies on solar energy for the power generation (which covers almost the bus avionics and communications) and the primary battery to cover for the remaining extra of the mission. For this design concept, a secondary battery is not included.

#### Concept E: Secondary battery + PDU.

Concept E relies solely on a rechargeable battery. The benefit is that the rechargeable battery is fully charged at B2 release whereas a primary battery is exposed to losses during the 3+ years of waiting. However considering the energy density of the rechargeable battery compared to the non-rechargeable battery, this option is likely to be higher mass than Concept C.

### **Rationale for the final selection**

The driving principles of probe B2 are: 24h mission, simple, low complexity, low mass, low cost and an increase in accepted risk.

An initial trade-off, considering higher estimates for the effective energy densities (namely 309 Wh/kg and 160 Wh/kg) led to the initial baselining of Concept C. This was selected as, for these higher effective energy densities, the effective power densities of the solar array options over 24 hours was much lower. This was particularly the case, given that the current B2 design does not include side panels, and as such supporting structure would have to be added to mount the cells.

Nonetheless, after the Study ended (and after the baselining of the Concept C), revised effective energy densities for the batteries became available, and the trade-off was performed again. The results of this trade-off are summarised here, **even though Concept C (primary batteries only) is maintained at System level and throughout the report for the B2 baseline.**

With the revised battery effective energy densities reported in Table 7-18 above, the results as indicated in Table 7-19 were obtained. Note that two cases were considered: a case with constant payload operation and communications over the full 24 hours, and a case with payload operation and communications only for the last 12 hours before closest approach.

Concept	Power architecture mass (full 24 h operations)	Power architecture mass – reduced operations (P/L + comms only last 12 h)	Other considerations
A (Solar arrays + secondary battery + PCDU)	Solar array [kg]: 3.18 Secondary battery [kg]: 8.72 PCDU [kg]: 0.40 <b>Total mass [kg]:12.30</b>	Solar array [kg]:3.18 Secondary battery [kg]:4.36 PCDU [kg]:0.40 <b>Total mass [kg]:7.94</b>	
B (Solar arrays + primary battery + secondary battery + PCDU)	Solar array [kg]:3.18 Secondary battery [kg]:0.48 Primary battery [kg]:3.31 PCDU [kg]:0.40 <b>Total mass [kg]:7.37</b>	Solar array [kg]: 3.18 Secondary battery [kg]:0.48 Primary battery [kg]:1.56 PCDU [kg]: 0.40 <b>Total mass [kg]:5.62</b>	System can provide reduced operations in event of the failure of e.g. the primary battery (e.g. approx. 20% cycling of payloads and communications).
C (Primary battery + PDU)	Primary battery [kg]:6.80 PDU [kg]:0.20 <b>Total mass [kg]:7.00</b>	Primary battery [kg]:4.99 PDU [kg]:0.20 <b>Total mass [kg]:5.19</b>	
D (Solar arrays + primary battery + PCDU)	Solar array [kg]3.18 Primary battery [kg]:3.50 PDU [kg]:0.40 <b>Total mass [kg]:7.09</b>	Solar array [kg]: 3.18 Primary battery [kg]:1.75 PDU [kg]: 0.40 <b>Total mass [kg]:5.33</b>	Despite receiving enough power from the solar arrays to power the bus avionics, the lack of a secondary battery would not allow enough power to support communications (even with payload off) for the sizing case of 45 deg solar offset. For cases with lower solar offsets, some limited duty cycling of payload and comms may be possible.
E (Secondary battery + PDU)	Secondary battery [kg]:16.93 PDU [kg]:0.20 <b>Total mass [kg]:17.13</b>	Secondary battery [kg]:12.42 PDU [kg]:0.20 <b>Total mass [kg]:12.62</b>	

**Table 7-19: Revised trade-off for power architecture mass of B2**

### **Conclusion**

Based on the earlier assumptions (higher battery effective energy densities), it seemed that solar power related concepts for B2 were less favourable, given the mass of the cells plus required supporting structure. A simple comparison of the total power architecture

mass for various solar array areas demonstrates that, under these assumptions, the primary battery case would be the most efficient solution (see Figure 7-13).

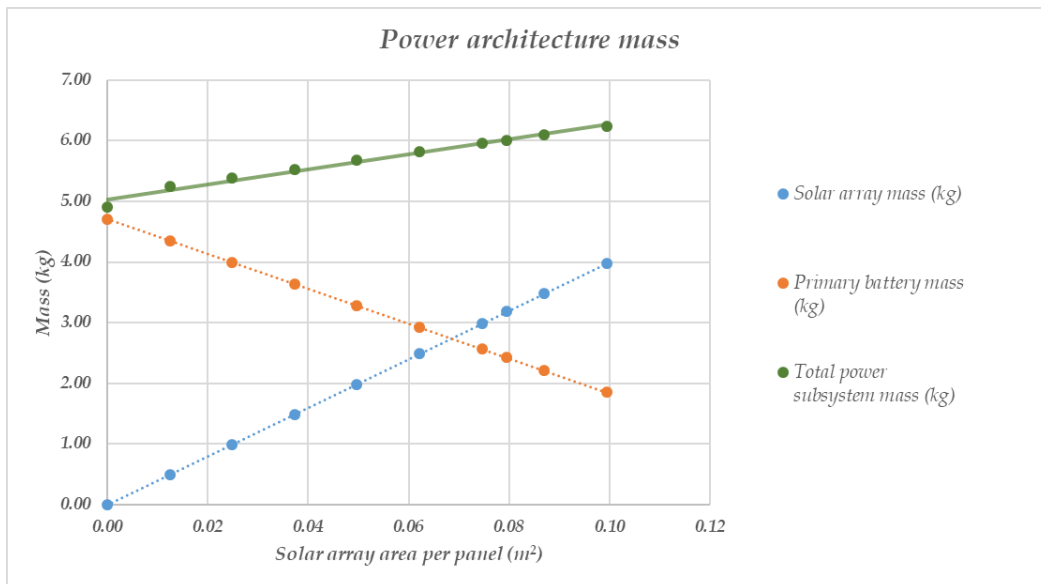


**Figure 7-13: Comparison of the power architecture mass as a function of SA area (for a 24h mission) (early assumptions)**

Based on these assumptions, **the baseline selected for the design, and as discussed in this report, was the Concept C (primary battery only) case**. Given the strict mass limitations of B2, and in order to bring the system closer to the 30 kg total mass target, a 5 kg mass limit was also imposed on the primary battery sizing. This resulted in an effective useable energy of 1068 Wh. This is broadly equivalent to the case of payload and communications only switched-on for the last 12 hours. As a result, the following “duty cycles” are considered for system sizing within this report:

Subsystem	Power ON (W)	Duty Cycle (hours)	Duty Cycle <sup>11</sup> (%)
<b>AOCS</b>	8.0	24	100%
<b>COMS</b>	13.0	13.5	56%
<b>DH</b>	5	24	100%
<b>PDU</b>	6	24	100%
<b>Instruments</b>	18.6	12	50%

**Table 7-20: Duty cycles of B2 subsystems to comply with the battery energy capacity**

<sup>11</sup> Note that the “Duty Cycle” shown here is between unit ON and OFF (not between ON and STANDBY, as typically applied in CDF reports). In addition, note that the ON power shown considers no system margin. For the calculation of the possible duty cycles within the 1068 Wh energy limit, note that a systems margin of 20% was added to the power demand.

Nevertheless, as discussed above, revised effective energy densities became available after the end of the Study, which would reduce the comparative advantage of primary battery only solutions relative to solar power-related solutions. As can be seen in Figure 7-14, for a 24 hour mission, the relative effectiveness of both solutions is comparable.

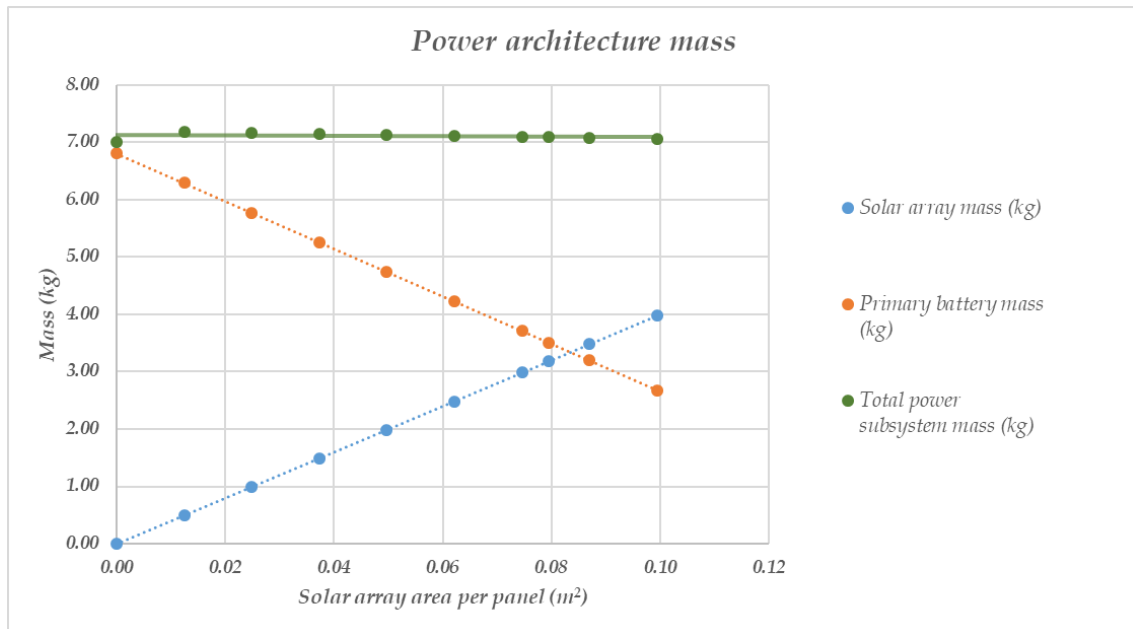


**Figure 7-14: Comparison of the power architecture mass as a function of SA area (for a 24h mission) (revised assumptions)**

These values are also supported by the comparative power architecture masses shown in Table 7-19 above. Under these revised assumptions, the power architecture masses of a case for primary battery only (Concept C) and for a case with solar panels (either with or without a secondary battery, i.e. Concepts B and D respectively) are broadly equivalent.

Considering this, the following points must also be taken into account:

- A solution relying only on one technology (e.g. primary battery) will likely be cheaper, and fits better with the “design-to-cost” approach of B2.
- Nonetheless, a solution relying only on one technology will be inherently less robust against failures during the mission.
- The addition of a secondary battery (along with the solar cells) would allow for a low payload or communications duty cycling (ca. 20%) even if the primary battery fails.
- The addition of a secondary battery (along with the solar cells) would also allow for a low payload or communications duty cycling (the same 20%) during the first 12 hours after separation, for the design case where the payloads and communications are nominally only turned on for the last 24 hours.
- Should later changes to the operational timeline result in a longer mission (>24 hours), or lower solar offset angles / distances to the Sun, then solar power-related solutions becoming more attractive.

- Conversely, should missions beyond 1.25 AU or with larger solar offset angles become part of the baseline options, solar power-related solutions become less attractive.

To summarise: the B2 baseline design considered in this report proposes a primary battery only solution, as earlier assumptions on the battery performance suggested that they were a much better option than solar array-powered solutions for this mission. A primary battery only solution would also be the option most compatible solution with the design-to-cost approach for B2. Nevertheless, on a mass basis, the revised trade-off suggests that the difference between primary battery and solar powered solutions may be much smaller than originally thought. As such, this trade-off should be re-evaluated in future phases.

### **7.2.2.3 Placement of the FGM boom and ISL antenna**

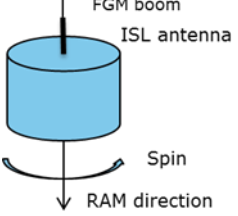
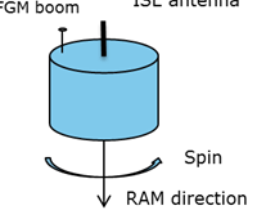
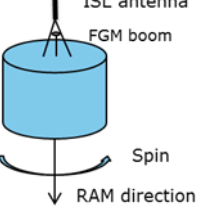
#### **Assumptions**

A trade-off regarding the placement of the ISL antenna and the FGM boom (payload magnetometer) on B2 was carried out under the following assumptions:

- Both the ISL antenna and the FGM boom are placed on the anti-RAM face of B2
- Any metallic part in the field of view of the ISL antenna has a negative impact on its performance

#### **Options**

The following configuration options were investigated. Preliminary findings are reported in Table 7-21:

Option	Configuration	Comments
<b>FGM boom on top of the ISL antenna</b>		Preliminary analysis shows that interference from the FGM boom affects the ISL performance. The option is not further retained for investigation.
<b>FGM boom on the same plane as the ISL but far away</b>		Preliminary analysis shows that interference from the FGM boom affects the ISL performance. The option is not further retained for investigation.
<b>ISL antenna on top of the FGM boom</b>		Preliminary analysis suggests that the solution could be feasible. Further analysis is required in order to establish a minimum height required for the ISL support structure.

**Table 7-21: FGM Boom and ISL Antenna Placement for B2**

### Conclusion

As discussed in the Telecommunication chapter (Section 16) and in Table 7-21 above, the current proposal is to place the ISL antenna on top of the FGM boom. However, it is noted that this may have significant RF or other (e.g. harness routing, structural) issues, which could not be assessed in detail. As such, significant further work is required to study this further, and also to investigate potential fall-back solutions.

#### **7.2.2.4 Radiation shielding**

### Assumptions

The following assumptions have been made for the trade-off for the probe B2 radiation shielding:

<b>Assumptions</b>	
1	The TIDS (Total Ionising Dose Sensitivity) for each unit in B2 is taken from the datasheet, where available.
2	For cases where the TIDS for a unit is not known, it has been assumed that the unit can withstand the TIDL seen by the internal S/C A units (namely 27.5 krad).
3	Radiation shielding can be performed at unit or spacecraft level
4	Shielding provided by other units is not taken into account
5	S/C A provides sufficient shielding in the interface ring direction for the majority of the mission
6	Al mass density = 2800 kg/m <sup>3</sup>

**Table 7-22: Assumptions for Radiation Shielding**

## **Rationale**

The B2 probe is placed on the +Z face of S/C A, using an interface ring. As a result, S/C A provides shielding for B2 only in the direction of this interface.

For mass reasons, the baseline design for B2 does not include external structural panels, and thus, there is no radiation shielding provided by the S/C external “structure”. Hence, it is important to assess the radiation levels experienced by the units, and two potential radiation shielding concepts to keep all units within their specified TIDS (Total Ionizing Dose Sensitivities). Note that other radiation effects were not considered in this analysis, and should be assessed in later phases.

## **Options**

### *Option 1 - Unit level shielding*

When a few units are sensitive to radiation and/or when the spacecraft configuration is not compact, individual shielding of the units can be considered. It allows to shield critical units/components without a great toll on the mass budget.

### *Option 2 - Probe B2 level shielding*

When most of the units are sensitive to radiation and the design is compact, shielding via external panels can provide protection to all units, with a reasonable mass impact.

For Option 1, two sub-options were assessed:

- Assuming that all units do not already include any equivalent local shielding
- Assuming that all units already include an additional 1 mm of Al shielding within their housing (which provides shielding on top of the TIDS specified for the unit)<sup>12</sup>

For Option 2, all units will experience the same TIDL behind the external shielding walls. As such, in order to size the shielding wall correctly, two sizing cases were considered (similar to the sub-options for Option 1):

- Setting the target TIDL to that assumed for the internal S/C A units (27.5 krad) and no shielding already included in the units mass.
- Setting the target TIDL to that assumed for the internal S/C A units (27.5 krad) but assuming 1 mm shielding already included in the units mass.

## **Model and TIDS description**

The TIDL after Al shielding are as reported in Chapter 6.3.1.1. A Radiation Design Margin of 2 has been applied, as specified in RD[17]. For the shielding mass estimations for Option 1, the thickness of Al needed per unit to meet the TIDS is added on all unit faces but the one placed in the interface direction. For Option 2, the probe B2 top and radial faces are designed with the additional shielding, but no shielding is considered as required for the interface plate to S/C A.

<sup>12</sup> I.e. if the TIDS for a unit suggests that it would require 4 mm of Al shielding for the estimated TIDL, an equivalent of 1 mm Al shielding is assumed to be provided by the unit housing. As such, the additional shielding mass would consider that only a further 3 mm Al must be provided.

Table 7-23 shows the list of radiation sensitive equipment considered in the analysis and their respective TIDS:

B2 unit	TIDS (krad)
Reaction Wheel	20
Inter Satellite Link Electronics	20
Onboard Computer & Power Distribution Unit	27.5 ( <i>assumed</i> )
DFP Dust Impact Sensor and Counter	27.5 ( <i>assumed</i> )
DFP Electronics Box	27.5 ( <i>assumed</i> )
EnVisS (Entire Visible Sky)	27.5 ( <i>assumed</i> )
OPIC (Optical Imager for Comets)	27.5 ( <i>assumed</i> )
Primary Battery	4000

**Table 7-23: B2 units TIDS for radiation shielding estimation**

### **Rationale for final selection**

#### *Option 1: the unit-level shielding concept*

If the unit masses do not include any shielding then the overall additional shielding mass is **4.22 kg**.

If the unit masses already include 1mm Al shielding then the overall additional shielding mass is **2.79 kg**.

#### *Option 2: the B2-level shielding concept*

For shielding up to **27.5 krad** TIDS, and no unit level shielding, the overall additional mass is **4.69 kg**.

For shielding up to **27.5 krad** TIDS, and 1 mm of unit level shielding already included, the overall additional mass is **3.02 kg**.

Considering the mass impact of all assessed options, it is clear that efforts should be undertaken to better understand the TIDS of units with missing values, and/or to assess units with greater radiation hardness. In particular the instrument TIDSs need to be refined, as only preliminary assumptions regarding TIDS were available at the time of the study. In particular, for the units with missing TIDS values, it should be considered that many CubeSat COTS components might be sensitive to TIDS of 20 krad, and as such the above values might be optimistic.

In any case, the above analysis suggests a trend that unit-level shielding will be preferable in all cases, and as such it was decided to baseline the unit level shielding concept.

*Note: a further trade-off is recommended in later phases, to consider whether some of the mass required for shielding could be regained by also using the required shielding (applied as external panels) to mount solar cells.*

## 7.3 Mission System Architecture

### 7.3.1 Mission Profile

The Comet Interceptor mission is designed for a 5 years mission lifetime with up to 6 months of nominal science operations after encounter. Based on the overall mission concept, the mission timeline is highly dependent on finding a suitable target and the planned fly-by encounter. The main mission phases are schematically shown in Figure 7-15 below:

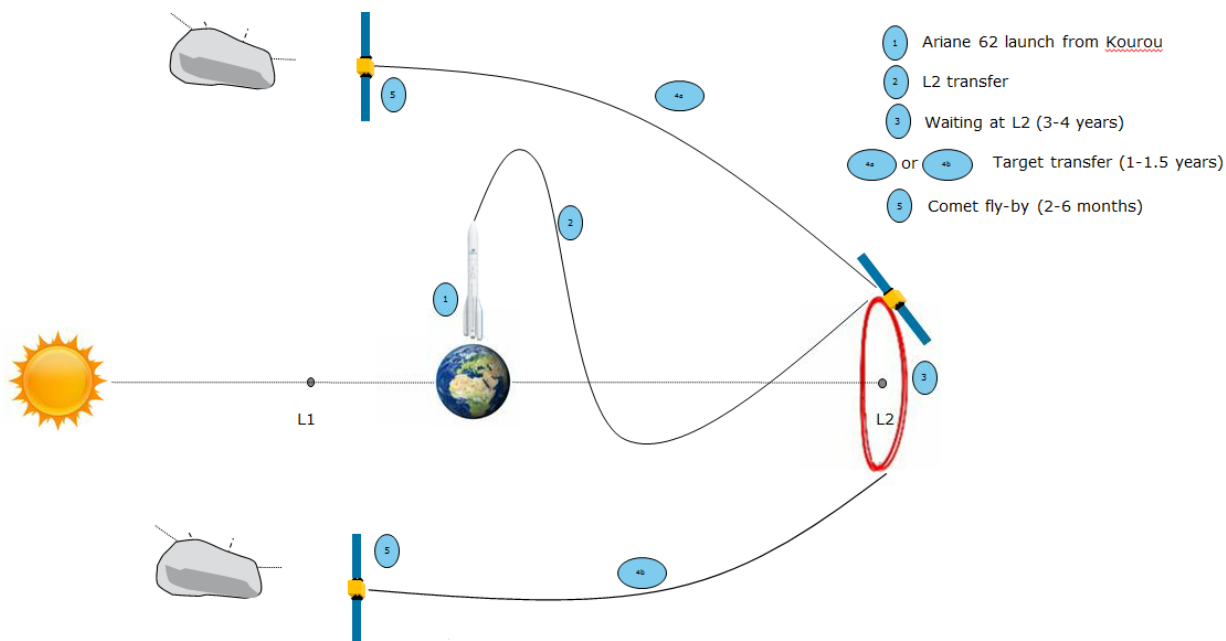


**Figure 7-15: Comet Interceptor Mission Profile**

The Fly-by phase is assumed to start 2–6 months before Closest Approach (CA) and is marked by the start of relative navigation to the comet. Approximately 56 hours before the spacecraft reaches the minimum distance to the comet, operations start becoming more active, and a more detailed timeline was derived (Figure 7-16) during which both probes are released and nominal science operations are performed.

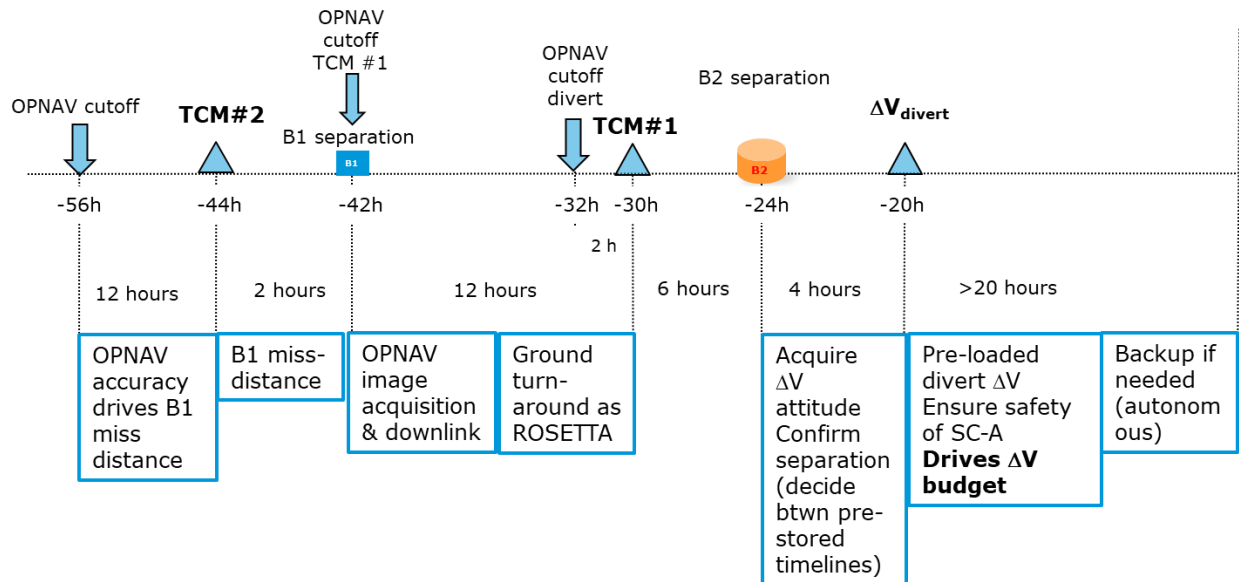


**Figure 7-16: Comet Interceptor Fly-by Timeline (from -56 hours up to 0 hours – Closest Approach)**

The geometry of the spacecraft and probes (A, B1 and B2) with respect to the comet during the Fly-by phase (with a focus on the closest approach) is presented in Figure 7-17.

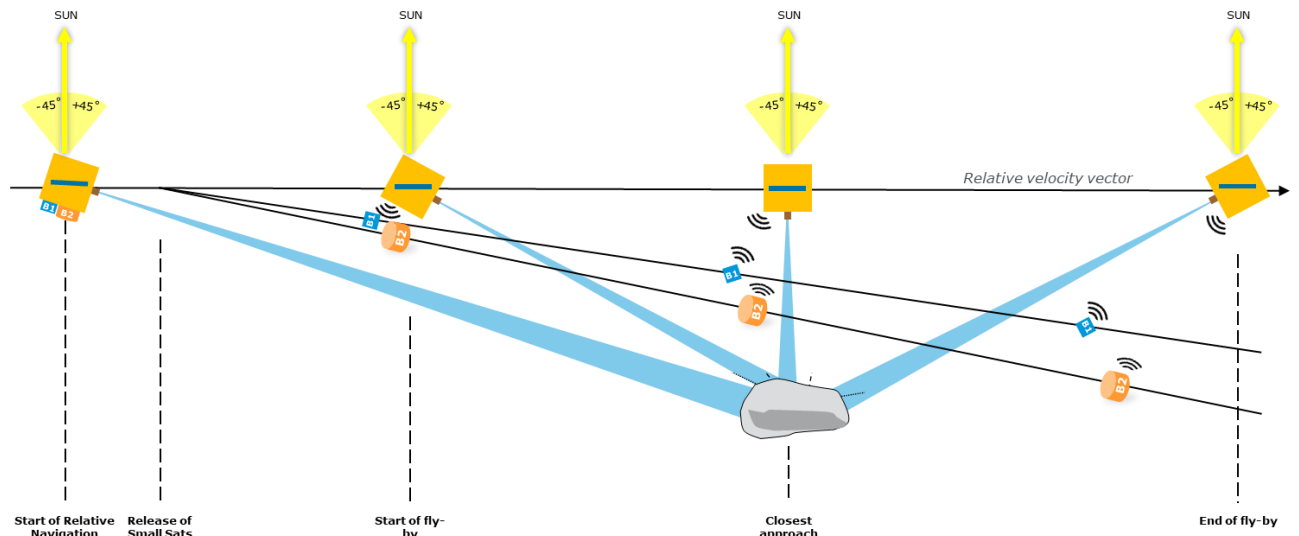


**Figure 7-17: Comet Interceptor Fly-by and Closest Approach Geometry**

### 7.3.2 System Modes

System mode	System mode description
<b>Launch Mode (LAU)</b>	From launch to spacecraft separation. Most equipment OFF (OBC and receiver potentially ON)

<b>System mode</b>	<b>System mode description</b>
<b>Sun Acquisition Mode (SUN)</b>	From spacecraft separation up to Sun pointing attitude Minimum units are ON (Sun sensors, TT&C up- and down-link via LGA) Instruments are OFF
<b>Safe Mode (SAFE)</b>	Minimum units ON to ensure prolonged safe state and communications to facilitate coming back to a nominal mode Instruments are OFF
<b>Standby Mode (STBY)</b>	Applicable when not thrusting, communicating with Earth, nor acquiring science data Instruments are OFF Most platform units are ON
<b>Communication Mode (COM)</b>	Applicable for communication with Earth Most platform units are ON and transmitter is ON
<b>EP Thrusting Mode (EPTH)</b>	Applicable for reaching the target object Instruments are OFF Most platform units are ON and EP thruster is ON
<b>Science Mode (SCI)</b>	Applicable for science acquisition during the fly-by at encounter Instruments are ON Most platform units are ON

**Table 7-24: System Modes**

## 7.4 System Baseline Design

### 7.4.1 System Decomposition

The breakdown of the Comet Interceptor system follows the classical decomposition into space segment, ground segment and launch segment.

The space segment is composed of three elements: one main S/C (S/C A) under ESA's responsibility and two probes, JAXA's probe (B1) and ESA's probe (B2), carried as payloads.

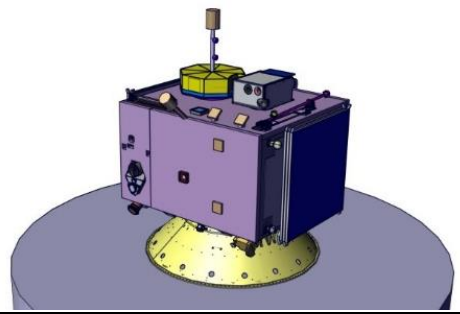
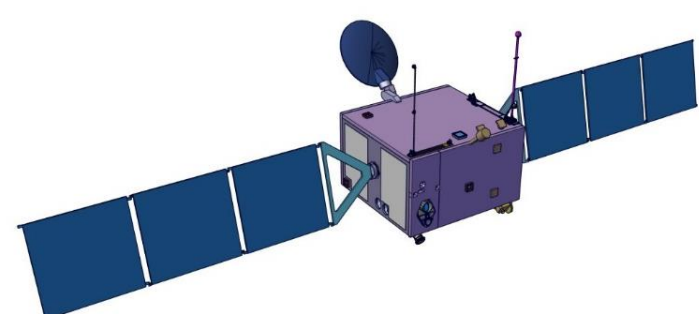
The ground segment is composed of two elements: the Mission Operations Centre (MOC) and the ESTRACK ground station network.

For B1, JAXA will provide a separate Mission Operations Centre.

The launch segment is composed of the baseline launcher Ariane 62 (as a dual launch with ARIEL).

### 7.4.2 Design Summary

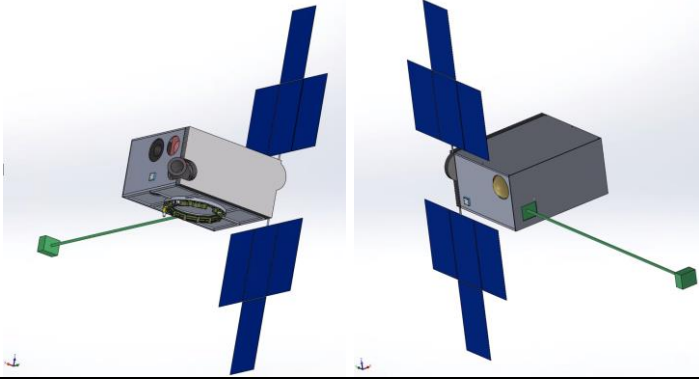
Table 7-25 shows the main characteristics of the S/C A baseline design.

Main S/C (S/C A, ESA) – System baseline summary		
Configuration stowed		
Configuration deployed		
Mass	Dry Mass (w/ margin)	655 kg
	Wet Mass	796 kg (incl. probes B1 and B2)
Dimensions	Stowed	1,974 mm x 2,073 mm x 1,976 mm
	Deployed	9,768 mm x 2,999 mm x 2,484 mm
Instruments	CoCa, DFP, MANiac (with rotating mechanism) and MIRMISS	
AOCS	6x Sun sensors (SS) 2x Star trackers (STR) 2x Inertial Measurement Unit (IMU) 2x Navcam 4x 4 Nms / 0.215 Nms Reaction Wheels (RW)	
Communications	1x 0.9 m diameter steerable X-band High Gain Antenna (HGA) 2x X-band Low Gain Antenna (LGA) 2x X-band Deep Space Transponder (DST) 2x S-band Inter-Satellite Link (ISL) transceivers 6x S-band ISL Low Gain Antenna (LGA)	
Data Handling	1x On-Board Computer (OBC) 1x Remote Interface Unit (RIU)	
Power	2x 3 m <sup>2</sup> solar arrays 1x Power Conversion and Distribution Unit (PCDU): MPPT for 28V non-regulated bus 1x 512 Wh Secondary Battery	
Chemical Propulsion	Monopropellant (Hydrazine) blow-down system 4(+4)x 5N thrusters 2x 33 L Hydrazine tank (usable)	

Electrical Propulsion	1x PPS-1350 Hall effect thruster 2x 32 L Xenon tank (usable)
Thermal	Radiators, SLI and MLI, heat pipes, paints, heaters and thermistors
Structures	Aluminium skin and honeycomb core central shear, side, baseplate and top panels Varying thicknesses of Al and honeycomb depending on the panel's shielding necessity. Primary micrometeoroid shielding on 3 panels.
Mechanisms	1x Launcher separation mechanism 1x B1 linear-separation mechanism 1x B2 linear-separation mechanism 1x 2 degrees of freedom Antenna Pointing Mechanism (APM) 2x Solar Array Driving Mechanism (SADM) 8x Solar panel Hold Down and Release Mechanism (HDRM)

**Table 7-25: S/C A summary**

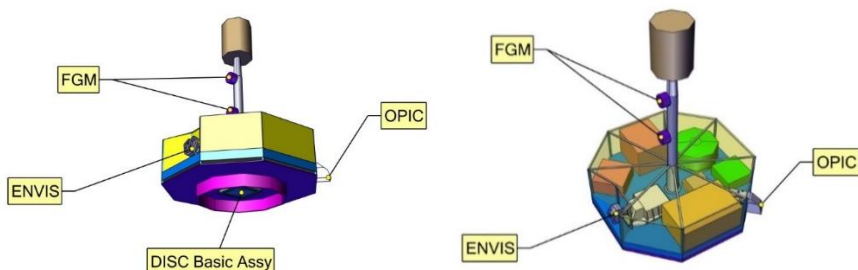
Table 7-26 shows the main characteristics of the probe B1 baseline design.

Probe B1 (JAXA) – System baseline summary		
Configuration		
Mass allocation	30 kg (including separation mechanism on B1 <b>and</b> A)	
Dimensions	Stowed	576 mm x 426 mm x 300 mm
	Deployed	1616 mm x 1489 mm x 534 mm
Instruments	HI, PS, WAC, Ion Mass Spectrometer & Deployable Magnetometer	

**Table 7-26: Probe B1 summary**

The baseline for probe B1 (JAXA) is a 3-axis stabilised satellite. The dimensions are based on a 24U cubesat design. The separation mechanism is attached to the bottom plane. HI and NAC have relatively narrow FoVs, whereas WAC has an approx. 45 deg half angle FoV. Those FoV shall not point directly at the Sun. The boresights of the two ISL antennas are, respectively, on the ram and anti-ram faces before closest approach. The boom of the magnetometer is deployable. The dust bumper shall be placed towards the relative velocity direction. The two solar arrays are mounted on 1-axis gimbals. JAXA is considering including a propulsion module.

Table 7-27 shows the main characteristics of the probe B2 baseline design.

Probe B2 (ESA) – System baseline summary	
Configuration	
Mass allocation	40 kg (including separation mechanism on B2)
Dimensions	851 mm x 600 mm x 600 mm
Payload	DFP, EnVisS, FGM and OPIC
AOCS	1x momentum wheel
Communications	1x S-band Inter-Satellite Link (ISL) 1x S-band toroidal antenna
Data Handling	1x On-board Computer (OBC)
Power	1x 1546 W.h Primary Battery 1x Power Distribution Unit (PDU)
Thermal	Radiators, SLI and MLI, paints, heaters and thermistors
Structures	Aluminium baseplate stiffened with Aluminium ribs and side walls MLI tent & Communication antenna support structure
Mechanisms	1x B2 linear-separation mechanism

**Table 7-27: Probe B2 summary**

#### 7.4.3 Mass Budget

The mass budget for both S/C A and probe B2 is presented in this section. Both account for a 5% allocation for harness as well as an overall 20% system margin.

It shall be noted that no mass allocation was considered for the launch adapter.

For S/C A, the breakdown by subsystem can be found in Table 7-28. Additional propellant tank shielding was considered for protecting from high impact velocity of dust particles. The mass of both probes was also taken into account in the S/C A budget, as they will remain attached for the majority of the mission. Mass for the propellants and pressurant was also taken into account to get the Total Wet Mass, as well as 2% margins to account for the residuals.

	Mass (kg)	
AOGNC		26.53
COM		33.47
CPROP		22.44
DH		19.43
EPROP		38.56
INS		37.07
MEC		33.41
PWR		57.93
STR		164.01
TC		12.96
Tank shielding		3.84
Dry Mass SC_B1		30.00
Dry Mass SC_B2		40.47
Harness	5%	26.00
<b>Dry Mass</b>	<b>546.10</b>	
System Margin	20%	109.22
<b>Dry Mass incl. System Margin</b>	<b>655.32</b>	
CPROP Fuel Mass		47.47
CPROP Fuel Margin	2%	0.95
CPROP Pressurant Mass		0.80
CPROP Pressurant Margin	2%	0.02
EPROP Fuel Mass		90.06
EPROP Fuel Mass Margin	2%	1.80
<b>Total Wet Mass</b>	<b>796.42</b>	

**Table 7-28: S/C A mass budget**

For probe B2, the breakdown by subsystem can be found in Table 7-29. Additional radiation shielding was considered. Structural mass for the ISL antenna support in B2 was not assessed (see Section 7.2.2.3 above).

	Mass (kg)	
AOGNC		2.84
COM		1.04
DH		1.10
INS		5.69
MEC		1.05
PWR		6.36
STR		6.20
TC		1.56
Radiation Shielding		6.29
Harness	5%	1.61
<b>Dry Mass</b>		<b>33.73</b>
System Margin	20%	6.75
<b>Dry Mass incl. System Margin</b>		<b>40.47</b>

**Table 7-29: Probe B2 mass budget**

Note that as per the considerations in the B2 radiation shielding analysis (section 7.2.2.4), a mass reduction of 3.5 kg (incl. margins) in B2 is to be considered, although not taken into account in the mass budget here presented.

In addition, the A/B2 interface was double counted in the budgets for both S/C A and B2, resulting in an additional reduction of 2 kg (incl. margins), also not taken into account in the mass budget here presented.

Hence, the final mass for probe B2 (iterated beyond the end of the Study) would consider a B2 system mass (incl. margins) of **35 kg**. Note that the earlier value of 40.47 kg was retained in the S/C A mass budget for consistency with the assumptions used by all subsystems.

	Mass (kg)	
AOGNC	2.84	
COM	1.04	
DH	1.10	
INS	5.69	
MEC	1.05	
PWR	6.36	
STR	6.20	
TC	1.56	
Radiation Shielding	2.79	
Harness	5%	0.53
<b>Dry Mass</b>	<b>29.16</b>	
System Margin	20%	5.83
<b>Dry Mass incl. System Margin</b>	<b>35</b>	

**Table 7-30: Revised probe B2 mass budget**

#### 7.4.4 Equipment List

The Equipment list of the Comet Interceptor study is presented in Table 7-31, for both S/C A and probe B2, listed by subsystem. For Spacecraft B1 only a mass allocation for the spacecraft is presented.

	Qty.	Mass (kg)	Mass Margin (%)	Mass incl. Margin (kg)
<b>SC_A (Spacecraft A)</b>				
<b>AOGNC</b>		<b>25.262</b>		<b>26.525</b>
A_DPU (A DTU Data Processing Unit)	1	0.560	5	0.588
A_IMU_LN200 (A IMU Northrop Grumman LN200 Core)	2	1.500	5	1.576
A_NAVCAM_OH (A DTU NAVCAM Optical Head )	2	0.752	5	0.790
A_STR_OH (A DTU STR Optical Head )	2	0.700	5	0.735
A_SUN_LENS_Bison64 (A SUN LENS Bison 64)	6	0.150	5	0.158
RW_RSI_4_215 (A RW Rockwell Collins RSI 4-215)	4	21.600	5	22.680
<b>COM</b>		<b>30.156</b>		<b>33.466</b>
XDST (X-Band DSTRASP)	2	7.200	5	7.560
XHGA (X-Band HGA)	1	6.050	10	6.655
XLGA (X-Band LGA)	2	0.600	5	0.630
XRFDN (X-Band RFDN)	1	10.000	20	12.000
XTWT (X-Band TWT)	2	1.600	5	1.680
XTWTA_EPC (X-Band TWTA EPC)	2	2.800	5	2.940

A_ISL_GOMx_board (A GOMx Electronics)	2	1.006	5	1.056
A_ISL_GOMx_Patch (A GOMx Antenna Patch)	6	0.900	5	0.945
<b>CPROP</b>		<b>20.940</b>		<b>22.437</b>
A_Lat_Val (A Latch Valves)	2	1.100	5	1.155
A_Pass_Valve (A Passivation_Valve)	1	0.070	5	0.074
A_Pipes (A Pipes)	1	3.000	20	3.600
A_Press_Trans (A Pressure Transducer)	3	0.660	5	0.693
A_Prop_Filt (A Propellant Filter)	1	0.110	5	0.116
A_Fil_Dr_Val (A Fill Drain Valve)	2	0.140	5	0.147
A_Test_Port (A Test_Ports)	2	0.140	5	0.147
A_Tk_CPROP (A Tank CPROP)	2	11.800	5	12.390
A_Thr_5N (A Thruster_MONARC 5N)	8	3.920	5	4.116
<b>DH</b>		<b>18.500</b>		<b>19.425</b>
A_OBC (A Onboard Computer)	1	6.500	5	6.825
A_RIU (A Remote Interface Unit)	1	12.000	5	12.600
<b>EPROP</b>		<b>36.725</b>		<b>38.561</b>
A_PPU (A Power Processing Unit)	1	10.660	5	11.193
A_Thruster_PPS1350 (A Thruster PPS1350)	1	4.350	5	4.568
A_BPRU (A BPRU)	1	2.750	5	2.888
A_FU (A FU)	1	0.675	5	0.709
A_Miscellaneous (A Miscellaneous)	1	3.500	5	3.675
A_PRE_Card (A PRE Card)	1	1.270	5	1.334
A_XFC (A XFC)	1	0.820	5	0.861
A_Prop_Tank (A Propellant Tank)	2	12.700	5	13.335
<b>INS</b>		<b>30.940</b>		<b>37.068</b>
A_CoCa_CSU (A CoCa Camera Support)	1	6.850	20	8.220
A_CoCa_ELU (A CoCa Electronics Unit)	1	2.100	20	2.520
A_DFP_DISC (A DFP Dust Impact Sensor and Counter)	1	0.350	20	0.420
A_DFP_E_Box (A DFP E-Box)	1	4.940	20	5.928
A_MIRMISS_TIRI (A MIRMISS Thermal InfraRed Imager)	1	5.600	20	6.720
A_DFP_SCIENA_ENA (A DFP Solar wind and Cometary Ions and Energetic Neutral Atoms-ENA sensor)	1	0.900	20	1.080
A_DFP_SCIENA_Ion (A DFP Solar wind and Cometary Ions and Energetic Neutral Atoms-Ion sensor)	1	0.000	0	0.000
A_DFP_LEES_1 (A DFP Low Energy Electron Spectrometer 1)	1	0.800	20	0.960
A_CoCa_PEU (A CoCa Proximity Electronics Unit)	1	0.850	20	1.020
A_CoCa_Rad (A CoCa Radiator)	1	0.200	5	0.210
A_DFP_COMPLIMENT_p_1 (A DFP COMetary Plasma Light Instrument probe #1)	1	0.000	0	0.000
A_MANiac_ELU (A MANiac Electronics Unit)	1	3.500	20	4.200
A_MANiac_NDG (A MANiac Neutral Density Gauge)	1	0.200	20	0.240
A_MANiac_SHU (A MANiac Sensor Head Unit)	1	0.900	20	1.080
A_MIRMISS_MIR (A MIRMISS Mid-InfraRed Sensor)	2	0.000	0	0.000

A_MIRMIS_NIR (A MIRMIS Near InfraRed Sensor)	1	0.000	0	0.000
A_MIRMIS_Rad (A MIRMIS Radiator)	1	0.200	5	0.210
A_DFP_COMPLIMENT_boom_1 (A DFP COMetary Plasma Light Instrument boom 1)	1	0.300	20	0.360
A_DFP_COM_FGM_boom_2 (A DFP COMPLIMENT+FGM+boom_2)	1	1.700	20	2.040
A_MANiaC_Harn (A MANiaC Harness)	1	0.350	20	0.420
A_MANiaC_Mec (A MANiaC Rotating Mechanisms)	1	0.500	20	0.600
A_CoCa_Harn (A CoCa Harness)	1	0.350	20	0.420
A_CoCa_MLI (A CoCa Thermal Insulation)	1	0.350	20	0.420
<b>MEC</b>		<b>31.100</b>		<b>33.405</b>
A_APM_HDRM_APME (A Antenna Pointing Mechanisms Subsystem with Driver and HDRM)	1	13.100	5	13.755
A_SA1_HDRM_1 (A SA1 HDRM #1)	8	4.000	10	4.400
A_SADM_1 (A SADM #1)	2	8.000	10	8.800
A_SADE (A SA drive electronics)	1	3.000	10	3.300
A_Clamp_Band (A Clamp Band Ejection System)	1	3.000	5	3.150
<b>PWR</b>		<b>52.660</b>		<b>57.926</b>
A_SA (A SolarArray)	2	29.260	10	32.186
A_Bat (A Battery)	1	4.900	10	5.390
A_PCDU (A PCDU)	1	18.500	10	20.350
<b>STR</b>		<b>136.676</b>		<b>164.011</b>
A_Misc_STR (A Miscellaneous STR)	1	5.000	20	6.000
A_RCS_Structure (A RCS Suport)	1	0.770	20	0.924
A_SecondarySTR (A Secondary Structure)	1	10.000	20	12.000
A_Inserts (A Inserts)	1	4.000	20	4.800
A_ShearW (A ShearWebs)	1	3.810	20	4.572
A_SA_yoke_1 (A Solar Array Yoke #1)	2	2.000	20	2.400
A_Baseplate (Baseplate)	1	28.880	20	34.656
A_ExtPanels_1 (A Closure Panels #1)	1	19.606	20	23.527
A_ShieldingPanels_1 (A ShieldingPanels #1)	1	59.610	20	71.532
A_PL_Panel (Payload Support Panel)	1	3.000	20	3.600
<b>SYE</b>		<b>3.200</b>		<b>3.840</b>
A_tank_shields (A_tank_shields)	4	3.200	20	3.840
<b>TC</b>		<b>10.800</b>		<b>12.960</b>
A_TC_FILLER (A TC Thermal Filler)	1	0.250	20	0.300
A_TC_HEATER (A TC Heater)	1	0.500	20	0.600
A_TC_MLI (A TC Multi Layer Insulation)	1	5.000	20	6.000
A_TC_PAINT (A TC Paint)	1	2.000	20	2.400
A_TC_RAD (A TC Radiator Panel)	1	1.000	20	1.200
A_TC_SO (A TC Stand Offs)	1	0.050	20	0.060
A_TC_STRAP (A TC Thermal Strap)	1	0.500	20	0.600
A_TC_T_SENS (A TC Temperature Sensor)	1	0.500	20	0.600
A_TC_HP (A TC Heat Pipes)	1	1.000	20	1.200

<b>SC_B1 (Spacecraft B1)</b>		<b>25.000</b>		<b>30.000</b>
SYE		25.000	20	30.000
<b>SC_B2 (Spacecraft B2)</b>		<b>27.433</b>		<b>32.122</b>
<b>AOGNC</b>		<b>0.000</b>		<b>0.000</b>
RW_RW250 (RW Astrofein RW250)	1	2.700	5	2.835
<b>COM</b>		<b>0.985</b>		<b>1.039</b>
ISL_T_LGA (ISL_ToroidalLGA)	1	0.514	5	0.540
B2_ISL_GOMx_board (B2 GOMx Electronics)	1	0.371	5	0.390
B2_ISL_GOMx_ActiveFE (B2 GOMx Active Antenna FE)	1	0.100	10	0.110
<b>DH</b>		<b>1.000</b>		<b>1.100</b>
B2_OBC (B2 Onboard Computer)	1	1.000	10	1.100
<b>INS</b>		<b>4.738</b>		<b>5.686</b>
B2_DFP_DISC (B2 DFP Dust Impact Sensor and Counter)	1	0.350	20	0.420
B2_DFP_E_Box (B2 DFP E-Box)	1	2.240	20	2.688
B2_EnvVisS (B2 Entire Visible Sky)	1	0.998	20	1.198
B2_OPIC (B2 Optical Imager for Comets)	1	0.350	20	0.420
B2_DFP_FGM_sensor(B2 DFP FGM )	2	0.260	20	0.312
B2_DFP_FGM_boom (B2 DFP FGM boom)	1	0.540	20	0.648
<b>MEC</b>		<b>1.000</b>		<b>1.050</b>
B2_Clamp_Band (B2 Clamp Band Ejection System)	1	1.000	5	1.050
<b>PWR</b>		<b>5.300</b>		<b>6.360</b>
B2_PDU (B2 PDU)	1	0.300	20	0.360
B2_Bat_1 (B2 Battery #1)	1	5.000	20	6.000
<b>STR</b>		<b>5.170</b>		<b>6.204</b>
B2_Baseplate (Baseplate B2)	1	2.622	20	3.146
B2_MLI_Tent_1 (MLI Tent B2 #1)	1	0.620	20	0.744
B2_Bumper (B2 bumper)	1	0.367	20	0.440
B2_COM_SupportSTR (COM_SupportSTR)	1	0.154	20	0.185
B2_IF_Ring (IF Ring B2)	1	1.407	20	1.688
<b>SYE</b>		<b>5.240</b>		<b>6.288</b>
B2_rad_shield (B2 Radiation Shielding)	1	5.240	20	6.288
<b>TC</b>		<b>1.300</b>		<b>1.560</b>
B2_TC_FILLER (B2 TC Thermal Filler)	1	0.050	20	0.060
B2_TC_HEATER (B2 TC Heater)	1	0.100	20	0.120
B2_TC_MLI (B2 TC Multi Layer Insulation)	1	0.600	20	0.720
B2_TC_PAINT (B2 TC Paint)	1	0.150	20	0.180
B2_TC_RAD (B2 TC Radiator Panel)	1	0.070	20	0.084
B2_TC_SO (B2 TC Stand Offs)	1	0.030	20	0.036
B2_TC_STRAP (B2 TC Thermal Strap)	1	0.100	20	0.120
B2_TC_T_SENS (B2 TC Temperature Sensor)	1	0.200	20	0.240

**Table 7-31: Equipment list**

#### 7.4.5 Power Budget

The power budget for Comet Interceptor 2 was assessed for both the S/C A, as well as for the B2 probe. The sizing cases are based on the System modes described in section 7.3.2.

The power budget for S/C A is presented in Table 7-32, and includes losses for the PCDU, Harness and LCLs. Additionally, survival heating power to be provided by S/C A to the probes while they remain attached to the main S/C is also considered in this power budget, in the relevant modes.

In addition, a 20% overall system margin was added to each mode's total power, except for the EPTH mode. In this specific mode, the EP thruster power is subtracted from the total power, as the thruster is physically not able to sustain a 20% increase in power requirement.

Please note that due to a misalignment in assumptions, the consumed power allocation for the PCDU in Spacecraft A considered in this budget (30 W) does not exactly match the assumption presented in the Power chapter (45 W).

A	LAU	SUN	SAFE	STBY	COM	EPTH	SCI
Total	0.0	273.4	314.4	262.9	484.3	1048.8	409.6
Survival heater B1	0.0	20.0	20.0	20.0	20.0	20.0	0.0
Survival heater B2	0.0	20.0	20.0	20.0	20.0	20.0	0.0
Losses PCDU	3%	9.4	10.6	9.1	15.7	32.7	12.3
Losses Harness	3%	9.4	10.6	9.1	15.7	32.7	12.3
Losses LCLs	1%	3.1	3.5	3.0	5.2	10.9	4.1
<b>Total w/ losses</b>	<b>0.0</b>	<b>335.3</b>	<b>379.2</b>	<b>324.1</b>	<b>561.0</b>	<b>1165.0</b>	<b>438.2</b>
						<b>363.4</b>	
System Margin	20%	0.0	67.1	75.8	64.8	112.2	72.7
<b>Total incl. Margin</b>		<b>0.0</b>	<b>402.3</b>	<b>455.0</b>	<b>388.9</b>	<b>673.2</b>	<b>1237.7</b>
							<b>525.9</b>

Table 7-32: S/C A power budget<sup>13</sup>

Please note that due to a misalignment in assumptions, the consumed power allocation for the PCDU in S/C A considered in this budget and in the remainder of the current chapter (30 W) does not exactly match the assumption presented in the Power chapter (45 W).

<sup>13</sup> As described in the text, the system margin of 72.7 W for the EPTH mode is calculated as 20% of the total power excluding the EP thruster, which is the 363.4 W shown.

A	LAU	SUN	SAFE	STBY	COM	EPTH	SCI
Total	0.0	288.4	329.4	277.9	499.3	1063.8	424.6
Survival heater B1	0.0	20.0	20.0	20.0	20.0	20.0	0.0
Survival heater B2	0.0	20.0	20.0	20.0	20.0	20.0	0.0
Losses PCDU	3%	0.0	9.9	11.1	9.5	16.2	33.1
Losses Harness	3%	0.0	9.9	11.1	9.5	16.2	33.1
Losses LCLs	1%	0.0	3.3	3.7	3.2	5.4	11.0
<b>Total w/ losses</b>	<b>0.0</b>	<b>351.3</b>	<b>395.2</b>	<b>340.2</b>	<b>577.0</b>	<b>1181.0</b>	<b>454.2</b>
						<b>379.4</b>	
System Margin	20%	0.0	70.3	79.0	68.0	115.4	75.9
<b>Total incl. Margin</b>		<b>0.0</b>	<b>421.6</b>	<b>474.3</b>	<b>408.2</b>	<b>692.5</b>	<b>1256.9</b>
							<b>545.2</b>

**Table 7-33: Updated S/C A power budget**

The power budget for probe B2 is presented in Table 7-34, and includes losses for the PCDU, Harness and LCLs. The only mode considered was Science (SCI) Mode, since B2 is operating only during the Fly-by phase. Periodic checks and calibrations prior to release were not assessed.

The B2 power demand for the SCI mode includes duty cycling on the equipment, (namely communications and instruments), which are assumed to not need to be operating continuously at peak power during the complete 24 h time after release (see Section 7.2.2.2, in particular Table 7-20, for more information).

B2	SCI
Total	35.6
Losses Regulation	1.8
Losses Harness	1.1
Losses LCLs	0.4
<b>Total w/ losses</b>	<b>38.8</b>
System Margin	7.8
<b>Total incl. Margin</b>	<b>46.6</b>

**Table 7-34: Probe B2 power budget**

At unit level, the power budget breakdown per mode for both S/C A and probe B2 is presented Table 7-35, before losses and system margin.

Power Budget	P_mean						
	LAU	SUN	SAFE	STBY	COM	EPTH	SCI
<b>SC_A (Spacecraft A)</b>	0.00	273.36	314.35	262.90	484.29	1048.77	409.58
<b>AOGNC</b>	0.00	12.00	12.00	12.00	84.30	16.30	97.00
A_DPU (A DTU Data Processing Unit)	0.00	0.00	0.00	0.00	3.60	3.60	3.60
A_IMU_LN200_1 (A IMU LN200 Core #1)	0.00	6.00	6.00	6.00	0.00	6.00	6.00
A_IMU_LN200_2 (A IMU LN200 Core #2)	0.00	6.00	6.00	6.00	0.00	6.00	6.00
A_NAVCAM_OH_1 (Optical Head #1)	0.00	0.00	0.00	0.00	0.00	0.00	0.35
A_NAVCAM_OH_2 (A NAVCAM OH #2)	0.00	0.00	0.00	0.00	0.00	0.00	0.35
A_STR_OH_1 (A STR Optical Head #1)	0.00	0.00	0.00	0.00	0.35	0.35	0.35
A_SUN_LENS_(#2)	0.00	0.00	0.00	0.00	0.00	0.00	0.00
A_SUN_LENS_3 (A SUN #3)	0.00	0.00	0.00	0.00	0.00	0.00	0.00
A_SUN_LENS_4 (A SUN LENS #4)	0.00	0.00	0.00	0.00	0.00	0.00	0.00
A_SUN_LENS_5 (A SUN LENS #5)	0.00	0.00	0.00	0.00	0.00	0.00	0.00
A_SUN_LENS_6 (A SUN LENS #6)	0.00	0.00	0.00	0.00	0.00	0.00	0.00
RW_RSI_4_215 (A RW)	0.00	0.00	0.00	0.00	20.00	0.00	20.00
RW_RSI_4_216 (A RW #2)	0.00	0.00	0.00	0.00	20.00	0.00	20.00
RW_RSI_4_217 (A RW #3)	0.00	0.00	0.00	0.00	20.00	0.00	20.00
RW_RSI_4_218 (A RW #4)	0.00	0.00	0.00	0.00	20.00	0.00	20.00
<b>COM</b>	0.00	113.69	87.92	32.00	160.07	32.00	61.76
A_ISL_board_1 (A Electronics #1)	0.00	0.00	0.00	0.00	0.00	0.00	4.08
A_ISL_board_2 (A Electronics #2)	0.00	0.00	0.00	0.00	0.00	0.00	4.08
A_ISL_Patch_1 (A Antenna Patch #1)	0.00	0.00	0.00	0.00	0.00	0.00	3.60
A_ISL_Patch_2 (A Antenna Patch #2)	0.00	0.00	0.00	0.00	0.00	0.00	3.60
A_ISL_Patch_3 (A Antenna Patch #3)	0.00	0.00	0.00	0.00	0.00	0.00	3.60
A_ISLPatch_4 (A Antenna Patch #4)	0.00	0.00	0.00	0.00	0.00	0.00	3.60
A_ISL_Patch_5 (A Antenna Patch #5)	0.00	0.00	0.00	0.00	0.00	0.00	3.60
A_ISL_Patch_6 (A Antenna Patch #6)	0.00	0.00	0.00	0.00	0.00	0.00	3.60
XDST_1 (X-Band DSTRASP #1)	0.00	24.00	24.00	16.00	24.00	16.00	16.00
XDST_2 (X-Band DSTRASP #2)	0.00	24.00	24.00	16.00	24.00	16.00	16.00
XHGA (X-Band HGA)	0.00	0.00	0.00	0.00	0.00	0.00	0.00
XLGA_1 (X-Band LGA #1)	0.00	0.00	0.00	0.00	0.00	0.00	0.00
XLGA_2 (X-Band LGA #2)	0.00	0.00	0.00	0.00	0.00	0.00	0.00
XRFDN (X-Band RFDN)	0.00	0.00	0.00	0.00	0.00	0.00	0.00
XTWT_1 (X-Band TWT #1)	0.00	28.34	15.46	0.00	51.53	0.00	0.00
XTWT_2 (X-Band TWT #2)	0.00	28.34	15.46	0.00	51.53	0.00	0.00
XTWTA_EPC_1 (X-Band TWTA EPC #1)	0.00	4.50	4.50	0.00	4.50	0.00	0.00
XTWTA_EPC_2 (X-Band TWTA EPC #2)	0.00	4.50	4.50	0.00	4.50	0.00	0.00
<b>CPROP</b>	0.00	57.71	25.61	17.90	17.90	17.07	0.65
A_Thr_5N_1 (A Thruster_MONARC 5N #1)	0.00	5.35	2.75	2.12	2.12	2.05	0.00
A_Thr_5N_2 (A Thruster_MONARC 5N #2)	0.00	5.35	2.75	2.12	2.12	2.05	0.00

A_Thr_5N_3 (A Thruster_MONARC 5N #3)	0.00	5.35	2.75	2.12	2.12	2.05	0.00
A_Thr_5N_4 (A Thruster_MONARC 5N #4)	0.00	5.35	2.75	2.12	2.12	2.05	0.00
A_Thr_5N_5 (A Thruster_MONARC 5N #5)	0.00	5.35	2.75	2.12	2.12	2.05	0.00
A_Thr_5N_6 (A Thruster_MONARC 5N #6)	0.00	5.35	2.75	2.12	2.12	2.05	0.00
A_Thr_5N_7 (A Thruster_MONARC 5N #7)	0.00	5.35	2.75	2.12	2.12	2.05	0.00
A_Thr_5N_8 (A Thruster_MONARC 5N #8)	0.00	5.35	2.75	2.12	2.12	2.05	0.00
A_Tk_CPROP_1 (A Tank CPROP #1)	0.00	0.00	0.00	0.00	0.00	0.00	0.00
A_Tk_CPROP_2 (A Tank CPROP #2)	0.00	0.00	0.00	0.00	0.00	0.00	0.00
A_Fil_Dr_Val_1 (A Fill Drain Valve)	0.00	0.00	0.00	0.00	0.00	0.00	0.00
A_Fil_Dr_Val_2 (A Fill Drain Valve)	0.00	0.00	0.00	0.00	0.00	0.00	0.00
A_Lat_Val_1 (A Latch Valves)	0.00	7.13	1.50	0.15	0.15	0.00	0.00
A_Lat_Val_2 (A Latch Valves)	0.00	7.13	1.50	0.15	0.15	0.00	0.00
A_Press_Trans_1_1 (A Pressure Transducer #1)	0.00	0.22	0.22	0.22	0.22	0.22	0.22
A_Press_Trans_1_2 (A Pressure Transducer #1)	0.00	0.22	0.22	0.22	0.22	0.22	0.22
A_Press_Trans_1_3 (A Pressure Transducer #1)	0.00	0.22	0.22	0.22	0.22	0.22	0.22
A_Pass_Valve (A Passivation_Valve)	0.00	0.00	0.00	0.00	0.00	0.00	0.00
<b>DH</b>	0.00	53.00	53.00	53.00	53.00	53.00	53.00
A_OBC (A Onboard Computer)	0.00	23.00	23.00	23.00	23.00	23.00	23.00
A_RIU (A Remote Interface Unit)	0.00	30.00	30.00	30.00	30.00	30.00	30.00
<b>INS</b>	0.00	0.00	0.00	0.00	0.00	0.00	71.16
A_CoCa_CSU (A CoCa Camera Support)	0.00	0.00	0.00	0.00	0.00	0.00	14.40
A_CoCa_ELU (A CoCa Electronics Unit)	0.00	0.00	0.00	0.00	0.00	0.00	0.00
A_CoCa_PEU (A CoCa Proximity Electronics Unit)	0.00	0.00	0.00	0.00	0.00	0.00	0.00
A_CoCa_Rad (A CoCa Radiator)	0.00	0.00	0.00	0.00	0.00	0.00	0.00
A_DFP_COM_FGM_boom_2 (A DFP COMPLIMENT+FGM+boom_2)	0.00	0.00	0.00	0.00	0.00	0.00	0.00
A_DFP_COMPLIMENT_boom_1 (A DFP COMetary Plasma Light Instrument boom 1)	0.00	0.00	0.00	0.00	0.00	0.00	0.00
A_DFP_COMPLIMENT_p_1 (A DFP COMetary Plasma Light Instrument probe #1)	0.00	0.00	0.00	0.00	0.00	0.00	0.00
A_DFP_DISC (Dust Impact Sensor and Counter)	0.00	0.00	0.00	0.00	0.00	0.00	0.00
A_DFP_E_Box (A DFP E-Box)	0.00	0.00	0.00	0.00	0.00	0.00	20.16
A_DFP_LEES_1 (A DFP Low Energy Electron Spectrometer 1)	0.00	0.00	0.00	0.00	0.00	0.00	0.00
A_DFP_SCIENA_ENA (Solar wind and Cometary Ions and Energetic Neutral Atoms-ENA sensor)	0.00	0.00	0.00	0.00	0.00	0.00	0.00
A_DFP_SCIENA_Ion (A DFP -Ion sensor)	0.00	0.00	0.00	0.00	0.00	0.00	0.00
A_MANiac_ELU (A MANiac Electronics Unit)	0.00	0.00	0.00	0.00	0.00	0.00	0.00
A_MANiac_NDG (A MANiac Neutral Density Gauge)	0.00	0.00	0.00	0.00	0.00	0.00	3.60
A_MANiac_SHU (A MANiac Sensor Head Unit)	0.00	0.00	0.00	0.00	0.00	0.00	21.60
A_MIRMISS_MIR_1 (Mid-InfraRed Sensor 1)	0.00	0.00	0.00	0.00	0.00	0.00	0.00
A_MIRMISS_MIR_2 (A MIRMISS Sensor 2)	0.00	0.00	0.00	0.00	0.00	0.00	0.00
A_MIRMISS_NIR (A MIRMISS Near InfraRed Sensor)	0.00	0.00	0.00	0.00	0.00	0.00	0.00
A_MIRMISS_Rad (A MIRMISS Radiator)	0.00	0.00	0.00	0.00	0.00	0.00	0.00
A_MIRMISS_TIRI (Thermal InfraRed Imager)	0.00	0.00	0.00	0.00	0.00	0.00	9.00

A_MANiaC_Harn (A MANiaC Harness)	0.00	0.00	0.00	0.00	0.00	0.00	0.00
A_MANiaC_Mec (A MANiaC Rotating Mechanisms)	0.00	0.00	0.00	0.00	0.00	0.00	2.40
A_CoCa_Harn (A CoCa Harness)	0.00	0.00	0.00	0.00	0.00	0.00	0.00
A_CoCa_MLI (A CoCa Thermal Insulation)	0.00	0.00	0.00	0.00	0.00	0.00	0.00
<b>MEC</b>	<b>0.00</b>	<b>6.96</b>	<b>9.80</b>	<b>3.00</b>	<b>53.00</b>	<b>9.80</b>	<b>35.00</b>
A_APM_HDRM_APME (A Antenna Pointing Mechanisms Subsystem with Driver and HDRM)	0.00	0.00	0.00	0.00	18.00	0.00	0.00
A_Clamp_Band (A Clamp Band Ejection System)	0.00	0.00	0.00	0.00	0.00	0.00	0.00
A_SA1_HDRM_1 (A SA1 HDRM #1)	0.00	0.00	0.00	0.00	0.00	0.00	0.00
A_SA1_HDRM_2 (A SA1 HDRM #2)	0.00	0.00	0.00	0.00	0.00	0.00	0.00
A_SA1_HDRM_3 (A SA1 HDRM #3)	0.00	0.00	0.00	0.00	0.00	0.00	0.00
A_SA1_HDRM_4 (A SA1 HDRM #4)	0.00	0.00	0.00	0.00	0.00	0.00	0.00
A_SA2_HDRM_1 (A SA2 HDRM #1)	0.00	0.00	0.00	0.00	0.00	0.00	0.00
A_SA2_HDRM_2 (A SA2 HDRM #2)	0.00	0.00	0.00	0.00	0.00	0.00	0.00
A_SA2_HDRM_3 (A SA2 HDRM #3)	0.00	0.00	0.00	0.00	0.00	0.00	0.00
A_SA2_HDRM_4 (A SA2 HDRM #4)	0.00	0.00	0.00	0.00	0.00	0.00	0.00
A_SADE (A SA drive electronics)	0.00	3.00	5.00	1.00	5.00	5.00	5.00
A_SADM_1 (A SADM #1)	0.00	1.98	2.40	1.00	15.00	2.40	15.00
A_SADM_2 (A SADM #2)	0.00	1.98	2.40	1.00	15.00	2.40	15.00
<b>PWR</b>	<b>0.00</b>	<b>30.00</b>	<b>30.00</b>	<b>30.00</b>	<b>30.00</b>	<b>30.00</b>	<b>30.00</b>
A_PCDU (A PCDU)	0.00	30.00	30.00	30.00	30.00	30.00	30.00
<b>STR</b>	<b>0.00</b>	<b>0.00</b>	<b>0.00</b>	<b>0.00</b>	<b>0.00</b>	<b>0.00</b>	<b>0.00</b>
A_Misc_STR (A Miscellaneous STR)	0.00	0.00	0.00	0.00	0.00	0.00	0.00
<b>TC</b>	<b>0.00</b>	<b>0.00</b>	<b>96.03</b>	<b>115.00</b>	<b>86.02</b>	<b>89.01</b>	<b>61.01</b>
A_TC_FILLER (A TC Thermal Filler)	0.00	0.00	0.00	0.00	0.00	0.00	0.00
A_TC_HEATER (A TC Heater)	0.00	0.00	96.03	115.00	86.02	89.01	61.01
A_TC_HP (A TC Heat Pipes)	0.00	0.00	0.00	0.00	0.00	0.00	0.00
A_TC_MLI (A TC Multi Layer Insulation)	0.00	0.00	0.00	0.00	0.00	0.00	0.00
A_TC_PAINT (A TC Paint)	0.00	0.00	0.00	0.00	0.00	0.00	0.00
A_TC_RAD (A TC Radiator Panel)	0.00	0.00	0.00	0.00	0.00	0.00	0.00
A_TC_SO (A TC Stand Offs)	0.00	0.00	0.00	0.00	0.00	0.00	0.00
A_TC_STRAP (A TC Thermal Strap)	0.00	0.00	0.00	0.00	0.00	0.00	0.00
A_TC_T_SENS (A TC Temperature Sensor)	0.00	0.00	0.00	0.00	0.00	0.00	0.00
<b>EPROP</b>	<b>0.00</b>	<b>0.00</b>	<b>0.00</b>	<b>0.00</b>	<b>0.00</b>	<b>801.59</b>	<b>0.00</b>
A_BPRU (A BPRU)	0.00	0.00	0.00	0.00	0.00	0.00	0.00
A_FU (A FU)	0.00	0.00	0.00	0.00	0.00	0.00	0.00
A_Miscellaneous (A Miscellaneous)	0.00	0.00	0.00	0.00	0.00	0.00	0.00
A_PPU (A Power Processing Unit)	0.00	0.00	0.00	0.00	0.00	801.59	0.00
A_PRE_Card (A PRE Card)	0.00	0.00	0.00	0.00	0.00	0.00	0.00
A_Prop_Tank_1 (A Propellant Tank #1)	0.00	0.00	0.00	0.00	0.00	0.00	0.00
A_Prop_Tank_2 (A Propellant Tank #2)	0.00	0.00	0.00	0.00	0.00	0.00	0.00
A_Thruster_PPS1350 (A Thruster PPS1350)	0.00	0.00	0.00	0.00	0.00	0.00	0.00

A_XFC (A XFC)	0.00	0.00	0.00	0.00	0.00	0.00	0.00
<b>SC_B2 (Spacecraft B2)</b>	0.00	0.00	0.00	0.00	0.00	0.00	35.59
<b>AOGNC</b>	0.00	0.00	0.00	0.00	0.00	0.00	8.00
RW_RW250 (RW)	0.00	0.00	0.00	0.00	0.00	0.00	8.00
<b>COM</b>	0.00	0.00	0.00	0.00	0.00	0.00	7.29
B2_ISL_ActiveFE (B2 Antenna FE)	0.00	0.00	0.00	0.00	0.00	0.00	4.05
B2_ISL_GOMx_board (B2 Electronics)	0.00	0.00	0.00	0.00	0.00	0.00	3.24
ISL_T_LGA (ISL_ToroidalLGA)	0.00	0.00	0.00	0.00	0.00	0.00	0.00
<b>DH</b>	0.00	0.00	0.00	0.00	0.00	0.00	5.00
B2_OBC (B2 Onboard Computer)	0.00	0.00	0.00	0.00	0.00	0.00	5.00
<b>INS</b>	0.00	0.00	0.00	0.00	0.00	0.00	9.30
B2_DFP_DISC (B2 DFP Dust Impact Sensor and Counter)	0.00	0.00	0.00	0.00	0.00	0.00	0.00
B2_DFP_E_Box (B2 DFP E-Box)	0.00	0.00	0.00	0.00	0.00	0.00	4.20
B2_DFP_FGM_1 (B2 DFP FGM #1)	0.00	0.00	0.00	0.00	0.00	0.00	0.45
B2_DFP_FGM_2 (B2 DFP FGM #2)	0.00	0.00	0.00	0.00	0.00	0.00	0.45
B2_DFP_FGM_boom (B2 DFP FGM boom)	0.00	0.00	0.00	0.00	0.00	0.00	0.00
B2_EnVisS (B2 Entire Visible Sky)	0.00	0.00	0.00	0.00	0.00	0.00	4.20
B2_OPIC (B2 Optical Imager for Comets)	0.00	0.00	0.00	0.00	0.00	0.00	0.00
<b>MEC</b>	0.00	0.00	0.00	0.00	0.00	0.00	0.00
B2_Clamp_Band (B2 Clamp Band Ejection System)	0.00	0.00	0.00	0.00	0.00	0.00	0.00
<b>PWR</b>	0.00	0.00	0.00	0.00	0.00	0.00	6.00
B2_Bat_1 (B2 Battery #1)	0.00	0.00	0.00	0.00	0.00	0.00	0.00
B2_PDU (B2 PDU)	0.00	0.00	0.00	0.00	0.00	0.00	6.00
<b>TC</b>	0.00	0.00	0.00	0.00	0.00	0.00	0.00
B2_TC_FILLER (B2 TC Thermal Filler)	0.00	0.00	0.00	0.00	0.00	0.00	0.00
B2_TC_HEATER (B2 TC Heater)	0.00	0.00	0.00	0.00	0.00	0.00	0.00
B2_TC_MLI (B2 TC Multi Layer Insulation)	0.00	0.00	0.00	0.00	0.00	0.00	0.00
B2_TC_PAINT (B2 TC Paint)	0.00	0.00	0.00	0.00	0.00	0.00	0.00
B2_TC_RAD (B2 TC Radiator Panel)	0.00	0.00	0.00	0.00	0.00	0.00	0.00
B2_TC_SO (B2 TC Stand Offs)	0.00	0.00	0.00	0.00	0.00	0.00	0.00
B2_TC_STRAP (B2 TC Thermal Strap)	0.00	0.00	0.00	0.00	0.00	0.00	0.00
B2_TC_T_SENS (B2 TC Temperature Sensor)	0.00	0.00	0.00	0.00	0.00	0.00	0.00

**Table 7-35: Unit-level S/C A and probe B2 power budgets (per mode)<sup>14</sup>**

Table 7-36 presents the power and redundancy scheme assumed for each unit, while Table 7-37 and Table 7-38 shows the unit duty cycles per mode for S/C A and probe B2, respectively.

---

<sup>14</sup> Note that the power values shown per mode are the mean power for each equipment. In the case of cold redundant units, the power value has been split across the units.

Equipment	P_stby	P_on	scheme	Redundancy		
				type	k	n
A_APM_HDRM_APME	0	18	Passive (or Cold or Standby)	Internal	1	2
A_CoCa_CSU	6	14.4	-	-	-	-
A_DFP_E_Box	12.12	20.16	-	-	-	-
A_DPU	0	3.6	-	-	-	-
A_IMU_LN200	0	12	Passive (or Cold or Standby)	External	1	2
A_ISL_GOMx_board	6.72	8.16	Passive (or Cold or Standby)	External	1	2
A_ISL_GOMx_Patch	1	7.2	Passive (or Cold or Standby)	External	1	2
A_Lat_Val	0	30	Passive (or Cold or Standby)	External	2	4
A_MANiaC_Mec	0	2.4	-	-	-	-
A_MANiac_NDG	0	3.6	-	-	-	-
A_MANiac_SHU	0	21.6	-	-	-	-
A_MIRMISS_TIRI	6.24	9	-	-	-	-
A_NAVCAM_OH	0	0.7	Passive (or Cold or Standby)	External	1	2
A_OBC	0	23	Passive (or Cold or Standby)	Internal	1	2
A_PCDU	0	30	-	-	-	-
A_PPU	0	1252	None	-	-	-
A_Press_Trans	0.216	0.216	None	-	8	8
A_RIU	0	30	Passive (or Cold or Standby)	Internal	1	2
A_RW_RSI_4_215	0	20	Active (or Hot)	External	3	4
A_SADE	1	5	Active (or Hot)	-	-	-
A_SADM	1	15	Passive (or Cold or Standby)	Internal	1	2
A_STR_OH	0	0.7	Passive (or Cold or Standby)	External	1	2
A_TC_HEATER	0	115	Passive (or Cold or Standby)	Internal	-	-
A_Thr_5N	4.1	18	Passive (or Cold or Standby)	External	4	8
B2_DFP_E_Box	9.96	8.4	-	-	-	-
B2_DFP_FGM_sensor	0	0.9	-	-	-	-
B2_EnVisS	0	8.4	-	-	-	-
B2_ISL_GOMx_ActiveFE	1	7.2	None	-	-	-
B2_ISL_GOMx_board	3.36	5.76	None	-	0	0
B2_OBC	0	5	None	-	-	-
B2_PDU	2	6	None	-	-	-
B2_RW_RW250	2	8	None	External	0	0
XPND_RX	16	16	Active (or Hot)	External	1	2
XPND_TX	0	16	Passive (or Cold or Standby)	External	1	2
XTWT	0	103.07	Passive (or Cold or Standby)	External	1	2
XTWTA_EPC	0	9	Passive (or Cold or Standby)	External	1	2

**Table 7-36: Unit-level S/C A and probe B2 nominal power and redundancy concept (where applicable)**

Equipment	P_stby	P_on	Duty cycle LAU	Duty cycle SUN	Duty cycle SAFE	Duty cycle STBY	Duty cycle COM	Duty cycle EPTH	Duty cycle SCI
A_APM_HDRM_APME	0	18	-1	-1	-1	-1	1	0	-1
A_CoCa_CSU	6	14.4	-1	-1	-1	-1	-1	-1	1
A_DFP_E_Box	12.12	20.16	-1	-1	-1	-1	-1	-1	1
A_DPU	0	3.6	-1	-1	-1	-1	1	1	1
A_IMU_LN200	0	12	-1	1	1	1	-1	1	1
A_ISL_GOMx_board	6.72	8.16	-1	-1	-1	-1	-1	-1	1
A_ISL_GOMx_Patch	1	7.2	-1	-1	-1	-1	-1	-1	1
A_Lat_Val	0	30	-1	0.475	0.1	0.01	0.01	0.0002	0
A_MANiaC_Mec	0	2.4	-1	-1	-1	-1	-1	-1	1
A_MANiac_NDG	0	3.6	-1	-1	-1	-1	-1	-1	1
A_MANiac_SHU	0	21.6	-1	-1	-1	-1	-1	-1	1
A_MIRMIS_TIRI	6.24	9	-1	-1	-1	-1	-1	-1	1
A_NAVCAM_OH	0	0.7	-1	-1	-1	-1	-1	-1	1
A_OBC	0	23	-1	1	1	1	1	1	1
A_PCDU	0	30	0	1	1	1	1	1	1
A_PPU	0	1252	-1	-1	-1	-1	-1	0.64	-1
A_Press_Trans	0.216	0.216	-1	1	1	1	1	1	1
A_RIU	0	30	-1	1	1	1	1	1	1
A_RW_RSI_4_215	0	20	-1	-1	-1	-1	1	-1	1
A_SADE	1	5	-1	0.5	1	0	1	1	1
A_SADM	1	15	-1	0.07	0.1	0	1	0.1	1
A_STR_OH	0	0.7	-1	-1	-1	-1	1	1	1
A_TC_HEATER	0	115	-1	-1	0.835	1	0.748	0.774	0.5305
A_Thr_5N	4.1	18	-1	0.475	0.1	0.01	0.01	0.0002	-1
XPND_RX	16	16	-1	1	1	1	1	1	1
XPND_TX	0	16	-1	1	1	-1	1	-1	-1
XTWT	0	103.07	-1	0.55	0.3	-1	1	0	-1
XTWTA_EPC	0	9	-1	1	1	-1	1	0	-1

 Table 7-37: Unit-level S/C A assumed duty cycles<sup>15</sup>

<sup>15</sup> Note that the duty cycles for the B2 payload units represent a delay in the switch-on of the units (i.e. the ratio of ON to OFF time, rather than switching between ON and STANDBY as for other units).

Equipment	P_stby	P_on	Duty cycle LAU	Duty cycle SUN	Duty cycle SAFE	Duty cycle STBY	Duty cycle COM	Duty cycle EPTH	Duty cycle SCI
B2_DFP_E_Box	9.96	8.4	-1	-1	-1	-1	-1	-1	0.5
B2_DFP_FGM_sensor	0	0.9	-1	-1	-1	-1	-1	-1	0.5
B2_EnVisS	0	8.4	-1	-1	-1	-1	-1	-1	0.5
B2_ISL_GOMx_ActiveFE	1	7.2	-1	-1	-1	-1	-1	-1	0.56
B2_ISL_GOMx_board	3.36	5.76	-1	-1	-1	-1	-1	-1	0.56
B2_OBC	0	5	-1	-1	-1	-1	-1	-1	1
B2_PDU	2	6	-1	-1	-1	-1	-1	-1	1
B2_RW_RW250	2	8	-1	-1	-1	-1	-1	-1	1

**Table 7-38: Unit-level probe B2 assumed duty cycles<sup>16</sup>**

#### 7.4.6 ΔV Budget

The delta-V budget for the Comet Interceptor study is presented in Table 7-39. The information on which manoeuvre is supported by chemical propulsion or by electric propulsion has also been added (in the right column).

Note that the delta-V budgeted for the attitude control during the mission (highlighted in the table with an \*) was found after the study to have increased to 57 m/s before margins, compared to the 41 m/s budgeted in the table below. This is due to the RCS thrusters getting placed closer to the centre of the thruster-mounting face than what was originally assumed (topic discussed in more detail in the AOCS chapter 14.2.2.6).

<sup>16</sup> Note that the duty cycles for the B2 payload units represent a delay in the switch-on of the units (i.e. the ratio of ON to OFF time, rather than switching between ON and STANDBY as for other units).

	Years	Delta-v [m/s]	Margin [%]	Delta-v (incl. margin)	PROP [m/s]
<b>Manoeuvre to L2</b>					
TCM#1 deterministic		15.0	10	16.50	CP
TCM#1 to TCM#3 stochastic		40.0	0	40.00	CP
L2 Orbit Insertion		0.0	10	0.00	CP
<b>Attitude Control</b>					
Mission*		41.0*	100*	82.00*	CP
<b>Approach Navigation</b>					
Navigation stochastic		14.1	5	14.81	CP
Divert manoeuvres deterministic		14.0	5	14.70	CP
<b>CP Total</b>				<b>168.0</b>	
<b>SK at L2</b>					
Station Keeping L2	3	5.0	50	22.50	EP
<b>Comet Interception</b>					
Allocation		1500.0	0	1500.00	EP
<b>EP Total</b>				<b>1522.5</b>	

**Table 7-39: ΔV budget**

#### 7.4.7 Payload Data Budget

The data volume generated by the payloads during the course of the fly-by by the instruments is summarized in Table 7-40. It is assumed that S/C A receives and stores also the data from probes B1 and B2 via ISL, and then downlinks the data to Earth. An overhead was applied to the total, as described in the communications chapter 16.2.5.

Data Volume (Gbit)		
<b>S/C A</b>		
CoCa		128.0
DFP		6.8
MANiaC		5.6
MIRMISS		4.5
<b>Payload Total (S/C A)</b>		<b>144.9</b>
<b>Probe B1</b>		
Allocation (per JAXA information)		14.4
<b>Payload Total (Probe B1)</b>		<b>14.4</b>
<b>Probe B2</b>		
DFP		0.32
EnVisS		4.32
OPIC		3.43
<b>Payload Total (Probe B2)</b>		<b>8.1</b>
<b>Total</b>		<b>167.4</b>
Overhead	10%	16.7
<b>Total (with overhead)</b>		<b>184.1</b>

**Table 7-40: Payload data volume**

In addition, a 5 kbps bandwidth is assigned to S/C A for real time housekeeping telemetry.

## 7.5 System Options

### 7.5.1 S/C A

Two system options were analysed during the study. The first one involved the use of the PPSXOO electric propulsion thruster instead of the baselined PPS1350 as a potential exercise to reduce the overall mass of S/C A. The second option investigated at system level an assessment of the probability to reach at least one LPC target using a chemical propulsion system only.

#### 7.5.1.1 Embarking PPSXOO

The use of the PPSXOO electric propulsion thruster instead of the PPS1350 for the transfer to the target object could lead to a reduction in the total wet mass of the spacecraft and hence provide a benefit overall for the mission. A preliminary assessment was carried out embarking the PPSXOO, which would lead to the following mass savings:

- Ca. 30% reduction (ca. 11kg) in dry mass saving for the overall electric propulsion subsystem
- Ca. 20% reduction (ca. 18kg) in the amount of required propellant compared to the PPS1350 baseline
- Ca. 7kg reduction of the solar array area (from 6m<sup>2</sup> baseline to 4.5m<sup>2</sup> required for the PPXOO option).

The option of embarking the PPSXoo thruster is deemed worthy of further investigation; however, the development of the thruster is on-going, and originally targets LEO constellations. The plan foresees subsystem coupling tests using EMs beginning of 2020, CDR in Q3 2021 and the QR in Q1 2023. The suitability of using the thruster for deep space missions needs to be further investigated.

### 7.5.1.2 Chemical propulsion only option

A system level assessment was carried out in order to investigate the impact on the probability of reaching at least one LPC using a chemical propulsion system only. The primary goal was to investigate this option as a means to reduce the cost of the overall mission.

The following assumptions were considered:

- All the manoeuvres are performed with a chemical propulsion system, either using
  - a:
  - Monopropellant system, Isp=210s (for a delta-V of 425m/s for the transfer to the target)
  - Bipropellant system, Isp=330s, (for a delta-V of 700m/s for the transfer to the target)
- The electrical propulsion system is removed, which allows a reduction of:
  - 38.6 kg for the EPS dry mass
  - 91.9 kg for the EPS propellant
  - ~30 kg (estimated) for the solar array mass, assuming a reduced peak power need of the system.
- A heavier chemical propulsion system needs to be embarked compared to the baseline to accommodate the larger tanks:
  - For the monopropellant system this led to an estimated increase of ~43kg dry mass for the propellant tanks and ~315 kg of propellant.
  - For the bipropellant system this led to an estimated increase of ~30kg dry mass for the propellant tanks and ~220kg of propellant.
- The following overall wet mass (1<sup>st</sup> order system-level assessment) at launch is therefore estimated for both options:
  - **945 kg wet mass** for a **monopropellant** system
  - **830 kg wet mass** for a **bipropellant** system

The two cases were considered for the analysis and the probability of reaching at least one LPC target for a 5 years mission lifetime as shown in Figure 7-18 below (as in the Mission Analysis chapter):

- Monopropellant system, Isp=210s, 425m/s for transfer to target → ca. **40%**
- Bipropellant system, Isp=330s, 700m/s for transfer to target → ca. **56%**

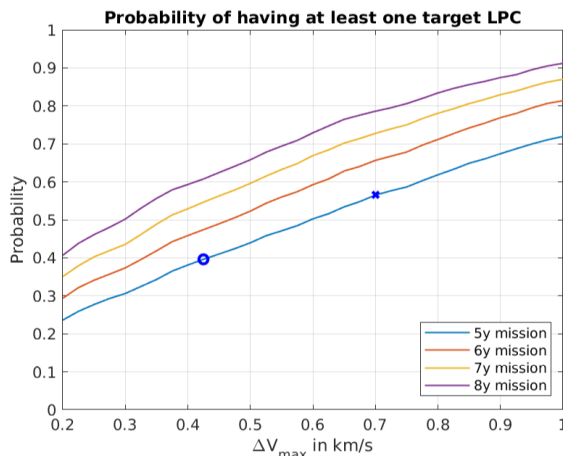


**Figure 7-18: Probability of reaching at least one LPC target with a CP system**

### 7.5.2 Probe B2

A system level assessment for probe B2 was done in order to assess the mass, power and accommodation aspects when embarking the Compliment payload. Embarking Compliment would imply the following additional mass and power needs:

- Total mass: 0.21 kg (including short booms)
  - Probe assemblies DFP-COMPLIMENT-Probes: 2 x 40 g = 80 g
  - Short (~10cm) rigid booms: 2 x 35 g = 70 g
  - 0.4 m harness @ 16g/m + 4 x 9 g connectors = 61 g
- Power:
  - 3.5 W stand-by
  - 4.3 W average
  - 4.3 W peak

Regarding operational constraints, the booms need to avoid the B2 wake and ideally should operate right after separation from the S/C A (and indeed before the CA), to characterise the spacecraft charging.

Two options were investigated for the Compliment placement and a high level system feasibility assessment was performed:

- Deployable booms: two 45 deg Compliment booms could be implemented if attachment to the ram shield is allowed. A deployment of the booms would be required, which is not preferred for B2.

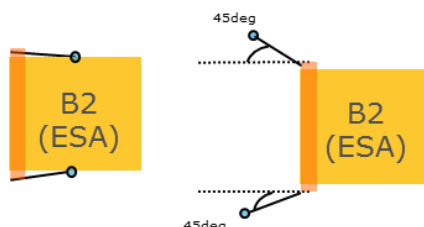


**Figure 7-19: Potential Compliment placement – Deployable Booms**

- Fixed booms (90deg perpendicular to the spin axis): the 90 deg solution is deemed to be suitable for the placement of Compliment, pending confirmation that available free area around B2 is available when B2 is attached to S/C A.



**Figure 7-20: Potential Compliment placement – Fixed Booms**

Nevertheless, it must be noted that the design for probe B2 is already considerably energy-constrained, as such the addition of any further instrument will reduce the available operating time of all other units. This is particularly the case for instruments which would intend to operate directly after release of B2 from S/C A (thus further increasing their energy requirements, relative to other instruments which are only operated closer to the comet).

## 7.6 Open Points

As identified above, one of the key areas still requiring further consolidation is the dust particle environment. This is discussed in greater detail in 6.1.2. The dust environment poses a key risk for all spacecraft, potentially leading to either significant loss of science (due to loss of desired pointing) or indeed full mission loss (i.e. catastrophic failure of any key system on S/C A).

Further to this, a major design change was considered in the Post-IFP delta-sessions. These two sessions assessed a system concept, whereby the S/C maintains a constant orientation during the fly-by, and only the payloads are rotated to observe the comet. This is discussed in further detail in Chapter 24 Scanning Mirror and Periscope Option.

This Page Intentionally Blank

## 8 CONFIGURATION

### 8.1 Requirements and Design Drivers

The following requirements apply to the Comet Interceptor (CI) configuration assessed in this study.

SubSystem Requirements		
Req. ID	Statement	Parent ID
CONF-010	The CI-ARIEL launch configuration shall fit within the Dual Launch System (with CI as upper passenger) constraints of the ARIANE 62 launcher fairing	
CONF-020	The CI interface to the launcher shall be based on the available existing standard interfaces	
CONF-030	The CI configuration shall accommodate two probes, B1 and B2	
CONF-040	The CI configuration shall accommodate all payloads and equipment required for the Mission Objectives	
CONF-050	The CI configuration shall take into account constraints and limitations due to AIV requirements.	
CONF-060	The CI configuration shall provide an unobstructed field of view for all instruments and equipment.	
CONF-070	The CI configuration shall provide unobstructed deployment for the mechanisms	
CONF-080	The CI configuration shall provide unobstructed position for the thrusters to fulfil the mission requirements without contamination of relevant parts of the spacecraft.	

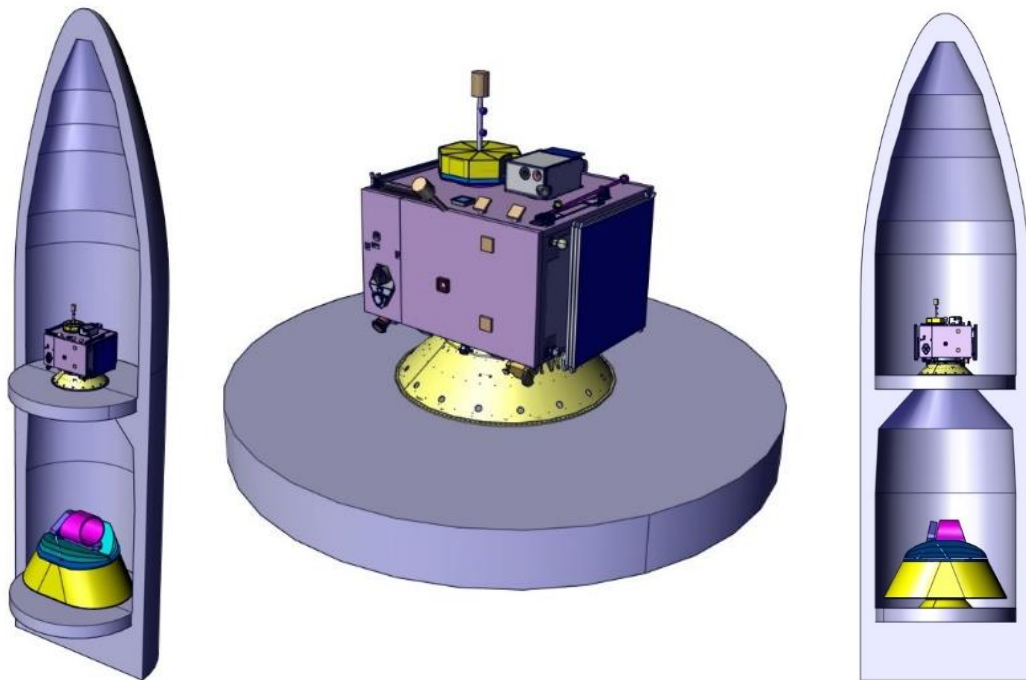
### 8.2 Assumptions and Trade-Offs

The following assumptions have been made.

Assumptions	
1	For the interface of CI with the launcher the 937 standard adapter has been selected.
2	A central “box” like structure has been selected based on structural panels for the Primary Structure of the satellite, which will provide a compact yet accessible configuration for the mission.
3	A meteoroid protection has been implemented on the relevant faces of S/C A, where the risk has been assessed as more relevant (described in more detail in the Structures chapter).

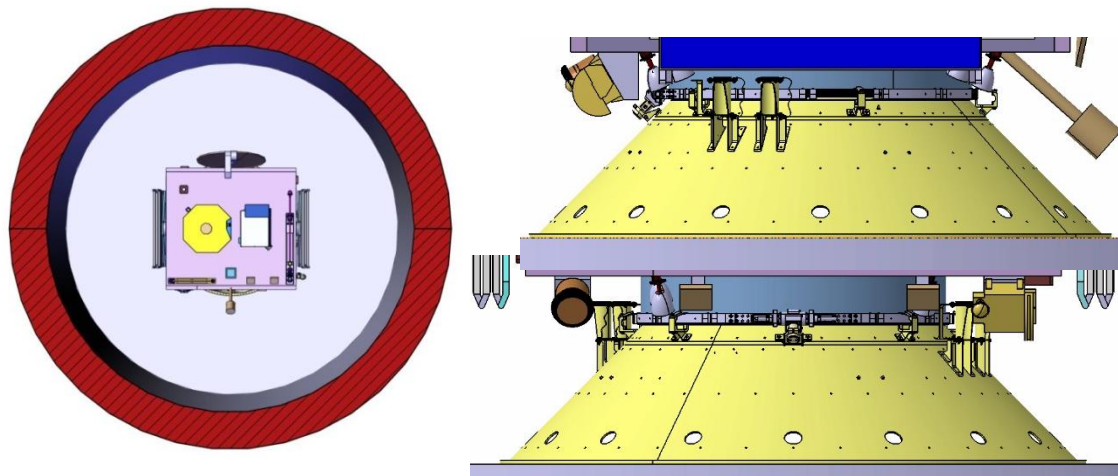
### 8.3 Baseline Design

Figure 8-1 shows the launch configuration of CI and ARIEL inside the Dual Launch System (DLS) of the Ariane 62 launch fairing. Clearly visible is that the available volume in the DLS is not a limiting factor for either spacecraft.



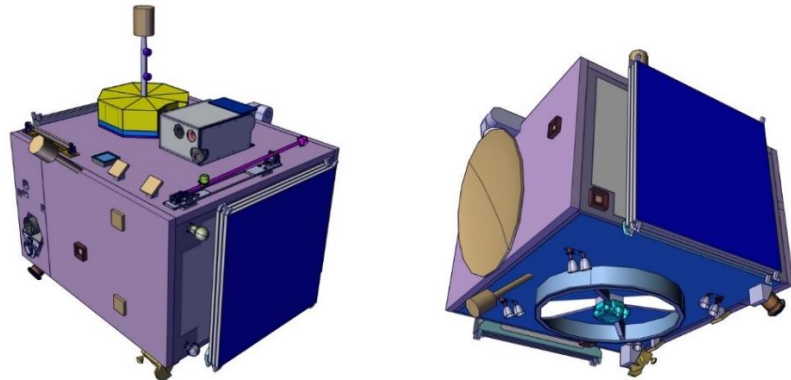
**Figure 8-1: Comet Interceptor and ARIEL in Ariane 62 DLS Fairing**

Figure 8-2 shows a top view of the launch configuration with a cut through the fairing. CI does not come close to the inner boundary of the fairing. In addition both front and side view show that the various appendages are free from the launcher adapter, and should not impede the launcher integration nor the release in orbit from the launch adapter.



**Figure 8-2: Comet Interceptor launch configuration**

Further views (front and back axonometric view) of CI can be seen in Figure 8-3, showing the complete assembly for launch, including the probes B1 and B2.



**Figure 8-3: Comet Interceptor in stowed configuration**

Figure 8-4 shows the stowed configuration with a mannequin for comparison. Figure 8-5 shows the three main spacecraft included in the CI mission: in the middle is spacecraft A, and on top to the right probe B1 and to the left probe B2.

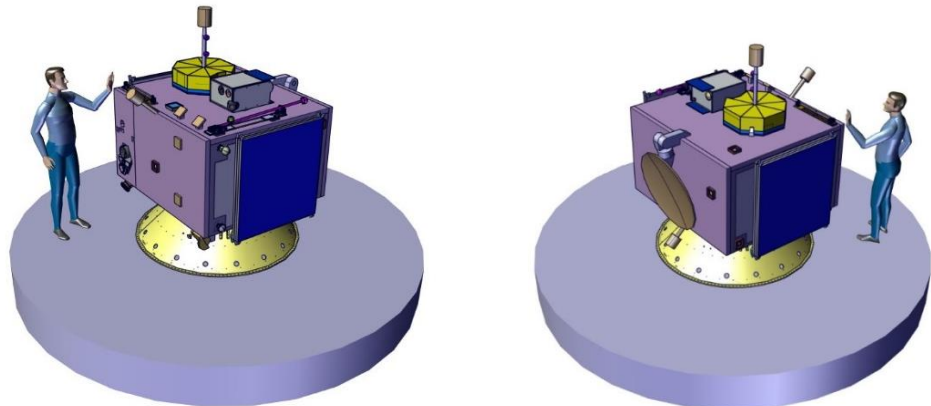


**Figure 8-4: Stowed spacecraft on launch adapter with mannequin**

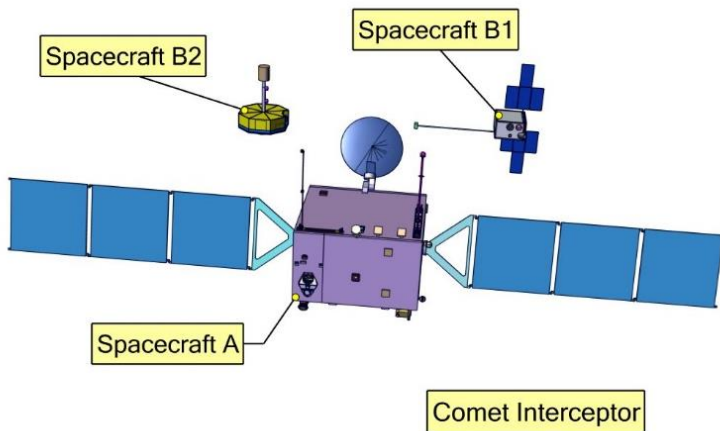
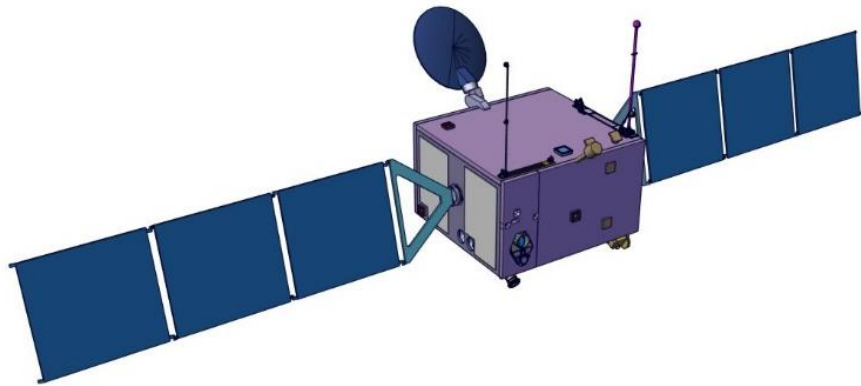


**Figure 8-5: S/C A and probes B1 and B2 deployed**

The next paragraphs show each spacecraft in some detail.

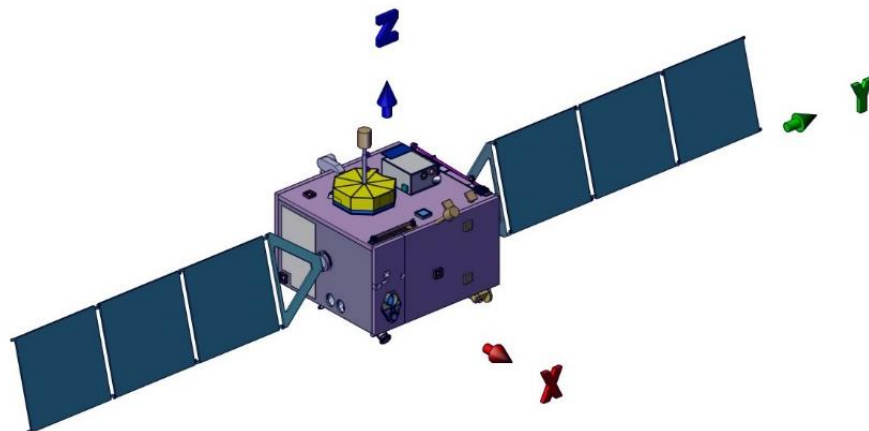
### 8.3.1 S/C A

Figure 8-6 shows spacecraft A with deployed Solar Arrays as well as the FGM and COMPLIMENT booms in deployed configuration. The High Gain Antenna is also deployed, and will be directed where relevant for communications.



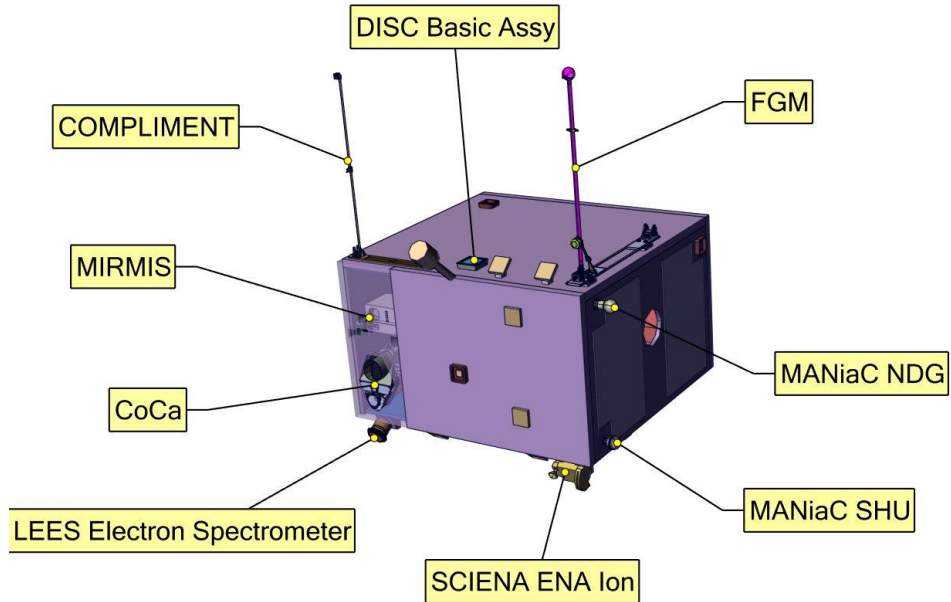
**Figure 8-6: S/C A, deployed**

Figure 8-8 shows the instruments proposed to fly on S/C A for the CI mission.



**Figure 8-7: Spacecraft Coordinate System**

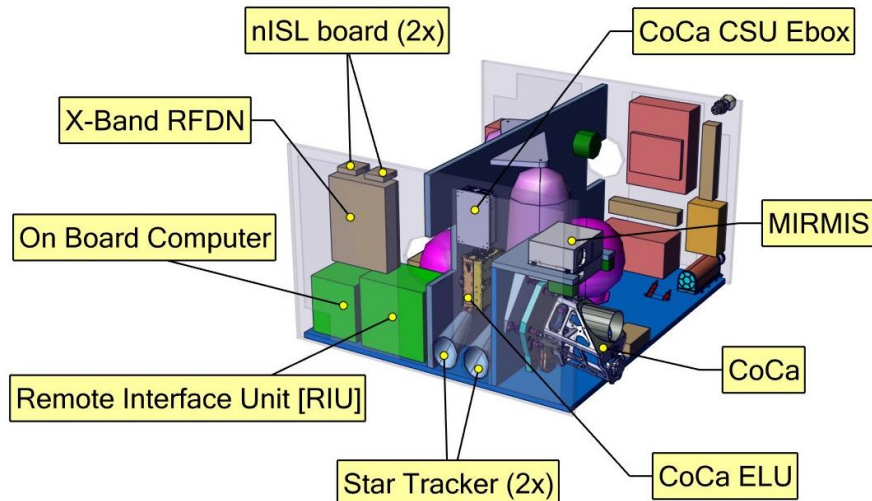
Figure 8-7 shows the coordinate system for the spacecraft in the Comet Interceptor study. The origin of this coordinate system is located on the interface plane to the launcher, and at the centre of the interface adapter ring.



**Figure 8-8: S/C A instruments**

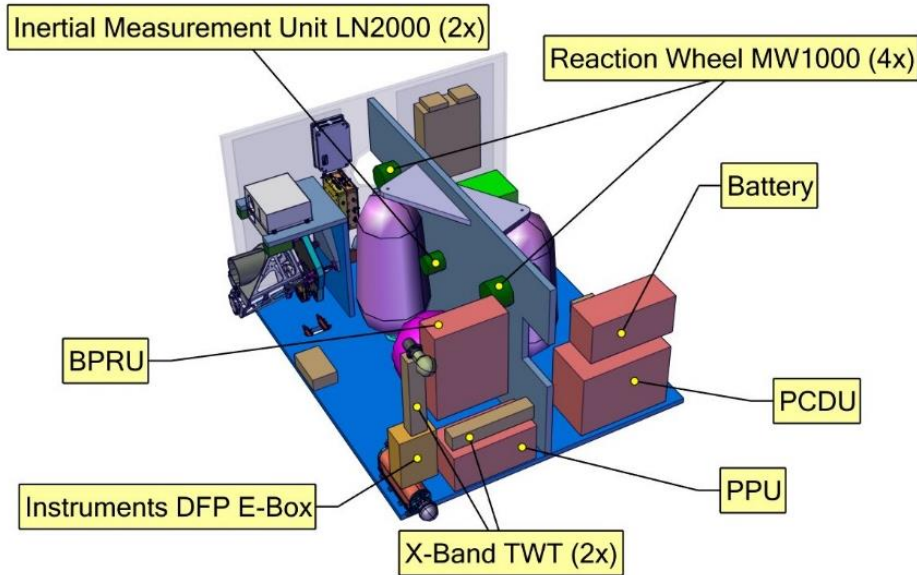
Inside the external panels of S/C A, various sub-systems are integrated to the structure of the spacecraft. Figure 8-9 shows the spacecraft without the external panels, and identifies a number of equipment.

Clearly visible is the Central Panel that has been adopted as the main structural load-path to support all the instruments and equipment.



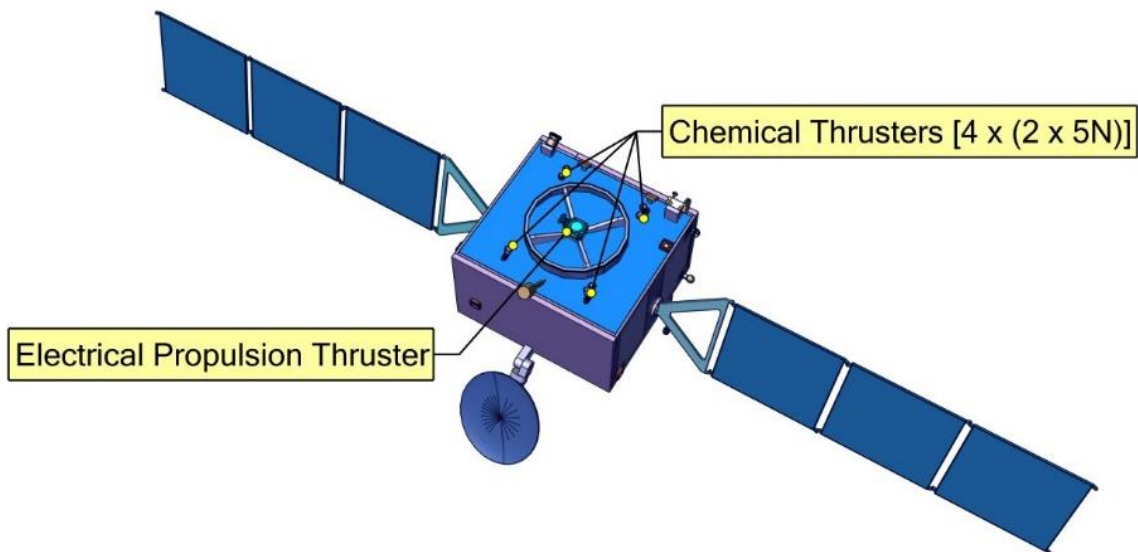
**Figure 8-9: S/C A Equipment (1)**

Figure 8-10 shows the other side of the equipment on S/C A.



**Figure 8-10: S/C A Equipment (2)**

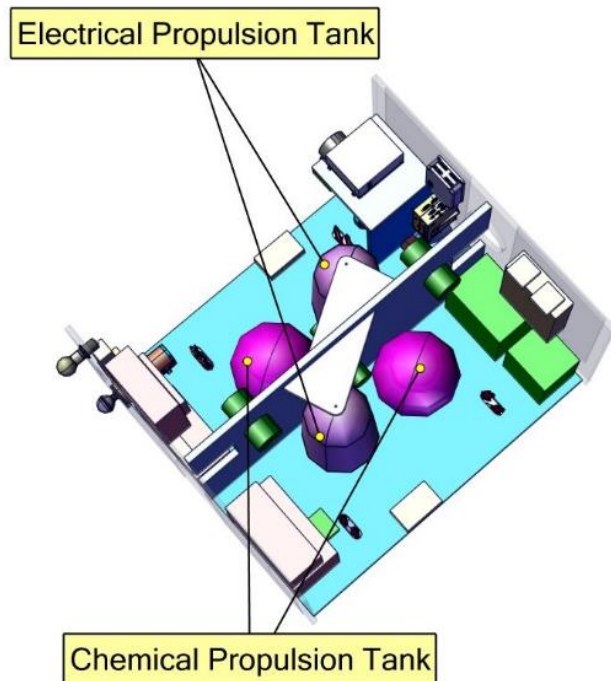
The propulsion sub-systems, both electrical and chemical, have their tanks located inside the main structure. The electrical PPS1350 thruster has been positioned on the central axis of the 937 interface adapter. The 8 (4 + 4 redundant) chemical 5N AOCS thrusters have been positioned right outside the 937 Interface Adapter on the bottom panel of the body of S/C A. Figure 8-11 shows the layout of the nozzles and engine.



**Figure 8-11: S/C A propulsion baseline layout**

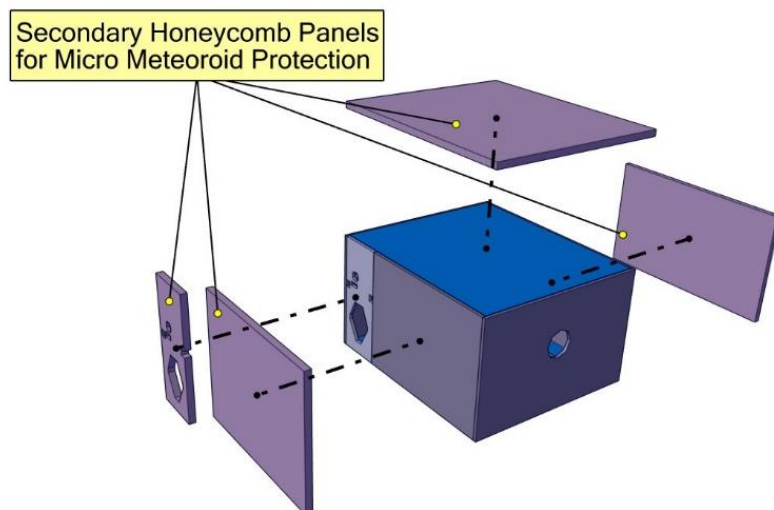
In the baseline design the two chemical propellant tanks and the 2 electrical propellant tanks have been positioned such that the CoG travel due to emptying of the tanks will be symmetric and have minimal impact on the attitude control considerations.

The layout of the tanks is shown in Figure 8-12. The tanks are located above the 937 interface adapter. The height of the adapter ring will have to be able to carry the load of these tanks.



**Figure 8-12: S/C A tank layout**

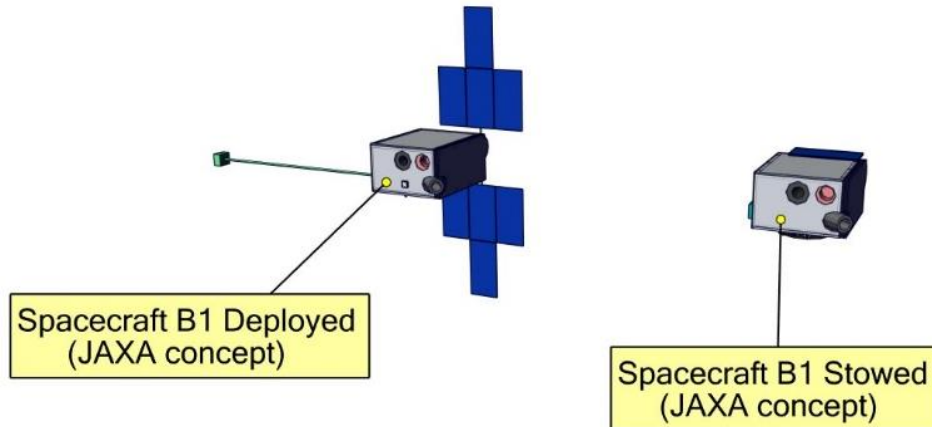
Figure 8-13 shows the planned micrometeoroid protection for the spacecraft on three main external panels.



**Figure 8-13: Three sides with additional structure as micrometeoroid protection**

### 8.3.2 Probe B1

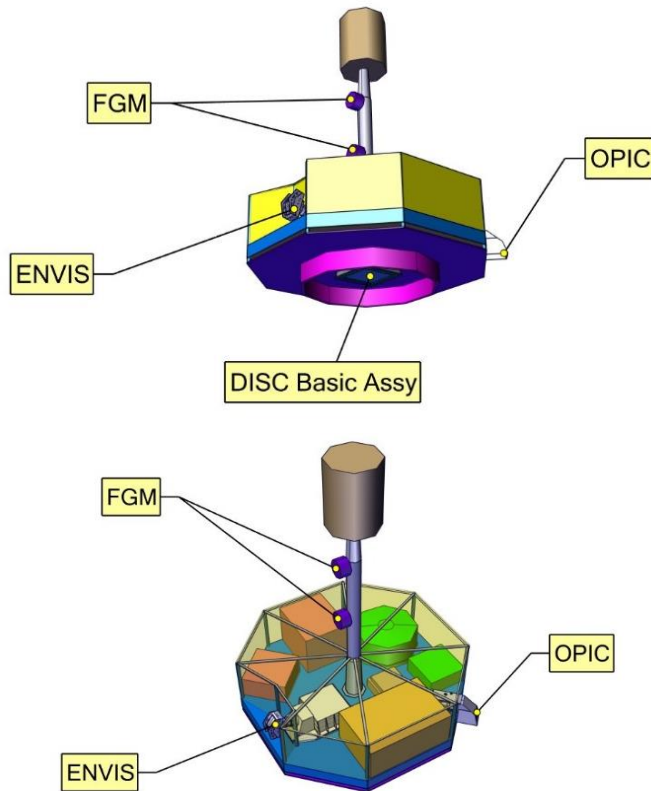
Probe B1 will be designed and developed by JAXA, and then integrated for the launch and transfer of the mission on S/C A. The current concept provided by JAXA is shown in Figure 8-14.



**Figure 8-14: Probe B1**

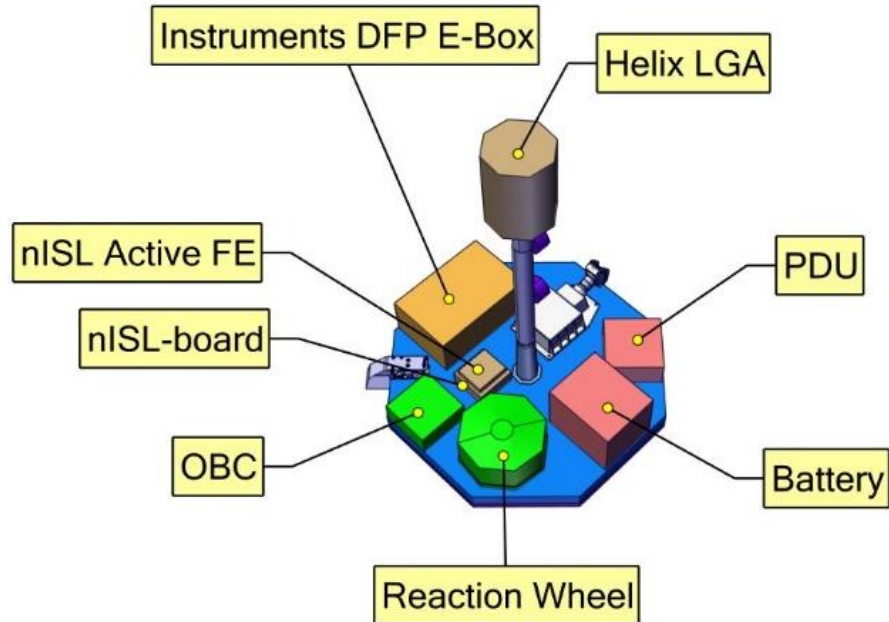
### 8.3.3 Probe B2

Probe B2 is an ESA spacecraft and is shown in Figure 8-15. The different proposed instruments have been identified.



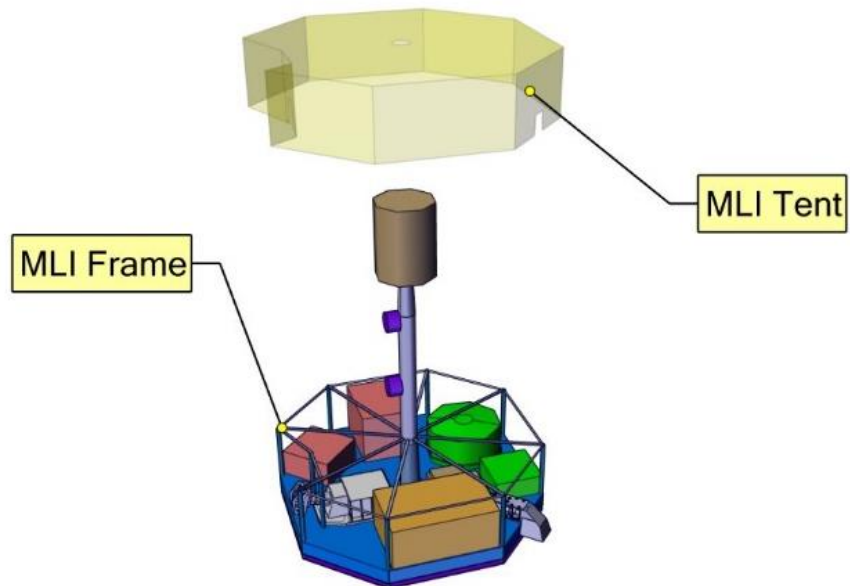
**Figure 8-15: Probe B2 Instruments**

Figure 8-16 shows the internal equipment of probe B2. The structure is an octagonal box, consisting of a baseplate with the instruments and equipment directly attached.



**Figure 8-16: Probe B2 Equipment**

The cover is a frame with MLI shown in Figure 8-17.



**Figure 8-17: Probe B2 MLI cover**

## 8.4 Overall Dimensions

The main dimensions of S/C A in launch configuration can be seen in Figure 8-18.

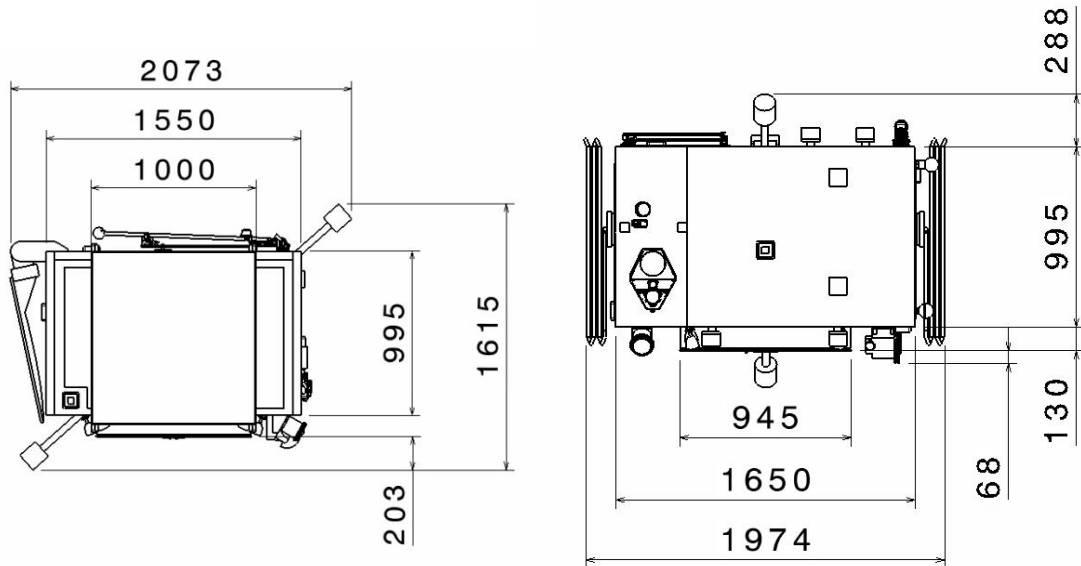


**Figure 8-18: S/C A main dimensions**

The overall stowed configuration of S/C A with the two probes B1 and B2 included, is shown in Figure 8-19.

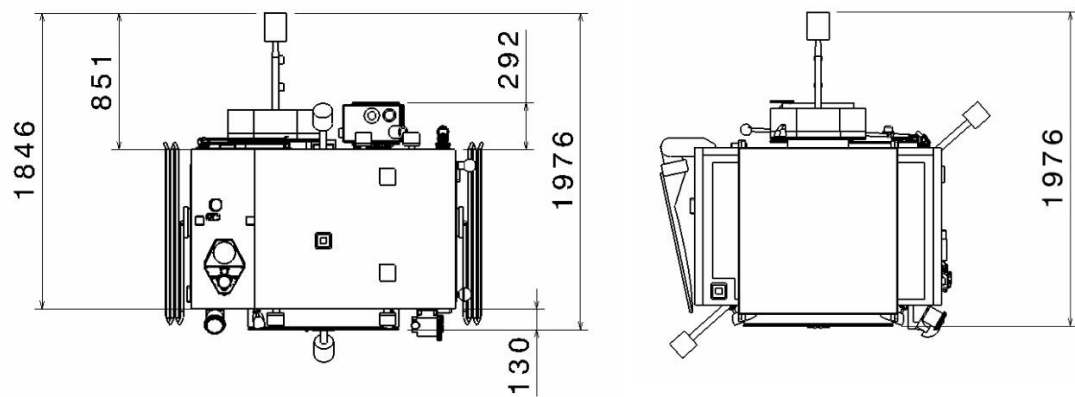


**Figure 8-19: Dimension of S/C A (with probes B1 and B2 included)**

The deployed configuration is shown in Figure 8-20 and Figure 8-21 for the front view dimensions.

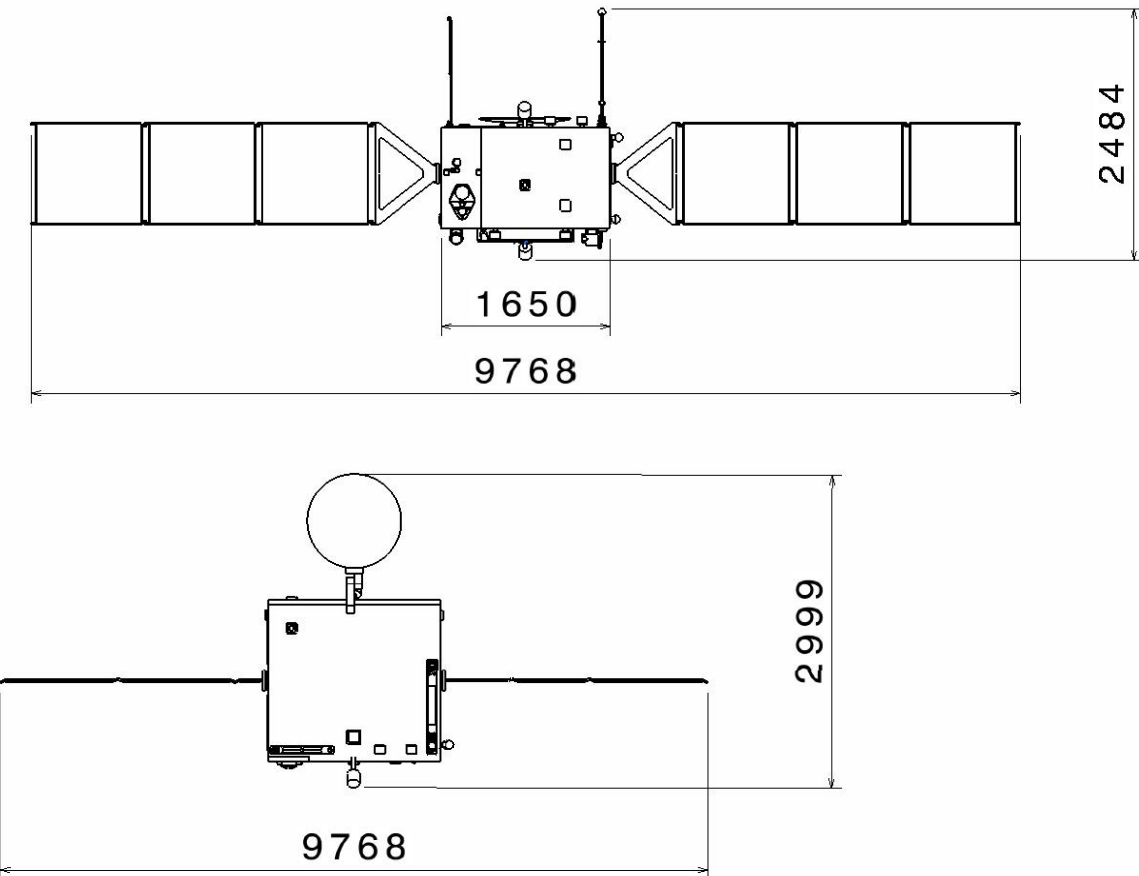


**Figure 8-20: Main dimensions of deployed S/C A**

The main dimensions of probe B1 are shown in Figure 8-21.

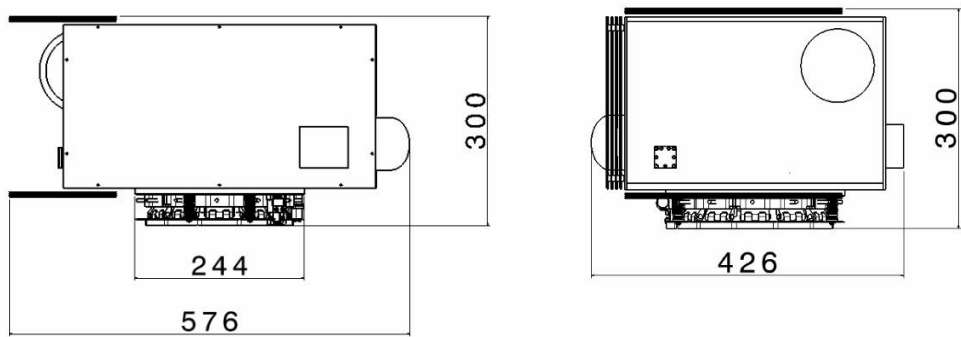


**Figure 8-21: Probe B1 initial dimensions**

The main dimensions of probe B1 in deployed configuration are shown in Figure 8-22.

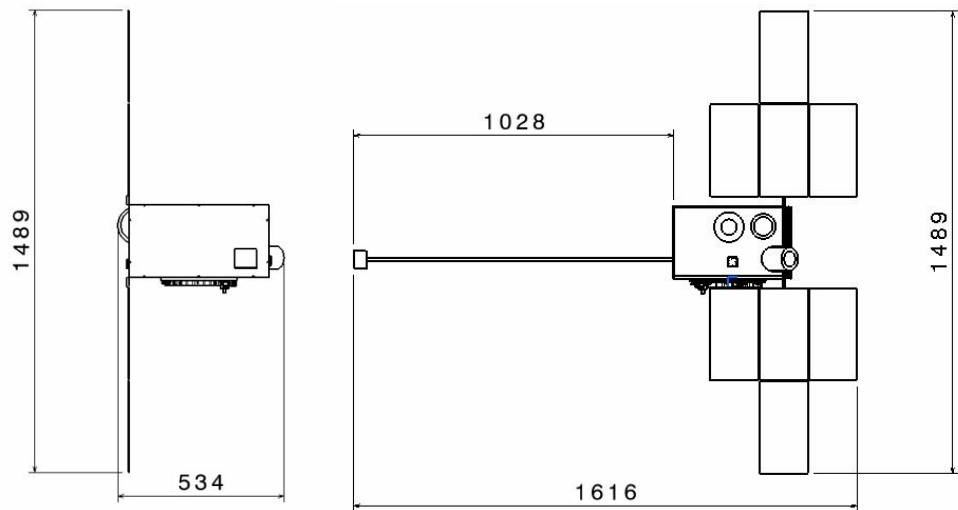


**Figure 8-22: Probe B1 deployed (concept by JAXA)**

The main dimensions of the body of probe B2 in stowed configuration are shown in Figure 8-23.

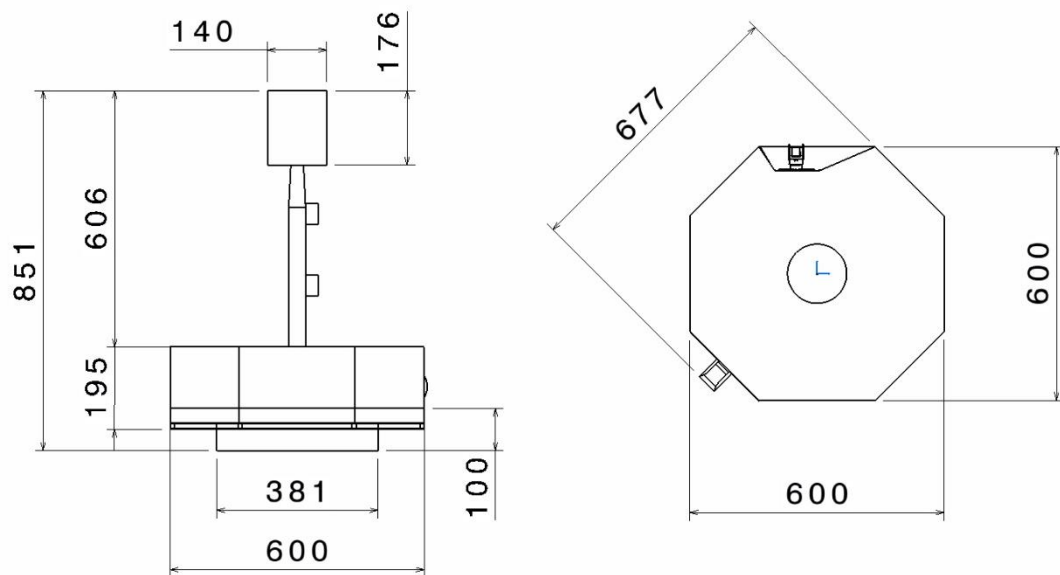


**Figure 8-23: Probe B2 stowed dimensions**

## 9 STRUCTURES

### 9.1 Requirements and Design Drivers

SubSystem Requirements		
Req. ID	Statement	Parent ID
STR-010	The Comet Interceptor structure shall be compatible with the launch environment as specified for Ariane 6	
STR-020	The S/C A (including the integrated probes B1 and B2), in launch configuration, shall have a first lateral frequency above 6Hz + 15%	
STR-030	The S/C A (including the integrated probes B1 and B2), in launch configuration, shall have a first axial frequency above 20Hz + 15%	
STR-040	The S/C A (including the integrated probes B1 and B2) CoG shall have an in-plane static offset of less than 30mm with respect to the LV I/F reference frame	
STR-050	The S/C A (including the integrated probes B1 and B2) CoG height shall be located between 0.4m and 3.4m from the LV interface plane	
STR-060	The S/C A structure shall provide shielding to comply with the reliability requirements considering the impact of particles of 100mg impacting at speeds up to 70 km/s.	
STR-070	The S/C A structure shall allow an independent integration of the propulsion subsystem and the instruments.	
STR-080	The materials considered for the structure design shall be compatible with the contamination requirements without dedicated bake outs.	
STR-B-090	Each secondary spacecraft (i.e. probes B1 and B2) shall have first lateral and axial modes higher than 110 Hz	
STR-B-100	Each secondary spacecraft (i.e. probes B1 and B2) shall be compatible with a QSL of 20 g in axial and lateral directions, simultaneously applied.	
STR-B-110	Each secondary spacecraft (i.e. probes B1 and B2) shall have a maximum in-plane static CoG offset below 30 mm (TBC) with respect to its interface reference frame (TBD).	

### 9.2 Assumptions and Trade-Offs

Assumptions	
1	The Ariane 6 requirements applied are those for payloads between 2000kg and 3,400 kg
2	LV interface can use any of the standard diameters (note that a 937 standard adapter was assumed)
3	Dual launch configuration together with ARIEL

### 9.3 S/C A Structure Design Definition

The S/C A structure is designed such that the launcher loads are transferred efficiently to the instruments, propulsion equipment, solar arrays and the probes B1 and B2.

In addition, the spacecraft structure shall provide shielding to allow a sufficient reliability considering micrometeoroid impacts of particles below 100mg and up to speeds of 70km/s.

The structure is composed of a baseplate, four lateral panels, a top panel and a central shear web, as shown in Figure 9-1.

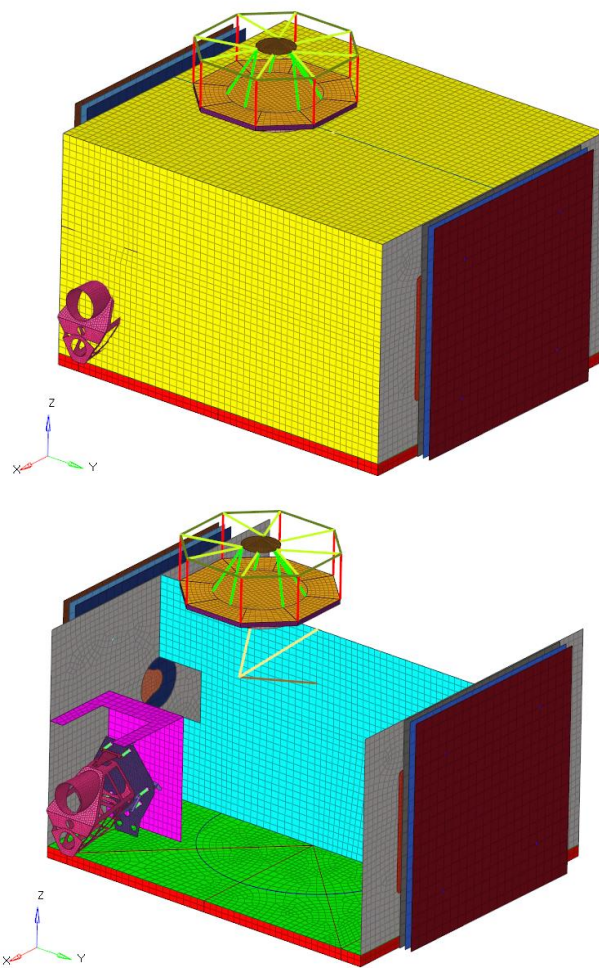


**Figure 9-1: S/C A structural design**

The baseplate, located in  $-Z$ , is designed as a 3 mm aluminium panel milled or cast, stiffened by ribs and including a launcher interface ring that provides the mechanical interface to the launch vehicle adapter. The baseplate also serves as the direct load path to the propellant tanks and the electric thruster.

The panels located at  $+/- Y$  serve as thermal radiators and structural support for several equipment, and for the solar arrays. Given that there is a substantial mass supported by these panels, they are designed as a 1 mm aluminium skin sandwich with 40 mm honeycomb core.

The panels at +/- X, as well as the top panel located at + Z must provide not only the mechanical stiffness, but also a sufficient level of micrometeoroid/dust shielding to prevent high risk of catastrophic damages for the mission during the flyby.

These panels are designed as a stuffed shield with a 0.3 mm aluminium external bumper, meant to vaporise the incoming particles, supported by a 50 mm ultra light honeycomb core. This panel is directly mounted on a 1.5 mm aluminium skin sandwich panel which provides the internal shielding protection as well as stiffness to the structure in the X direction.

The full schematic is as follows (with reference to Figure 9-2 below):

- Outer bumper: 0.3 mm Al
- Outer honeycomb (*S<sub>1</sub>* in Figure 9-2): 50 mm ultra-light honeycomb core
- Inner bumper: 1.5 mm Al
- Inner honeycomb (*S<sub>2</sub>* in Figure 9-2): 25 mm ultra-light honeycomb core
- Front wall: 1.5 mm Al

The dimensions of the shield were derived from the triple plate ballistic limit equation (BLE) that was introduced by Schaefer et al. (2008) and is based on numerous hypervelocity impact test campaigns. Different designs of single HC with Kevlar reinforced MLI as well as double honeycomb construction with toughened MLI was considered (Figure 9-2). The latter was taken into account as it provides high relative protection efficiency compared to the other solutions. The set properties of the shielding enable to withstand the considered meteoroid particles, as seen in Figure 9-3.

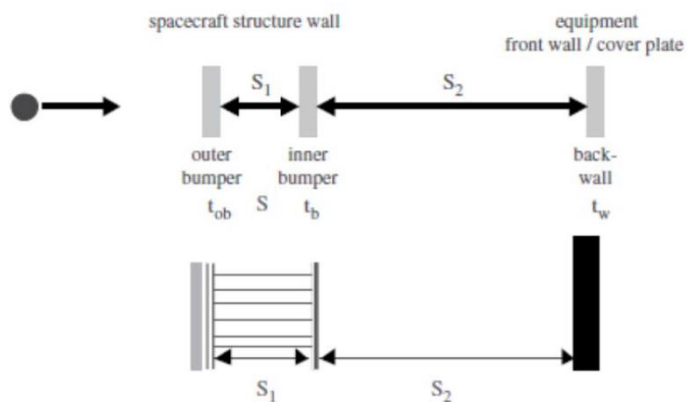
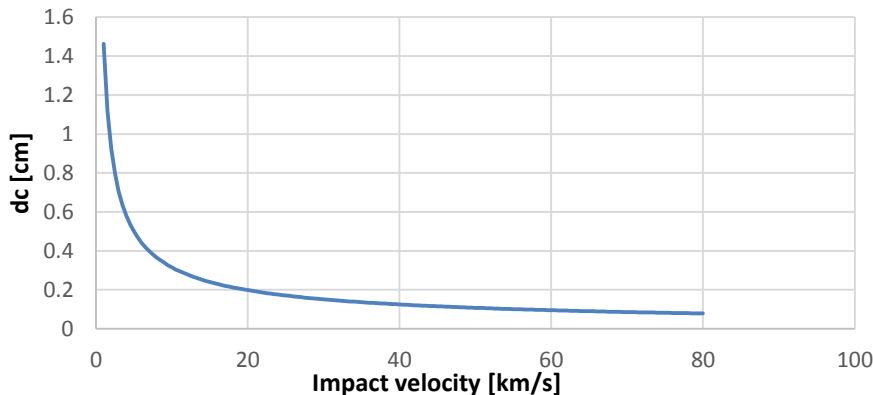


Figure 3: Geometrical configuration and nomenclature for the SRL ballistic limit equation.

**Figure 9-2: Geometrical configuration and nomenclature for the applied BLE (Schaefer et al., 2008)**



**Figure 9-3: Critical projectile diameter for failure of rear wall dc dependent on the impact velocity of the micrometeoroids of the considered shield taking the BLE into account.**

The (central) shear panel provides a second load path from the LV adapter into the Y panels and provides support for Propulsion and AOCS equipment. As such, the panel is composed of 0.3 mm aluminium skin and 20mm HC sandwich.

Last, considering the nominal field of view for the science instruments is towards +X, a dedicated payload panel is required. This panel shall provide a stiff interface to CoCa and MERMIS, in order to meet their co-alignment requirements. Therefore, in order to avoid a significant dynamic coupling it is composed of 1.5 mm aluminium skin and 40 mm HC sandwich.

### 9.3.1 Material Justification

A monolithic aluminium baseplate is considered for the LV interface as it is considered more cost effective and more accurate to estimate in the current Phase. An aluminium baseplate can be locally optimised to transfer the loads effectively to the external panels without a significant mass penalty and avoids the uncertainty associated with the interfaces of sandwich panels, in particular towards the LV adapter ring.

For the external panels aluminium sandwich has been selected due to its lower manufacturing cost and outgassing limited to the adhesives.

Aluminium sandwich also eliminates thermoelastic problems with adjacent structures (baseplate and electronic equipment).

An alternative option would be to consider CFRP skin sandwich. Thanks to its higher stiffness and lower density, a mass benefit can be expected but limited by the minimum feasible thicknesses and the need to account for complex interface inserts to avoid CTE (Coefficient of Thermal Expansion) problems. In addition, the CFRP alternative will result in higher costs for the panels and may probably require dedicated bake outs to prevent payload contamination in orbit.

## 9.4 Probe B2 Design Definition

### 9.4.1 Definition

The baseline structural design of probe B2 consists of an aluminium baseplate that is stiffened with aluminium ribs and edge frame. A central ring also provides the connection to the S/C A via a 381mm diameter clamp band. The MLI tent (functioning as the outer upper “structure”) is simplified modelling the load carrying outer frames of the tent using squared aluminium profiles.

All instruments as well as the corresponding equipment of the AOCS, DHS and PWR are modelled as point masses in accordance to the current configuration. The low gain antenna support structure is designed as an aluminium skin sandwich supported by rods that are connected to the baseplate. Both the antenna itself as well as the proximity electronics are mounted on this panel and added to the FE model as non-structural mass. In addition, the portion of the clamp band that remains attached to B2 hardware is added as non-structural masses to the adapter ring. Thermal hardware mass is distributed over the MLI tent support structure.

Concerning the shielding, the same concept as for S/C A is used. As an outer shield against micrometeoroids, only the ram-facing structure is shielded. The shielding is provided as a 0.3 mm aluminium bumper placed 50 mm in negative z-direction away from the baseplate, while the inner bumper contains a Kevlar/Nextel stiffening before the 3mm baseplate shell. The bumper mass is also added as non-structural mass to the baseplate ribs.

As such, the probe B2 has a double-wall shielding of:

- Outer bumper: 0.3 mm Al
- Honeycomb: 50 mm ultra-light honeycomb core
- Inner bumper (= baseplate shell): 3 mm Al

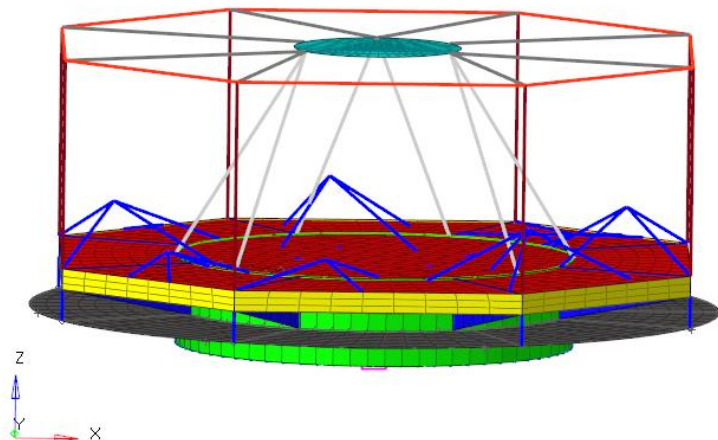


**Figure 9-4: FEM model of B2, showing the shielding. It has to be noted that the shield is added as NSM and only visible here for illustration purposes**

#### 9.4.2 Dimensioning Analysis Results

A preliminary structural analysis has been performed to confirm the compliance to the defined requirements. A preliminary FE model has been developed where the primary structure is physically modelled. Also, the probe B2, the solar array panels and the CoCa instrument have been explicitly modelled. Other units are modelled as point masses attached through rigid elements to the primary structure.

The mass associated to harness, thermal hardware and system margin is distributed over the primary structure panels.

Overall FE model properties are reported in the following table:

	<b>Value</b>	<b>Requirement</b>
FE model Mass	743kg	OCDT mass: 796.42kg (+7%)
CoG height	0.53 m	$0.45 < h < 3.4$ m
Cog X,Y offset	X:9.8mm,Y:2.3mm	<30mm
First lateral mode	8.85Hz	6.9Hz
First axial mode	38.9Hz	23Hz

**Table 9-1: Compliance matrix to structural requirements**

##### 9.4.2.1 S/C A - Modal analysis

A modal analysis has been performed considering a rigid LV interface.

The following table shows the percentage of modal mass per mode.

<b>Mode</b>	<b>Freq. Hz</b>	<b>M<sub>xx</sub></b>	<b>M<sub>yy</sub></b>	<b>M<sub>zz</sub></b>	<b>I<sub>xx</sub></b>	<b>I<sub>yy</sub></b>	<b>I<sub>zz</sub></b>
1	8.9	366.6	0.6	0	1.4	517.1	0
2	19.0	1.2	334.8	0.1	555.7	0.6	0
3	38.9	0	0	664.5	0	0.1	0
12	95.5	4.8	3.9	0	0	0.1	17.8
13	98.0	1.8	13.8	0	0.1	0	6.6

**Table 9-2: Modal mass per mode**

##### 9.4.2.2 Probe B2 - Modal analysis

The MLI tent possesses a first eigenfrequency below 120 Hz but with a very low effective mass (well below 5%). Therefore, it is not considered for the requirement verification.

The first eigenfrequency of the probe B2 is at 121 Hz showing that the B2 stiffness requirement is met.

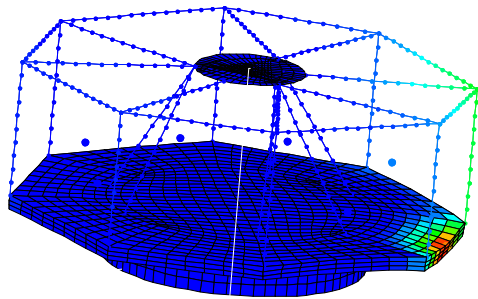


**Figure 9-5: First mode of probe B2**

#### 9.4.3 Mass Budget

The mass budget is presented in the following tables for the S/C A and B2 structures. Currently, the S/C A mass is driven by the shielding requirements with an approximate impact of 30 kg (10kg per panel of shielding). The +/- Y panels are currently sized by the stiffness required to provide stiff interfaces to the solar array and the P/L and avionics equipment. The mass of this panel can be optimised to only locally stiffen the interface areas and reduce the skin and core stiffness where not required.

In addition to those elements sized based on the mathematical model, additional allocations are estimated for fasteners and other attachment hardware (“Miscellaneous STR”), for not modelled secondary structure (e.g. brackets, local supports) and for inserts which are not included in the sandwich panels.

Item	Mass [kg]	Margin [%]	Mass, including margin [kg]
Baseplate	28.9	20	34.656
+/- Y panels	19.6	20	23.5272
Inserts	4.0	20	4.8
Miscellaneous STR	5.0	20	6
Propulsion support	0.77	20	0.924
Solar Array yoke #1	1.0	20	1.2
Solar Array yoke #2	1.0	20	1.2
Secondary structure	10	20	12
Shear Web	3.81	20	4.572
Shielding Panels	59.61	20	71.532
PL_Panel	3.00	20	3.6
<b>Total</b>	<b>136.68</b>		<b>164.01</b>

**Table 9-3: S/C A Structure Mass budget**

The probe B2 structural mass is driven by the baseplate that is the only load carrying structure.

As the baseplate is the main driver concerning structural mass of B2, topology and sizing optimization were performed on the baseplate including the ribs and the edges. A topology algorithm was used to meet the first eigenfrequency requirement ( $> 120$  Hz) while minimising the mass. As design space the ribs as well as the side panel were chosen, while the baseplate itself as well as the launch adapter ring were set as non-design space in order not to influence the equipment and the basic dimensions of the MLI tent. As a starting point the aluminium ribs, baseplate and edges were defined as 3 mm thick.

The result shows that the thickness of the ribs and the edge can be reduced with increasing distance from the launch adapter ring. Therefore, the overall height dimensions of the ribs as well as the edges were reduced towards the external perimeter of the baseplate maintaining a constant thickness.

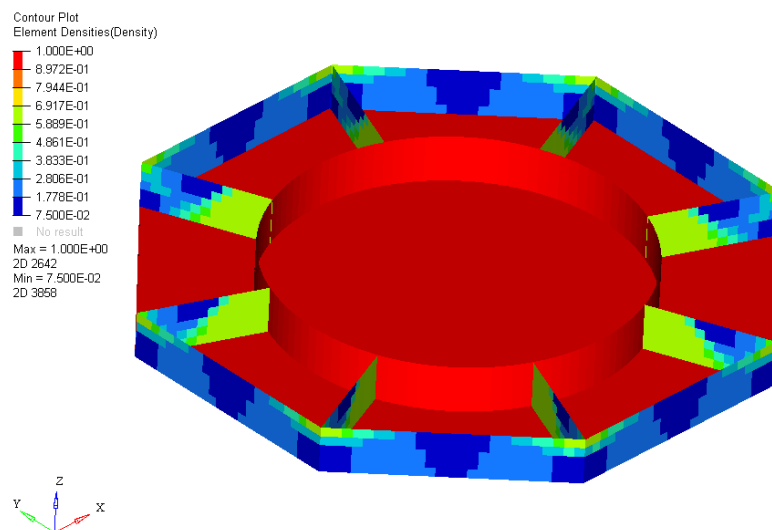


**Figure 9-6: Results of topology optimisation for baseplate of B2**

The final design of the baseplate led to a baseplate thickness of 2.7 mm, ribs of 1.7 mm thickness and an external edge of 1.0 mm. The probe B2 in hard mounted conditions and considering the overall mass with margins obtains a first eigenfrequency of 121 Hz ( $> 120$  Hz). The mass of the baseplate was decreased from 3.35 kg to 2.62 kg, representing a reduction of 20 % of its structural mass.

This can be further improved by more complex rib patterns that can help in reducing the thickness of the shell.

Note that the mass budget of the separation system is currently included twice in the FEM (mechanism: 1.0 kg as NSM in the SC/I Ring and structure of SC/I Ring; 1.41 kg). The current mass-budget of the FEM model therefore is 1.41 kg higher than specified in Table 9-4.

Item	Mass [kg]	Margin [%]	Mass, including margin [kg]
Baseplate	2.62	20	3.15
Bumper	0.37	20	0.44
Antenna Support Structure	0.15	20	0.18
MLI Tent	0.62	20	0.74
<b>Total</b>	<b>3.76</b>		<b>6.20</b>

**Table 9-4: B2 Structure Mass budget**

This Page Intentionally Blank

## 10 CHEMICAL PROPULSION

Note that, as indicated in the introduction, the CDF study baseline assumed a combination of CP and EP. After the Study, it was concluded that a mission design based only on chemical propulsion (CP) better matches the strict programmatic boundaries of the F-mission. Nonetheless, the chapter below highlights important considerations and provides a comparative sizing case for a CP+EP solution.

### 10.1 Requirements and Design Drivers

SubSystem Requirements		
Req. ID	Statement	Parent ID
PROP -010	The chemical propulsion subsystem shall be able to deliver a gross velocity increment of $\Delta v = 168 \text{ m/s}$	
PROP -020	The chemical propulsion subsystem shall also be used for performing AOCS functionality	
PROP -030	The contamination of the spacecraft by the plume of the thrusters shall be minimised	
PROP -040	The propulsion subsystem shall make use of European COTS components where available	
PROP -050	All components of the propulsion subsystem shall have reached TRL 6 or more by Mission Selection (Q1 2020) and TRL 7 by Mission Adoption (Q4 2022)	
PROP -060	<i>Deleted</i>	
PROP -070	The CP shall be used for TCM (deterministic and stochastic), L2 insertion and AOCS manoeuvres	

### 10.2 Assumptions and Trade-Offs

The following assumptions have been made for the chemical propulsion subsystem.

Assumptions	
1	The amount of unusable residual propellants remaining in the subsystem at end of life is assumed to be 2% of the total propellant loading
2	The propellant for AOCS manoeuvres in support of the EP during transfer are calculated, assuming half the EP propellant still on board.
3	The thrusters (5N) for the baseline design are ITAR restricted but are assumed to be available for this mission.
4	Propellant margins are covered by margins in $\Delta v$ demand, therefore no additional margin is applied to the propellant mass

A trade-off has been performed to analyse the propellant consumptions and tank sizes for different configurations. The velocity increments used for this trade-off study are reported in Table 10-1.

Manoeuvre	$\Delta v$ [m/s]	Margin [%]	Total [m/s]
TCM Stochastic	40	0	40
TCM Deterministic	15	10	16.5
L2 Orbit Insertion	0	10	0
Mission - AOCS	41	100	82
Navigation Stochastic	14.1	5%	14.8
Divert Maneouvres Deterministic	14	5	14.7
<b>Total</b>			<b>168</b>

**Table 10-1: Delta-V budget for trade-off analysis**

The baseline design for the spacecraft was sized assuming 5N MONARC-5 thrusters, which are ITAR restricted. Further options were also investigated. For this trade-off, the propellant mass was kept constant as for the baseline assumption of the 5N MONARC-5 thrusters. This mass was iterated with the EP system to be half of the 91.87 kg before the mission AOCS manoeuvres and the other half of the 91.87 kg afterwards.

The other options investigated were:

- A. IHI-4N thruster (Japanese)
- B. LT-5N thruster (Rafael Aerospace)
- C. Aerojet 5N thruster (ITAR restricted)
- D. Ariane Group 5N thruster (Discontinued).

Option C has the same issue as the assumed baseline (i.e. ITAR-restriction), along with not much data being available for the Aerojet thrusters. Option D would have been ideal as the provider is a European company, but the 5N thruster has been discontinued. The production of these thrusters could be revived but this would potentially come with a significant price tag. Option B is similar to the assumed baseline but the thruster requires higher power consumption during standby mode as well as the LT-5N thruster having issues with spitting catalyst parts from the nozzle. Option A would be the ideal back up to the assumed baseline as it is not known to have any performance issues nor is the power requirement ominously higher but this thruster configuration would add significant mass to the chemical propulsion subsystem.

Thruster Options	Propellant Mass [kg]	Tank Mass [kg]	Power Requirement [W] On / (standby)	Additional Thruster Mass [kg]	Total CP system additional mass [kg]
MONARC-5 (5N)	48.42	11.8	18 (4.1)	-	-
LT-5N (5N)	51.64	11.8	19.2 (9)	-1.6	1.62
IHI-4N (4N)	50.9	11.8	19.6 (4.6)	4	7.28

**Table 10-2: Thruster Mass and Power Consumption Trade-Off Analysis (Baseline, Option A & B)**

Options A and B impose a higher power requirement whilst also commanding more mass. Not enough data was available for Options C & D to warrant a trade-off therefore the baseline design was sized utilising the Monarc-5 thrusters, with considered IHI-4N as backup. The tank mass in either case does not change and provides a better blow-down ratio in the baseline design. LT-5N, having the benefit of weighing less than the MONARC-5 engine, ends up costing the spacecraft more propellant mass along with additional power requirement.

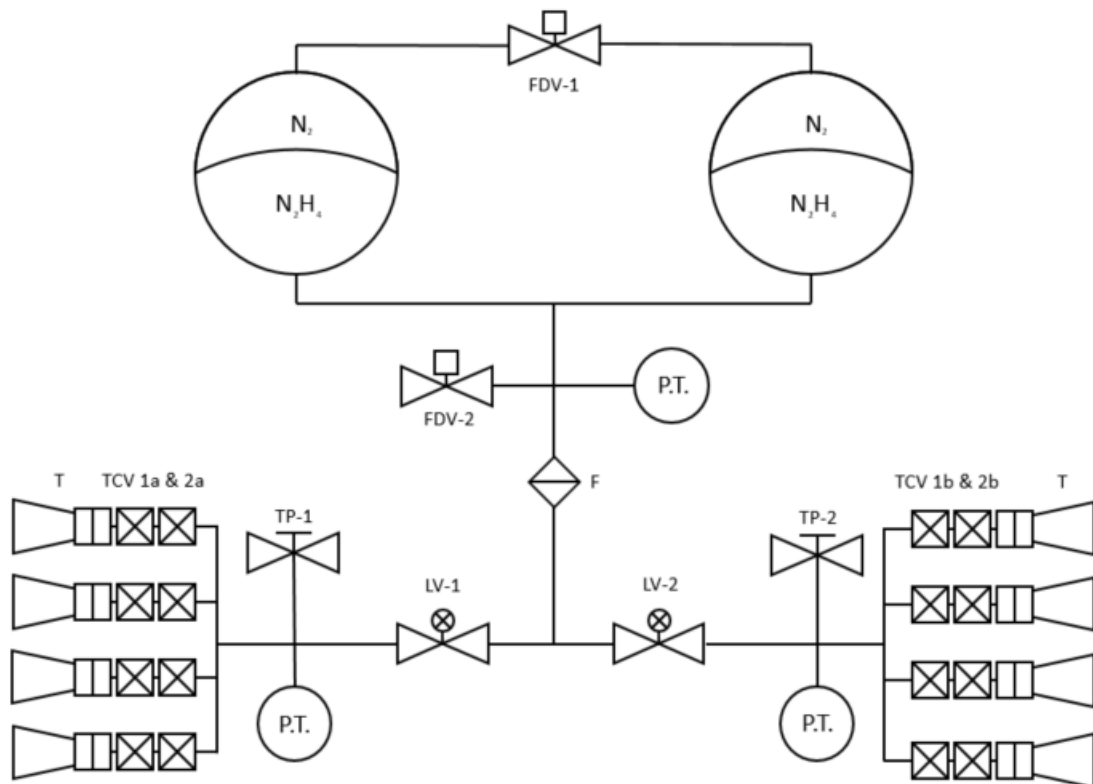


**Figure 10-1: Propulsion Sub-system schematic**

The propulsion system for either of the aforementioned options would require the use of 8 thrusters. The proposed system consists of dual modular redundancy with 2 chains of 4 thrusters each and 3 barriers between the tank and the thrusters in the form of a latch valve and 2 solenoid valves on the thruster itself.

## 10.3 List of Equipment

The following equipment was used to size the baseline design:

### 10.3.1 Hydrazine Tank D-358

The diaphragm tank D-358 from Northrop Grumman (RD[20]) has been selected as sizing case for the hydrazine tank. The spacecraft would have 2 of these tanks.

<b>Propellant Management</b>	Diaphragm
<b>MEOP</b>	27.3 bar
<b>Total Volume</b>	38.32 l
<b>Propellant Volume</b>	32.74 l
<b>Tank Diameter</b>	419 mm
<b>Tank Length</b>	419 mm
<b>Material</b>	Ti-6Al-4V
<b>Mass (dry)</b>	5.9 kg

**Table 10-3: Hydrazine tank properties**

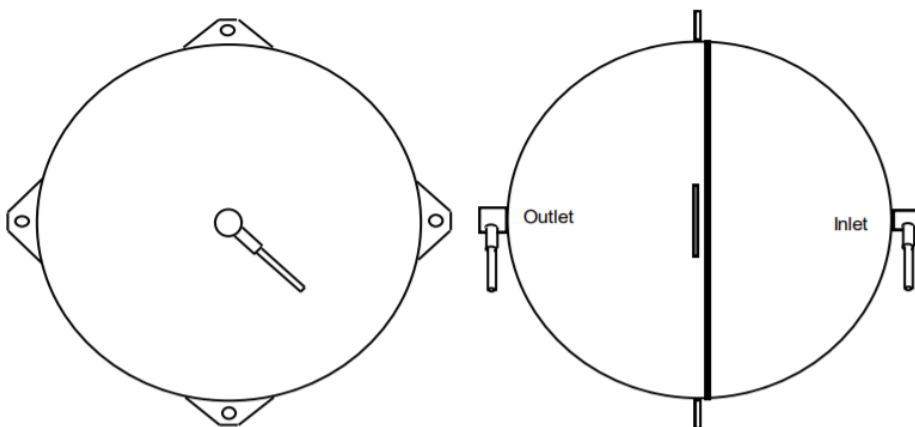


**Figure 10-2: D358 Northrop Grumman Tank. Drawing Courtesy of Northrop Grumman**

### 10.3.2 Thruster MONARC-5

As discussed above, the 5N thruster MONARC-5 from Moog Isp RD[21] were selected as sizing case for the RCS thruster operation.

<b>Propellant</b>	Hydrazine
<b>Thrust (range)</b>	1.8 N – 4.9 N
<b>Inlet pressure (range)</b>	5.5 bar - 29 bar
<b>Nozzle Expansion Ratio</b>	135
<b>Specific impulse</b>	225 s - 231 s
<b>Mass flow</b>	0.8 g/s - 2.1 g/s
<b>Maximum throughput</b>	125 kg
<b>Chamber Material</b>	Platinum
<b>Mass</b>	490 g

**Table 10-4: 5N MONARC-5 thruster properties**



**Figure 10-3: 5N thruster MONARC-5. Photo courtesy of MOOG Isp RD[21]**

### 10.3.3 Latch Valve LPLV

The LPLV from Ariane Group RD[22] was selected as an example for design purposes as latch valves.

<b>Propellants</b>	Hydrazine, MMH, NTO
<b>Tubing interface</b>	1/4"
<b>Back relief pressure</b>	8 bar - 14 bar
<b>Material</b>	Stainless steel
<b>Mass</b>	545 g

**Table 10-5: LPLV Latch Valve**

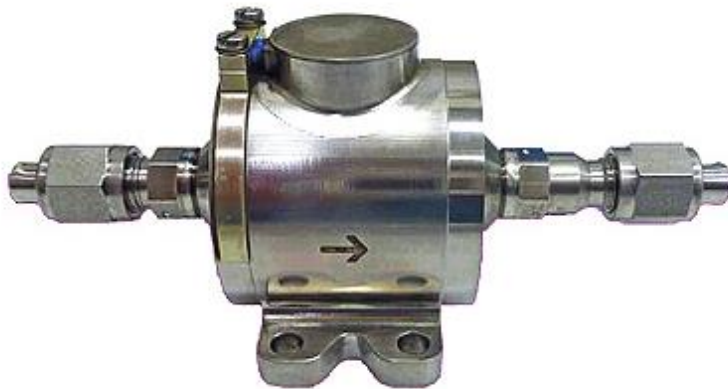


**Figure 10-4: Latch Valve LPLV. Photo courtesy of Ariane Group**

### 10.3.4 Miscellaneous Equipment

#### 10.3.4.1 Pipework

The 1/4" pipework is assumed to be 3 kg, based on similar spacecraft. This includes mass for transition joints as well. A margin of 20% applies.

#### 10.3.4.2 Pressuring gas

Nitrogen is used as pressuring gas. The required mass is calculated based on the propellant volume and the volume available in the chosen diaphragm tanks. The pressurising gas is treated as part of the propulsion system dry mass in the mass budget, although it's actual mass varies based on the required propellant mass. It is in the order of 0.80kg.

#### 10.3.4.3 Full Equipment List

Below is the equipment list and power budget used for sizing at system level:

Description	Type	Amount	Mass per unit	Margin	Mass incl. margin
Pipes	Pipes – ¼ ``	1	3.00	20%	3.60
Fill & drain valve	AST-FFVV	2	0.07	5%	0.15
Pressure transducer	SAPT-250	3	0.22	5%	0.68
Test Port		2	0.07	5%	0.15
Latch valves	LPLV 3554258	2	0.55	5%	1.16
5N thruster	Monarc-5	8	0.49	5%	4.12
Propellant Filter	430-PF2	1	0.11	5%	0.12
Passivation Valves	vgl. Bar mit Test Ports	1	0.07	5%	0.07
Tank	D358	2	5.9	5%	12.39
Chemical propulsion system			10.49		22.44
Propellant	Hydrazine	1	47.47	2%	48.42
Pressurant	Nitrogen	1	0.80	2%	0.82
					71.68

Table 10-6: CP Equipment list

Product/Function	Product	
Element Owner	CPROP	
Power (W)	P_on	P_stby
SC_A (Spacecraft A)	204.65	33.45
A_Fil_Dr_Val_1 (A Fill Drain Valve)	0.00	0.00
A_Fil_Dr_Val_2 (A Fill Drain Valve)	0.00	0.00
A_Lat_Val_1 (A Latch Valves)	30.00	0.00
A_Lat_Val_2 (A Latch Valves)	30.00	0.00
A_Pass_Valve (A Passivation_Valve)	0.00	0.00
A_Press_Trans_1_1 (A Pressure Transducer #1)	0.22	0.22
A_Press_Trans_1_2 (A Pressure Transducer #1)	0.22	0.22
A_Press_Trans_1_3 (A Pressure Transducer #1)	0.22	0.22
A_Tk_CPROP_1 (A Tank CPROP #1)	0.00	0.00
A_Tk_CPROP_2 (A Tank CPROP #2)	0.00	0.00
A_Thr_5N_1 (A Thruster_MONARC 5N #1)	18.00	4.10
A_Thr_5N_2 (A Thruster_MONARC 5N #2)	18.00	4.10
A_Thr_5N_3 (A Thruster_MONARC 5N #3)	18.00	4.10
A_Thr_5N_4 (A Thruster_MONARC 5N #4)	18.00	4.10
A_Thr_5N_5 (A Thruster_MONARC 5N #5)	18.00	4.10
A_Thr_5N_6 (A Thruster_MONARC 5N #6)	18.00	4.10
A_Thr_5N_7 (A Thruster_MONARC 5N #7)	18.00	4.10
A_Thr_5N_8 (A Thruster_MONARC 5N #8)	18.00	4.10
<b>Grand Total</b>	<b>204.65</b>	<b>33.45</b>

**Table 10-7: CP Power budget**

This Page Intentionally Blank

## 11 ELECTRIC PROPULSION

Note that, as indicated in the introduction, the CDF study baseline assumed a combination of CP and EP. After the Study, it was concluded that a mission design based only on chemical propulsion (CP) better matches the strict programmatic boundaries of the F-mission. Nonetheless, the chapter below highlights important considerations and provides a comparative sizing case for a CP+EP solution.

### 11.1 Requirements and Design Drivers

The EP subsystem requirements are listed in the table below.

SubSystem Requirements		
Req. ID	Statement	Parent ID
EP-010	The EP subsystem shall be used for station keeping in L2	
EP-020	The EP subsystem shall be used for the transfer to the comet.	
EP-030	The EP subsystem shall provide a total $\Delta v$ of 1522.5 m/s (SK: 22.5 m/s, comet interception: 1500 m/s).	
EP-040	All EP equipment shall be at least TRL6 by Mission Selection (Q1 2020) and TRL 7 by Mission Adoption (Q4 2021)	

The following design drivers have been identified:

1. An EP thruster technology with a high thrust-to-power ratio shall be selected in order to maximise the thrust at a given power level. Therefore a Hall Effect Thruster (HET) has been selected since it has a higher thrust-to-power ratio than gridded ion engines.
2. The EP subsystem mass shall be minimised. Therefore a non-redundant EP subsystem has been selected.

Note: The single string EPS baselined does already include some internal redundancy. The BPRU valves are duplicated, protecting against single failures in the pressure regulation valve chain. The power connection, between the EPS and the spacecraft power bus, is also duplicated, as are the thruster hollow cathodes and their appropriate XFC connection. Also included is a redundant BPRU heater.

Furthermore, the PPS®1350-G thruster has significant flight heritage: it has been operated for more than 5000 hours on SMART1, on AlphaSat the 4 thrusters have accumulated more than 1800 hours of operation. There has been no in-orbit failure of the PPS®1350-G to date.

### 11.2 Assumptions and Trade-Offs

The following assumptions are made for the sizing of the EP subsystem:

### Assumptions

- 1 A maximum power of ~800 W is available for the EP system.
- 2 The full CP propellant mass is taken into account for the EP SK propellant mass determination (at L2)
- 3 Only a part of the CP propellant mass is taken into account for the EP comet interception propellant mass determination (discussed in Section 11.3.1)

## 11.3 Baseline Design

An EP subsystem similar to the one flown on SMART-1 (RD[23]) has been assumed as the baseline sizing case. The only difference is the selected propellant tanks. All proposed units are fully qualified and have flight heritage. Two tanks have been proposed for configuration reasons in order to simplify the accommodation of the tanks inside the spacecraft.

The assumed EP subsystem is composed of:

- 2 Propellant Tanks (32 L capacity each)
- 1 Bang-bang Pressure Regulator Unit (BPRU)
- 1 Xenon Flow Control unit (XFC)
- 1 Power Processing Unit (PPU)
- 1 Electrical Filter Unit (FU)
- 1 Pressure Regulation Electronics Card (PRE Card)
- 1 1.5 kW Hall Effect Thrusters (HET).

A functional diagram of the transfer EP subsystem is shown in Figure 11-1.

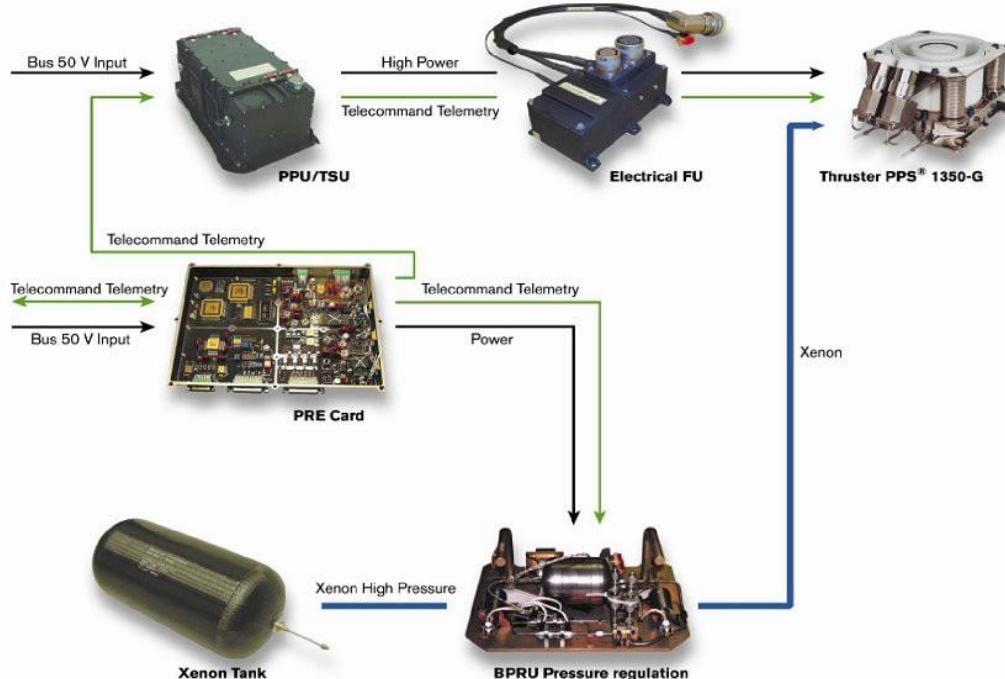


**Figure 11-1: Functional diagram of the transfer EPS (one single branch shown)**

The EPS proposed would consist of three main sections: the Xenon system, the electrical power and thruster system, and the digital interface and communication system.

The xenon is stored under high pressure (up to 187 bar) in two propellant tanks with a volume of 32 litres each (i.e. a total propellant capacity of 108 kg of Xenon). A pressure regulator (BPRU) is used to regulate the xenon down to a constant low pressure of around 2 bar at the beginning of the mission and configurable later to extend the lifetime of the thrusters when the pressure in the main tank drops to lower levels. The low-pressure xenon is then fed into the adjustable flow regulator (XFC). A simple and robust control loop algorithm, located in the PRE Card, is used to control the constant pressure delivered by the BPRU. The XFC is used to fine control the xenon mass flow rate in order to operate the HET at a constant discharge current and hence a constant power. The HET is controlled and powered by the Power Processing Unit (PPU). All Telemetry (TM) and Telecommands (TC) are interfaced to the EP subsystem through the PRE Card. If necessary, the PRE Card can be integrated in other interface units. Commands reaching the PRE Card are either executed by the PRE Card (if relating to the BPRU control) or passed to the PPU. An electric filter (FU) is included to reduce the electrical thruster oscillations and to protect the electronics of the PPU.

### 11.3.1 Propellant Budget

The EP propellant budget has been calculated together with CP using a mixed manoeuvre strategy.

For the EP Station Keeping (SK) propellant mass determination, the full CP propellant mass (48.4 kg) has been accounted for.

For the EP propellant mass associated with the transfer to the comet only the following contributions to the CP propellant mass have been accounted for:

- Half of the CP propellant required for mission AOCS manoeuvres (24.2 kg),
- All of the CP propellant required for the navigation stochastic manoeuvres (14.8 kg),
- All of the CP propellant required for the divert manoeuvres deterministic (14.7 kg).

A dry mass of 644.1 kg<sup>17</sup> has been considered for the propellant budget.

In line with the maximum power available for the EP subsystem at 1 AU, the following operating point has been selected since EP thrust arcs of the transfer trajectory for most scenarios will occur around 1 AU:

- Input power to the PPU: 801.6 W
- Thrust: 40.1 mN
- Specific impulse: 1219 s

<sup>17</sup> The dry mass assumed for the propellant budget is slightly different to the final dry mass assumed in the system budget (655.1 kg) due to late changes in the design. This difference however has no impact on the subsystem design and resulting increase in propellant mass is still within the capacity of the selected propellant tank.

The resulting propellant budget is presented in Table 11-1.

Manoeuvre	$\Delta V$ incl. margins [m/s]	Propellant mass [kg]	Residuals [kg]	Propellant volume [L]
Station keeping (3 years)	22.5	1.47	0.03	
Comet interception	1500	88.59	1.77	
<b>Total</b>	<b>1522.5</b>	<b>90.06</b>	<b>1.8</b>	<b>54.25</b>

**Table 11-1: EP propellant budget**

The total propellant volume amounts to 54.25 L. This is smaller than the total propellant volume of 64 L.

## 11.4 List of Equipment

The list of equipment for the sizing case EP subsystem, the number of units installed and the mass of each of this equipment is presented in Table 11-2. The total mass of the subsystem is also included.

EPROP						
Unit	Unit mass [kg]	Qty	Total Mass [kg]	Equipment Cat	Margin	Total mass with margin [kg]
Hall Effect Thruster	4.35	1	4.35	A	5%	4.57
Xenon Flow Controller	0.82	1	0.82	A	5%	0.86
Pressure Regulator Assembly	2.75	1	2.75	A	5%	2.89
Pressure Regulator Electronics	1.27	1	1.27	A	5%	1.33
PPU	10.66	1	10.66	A	5%	11.19
Filter Unit	0.68	1	0.68	A	5%	0.71
Miscellaneous (piping, harness, etc.)	3.50	1	3.5	A	5%	3.68
Tank	6.35	2	12.7	A	5%	13.34
<b>Total Dry Mass excluding margins</b>						<b>36.73</b>
<b>Total Dry Mass including margins</b>						<b>38.57</b>

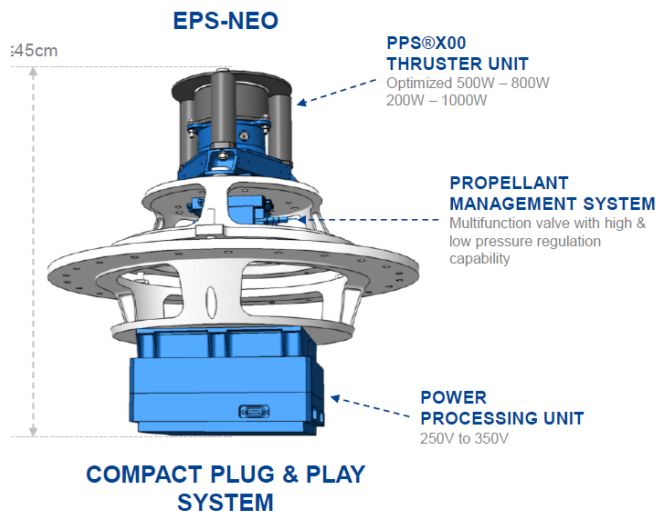
**Table 11-2: EP Subsystem Equipment list and mass budget**

## 11.5 Options

Due to the power limitation of the spacecraft, the assumed baseline thruster would be operated at a lower power operating point than its nominal operating point. It thus might be beneficial to consider a smaller thruster that is better optimised for this lower power range in order to reduce the EP subsystem mass and the propellant mass.

There is currently a Safran led development of an EP subsystem (EPS-NEO) based on the low power PPS®Xoo Hall effect thruster. This development is funded by a H2020 program as well as an ARTEMIS program. The EPS-NEO is a compact plug-and-play system that is mainly developed for LEO constellation applications. This compact propulsion system would lead to a reduction of ~30% of the subsystem mass, compared to the sizing case above.

An overview of the EPS NEO is shown in Figure 11-2.



**1.5 MN.s**

First European HET EPS  $\leq 1\text{kW}$   
with Total Impulse  $\geq 1\text{MN.s}$

**200 k€**

Target price for satellite constellation

**Xe-Kr**

Target optimization with Xenon  
and compatible with Krypton

**Figure 11-2: Main features of the EPS-NEO propulsion system**

The current EPS-NEO development plan foresees subsystem coupling tests using EMs beginning of 2020, CDR in Q3 2021 and the QR in Q1 2023.

At an input power of  $\sim 800\text{ W}$ , the EPS-NEO is expected to deliver a thrust of  $\sim 53\text{ mN}$  and Isp of  $\sim 1500\text{ s}$ . The higher specific impulse compared to the baseline thruster would lead to propellant mass savings of the order of 21%.

## 11.6 Open Issues

The proposed baseline used for the system sizing foresees to have both the CP and the EP thrusters on the same side of the spacecraft (-Z). In order to dump momentum, the RCS CP thrusters might need to be fired every 35 min during EP thrusting mode. Given that the RCS thrusters would need to be fired very frequently, it is not possible to switch off the EP thrusters during the RCS firings since there is a minimum off time of  $\sim 23$  minutes between two consecutive HET firings. Simultaneous operation of CP and EP thrusters might lead to intersection of the plumes and can result in a contamination risk of the EP thruster by the CP propellant. The most critical component of the EP subsystem with respect to contamination is the cathode since the LaB6 emitter inside the cathode is very sensitive to contamination especially when it is hot during operation ( $\sim 1750^\circ\text{C}$ ).

A detailed plume analysis would be required to assess potential issues due to CP and EP plume intersections and contamination of the EP thruster components. This analysis is out of the scope of the current CDF study.

## 11.7 Technology Needs

Technology Needs						
*	Equipment Name & Text Reference	Technology	Supplier (Country)	TRL	Funded by	Additional Information
✓	EPS-NEO		Safran		H2020 Program & ARTES	EM 2020, CDR in Q3 2021
✓	PPS Xoo	Hall Effect EP Thruster	Safran		H2020 Program	

## 12 MECHANISMS

### 12.1 Requirements and Design Drivers

#### 12.1.1 Separation/Release Mechanisms

##### 12.1.1.1 Launcher adaptor clamp band for S/C A

The mechanism is considered to belong to the launcher adaptor and the mass for the part retained by the satellite is included in the structures mass budget of S/C A. Nonetheless, the following preliminary requirements have been identified:

Subsystem Requirements		
Req. ID	Statement	Parent ID
MEC-010	The S/C A separation / release mechanism shall sustain the launch environment.	
MEC-020	The S/C A separation / release mechanism(s) shall provide the Comet Interceptor with a separation velocity in the range of TBD m/s.	
MEC-030	The S/C A separation / release mechanism(s) shall provide I/F diameter of Ø937mm between the Launch Structure and the Comet Interceptor.	

##### 12.1.1.2 Probe separation/release mechanisms from S/C A

###### 12.1.1.2.1 Probe B1:

Not included: the mass is considered to belong to the probe B1 payload, while dedicated interface requirements will be covered in an ICD.

###### 12.1.1.2.2 Probe B2:

Subsystem Requirements		
Req. ID	Statement	Parent ID
MEC-200	The probe B2 separation / release mechanism shall sustain the launch environment	
MEC-210	The probe B2 separation / release mechanism shall provide a separation velocity in the range of TBD m/s	
MEC-220	The probe B2 separation / release mechanism shall provide thermo-mechanical and an electrical (i.e. data/power) interface to the S/C A	

### **12.1.2 Antenna (Deployment and) Pointing Mechanism & HDRM on S/C A**

Subsystem Requirements		
Req. ID	Statement	Parent ID
MEC-300	The Antenna Pointing Mechanism (APM) shall deploy the antenna from the stowed position to the deployed configuration	
MEC-310	The Antenna Pointing Mechanism shall provide 2DoF (TBC) motion capability to point the antenna towards the Earth during operational phase.	
MEC-320	The Antenna Pointing Mechanism accuracy shall be TBD deg and resolution shall be TBD deg	
MEC-330	The antenna Hold-Down and Release Mechanism (HDRM) on S/C A shall sustain the launch environment	
MEC-340	The Antenna Pointing Mechanism shall sustain the inertial loads generated by the spacecraft manoeuvres	
MEC-350	The antenna mechanisms shall provide thermo-mechanical and electric interfaces for the antenna to the main spacecraft	

### **12.1.3 SA Mechanism: HDRM and Hinges/Synchronization Device on S/C A**

Subsystem Requirements		
Req. ID	Statement	Parent ID
MEC-400	The solar array HDRM shall sustain the launch environment	
MEC-410	The solar array hinges and synchronization devices shall ensure the 180° deployment of the panels wrt the other panel from the stowed position to the deployed configuration.	
MEC-420	The solar array hinges and synchronization devices shall interface with the solar array mechanical linkage between the solar array wing and the yoke/panels	
MEC-430	The solar array hinges and synchronization devices shall lock the solar arrays in deployed configuration	
MEC-440	The solar array HDRM shall provide thermo-mechanical interface to the main spacecraft in stowed configuration	

## 12.1.4 Solar Array Drive Mechanism (SADM) on S/C A

SubSystem Requirements		
Req. ID	Statement	Parent ID
MEC-500	The SADM shall link mechanically the solar array to the platform : <ul style="list-style-type: none"> <li>• To maintain the solar array along its axis</li> <li>• To allow solar array rotation around its main axis (to maintain the solar array pointed toward the sun)</li> </ul>	
MEC-510	The SADM shall transfer the solar array generated power to the platform	
MEC-520	The SADM shall provide the solar array/SADM grounding to the platform	
MEC-530	The SADM shall transfer the solar array data communications to the platform (TMs and TCs)	
MEC-540	The SADM shall be able to accelerate up to (and decelerate from) an angular rate of 4deg/s in 50s (TBC)	
MEC-550	The SADM shall provide thermo-mechanical and electrical interfaces between the solar array and the main spacecraft	

## 12.2 Assumptions and Trade-Offs

### 12.2.1 Separation/Release Mechanisms

#### 12.2.1.1 S/C A separation/release mechanism

This separation mechanism is not included in the mechanisms mass budget, because it is formally an integral part of the launcher's separation system adaptor.

In summary, no major technical elements make the difference in the trade-off among the available standard launcher clamp band diameters and launchers' adapter systems, because they all can provide sufficient performance. The total mass of these types of separation systems is about 19-22kg, of which the upper ring is ejected with the spacecraft (mass is about 6-7kg - this mass is accounted in the structural mass budget of S/C A). For completeness, the range of considered options is shown below:

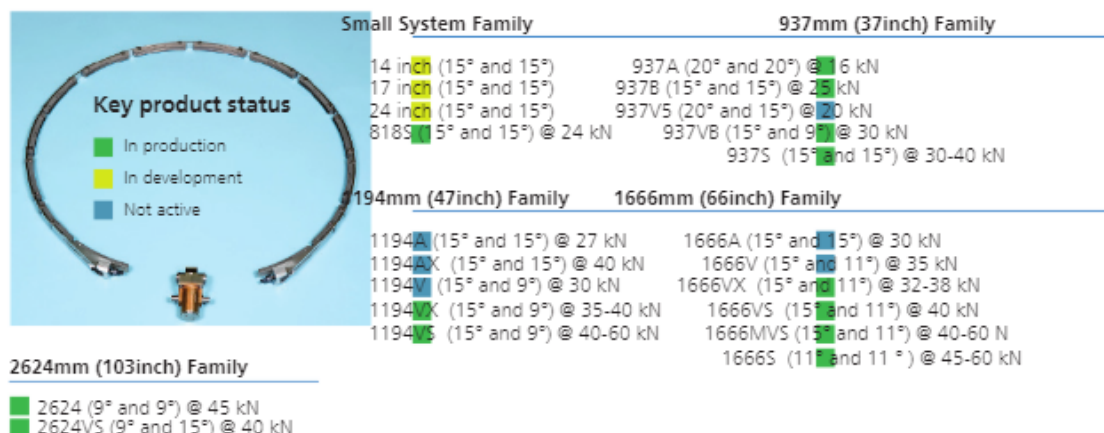


Table 12-1: Clamp band mechanisms range of options considered

### 12.2.1.2 Probe separation/release mechanisms

#### 12.2.1.2.1 Probe B1:

The B1 interfaces will be governed by an ICD.

#### 12.2.1.2.2 Probe B2:

Assumptions	
1	Mass of probe B2: 30-50 kg
2	Mass of S/C A (wet at launch) : 650 kg to 800 kg
3	S/C A & B2 separation velocity are TBD
4	Spin capability of B2 is not required. <i>Note that the original consideration was to provide the required spin for B2 only via the separation mechanism; however, after a trade-off at system level (detailed in the AOCS chapter), it was decided to provide the spin instead by an internal B2 reaction wheel.</i>
5	The mechanism shall be compatible with torsional loads $M_x=1\text{Nm}$ (TBC)
6	Efficiency of the separation springs 0.9
7	System consolidation will meet performances of existing product

The trade-off for the B2 separation mechanism aims to identify the available alternatives, types, performances (range of force values, unbalance, mass, complexity), preliminary assessment of pros and cons, and risk considerations.

The approach followed was to consider as far as possible qualified, off-the-shelf equipment, in order to reduce cost, procurement time and development risks.

Considered were the separation mechanisms for the following missions:

- Cassini/Huygens
- ExoMars/Schiaparelli
- Mars Express/Beagle-2
- And two additional conventional solutions for launcher separation.

The high-level overview of the assessment is provided in the table hereafter:

DEVICE	Mass [kg]	Reference	Comments
Cassini HUYGENS	23	o, RD[28]	Spin capability included Mass too heavy for mission
EXOMARS	39.3	RD[29]	Spin capability included Mass too heavy for mission
BEAGLE SUEM	4.2	RD[30]	Spin capability included Beagle overall mass: limited to 72 kg by Mars Express Compatible with B2 requirements
RUAG PAS 381S	3.7	RD[41]	15" clamp band, no spin capability Overall payload mass: limited to 180 kg Compatible with B2 requirements
PSC LightBand	2.1	RD[42]	11" clamp band, no spin capability

DEVICE	Mass [kg]	Reference	Comments
Mark II			Overall payload mass: limited to 100 kg Compatible with probe B2 requirements

**Table 12-2: Overview separation/release mechanisms for probe B2**

### 12.2.2 Antenna Pointing Mechanisms and HDRM

Assumptions	
1	The antenna reflector diameter is 0.9m
2	Pointing requirements (resolution, accuracy, range, ...) are TBD
3	The required DoF is expected to be 2 for the APM (and considered as the worst case for the mechanisms design)
4	2 HDRMs will be required, together with the APM to stow the antenna of 0.9 meters diameter during launch

For an antenna pointing mechanism with 2DoF, such a mechanism is mainly composed of two identical rotary actuators powered and controlled by dedicated electronics. The two actuators are in general oriented 90° to each other and have the rotational ranges, called azimuth ±TBD° and elevation ±TBD°. The antenna pointing is carried out by a stepper motor with an integrated planetary gear, an anti-backlash pinion and a main gear with a reduction of TBD. The absolute position is measured with a potentiometer or an optical encoder. Integrated into the APM are rotary joints for the routing of the waveguides and the coaxial cable as well as cable wraps for a stress free routing of the electrical harness.

The pointing accuracy of the mechanism is TBD°. The total accuracy is also linked to the design of the brackets under thermal behaviour and can be a factor 2 or 3 of the actuator capability. The antenna pointing mechanism will deploy the antenna to its required operational position.

No additional device is required, and the deployment can be achieved within a few minutes after release of the HDRM.

Two standard hold-down and release points can be used to stow the antenna and the pointing mechanism together on the spacecraft during launch in order to provide adequate stiffness and strength capabilities.

Each HDRM will be based, at each point, on a pyro (or similar release device) to initiate the separation and a spring pusher.

The option assessment aimed to identify available alternatives, types, performances (range of force values, unbalance, mass, complexity), preliminary assessment of pros and cons, and risk considerations.

The approach followed was to consider as far as possible qualified, off-the-shelf equipment, in order to reduce cost, procurement time and development risks.

Solutions analysed for the Antenna Pointing Mechanism are the following:

Equipment	Number of mechanism axes	Antenna diameter [m]	Comment	Reference
Solar Orbiter - HGAMA	2	1.1	SENER	RD[34], RD[35]
Solar Orbiter - MGAMA	1	?	SENER	RD[34], RD[35]
Bepi Colombo HTHGA	1	1.5	SENER	RD[33]
Bepi Colombo Unknown product name	2 axis with boom	1.5	SENER	RD[33]
Rosetta HGA	2 axis	2.2	HTS AG	RD[36], RD[37]
ExoMars HGA APM	2 axis	2.2m	MDA, US Rotary actuator	RD[31], RD[32]

Table 12-3: Overview Antenna Pointing Mechanisms for S/C A

### 12.2.3 Solar Array Mechanism: HDRM and Hinges/Synchronization Device

Assumptions	
1	The solar arrays are rigid panels
2	4 HDRM will be use per solar array
3	There are 2 solar arrays
4	The yoke is covered by the Structural domain
5	Architecture as shown in Figure 12-1

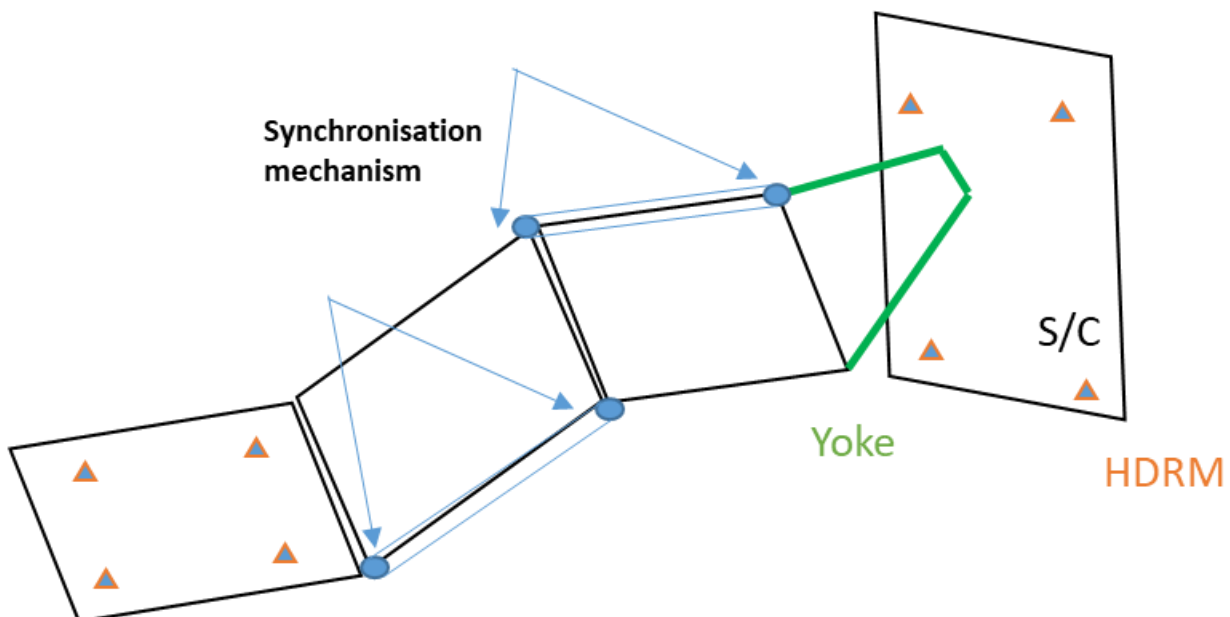


Figure 12-1: Schematic view of synchronisation mechanisms for Solar Array Deployment

## 12.2.4 Solar Array Drive Mechanisms

Assumptions	
1	The solar array generated power to be transferred could be up to around 2kW (collector or cable wrap sizing)
2	2 panels of 3m <sup>2</sup> (inertia capability)
3	Maximum angular rate = 4 deg/s

The assessment aims to identify available alternatives, types, performances (range of force values, unbalance, mass, complexity), preliminary assessment of pros and cons, and risk considerations.

The approach followed was to consider as far as possible qualified, off-the-shelf equipment, in order to reduce cost, procurement time and development risks.

The main outcome of this assessment is summarised in the table hereafter:

Product	Company	Max power capability	Mass	Comments
SEPTA 32	RUAG RSSZ (CH)	2-3kW	3,5kg	Flying on Cosmos Skymed. RD[38]
SADM Constellation 2 <sup>nd</sup> Generation	Thales Alenia Space (F)	2.1 kW	3.4kg	Flying on constellation US actuator. RD[38]
E2SADM	Airbus Defence & Space Ltd (UK)	0,8-5,6kW	5.6kg	Various Telecom satellites (56 units in space). RD[38]
KARMA 4 TC	KONGSBERG (N)	4kW	3kg	Qualified for SENTINEL 1. Design integrating a Cable Wrap from RUAG. RD[38]
KARMA 4 SR	KONGSBERG (N)	4kW	3.6kg	Qualified for SENTINEL 3. Design integrating a Slip Ring from RUAG. RD[38]

## 12.3 Baseline Design

### 12.3.1 Separation/Release Mechanisms

#### 12.3.1.1 S/C A (Comet Interceptor) launcher separation system

Among the analysed options, considerations regarding structural and accommodation constraints led to selecting a smaller clamp band (similar to 937VB from RUAG Space AB) as sizing case. The device is a European low shock separation system with extensive successful heritage.

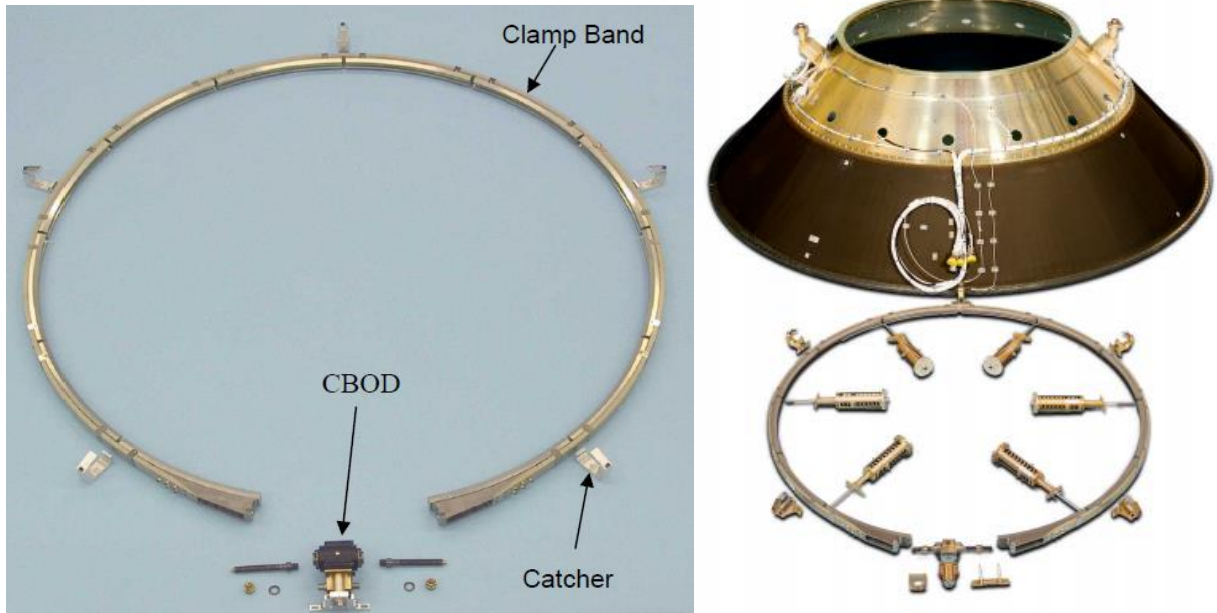


**Figure 12-2: Picture of proposed baseline separation system - release mechanisms for Comet Interceptor (e.g. RUAG 937VB)**

### 12.3.1.2 Probe separation/release mechanisms

#### 12.3.1.2.1 Probe B1:

The proposed system should follow the guidelines hereafter:

- 3 contact points between dispenser-structure and S/C
- A pyro-nut and a spring pusher at each point.

Even if no known heritage option has been used for the low speed required, no criticality is expected to meet the low speed objective, as:

- The spring pusher stiffness can be adapted
- Spring stroke can be reduced through stroke limiter.

#### 12.3.1.2.2 Probe B2:

For the selection of an option for the sizing case, the mass is a key parameter of the trade-off.

As such, the proposed option for the system sizing is a solution based on a 15" ring, for example the RUAG PAS 381S separation mechanism. The main performances of this product are recalled hereafter:

- |                    |  |
|--------------------|--|
| • Ejection energy: | 4.4 J to 6.4 J (4 to 24 springs, 1.1 J each) |
| • Mass:            | 3.7 kg <sup>18</sup> (0.98 kg separated)     |
| • Payload:         | 180 kg at 0.5m                               |

<sup>18</sup> Excluding bolts, harness, etc. Hence 4 kg used at system level.

The above values for energy would determine the relative ejection velocity of probe B2. Doubling the velocity corresponds to a fourfold increase in ejection energy. This separation mechanism would be oversized with the mass of probe B2 being in the order of 30-50 kg; however, no smaller European alternatives are currently available on the market. It may be technically interesting to look into the option of scaling down the 15" design to an 11" design, with the objective to reduce mass and the delivered ejection energy. The expected effort is not considerable; on the other hand, the new unit may not enjoy the same confidence of proven flight heritage as the proposed product.



**Figure 12-3: Picture of the baseline design separation/release mechanisms for probe B2 (e.g. RUAG PAS 381S)**

From a risk analysis prospective, the risk associated with this product would be very low, because it is considered COTS with extensive flight heritage.

### 12.3.2 Antenna Pointing Mechanisms and HDRM

The HGAMA APM of Solar Orbiter is presented as an example for the baseline design, considering both the reflector diameter (inertia capabilities) and the worst case considered for DoF (2-axis).



**Figure 12-4: Picture of the baseline design Antenna pointing Mechanism in the Solar Orbiter configuration HGAMA**

### 12.3.3 Solar Array Mechanism: HDRM and Hinges/Synchronization Device

HDRM are standard units, composed by a pyro-nut, low shock unit or thermal knife system (longer release, and more power consuming than standard pyro-nut / low shock unit) and a spring pusher at each point.

The deployment mechanisms can consist of COTS hinges with redundant deployment springs (typical stiffness of 5000 Nm/rad) manufactured, for example, by Sener or Dutch Space. It is provided with synchronisation mechanisms (hinges and pulleys) to control the motion of the SA in deployment. Viscous fluid deployment dampers are dedicated to the control of the deployment speed, a purely passive system. Finally, the latching mechanisms embedded in the hinges will ensure a stiff deployed configuration.

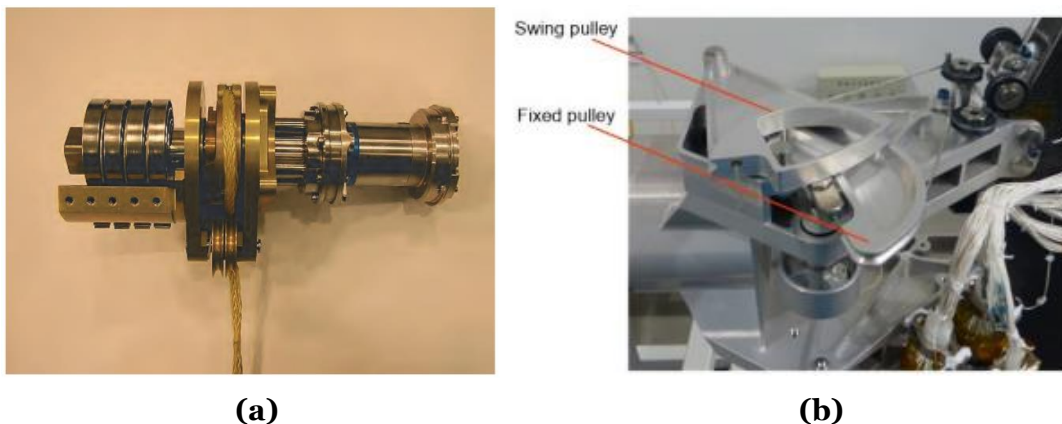


**Figure 12-5: (a): Damper Spring Unit of Sentinel 1 solar Array (b): Synchronization mechanism**

### 12.3.4 Solar Array Drive Mechanism

The solution selected as an example for the sizing case was the SADM from KONGSBERG (NO), due to its lower mass and compatibility with the 2 kW requirement. There is also generous margin on power capability in case of growth in the generated power requirement. During ground life testing, this product has already been driven to angular rates up to 10deg/s, which provides some level of confidence for reaching the required in-orbit slew rate.

Delta qualification of the product to demonstrate the high accelerations and angular rate is to be expected.

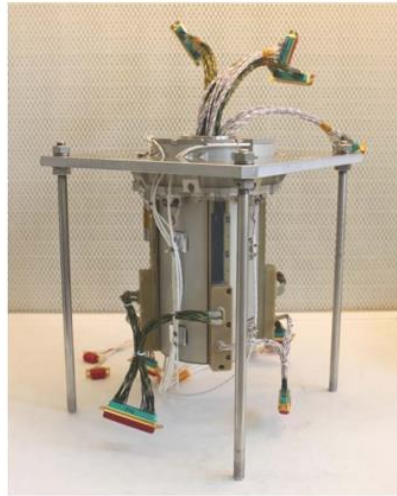


**Figure 12-6: Picture of the KARMA4 product, RD[39]**

## 12.4 List of Equipment

### 12.4.1 Separation/Release Mechanisms

#### 12.4.1.1 S/C A (Comet Interceptor) Launcher separation system

Not included, but the mass of the part remaining on the S/C A after release is accounted for in the structural design.

#### 12.4.1.2 Probe separation/release mechanisms

##### 12.4.1.2.1 Probe B1:

Not included, considered in the B1 design.

##### 12.4.1.2.2 Probe B2:

Unit name	Quantity	Mass per quantity excluding margin kg	Maturity level	Margin %	Total mass including margin kg
RUAG PAS 381S	1	4 (1 kg on B2, 3 kg on S/C A)	Fully developed	5	4.2
SUBSYSTEM TOTAL					4.2

**Table 12-4: Mass budget for probe B2 separation/release mechanisms**

## 12.4.2 Antenna Pointing Mechanisms and HDRM

Unit name	Quantity	Mass per quantity excluding margin kg	Maturity level	Margin %	Total mass including margin kg
APM	1	7	Fully developed, design adjustment to meet specificity of the mission	5	7.4
APM electronic, redundancy included	1	4.4	Fully developed	5	4.6
HDRM	2	0.5	To be adapted	10	1.1
SUBSYSTEM TOTAL				5	13.755

**Table 12-5: Mass budget for APM**

Note 1: typical power consumption of an APM is in between 15 and 18 W.

## 12.4.3 Solar Array Mechanism: HDRM and Hinges/Synchronization Device

### Solar Array 1

Unit name	Quantity	Mass per quantity excluding margin kg	Maturity level	Margin %	Total mass including margin kg
Light Hinges*	4	0.260	High TRL but standard adaptation need (stiffness, allocated volume)	20	1.25
Synchronized Hinges*	4	1	To be adapted	10	4.4
HDRM	4	0.5	To be adapted	10	2.2
SUBSYSTEM TOTAL					2.2*

**Table 12-6: Mass budget for solar array 1: HDRM and hinges**

### Solar Array 2

Unit name	Quantity	Mass per quantity excluding margin kg	Maturity level	Margin %	Total mass including margin kg
Light Hinges*	4	0.260	High TRL but standard adaptation need	20	1.25

Unit name	Quantity	Mass per quantity excluding margin kg	Maturity level	Margin %	Total mass including margin kg
			(stiffness, allocated volume)		
Synchronized Hinges*	4	1	To be adapted	10	4.4
HDRM	4	0.5	To be adapted	10	2.2
SUBSYSTEM TOTAL					2.2*

**Table 12-7: Mass budget for solar array 2: HDRM and hinges**

\*Note: mechanism of solar arrays panels (hinges inter panels) are included in the Solar Array budget, under the Power domain.

#### 12.4.4 Solar Array Drive Mechanism

Unit name	Quantity	Mass per quantity excluding margin kg	Maturity level	Margin %	Total mass including margin kg
SADM	2	4	Delta qualification to meet specificity of the mission	10	8.8
SADE	1	3	<i>To be adapted</i>	10	3.3
SUBSYSTEM TOTAL					12.1

**Table 12-8: Mass budget for SADM mechanism**

### 12.5 Options

#### 12.5.1 Electric Propulsion Pointing Mechanism (EPPM)

##### 12.5.1.1 Requirements and Design Drivers

SubSystem Requirements		
Req. ID	Statement	Parent ID
MEC-900	The EPPM shall connect mechanically the EP thruster to the platform	
MEC-910	The EPPM shall direct the EP thruster along the thrust vector axis	
MEC-920	The EPPM shall provide a pointing accuracy of TBD, with repeatability of TBD	
MEC-930	The EPPM shall provide EP thruster grounding to platform	
MEC-940	The EPPM shall transfer electric power and propellant from the platform to the EP thruster	
MEC-950	The EPPM shall be compatible with a 3(TBC) kW EP thruster	

### 12.5.1.2 Assumptions and Trade-Offs

Assumptions	
1	EP thruster mass up to 10kg, power up to 5kW
2	2 axes gimbal, angular pointing range of +/-15deg (TBC), with accuracy of 0.2deg (TBC)

Solutions analysed:

Product	Company	Max power capability	Mass	Comments
Bepi-TPM	RUAG RSA (A)	1 thruster x 5kW	13.5kg	Flying on BepiColombo
C-EPPM	RUAG RSA (A)	1 thruster x 5kW or 1 thruster x 1.5kW	12kg	Galileo SG, new-space constellations
EPMEC	RUAG RSSZ (CH)	1 thruster x 1.5kW	10kg	Flown on Smart-1, deep space missions
ETHM	TAS (F)	1 thruster x 5kW	19.1kg	TAS NEOSAT baseline mechanism
P-ATMA	RUAG RSA (A)	2 thrusters x 1.5kW	18.5kg	Flying on Airbus E3000 telecom platforms
EPPM-MSR	RUAG RSA (A)	1 thruster x 5kW	15kg	Baseline for Mars Sample Return

**Table 12-9: Electric Propulsion Pointing Mechanism**

Among the analysed European options, EPMEC would have the closest heritage to the foreseen application, as well as the lightest product. The main drawback is related to materials and technology obsolescence: ultimately, recent lessons learnt show that the effort and cost to re-design and upgrade an obsolescent mechanism easily escalates far beyond the effort of adapting more recent references (such as ETHM, Bepi-TPM or C-EPPM).

### 12.5.1.3 Solution considered for potential sizings

The solution selected as an example for system sizings (although the EPPM is not in the design baseline) is a design similar to C-EPPM, which embeds all the lesson learnt from the Bepi-TPM and ARTE-8 development, while aiming to maximise competitiveness and minimise lead time. For reference, the qualification model of the C-EPPM is expected to be completed by the end of 2020.

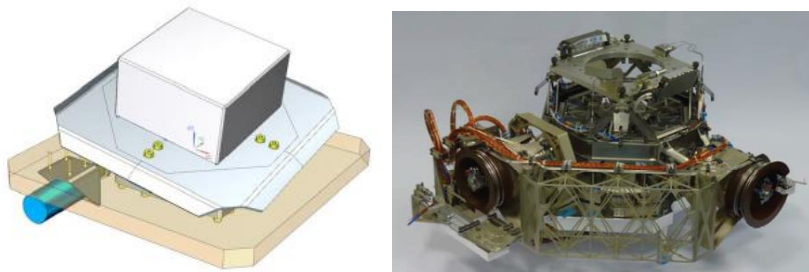


**Figure 12-7: Examples of RUAG EPPMs**

Unit name	Quantity	Mass per quantity excluding margin kg	Maturity level	Margin %	Total mas including margin kg
C-EPPM	1	12	in development, qualification pending	10	13.2
<i>C-EPPM driver</i>	1	4.5	<i>To be adapted</i>	10	5
SUBSYSTEM TOTAL					18.2*

**Table 12-10: Mass budget for C-EPPM mechanism**

\*Note: the mass of the EP mechanism electronic driver is standardly included in the power electronics budget, but is included here for ease of reference (a 5kg, 100\*50\*200mm box could be a conservative assumption).

## 12.6 Technology Needs

Technology Needs						
s*	Equipment Name & Text Reference	Technology	Supplier (Country)	TRL	Funded by	Additional Information
*	SADE	Engineering and qualification extension to higher frequency commanding	TBD	4	TBD	Extension of the fast mode drive (high stepping frequency) of SADM according to the mission profile
*	11" separation device	Design scaling	RUAG (S)	6	TBD (GSTP?)	Family extension by down-sizing the existing 15" clampband

This Page Intentionally Blank

## 13 GUIDANCE, NAVIGATION AND CONTROL SYSTEM

### 13.1 Requirements and Design Drivers

SubSystem Requirements		
Req. ID	Statement	Parent ID
GNC-010	The GNC subsystem shall be able to acquire images with a dedicated navigation camera that permits a ground-based orbit determination accuracy compatible with the B-plane accuracy required by the probes and the S/C A considering 12 hours of ground turn-around time.	
GNC -020	The GNC subsystem shall be able to autonomously process images from the navigation camera and estimate the S/C A relative position at the closest distance in the B-plane.  Note: the time-of-arrival does not have to be estimated autonomously.	
GNC -030	The GNC subsystem shall be able to update the attitude profile based on the on-board vision-based navigation to ensure imaging the comet nucleus.	
GNC -040	The GNC subsystem shall be compatible with a probe separation sequence requiring divert delta-Vs lower than 10 m/s.  Note: the requirement affects the maximum individual delta-V not the total delta-V budget.	
GNC-050	The GNC subsystem shall be able to execute autonomously the delta-V manoeuvres of the separation sequence previously uploaded by ground.	
GNC-060	During the science phase, the contribution of the S/C A GNC subsystem to the APE of the CoCa instrument boresight wrt the nucleus of the active comet shall not exceed 0.2 deg <sup>19</sup> (TBC) half cone (with 95% probability at 90% confidence level).	
GNC-070	The GNC autonomous navigation function shall be compatible with the ram velocities and comet nucleus size and activity defined in the mission scenario.	

#### 13.1.1 Design Drivers

The following design drivers were identified:

- Very demanding APE due to very narrow FoV of the CoCa instrument (0.69 x 0.92 deg).
- APE is driven by the relative position knowledge accuracy which requires autonomous tracking of the target from very long distances (comet orbit uncertainty does not allow pre-planned operations with such accuracy).

<sup>19</sup> Note that the specification of CoCa (see Section 4.1.1) is to have the “nucleus <0.1° from detector centre”. This should be assessed further in later phases.

- Flight heritage (ROSETTA) and technology developments for on-board autonomous target tracking are focused on asteroids. The capability to identify and track the nucleus of an active comet complicates significantly the image processing performances as well as its validation and verification.
- The Delta-V limitation coupled with the long ground turnaround time and the very high flyby velocities constrain significantly the separation sequence and the delivery error of the probes.
- The navigation camera high TRL, low cost and low mass requirements, constrain the angular resolution that is the critical parameter for the navigation performance and therefore the delivery error of the different spacecraft.
- Due to schedule and cost constraints, there is a limitation in the on-board autonomy that prevents the autonomous computation of delta-V.

## 13.2 Assumptions and Trade-Offs

### 13.2.1 Assumptions

Assumptions	
1	The maximum comet fly-by relative velocity is 70 km/s and the closest approach for the S/C A is 1000 km.
2	The sequence of deployment of the probes (B1 and B2) and retargeting manoeuvre for the S/C A will be pre-planned by ground (no autonomous trajectory guidance)
3	The closest approach to be considered for the B2 probe is 100 km, though risk of pointing violations may be acceptable if occurring near closest approach.
4	The S/C A shall rotate to point the payload towards the comet.
5	During waiting at L2 and cruise phases there is no need of autonomous trajectory guidance.
6	The increase of autonomy period during cruise might be achieved via autonomous trajectory navigation for monitoring the EP performance. In that case, no extra HW will be used, i.e. the same navigation camera required for fly-by will be used for interplanetary navigation.
7	Ground based Image processing error for unresolved comet nucleus is 0.2 pixel (white Gaussian, 1-sigma). The IP does not have systematic errors. Note: sub-pixel accuracy requires special image processing as in EPOXI/Deep Impact
8	On-board image processing accuracy <ul style="list-style-type: none"><li>• Unresolved nucleus 1 pixel (1-sigma), white Gaussian noise</li><li>• Resolved nucleus: nucleus angular size (3-sigma), bias or ECRV (long correlation time)</li></ul>
9	Time of arrival (TOA) is not estimated or updated on-board Note: based on previous missions, the TOA estimate is few seconds and remains constant during the approach and fly-by phase

### 13.2.2 Trade-Offs

#### 13.2.2.1 Dedicated NavCam vs CoCa for optical navigation

Due to the uncertainty in the comet ephemerides, the use of optical navigation is required for both ground and on-board operations. The use of CoCa would reduce the amount of HW to be used on board (although due to redundancy it might not reduce the total mass) and can improve the navigation performances as seen in the figure below.

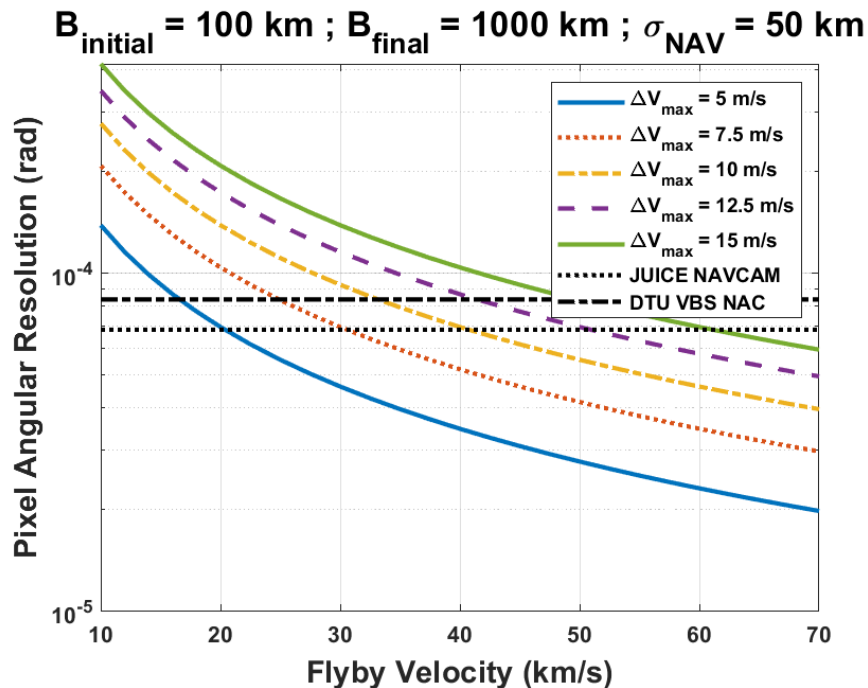


**Figure 13-1: Theoretical image resolution to perform a given divert delta-V from B2 fly-by distance (100 km) to S/C A nominal flyby distance (1000 km). No delays included (for instance ground turn-around). CoCa angular resolution is below the 5 m/s line**

However, the development and operations of a science instrument as mission critical equipment is riskier than high TRL equipment from GNC/AOCS suppliers. This programmatic risk is considered unacceptable at this moment and a dedicated navigation camera is the preferred option.

#### 13.2.2.2 Comet tracking strategy

The trade-off involves multiple system level aspects. In this section, only the GNC implications are outlined. The following options are considered:

- **Ground-based attitude profile** implies that at the last ground contact, the attitude to be followed by the spacecraft during the fly-by is uploaded from ground (so there are no on-board corrections)
- **NavCam-based autonomous update** means that the image processing and on-board navigation provides corrections after the last ground contact and improves the attitude profile with more accurate measurements. In this option, the entire spacecraft is rotating to track the comet.

- **NAVCAM-based scanning mirror attitude control** means that the NAVCAM is fixed-mounted on the spacecraft and is imaging the nucleus while it is in the FoV. The on-board navigation is updating the mirror scanning law, as well as the platform out-of-plane deviation. In this option, only the payload is rotating (via the scanning mirror) to view the comet. *Note: this is only for the system option discussed in Chapter 24.8.*
- **NAVCAM+CoCa mounted in the scanning mirror** means that both units are rotating with the scanning mirror and can track the comet in closed-loop control. *Note: this is only for the system option discussed in Chapter 24.*

Strategy	Pros	Cons
• Ground-based attitude profile	<ul style="list-style-type: none"> <li>• Simplest AOGNC (no on-board navigation)</li> </ul>	<ul style="list-style-type: none"> <li>• Very low probability of tracking the nucleus</li> </ul>
• NAVCAM-based autonomous update (full S/C rotation)	<ul style="list-style-type: none"> <li>• Similar ground &amp; autonomous algorithms (easier in-flight verification), when nucleus unresolved (less than few pixels)</li> <li>• Simple controller architecture</li> </ul>	<ul style="list-style-type: none"> <li>• Very high demand on the actuators (torque and angular momentum)</li> <li>• Autonomous on-board navigation &amp; attitude guidance</li> <li>• Difficult performance validation when nucleus resolved</li> </ul>
• NAVCAM based scanning mirror attitude control (CoCa not in closed-loop)	<ul style="list-style-type: none"> <li>• Low demand on actuators (platform inertial pointing)</li> <li>• NAVCAM only when nucleus unresolved <math>\Rightarrow</math> easier validation &amp; in-flight verification</li> <li>• Simple scanning mirror controller</li> </ul>	<ul style="list-style-type: none"> <li>• More complex controller architecture (but scanning mirror in open-loop)</li> <li>• Autonomous on-board navigation &amp; attitude guidance</li> <li>• Potential (TBC) temporary loss of nucleus in CoCa (period between 4 to 30 sec time-to-go) depending on accuracy at last NAVCAM update</li> </ul>
• NAVCAM+CoCa mounted in scanning mirror	<ul style="list-style-type: none"> <li>• Low demand on actuators (platform inertial pointing)</li> <li>• Continuous monitoring of nucleus in CoCa images</li> </ul>	<ul style="list-style-type: none"> <li>• Complex navigation and controller architecture (two navigation <b>chains</b> and two controller actuators)</li> <li>• Complex AOGNC qualification (must include CoCa and periscope in ATB and PFM tests)</li> </ul>

The on-board image processing accuracy is not expected to be as accurate as ground-based. In this case, using the brightest pixel to define the nucleus is expected to provide 1 pixel accuracy, compared to more complex correlation or template matching for ground processing that provide sub-pixel accuracy, according to EPOXI/DeepImpact literature. The B-plane error is depicted in Figure 13-4. Note that when the nucleus is

resolved, the error remains constant at the nucleus size due to the gas jets and the extended nucleus (the brightest pixel is expected close to the limb). Nevertheless, this ‘simple’ on-board image processing (for instance until 1 hour before closest approach) still provides better accuracy than the orbit determination at the time of the divert delta-V cut-off, several hours before the closest approach.

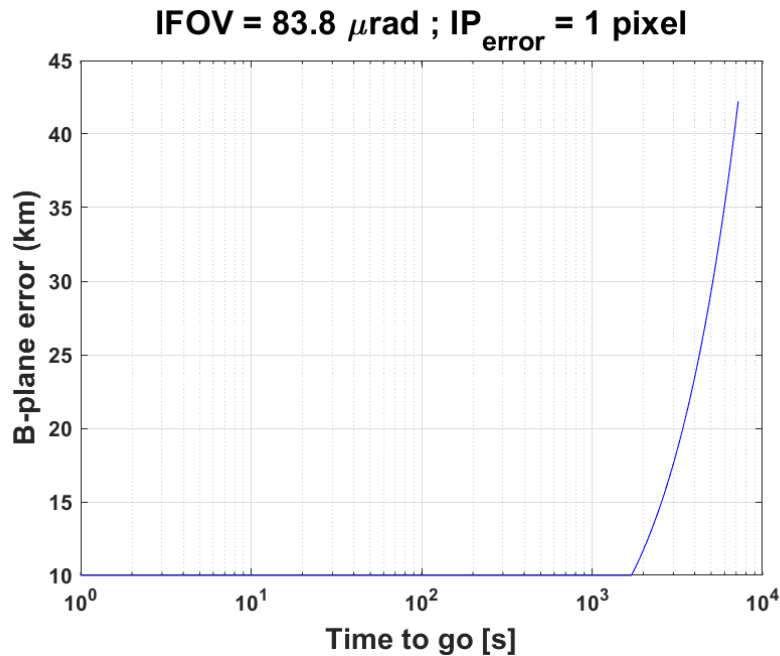


**Figure 13-2: On-board navigation accuracy**

### 13.2.2.3 Separation sequence

The separation sequence has an impact on the delta-V budget and in the delivery error. The delta-V to achieve the distance between the probe B2 miss distance and the S/C A miss distance decreases with the distance to the closest approach. This can be seen in Figure 13-3 for a probe B2 miss distance of 100 km.

The closer to the closest approach, the higher the required divert delta-V. However, the further the divert delta-V, the larger the error due to the navigation accuracy (see Figure 13-4).

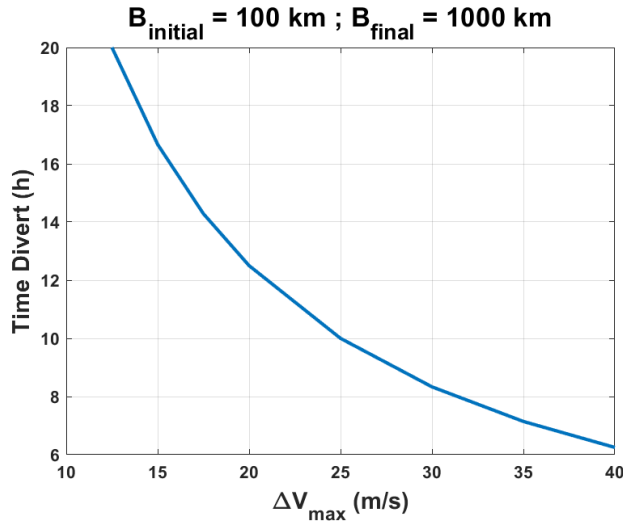


**Figure 13-3: Divert delta-V to achieve 900 km miss distance variation**

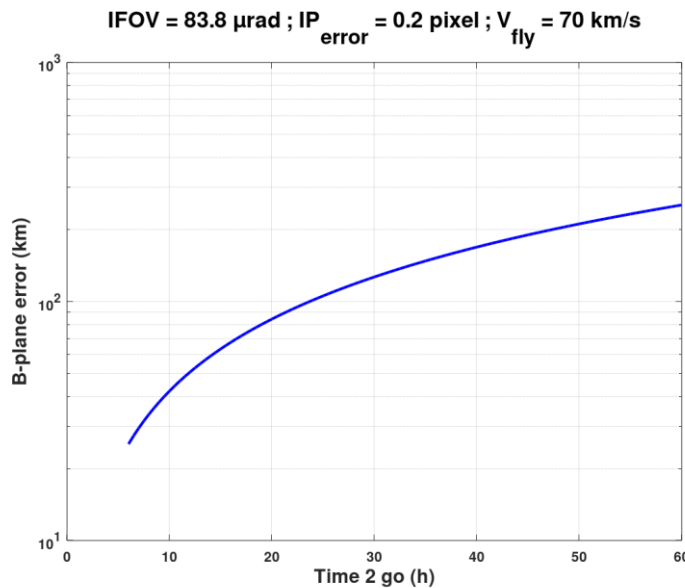


**Figure 13-4: B-plane navigation error as function of the time to closest distance**

Given that the delta-V execution error remains constant (the assumption is that the entire S/C A slews to perform the divert delta-V) and much smaller than the navigation error, and the above relations, the smaller the divert delta-V, the larger the miss distance dispersion.

The navigation uncertainty is the main source of B-plane delivery error. The navigation camera resolution can be calculated in order to achieve a certain S/C A miss distance with a given dispersion ( $\sigma_{\text{NAV}}$ ) with a fixed divert delta-V (Figure 13-1). With existing Narrow Angle Cameras (NAC), the minimum delta-V covering all fly-by velocities can be very high (higher than in the plot because the ground turn-around time includes additional delays that penalise the navigation accuracy).

To reduce the delta-V while maintaining the operational constraints (no autonomous divert delta-V computation), the only possibility is to increase the B2 miss distance and accept higher navigation errors at the cut-off time for B2 separation and for divert delta-V computation. Increasing the B2 miss distance to 250 km and the navigation error at cut-off of divert delta-V to 135 km, the angular resolution is calculated (Figure 13-5) and shows that with current NAC, the final divert delta-V to cover all possible fly-by velocities is 10 m/s.

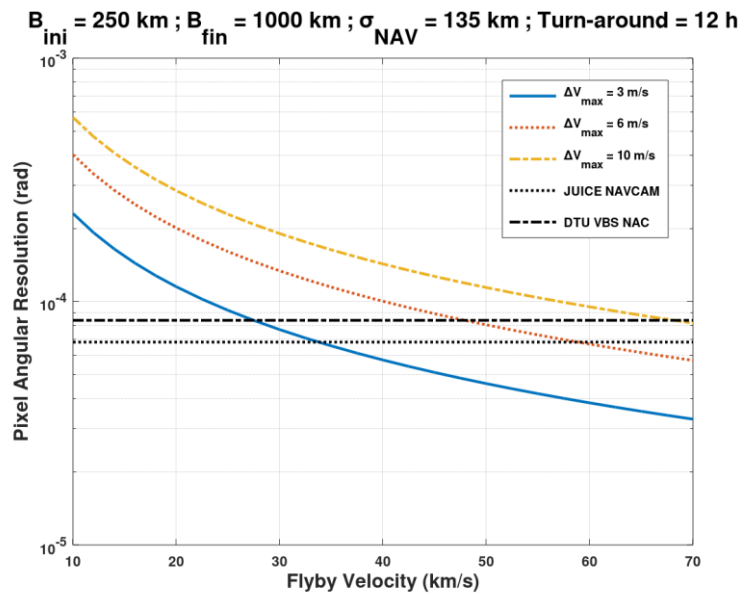


**Figure 13-5:** Navigation camera IFOV for different divert delta-V including ground time around

### 13.3 Baseline Design

#### 13.3.1 Separation Sequence

Given the ground turn-around time and the operations constraints, the separation sequence is defined as per Figure 13-6.

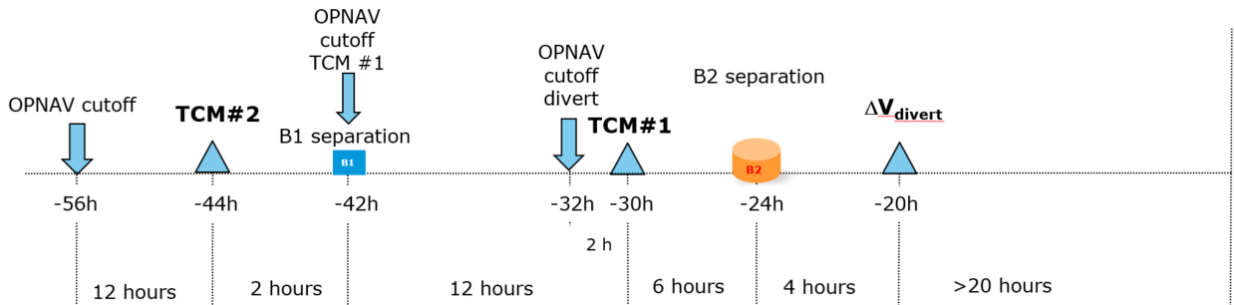


**Figure 13-6:** Separation sequence

Given this sequence and the conclusions from Section 13.2.2.3, the probability of a spacecraft to pass closer than a certain distance to the nucleus can be computed.

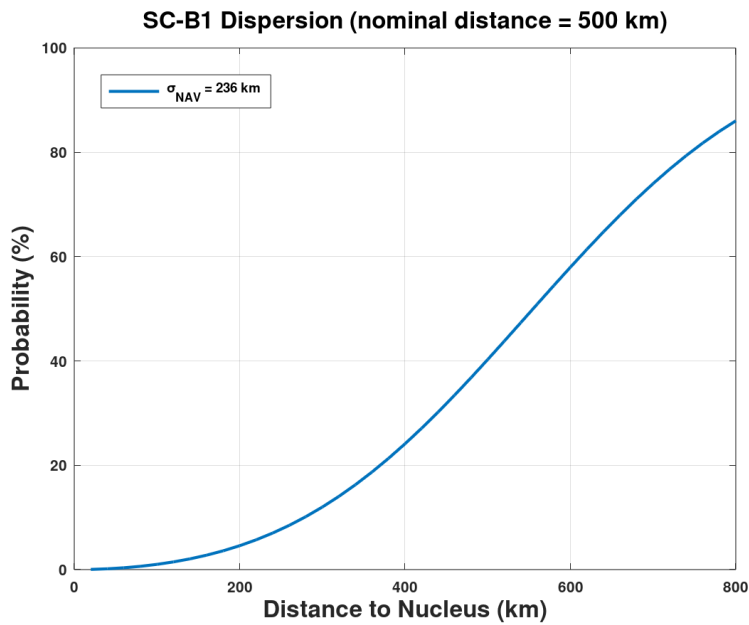


**Figure 13-7: Probability of probe B1 passing closer than a certain distance to the nucleus**

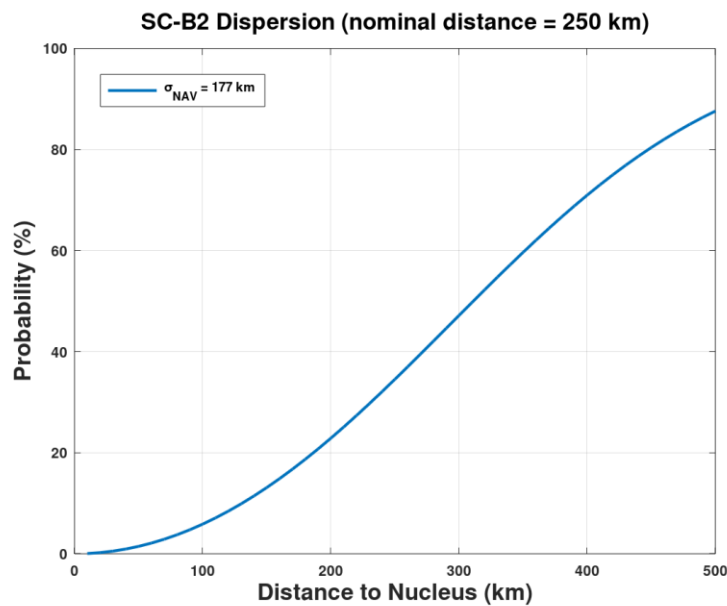


**Figure 13-8: Probability of probe B2 passing closer than a certain distance to the nucleus**

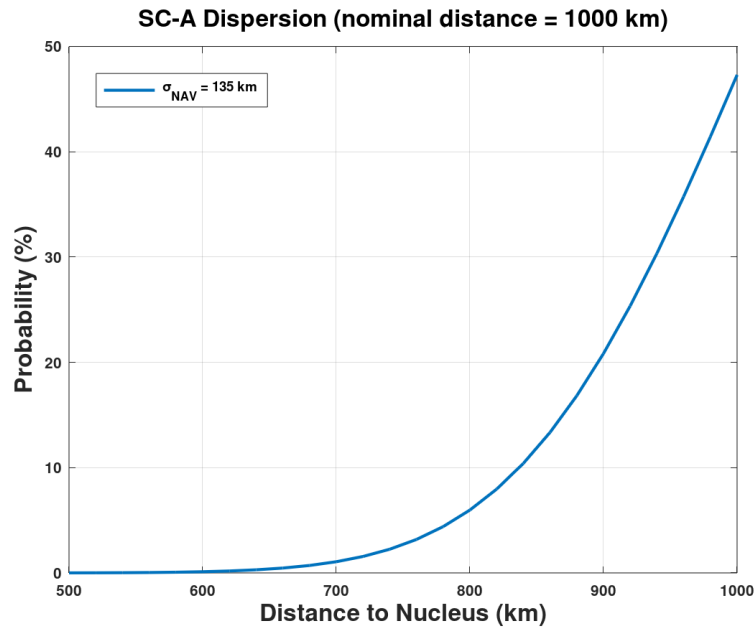


**Figure 13-9: Probability of S/C A passing closer than a certain distance to the nucleus**

The probability of the probe B2 colliding with the nucleus can also be computed, and it is very small (Figure 13-10).

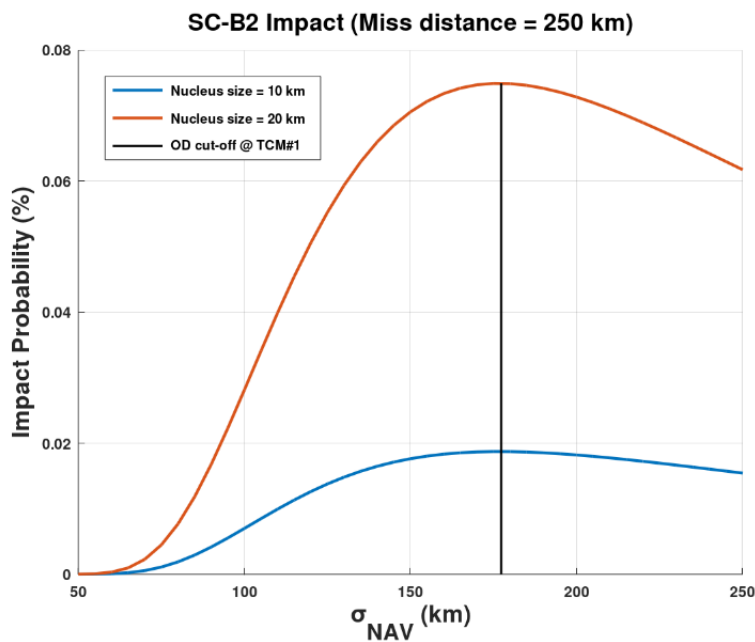


**Figure 13-10: Probability of probe B2 collision with the nucleus**

### 13.3.2 GNC Architecture

The basic GNC architecture is depicted in Figure 13-11. Blue and red boxes are on-board functionalities, blue are ‘standard’ AOCS services while red are specific functionalities

for the Comet Interceptor mission that require some special developments. The on-board functionalities have been optimised for simplicity considering the ground and space segments previous flight heritage and the objectives of the comet interceptor mission. The share of responsibilities is:

- Ground-based manoeuvre plan (translational guidance)
  - Cruise (including EP arcs)
  - Fly-by phase, including probes deployment sequence
- On-board relative navigation for attitude pointing during fly-by
  - Compensate relative trajectory errors to ensure proper imaging (see Figure 13-12, which shows that the dispersion in the trajectory due to the navigation error at the cut-off time for the divert delta-V induces an off-pointing of the instruments 1 order of magnitude larger than the FoV of CoCa).
- On-board attitude guidance to maximise the time of the comet nucleus in the FOV
  - ‘Semi-autonomous’ guidance is already being implemented for e.g. the HERA mission. There are some modifications to be performed in order to consider the impact of the active nucleus in the image processing.
- On-board attitude determination and control (‘standard’ platform services).

In case longer autonomy periods are desired for the EP arcs during cruise, then an autonomous navigation function should be included to monitor the behaviour of the EP. This is not considered in the baseline.

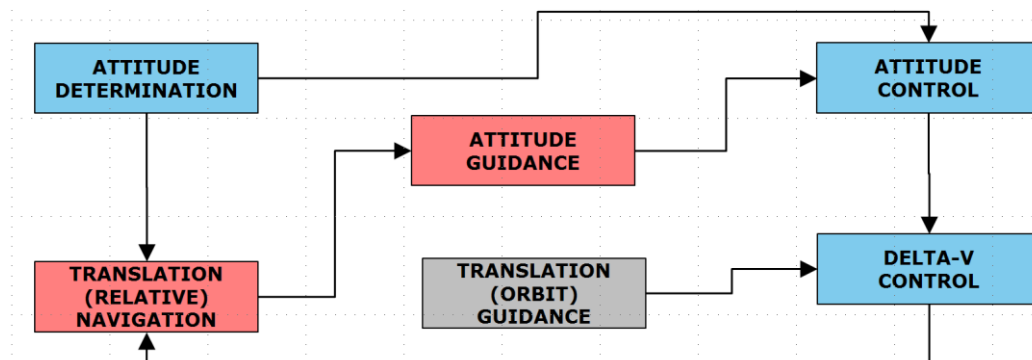


**Figure 13-11: GNC architecture**

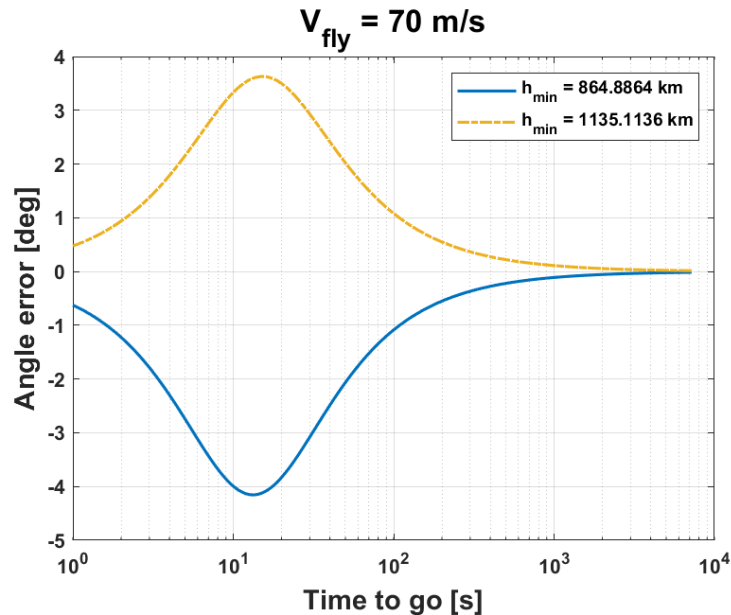


**Figure 13-12: Maximum error due to dispersion @ divert cut-off (error in the Time-Of-Arrival not included)**

The proposed algorithms for autonomous pointing are based on the HERA GNC development, which considers the ROSETTA heritage. However, some major updates are needed due to the active nucleus and the high torque demand. The core of the on-board system is the use of the NAVCAM images for vision-based navigation with two main differences with respect to previous missions (ROSETTA, HERA):

- Image processing algorithm shall be able to differentiate the nucleus from the coma (see difference between validation image in HERA Figure 13-13 and a GIOTTO image of comet Halley, Figure 13-14)
- ‘Semi-autonomous’ attitude guidance that computes small corrections to the pointing profile defined by ground, based on the navigation solution. These corrections shall consider the torque limitation and the final constraint of imaging the nucleus at the closest distance.

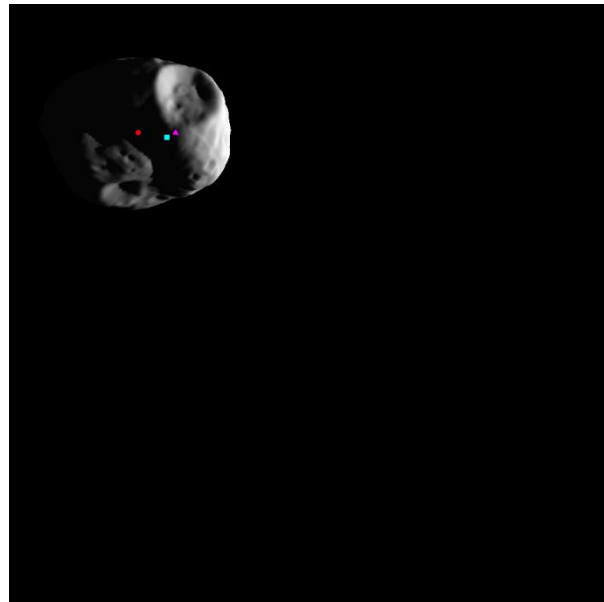


**Figure 13-13:** Example of IP and navigation results in HERA

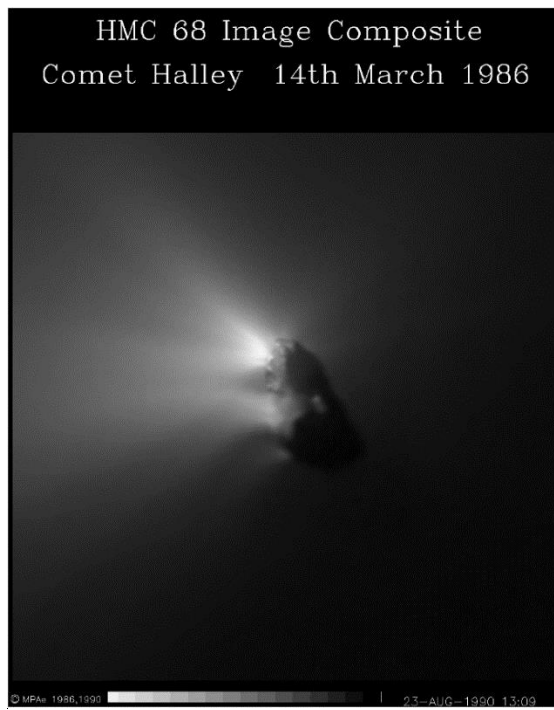


**Figure 13-14:** GIOTTO image of comet Halley

### 13.4 List of Equipment

A list of space-qualified, off-the-shelf equipment, suitable for a low-cost mission has been proposed for the system sizing case.

### 13.4.1 Visual Navigation Camera

The baseline proposed visual camera for the sizing at system level is DTU's PRISMA VBS. The two optical heads would be connected to the same DPU managing also the STR.

- FoV : 9 x 7 deg half-angle
- Detector : 752 x 580 (CCD)
- Mass < 1 kg<sup>20</sup>
- Power < 2 W<sup>20</sup>
- TRL 9

### 13.5 Options

In principle, there are several European suppliers who could potentially provide narrow angle navigation cameras fulfilling the Comet Interceptor requirements. The mass and cost of each option should be considered in a future trade-off. A brief summary of potential options is provided here below for information only and may not be complete or exhaustive:

- Sodern: developed the JUICE NAVCAM and the NAC Engineering Model for Mars Sample Return Orbiter.
- Jena-Optronik: Astrohead-X derived from AstroXP high-accuracy STR has a narrower FOV than JUICE NAVCAM.
- 3Dplus: offers a small space-qualified detector and electronics, but the optics for the narrow angle camera have a lower TRL.
- OIP: developed the camera for PILOT (Lunar Lander navigation experiment), but the FoV is too large and optics would require to be redesigned and qualified.
- LEONARDO: developed the ROSETTA NAVCAM but the design is obsolete and a re-design would be needed.

### 13.6 Technology Needs

Technology Needs						
*	Equipment Name & Text Reference	Technology	Supplier (Country)	TRL	Funded by	Additional Information
*	GNC system (section 1.3)	Semi-autonomous attitude guidance based on LOS navigation with active comets	ADS, GMV	3		ROSETTA and HERA experience

\* Tick if technology is baselined

<sup>20</sup> Including the DPU

This Page Intentionally Blank

## 14 ATTITUDE AND ORBIT CONTROL SYSTEM

### 14.1 Requirements and Design Drivers

SubSystem Requirements		
Req. ID	Statement	Comments
AOCS-010	The S/C A AOCS shall provide hardware and associated on-board software to acquire, control and measure the required spacecraft attitude during all phases of the mission, and to control and monitor all the necessary Delta-V for the complete mission according to the specified system requirements.	
AOCS-020	The AOCS shall ensure that the S/C A is capable of being 3-axis stabilised	
AOCS-030	For all mission phases, the S/C A AOCS shall have the autonomous capability to maintain the required attitude and to perform attitude manoeuvres, including when contact with ground is not available or ground response time is inadequate.	
AOCS-040	The S/C A AOCS shall be able to maintain, during Safe mode, the solar arrays pointing to the Sun using a minimum of the on-board resources ensuring power generation and ground communication.	
AOCS-050	The AOCS shall detumble the S/C A after launcher separation in less than 5 minutes, for a worst-case tip-off rate of 5 deg/sec along any spacecraft axis	Assumed launcher tip-off rate
AOCS-051	After solar array deployment, the S/C A AOCS shall point solar arrays to the Sun within 15 minutes.	Constraint assumed for power budgeting
AOCS-060	During thrust arcs performed with electrical propulsion or RCS, the contribution of the S/C A AOCS to the APE of the thrust vector shall not exceed 1.5 deg (TBC) half cone 95% of the time.	Assumed value
AOCS-070	During communication windows in nominal operations, the contribution of the S/C A AOCS to the APE of the HGA shall not exceed 0.5 deg (TBC) half cone 95% of the time.	From communication design
AOCS-071	During communication windows in safe mode, the contribution of the S/C A AOCS to the APE of the HGA shall not exceed 2.8 deg (TBC) half cone 95% of the time.	Agreed compromise value with communication subsystem
AOCS-080	The S/C A AOCS shall ensure a safe attitude between orbital manoeuvres or communication events; i.e. during L2 station keeping. As a goal, the need for ground operations/monitoring should be minimised during this	

SubSystem Requirements		
Req. ID	Statement	Comments
	phase.	
AOCS-090	During the comet fly-by, the S/C A AOCS/GNC shall maintain the comet nucleus inside the field of view of the CoCa instrument (narrow angle camera). This implies an APE better than $0.46^\circ$ 95% of the time.	Science requirement
AOCS-091	Star trackers shall be placed to avoid incoming dust impinging inside the baffle during the fly-by	To ensure they are functioning after the fly-by, to allow setup of comms attitude with Earth for science downlink
AOCS-092	The S/C A AOCS design shall consider up to 1 hour of star tracker outage during fly-by due to dust particle reflections	This requirement derives from a Rosetta lesson learned. Time horizon chosen arbitrarily.
AOCS-093	RCS firings shall be inhibited during the last 12 hours of fly-by to avoid contamination of science instruments	Based on some instruments which require a long period for propellant contamination to dissipate prior to making measurements.
AOCS-100	The S/C A reaction wheels offloading during setup of the fly-by shall produce a parasitic delta-V introducing a variation of the closest distance lower than 5% (TBC) and with trajectory impact compatible with the comet pointing APE requirements	To constrain trajectory deviations, for science.
AOCS-200	The probe B2 shall provide passive attitude control capable of limiting off-pointing to < 20 deg (with 95% probability at 90% confidence level).	Agreed value with systems team
AOCS-210	The probe B2 shall be spin about it's ejection axis with 6 – 15 rpm	Derives from science needs

#### 14.1.1 Design Drivers

The following design drivers were identified:

- Significant RCS propellant is required to counteract EP thruster misalignment with respect to the centre of gravity due to lack of thrust orientation mechanism. Previous EP missions (SMART-1 and BepiColombo) used thruster orientation mechanisms to compensate misalignment perturbation torques.

- Higher autonomy periods during waiting phase at L2 and during cruise are desirable. Lessons learned from Bepi Colombo could allow increase in autonomy with respect to orbit determination and monitoring. Note that these activities are assumed to be done once per week and the EP must be switched-off during the ground station communication.
- Very high demand of torque and angular momentum capacity during the fly-by due to the high velocity and short closest distance.
- The achievable APE during fly-by will be driven by the relative position accuracy (knowledge) which requires autonomous tracking of the target from very long distances (comet orbit uncertainty does not allow pre-planned operations with such accuracy). This is further investigated in the GNC chapter.
- Flight heritage (Rosetta) and technology developments for on-board autonomous target tracking are focused on asteroids. The capability to identify and track the nucleus of an active comet complicates the achievement of the APE requirement. This is further investigated in the GNC chapter.
- The star tracker placement requirement is necessary to avoid damage to the optical heads during the fly-by, since the S/C must also be capable of fine pointing after the fly-by to downlink all the science data to Earth. This requirement, combined with general Sun and illuminated-structure exclusion angles, leaves very few feasible boresight directions for the star trackers. The positioning of the tracker is further complicated by potential contamination from RCS or EP.
- The requirement to handle star tracker outages (based on lessons learned from Rosetta) and the need to acquire the Earth via communication-beacon strobining drives the need to include a medium to high accuracy gyro.
- The payload contamination requirement prevents a fully RCS-based design. This drives the need to include high torque reaction wheels, which adds significant mass.

## 14.2 Assumptions and Trade-Offs

### 14.2.1 Assumptions

Assumptions	
1	In case of a single actuator failure, a period of science outage at closest approach may be acceptable (to avoid driving actuator mass too high).
2	The maximum comet fly-by relative velocity is 70 km/s.
3	The maximum comet activity is 3000 kg/s.
4	The closest approach for the S/C A is 1000 km.
5	The closest approach to be considered for the probe B2 is 100 km, though risk of pointing violations may be acceptable if occurring near closest approach
6	The dust field in the vicinity of the comet is treated as being divided in two separate groups: <ul style="list-style-type: none"> <li>(a) Large particle impacts (<math>&gt; 10</math> mg) that do not hit in a uniform manner                              The probability of encountering large particles is relatively low. The largest particle encountered by Giotto was 40 mg. For this CDF study, a single 100 mg particle impact was considered. Note that probability of the S/C A</li> </ul>

### Assumptions

encountering a 100 mg particle at 1000 km is similar to the probability of probe B2 encountering a 100 mg particle at 100 km, due to the different cross-section areas. Particles even larger than 100 mg are not considered in the AOCS design due to low probability and the fact that they may catastrophically damage the spacecraft.

- (b) Small particle impacts ( $\leq 10$  mg) that hit the spacecraft with a quasi uniform distribution

The density ( $\text{kg/m}^3$ ) of the small particle field is assumed to be:

$$\rho = \frac{Cf}{4\pi r^2}$$

$r$  – distance from comet (m)

$f$  – factor representing portion of total mass that are considered ‘small’

$C$  – comet activity ( $\text{kg/s}$ )

$f = 0.01$  was considered based on dust models that show that 1% of total dust mass is contained in particles of size 10 mg or smaller<sup>21</sup>

Note that this density model makes assumptions about ejection velocity of material from the comet

7 Dust particle impacts are assumed to be plastic; particles transfer their entire momentum to the spacecraft. Note that this may only be true for surfaces covered in MLI. Some materials can lead to elastic collisions where greater momentum is transferred.

8 The fly-by slew is about the minimum inertia axis (the solar panel long axis).

9 The solar panel is maintained edge-on to the incoming dust flow during fly-by in order to minimise cross-sectional exposure; assumed S/C A cross-sectional area:  $2.75 \text{ m}^2$  (the true value should be closer to the range  $1.6 - 2.3 \text{ m}^2$  given the final design but this assumption was taken early on and thus includes margin).

10 The maximum moment arm for a single particle impact is considered to be the edge of the main S/C body (i.e. not the solar panels).

11 The moment arm between the centre of pressure and the c.g. due to the dust pressure from the small particles is considered to be 5% of the total exposed S/C dimension.

12 S/C A inertia at fly-by (EoL): [225, 128, 223]  $\text{kg.m}^2$  based on 526 kg,  $1.2 \times 1.2 \times 1.2$  box and two 12 kg,  $2.5 \times 1.0 \times 0.01$  m solar panels

13 Probe B2 inertia:  $1.35 \text{ kg.m}^2$  spin-axis,  $0.9 \text{ kg.m}^2$  transverse-axes based on a 30 kg,  $\phi 0.6 \times 0.3$  m cylinder

The assumed S/C A spacecraft AOCS reference frame is shown below, with the origin at the centre of the launch vehicle separation plane:

<sup>21</sup> Note that the current estimate from the model is  $f=0.016$ , however this should be revised in later work.

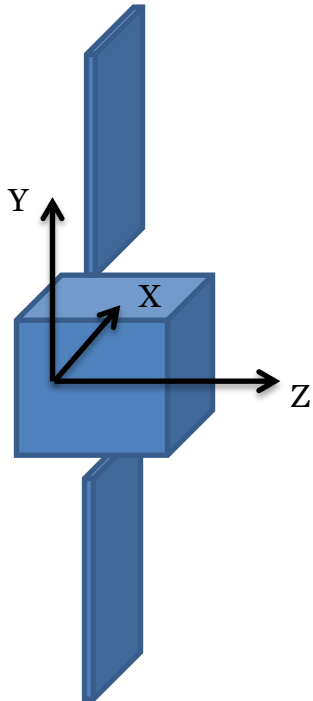


**Figure 14-1: AOCs reference frame assumed**

During the fly-by the spacecraft attitude is as follows:

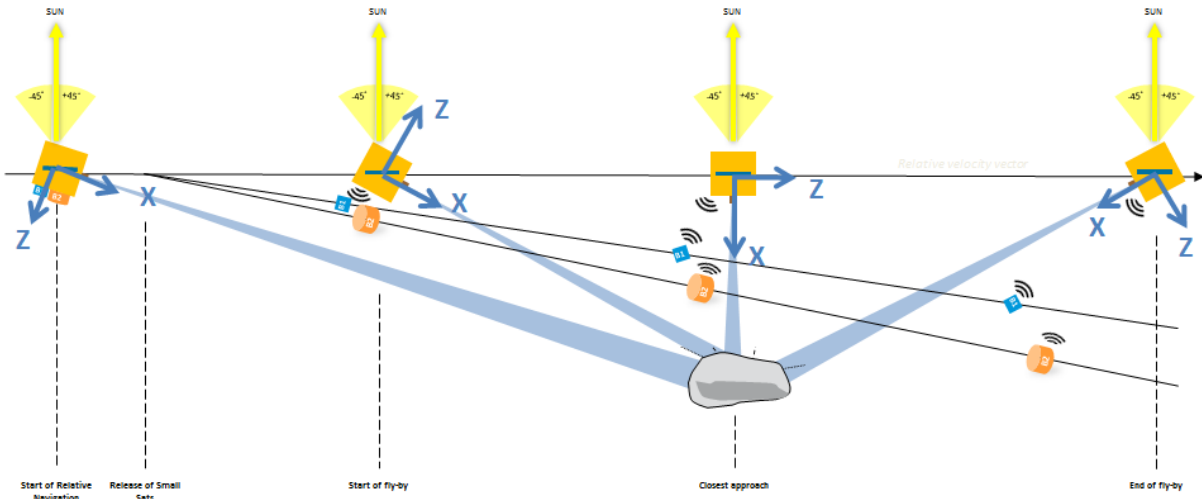


**Figure 14-2: Fly-by attitude profile**

Note that the burn attitude during the last TCM, after release of the probes, is not shown since it is design dependant.

### 14.2.2 Trade-Offs

#### 14.2.2.1 Star tracker redundancy and layout

The APE requirements can be satisfied with a single star tracker head in cold redundancy.

As per ESA practice, the design shall consider a single failure of each hardware unit. Therefore, 2 optical heads shall be embarked and their boresights can be parallel if this simplifies configuration design. Non-parallel boresights may reduce the risk of a common visibility issue impacting both heads (e.g. illuminated dust cloud on a certain side of the spacecraft) but a gyro is embarked to handle outages (req. AOCS-092).

The layout constraints are as follows:

- Optical heads shall not be placed on the same face as EP or RCS thrusters in order to minimise contamination
- Optical head boresight
  - Shall be in the  $-Z/\pm Y$  half-plane to avoid dust particles impinging into the baffle during fly-by (note that dust will initially impinge on  $+X$ , then  $+Z$ , then  $-X$ ) to satisfy req. AOCS-091
  - Shall be at least  $30^\circ$  away from the  $XZ$  plane to avoid the Sun, which is constrained to be in this plane by attitude guidance (for thermal design and power maximisation).
  - Shall be at least  $30^\circ$  away from any S/C hardware to avoid straylight reflections
  - Shall be at least  $45^\circ$  (TBC - value proposed is approximate) away from any EP or RCS nozzle vectors to minimise risk of star tracking outages caused by propellant plume particles in field of view.

Given that EP and RCS thrusters are placed on the  $-Z$  face (see 14.2.2.6), the feasible solution was to mount the optical heads on one of the  $Y$  faces, pointing roughly diagonally between the  $-Z$  and  $Y$  axes. However, depending on the specific canting of RCS thrusters, the plume avoidance constraint may be violated. It is not clear if a feasible design exists satisfying all these constraints as well as the need to cant the RCS thrusters for  $Z$ -axis rotation control and position the thrusters sufficiently far from the centre for adequate torque control fuel efficiency. Canting could be constrained to the  $XZ$  plane but then contamination of the payload may suffer if RCS is ultimately needed to desaturate the wheels during fly-by due to an unexpectedly large particle impact.

The presence of the solar panels on the  $\pm Y$  panels also means that the star trackers would not be available in case of a single deployment failure, as they would be underneath the stowed array. However, most likely the mission would be lost anyway if a deployment failure could not be resolved.

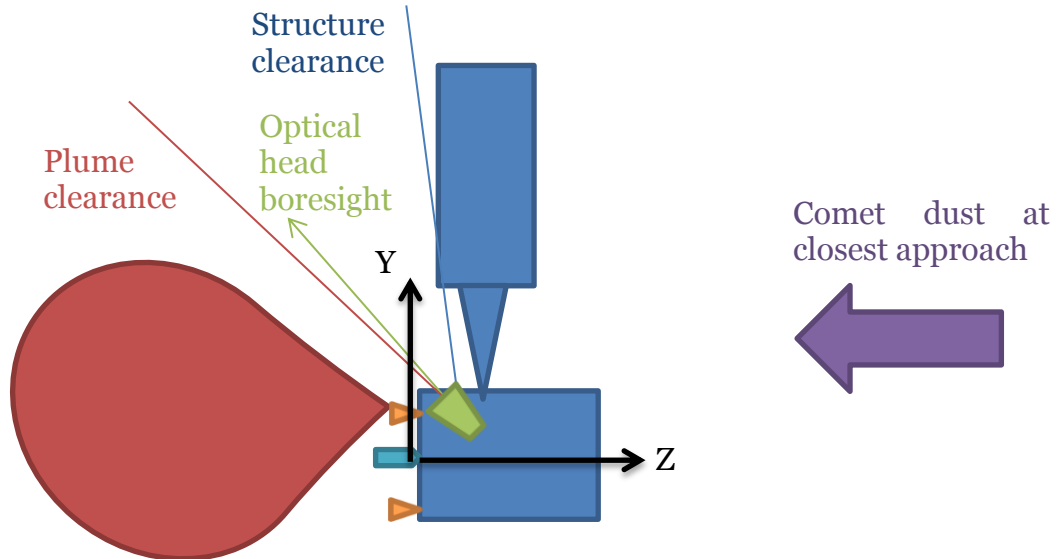


**Figure 14-3: Star tracker layout constraints**

The baseline design has the heads and baffles recessed in a Y-panel cutout. It needs to be assessed in the next design phase if this is truly feasible from an AIT, structural and configurations viewpoint.

#### 14.2.2.2 Fly-by slew actuator sizing

The fly-by kinematics can be written analytically, which allows for parametric mapping of actuator requirements as a function of fly-by velocity and closest approach distance.

Angular offset from closest-approach vector	$\theta = \tan^{-1}\left(\frac{vt}{d}\right)$
	$v$ = relative velocity (along fly-by direction) during fly by
	$t$ = time elapsed since passing closest approach point
	$d$ = closest approach distance to fly-by target
Angular rate	$\omega = \frac{vd}{v^2 t^2 + d^2}$
Angular acceleration	$\dot{\omega} = \frac{-2tv^3}{d^3 \left( \frac{t^2 v^2}{d^2} + 1 \right)^2}$
Maximum angular rate	$\omega_{max} = \frac{v}{d}$
Maximum angular acceleration	$\dot{\omega}_{max} = \frac{3\sqrt{3}}{8} \left( \frac{v}{d} \right)^2$

These equations have been validated by comparison to simulation. They represent a straight line fixed relative velocity fly-by.

For the S/C A fly-by at 70 km/s with 1000 km closest approach, the kinematics and necessary slew-axis command authority are shown below.

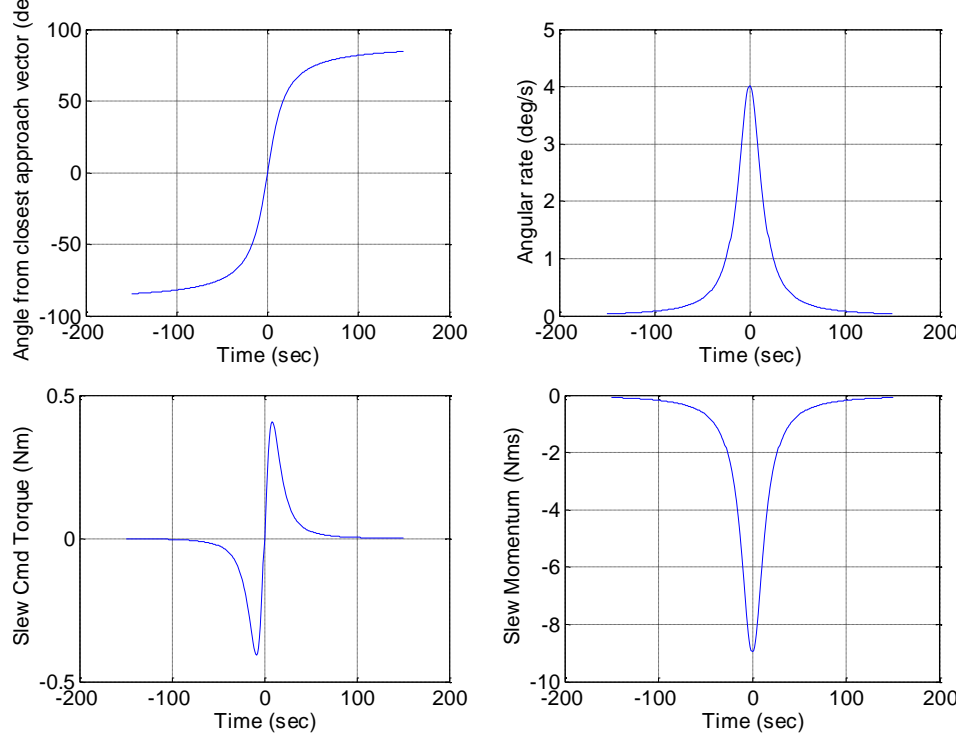


**Figure 14-4: Fly-by slew kinematics for worst case comet relative velocity**

In addition to the torque required to follow the above pointing profile, the actuators must also reject disturbance torques from the solar pressure torque and particle impacts from the comet dust field. For solar pressure and small-particle dust impacts, a conservative moment arm of 0.3 m was assumed (5% of total S/C dimension).

Starting at 100 000 km from the comet, the fly-by was simulated for a worst case comet (dust emission 3000 kg/s) and the cumulative small-particle ( $\leq 10$  mg) dust impacts were evaluated. The figure below shows that for the baseline mission (1000 km closest approach) the total cumulative mass is 0.014 grams. However, the Giotto S/C, which performed fly-by of a comet with similar activity, was hit by  $\sim 2$  grams in total. It seems unlikely that the bulk of the mass discrepancy would be covered by the particles between 10 and 40 mg (the max size encountered by Giotto). This brings into question the factor 0.01 assumption when converting the total mass density into the assumed density for the uniform-impact particle field. This should be re-examined in the next design phase.

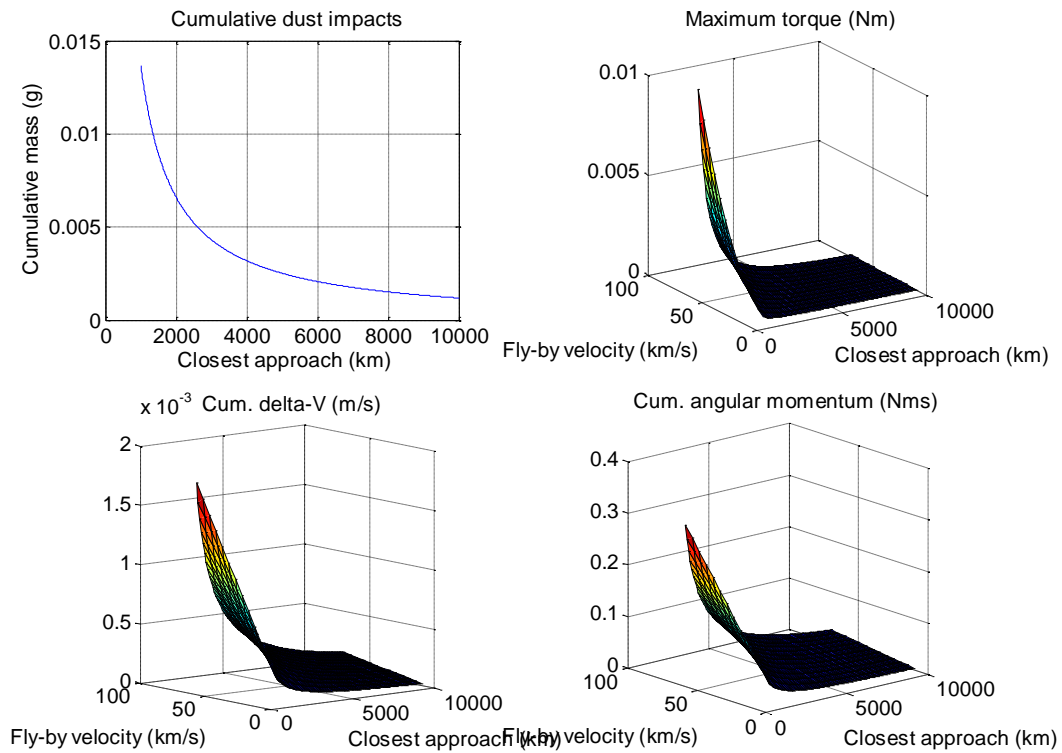


**Figure 14-5: Accumulation of small particle impacts on S/C A during fly-by**

The single worst case impact considered is a 100 mg particle hitting at the edge of the main S/C box. Such an event would have the following consequences:

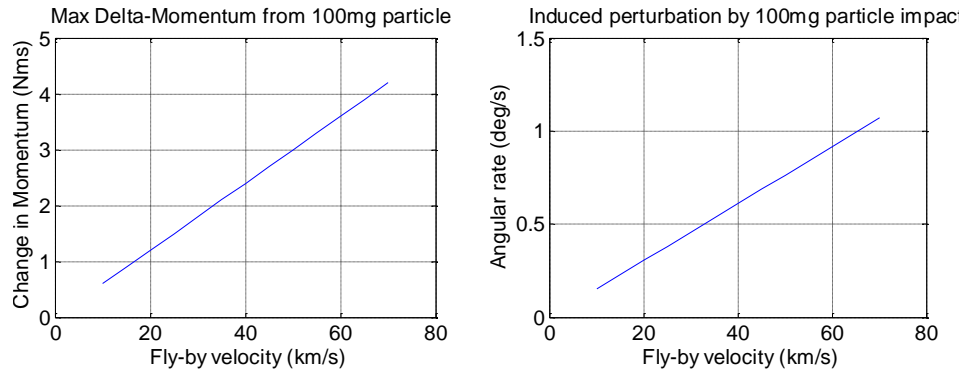


**Figure 14-6: Perturbation induced by 100 mg single particle impact at worst case location on main S/C body**

Note that momentum and angular rate scales linearly with the mass of the particle if the designer wishes to consider a different worst case.

The induced de-pointing and time to recover comet-pointing depends on the available actuator torque. The performance for several actuation options is presented below:

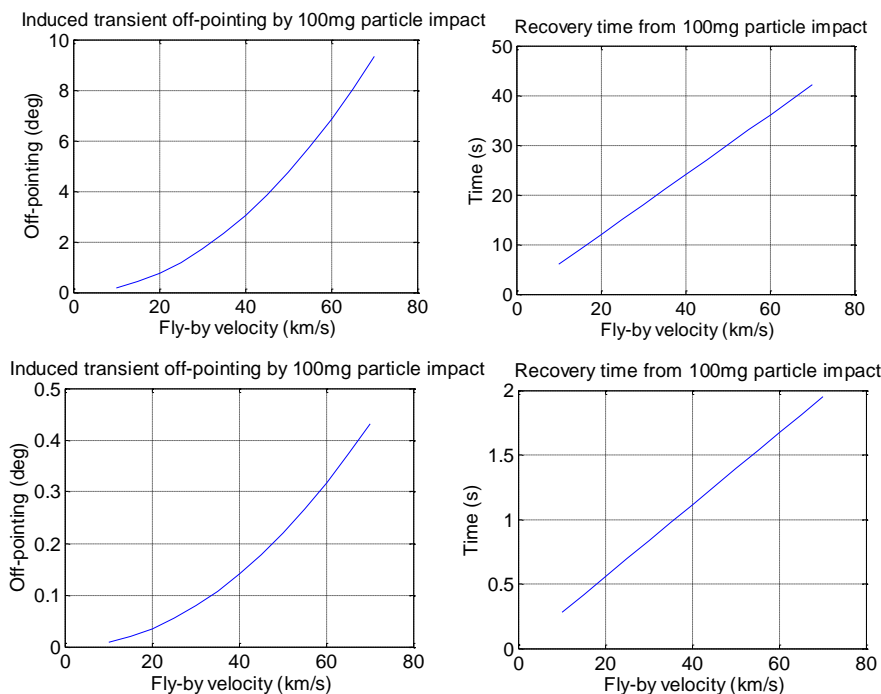


**Figure 14-7: Recovery from large particle impact about Y-axis; top – with 0.25 Nm Y-torque allocation (compatible with 1N RCS or 4 x 0.2 Nm wheels), bottom – with 7 Nm (compatible with 20N RCS)**

To avoid significant visible and infrared science outage in case of impact, large RCS thrusters (e.g. ~20 N) are essential. However, firing thrusters violates req. AOCS-093.

Based on the worst case fly-by (70 km/s & 3000 kg/s dust activity) the torque and momentum requirements for the primary actuator assembly are:

	Torque (Nm)			Momentum (Nms)		
	X	Y	Z	X	Y	Z
Solar pressure (at 0.7 AU) mitigation	3e-5	3e-6	0	1.3 (12 hrs without dumping, will automatically dissipate after closest approach via 180° change in attitude)	0.3	0
Small-particle (10 mg or less) dust pressure mitigation	0	0.00	0.01	0	0.01	0.14
Large-particle (100 mg) single impact recovery	0.25 (allocation for ~45 sec recovery)	0.12 (allocation for ~45 sec recovery)	0.25 (allocation for ~45 sec recovery)	4.2	4.2	4.2
Slew guidance profile	0	0.41	0	0	9	0
<b>TOTAL</b>	<b>0.25</b>	<b>0.53</b>	<b>0.26</b>	<b>5.5</b>	<b>13.5</b>	<b>4.3</b>

**Table 14-1: Body-frame torque and momentum budgets for fly-by**

The Cartesian actuation demands are then converted into actuator needs below.

For the option of using reaction wheels as primary actuator, a 4-wheel pyramid with 60° canting of the wheel spin axes away from the XZ plane (toward Y) is assumed, since most of the authority is required on the slew axis (Y). Wheel spin-axis directions:

	RW1	RW2	RW3	RW4	Total authority per axis
x	0.354	-0.354	-0.354	0.354	1.4
y	0.866	0.866	0.866	0.866	3.5
z	0.354	0.354	-0.354	-0.354	1.4

If the fly-by slew was a multi-axis slew a more isotropic wheel pyramid would be required and this would drive up the required wheel sizes and mass.

For the option of using RCS as primary actuators (which would save mass but violate requirement AOCS-093), 4 thrusters in a box configuration with a layout described in section 14.2.2.6 is assumed. The mean moment arm per axis is:

	Total mean RCS moment arm (m)
X	1.3
Y	0.9
Z	0.3

Since the system is only being sized for a single large particle impact (about an unknown axes) the wheel sizing is computed per-axis rather than assuming that all torques and momenta of Table 14-1 are simultaneously required on all three axes.

	X sizing case	Y sizing case	Z sizing case
Wheel torque required (Nm)	0.18	0.16	0.19
Wheel momentum required (Nms)	3.9	3.9	3.1
RCS thruster size required (N)	0.2	0.6	0.9

**Table 14-2: Actuator sizing**

Therefore, a 4 Nms high-torque (~0.2 Nm) wheel or 1 N monoprop thrusters would suffice, albeit with negligible margin. This sizing assumes no wheel failures.

If wheels are embarked, note that the required wheel assembly mass can be illustrated as a function of fly-by velocity based on wheels available on the market. These plots were computed based on a list of possible types/configurations including 4 wheel (as above) and 6 wheel (isotropic pyramid + 2 extra Y-axis wheels) configurations. Hybrid configurations with 3 small wheels and 2 large wheels were also studied but not found to

be mass optimal. If the project wishes to cater for the case of wheel failure without science degradation, the assembly mass may go up – as shown on the rightmost plot below. However, for the 70 km/s fly-by the mass stays the same since it is based on a 6 wheel 4 Nms / 0.1 Nm product (e.g. Astrofein RW250) which is slightly oversized for the no-failure case.

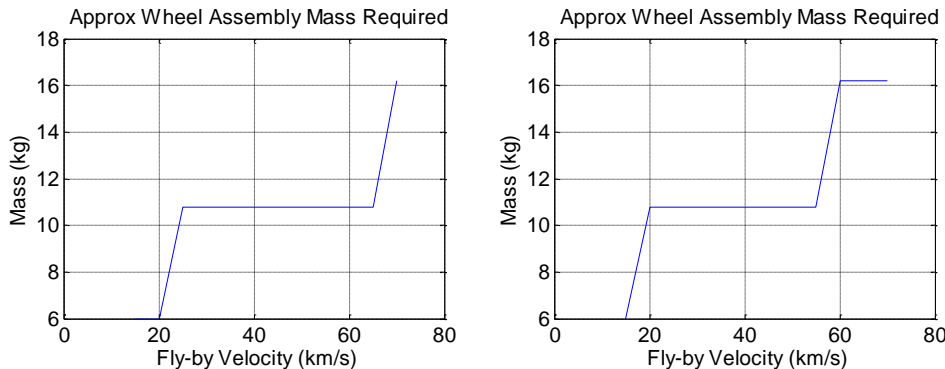


**Figure 14-8: Wheel assembly mass required; left – using full assembly, right – assuming 1 failed wheel**

Despite the above plot, the baseline configuration chosen during the study was actually a 4-wheel configuration (e.g. Rockwell Collins Deutschland RSI 4-215, total mass 21.6 kg) for simplicity and presumed cost minimisation. However, there may be mass and failure-tolerance advantages to switching to a 5 or 6 wheel configuration with a lower torque wheel (e.g. Astrofein RW250).

Since the wheel-based solution is less robust to large particle impacts than the RCS-based one (due to potential momentum saturation if multiple large particles hit), an algorithm to minimise science outage was investigated in this study (section 14.2.2.3). This is especially important in case of a wheel failure or multiple large particle impacts, where the actuator sizing margin may be negative at closest approach.

Note that the current dust models predict a 1.4% chance of encountering a 100 mg particle at closest approach. There is a 12% chance of a 10 mg particle encounter.<sup>22</sup>

#### 14.2.2.3 Guidance optimisation

The main goal of this section is to outline a method to perform on-board optimisation of slew profile subject to torque and wheel momentum constraints. The procedure could maximise the science time in the event of wheel failure, or unexpected wheel saturation due to dust impacts, by performing autonomous redesign of the guidance profile. It represents a way to boost mission robustness in the face of limited actuator authority (due to mass and cost constraints). Algorithms similar to the one proposed here are frequently used in terrestrial applications and also recently in space applications (launch vehicle guidance).

<sup>22</sup> Note that the revised analysis reported in Section 7.2.1.3 suggests probabilities an order of magnitude higher, namely a 9.9 % chance of impacting a 100 mg particle and a 98.9% chance of impacting a 10 mg particle. Nonetheless, the general design principle still applies.

The algorithm relies on solving a series of convex optimisations to produce the necessary torque profile. Convex optimisation is a subfield of mathematical optimisation that can handle problems with several thousand variables in an efficient manner with established theoretical convergence rates as well as good numerical properties. Many classes of convex optimisation problems admit polynomial-time algorithms, whereas mathematical optimisation is in general NP-hard. For this reason, efficient tools have been developed that are able to solve these problems on typical on-board flight computers.

Let  $F_I := (O_I; \vec{x}_I, \vec{y}_I, \vec{z}_I)$  represent the coordinate frame with the origin  $O_I$  fixed to the comet location and  $F_B := (O_B; \vec{x}_B, \vec{y}_B, \vec{z}_B)$  a body fixed frame fixed to centre of the mass of the spacecraft. The vector  $\boldsymbol{\omega} := [\omega_x \ \omega_y \ \omega_z]^T$  represents the angular velocity in the body frame while the unit quaternion  $\mathbf{q}(t) \in \mathbb{R}^4$  with  $\mathbf{q}^T \mathbf{q} = 1$  is used to rotate from the inertial frame to the body frame. Considering that the spacecraft is actuated by a set of  $n_w$  reaction wheels, the attitude kinematics and dynamics can be expressed as:

$$\begin{aligned}\dot{\mathbf{q}}(t) &= \frac{1}{2} \mathbf{q}(t) \otimes \begin{bmatrix} \boldsymbol{\omega}(t) \\ 0 \end{bmatrix} \\ J\dot{\boldsymbol{\omega}}(t) &= [J\boldsymbol{\omega}(t) + L\mathbf{h}(t)] \times \boldsymbol{\omega}(t) - Lu(t) \\ \dot{\mathbf{h}}(t) &= u(t)\end{aligned}$$

where the operator  $\otimes$  denotes the quaternion product,  $J \in \mathbb{R}^{3 \times 3}$  is moment of inertia in the body frame,  $\mathbf{h}(t) \in \mathbb{R}^{n_w}$  is vector containing the angular momentum stored in each of  $n_w$  wheels,  $\mathbf{u}(t) \in \mathbb{R}^{n_w}$  is the motor torque applied to the wheels and  $L \in \mathbb{R}^{3 \times n_w}$  is reaction wheel torque distribution matrix. The matrix representation of the quaternion is defined as  $\mathbf{q} = [\mathbf{q}_v^T \ q_s]^T$  where  $q_s \in \mathbb{R}$  denotes the scalar part and  $\mathbf{q}_v(t) \in \mathbb{R}^3$  denotes the vector part. In a more compact notation, dynamics and kinematics can be written as:

$$\dot{\mathbf{x}}(t) = f(\mathbf{x}(t), \mathbf{u}(t)) \text{ with } \mathbf{x} = [\mathbf{q}^T \ \boldsymbol{\omega}^T \ \mathbf{h}^T]^T$$

Consider two unit vectors  $\vec{r}$  and  $\vec{v}$  centred at the spacecraft's centre of mass as shown in Figure 14-9. The vector  $\vec{r}$  points towards the target comet and has known coordinates  $\mathbf{r}_I$  in the inertial frame while the vector  $\vec{v}$  is aligned along the sensor's boresight direction and has known coordinates  $\mathbf{v}_B$  in the body frame.

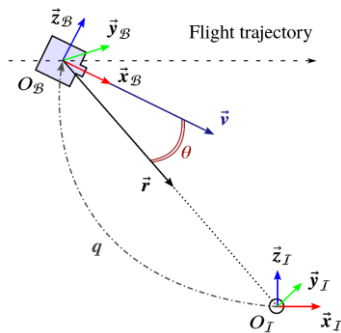


**Figure 14-9: Illustration of the coordinate frames together with the instrument pointing unit vector  $\vec{v}$  and the comet pointing unit vector  $\vec{r}$**

In order to conduct scientific observations, the pointing error angle  $\theta$  between these two unit vectors must be kept below a maximum value  $\theta_{vi}$  for the visual camera. In terms of cosines, this constraint is equivalent to:

$$\cos \theta \geq \cos \theta_{vi} \quad \text{or} \quad \mathbf{r}_B^T \mathbf{v}_B \geq \cos \theta_{vi}$$

where  $\mathbf{r}_B$  represents the body frame components of  $\tilde{\mathbf{r}}$  and can be computed from the known inertial frame coordinates  $\mathbf{r}_I$  and quaternion  $\mathbf{q}$  using:

$$\begin{bmatrix} \mathbf{r}_B \\ 0 \end{bmatrix} = \mathbf{q}^* \otimes \begin{bmatrix} \mathbf{r}_I \\ 0 \end{bmatrix} \otimes \mathbf{q}$$

Where  $\mathbf{q}^*$  represents the quaternion conjugate of  $\mathbf{q}$ . The multiplication between two quaternions  $\mathbf{q}$  and  $\mathbf{p}$  can be represented in matrix form as:

$$\mathbf{p} \otimes \mathbf{q} = [\mathbf{p}]_\otimes \mathbf{q} = [\mathbf{q}]_\otimes \mathbf{p} \quad \text{with}$$

$$[\mathbf{q}]_\otimes = \begin{bmatrix} q_s \mathbf{I}_3 + [\mathbf{q}_v]^\times & \mathbf{q}_v \\ \mathbf{q}_v^T & q_s \end{bmatrix} \quad \text{and} \quad [\mathbf{q}]_\otimes = \begin{bmatrix} q_s \mathbf{I}_3 - [\mathbf{q}_v]^\times & \mathbf{q}_v \\ \mathbf{q}_v^T & q_s \end{bmatrix}$$

where the operator  $[\mathbf{r}]^\times$  with  $\mathbf{r} = [x \ y \ z]^T$  is equal to the left-hand side equivalent of the vector cross product in matrix form, i.e.

$$[\mathbf{r}]^\times = \begin{bmatrix} 0 & -z & y \\ z & 0 & -x \\ -y & x & 0 \end{bmatrix}$$

If both  $\mathbf{p}$  and  $\mathbf{q}$  are pure quaternions (i.e. with scalar part  $p_s = q_s = 0$ ), then quaternion multiplication reduces to the cross-product and the dot product between the vectors parts:

$$\mathbf{p} \otimes \mathbf{q} = \begin{bmatrix} \mathbf{p}_v \times \mathbf{q}_v \\ -\mathbf{p}_v^T \mathbf{q}_v \end{bmatrix}$$

Using the notations  $\tilde{\mathbf{v}}_B = [\mathbf{v}_B^T \ 0]^T$  and  $\tilde{\mathbf{r}}_I = [\mathbf{r}_I^T \ 0]^T$ , the dot product relationship  $\cos \theta = \mathbf{r}_B^T \mathbf{v}_B$  can be redefined as

$$\begin{aligned} \cos \theta &= -\mathbf{q}^T [\tilde{\mathbf{r}}_I]_\otimes [\tilde{\mathbf{v}}_B]_\otimes \mathbf{q} \\ &= \mathbf{q}^T \mathbf{q} - \mathbf{q}^T ([\tilde{\mathbf{r}}_I]_\otimes [\tilde{\mathbf{v}}_B]_\otimes + \mathbf{I}) \mathbf{q} \\ &= 1 - \mathbf{q}^T \mathbf{M} \mathbf{q} \end{aligned}$$

where the fact that  $\mathbf{q}^T \mathbf{q} = 1$  was used. In this case, the matrix  $\mathbf{M} = [\tilde{\mathbf{r}}_I]_\otimes [\tilde{\mathbf{v}}_B]_\otimes + \mathbf{I}$  is positive semidefinite with eigenvalues 0 and 2. Based on the previous equation, the field of view constraint  $\cos \theta \geq \cos \theta_{vi}$  can be equivalently expressed as:

$$\mathbf{q}^T \mathbf{M} \mathbf{q} \leq 1 - \cos \theta_{vi} \quad \text{or} \quad \|\mathbf{N} \mathbf{q}\|_2 \leq \sqrt{1 - \cos \theta_{vi}} \quad \text{with} \quad \mathbf{N}^T \mathbf{N} = \mathbf{M}$$

where the factorization term  $\mathbf{N}$  can be obtained using an eigen decomposition of the matrix  $\mathbf{M}$ . The goal of the optimisation problem is to find a command  $\mathbf{u}(t)$  such that the previous constraint holds for all  $t \in [t, t_{max}]$ . However, in some circumstances, such as wheel failures, this constraint can be too demanding and no feasible control solutions exist. To resolve this issue, the hard constraint given in the previous equation is replaced by the following soft constraint version:

$$\|\mathbf{N}(t) \mathbf{q}(t)\|_2 \leq \sqrt{1 - \cos \theta_{vi}} + \gamma(t); \quad \gamma(t) \geq 0$$

Where  $\gamma(t)$  is a measure of the constraint violation magnitude at time  $t$ . Minimizing  $\gamma$  throughout the trajectory therefore enforces the field of view constraint to the maximum

degree possible. A similar cost  $\zeta(t)$  can be introduced for deviations outside the field of view limit  $\theta_{ir}$ .

Using the previous equations, the constrained pointing optimisation can be formulated as follows:

$$\begin{aligned}
 \text{minimize } J_{nl}(\mathbf{x}, \mathbf{u}) &:= \int_0^{t_{max}} \boldsymbol{\beta} [\mathbf{card}(\gamma(t)) \quad \mathbf{card}(\zeta(t)) \quad \boldsymbol{\eta}(t) \quad \|\mathbf{u}(t)\|_2]^T dt \quad \text{subject to} \\
 \mathbf{x}(0) &= \mathbf{x}_{init} \quad \text{initial conditions} \\
 \dot{\mathbf{x}}(t) &= \mathbf{f}(\mathbf{x}(t), \mathbf{u}(t)) \quad \text{nonlinear dynamics} \\
 \|\mathbf{N}(t)\mathbf{q}(t)\|_2 &\leq \sqrt{1 - \cos \theta_{vi}} + \gamma(t); \quad \gamma(t) \geq 0 \\
 &\leq \sqrt{1 - \cos \theta_{ir}} + \zeta(t); \quad \zeta(t) \geq 0 \\
 &\leq \boldsymbol{\eta}(t); \quad \boldsymbol{\eta}(t) \geq 0
 \end{aligned}$$

where the cardinality function  $\mathbf{card}(\mathbf{v})$  denotes the number of nonzero elements in  $\mathbf{v} \in \mathbb{R}^m$ , the operator  $\leq$  denotes element-wise inequality,  $\mathbf{x}_{init}$  represents the initial state,  $\omega_{\bullet}^{max}$  the maximum angular rates around each axis,  $u_{\bullet}^{max}$  and  $\mathbf{h}_{\bullet}^{max}$  the maximum motor torque and the maximum momentum for each of the  $n_w$  wheels and  $\bullet$  is used to denote any of the possible subscripts (for example  $\omega_{\bullet}^{max}$  can mean  $\omega_x^{max}$ ,  $\omega_y^{max}$  or  $\omega_z^{max}$ ). The vector  $\boldsymbol{\beta} \in \mathbb{R}^4$  contains the weights that determine the relative importance of the different terms in the cost function. The values  $\boldsymbol{\beta}(1)$  and  $\boldsymbol{\beta}(2)$  multiplying the  $\mathbf{card}(\gamma(t))$  and  $\mathbf{card}(\zeta(t))$  terms determine the cost of violating at time  $t$  the field of view constraint of the visual and infrared camera respectively.  $\boldsymbol{\beta}(3)$  introduces a small cost proportional to the pointing error and is used to bring this error close to zero when the field of view constraints are satisfied and the previous two terms are zero.  $\boldsymbol{\beta}(4)$  places a small cost proportional to the energy of the control energy and is used to reduce the chattering in  $\mathbf{u}$  without significantly impacting the pointing performance.

This optimisation problem is challenging to solve directly since it contains the nonlinear kinematics and dynamics equations. Additionally, the problem is optimised for all  $t \leq t_{max}$  and is therefore infinite dimensional. To tackle these issues, the first idea is to first approximate the function  $\mathbf{f}(\mathbf{x}(t), \mathbf{u}(t))$  using a first-order Taylor expansion around a previously-computed trajectory denoted by  $\bar{\mathbf{x}}(t), \bar{\mathbf{u}}(t)$ , i.e.

$$\begin{aligned}
 \dot{\mathbf{x}}(t) &\approx \mathbf{A}(t)\mathbf{x}(t) + \mathbf{B}(t)\mathbf{u}(t) + \mathbf{z}(t) \quad \text{where} \\
 \mathbf{A}(t) &= \left. \frac{\partial \mathbf{f}}{\partial \mathbf{x}} \right|_{\bar{\mathbf{x}}(t), \bar{\mathbf{u}}(t)}, \mathbf{B}(t) = \left. \frac{\partial \mathbf{f}}{\partial \mathbf{u}} \right|_{\bar{\mathbf{x}}(t), \bar{\mathbf{u}}(t)}, \mathbf{z}(t) = -\mathbf{A}(t)\bar{\mathbf{x}}(t) - \mathbf{B}(t)\bar{\mathbf{u}}(t)
 \end{aligned}$$

This linearization is only valid if the new trajectory stays relatively close to the previous one. Therefore, a new trust region constraint will be introduced to the original optimisation problem to keep the solution in a region where the linear approximation is valid.

The infinite dimensional optimisation is also discretized to render the problem tractable by numerical tools. To do this, the time interval  $t \in [0, t_{max}]$  is subdivided into a grid of  $N$  sampling times. For each subinterval  $t \in [t_k, t_{k+1}]$  with  $k \in 0, \dots, N - 1$ , the trajectory  $\mathbf{x}(t)$  satisfying the linearized equations is given by

$$\mathbf{x}(t) = \Phi(t, t_k)\mathbf{x}(t_k) + \int_{t_k}^t \Phi(t, \xi)\mathbf{B}(\xi)\mathbf{u}(\xi)d\xi + \int_{t_k}^t \Phi(t, \xi)\mathbf{z}(\xi)d\xi$$

where  $\Phi(\xi, t_k)$  is the state transition matrix defined for  $\xi \in [t_k, t_{k+1}]$  as:

$$\Phi(\xi, t_k) = \int_{t_k}^{\xi} \mathbf{A}(\tau)\Phi(\tau, t_k)d\tau$$

Between sample times, the control signal  $\mathbf{u}(t)$  is assumed to be linearly interpolated using a first-order-hold (FOH), i.e.

$$\begin{aligned} \mathbf{u}(t) &= \lambda_k^-(t)\mathbf{u}_k + \lambda_k^+(t)\mathbf{u}_{k+1}, \quad \forall t \in [t_k, t_{k+1}), \\ \lambda_k^-(t) &= \frac{t_{k+1} - t}{t_{k+1} - t_k}, \quad \lambda_k^+(t) = \frac{t - t_k}{t_{k+1} - t_k} \end{aligned}$$

where  $\mathbf{u}_k := \mathbf{u}(t_k)$ . Using the fact that  $\Phi(t_{k+1}, \xi) = \Phi(t_{k+1}, t_k)\Phi(\xi, t_k)^{-1}$ , for all  $t_k, t_{k+1}, \xi \in \mathbb{R}$ , the state propagation equation can be restated as:

$$\begin{aligned} \mathbf{x}_{k+1} &= \mathbf{A}_k\mathbf{x}_k + \mathbf{B}_k^-\mathbf{u}_k + \mathbf{B}_k^+\mathbf{u}_{k+1} + \mathbf{z}_k \quad \text{with} \\ \mathbf{A}_k &= \Phi(t_{k+1}, t_k), \\ \mathbf{B}_k^- &= \mathbf{A}_k \int_{t_k}^{t_{k+1}} \Phi(\xi, t_k)^{-1}\lambda_k^-(\xi)\mathbf{B}(\xi)d\xi, \\ \mathbf{B}_k^+ &= \mathbf{A}_k \int_{t_k}^{t_{k+1}} \Phi(\xi, t_k)^{-1}\lambda_k^+(\xi)\mathbf{B}(\xi)d\xi, \\ \mathbf{z}_k &= \mathbf{A}_k \int_{t_k}^{t_{k+1}} \Phi(\xi, t_k)^{-1}\mathbf{z}(\xi)d\xi \end{aligned}$$

For each subinterval, the precise value of  $\mathbf{A}_k, \mathbf{B}_k^-, \mathbf{B}_k^+$  and  $\mathbf{z}_k$  can be calculated to arbitrary precision using numerical integration tools using the known functions  $\mathbf{A}(t), \mathbf{B}(t)$  and  $\mathbf{z}(t)$ . Based on the previous considerations, the original nonlinear optimisation problem is approximated using the following convex form:

$$\begin{aligned} \text{minimize } J(\mathbf{x}, \mathbf{u}) &:= \sum_{k=0}^N \boldsymbol{\beta} [\mathbf{c}_{\gamma, k}\gamma_k \ \mathbf{c}_{\zeta, k}\zeta_k \ \boldsymbol{\eta}_k \ \|\mathbf{u}_k\|_2]^T \quad \text{subject to} \\ \mathbf{x}_0 &= \mathbf{x}_{init} \quad \text{initial conditions} \\ \mathbf{x}_{k+1} &= \mathbf{A}_k\mathbf{x}_k + \mathbf{B}_k^-\mathbf{u}_k + \mathbf{B}_k^+\mathbf{u}_{k+1} + \mathbf{z}_k \quad \text{linearized dynamics around } \bar{\mathbf{x}}, \bar{\mathbf{u}}, \text{ for } k \in 0, \dots, N - 1 \\ &\quad \text{for } k \in 0, \dots, N: \\ \|\mathbf{N}_k \mathbf{q}_k\|_2 &\leq \sqrt{1 - \cos \theta_{vi}} + \gamma_k; \quad \gamma_k \geq 0 \end{aligned}$$

$$\begin{aligned}
 & \leq \sqrt{1 - \cos \theta_{ir}} + \zeta_k; \quad \zeta_k \geq 0 \\
 & \leq \eta_k; \quad \eta_k \geq 0 \\
 |\mathbf{u}(t)| & \leq [u_1^{max} \dots u_{n_w}^{max}]^T \text{ max motor torque} \\
 |\mathbf{h}(t)| & \leq [h_1^{max} \dots h_{n_w}^{max}]^T \text{ max wheel momentum} \\
 |\boldsymbol{\omega}(t)| & \leq [\omega_x^{max} \omega_y^{max} \omega_z^{max}]^T \text{ max angular rates} \\
 |\mathbf{u}_k - \bar{\mathbf{u}}_k| & \leq \rho \text{ trust region}
 \end{aligned}$$

The proposed method works by repeatedly solving this convex optimisation problem, using the previous solution as the new linearization trajectory. The iterations are stopped when the improvements in the cost function drop below a certain threshold. For the first iteration, the scaling factors  $\mathbf{c}_{\gamma,k}$  and  $\mathbf{c}_{\zeta,k}$  are fixed to  $\mathbf{c}_{\gamma,k}^{\{1\}} = \mathbf{c}_{\zeta,k}^{\{1\}} = 1$ . During the  $n$ -th iteration, these factors are reset to:

$$\mathbf{c}_{\gamma,k}^{\{n\}} = \frac{1}{\epsilon + |\mathbf{c}_{\gamma,k}^{\{n-1\}}|}$$

and analogous for  $\mathbf{c}_{\zeta,k}$ . The notation  $\mathbf{c}_{\gamma,k}^{\{n-1\}}$  denotes the  $\mathbf{c}_{\gamma,k}$  values obtained during the  $n-1$  iteration and  $\epsilon$  is a small term controlling the maximum scaling when  $\mathbf{c}_{\gamma,k}^{\{n-1\}} = 0$ . In this way, small values of  $\gamma_k$  and  $\zeta_k$  are weighted more while small values are weighted less. This strategy effectively approximates the cardinality function **card**.

The speed of convergence and the quality of the solution is significantly influenced by the size of the trust region. If  $\rho$  is chosen too big, the linear approximations will be poor, leading to a bad solution. On the other hand, if  $\rho$  is chosen too small, progress is slow. Let  $\rho^{\{n\}}$  denote the trust region size used to constrain the optimisation during the  $n$ -th iteration. To achieve a balance between robustness and speed of convergence of the sequential method, the following policy (inspired by the work in *Mao, Y., Szmuk, M., and Acikmese, B. (2016). Successive convexification of non-convex optimal control problems and its convergence properties. In 2016 IEEE 55th Conference Conference on Decision and Control (CDC), 3636–3641*) was adopted in this study:

1. Compute the control signal  $\tilde{\mathbf{u}}$  and state trajectory  $\tilde{\mathbf{x}}$  as the preliminary solution to the convex problem using the trust region size  $\rho^{\{n\}}$  and the linearization trajectory  $\mathbf{x}^{\{n\}}, \mathbf{u}^{\{n\}}$ . Here,  $\mathbf{u}^{\{n\}}$  and  $\mathbf{x}^{\{n\}}$  refer to the control signal and state trajectory solution obtained after  $n$  iterations.
2. Using the control signal  $\tilde{\mathbf{u}}$  and the nonlinear state propagation equation, compute by numerical integration, the true trajectory  $\tilde{\mathbf{x}}_{nl}$  containing the states at each of the  $N$  sampling times used in the discretization.
3. Compute the absolute difference  $\epsilon = |J(\tilde{\mathbf{x}}, \tilde{\mathbf{u}}) - J(\tilde{\mathbf{x}}_{nl}, \tilde{\mathbf{u}})|$  between the true cost function  $J(\tilde{\mathbf{x}}_{nl}, \tilde{\mathbf{u}})$  and the one obtained in the convex optimisation  $J(\tilde{\mathbf{x}}, \tilde{\mathbf{u}})$ .
4. If  $\epsilon \geq \epsilon_{max}$  then reject solution (i.e. set  $\mathbf{x}^{\{n+1\}} = \mathbf{x}^{\{n\}}$  and  $\mathbf{u}^{\{n+1\}} = \mathbf{u}^{\{n\}}$ ), contract the trust region size for the next iteration ( $\rho^{\{n+1\}} = \beta^- \rho^{\{n\}}$  with  $\beta^- \in [0, 1)$ ) and go back to step 1. Otherwise, accept solution (i.e. set  $\mathbf{x}^{\{n+1\}} = \tilde{\mathbf{x}}$  and  $\mathbf{u}^{\{n+1\}} = \tilde{\mathbf{u}}$ ) and expand the trust region size ( $\rho^{\{n+1\}} = \beta^+ \rho^{\{n\}}$  with  $\beta^+ \geq 1$ ).

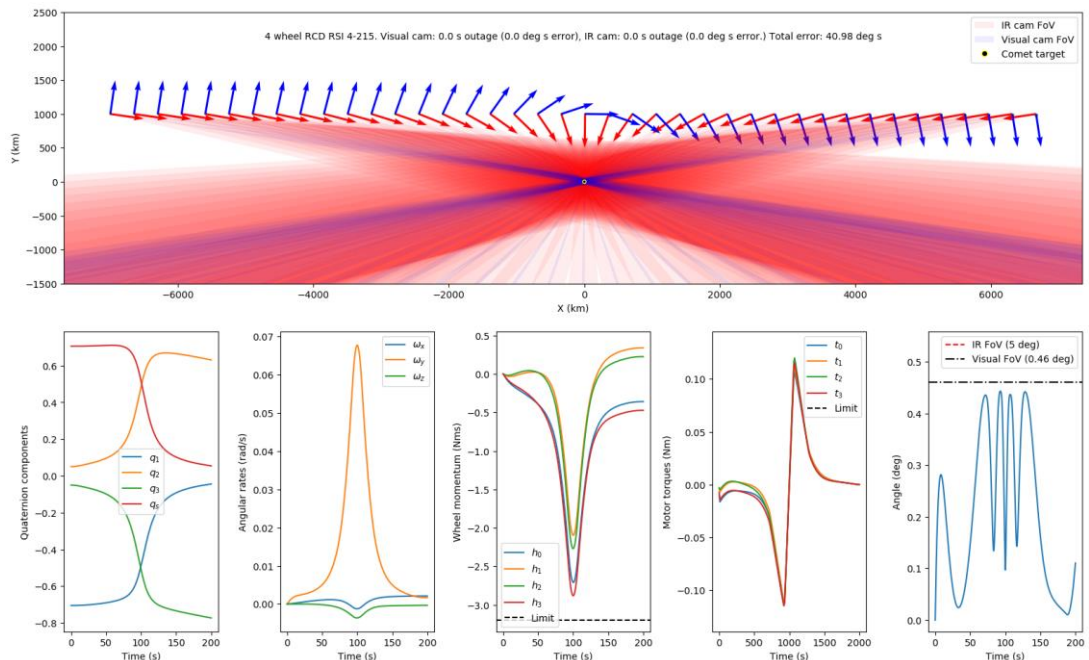
5. If the relative improvement in the cost function between subsequent iterations drops below a certain threshold i.e. if  $|J(\mathbf{x}^{n+1}, \mathbf{u}^{n+1}) - J(\mathbf{x}^n, \mathbf{u}^n)| \leq \alpha$ , stop and return the pair  $\tilde{\mathbf{x}}, \tilde{\mathbf{u}}$  as the solution. Otherwise, go back to step 1.

The algorithm was implemented using only open source tools: Python as programming language, CVXPY as the optimisation modelling language and ECOS as the convex solver. The numerical values for all the parameters are provided in Table 14-3.

Parameter	Value
<b>Spacecraft</b>	
Initial position in the inertial frame	[−7000 1000 0] km
Velocity in the inertial frame	[70 0 0] km/s
Initial pointing error	0 rad
Initial angular velocity $\omega(0)$	[0 0 0] rad/s
Initial wheel momentum $\mathbf{h}(0)$	[0 0 0] Nms
Moment of inertia $\mathbf{J}$	$\begin{bmatrix} 255 & 10 & -10 \\ 10 & 128 & 10 \\ -10 & 10 & 223 \end{bmatrix}$ kg m <sup>2</sup>
Reaction wheel torque distribution matrix $\mathbf{L}$ 4 wheel pyramid configuration	$\frac{\sqrt{2}}{4} \begin{bmatrix} 1 & -1 & -1 & 1 \\ \sqrt{6} & \sqrt{6} & \sqrt{6} & \sqrt{6} \\ 1 & 1 & -1 & -1 \end{bmatrix}$
Reaction wheel torque distribution matrix $\mathbf{L}$ 5 wheel hybrid configuration	$\begin{bmatrix} 1 & 0 & 1/\sqrt{2} & 0 & 0 \\ 0 & 0 & 0 & 1 & 1 \\ 0 & 1 & 1/\sqrt{2} & 0 & 0 \end{bmatrix}$
Reaction wheel torque distribution matrix $\mathbf{L}$ 6 wheel hybrid configuration	$\frac{\sqrt{2}}{4} \begin{bmatrix} 1 & -1 & -1 & 1 & 0 & 0 \\ \sqrt{6} & \sqrt{6} & \sqrt{6} & \sqrt{6} & 0 & 2\sqrt{2} \\ 1 & 1 & -1 & -1 & 2\sqrt{2} & 0 \end{bmatrix}$
<b>Optimisation constraints</b> (using RCD RSI 4-215 wheels)	
Maximum wheel motor torque $u_{\max}^{max}$	0.172 Nm (includes 20% margin)
Maximum wheel angular momentum $h_{\max}^{max}$	3.2 Nms (includes 20% margin)
Maximum angular rates $\omega_{\max}^{max}$	$\infty$ rad/s
Visual camera half field of view angle $\theta_{vi}$	0.46 deg
Infrared camera half field of view angle $\theta_{ir}$	5 deg
<b>Sequential convex optimisation parameters</b>	
Number of sample points $N$	200
Total time $t_{max}$	200 s
Weighting vector $\beta$	[1 1 1.5 0.1]
Factor in the linear approximation of the cardinality function <b>card</b>	$10^{-3}$
Initial trust region size $\rho^{[0]}$	$10^{-3}$ Nm
Trust region update parameters $[\beta^- \quad \beta^+]$	[0.5 1.5]
Maximum absolute difference $\epsilon_{max}$	1
Cost improvement termination threshold $\alpha$	$10^{-4}$

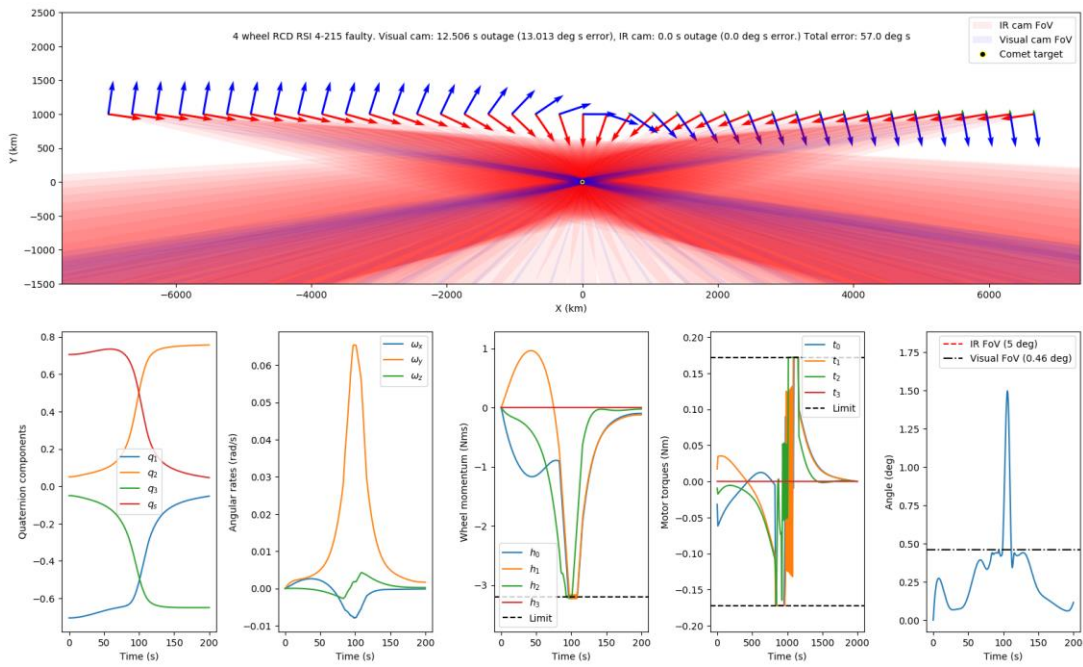
**Table 14-3: Numerical values for the parameters used during the guidance optimisation procedure**

Figure 14-10 shows the result of the attitude guidance optimisation procedure for a nominal scenario, using a set of 4 x RCD RSI 4-215 wheels (as an example) arranged in a pyramid configuration. In this case, the angular rates are left unconstrained (i.e.  $\omega_{\text{max}} = \infty$ ) allowing for nonplanar rotations. The sequential convex programming method typically converges in about 5-10 iterations from random initial conditions. In this case, the resulting trajectory is very close to the optimal one that can be derived analytically – since the actuator authority is sufficient to avoid encountering constraints. Small differences occur due to the fact the convex optimisation method accounts for the full nonlinear dynamics and the resulting complex kinematics.



**Figure 14-10: Guidance profile for a nominal 4 wheel RCD RDS-4-215 configuration**

In Figure 14-11, the torque on the 4<sup>th</sup> reaction wheel is kept at zero throughout the flyby, corresponding to a wheel failure scenario. It can be observed that the method converges towards a slightly nonplanar solution satisfying all the momentum and torque constraints while also minimising the total amount of time spent outside the field of view of the visual camera to just 12.5 sec (as opposed to 110 sec when using a modified PD controller outlined later in this subsection).



**Figure 14-11: Guidance profile for a 4 wheel RCD RDS-4-215 configuration with one failed wheel**

Table 14-4 presents the results of a similar nominal & failure-case analysis performed for multiple wheel models and arrangements. The list of wheel configurations was chosen to cover a broad range of actuator torques and momentum, but is not intended to be a complete list of possible suppliers/designs. For comparison to more classical methods, a conventional quaternion PD tracking controller (with 0.5 Hz bandwidth and tuned for minimum unconstrained response time) was also implemented, augmented with a proportional error saturation (set to the visual camera FoV half-angle) to reduce overshoot in case of torque or momentum saturation. Note that science outage is sensitive to the proportional error saturation threshold, but this was not optimised in this CDF study.

Test case	1	2	3	4	5	6	7	8	9	10
<b>Manufacturer</b>	MSCI Canada	RCD Germany	RCD Germany	RCD Germany	<b>RCD Germany</b>	RCD Germany	RCD Germany	RCD Germany	RCD Germany	TAMAM Israel
<b>Model</b>	Micro-wheel 1000	RSI 4-75/60	RSI 4-75/60 & 12-220/45	RSI 4-75/60	<b>RSI 4-215</b>	RSI 12-220/45	RSI 12-220/45	RSI 30-280/30	RSI 30-280/30	15 Nms wheel
<b>Assumed configuration</b>	4 wheel pyramid	4 wheel pyramid	5 wheel hybrid config (two wheel types)	4 wheel pyramid + 2 extra wheels to improve instrument slews	<b>4 wheel pyramid</b>	4 wheel pyramid	4 wheel pyramid + 2 extra wheels to improve instrument slews	4 wheel pyramid	4 wheel pyramid + 2 extra wheels to improve instrument slews	4 wheel pyramid
<b>Max torque per wheel (Nm)</b>	0.03	0.075	0.075 & 0.22	0.075	<b>0.215</b>	0.22	0.22	0.28	0.28	0.4
<b>Max momentum per wheel (Nms)</b>	1.1	4	4 & 12	4	<b>4</b>	12	12	30	30	15

Quaternion tracking with PD control & proportional error limiter (i.e. no guidance optimisation)									
IR cam science outage (s)	93	71	0	21	0	0	0	0	0
Vis. cam science outage (s)	137	101	27	53	0	0	0	0	0
Quaternion tracking with PD control & proportional error limiter (i.e. no guidance optimisation) in wheel failure case									
IR cam science outage (s)	131	82	80	39	85	0	0	0	0
Vis. cam science outage (s)	200	111	108	78	110	0	0	0	0
Performance with guidance optimisation									
IR cam science outage (s)	90	20	0	0	0	0	0	0	0
Vis. cam science outage (s)	115	41	0	26	0	0	0	0	0
Performance with guidance optimisation in wheel failure case (re-optimised)									
IR cam science outage (s)	113	35	47	16	0	0	0	0	0
Vis. cam science outage (s)	122	58	21	43	13	0	0	0	0

**Table 14-4: Pointing performance obtained for different sets of wheels using the convex guidance approach vs classic simple approach, for 70 km/s fly-by with 1000 km closest approach**

It can be seen that the proposed optimisation technique outperforms or matches the classical methods in all situations. The method dramatically improves the science time in the cases where the actuators are undersized or a wheel failure or unexpectedly large dust particle impact occurs.

This optimisation technique can be implemented on standard flight processors, either with regular re-optimisation at the AOCS frequency (TBC) or at less regular intervals (or even just once before the fly-by or after a saturation/failure event) along with a high frequency trajectory tracking controller. This algorithm represents an elegant way to improve robustness when actuator mass is highly constrained during the design – as is the case with this mission.

#### 14.2.2.4 Primary actuator trade-off

Reaction wheels were traded against RCS (1N and 20N) in the following table. It is assumed that 1N RCS thrusters (or slightly larger) would be required anyway for dumping momentum. Therefore, wheels or an upgrade to 20 N thrusters will introduce extra mass/power/volume penalties.

Primary attitude actuator	4 x Reaction wheels	2 x 4 x 20 N RCS	2 x 4 x 1 N RCS
Cost beyond 1N RCS (needed anyway for dumping wheel momentum)	Medium	Low	0
Additional assembly mass beyond 1N RCS	21.6 kg	2.7 kg	0
Assembly power average	24 W (~200 W during slew)	120 W	72 W
Additional volume beyond 1N RCS	48 000 cm <sup>3</sup>	6100 cm <sup>3</sup> (external)	0
Science impact	EMC noise	Potential plume disturbances to mass spectrometer  Additional micro-vibrations during slew	Potential plume disturbances to mass spectrometer  Additional micro-vibrations during slew (but less than 20N RCS)
Recovery from 100 mg impact at 70 km/s	42 sec Robust to 1 worst case impact only!	Negligible	42 sec
Total att. control prop. (mostly to compensate EP 1cm+1deg thrust misalign)	10.8 kg + 100% = 21.6 kg	12.2 kg + 100% = 24.4 kg	10.9 kg + 100% = 21.6 kg

**Table 14-5: Primary attitude actuator trade-off**

Note that the propellant consumption for attitude control does not change much by adding reaction wheels, since most of the propellant is required to compensate the EP thruster misalignments. During EP firing the attitude control will be via RCS, which will induce a one-sided limited cycle thus consuming no more propellant than if control was done with wheels and regular (every 35 minutes with 4 Nms wheels) momentum dumping. Reaction wheels reduce the propellant required for slews and attitude hold during Earth comms events. However, this is negligible given the small minimum impulse bit of 1N thrusters (0.001 Ns assumed). The 20 N thrusters consume 1.3 kg extra (+100% margin) due to their large minimum impulse bit (0.02 Ns assumed). Propellant budget details can be found in section 14.3.2.

Pure RCS-based attitude control is used on many NASA missions, such as the New Horizons probe. It may introduce additional microvibrations due to frequent pulsing around the closest approach, however this is expected to be tolerable for the science cameras on basis of the success of the New Horizons probe. The large solar panels on Comet Interceptor may lead to worse microvibrations than New Horizons but this issue is expected to be solvable – via controller design or with the addition of isolators.

The other key disadvantage of RCS firings are possible contamination of the instruments, such as the mass spectrometer. Requirement AOCS-093 was defined for this reason.

Despite RCS-based control having improved slew robustness, reduced system mass, volume and EMC, the wheel solution remains the baseline due to requirement AOCS-093. This trade should be discussed at payload/system level in the next design phase.

#### 14.2.2.5 RCS sizing

Given that wheels are baselined as primary actuators, the RCS just needs to be big enough to perform the translational manoeuvres in a suitable amount of time.

The final TCM burn before the fly-by is ~10 m/s.

Assuming 30 deg canting of thrusters (required for 3-axis attitude control) and a 75% reduction in thrust output due to pressure reduction at end of life, the following burn times vs thruster size are calculated:

- 4 x 1 N → 1.8 hrs
- 4 x 5 N → 22 mins

Since there are several navigation-related activities surrounding this burn and the operations timeline is fairly tight, the project decision was to embark the 5 N monoprop thrusters as baseline.

#### 14.2.2.6 RCS layout

A trade-off was made to determine the number of RCS thrusters and the layout thereof:

RCS configuration	2 x 4 on -X face	2 x 4 on -Z face	2 x 8 on -Z/+Z faces
Additional h/w mass (assuming 5N RCS)	0	0	4 kg + piping, etc.
AIT complexity	Low (single integrated unit)	Low (single integrated unit)	Medium
Science impact	Exposure of payload face to Sun during final TCM prior to fly-by  Presumed negligible contamination even if firing during science phase (TBC)	Possible spectrometer contamination if firing during science phase (depends on wheel/RCS choices)  Payload hemisphere pluming minimized by avoiding nozzle pointing toward +X	Possible spectrometer contamination if firing during science phase (depends on wheel/RCS choices)  Payload hemisphere pluming minimized by avoiding nozzle pointing toward +X
Configuration complexity	Low	Medium, tricky to accommodate thrusters without pluming -Z instruments	Difficult, too many instruments already on +/- faces
Trajectory impact during EP thrustings or accompanying momentum dumps	35 m/s (excluding margin) orthogonal to EP delta-V direction  But this is considered correctable via the EP (in the propellant margin)	Negligible	Null
Trajectory impact outside EP transfer (e.g. safe mode, L2 station keeping)	3 m/s (excluding margin)  Can possibly be distributed inertially by optimising timing of firings and/or attitude	3 m/s (excluding margin)  Can possibly be distributed inertially by optimising timing of firings and/or attitude	Null
Trajectory impact during comet fly-by	Negligible (timing modification only)	0.09 m/s orthogonal to comet-relative flight path for mitigation of 100 mg dust particle with RCS	Null

Table 14-6: RCS layout trade-off

From an operations standpoint, force-free torques are preferred as they remove the impact to the trajectory/orbit during events such as safe mode, hibernation in L2 or any emergency wheel de-saturation firings needed during the fly-by. However, these impacts are fairly small and a force-free configuration would necessitate thrusters on two opposing faces. From a configurations standpoint there is insufficient space to accommodate these thrusters on both -Z and +Z due to instruments located near the edge of the Z/X faces. Using both +X and -X is not an option as the +X face houses the majority of the instruments. Y faces are not an option due to the solar panels.

A standard 4 thruster configuration was baselined due to low AIT complexity and because a force-free configuration may not be feasible due to positioning constraints. The preferable mounting face is -Z as any firings during the EP-phase will primarily

contribute to desired delta-V rather than perturb the orbit in an unwanted direction (as would be the case with X thrusters). Z thrusters also avoid having to slew the spacecraft for the final TCM prior to fly-by; X thrusters would imply exposing the instrument to the Sun during this burn as the required delta-V direction is orthogonal to the comet relative velocity vector.

Note that if RCS were to be used during the fly-by the -Z thruster placement may not be ideal since the payload will be slewing toward the ejected plume.

For sizing calculations during the CDF study, thrusters were assumed to be 0.55 m from the centreline and canting of thrusters by 30 deg was assumed in order to permit Z-axis control. The final layout chosen by the configurations engineer is presented in 14.3.2.

#### **14.2.2.7 Probe B2 gyroscopic stabilization**

The probe B2 is intended to maintain attitude control via passive means (req. AOCS-200) and spin at  $\omega_s = 6 - 15$  rpm (req. AOCS-210). This implies use of either spin stabilization or a combination of spin & momentum-wheel ( $h_w$ ) stabilization.

Assuming particles  $\leq 10$  mg hit the spacecraft in a uniform distribution, they will induce a torque proportional to the offset of the centre of dust pressure from the c.g. For B2, we assume a 3 cm offset (5% of body size). The body-fixed torque  $T_d$  will induce nutation (wobble) but will not precess (inertially shift) the spin-axis since the theoretical average inertial-frame torque over the spin period is zero. The nutation amplitude is governed by the formula:

$$\frac{2T_d I_t}{((I_s - I_t)\omega_s + h_w)(I_s\omega_s + h_w)}$$

where  $I_s$  and  $I_t$  are the spin and transverse axis inertias respectively. This equation comes from Sidi (1997, "Spacecraft Dynamics & Control"), modified to include wheel momentum.

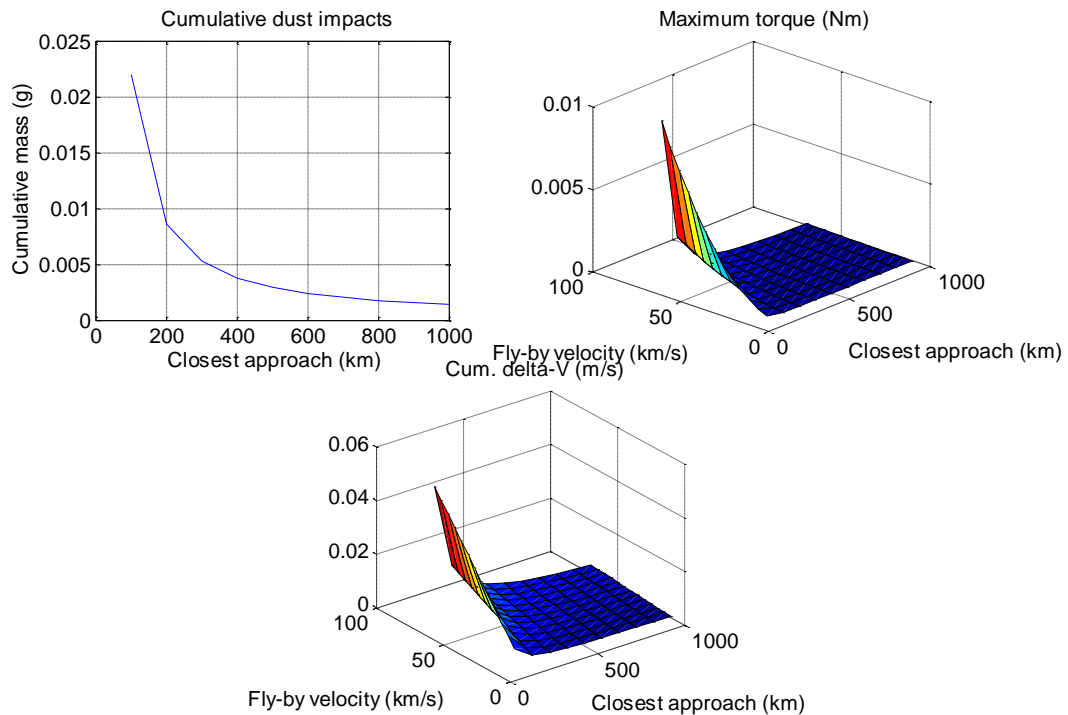


**Figure 14-12: Accumulation of small particle impacts on B2 during fly-by; cumulative dust mass encountered, maximum torque, maximum accumulated momentum**

The small-dust-field related nutation build-up is given for two candidate designs below:

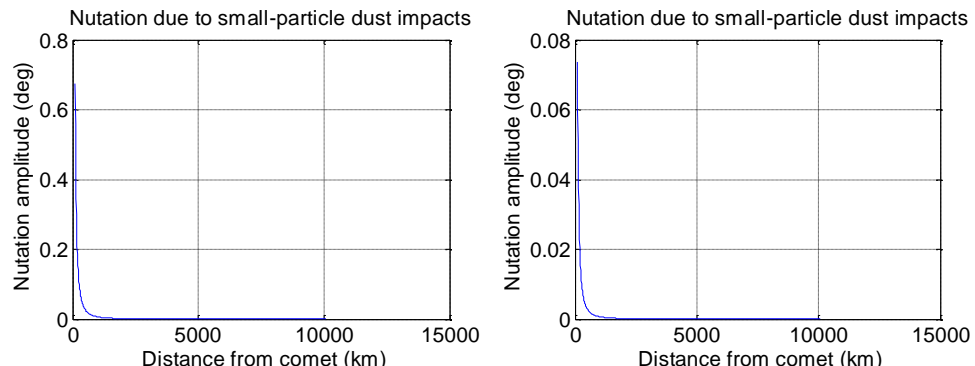


**Figure 14-13: Nutation induced by small dust particles; left – 15 rpm spin, right – 6 rpm spin + 3 Nms from momentum wheel**

Single large particle impacts will precess the spin-axis by an angle of  $\frac{\Delta h}{(I_s \omega_s + h_w)}$  and potentially increase nutation by the same amount if the impact is phased with the worst-case timing within the nutation cycle. This is considered unlikely but is still accounted for in the budgeting process. To examine the impact on pointing, an allocation budget is constructed as follows:

Contributor	Absolute pointing error (95% confidence level with temporal statistical interpretation) [deg]
Inertia imbalance (coning)	4
Nutation from small ( $\leq 10$ mg) particle impacts	1
Precession & nutation from large ( $> 10$ mg) particle impacts	15
<b>Total</b>	<b>20</b>

**Table 14-7: B2 Pointing Budget**

To satisfy the allocation for coning requires configurations balancing and possible inclusion of dummy masses to maintain principal inertia axis within 4 deg of the geometrically-desired spin-axis (B2 probe Z direction).

To meet the 15 deg allocation for a single large particle impact, impact is assumed at the worst case location and phasing within the nutation cycle. These assumptions may be conservative and should be re-evaluated in the next design phase. The total angular momentum of the spacecraft required to meet the 15 deg allocation is given below:

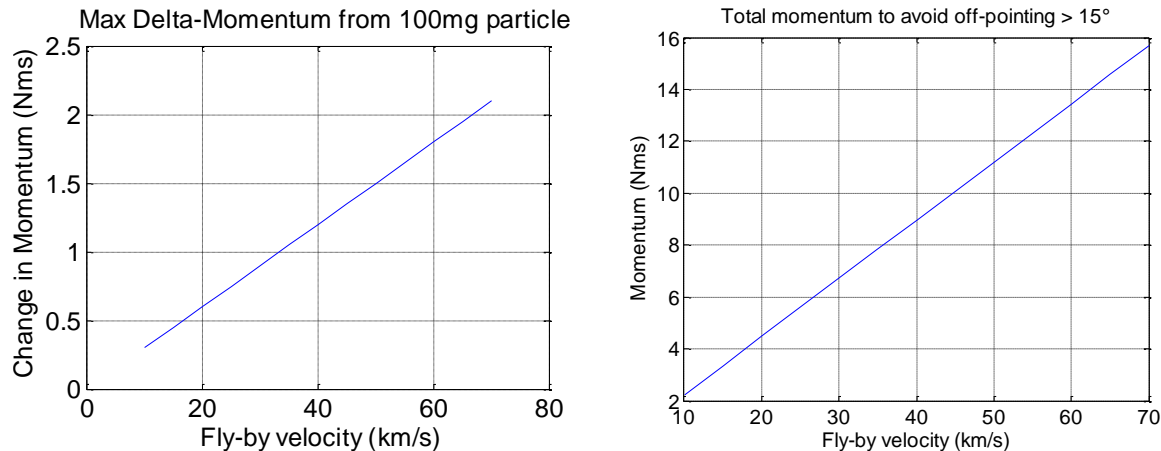


**Figure 14-14: B2 momentum required to handle large particle impact**

Note that the current dust models predict a 0.7% chance of encountering a 100 mg particle at closest approach (100 km). There is a 6% chance of a 10 mg particle encounter.<sup>23</sup> Therefore, using 100 mg as a design case may be unnecessarily conservative especially given the low cost / elevated-risk nature of the B2 mission.

For the 70 km/s fly-by velocity, 16 Nms would be required to cater for a 100 mg worst case impact. The spin of the probe generates 0.8 Nms at 6 rpm and 2.1 Nms at 15 rpm. 2.1 Nms would only be sufficient to cover a single worst case 13 mg particle impact. Therefore, in order to provide robustness to larger particles, a momentum wheel is required.

<sup>23</sup> Note that the revised analysis reported in Section 7.2.1.3 suggests probabilities an order of magnitude higher, namely a 4.8 % chance of impacting a 100 mg particle and a 48.0% chance of impacting a 10 mg particle. Nonetheless, the general design principle still applies.

Due to mass and power constraints, it was decided not to embark a 14 - 16 Nms wheel but to compromise and cater for a reduced worst case. A single 4 Nms wheel is included in the baseline, to be used both for additional gyroscopic stability and for inducing the spin rate on the probe – which removes the need for a spin-up ejection spring development. There is no wheel redundancy due to mass constraints.

The baseline concept is to spin the wheel to maximum speed (4 Nms) before ejection, using power from the main spacecraft. Note that acceleration could require up to 100 W, depending on friction levels at wheel switch-on. After B2 ejection, the wheel will be controlled to a lower speed set point (3.2 Nms) which will cause B2 to spin-up to 6 rpm in the same spin-direction as the wheel due to conservation of angular momentum. The power budget includes 8 W for speed maintenance at 3.2 Nms. This figure seems feasible from historical data from various wheel manufacturers but it requires confirmation in the next phase. It is possible that thermal conditions on the probe and wheel lubricant state (which affects friction) may lead to higher power consumption.

The baseline fly-by will have the probe spinning at 6 rpm, which infers a spin period of 10 secs and a nutation period of 4.2 secs - driven by the inertias and total B2 angular momentum. The 4 Nms total momentum during the fly-by will provide robustness to a single worst case impact (70 km/s at edge of probe) of a 25 mg dust particle. The likelihood of encountering larger particles is low and if it does occur it would most likely be at closest approach - after the majority of B2 science has been collected.

Note that a ~1 kg viscous-fluid nutation damper could mitigate up to half of the off-pointing (the wobble component) induced by a large particle impact, with a ~2 minute transient decay time to 10% amplitude. NASA has tested nutation dampers in this class but a European solution would require a new development since the last European nutation damper was built for Cluster (launched in 2000) and was significantly larger. Due to cost and mass constraints a nutation damper was not included in the baseline.

## 14.3 Baseline Design

### 14.3.1 AOCS Modes

The following AOCS modes for S/C A were defined and equipment usage per mode is also presented below:

Mode	Sun acquisition mode			Normal mode			Orbit Control Mode			Hibernation mode		Safe mode			
	Sub-mode	Rate damp	Sun acquisition	Sun hold	Slew	Inertial pointing	Comet tracking	Slew	Attitude hold	RCS Delta-V	Rate control	Idle	Rate damp	Sun acquisition	Earth strobe
Sun sensor		X	X										X	X	X
Gyro	X	X	X			(X)					X		X	X	X
Star tracker				X	X	X	X	X	X						
Nav camera					(X)	X									
Reaction Wheels				X	X	X	X	(X)	(X)						
RCS	X	X	X		(X)	(X)		X	X	X		X	X	X	X
EP Thruster								(X)							

**Table 14-8: AOCS modes, sub-modes and equipment usage**

These map to system modes as follows:

- **Launch:** Hibernation mode → Idle
- **Sun:** Sun acquisition mode

- **Safe:** Safe mode
- **Standby:** Hibernation mode
- **Communications:** Normal mode → Inertial pointing
- **EP Thrust:** Orbit control mode → Attitude hold
- **Science:** Normal mode → Comet tracking

#### 14.3.1.1 Sun acquisition mode

This mode includes three phases: rate damp, slew toward Sun, Sun-pointing hold.

The Sun position is obtained from non-redundant fine Sun sensors – also needed for delivering sufficient accuracy for the Earth-comms strobing in Safe mode. A Sun sensor failure could be covered by inducing a Sun search if the Sun is not found after a specified amount of time. For the face that will remain Sun pointing during the Sun hold, extra redundancy or sensor overlap could be considered.

RCS is used for primary actuation to avoid requiring multiple active actuator types (as is the case if reaction wheels are used). Sun hold is envisaged as a two-axis pointing controller with 3-axis rate damping.

Communications in this mode are possible via S-band only when the spacecraft is close to the Earth. For FDIR events when the S/C is far from Earth, or for any severe FDIR events, the Safe mode has to be used to re-establish communications.

#### 14.3.1.2 Normal mode

Normal mode will be used to slew to inertial pointing attitudes (e.g. for Earth comms or early imaging of the comet) or for comet tracking during the fly-by.

Wheels provide primary actuation but RCS will be used intermittently (~once per day) for momentum dumping. Star trackers provide the 3-axis attitude determination capability.

During comet tracking the gyro is active but only used in the control loop in case of a star tracker outage caused by confusion from dust reflections. Corrections of pointing with respect to the comet will be made via filtering of navigation camera centroid measurements. See the GNC chapter for more details. RCS is not baselined for use in the comet tracking phase, but if an unexpectedly large particle causes wheel saturation and loss of pointing control it could be decided during FDIR design to allow the RCS to desaturate the wheels to avoid losing optical/infrared science at the possible expense of in-situ science (due to plume contamination of some payloads).

In inertial pointing sub-mode, the navigation camera may be used intermittently to image the comet.

#### 14.3.1.3 Orbit control mode

This mode is used for slewing to manoeuvre attitudes and maintaining those attitudes before, after and during a burn.

The slew sub-mode is identical to that in Normal mode.

During EP burns, the attitude hold sub-mode is envisaged for use. Due to the relatively high misalignment torques from the EP thruster, this mode would drive the momentum

sizing of the wheels. To avoid this becoming the sizing case and/or avoiding very frequent momentum dumps (possibly multiple times per hour), RCS is used in on-pulse mode for primary actuation in attitude hold. Wheel speed could be maintained at a constant level to avoid switching the wheels off and on. During EP firings it is envisaged to turn the wheels off completely, which will also reduce the total power burden. Note that the RCS is expected to induce a one-sided limit cycle ( $>200$  sec period), which means the required fuel for attitude control is similar to a mode design where it is only used to dump momentum.

During RCS Delta-V, attitude control is maintained via off-pulsing of the RCS thrusters.

#### **14.3.1.4 Hibernation mode**

During long periods of waiting (e.g. L2 station keeping) an extra mode is envisaged to allow power consumption minimisation and still enable necessary intermittent ground contacts. This is achieved via a spin-stabilized attitude, which does not require active attitude control.

The spin-axis must be close to the principal axis of inertia. The baseline is to spin about the S/C X axis. Before the spin-up manoeuvre, the solar panels will orient such that the normal is along -X and then Normal mode will be used to setup an initial Sun-pointing attitude. Hibernation mode, with rate control sub-mode, will be engaged to drive the rate to 5 deg/s (for example) about X. Lower rates could also be considered in order to save RCS propellant.

Note that fuel consumption is not expected to be reduced (compared to a 3-axis stabilized hibernation) because the spin will need to be removed everytime a ground contact is desired or the spin-axis needs re-orienting toward the Sun to meet minimum power needs.

#### **14.3.1.5 Safe mode**

This mode allows establishing contact with Earth by acquiring the Sun and then using the on-board Earth-ephemeris knowledge to perform a conical Earth search with the HGA at a fixed angle from the Sun. The HGA is activated and will strobe the Earth intermittently during this search. The maximum allowed pointing error for this search is  $\sim 2.8$  deg as per AOCS-060. This is deemed feasible using a fine sun sensor and a medium performance gyro. The same gyro that is used in sun acquisition mode and comet fly-by (in case of star tracker outage) is also used in safe mode due to cost and mass constraints. However, this should be examined in the next design phase as it could be considered to violate ESA's policy to use different equipment in safe mode.

Once the ground station receives the signal, they send a command to the S/C to stop the strobing at a future cycle such that the HGA is pointing to Earth. Once communications lock is re-established, the star tracker can be activated to correct pointing bias or switch to Normal mode to continue with communications in a more precisely controlled attitude.

Safe modes similar to this are used on Rosetta and Solar Orbiter, for example.

### 14.3.2 Attitude Control Propellant Budget

The final RCS layout used by the configurations engineer was used to update the attitude control propellant budget. The approximate assumed positions and directions in AOCS reference frame are given below:

Position X (m)	Position Y (m)	Position Z (m)	Force Direction X	Force Direction Y	Force Direction Z
0.41	0.41	0	-0.174	0.492	0.853
0.41	-0.41	0	-0.174	-0.492	0.853
-0.41	-0.41	0	0.174	-0.492	0.853
-0.41	0.41	0	0.174	0.492	0.853

**Table 14-9: Thruster positions and directions**

Several assumptions for generating the propellant budget were:

- 5 year mission
- 0.3 m offset between centre of solar pressure and c.g.
- 6 safe mode events over the lifetime
- 4 S/C hibernation cycles (spin-up, hibernate, spin-down)
- 1522 m/s EP delta-V
- 1 deg + 0.01 cm thruster misalignments with respect to c.g.
- 5 N thrusters, 0.005 Ns minimum impulse bit, 200 s specific impulse

	Events over lifetime	Mean per thruster tot. on time (min)	Propellant (kg)
Orbit maneuvers		43.2	13.223
Slew maneuvers	7	0.0	0.002
Spin up / recovery	15	0.4	0.113
Hold attitude		0.1	0.020
Momentum dump		6.0	1.850
Total			15.21 kg
Delta-V equivalent			57.35 m/s

**Table 14-10: RCS attitude control propellant budget without margin**

Note that the required fuel for attitude control has increased compared to the 41 m/s budgeted during the final presentation of the Study. This is due to the RCS thrusters getting placed closer to the centre of the thruster-mounting face (0.41 m offset per axis) than originally assumed (0.55 m per axis) and additional thruster canting, both introduced to reduce pluming on the payloads. However, since the payloads are not expected to be operating during RCS firings the need for this should be re-assessed in the next design phase.

The bulk of the attitude control propellant is used during EP firings (13.2 kg). The selected EP thruster has a 1 deg thrust vector direction error relative to the mounting interface. An additional 1 cm lateral offset of the thrust line from the centre of gravity

has been assumed. At a thrust level of 65 mNm the misalignments lead to 1.3 mNm disturbance torque that has to be mitigated via RCS. Lower thrust levels induce less torque but the same overall RCS propellant is required because the EP burns become longer. In the interest of mass savings, it is recommended to re-assess the possibility to include a gimbal mechanism or two extra thrusters, to minimise disturbance torque by tuning duty cycles.

Note that the EP thruster does not have any capability for AIT engineers to adjust the thrust direction to aim at the expected mean centre of gravity over the mission (as measured during AIT). Therefore, the baseline assumes some adjustable bracket/mounting screws will be implemented at S/C-level for this purpose. Without this, a higher translational offset should be assumed.

The systems budget contains the old 41 m/s delta-V figure rather than 57 m/s, but includes a 100% margin.

## 14.4 List of Equipment

A list of space-qualified, off-the-shelf equipment suitable for a low-cost mission has been selected. **The selections below are just examples used for system sizing purposes. Alternative equipment is available for all the selected units both inside and outside Europe.**

	mass (kg)	mass margin (%)	mass incl. margin (kg)	P_on (W)
SC_A (Spacecraft A)	25.26	5.00	26.53	110.40
+ A_DPU (A DTU Data Processing Unit)	0.56	5.00	0.59	3.60
+ A_IMU_LN200_1 (A IMU Northrop Grumman LN200 Core #1)	0.75	5.00	0.79	12.00
+ A_IMU_LN200_2 (A IMU Northrop Grumman LN200 Core #2)	0.75	5.00	0.79	12.00
+ A_NAVCAM_OH_1 (A DTU NAVCAM Optical Head #1)	0.38	5.00	0.39	0.70
+ A_NAVCAM_OH_2 (A DTU NAVCAM Optical Head #2)	0.38	5.00	0.39	0.70
+ A_STR_OH_1 (A DTU STR Optical Head #1)	0.35	5.00	0.37	0.70
+ A_STR_OH_2 (A DTU STR Optical Head #2)	0.35	5.00	0.37	0.70
+ A_SUN_LENS_Bison64_1 (A SUN LENS Bison 64 #1)	0.03	5.00	0.03	0.00
+ A_SUN_LENS_Bison64_2 (A SUN LENS Bison 64 #2)	0.03	5.00	0.03	0.00
+ A_SUN_LENS_Bison64_3 (A SUN LENS Bison 64 #3)	0.03	5.00	0.03	0.00
+ A_SUN_LENS_Bison64_4 (A SUN LENS Bison 64 #4)	0.03	5.00	0.03	0.00
+ A_SUN_LENS_Bison64_5 (A SUN LENS Bison 64 #5)	0.03	5.00	0.03	0.00
+ A_SUN_LENS_Bison64_6 (A SUN LENS Bison 64 #6)	0.03	5.00	0.03	0.00
+ RW_RSI_4_215 (A RW Rockwell Collins RSI 4-215)	5.40	5.00	5.67	20.00
+ RW_RSI_4_216 (A RW Rockwell Collins RSI 4-#216)	5.40	5.00	5.67	20.00
+ RW_RSI_4_217 (A RW Rockwell Collins RSI 4-#217)	5.40	5.00	5.67	20.00
+ RW_RSI_4_218 (A RW Rockwell Collins RSI 4-#218)	5.40	5.00	5.67	20.00
SC_B2 (Spacecraft B2)	2.70	5.00	2.84	8.00
+ RW_RW250 (RW Astrofein RW250)	2.70	5.00	2.84	8.00
<b>Grand Total</b>	<b>27.96</b>	<b>5.00</b>	<b>29.36</b>	<b>118.40</b>

Table 14-11: AOCS & GNC equipment list

### 14.4.1 Reaction Wheels

The proposed S/C A reaction wheels are 4 x Rockwell Collins Deutschland 4-215 (4 Nms / 0.215 Nm) wheels in biased tetrahedral configuration (see 14.2.2.2). This choice is driven by the high torque requirements for the comet fly-by slew.

For the B2 probe, the Astrofein RW250 (4 Nms, 0.1 Nm) have been proposed for mass minimisation.

There may be a cost advantage to procuring wheels for both spacecraft from a single manufacturer thus this should be examined in a future design phase.

#### 14.4.2 Star Tracker

The example star tracker is DTU Masc (Advanced Stellar Compass), which has been flown on deep-space missions (in Juno, not as main STR but as part of a payload). The Masc is composed of the following elements:

- Two Camera Head Units: comprising of optics and detector (0.4Mpixels)
- Redundant Digital Processing Unit (DPU)
- Two baffles: this is a passive element intended to reduce straylight from Earth/Sun and comet.



**Figure 14-15: DTU Masc star tracker (left: Camera Head Unit, middle: DPU, right: baffle)**

Note that the Navigation cameras can also be hosted on the same DPU.

It should be investigated in future phases if there is any significant mass/cost advantage to removing the DPU and interfacing the optical heads and navigation cameras directly with the OBC. Many star tracker manufacturers currently provide the option of hosting star tracker software on the OBC.

#### 14.4.3 Sun Sensors

The proposed Sun sensor examples are the Bison-64 by Lens R&D, shown in Figure 14-16.

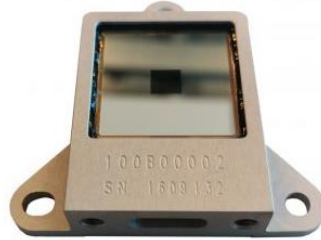


**Figure 14-16 : LENS R&D Bison-64**

This Sun sensor would have the following performance characteristics:

- AKE 0.5 deg (after calibration) or 3.5 deg (without calibration)
- Full FoV: 128 degrees diagonal

Note that the Sun sensors on the  $\pm Y$  faces may need to be mounted on the solar panels to avoid straylight from solar panel reflections.

#### 14.4.4 Gyroscope

Requirement AOCS-092 demands that gyro propagation be relied upon for 1 hour during fly-by. Therefore a bias drift <0.1 deg/hour (approx.) is required to meet the 0.46° APE requirement (AOCS-090).

The proposed gyro example is the Northrup Grumman LN-200S due to low mass and to heritage in multiple interplanetary missions. However, it must be noted that it is ITAR-restricted and the radiation limit is 10 krad.

#### 14.4.5 Navigation Camera

The proposed example is to use the same DTU DPU as used for the star trackers as well as embarking two additional camera head units. See GNC chapter for more details.

### 14.5 Options

There are several key trades that should be re-investigated in the next design phase:

- Parallel or non-parallel optical heads
  - Parallel [baseline] slightly simplifies configuration design but non-parallel may reduce reliance on gyro in case star tracker outage is caused by presence of illuminated dust particles non-homogeneously around the spacecraft.
- 4 or 6 reaction wheels
  - A 4 high-torque wheels design [baseline] possibly saves cost and volume but a 6 medium-torque wheels design is less massive and permits no science outage in case of wheel failure. With a wheel failure, the 4 wheel design experienced ~20 secs science outage using an on-board convex optimisation algorithm to minimise outages.
- Wheel or RCS-based attitude control
  - Several NASA spacecraft fly without reaction wheels, such as New Horizons.
  - Removing wheels from the S/C A design saves mass, cost, volume and makes the S/C robust to multiple large particle impacts. However, RCS-firings during

the fly-by may lead to potential instrument contamination and possibly greater micro-vibrations.

- The robustness of the baseline design could be improved by allowing RCS firings only if the wheels become saturated. This would improve robustness for visual/IR science at the possible expense of mass spectrometer science.
- Replacing star tracker DPU with OBC-hosted software
  - Would save mass with respect to baseline.
  - Needs to be investigated if this would save cost. It may be associated with more development effort on the S/C software side.
  - It is also unclear whether the navigation camera software can be hosted on the OBC.
- EP thruster on gimbal or embarking 3 EP thrusters to allow cancelling of misalignment torques via duty cycle tuning.
  - Baseline is a single fixed EP thruster that induces significant misalignments to be compensated via RCS propellant expenditure.
  - The potential propellant saving of 13 kg (+100% margin) needs to be compared to the mass and development cost of a gimbal or extra thrusters.
- Spin-stabilized [baseline] or 3-axis stabilized hibernation
  - Fuel consumption is expected to be similar for both solutions. Trade-off is largely an operations and FDIR design tradeoff.
- Single gyro type or a separate gyro for safe mode
  - Design to cost rationale has driven embarkation of a single gyro type but this may be considered to violate ESA's policy of using different equipment in safe mode.

## 14.6 Technology Needs

Technology Needs						
*	Equipment Name & Text Reference	Technology	Supplier (Country)	TRL	Funded by	Additional Information
*	AOCS GNC SW (section 14.2.2.3)	Convex attitude guidance optimisation during fly-by		4 at ESA (space vehicle convex guidance optimisation TRL 9 in US)		Concept proven on flight processor in ongoing ESA-funded Embotech study  This allows for optical/infrared science outage minimisation in case of wheel failure or an unexpectedly large dust impact.

						Attitude trajectory optimisation can be performed on-board regularly during fly-by.
--	--	--	--	--	--	---

\* Tick if technology is baselined

This Page Intentionally Blank

## 15 POWER

### 15.1 S/C A

#### 15.1.1 Requirements and Design Drivers

The main function of the power subsystem for S/C A is to generate, store and distribute electrical energy to all equipment of the Comet Interceptor mission and provide a clear power interface to the probes attached (B1 and B2) during transportation and deployment.

SubSystem Requirements		
Req. ID	Statement	Parent ID
POW-010	The power subsystem of S/C A shall be able to generate, store, condition, distribute and monitor the electrical power used by the spacecraft throughout all mission phases in the presence of all environments actually encountered and during the complete lifetime of the mission.	
POW-020	When in sunlight at 1.0 AU, the solar array shall be able to provide 1237 W of total power (including 20% margin on the total spacecraft power, minus the power for the EP <sup>24</sup> ).	
POW-030	The battery shall be able to provide the energy required (including margins) during all phases of the Sun acquisition mode: high de-tumbling, initialisation and waiting.	
POW-040	The battery shall be rechargeable.	
POW-050	The power subsystem design shall be compliant with a 5-year lifetime.	

**Table 15-1: Power subsystem requirements for S/C A**

#### 15.1.2 Assumptions and Trade-Offs

The following table reports the assumptions made at subsystem level.

Assumptions	
1	The spacecraft does not require power during launch, until the beginning of the Sun acquisition mode.
2	There is no power generation by the solar array during Sun acquisition; this can be regarded as a conservative assumption.
3	Additional heater power is not required during the Sun acquisition phase for S/C A. S/C A is assumed to provide survival heating power to probes B1 and B2 during this phase.
4	During the study, a mode for operations during the lunar eclipse in the lunar swing-by was not defined; however, this situation is not assumed to be the driving case. <sup>25</sup>

<sup>24</sup> See Section 7.4.5 for more details.

Assumptions	
5	A SADM is included in the spacecraft design.

**Table 15-2: Power subsystem assumptions for S/C A**

### 15.1.3 Baseline Design

The power subsystem for S/C A consists of three main elements: solar arrays, a secondary (or rechargeable) battery, and a Power Conditioning and Distribution Unit (PCDU).

A power bus voltage of 28V has been selected considering the heritage of the subsystems and units used in this spacecraft.

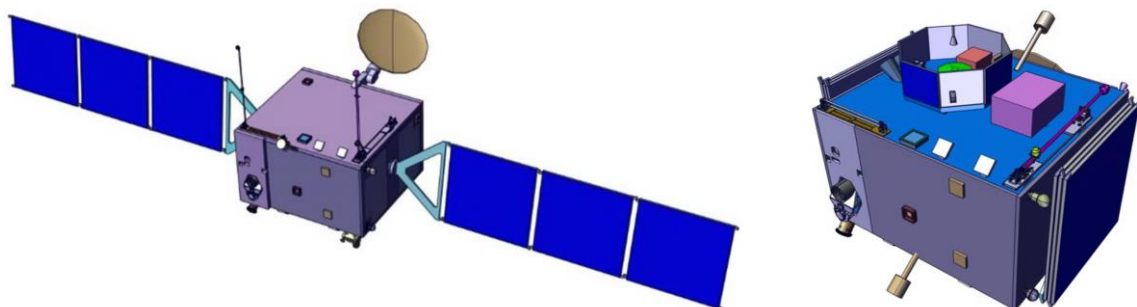


**Figure 15-1: Comet Interceptor (left: with solar panels deployed; right: in stowed configuration)**

#### 15.1.3.1 Battery

The sizing case for the rechargeable battery is the Sun acquisition mode during LEOP, which has an assumed total duration of 50 minutes and a total energy requirement of 335.3 Wh.<sup>25</sup>

<sup>25</sup> It was decided at system level that the battery design should be driven by the LEOP sizing, and the potential lunar eclipse was not assessed in detail. As indicated in the Mission Analysis chapter, a lunar swingby is expected to have an eclipse of around 1 hour. The battery design, driven by the LEOP, should be able to provide an average power equivalent close to the safe mode consumption. As such, it is expected that a suitable eclipse mode could be found in future phases.

	Sun Acquisition: High Detumbling	Sun Acquisition: Initialization	Sun Acquisition: Waiting	Total duration (min)
Duration (min)	5	25	20	50
# attempts	1	1	1	
AOGNC	12.0	12.0	12.0	
COM	113.7	113.7	113.7	
CPROP	102.6	81.2	17.0	
DH	53.0	53.0	53.0	
INS	0.0	0.0	0.0	
MEC	3.0	9.8	4.4	
PWR	30.0	30.0	30.0	
STR	0.0	0.0	0.0	
TC	0.0	0.0	0.0	
EPROP	0.0	0.0	0.0	
Surv B1	20.0	20.0	20.0	
Surv B2	20.0	20.0	20.0	
Total w/o losses	354.3	339.7	270.1	
Harness + LCL+ PCDU losses	1.07	1.07	1.07	
Total w losses	379.1	363.5	289.0	
System margin	1.2	1.2	1.2	
Total Power (W)	455.0	436.2	346.9	
Total Energy (Wh)	37.91	181.76	115.62	
Battery Sizing	computed	335.3 Wh		

**Table 15-3: Energy and power requirements for the battery sizing of S/C A**

Including 5% for power conditioning losses, 80% as maximum DoD and a 10% for battery string redundancy, the energy that must be provided by the rechargeable battery is 485 Wh.

Energy requirement (from Systems)	Wh	335.3
5% power cond. losses	Wh	352.9
80% DoD	Wh	441.2
10% battery string redundancy	Wh	485.3
<b>Total energy required</b>	<b>Wh</b>	<b>485</b>

**Table 15-4: Battery sizing calculations**

A battery with 32 Li-ion cells (8S-4P configuration), supplying a total energy of 512 Wh at 20°C, would be able to meet the energy requirement.

As previously stated, the operations during the lunar eclipse are not expected to be the driving case for the battery sizing. It has been assumed that the current LEOP sizing case should also allow for the 1 hour eclipse duration; this would imply, in later design phases, either having a low-power eclipse mode, or else limiting the allowable eclipse duration.

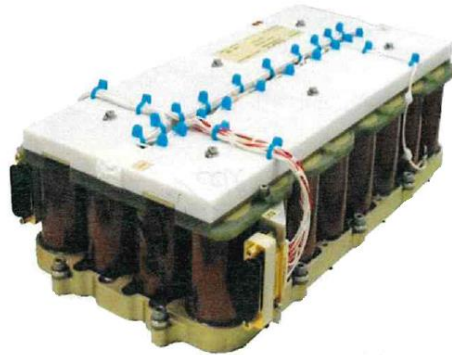


**Figure 15-2: 8S-4P battery**

### 15.1.3.2 Solar Arrays

The power subsystem was implemented in EcosimPro software using PEPS: this allows dynamic modelling of full power system with a load profile of unlimited complexity. Simulations have been done with the orbit of the mission using the orbit/geometry model implemented in PEPS.

The following table presents the sizing options made for the SA sizing:

Size	Power available
3 m <sup>2</sup>	693.54 W
4 m <sup>2</sup>	924.72 W
5 m <sup>2</sup>	1156.1 W
6 m <sup>2</sup>	1387.4 W

**Table 15-5: Sizing options for SA sizing**

The solar array has been sized based on the worst case of the required power: at 1.0 AU, ~1237 W of total power (including 20% margin on the total spacecraft power, except on the power for the EP, as discussed in Section 15.1.2 above). The calculation also considered 2 strings failed, 1% harness loss, 85% effective cell area, and the 3% losses for power conversion (in the PCDU). The PCDU is based on a MPPT SAR with a non-regulated bus of 28 V.

The final baseline size of the 2 solar panels was decided to 6 m<sup>2</sup>. The high efficiency 4G32 cell, assuming it has been integrated with the standard CMX 100µm AR cover glass, has been selected. Preliminary test result shows that the efficiency of the 4G32 cells is 30.6% BoL and 27.6% 1E15.

The following table reports the assumptions made for the SA sizing calculations.

Assumptions for SA sizing	
1	Maximum temperature of the solar array is around 90°C given in the mission characteristics.
2	Radiation effects for the solar cells have been extracted from the datasheet.

Assumptions for SA sizing	
3	0.85 packing factor in the solar panels surface.
4	Distance from the Sun: 1.0 AU.
5	3% losses harness.
6	2% losses power distribution.
7	5% losses MPPT.
8	Loss of 1 string per wing of solar panel.

**Table 15-6: Assumptions for SA sizing**

The schematic representation of the power system model is shown in Figure 15-3.

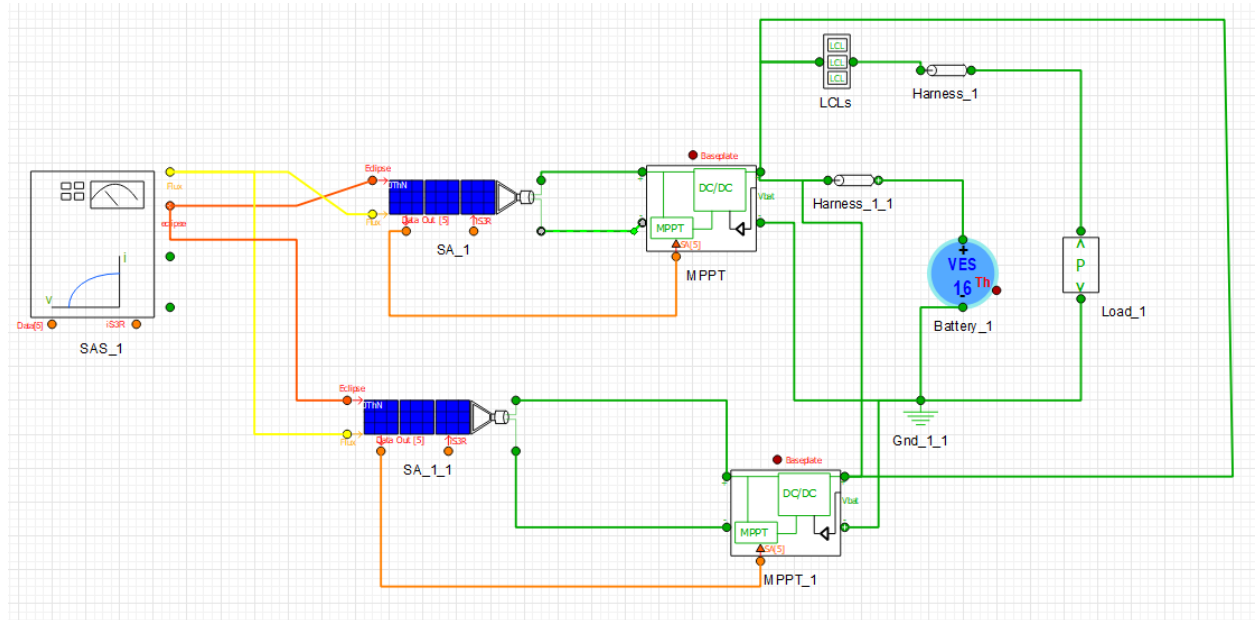


**Figure 15-3: EcosimPro Comet Interceptor 2 model**

A low solar array mass calculation factor of 4.91 kg/m<sup>2</sup> has been used to calculate the total SA mass. The following table describes the assumptions in the breakdown of the 4.91 kg/m<sup>2</sup> total value.

Solar Panel Mass System breakdown	
1	Panel mass 3 m <sup>2</sup> = 7.2 kg (including synchronisation and hinges)
2	PVA mass 3 m <sup>2</sup> = 4.7 kg
3	Total cable 1x wing = 2.73 kg

**Table 15-7: Assumptions for SA mass breakdown**

### 15.1.3.3 PCDU

A trade-off for the power architecture implemented in the Power Conditioning and Distribution Unit is given in the next sections:

- 28 V unregulated bus and MPPT: some trade-offs exist for deciding on the power systems architecture, including which type of bus is used. The most common is regulated vs unregulated bus. Adopting an unregulated bus has a benefit on the power system because the solar cells and battery design can be optimised. The EPS architecture related trade-off that needs to be considered has to do with the Solar Array Regulator (SAR) converter type, which can be either a Maximum Power Point Tracker (MPPT) or a Sequential Switching Shunt Regulator (S3R). The first is heavier and less efficient, but able to extract all the available power from the solar arrays under a large range of conditions (BoL, EoL, temperature, etc.). The latter is simpler, lighter, cheaper and more efficient, but is very rigid in the way it extracts power and dependent of the battery level. Under the varying conditions (e.g. temperature, incoming solar power), the S3R is unable to extract all available power, which negatively influences the SA sizing. Therefore, the MPPT option is selected as most suitable SAR converter. The solar cells work during the entire mission at the same voltage, therefore it is possible to optimise the design of the Solar Array in terms of power generated. This advantage has less impact when MPPT is the solution preferred for an unregulated bus in the Comet Interceptor mission.
- With an unregulated bus there is also a great benefit as the PCDU requires less complexity on the battery manager system, as no BCR and BDR are needed.
- TMTC and protections implemented.
- Fixed power dissipated: 45 W.
- Mass: 18.5 kg.
- Dimensions: 436 x 317 x 240 mm.

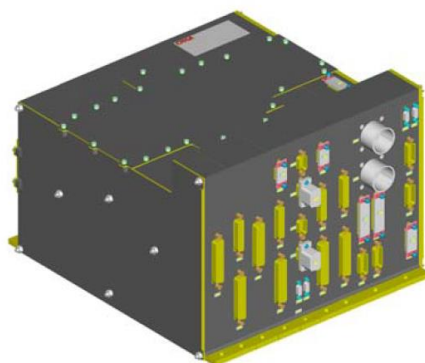


**Figure 15-4: PDCU MPPT**

#### 15.1.4 Technology Needs

Technology needs					
*	Equipment Name & Text Reference	Technology	Supplier (Country)	TRL	Additional Information
✓	PCDU	MPPT and unregulated bus	Airbus Spain,	7	Heritage from Bepicolombo and

Technology needs					
*	Equipment Name & Text Reference	Technology	Supplier (Country)	TRL	Additional Information
			Thales Alenia Space Belgium, TERMA Denmark		SWARM
✓	Battery	Battery 8S4P VES16	SAFT France	7	
✓	Solar Array	Cells	LEONARDO, Thales Alenia Space, Airbus	7	Heritage from Proba 3, Euclid, Cheops, EDRS-C, MTG

## 15.2 Probe B1

This spacecraft is the responsibility of JAXA.

S/C A is expected to provide power to probe B1, for example to charge its secondary battery up to TBD% of DoD.

## 15.3 Probe B2

### 15.3.1 Requirements and Design Drivers

SubSystem Requirements		
Req. ID	Statement	Parent ID
POW-060	The power subsystem of probe B2 shall be able to provide power to the probe throughout 24 hours of lifetime.	
POW-070	The probe B2 shall be deployed from S/C A at a Sun distance of up to 1.25 AU.	
POW-080	The worst sun light condition during operation shall have a maximum inclination of $\pm 45^\circ$ with respect to the Sun.	
POW-090	The probe B2 shall be spinning in one axis during the 24h operation.	
POW-100	The probe B2 shall not have eclipse during the 24 hours of lifetime.	
POW-110	No redundancy of the power functions shall be implemented as baseline design.	

SubSystem Requirements		
Req. ID	Statement	Parent ID
POW-120	Duty cycle is not allowed to be implemented in the science load during the 24 hours of lifetime, the instrument shall be permanently ON during operation. <sup>26</sup>	

**Table 15-8: Power subsystem requirements for probe B2**

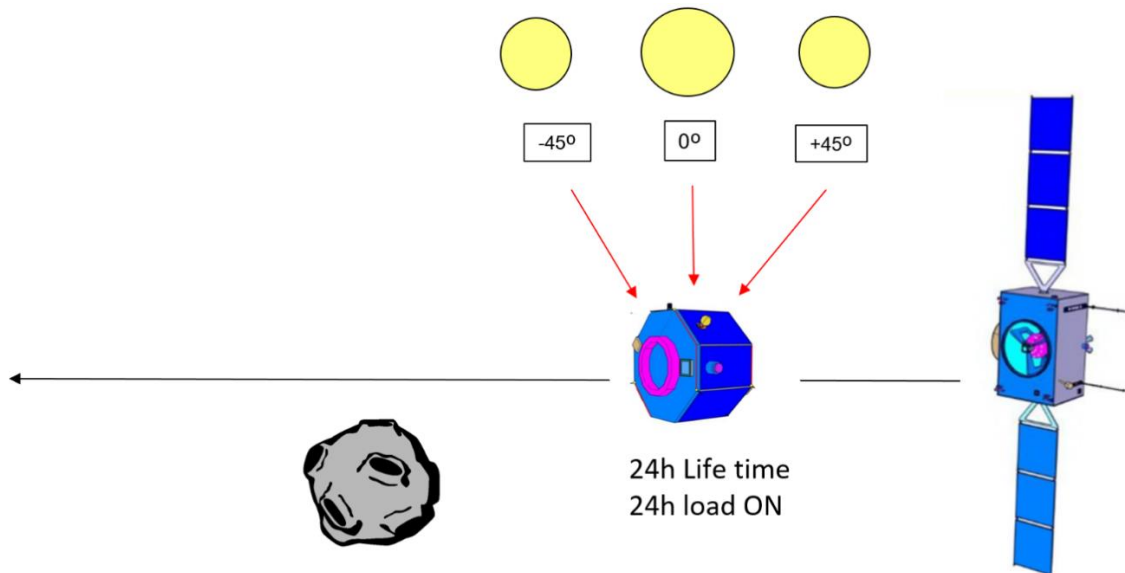


**Figure 15-5: Illustration of probe B2 after deployment**

### 15.3.2 Assumptions and Trade-Offs

The probe B2 requires energy to power the avionics systems and the scientific instruments. In order to achieve this goal, a combination of five different types of power equipment can be implemented:

1. Solar panels: body mounted solar panels have been considered, so that the eight faces available could be populated with solar cells. However, since the current design for B2 does not have structural panels, body mounted solar panels would require an additional structural support.
2. Rechargeable battery: based on Li-ion cells.
3. Primary battery: based on Li-SOCl cells. This type of cells has been used before in space missions, in particular in the Rosetta-Philae lander mission; they provide an energy density in the range 390-410 Wh/kg. This technology is very useful when a high demand in peak power is required in a short period of time; additionally, it provides a backup option in case the environment conditions (illumination or dust) limit the harvesting of energy from the solar panels.

<sup>26</sup> Note that requirement POW120 was removed at the end of the study, however there was not enough time to assess and redesign the power architecture in full.

4. Power Distribution Unit (PDU): Power module with LCLs and BDR, needed to regulate the power coming from the battery to main bus.
5. Power Conditioning Unit (PCU): Power module that integrates the power regulation from the energy harvested in the solar panels string into the battery.

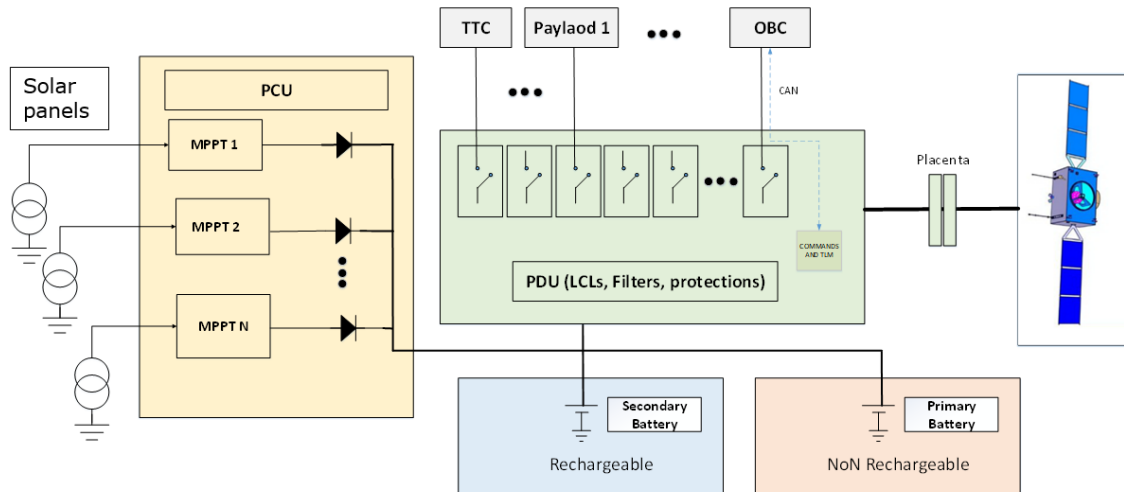


**Figure 15-6: Power system for probe B2**

### 15.3.3 B2 Electrical Architecture

A total of 5 different concepts could be implemented, based on the equipment described in the previous chapter. The following table summarises the concepts considered for the trade-off, depending on what power functions are needed to fulfil the requirements.

Concept	Solar Panels	- Rechargeable battery	Primary battery (non rechargeable)	PDU	PCU
A	YES	YES	NO	YES	YES
B	YES	YES	YES	YES	YES
C	NO	NO	YES	YES	NO
D	YES	NO	YES	YES	YES
E	NO	YES	NO	YES	NO

**Table 15-9: B2 electrical architecture concepts**

#### 15.3.3.1 Solar panels

The sizing of the potential solar panels has taken into account the following assumptions and considerations.

Assumptions for SA sizing (B2)	
1	Maximum temperature of the solar array is around 90°C given in the mission characteristics.

Assumptions for SA sizing (B2)	
2	Radiation effects for the solar cells have been extracted from the datasheet.
3	0.85 packing factor in the solar panels surface.
4	Distance from the Sun: 1.25 AU.
5	3% losses harness.
6	2% losses power distribution.
7	5% losses MPPT.
8	Loss of 1 string per wing of solar panel.
9	The PDU is based on a MPPT SAR with a non-regulated bus of 28 V.
10	The spacecraft is spinning in one axis, so it means that at least 3 of 8 panels are illuminated and the effective surface is always the same but distributed dynamically over the three panels (SPA 1, SPA2, and SPA 3).
11	The worst case of inclination is 45°.

**Table 15-10: Assumptions for SA sizing (B2)**

With these assumptions implemented in the EcosimPro simulator, the following table shows the results of the sizing exercise with the body mounted solar panels.



**Figure 15-7: Illustration of B2 spinning with inclination respect of the Sun**

Size per solar panels [m <sup>2</sup> ]	Sun pointing inclination [deg]	Contribution SPA 3 power [W]	Contribution SPA 2 power [W]	Contribution SPA 1 power [W]	Total supply power after PCU [W]
0.2	0	24.1	34.1	24.1	82.32
0.2	45	17.04	24.11	17.04	58.2
0.1	0	12.05	17.05	12.05	41.16
0.1	45	8.52	12.05	8.52	29.1
0.08	0	9.64	13.64	9.64	32.9
0.08	45	6.8	9.6	6.8	23.2
0.05	0	6.02	8.52	6.02	20.58
0.05	45	4.2	6.02	4.2	14.55

**Table 15-11: Body mounted solar panels**

The following conclusions can be drawn from the table above:

- With the implementation of an area of about  $0.08 \text{ m}^2$  per body mounted panel, the energy generated in the solar panels is about 23.2 W in the worst case scenario. This would not be sufficient to power up a total load of 58.3 W (as calculated during the study) permanently during the 24 hours of operations.
- Therefore, for this case, the power subsystem baseline design should also include either primary batteries, such as in proposed concepts B and C, or solar panels as big as, or bigger than,  $0.2 \text{ m}^2$  each.

### 15.3.3.2 Trade-off options: B versus C

Only concepts B and C have been taken into account because A, D and E exceed the requirements in mass, volume, complexity and cost. The following table shows a comparison between B and C.

	B	C
Reliability in case of failure	<p>In case of failure or anomaly on the electrical system during the 24h operation, it is possible to implement a contingency plan: for instance, one of the solar panels or string can be used to place the probe B2 into a safe mode for the time needed to see what is wrong, assess the failure and perform operations to recover the spacecraft.</p> <p>Note however, that the current communications design does not allow two-way communication with the probe B2, and so this would not be possible with the current baseline.</p>	<p>By relying on only one type of energy source, in case of failure the chances of implementing a contingency plan are very limited (if a failure occurs after the release from S/C A, the electrical architecture via option C could potentially not provide enough power or place the bus into a safe mode).</p> <p>If the probe enters in safe mode there are two options: 1) Uplink available: The failure is assessed on ground and actions are performed to recover the probe to nominal.</p> <p>2) No Uplink: there is a dedicated function targeted to analyse the issue on site and isolate the failure and continue to nominal operations</p> <p>(Note that a failure in the primary battery or in BDR can not be covered by the safe mode).</p>
Flight proven	Yes (heritage from electrical architecture in Philae).	Yes (but not with the latest technology in cells Li-SOCl).
Flexibility	High	Limited
Power budget	In case the primary battery fails, it would be possible to implement a duty cycle and switch on instrument periodically.	Need to implement duty cycle on the payload.
Cost	Medium	Low
Complexity	Medium, heritage from electrical	Medium, because it will require the

	<b>B</b>	<b>C</b>
	architecture and the design in Philae can be re-used.	trade off and development of a PDCU with a BDR suitable for primary battery technology (it will require the design of a dedicated Battery Discharge Regulator that provides regulation with a significant efficiency in all cases).
Mass	High, the solar panels would require additional structural support (not included in the current design).	Medium
Volume	High, the solar panels would increase the external volume.	Lower

**Table 15-12: Architecture comparison of options B versus C**

#### 15.3.4 Baseline Design

From a mere power subsystem point of view, the recommended concept would be B; however, concept C has been selected, prioritizing the reduction in volume, mass (one of the initial goals of the study was a maximum mass of 30 kg for B2), and cost, at the expense of reliability, power availability and flexibility.

##### 15.3.4.1 Battery

The primary battery is based on Li-SOCl<sub>2</sub> cells. Although they have a wide operating temperature range (-60°C / +85°C), 20°C is recommended as the optimal operating temperature, both during the cruise (where heat is supplied by S/C A) and after the release. While performances at higher temperatures would slightly improve, lower temperatures would have a more significant degradation effect. The battery has been sized assuming the battery properties at 20°C: it should be possible to maintain the battery close to 20°C, by placing warmer units, such as DHS, in its proximity without requiring additional heat. This assumption will have to be checked in further studies.

Due to mass constraints at system level, the primary battery has been sized considering the system-imposed design constraint of a 5 kg maximum battery mass (without margin). This mass value implies an average power of 44.5 W available at system level over 24 hours. With all equipment ON a required calculated load of 63 W (including the reaction wheels) would have to be supplied for the 24h lifetime. Therefore, concept C (primary battery only) forces to implement a duty cycle in some loads, resulting in the 44.5 W average power requirement (=1068 Wh energy requirement).

<b>Total power (available to SYS)</b>	<b>W</b>	<b>44.5</b>
<b>Time</b>	<b>hours</b>	<b>24</b>
Energy requirement	Wh	1068
5% power cond. losses	Wh	1124
80% DoD	Wh	1405
10% battery string redundancy	Wh	1546
<b>Total energy required</b>	<b>Wh</b>	<b>1546</b>
Self-discharge rate	per year	0.03
Mission duration	years	5
Nominal capacity	Ah	13
Nominal voltage	V	3.6
Cell mass	kg	0.1
Cell energy density @ BOM	Wh/kg	468
Cell energy density @ EOM	Wh/kg	402
Packing factor cells-to-battery	-	1.3
Battery energy density @ EOM	Wh/kg	309
<b>Total battery mass</b>	<b>kg</b>	<b>5.0</b>
Battery density	g/cc	1.5
Battery volume	litres	3.3
Battery height	mm	125.0
Battery width	mm	170.0
Battery length	mm	156.9

**Table 15-13: B2 battery sizing**

#### 15.3.4.2 PDU

In order to save mass, it was decided to integrate the PDU with the OBC required for DHS. The dimensions defined take into account this assumption. However, the need for radiation shielding and, therefore, additional mass for the electronics is yet to be investigated.

#### 15.3.5 Conclusions and follow up

As stated above, the Concept C (primary battery only) was preferred and selected at systems level, in order to meet the system requirements for B2 (except requirement POW-120 since this option would impose to the science instruments to be duty cycled). Concept B (primary battery, rechargeable and solar arrays) is nonetheless favoured by the power domain experts, and a further trade-off in later phases is recommended by the power team with regards to the baseline.

As well, it would be an added value to explore other materials in the panels design, including the state-of-art for small satellites and new space technologies. Nowadays, such panels do not require having panel substrates based on metals or heavy materials. Potentially, using only PCBs, plastics for space or lighter materials like carbon fibre may be considered to for mounting the solar cells and strings. In this case, the overall mass impact would be lower, while making the baseline design more reliable than concept C and not require implementing a duty cycle on the science instrument (at current load assumptions).

In addition, should the design for probe B2 later change to 3-axis stabilised, the required solar panels areas could be substantially reduced since a sun pointed attitude could potentially be achieved for the entire area of the installed solar array.

In addition, it would be an added value to consider for the concept B the deployment of solar panels. At the time the assessment was done, the cost of those deployment systems for solar panels within the small satellite industry has been reduced significantly enough to consider in future phases as complementary energy power source. However current issues with regards to deployable volume and mass rendered this unfeasible from a system-perspective.

### 15.3.6 Technology Needs

Technology needs					
*	Equipment Name & Text Reference	Technology	Supplier (Country)	TRL	Additional Information
✓	PCDU	For S/C (Concept C) it is required to develop a complete new PCDU	NA	2	
✓	Battery cell	Li-SOCl2	SAFT France	7	
✓	Battery	For S/C (Concept C) it is required to develop a complete new Battery	SAFT France	2	

## 15.4 Budgets

### 15.4.1 Mass Budget

	Mass (kg)	Mass margin (%)	Mass incl. margin (kg)
<b>SC_A (Spacecraft A)</b>	<b>52.66</b>		<b>57.93</b>
A_SA (A SolarArray)	14.63	10.00	16.09
A_SA_2 (A SolarArray #2)	14.63	10.00	16.09
A_Bat (A Battery)	4.90	10.00	5.39
A_PCDU (A PCDU)	18.50	10.00	20.35
<b>SC_B2 (Spacecraft B2)</b>	<b>5.30</b>		<b>6.36</b>
B2_Bat (B2 Battery)	5.00	20.00	6.00
B2_PDU (B2 PDU)	0.30	20.00	0.36

Table 15-14: Mass budget for Power equipment

### 15.4.2 Power Budget

	P_stby	P_on
<b>SC_A (Spacecraft A)</b>	<b>0.00</b>	<b>45.00</b>
A_PCDU (A PCDU)	0.00	45.00
<b>SC_B2 (Spacecraft B2)</b>	<b>0.00</b>	<b>6.00</b>
B2_Bat (B2 Battery)	0.00	0.00
B2_PDU (B2 PDU)	0.00	6.00

**Table 15-15: Power budget for Power equipment**

This Page Intentionally Blank

## 16 TELECOMMUNICATIONS

### 16.1 Requirements and Design Drivers

SubSystem Requirements		
Req. ID	Statement	Notes
COM-TTC-010	<p>The telecommunication subsystem of S/C A shall be able to perform the following functions regardless of the spacecraft's attitude, throughout all the mission phases:</p> <ul style="list-style-type: none"> <li>• Receive and demodulate the uplink signal from the ground segment and transmit the telecommands (TC) to the data handling system as defined in RD[43] and RD[44].</li> <li>• Receive a telemetry (TM) data stream from the data handling system and transmit this data to the ground segment as defined in RD[43] and RD[45],</li> <li>• Receive, transponder, and re-transmit a ranging signal (both PN (TBC) and ESA standard as defined in RD[46]),</li> <li>• Provide two-way Doppler,</li> <li>• Provide DDOR for navigation (TBC).</li> </ul>	
COM-TTC-020	Active (hot) redundancy shall be provided for telecommand (uplink) and passive (cold) redundancy for telemetry (downlink).	
COM-TTC-030	<p>The link budget margins shall be as defined in RD[43]:</p> <ul style="list-style-type: none"> <li>• Nominal &gt; 3 dB</li> <li>• Mean 3*sigma &gt; 0 dB</li> <li>• RSS worst case &gt; 0 dB</li> </ul>	
COM-TTC-040	<p>The frequency assignment shall be done in coordination with the Space Frequency Coordination Group (SFCG) and in compliance to its recommendations and resolutions RD[47].</p> <p>Note: Comet Interceptor follows the frequency allocation rules of a deep space mission (Cat B)</p>	
COM-ISL-010	<p>Maximum distance between the probes and S/C A:</p> <p>The ISL shall support telemetry and telecommand capabilities for a maximum distance of 3000 km (TBC)</p> <p><i>ISL is assumed being in a star network configuration.</i></p>	
GOAL-COM-ISL-020	<p>Ranging capabilities:</p> <p>The probe ISL shall provide ranging capabilities with the S/C A for a maximum distance as per COM-ISL-010.</p>	Goal, not driving mission success or feasibility.
GOAL-COM-ISL-030	<p>Ranging accuracy:</p> <p>The ISL shall allow ranging accuracy of at least 1.0 m at 95% probability with 90% confidence level.</p>	Goal, not driving mission success or feasibility.

SubSystem Requirements		
Req. ID	Statement	Notes
GOAL-COM-ISL-040	<p>Doppler capabilities:</p> <p>The ISL shall be able to perform Doppler measurements at the maximum distance as per COM-ISL-010. Doppler measurements shall be provided at programmable interval of minimum 1 s (TBC).</p> <p>Note: coherent link is not required.</p>	Goal, not driving mission success or feasibility.
GOAL-COM-ISL-060	<p>Time transfer accuracy:</p> <p>The ISL design shall allow a time transfer with an accuracy of at least TBD ms between nodes at the maximum distance as per COM-ISL-010.</p>	Goal, not driving mission success or feasibility.
COM-ISL-070	<p>Adaptable data rate:</p> <p>The ISL design shall be capable to autonomously adapt the data rate to the channel conditions. At least the following net data rates shall be made available:</p> <ul style="list-style-type: none"> <li>• 460 kbps (TBC)</li> <li>• 200 kbps (TBC)</li> <li>• 100 kbps (TBC)</li> <li>• 50 kbps</li> <li>• 20 kbps (TBC)</li> <li>• 2 kbps (TBC)</li> </ul> <p>Manual rate change via telecommand shall be available and shall override the autonomous data rate adaptability.</p> <p>Note: <i>net data rate</i> refers to the data rate available for platform and payload data transmission before encoding. Transmission of ISL protocol overhead bits shall be accounted in addition to the net data rate.</p> <p>Note: <i>autonomously</i> refers to the capability of the ISL transceivers to vary the data rate without the need of a dedicated external issued telecommand (manual rate change).</p>	
COM-ISL-075	<p>Communications redundancy scheme:</p> <p>The ISL design shall provide at least 2 receivers working in hot redundancy during nominal operations.</p> <p>Note: provision of full redundancy ISL equipment can be waived only for probe B2.</p>	
COM-ISL-080	<p>ISL compatibility with probes stabilization mode:</p> <p>ISL shall be compatible with:</p> <p>A three-axis stabilised spacecraft</p> <p>A spin-stabilised spacecraft, that spins and wobbles max +/- 20 deg around the RAM direction.</p>	
COM-ISL-100	<p>ISL minimum real time data rate:</p> <p>The ISL shall support a minimum real time net data rate of 50 kbps @ 900 km (TBC) simultaneously from two probes to the main S/C and net data rate of 4 kbps @ 900 km (TBC) from</p>	

SubSystem Requirements		
Req. ID	Statement	Notes
	the main S/C to the probe. Note: <i>net data rate</i> refers to the data rate available for platform and payload data transmission before encoding. Transmission of ISL protocol overhead bits shall be accounted in addition to the net data rate.	
COM-ISL-110	The minimum net data rate shall be provided continuously during the slew manoeuvre of S/C A at encounter (180 deg rotation around one axis at max average rate 1.5 deg/s, max peak rate 4 deg/s).	

### 16.1.1 Design Drivers

The main driver for this mission is the design-to-cost.

For what concerns S/C A, highest TRL technologies have been considered.

For what concerns the ISL, the design drivers are:

- Simplest redundant design
- Low mass and power consumption
- Reuse as much as possible of existing equipment
- Ranging and time transfer capabilities desired for science but not driving mission success or feasibility.

### 16.2 Assumptions and Trade-Offs

Assumptions	
1	In the nominal case, S/C A generates 167 Gbit + 10% overhead of scientific data to be stored onboard and transmitted to Earth after the encounter.
2	The scientific data volume can be reduced in the case where the ground station time needed to downlink the data exceeds 6 months.
3	The range of distances from Earth to S/C A is up to 2.25 AU with the nominal mean worst case at 2 AU.
4	ESTRACK 35m G/S is available for communications sessions with the S/C A for 10h/day after the encounter.
5	The bandwidth assigned to S/C A for real time housekeeping telemetry transmission is 5 kbps.
6	The reference encounter geometry for the three spacecraft is applicable (see below). Both probes are equipped with the same ISL and the channel is shared between the two.
8	The bandwidth assigned to the overhead due to the link protocol over the ISL link is 10%.
9	Probe B1 points one ISL antenna towards S/C A during ISL communication with an accuracy of +/- 5 deg.

Assumptions 1 and 2 are in line with the figures for the nominal scientific data volume provided during the study and the approach to limit the ground station booking time. The following reference data volume has been derived:

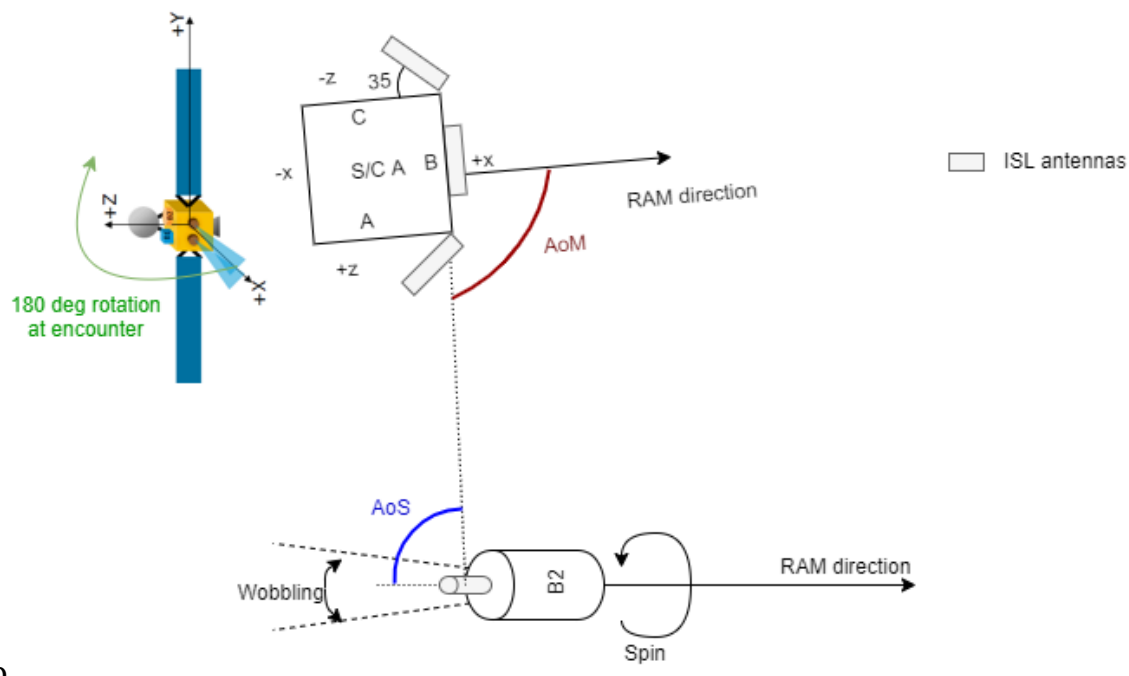
- 145 Gb for S/C A
- 8 Gb for probe B2
- 14 Gb for probe B1.

Assumption 3 is in line with the statistics of the possible encounters provided by Mission Analysis in Chapter 5. For the 99% of the simulated comet encounters, the maximum mean distance to Earth for the six months after the encounter is 2 AU.

Assumption 4 is based on an assumed availability of ESTRACK stations.

Assumption 5 is based on a preliminary assessment considering previous missions.

Assumption 6 refers to the fact that the reference encounter geometry produced in the study has been used to provide the ISL capabilities and to drive the choice of specific antenna types. After the release, the three S/C travel almost parallel and the viewing angle from the probe B2 to the S/C A is ~90 deg during the full flyby duration. S/C A performs a 180 deg slew at the encounter around the Y-axis and three pairs of antennas are required to continuously cover the encounter slew manoeuvre. The geometry is schematized in Figure 16-1.



p

**Figure 16-1: Link geometry after the probes release and after S/C A divert manoeuvres. The 180 deg slew is performed by S/C A at the comet encounter. B1 is not shown since its attitude is under JAXA responsibility and not consolidated in**

**the study; however, B1 can be imagined travelling in a region between S/C A and probe B2 with a similar RAM direction.<sup>27</sup>**

The view angle of probe B2 as seen from the normal to the face B of the S/C A (“Angle offset from main S/C”, AoM) and the view angle of S/C A as seen from the spin axis of probe B2 are shown in the following figure starting from the time of the release (“Angle offset from probe”, AoS).

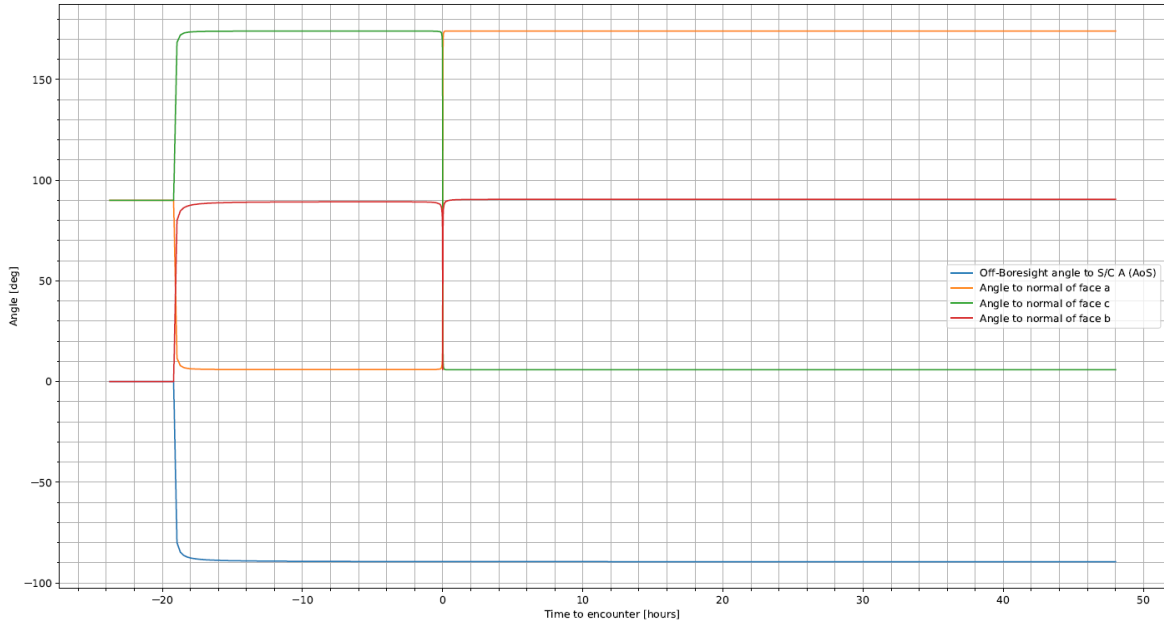


**Figure 16-2: Reference link geometry used for the ISL analysis. AoM (angles for different S/C A faces) and AoS angle (ref. Figure 16-1) for the relative geometry of S/C A and probe B2.**

<sup>27</sup> Note that B1 may be travelling out-of-plane from S/C A and B2, i.e. it may be travelling out-of-plane, of the plane formed by the ram vectors and the S/C A-comet vector. There are two considerations here: firstly, B1 has the advantage of likely not rotating during the fly-by (TBC), allowing for optimisation of the antenna pointing on B1. However, the current antenna pointing on S/C A is not optimised for the out-of-plane motion of B1, and so this would need to be considered in more detail, as to how much the design optimisation on B1 could account for this.

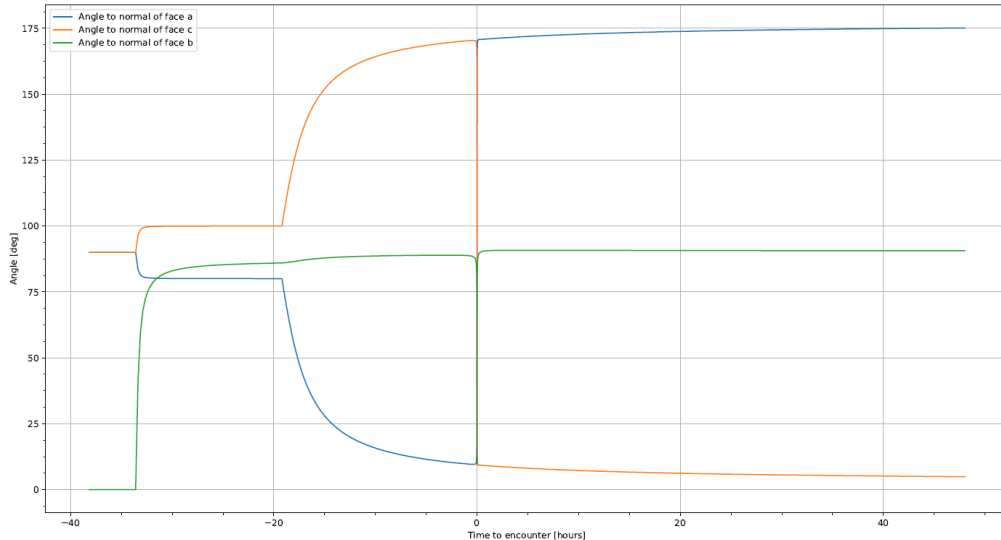


**Figure 16-3: Reference link geometry used for the ISL analysis. AoM angles for different S/C A faces (ref. Figure 16-1), relative geometry of S/C A and probe B1. B1 is assumed pointing towards S/C A so the depoint angle AoS is fixed at the assumed worst (5 deg).**

The evolution of the distance between the three spacecraft is shown later in Figure 16-9 and in Figure 16-11 on the left hand axis.

Assumption 7 allows to make use of a single ISL subsystem onboard the S/C A. The assumption has to be consolidated at programmatic level since, if confirmed, it has to be taken into account also in the design of the JAXA probe B1.

Assumption 8 is based on an estimation of a potential ISL protocol overhead used to derive the ISL net data rates from the gross data rates.

Assumption 9 is based on the fact that probe B1 is a three axis stabilised probe with an active AOCS. The assumption shall be further evaluated in the next program phases based on more refined capabilities and constraints (JAXA).

### 16.2.1 TT&C Bandwidth Trade-Offs

The main communication sessions are performed while the S/C is in deep space around the comet encounter phase (distance to Earth greater than 2 million km). Even if the S/C would remain below 2 million km even for more than half of the overall duration of the mission, during those mission phases only periodical S/C checks and navigation telecommunication sessions are performed. Comet Interceptor can hence be considered a Cat. B mission.

For the S/C A TT&C, the following options have been considered for the available deep space frequency bands:

- S-band usage is discouraged by the international standards. Moreover, this may pose other limitations for the ISL that share similar frequencies.
- Ka-band usage is an asset that allows reaching greater downlink data rates. However a Ka-band only TT&C is lacking the G/S support and has an increased cost w.r.t. the standard X-band system.

- X-band usage is standard for deep space missions and hence is used as baseline for Comet Interceptor, given the available high TRL and low cost.
- A dual band X + Ka system has been considered and traded-off.

### 16.2.2 TT&C Antenna Trade-Offs

Considering as a starting point a 65 W X-band TWTA, the ground station contact times as per Assumption 4 and the real time housekeeping rate as per Assumption 5, the number of days necessary to downlink all the scientific data in Assumption 1 have been computed for various HGA antenna sizes and distances to Earth as shown in Table 16-1.

Days to downlink all 183.7 Gbit of data [days]. RF power = 65 W, Contact time = 10 h/day										
Antenna diameter [m]	0.2	0.3	0.4	0.5	0.6	0.7	0.8	0.9	1	1.1
Distance [AU]										
0.3	149.7	61.5	33.7	21.3	14.7	10.8	8.2	6.5	5.2	4.3
0.4	300.4	114.8	61.5	38.5	26.5	19.3	14.7	11.6	9.4	7.7
0.5	562.6	191.4	99.5	61.5	42.0	30.5	23.2	18.2	14.7	12.1
0.6	1069.5	300.4	149.7	91.0	61.5	44.5	33.7	26.5	21.3	17.6
0.7	2341.9	457.6	215.2	128.0	85.6	61.5	46.5	36.4	29.2	24.1
0.8	10281.0	692.7	300.4	173.9	114.8	81.9	61.5	48.0	38.5	31.6
0.9	-7764.3	1069.6	412.5	230.5	149.7	105.9	79.1	61.5	49.3	40.4
1	-3442.1	1750.9	562.6	300.4	191.4	134.0	99.5	77.0	61.5	50.3
1.1	-2438.3	3311.7	769.9	387.5	241.1	166.7	122.9	94.7	75.4	61.5
1.2	-1995.5	10285.0	1069.6	497.0	300.4	204.7	149.7	114.8	91.0	74.1
1.3	-1748.4	-16102.1	1534.5	637.2	371.6	249.0	180.3	137.4	108.5	88.0
1.4	-1592.0	-5304.2	2342.3	820.9	457.6	300.4	215.2	162.8	128.0	103.5
1.5	-1484.5	-3442.1	4071.5	1069.6	562.6	360.6	255.0	191.4	149.7	120.7
1.6	-1407.1	-2673.8	10286.4	1422.4	692.7	431.3	300.4	223.6	173.9	139.6
1.7	-1348.9	-2256.4	-38801.4	1957.4	857.0	514.9	352.6	259.7	200.7	160.4
1.8	-1303.6	-1995.4	-7761.7	2858.3	1069.6	614.9	412.5	300.4	230.5	183.3
1.9	-1267.6	-1817.5	-4628.3	4682.3	1353.8	735.7	481.9	346.4	263.6	208.5
2	-1238.4	-1688.9	-3442.0	10287.1	1751.0	884.0	562.6	398.4	300.4	236.2
2.1	-1214.3	-1592.0	-2819.9	-341732.8	2342.4	1069.6	657.4	457.6	341.5	266.8
2.2	-1194.3	-1516.5	-2438.0	-11145.8	3311.9	1307.5	769.9	525.2	387.5	300.4
Mean value [days]	-736	-1007.7	-1899.1	-16360.1	699.9	366.4	241.3	174.9	134.0	106.6

**Table 16-1: No. of days (worst case) after encounter necessary to downlink science generated data with a 65 W TWTA, as a function of HGA dish diameter and mean S/C to Earth distance. The subsystem DC peak power consumption is 160 W<sup>28</sup>**

A 0.9 m HGA has been selected as baseline. Preliminary results show no great mass benefit in reducing the antenna diameter while maintaining the same data rate as per

<sup>28</sup> The values highlighted in red indicate that with the design choice of the 0.9 m antenna, the maximum distance that would allow to downlink the full science data within 6 months is between 1.4 AU and 1.5 AU.

the 0.9 m case, as this would result in a quick increase of the TWTA output power. With 0.7 m HGA, the required RF output power would be more than 100 W (deep space heritage).

One can see that above 1.4 AU the number of days necessary to downlink all the science data is more than 180 (6 months). The net data volume that can be downlinked in 180 days is shown in Table 16-2.

Data volume that fits within 180 days of downlink [Gb]. RF power = 65 W, Contact time = 10 h/day										
Antenna diameter [m]	0.2	0.3	0.4	0.5	0.6	0.7	0.8	0.9	1	1.1
Distance [AU]										
0.3	198.8	483.7	882.6	1395.4	2022.2	2763.0	3617.7	4586.4	5669.1	6865.7
0.4	99.1	259.3	483.7	772.2	1124.7	1541.4	2022.2	2567.1	3176.1	3849.2
0.5	52.9	155.5	299.1	483.7	709.3	976.0	1283.7	1632.5	2022.2	2453.0
0.6	27.8	99.1	198.8	327.0	483.7	668.9	882.6	1124.7	1395.4	1694.6
0.7	12.7	65.0	138.3	232.5	347.6	483.7	640.7	818.6	1017.5	1237.2
0.8	2.9	43.0	99.1	171.2	259.3	363.5	483.7	619.9	772.2	940.4
0.9	-3.8	27.8	72.1	129.1	198.8	281.1	376.0	483.7	604.0	736.9
1	-8.6	17.0	52.9	99.1	155.5	222.1	299.1	386.2	483.7	591.4
1.1	-12.2	9.0	38.7	76.8	123.4	178.5	242.1	314.1	394.7	483.7
1.2	-14.9	2.9	27.8	59.9	99.1	145.3	198.8	259.3	327.0	401.8
1.3	-17.0	-1.8	19.4	46.7	80.1	119.5	165.1	216.6	274.3	338.0
1.4	-18.7	-5.6	12.7	36.3	65.0	99.1	138.3	182.8	232.5	287.4
1.5	-20.0	-8.6	7.3	27.8	52.9	82.5	116.7	155.5	198.8	246.6
1.6	-21.1	-11.1	2.9	20.9	43.0	69.0	99.1	133.1	171.2	213.2
1.7	-22.1	-13.2	-0.8	15.2	34.7	57.8	84.4	114.6	148.3	185.6
1.8	-22.8	-14.9	-3.8	10.4	27.8	48.4	72.1	99.1	129.1	162.4
1.9	-23.5	-16.4	-6.4	6.4	22.0	40.5	61.8	85.9	112.9	142.7
2	-24.0	-17.6	-8.6	2.9	17.0	33.7	52.9	74.7	99.1	126.0
2.1	-24.5	-18.7	-10.6	-0.1	12.7	27.8	45.3	65.0	87.1	111.6
2.2	-24.9	-19.6	-12.2	-2.7	9.0	22.8	38.7	56.7	76.8	99.1

**Table 16-2: Total net scientific data (worst case) downlinkable in 180 days with a 65 W TWTA, as a function of HGA dish diameter and mean S/C to Earth distance**

Note that to produce the previous tables, the elevation over the G/S has been considered constant at 10 deg for the simplified CDF design, so the numbers shown represent the worst case. Further refinement considering typical ground station passes as function of the possible encounters shall be carried out in the next study phase. Improvement of around roughly 20% could be expected considering the elevation change over a pass.

At system level, a fixed HGA w.r.t. a steerable HGA has been traded-off. A steerable HGA has been considered necessary, due to the unknown S/C and Earth position at the comet encounter. APM pointing losses have been taken into account in the link budgets.

### 16.2.3 TT&C RF Power Amplification Trade-Off

The number of days required to downlink the scientific data reduces by increasing the transmitted power. This is an interesting case assuming that there is enough generated power available (could be the case with the electric propulsion subsystem requiring high-power during its usage). In addition to the 65 W baseline, the 100 W case has been considered as an option, and the downlink times are reported in Table 16-3.

Days to downlink all 183.7 Gbit of data [days]. RF power = 100 W, Contact time = 10 h/day										
Antenna diameter [m]	0.2	0.3	0.4	0.5	0.6	0.7	0.8	0.9	1	1.1
Distance [AU]										
0.3	92.6	39.2	21.7	13.8	9.5	7.0	5.3	4.2	3.4	2.8
0.4	177.0	71.8	39.2	24.7	17.0	12.5	9.5	7.5	6.1	5.0
0.5	306.5	116.8	62.5	39.2	26.9	19.6	14.9	11.8	9.5	7.9
0.6	508.6	177.0	92.6	57.4	39.2	28.5	21.7	17.0	13.8	11.3
0.7	844.2	257.1	130.3	79.7	54.1	39.2	29.7	23.3	18.8	15.5
0.8	1476.5	363.8	177.0	106.6	71.8	51.8	39.2	30.7	24.7	20.3
0.9	3035.2	508.6	234.9	138.8	92.6	66.4	50.1	39.2	31.5	25.9
1	12392.3	711.1	306.5	177.0	116.8	83.3	62.5	48.8	39.2	32.2
1.1	-9674.2	1007.9	395.9	222.3	144.8	102.5	76.7	59.6	47.8	39.2
1.2	-4109.1	1476.7	508.7	276.0	177.0	124.4	92.6	71.8	57.4	47.0
1.3	-2838.4	2314.4	653.5	339.9	214.2	149.1	110.4	85.3	68.0	55.5
1.4	-2279.2	4209.3	844.3	416.3	257.1	177.0	130.3	100.2	79.7	65.0
1.5	-1966.6	12398.0	1104.4	508.7	306.5	208.6	152.4	116.8	92.6	75.3
1.6	-1768.1	20936.0	1476.7	621.4	363.8	244.2	177.0	135.0	106.6	86.6
1.7	-1631.6	6485.0	2049.3	761.3	430.5	284.5	204.4	155.0	122.0	98.8
1.8	-1532.5	-4108.0	3035.8	938.2	508.7	330.1	234.9	177.0	138.8	112.1
1.9	-1457.6	-3136.0	5122.6	1168.0	600.9	381.9	268.8	201.3	157.1	126.5
2	-1399.1	-2608.0	12400.0	1476.7	711.1	440.9	306.6	227.8	177.0	142.0
2.1	-1352.5	-2279.0	-55708.7	1911.6	844.3	508.7	348.7	257.1	198.7	158.9
2.2	-1314.5	-2054.0	-9670.3	2566.8	1007.9	586.8	395.9	289.3	222.3	177.0
Mean value [days]	-624.5	-897.0	-1836.2	592.2	299.7	192.3	136.6	102.9	80.8	65.2

**Table 16-3: Number of days (worst case) after the encounter necessary to downlink the science generated data with a 100 W TWTA, as a function of HGA dish diameter and S/C to Earth distance. The subsystem DC peak power consumption is 220 W**

The net data volume that can be downlinked in 180 days is shown in the following table.

Data volume that fits within 180 days of downlink [Gb]. RF power = 100 W, Contact time = 10 h/day										
Antenna diameter [m]		0.3	0.4	0.5	0.6	0.7	0.8	0.9	1	1.1
Distance [AU]										
0.9	9.8	58.5	126.7	214.4	321.5	448.1	594.2	759.8	944.9	1149.5
1	2.4	41.9	97.1	168.1	254.9	357.4	475.8	609.9	759.8	925.5
1.1	-3.1	29.5	75.2	133.9	205.6	290.3	388.2	499.0	622.9	759.8
1.2	-7.2	20.2	58.5	107.8	168.1	239.3	321.5	414.6	518.7	633.8
1.3	-10.5	12.9	45.5	87.6	138.9	199.6	269.6	349.0	437.7	535.7
1.4	-13.1	7.1	35.2	71.5	115.8	168.1	228.5	296.9	373.4	457.9
1.5	-15.1	2.4	26.9	58.5	97.1	142.7	195.3	254.9	321.5	395.1
1.6	-16.8	-1.4	20.2	47.9	81.8	121.9	168.1	220.5	279.0	343.8
1.7	-18.2	-4.6	14.5	39.1	69.1	104.6	145.6	192.0	243.8	301.2
1.8	-19.4	-7.2	9.8	31.7	58.5	90.2	126.7	168.1	214.4	265.5
1.9	-20.4	-9.5	5.8	25.5	49.5	77.9	110.7	147.9	189.4	235.3
2	-21.3	-11.4	2.4	20.2	41.8	67.5	97.1	130.6	168.1	209.5
2.1	-22.0	-13.1	-0.5	15.6	35.2	58.5	85.3	115.8	149.7	187.3
2.2	-22.6	-14.5	-3.1	11.6	29.5	50.7	75.2	102.9	133.9	168.1

**Table 16-4: Total net scientific data volume (worst case) downlinkable in 180 days with a 100 W TWTA, as a function of HGA dish diameter and mean S/C to Earth distance**

The 100 W solution is currently not baselined. However, further iterations are needed in the next program phases also considering potential reduction of the scientific data volume.

#### 16.2.4 TT&C Addition of Ka-Band Downlink Trade-Off

The addition of a Ka-band downlink in parallel to the X-band system has several implications:

- Higher cost (at subsystem level), mass and power consumption
- Dual frequency DST X/X-Ka is required
- Two Ka TWTA (35 W European heritage) are required for redundancy
- Additional mass in the RFDN
- Dual frequency HGA and APM needed
- Mass: + 6.2 kg w/o margin (w/o APM)
- Power: + 64.7 W power consumption to be added on top of X-band consumption (only for science data downlink)
- Higher accuracy required to point HGA to Earth. Considering 0.9 m diameter HGA, Ka: +/- 0.15 deg w.r.t the +/- 0.6 deg of X-band
- AIT complexity.

The advantage is that higher downlink data rates are achievable. With a 0.9m HGA, all data can be downlinked in 132 days from 2 AU. However, Ka downlink is not baselined at this stage due to the higher complexity, mass and cost.

### 16.2.5 ISL Trade-Offs

For the ISL, the first trade-off is between a RF communication system and a laser-based one. Considering the low maturity of miniaturised laser equipment in Europe and the different design of the two probes, a laser ISL has been not considered further for Comet Interceptor.

Two RF frequency bands are considered for the ISL: S-band and UHF-band.

The advantages of an S-band over a UHF-band system can be summarised as follows:

- Wider available deep-space heritage (Rosetta, Deep Impact)
- Smaller non-deployable antennas
- Ranging and time transfer already implemented.

The advantages of a UHF link over an S-band link are the lower directivity of the antennas and the higher data rates due to lower free space propagation losses. However ranging and time transfer are not available in the known ISL UHF architectures.

Today the state of the art is S-band for the probe ISL. Preliminary estimations indicate that developing full ISL functionalities in UHF band would require significant effort and extensive re-design of existing equipment. Furthermore, mass constraints do not allow usage of big UHF antennas. For this reasons, UHF is not considered further.

Two architectures for the S-band ISL are of interest for Comet Interceptor: one based on SDR and active antennas COTS equipment and one with passive antennas and “classical” transceivers.

#### 16.2.5.1 ISL with SDR and active antennas

A SDR ISL system with active antenna has the following characteristics:

- Pros:
  - No high RF power loss because of absence of passive coupling
  - Each probe has its own dedicated channel (FDM), no sharing of the bandwidth
  - Cheap COTS based solutions are available
- Cons:
  - Additional mass to cope with redundancy
  - COTS based solutions shall be adapted for deep space (dedicated qualifications).

The front end electronics with RF power amplifier for transmission and the LNA for reception are either embedded in the antenna (for patch antennas) or integrated in the proximity of the base of the antenna (for toroidal antennas).

The subsystem design varies on the three spacecraft and it is schematised in the following figures.

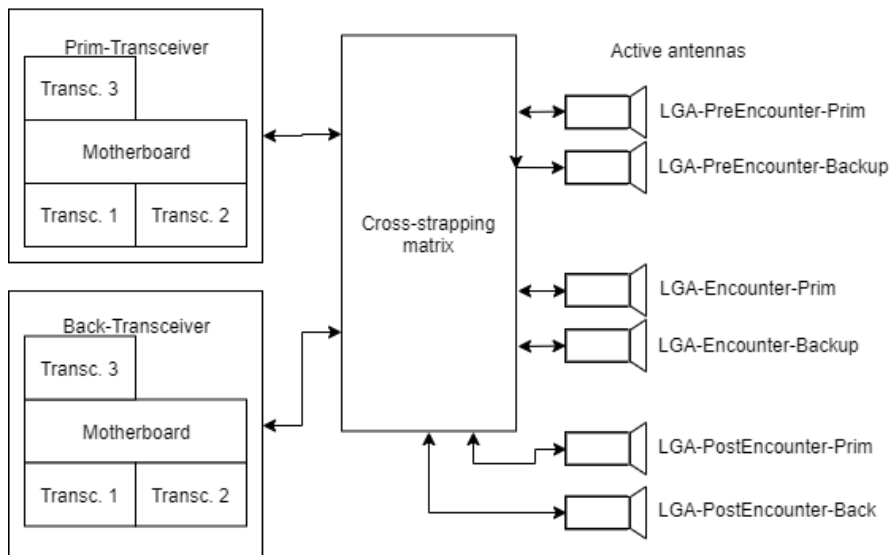


**Figure 16-4: Concept of active antenna S-band ISL for S/C A**

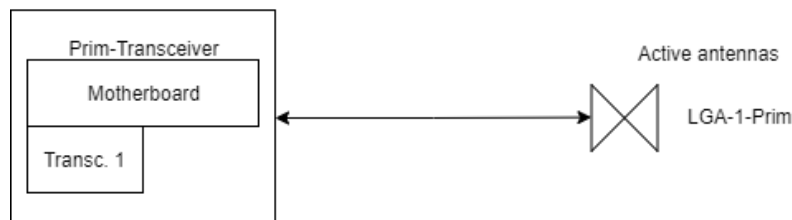


**Figure 16-5: Concept of active antenna S-band ISL for probe B2**

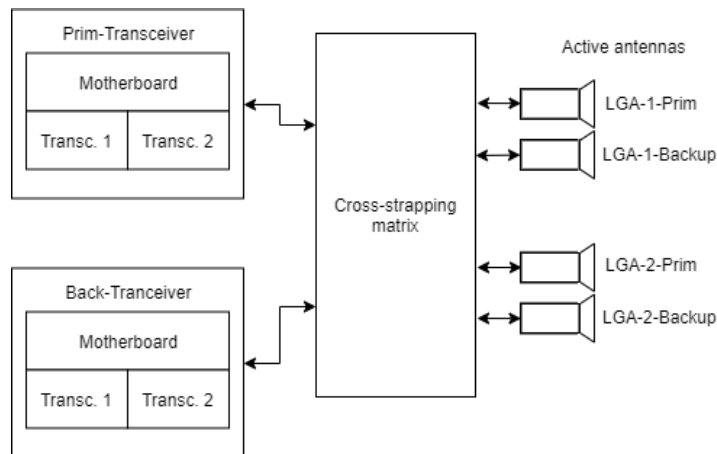


**Figure 16-6: Concept of active antenna S-band ISL for probe B1**

In the S/C A, the ISL system is considered fully redundant. Three low gain antennas (the same considered for the probes, Figure 16-8) are connected to two ISL transceivers: the receivers work in hot redundancy and the transmitters in cold redundancy.

The selection of the antennas is based on the link geometry (assumption 6). A different design has been considered for the two probes.

For the spin-stabilised B2 probe, a toroidal low gain antenna has been included (Figure 16-7). The subsystem is not redundant for mass and power limitations.

For the three axis stabilised B1 probe, two couples of low gain antennas are accommodated on two opposite faces of the probe (Figure 16-8).

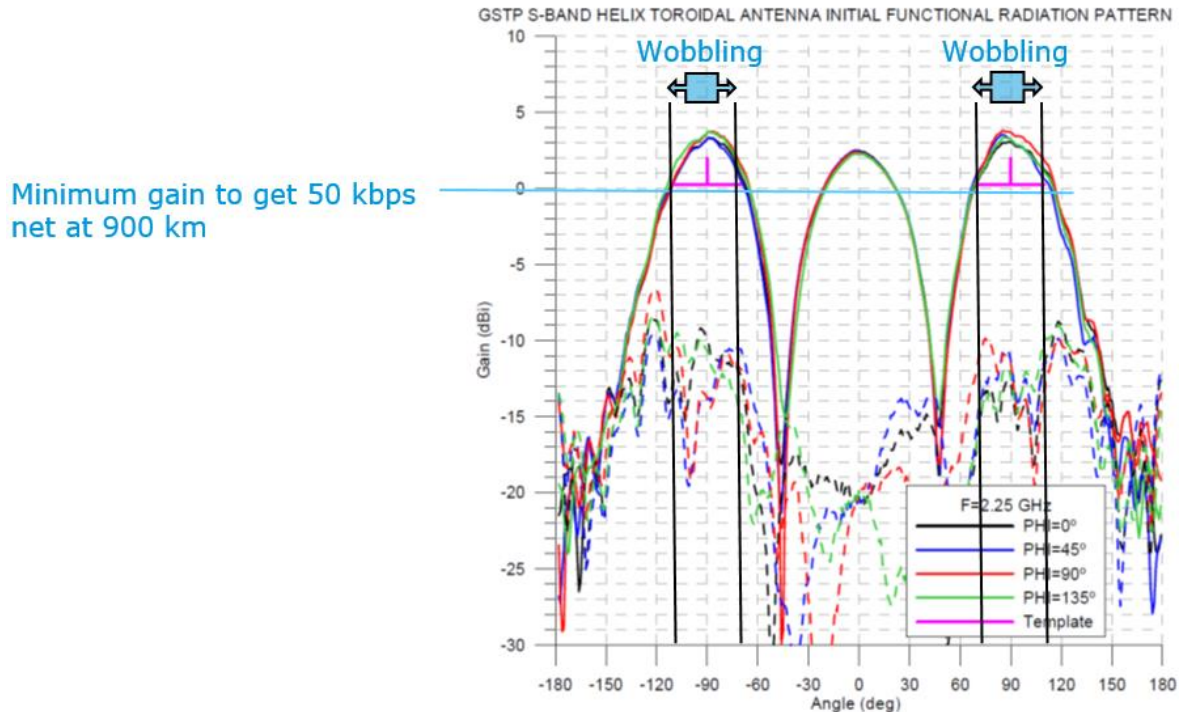


**Figure 16-7: Assumed performance of S-band ISL toroidal antenna (Sener Aerospacial, former Rymsa). The effect of +/- 20 deg wobbling is also shown**

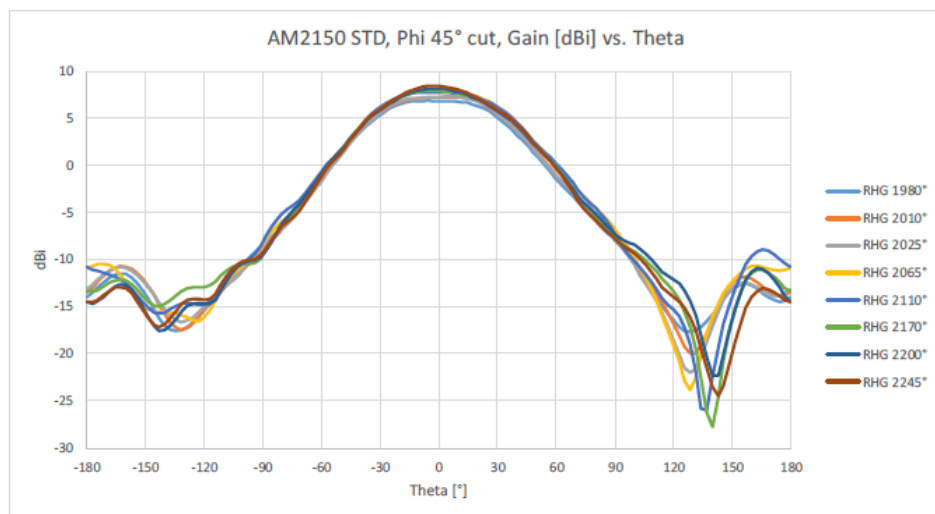


**Figure 16-8: Assumed performance of S-band ISL patch antenna (GOM Space patch antenna)**

The concept link budget (B2 to S/C A) is shown in Table 16-5.

PARAMETER	Value	Notes
RANGE [km]	900.0	
FREQUENCY [MHz]	2245	
TX POWER [W]	2	S band output power
TX ANTENNA GAIN [dB]	0	Toroidal antenna 20 deg off-boresight
TX LOSSES [dB]	0	Antenna itself is radiating
TX EIRP [dBW]	3.01	Calculated
PATH LOSSES [dB]	158.55	Calculated
ATMOSPHERE LOSS [dB]	0.00	NA in space
RX POL. LOSS [dB]	0.60	Estimation including some xpol
RX G/T [dBK]	-18.40	Patch antenna 23 deg offpoint 6.55 dBi
DEMOD. LOSS [dB]	1.00	Estimation
MOD. LOSS [dB]	0.00	Suppressed carrier modulation
S/No [dB]	53.06	
REQUIRED Eb/No [dB]	2.60	Concatenated
MINIMUM MARGIN [dB]	3.00	Standard ESA
MAX BIT RATE [dBHz]	47.46	
MAX BIT RATE [kbps]	55.71	
<b>MAX NET BIT RATE [kbps]</b>	<b>50.14</b>	Includes 10% packetization overheads

**Table 16-5: Concept of active antenna S-band link budget, probe B2 to S/C A**

A dynamic simulation based on the reference link budget and on the reference geometry has been performed and the results are shown in Figure 16-9 and Figure 16-10 for the ISL between probe B2 and S/C A. The 50 kbps net data rate can be maintained up to 1.5 hours after the encounter, switching between the three antennas on the S/C A. Then the rate has to be reduced (in the example figure to 20 kbps) and the ISL can be used to retransmit the most valuable science data recorded during the encounter. Finally, a lower rate (in the example figure 2 kbps) is maintained to continue retransmit further data up to 3000 km.

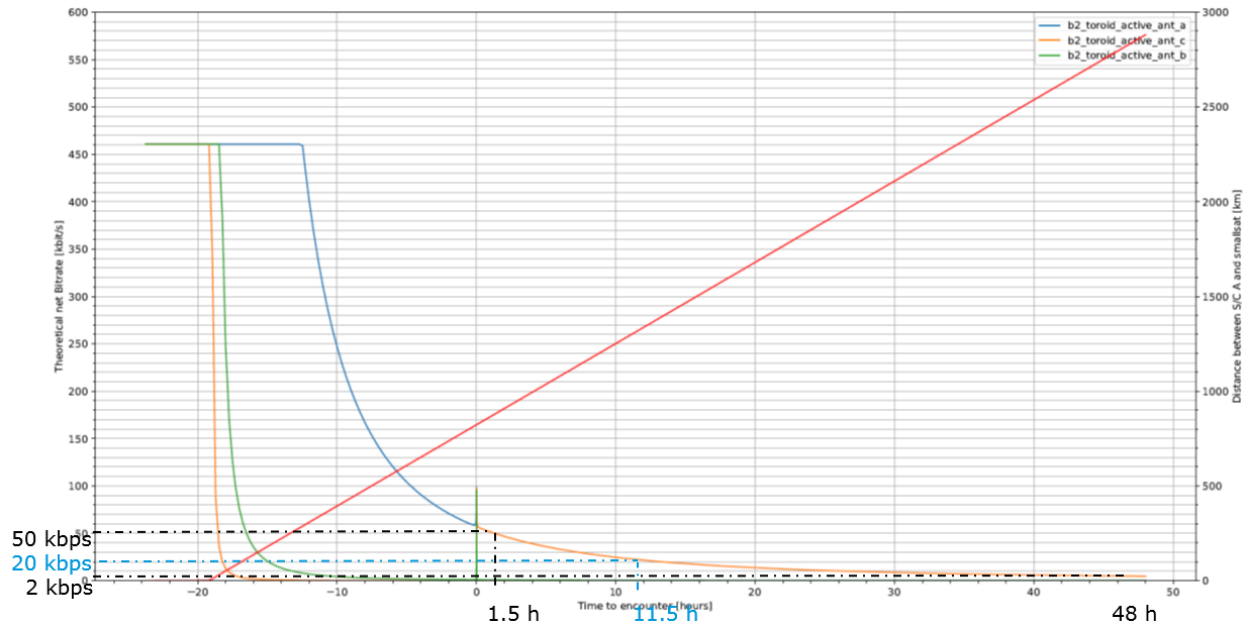


**Figure 16-9: ISL theoretical performance for the link probe B2 to S/C A in the reference geometry. Red line is relative distance with the axis on the right**

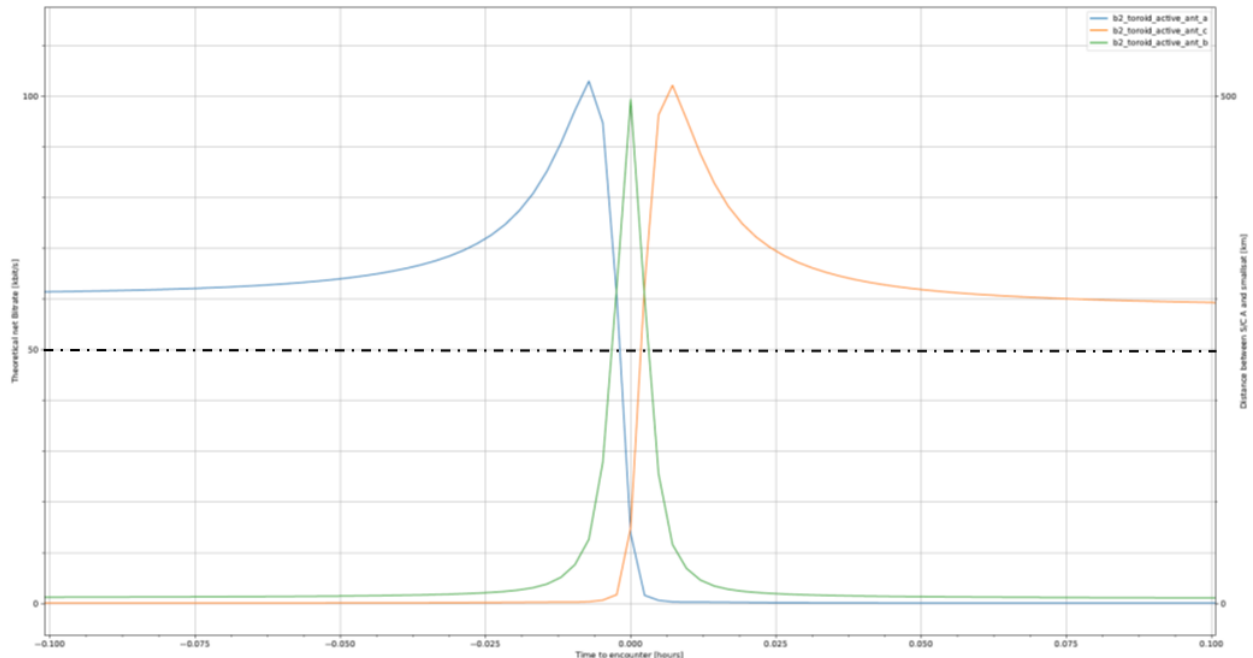


**Figure 16-10: ISL theoretical performance for the link probe B2 to S/C A in the reference geometry. Zoom around the encounter (abscissa = 0)**

For probe B1, the theoretical data rates in Figure 16-11 and Figure 16-12 can be achieved, based on Assumption 9 (one ISL antenna is pointed towards S/C A with +/- 5 deg).

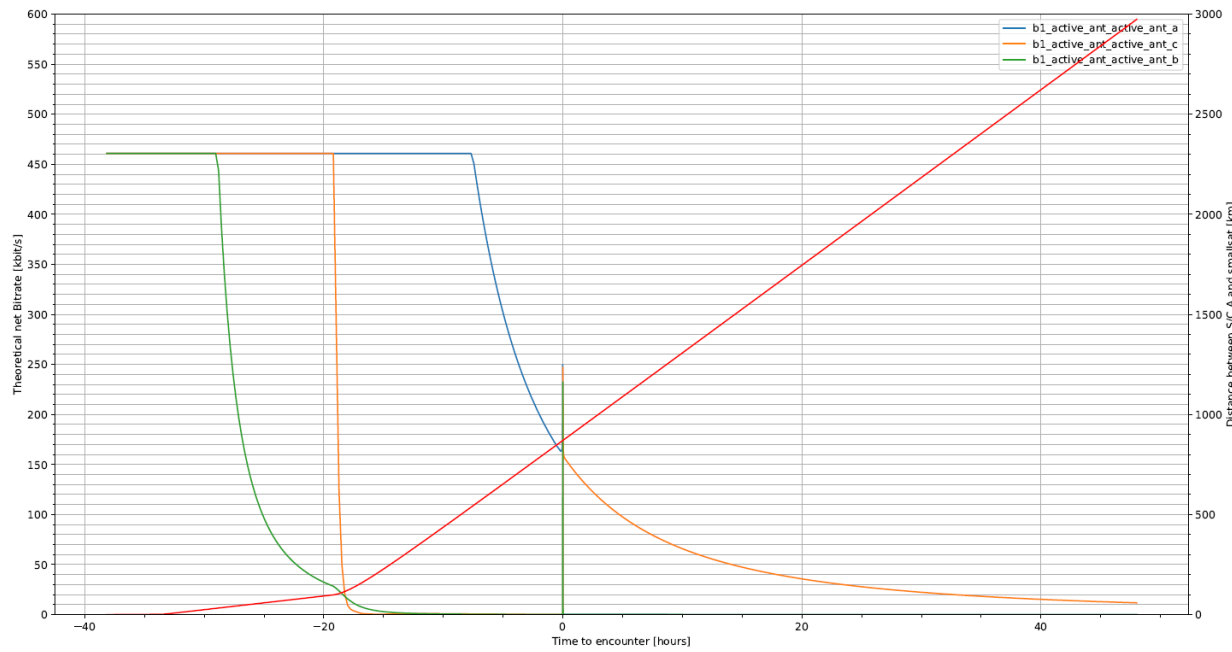


**Figure 16-11: ISL theoretical performance for the link probe B1 to S/C A in the reference geometry. Red line is relative distance with the axis on the right.  
Assumed probe B1 pointing ISL antenna +/- 5 deg towards S/C A**

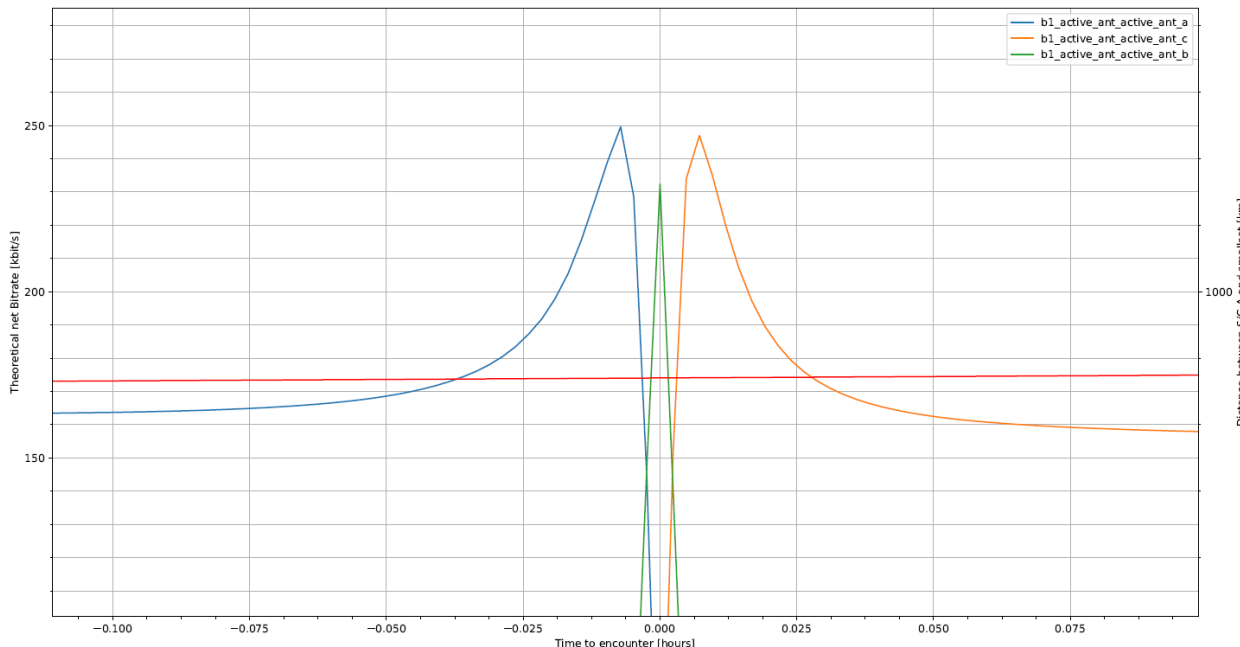


**Figure 16-12: ISL theoretical performance for the link probe B1 to S/C A in the reference geometry. Zoom around the encounter (abscissa = 0). Assumed probe B1 pointing ISL antenna +/- 5 deg towards S/C A**

### 16.2.5.2 ISL with passive antenna coupling

An ISL system with passive antenna has the following characteristics:

- Pros:
  - Deep space heritage, ranging and time transfer already implemented
- Cons:
  - Half of RF power is lost when using coupling
  - Time division multiplex is implemented, this means that the available bandwidth has to be shared between the probes (TDMA)
  - In some architectures, the link is established by the main node (S/C A) with either one or the other probes employing a handshaking protocol.

In this design there is no antenna frontend, the transmitter amplifier and the receiver LNA are inside the transceiver unit.

The handshaking strategy currently implemented in some equipment of this kind is preliminarily not considered compatible with Comet Interceptor needs due to the short duration of the probes mission and the high ISL data rates required. A TDMA approach based on switching over “hard-coded” time-slots for the two probes, if fast enough to guarantee 50 kbps simultaneously from two probes, can be considered.

The subsystem design varies on the three spacecraft and it is schematised in the following figures.

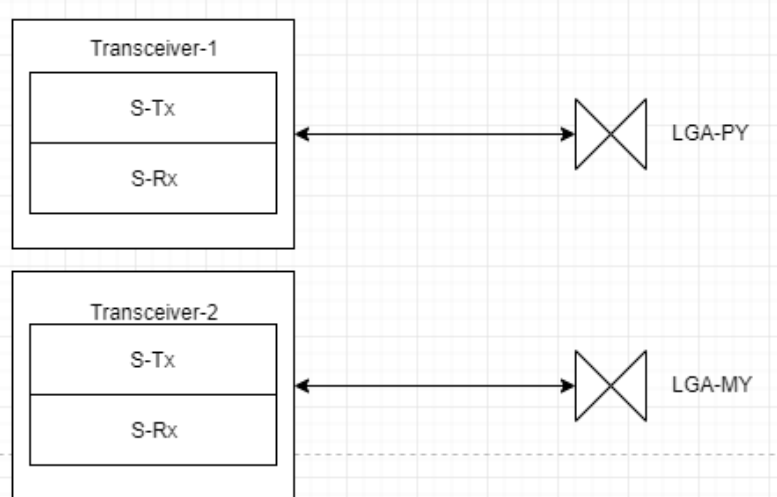


**Figure 16-13: Concept of passive antennas S-band ISL for S/C A**

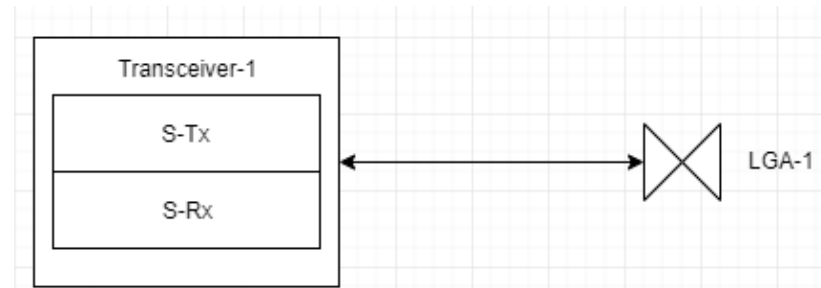


**Figure 16-14: Concept of passive antennas S-band ISL for probe B2**

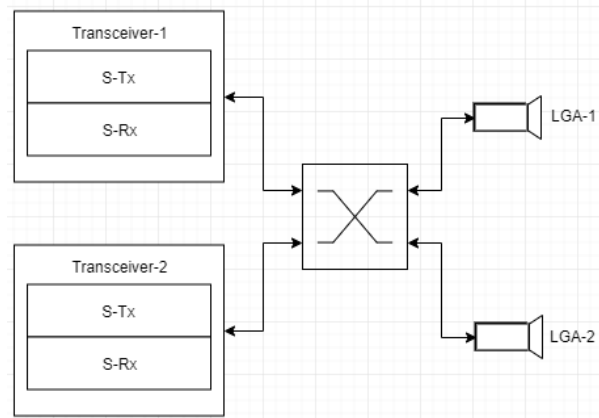


**Figure 16-15: Concept of passive antennas S-band ISL for probe B1**

In the S/C A, the ISL system is considered fully redundant. Two toroidal antennas are located on the +Y and -Y panels of S/C A (eventual interference with folded solar arrays is TBC) and are connected to two ISL transceivers: the receivers work in hot redundancy and the transmitters in cold redundancy.

A different design has been considered for the two probes.

For the spin stabilised B2 probe, a toroidal low gain antenna has been included (Figure 16-7). The subsystem is not redundant for mass and power considerations.

For the three axis stabilised B1 probe, two couples of low gain antennas are accommodated on two opposite faces of the probe (Figure 16-16).

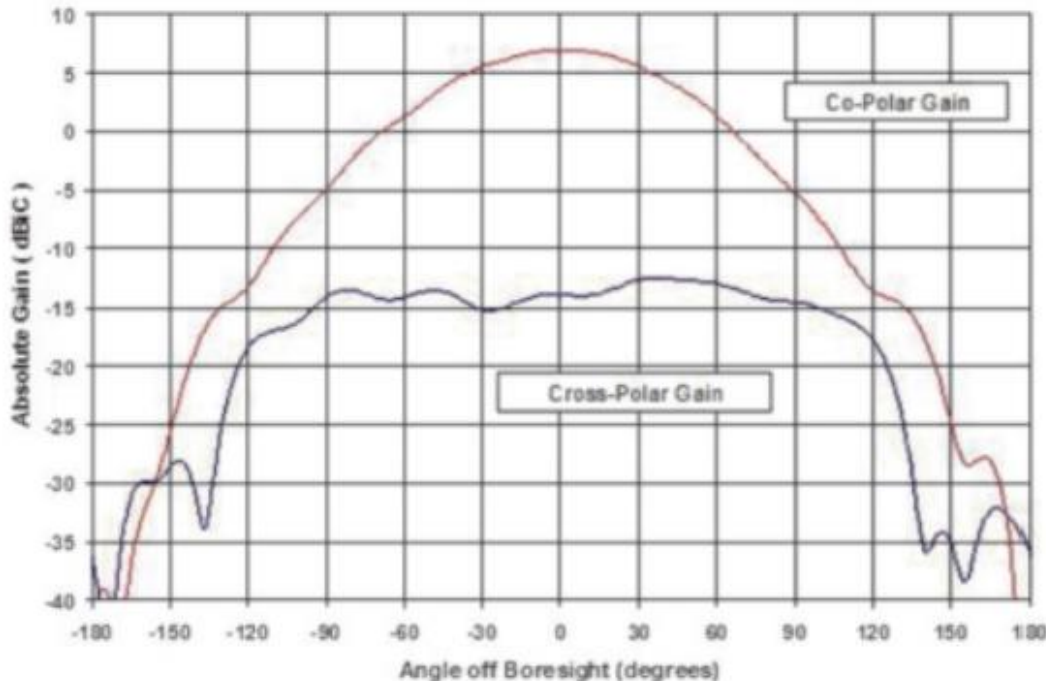


**Figure 16-16: Assumed performance of S-band ISL patch antenna (Surrey patch antenna), for probe B1 only**

The selection of the antenna is based on the link geometry. After the release, the three spacecraft travel almost parallel and the viewing angle from the probe B2 to the S/C A is around 90 deg throughout the mission. S/C A performs a 180 deg slew at the encounter around the y axis, so the same toroidal antenna on S/C A ensures smooth coverage of the encounter without the need to switch to another antenna.

The reference link budget (probe B2 to S/C A) is shown in Table 16-6 and shows that with the standard 2 W of RF output power the required 50 kbps cannot be achieved.

PARAMETER	Value	Notes
RANGE [km]	900.0	
FREQUENCY [MHz]	2250	
TX POWER [W]	2	Transmitter
TX ANTENNA GAIN [dB]	0	Toroidal antenna on B2 20 deg wobbling
TX LOSSES [dB]	0.5	Preliminary Estimated Value (cables)
TX EIRP [dBW]	2.51	Calculated
PATH LOSSES [dB]	158.57	Calculated
ATMOSPHERE LOSS [dB]	0.00	NA in space
RX POL. LOSS [dB]	0.60	Estimation including some xpol
RX G/T [dBK]	-21.40	S/C A antenna toroidal 3 dBi, no coupl.
DEMOD. LOSS [dB]	1.00	Estimation
MOD. LOSS [dB]	0.00	Suppressed carrier modulation
S/No [dB]	49.54	
REQUIRED Eb/No [dB]	2.60	Concatenated
MINIMUM MARGIN [dB]	3.00	Standard ESA
MAX BIT RATE [dBHz]	43.94	
MAX BIT RATE [kbps]	24.75	
<b>MAX NET BIT RATE [kbps]</b>	<b>22.27</b>	Includes 10% packetization overheads

**Table 16-6: Reference passive antenna S-band link budget, probe B2 to S/C A**

Counter actions are necessary to reach 50 kbps in this design for B2, for example:

- To increase the transmitted power, or
- To modify the antenna, or
- To implement more complicated coding/decoding algorithms in the transceivers, or
- To employ a combination of the three aforementioned counteractions.

However, considering also that the channel has to be time shared between the probes (TDMA) in order to provide 50 kbps simultaneously from two probes, the link shall be sized for  $50 \times 2 = 100$  kbps.

As probe B2 is power limited, any increased output power shall be carefully evaluated. Higher power might also mean re-design of the power amplification stage of the transmitter.

For probe B1 the link is more favourable: the absence of wobbling and the increased gain of the patch antenna makes it possible to reach 50 kbps at the encounter with the standard 2 W RF output power. However due to the TDMA, a re-design for 100 kbps shall be targeted.

For this reasons the solution based on passive antennas and TDMA approach is not baselined.

### 16.2.6 Probe B2 Magnetometer Boom and ISL

The effect of the presence of the probe B2 magnetometer boom on the ISL performance has been analysed using as a reference case a simple monopole antenna (Figure 16-17).

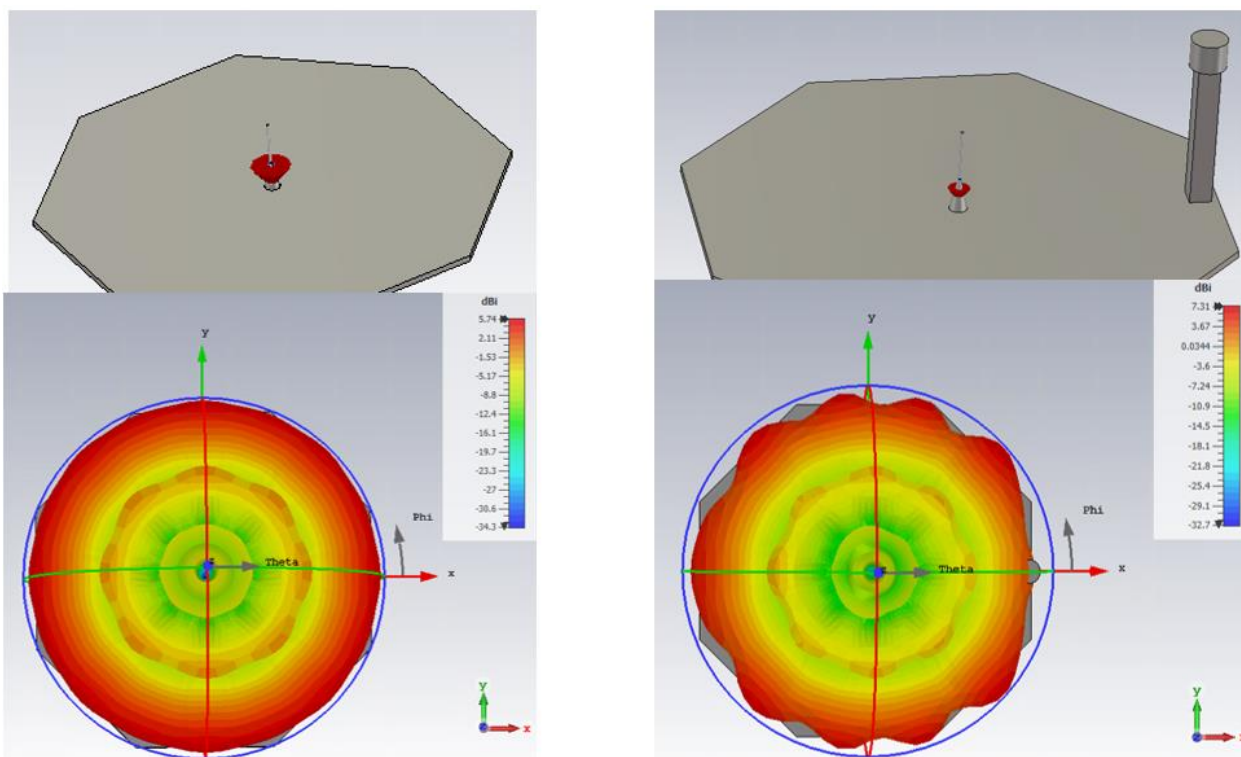


**Figure 16-17: EM simulations of a monopole antenna with the magnetometer boom in its proximity**

The phi cuts of the electromagnetic simulations show a 3 dB degradation on the antenna gain due to ripples in the antenna pattern – that spins around the Z-axis – formed by the reflections of the radio waves on the magnetometer. Higher losses are expected when the magnetometer is closer to the antenna.

Assuming that the same losses are valid for the boom illuminated by the toroidal helix (TBC by detailed EM simulations), this additional 3 dB loss does not allow to close the link budget for 50 kbps at 900 km. Two solutions are hence proposed:

- a) The antenna is placed on top of the boom (no loss)
- b) If solution a) above is not feasible, it would be necessary:
  - o To review the EM simulations using a more representative antenna model, and
  - o To increase the transmitted power, or
  - o To modify the antenna, or
  - o To implement more complicated coding/decoding algorithms in the transceivers, or
  - o To employ a combination of the three aforementioned counteractions.

For this study, the solution a) is preliminarily considered feasible, to be further investigated in the next phases.

### 16.3 Baseline Design

The baseline design for the TT&C on board S/C A is shown in Figure 16-18. It includes:

- Two X/X transponders
- Two LGAs
- One HGA
- Two X-Band TWTAs
- The RF DN that interconnects all the aforementioned devices
- Two S-Band ISL transceivers
- Six S-band ISL antennas
- RF cables ISL receivers to the ISL antennas.

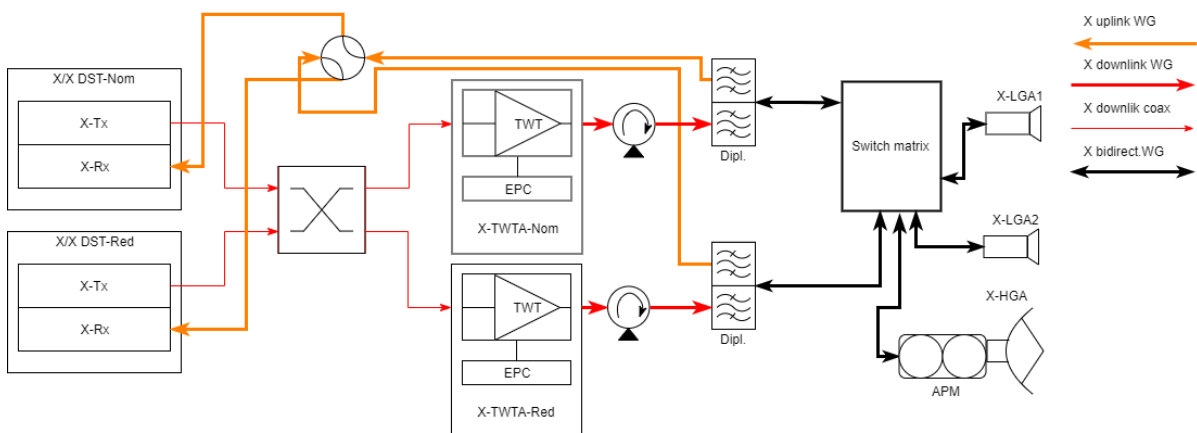


**Figure 16-18: Baseline design of the S/C A TT&C (X-band). The ISL part (S-band) is shown in Figure 16-4.**

Of the two transponders and ISL transceivers, only one is adopted for nominal operation. The second transponder and transceiver are used for redundancy: their transmitter is operating in cold mode and its receiver in hot mode (see requirements COM-020 and COM-ISL-075).

The output TM signal from the active transmitter is amplified by means of TWTAs. The TWTA RF output power is 65 W for X-Band.

The uplink and downlink telemetry signals are routed between the transponders and the LGAs (for low bit rate TM) or the HGA (for high bit rate TM) by means of the RFDN. The two LGAs are on opposite directions for obtaining an almost omnidirectional coverage.

The RFDN consist of hybrids, switches, and waveguides that interconnect all the aforementioned equipment. A possible configuration of the RFDN is provided in Figure 16-18, but it is pointed out that a more detailed RFDN design shall be performed during the next phases by trading off reliability, dimension, mass, and power losses and its optimisation is out of the scope of the CDF study.

Note that loss of contact with Earth is expected during the slew manoeuvre at the closest comet encounter. This is based on the following assumptions: 1) the APM is assumed not able to cope with the maximum slew rate of 4 deg/s and 2) the slew is performed without APM steering, to avoid the CoM change due to the HGA movement.

LEOP is carried out using LGA and the DST working in “clamped” mode: the nominal DST output power is reduced by ~30 dB to reduce the TWTA RF output power (backoff). The TWT power consumption is reduced (~55% reduction has been considered for this study). Dedicated analysis to comply with PFD limits at ground during LEOP shall be carried out in the next program phase.

Safe mode is assumed to be carried out by using the HGA, moving it in stowed position and strobing the entire S/C to look for the Earth in the HGA main lobe (+/- 2.8 deg) with the support of ESTRACK 35 m G/S.

Full support of survival mode (TC and low rate TM) is possible via LGA and ESTRACK 35 m G/S up to 0.6 AU distance. Beyond this distance, support of bigger G/S (NASA 70m or JAXA’s Usuda 64 m station) is required.

For what concerns the ISL equipment on the three spacecraft, refer to section 16.2.5.1.

### 16.3.1 Telecommunications Mass Budgets

The mass budget for the telecommunication equipment is shown in Table 16-7.

	Mass (kg)	mass margin (%)	mass margin (kg)	incl.
<b>SC_A (Spacecraft A)</b>	<b>30.16</b>	<b>10.98</b>		<b>33.47</b>
<b>XDST_1 (X-Band DSTRASP #1)</b>	<b>3.60</b>	<b>5.00</b>		<b>3.78</b>
<b>XDST_2 (X-Band DSTRASP #2)</b>	<b>3.60</b>	<b>5.00</b>		<b>3.78</b>
<b>XHGA (X-Band HGA)</b>	<b>6.05</b>	<b>10.00</b>		<b>6.66</b>
<b>XLGA_1 (X-Band LGA #1)</b>	<b>0.30</b>	<b>5.00</b>		<b>0.32</b>
<b>XLGA_2 (X-Band LGA #2)</b>	<b>0.30</b>	<b>5.00</b>		<b>0.32</b>
<b>XTWT_1 (X-Band TWT #1)</b>	<b>0.80</b>	<b>5.00</b>		<b>0.84</b>
<b>XTWT_2 (X-Band TWT #2)</b>	<b>0.80</b>	<b>5.00</b>		<b>0.84</b>
<b>XTWTA_EPC_1 (X-Band TWTA EPC #1)</b>	<b>1.40</b>	<b>5.00</b>		<b>1.47</b>

	Mass (kg)	mass margin (%)	mass margin (kg)	incl. margin (kg)
<b>XTWTA_EPC_2 (X-Band TWTA EPC #2)</b>	<b>1.40</b>	<b>5.00</b>		<b>1.47</b>
<b>XRFDN (X-Band RFDN)</b>	<b>10.00</b>	<b>20.00</b>		<b>12.00</b>
<b>A_ISL_board_1 (A Electronics #1)</b>	<b>0.50</b>	<b>5.00</b>		<b>0.53</b>
<b>A_ISL_board_2 (A Electronics #2)</b>	<b>0.50</b>	<b>5.00</b>		<b>0.53</b>
<b>A_ISL_Patch_1 (A Antenna Patch #1)</b>	<b>0.15</b>	<b>5.00</b>		<b>0.16</b>
<b>A_ISL_Patch_2 (A Antenna Patch #2)</b>	<b>0.15</b>	<b>5.00</b>		<b>0.16</b>
<b>A_ISL_Patch_3 (A Antenna Patch #3)</b>	<b>0.15</b>	<b>5.00</b>		<b>0.16</b>
<b>A_ISL_Patch_4 (A Antenna Patch #4)</b>	<b>0.15</b>	<b>5.00</b>		<b>0.16</b>
<b>A_ISL_Patch_5 (A Antenna Patch #5)</b>	<b>0.15</b>	<b>5.00</b>		<b>0.16</b>
<b>A_ISL_Patch_6 (A Antenna Patch #6)</b>	<b>0.15</b>	<b>5.00</b>		<b>0.16</b>
<b>SC_B2 (Spacecraft B2)</b>	<b>0.99</b>	<b>5.51</b>		<b>1.04</b>
<b>ISL_T_LGA (ISL_ToroidalLGA)</b>	<b>0.51</b>	<b>5.00</b>		<b>0.54</b>
<b>B2_ISL_board (B2 Electronics)</b>	<b>0.37</b>	<b>5.00</b>		<b>0.39</b>
<b>B2_ISL_ActiveFE (B2 Active Antenna FE)</b>	<b>0.10</b>	<b>10.00</b>		<b>0.11</b>
<b>Grand Total</b>	<b>31.14</b>	<b>10.80</b>		<b>34.51</b>

**Table 16-7: Telecomm mass budget**

### 16.3.2 Telecomms Power Budgets

The power budget for the units is shown in Table 16-8.

Power (W)	P_on	P_stby
<b>SC_A (Spacecraft A)</b>		
<b>XDST_1 (X-Band DSTRASP #1)</b>	<b>32.00</b>	<b>16.00</b>
XPND_RX (Transponder Receiver)	16.00	16.00
XPND_TX (Transponder Transmitter)	16.00	0.00
<b>XDST_2 (X-Band DSTRASP #2)</b>	<b>32.00</b>	<b>16.00</b>
XPND_RX (Transponder Receiver)	16.00	16.00
XPND_TX (Transponder Transmitter)	16.00	0.00
<b>XHGA (X-Band HGA)</b>	<b>0.00</b>	<b>0.00</b>
<b>XLGA_1 (X-Band LGA #1)</b>	<b>0.00</b>	<b>0.00</b>
<b>XLGA_2 (X-Band LGA #2)</b>	<b>0.00</b>	<b>0.00</b>
<b>XTWT_1 (X-Band TWT #1)</b>	<b>163.41</b>	<b>0.00</b>
<b>XTWT_2 (X-Band TWT #2)</b>	<b>163.41</b>	<b>0.00</b>
<b>XTWTA_EPC_1 (X-Band TWTA EPC #1)</b>	<b>9.00</b>	<b>0.00</b>

Power (W)	P_on	P_stby
XTWTA_EPC_2 (X-Band TWTA EPC #2)	9.00	0.00
XRFDN (X-Band RFDN)	0.00	0.00
A_ISL_board_1 (A Electronics #1)	8.16	6.72
A_ISL_board_2 (A Electronics #2)	8.16	6.72
A_ISL_Patch_1 (A Antenna Patch #1)	7.20	1.00
A_ISL_Patch_2 (A Antenna Patch #2)	7.20	1.00
A_ISL_Patch_3 (A Antenna Patch #3)	7.20	1.00
A_ISL_Patch_4 (A Antenna Patch #4)	7.20	1.00
A_ISL_Patch_5 (A Antenna Patch #5)	7.20	1.00
A_ISL_Patch_6 (A Antenna Patch #6)	7.20	1.00
SC_B2 (Spacecraft B2)	12.96	4.36
ISL_T_LGA (ISL_ToroidalLGA)	0.00	0.00
B2_ISL_board (B2 Electronics)	5.76	3.36
B2_ISL_ActiveFE (B2 Active Antenna FE)	7.20	1.00
<b>Grand Total</b>	<b>481.31</b>	<b>55.80</b>

**Table 16-8: Telecomm power budget**

### 16.3.3 Telecomms Link Budgets

The link budget for the S/C A downlink to Earth is shown in Table 16-9.

PARAMETER	Value	Notes
ALTITUDE [AU]	2.0	
ELEVATION ANGLE [deg]	20.0	
RANGE [km]	299200196.5	
FREQUENCY [MHz]	8400	
TX POWER [W]	65	ExoMars 2016 TWTA
TX ANTENNA GAIN [dB]	35.3164195	0.9 m diameter dish pointing acc.: 0.56 deg
TX LOSSES [dB]	2	Preliminary Estimated Value (RFDN)
TX EIRP [dBW]	51.45	Calculated
PATH LOSSES [dB]	280.45	Calculated
ATMOSPHERE LOSS [dB]	0.50	X-band
RX POL. LOSS [dB]	0.00	Already included in Antenna Gain
RX G/T [dBK]	50.10	ESTRACK New Norcia 35 m

PARAMETER	Value	Notes
DEMOD. LOSS [dB]	2.00	Estimation
MOD. LOSS [dB]	1.20	Residual carrier modulation
S/No [dB]	46.00	
REQUIRED Eb/No [dB]	0.50	Turbo 1/4, FER=1e-6
MINIMUM MARGIN [dB]	3.00	Standard ESA
MAX BIT RATE [dBHz]	42.50	
<b>MAX BIT RATE [kbps]</b>	<b>17.78</b>	

**Table 16-9: X-band reference link budget, S/C A with Earth**

The ISL link budget is shown in Table 16-5 (baseline S-band).

## 16.4 List of Equipment

The transponder considered as example for the baseline design sizing is the X/X-Band deep space transponder developed by Thales-Italy. The transponder, shown in Figure 16-19, has TRL 9 and would meet all performance and functional requirements foreseen for Comet Interceptor.

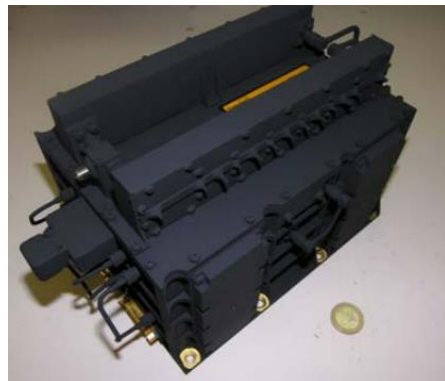


**Figure 16-19: X-Band Transponder**

An example solution for the X-Band LGAs is manufactured by TRY O and is shown in Figure 16-20. Their mass is 0.4 kg, diameter 90 mm, and height 240 mm, and they have TRL 9.



**Figure 16-20: X-Band LGA**

The figures for the 0.9 meters HGA have been derived assuming a resized version of the one adopted in Solar Orbiter. TRL is considered hence 8.

A possible solution for the TWTA in X-Band is the one developed by Thales and used for the ExoMars 2016 TGO. It is TRL 9.

Concerning active ISL equipment, an example is GOMspace NanoCom SR2000 (Figure 16-21):



**Figure 16-21: Example of ISL electronics (GOMspace)**

An example of ISL antenna on both S/C A and probes is shown in Figure 16-22, from SSTL. It is a small patch 8x8x2 cm, TRL is 9. Also GOMspace has a similar solution with an embedded active frontend.

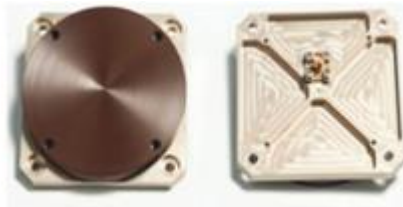


**Figure 16-22: S-band ISL patch antenna (Surrey Satellite Technologies Ltd. Patch antenna)**

Due to the spinning nature of the probe B2, a toroidal antenna has been added. The one considered as example for this study is qualified by Rymsa (now Sener Aerospace) at EQM level, has a mass of 514 g, dimensions 140.0 ( $\varnothing$ ) x 175.8 mm and its TRL is 8 (Figure 16-23).



**Figure 16-23 – S-band ISL toroidal antenna (Sener Aerospace)**

## 16.5 Options for S/C A TT&C

The long time required to downlink the scientific data after the encounter is an important issue when the distance is above 1.4 AU.

While the downlink time and data volume estimations shall be refined in the next phases considering the varying of the ground station performances when varying the S/C elevation, the following options can be considered to reduce the downlink time:

- X-band: G/S arraying (use of two 35m stations in parallel). This would mean half of D/L time, to be traded off with operation constraints and cost.
- X-band: usage of 64 m Usuda JAXA G/S during the nominal downlink. The downlink data rate increases 3 times for the pass. This translates roughly into 30% less downlink time assuming 1 over 3 passes is with Usuda G/S. To be further investigated considering G/S visibility and including in the analysis the variation of the G/S performance with the elevation.
- X-band: Increase power to 100 W (no mass penalty, +60 W peak power). TBC the impacts at system level.
- X-band: transmission of both RHCP and LHCP in parallel using the two TWTAs. This would mean half of D/L time, to be traded off in terms of complexity and cost of the RFDN, reliability and at system level for the increased power consumption (+120 W peak power).

## 16.6 Options for ISL

The main option for the ISL is to use a solution based on passive antennas coupling. This option is described in section 16.2.5.2.

## 16.7 Technology Needs

The following developments have been identified:

Technology Needs						
*	Equipment Name & Text Reference	Technology	Supplier (Country)	TRL	Funded by	Additional Information
*	S-band ISL with active antennas	Increase maximum distance to 3000 km; Addition of adaptable data rate; COTS qualification for deep space.	Portugal, France, Denmark	5	TRP, GSTP	Ranging and time transfer to be added or improved as a goal (not mandatory for mission objectives).
	S-band ISL with active antennas	Increase RF output power.	Portugal, France, Denmark	5	TRP, GSTP	More link margin and accommodation of magnetometer boom on the same face of the antenna.

Technology Needs						
*	Equipment Name & Text Reference	Technology	Supplier (Country)	TRL	Funded by	Additional Information
						Impact to be evaluated at system level.
	S-band ISL with passive antennas	Upgrades to reach 50 kbps from 900 km simultaneously from 2 probes; Addition of adaptable data rate; Removal of handshaking protocols when establishing the link in TDMA.	Portugal, France, Denmark	5	TRP, GSTP	To support 50 kbps simultaneous stream of data from two probes to the main S/C from 900 km distance. Impact of increased RF power to be evaluated at system level.

\* Tick if technology is baselined

## 17 DATA HANDLING

### 17.1 Requirements and Design Drivers

Subsystem Requirements		
Req. ID	Statement	Parent ID
DHS-010	The DHS shall manage S/C A modes, platform and payload equipment and offer enough storage capability for the science data from all three spacecraft (A, B1 and B2).	
DHS-020	The DHS of S/C A shall be dual lane with cold redundancy.	
DHS-030	The DHS shall perform thermal control of S/C A.	
DHS-040	The DHS of S/C A shall perform thermal control of probes B1 and B2 before release.	
DHS-050	The DHS of S/C A shall be based on radiation-hardened components.	
DHS-060	The DHS for S/C A shall be compact and have a high TRL.	
DHS-100	The DHS for probe B2 shall be able to manage the power and thermal subsystem through PDU commanding.	
DHS-110	The DHS of probe B2 may be based on radiation-tolerant or COTS components.	
DHS-120	The probe B2 platform bus should be isolated from S/C A platform bus to avoid failure propagation.	
DHS-130	The DHS of probe B2 shall be compact and lightweight.	
DHS-200	Both DHS for S/C A and probe B2 shall connect to the payload equipment via SpaceWire links.	
DHS-210	Time Synchronisation accuracy requirements between S/C A and probe B2 are in the order of 50 ms.	
DHS-220	The DHS subsystems of S/C A and probe B2 shall be compatible with the mission total dose which is estimated at about 30 kRads.	

### 17.2 Assumptions and Trade-Offs

Assumptions	
1	As far as possible, off-the shelf components with high TRL shall be used for the DHS on both S/C A and probe B2.
2	The science data volumes for S/C A, B1 and B2 are assumed to be 161 Gbits, 50 Gbits and 50 Gbits respectively.
3	Due to the size, mass, and power constraints of probe B2, the DHS must be reduced to a single board computer design.
4	In the nominal functionality, the science data storage capability on probe B2 is assumed to be transmitted in real time through the ISL.
5	Miniaturised solid state mass memory will also be supported on the probe B2 DHS

### Assumptions

for potential retransmissions.

6 In order to reuse existing developments and to keep size/power/mass budgets low, it is assumed that the payloads of probe B2 will support HK TC/TM through the Payload Link (SpW).

## 17.3 Top level Design

A block diagram of the S/C A - probe B2 pair is shown in Figure 17-1.

S/C A is responsible for:

- Telemetry and telecommand (TM/TC) handling
- Modes, Reconfiguration management
- Management of the thermal, power, AOCS and propulsion subsystems
- Management of the S/C A payload instruments
- Storage of S/C A payload data to the Mass Memory
- Reception of probes B1 and B2 data storage to the Mass Memory.

S/C A is built around a platform bus used to control Mass Memory, RIU, the payloads and the power subsystem.

The OBC is the overall coordinator, acting as Bus Controller and controlling the Mass Memory, RIU and Power Subsystem.

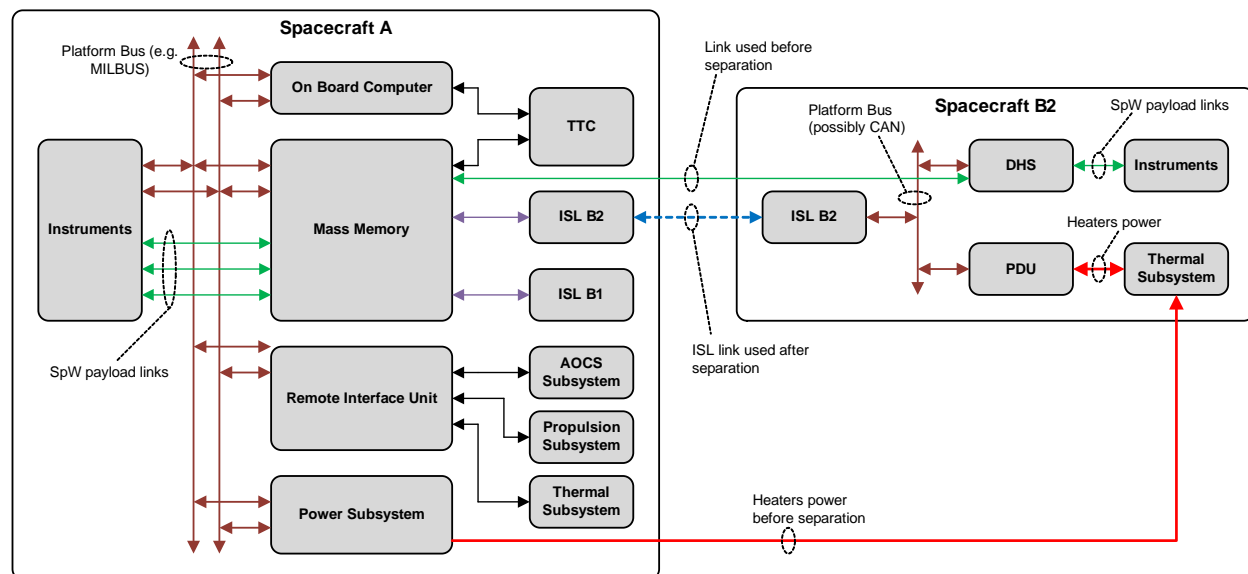


Figure 17-1: Top Level architecture<sup>29</sup>

The Mass Memory stores the science data coming from S/C A instruments as well as probes B1 and B2 through the ISLs. The direct connections between the Mass Memory

<sup>29</sup> Note that the ISL and heater links to probe B1 are not shown here, but would be present. In addition, the interface from the B2 DHS to the AOCS reaction wheel on probe B2 is not shown.

and the ISLs, shown in Figure 17-1, are conceptual and in reality, depending on the availability of existing units, this may be performed through the OBC.

The RIU is responsible for acquiring sensor data and controlling actuators of the AOCS, Propulsion and Thermal subsystems with potential contribution from the Power Subsystem (for heaters supply). The heaters of probes B1 and B2 are also supplied with power before probe separation.

Before separation there are two direct interfaces each with probes B1 and B2: one for data communication for periodic checks, and one for heaters management. Acquisition of sensors that have to do with temperatures is assumed to take place by S/C A directly, as B1 and B2 will be nominally off before release.

## 17.4 List of Equipment

### 17.4.1 S/C A

For the implementation of the DHS of S/C A different options exist. The document herein does not propose specific units for its implementation, but rather it presents different examples in order to demonstrate that the budgets that are presented in the end are feasible.

#### 17.4.1.1 On Board Computer and Mass Memory

##### 17.4.1.1.1 Example 1: ADS OSCAR

A classical architecture of a DHS subsystem could consist of separate OBC, SSMM and RIU units. An example of such an architecture (for the OBC and SSMM units only – the RIU is addressed in section 17.4.1.2) is presented herein, based on ADS OSCAR and a standalone SSMM.

OSCAR OBC is a fully redundant computer core based on SCoC3 ASIC made up of two types of boards (RD[48], RD[49]):

- Processor Board: A board implementing the processor module (PM) and its IO (Mil Bus, Space Wire links, UART's), the TM/TC and the reconfiguration unit (RU).
- DC/DC Converter board: A board which generates all the power rails required by the Processor Board and in addition embeds all the power interfaces for a number of HPC and LLC commands and a small number of RSA, BLD interfaces.

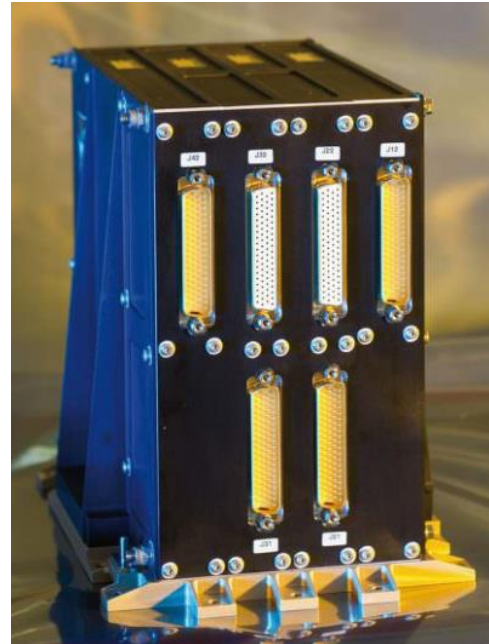
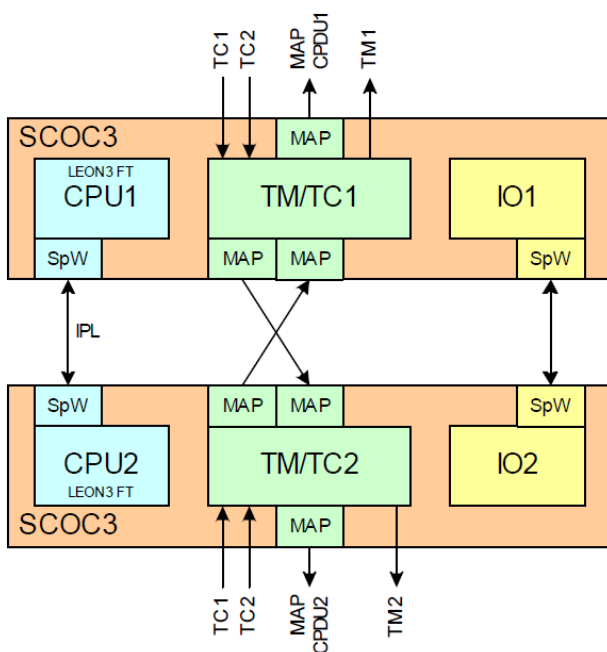


**Figure 17-2: The OSCAR OBC architecture and unit**

The OSCAR OBC consists of:

- Two PM based on Leon3FT core
- Two 512Mbytes Exchange/Mass memory areas
- Two safeguard memories implemented in 512kbytes EEPROM
- Two datation modules
- Two decoders with a 128kbytes Authentication EEPROM
- Two transfer frame generators
- Two reconfiguration units named implemented RadHard FPGA.

Cross-strapping is implemented between:

- The PM and the exchange/mass memories (SDRAM area)
- The PM and the safeguard memories through a SpaceWire link
- The PM and the decoders through MAP links and CLCW links
- The PM and the reconfiguration unit through UART link and “PM Alive” discrete signals
- The PM and the datation modules through discrete signals and a SpW link
- The PM and the transfer frame generators through TFG Data links.

During all mission phases both OBC sides are powered even if the redundant PM does not execute its SW. The reasons are:

- The TC Decoder part is integrated in the SCoC3 ASIC, so the ASIC on the redundant part is also powered

- The cross strapping for the SGM and Exchange/Mass Memory passes through the SCoC3 ASIC
- The Reconfiguration Units operate in hot redundancy.

To this respect the consumption of the redundant side is similar to the nominal side's consumption.

OSCAR OBC has a mass of around **6 kg**, and a consumption of around **20 W**. Its dimensions are **160x200x230 mm<sup>3</sup>**.

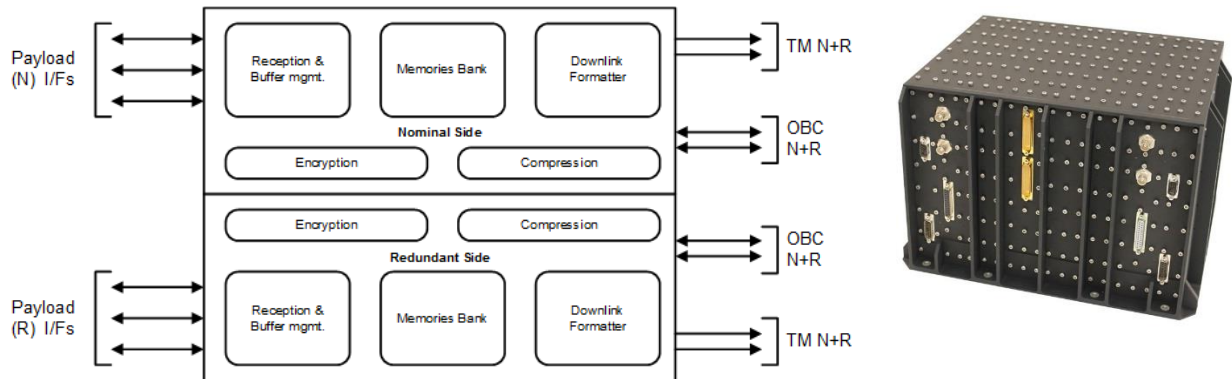


**Figure 17-3: The DSI compact high performance PDHU**

For the SSMM one of the compact ones is the compact high performance PDHU produced by DSI with 1-4 Tbits BoL (RD[50]) of non-volatile storage which has the following characteristics:

- Data storage from different independent input interfaces (up to 1 Gbit/s total)
- Data downlink formatting up to 1 Gbit/s
- CCSDS conform Image Data Compression additional module available (wavelet based)
- Data Encryption (AES, 256 Bit)
- Channel Coding Functionalities (e.g. transfer frame generation, Reed-Solomon)
- CFDP support.

The size of the PDHU is **195x135x195m<sup>3</sup>**.

#### 17.4.1.1.2 Example 2: RUAG Next Generation OBC

Another example with SSMM integrated with the OBC is based on RUAG Next Generation OBC. It is based on a System-on-Chip (SoC) called CREOLE (RD[51], RD[52]), which includes the TM/TC handler. The SoC is based on a LEON2FT processor, provides 7 SpaceWire interfaces, 2 CAN bus interfaces, 2 MIL-STD-1553B bus interfaces, 2 PPS inputs, and the telecommunication interface.

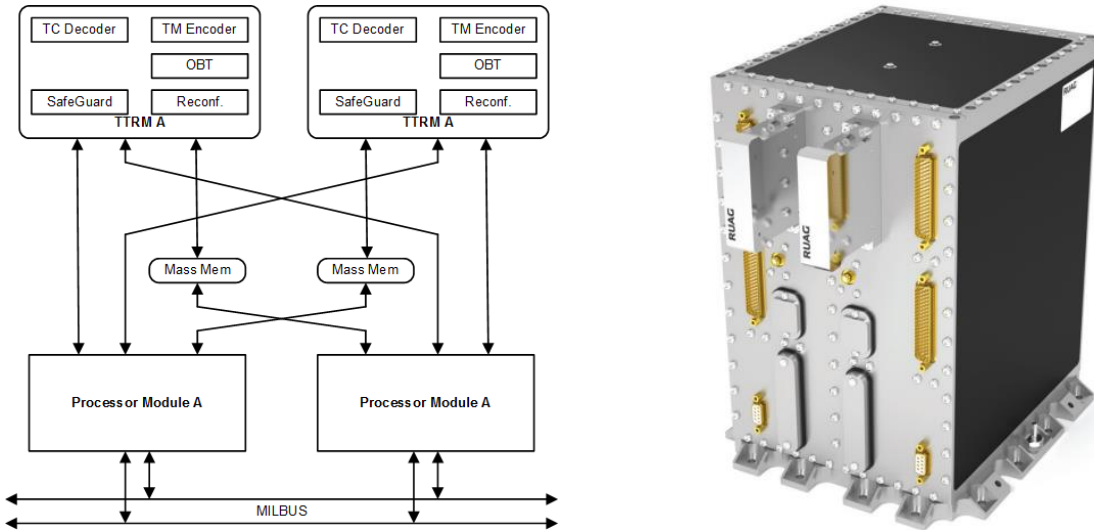


**Figure 17-4: RUAG Next generation OBC architecture and unit**

As shown in Figure 17-4, the OBC is a fully redundant unit with internal cross-coupling between all important sub-systems. The unit provides 374 Gbits of data storage (with EDAC included) in its default configuration, which covers the requirements for payload storage.

From the implementation point of view, the solution is similar to OSCAR since:

- Each string consists of two boards, the Core Processing and the Power Supply boards
- Both strings are continuously powered since TC/TM/PM are integrated in the CREOLE ASIC and there are two hot redundant Reconfiguration Modules.

This solution has the advantage that it integrates 7 SpW interfaces on each lane for connectivity to the payloads and has storage capacity of 374 Gbits, which covers the needs of  $161+50+50 = 261$  Gbits for S/C A, B1 and B2 respectively.

RUAG CREOLE based OBC has a consumption of **23W**, a mass of **6.5 kg**, and external dimensions **208x242x278 mm<sup>3</sup>**.

#### 17.4.1.1.3 Example 3: Thales IPAC

The current assumption for the total amount storage requirements for S/C A, B1 and B2 is 261 Gbits, including margins, which could be supported by the RUAG Next Generation OBC. In case higher amount of storage is required, a solution could be found through the use of TAS IPAC OBC (RD[53]) which is an integrated solution, integrating OBC, SSMM and RIU functionalities.

IPAC is a fully redundant computer with 512 Gbits platform memory and an option for up to 2Tbit Payload Mass Memory. It is based on GR740 which is a quad core LEON4 processor delivering up to 1700 MIPS and integrates a SpW Router with 8 SpW links, CAN and MILBUS interfaces. Except for the OBC module (core module) which integrates TM/TC, CPDU for autonomous HPC generation, HPTM for essential TM, 512 Gbits memory, IPAC has two additional options which result in high integration:

- Mass Memory option: It offers up to 2+2 Tbits NAND flash memory for science storage offering 2 HSSL up to 1.2 Gbps and high speed TM links (600 Mbps).
- AOCS and I/O option: it offers acquisition of 4 FSS, 12 CSS, 2 MGM, 4 STR, control of 3 MTQ, 4 RW, propulsions and Solar Array subsystem management interfaces.

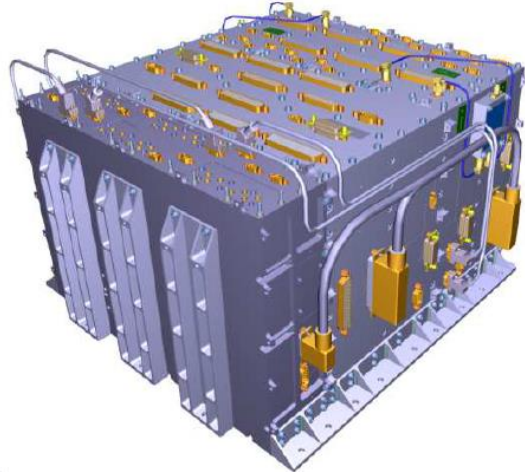


**Figure 17-5: The Thales IPAC OBC**

#### **17.4.1.2 Remote Interface Unit**

The RIU provides a diversity of interfaces to support connection to sensors and actuators that are not connected to the platform and payload buses. These sensors/actuators have to do with AOCS, GNC, and Housekeeping.

The functionality of the RTU is to:

- Condition the analog sensors signals and perform the acquisition
- Acquire digital telemetry
- Provide High Priority and Low Level commands for units ON/OFF and reconfigurations
- Control the propulsion actuators
- Control AOCS actuators and sensors
- Distribute power to thermal control heaters (including probe B1 and B2 heaters for the time before separation)
- Provide communication with the OBC providing the acquired telemetry and receiving the actuator commands.

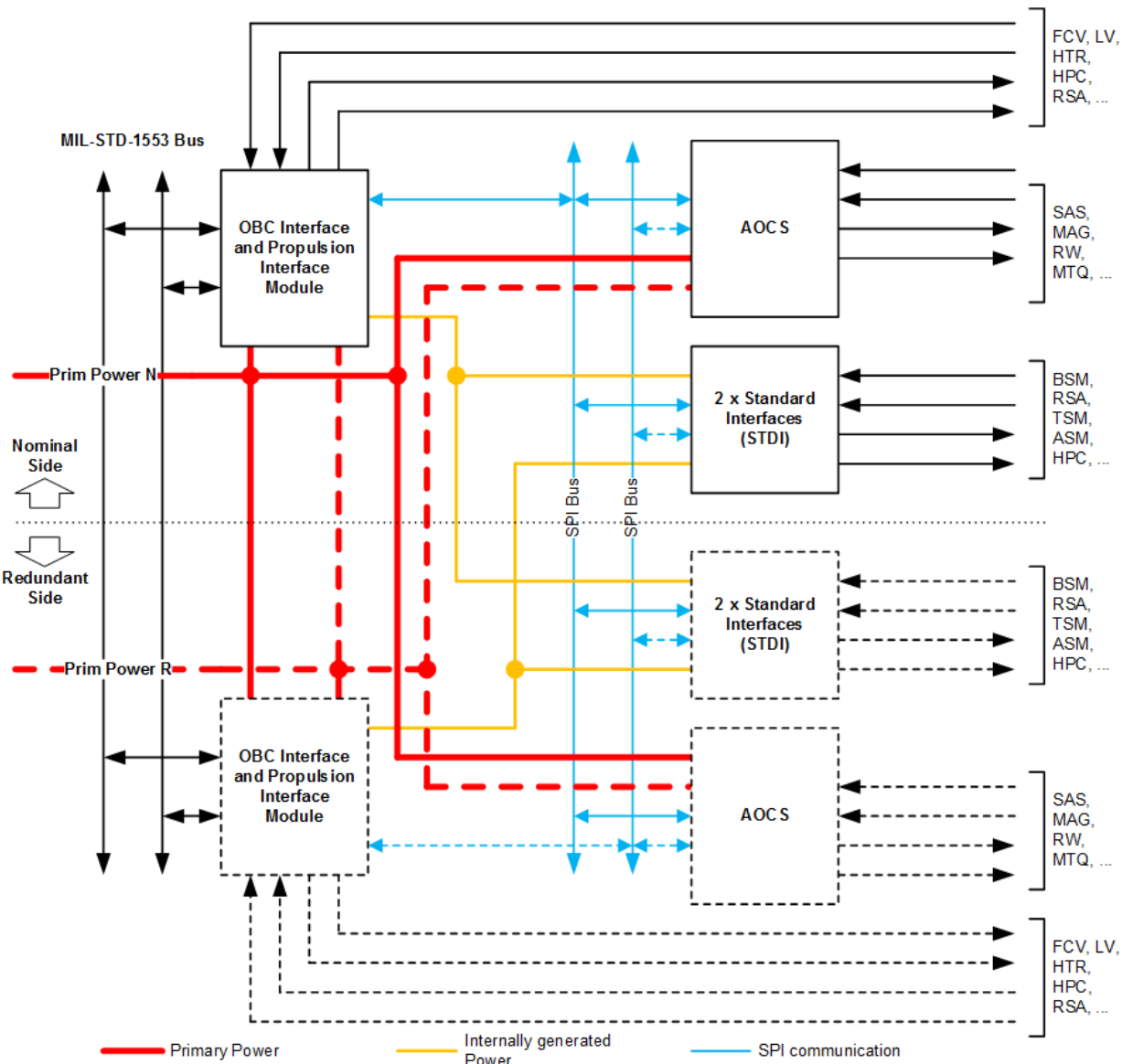


**Figure 17-6: RIU Architecture (redundant boards & I/Fs in dashed)**

The sizing of the RIU has been performed with a comparative evaluation with similar missions in order to define the types and number of interfaces anticipated for the Comet Interceptor mission.

The CRISA RIU (RD[54]) is modular allowing a different mix of boards to be installed in the unit to compensate for mission needs. Communication inside the units is performed through SPI and the unit supports two sides, both sides being commandable either by the nominal or redundant OBC C&C interface module. A typical configuration for the CRISA AS250 RIU is presented in Figure 17-6. There are 4 functions:

- OBC Interface function
- Standard Interfaces function
- AOCS Interfaces function

- Propulsion function.

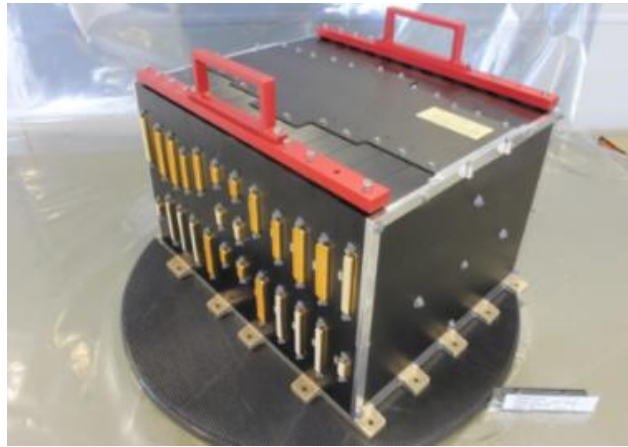


**Figure 17-7: AS250 RIU by ADS**

The budgets for AS250 RIU can be found in Table 17-1.

Remote Interface Unit Budgets	
Unit Size	336 x 230 x 338 mm
Mass	12 kg
Power Consumption	30 W
Configuration	1 OBC and Propulsion Interface Module 2 Standard Interface Module 1 AOCS Interface Module

**Table 17-1: RIU Budgets**

#### 17.4.1.3 Comparison and conclusions for S/C A

A summary of the pros and cons of the examples presented above can be found in Table 17-2.

Example		Mass (kg)	Margin	Total (kg)	Power (W)
Separate SSMM	OBC	6	5%	6.3	20
	SSMM	6	20%	7.2	12
	RIU	12	20%	14.4	28
<b>TOTAL</b>				<b>27.9</b>	<b>60</b>
OBC & SSMM integrated	OBC+SSMM	6.5	20%	7.8	23
	RIU	12	20%	14.4	30
<b>TOTAL</b>				<b>22.2</b>	<b>53</b>

Example		Mass (kg)	Margin	Total (kg)	Power (W)
All integrated	OBC & SSMM & RIU	16	20%	19.2	<70
<b>TOTAL</b>				<b>19.2</b>	<b>&lt;70</b>

**Table 17-2: S/C A DHS examples comparison**

From the above it becomes clear that a solution is feasible, with the values indicated in Table 17-3 being used at system level for the sizing case.

Estimated budgets for the DHS of S/C A	
Mass	22.2 kg
Power Consumption	< 70 W

**Table 17-3: S/C A DHS budgets<sup>30</sup>**

#### 17.4.2 Probe B2

Probe B2 is constrained by mass, size and power. Its lifetime is short so COTS components are also an option provided that there are reliability data available. It must be noted that the B2 mission is a single-shot mission, with no opportunity for ground intervention in case of failures; in addition, while the lifetime is short, it also takes place after up to 5 years in deep space.

Example solutions (discussed further below) are:

- MASCOT which is based on radiation hardened and radiation tolerant components and has already flight heritage. Minor modifications would be required here.
- GomSpace Nanomind Z7000 which is a module used on cubesats. Radiation performances are unknown but an activity is running which will provide data.
- GR716 computer board which targets GomX5, is based on Cobham-Gaisler GR716 microcontroller and is currently under development.

##### 17.4.2.1 Example 1: MASCOT

MASCOT is a computer consisting of two boards, the computer board and the Mass Memory and I/O board. MASCOT provides 4 SpW links, two of which are connected to the computer board and two on the Mass Memory and IO board, provides 7 UART RS-422 interfaces, 16 digital and 16 analog I/Os. In its original configuration it is redundant and one SpW link from each board is used for cross strapping with the redundant side, thus reducing the number of available SpW links for connection to the payload to 2 (RD[55]).

MASCOT also incorporates 1 Gbit NAND Flash memory with Reed Solomon correction on the Memory and IO board, which can be used as Mass Memory.

<sup>30</sup> Note that in the System modelling, a total DHS mass of 19.4 kg is assumed, with a power of 53 W.

The Computer board of MASCOT is based on GR712 which is radiation hardened, whereas the Memory and IO board is built around a ProASIC3 FPGA, which although not hardened, has good radiation performance for the Comet Interceptor and is being used in many missions. It does not present any degradation up to 22 kRads, 7% degradation up to 40 kRads, 15% degradation up to 55 kRads and it is SEL free up to 55 MeVcm<sup>2</sup>/mg (RD[58], RD[59]).



**Figure 17-8: MASCOT Computer board and Mass Memory and IO board**

The MASCOT OBC would require some modifications for probe B2 for the following reasons:

- The instruments have baseline SpW links as payload I/F
- The baseline choice for the RF is CAN bus (potentially I2C)
- Isolation between S/C A and probe B2 platform buses is required in order to avoid failure propagation
- It is preferred to gather all SpW links to the Mass Memory and IO board for storage rather than using links scattered between Computer and Memory and IO boards.

To this respect, one example option is the one shown in Figure 17-9, in which the Payload SpW links are all connected to the Memory and IO board, two SpW links are used for connection to S/C A, and a modification to add CAN bus inside the ProASIC FPGA of the Memory and IO board is proposed in order to provide communication with the ISL and potentially the PDU. For the PDU the RS-422 UART links can also be used.

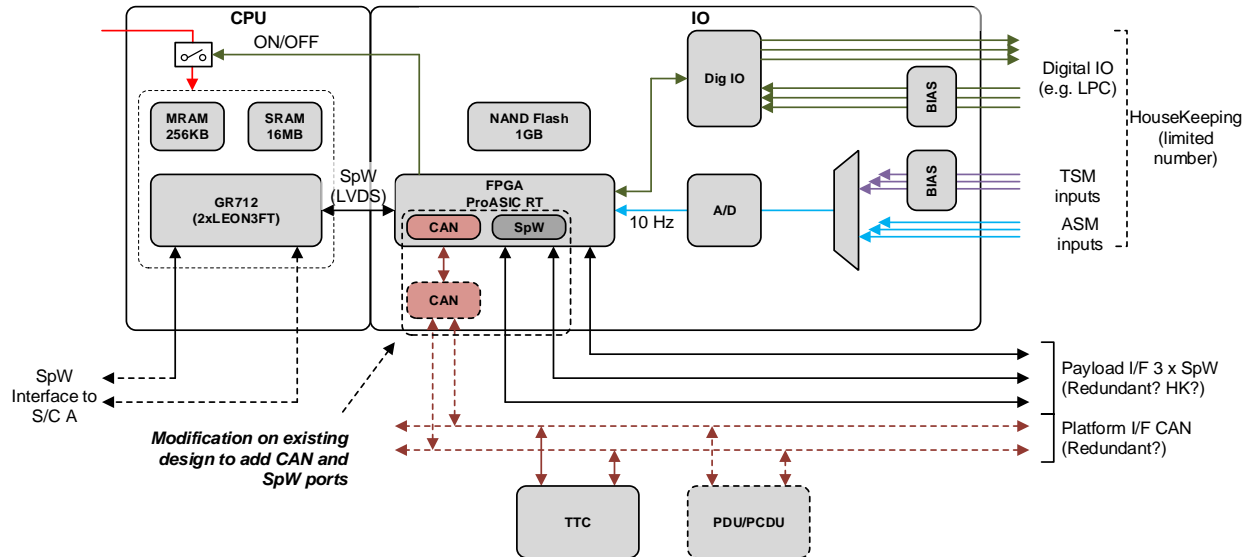


**Figure 17-9: MASCOT example modifications**

#### 17.4.2.2 Example 2: GomSpace Z7000 board

The Z7000 board (RD[56]) is based on Xilinx Zynq 7000 APSoC which is the integration of a dual A9 ARM processor with programmable logic array and as such has inherent advantages regarding flexibility, processor performance, throughput performance, thanks to the integration of processors and logic in the same die etc.

The board offers 1 GB of DDR3 memory and 32 GB storage and also offers CAN/I<sup>2</sup>C interfaces implementing the CSP protocol, which is also adopted by the baseline ISL module. The processor runs up to 1 GHz delivering up to 2.5 MIPS/MHz when no SW mitigation techniques are used.

The main component used, although not radiation hardened does not present latch ups. It presents though micro latch ups over 13.8 MeVcm<sup>2</sup>/mg which are not destructive, do not halt the operation of the module, but for sure they shall be handled for graceful processor operation upon their detection. Regarding SEFIIs/SEUs the programmable logic part behavior is known as there is a lot of data in the literature (presenting among others multi-bit upsets in the configuration memory and cluster upsets in the Block RAMs as reported in RD[60], RD[61], RD[62], RD[63]) but for the processor part little data is available in the literature (RD[64]). In addition, it is a COTS component, so all data above are indicative and can depend per lot.

An example architecture of the DHS system based on Z7000 is shown in Figure 17-10, along with a picture of the module.

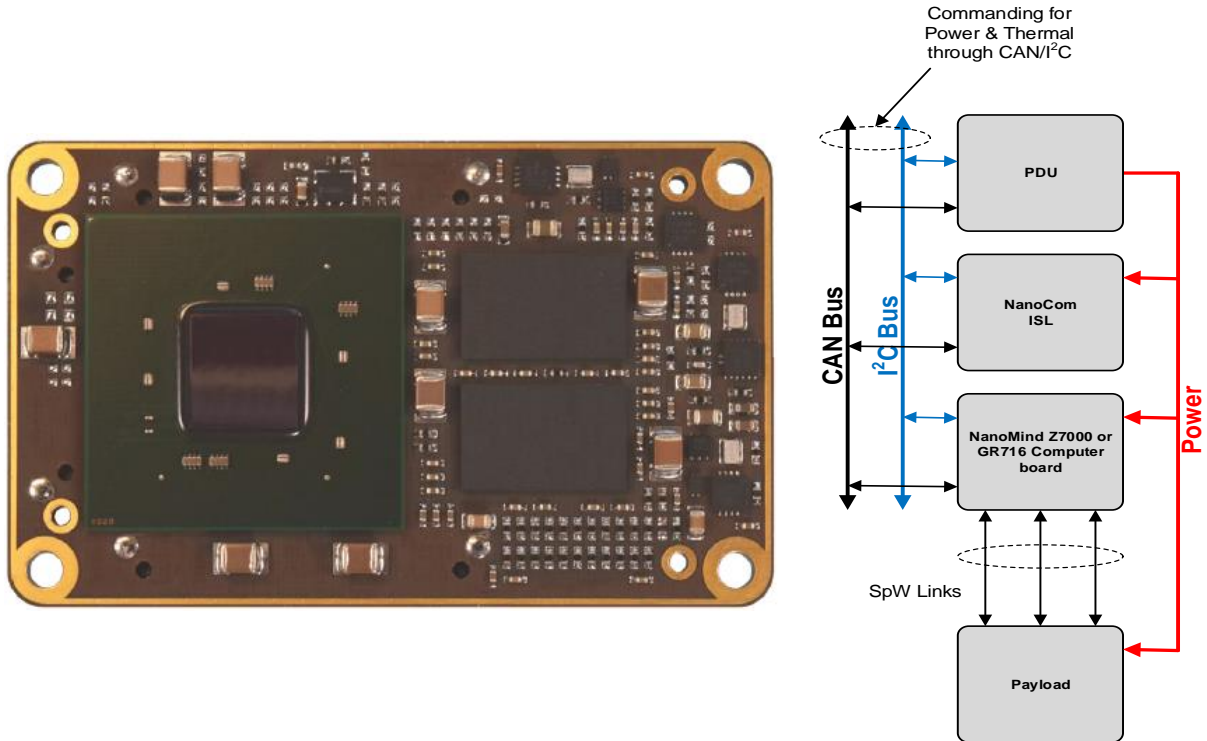


**Figure 17-10: Z7000 module and respective architecture**

#### 17.4.2.3 Example 3: GR716 Computer board

The third example lies in between the two previous ones. It is based on a GSTP activity which develops a computer board which, on one hand is targeting GomX5 so the same architecture as shown in Figure 17-10 can be adopted, but on the other hand is based on the radiation hardened GR716 microcontroller. The board will reach TRL4 readiness and is planned for flight in GomX5 in 2021 and it will integrate SpW, I<sup>2</sup>C, SPI, CAN interfaces as well as SDRAM for storage. The GR716 microcontroller (RD[56]) is originally designed for applications such as RIU central controller, Instrument control, mechanisms/power control or robotic applications but has the workload to satisfy the requirements of the B2 probe and offers significant advantage in terms of reliability compared to COTS implementation. Its main characteristics are the following:

- MILBUS interface
- CAN 2.0B interface
- UARTs, SPI, GPIOs
- SpaceWire interfaces up to 100 Mbps
- Boot from external SRAM/PROM/SPI memory protected by EDAC and dual memory redundancy
- PROM/SRAM interface with BCH EDAC.

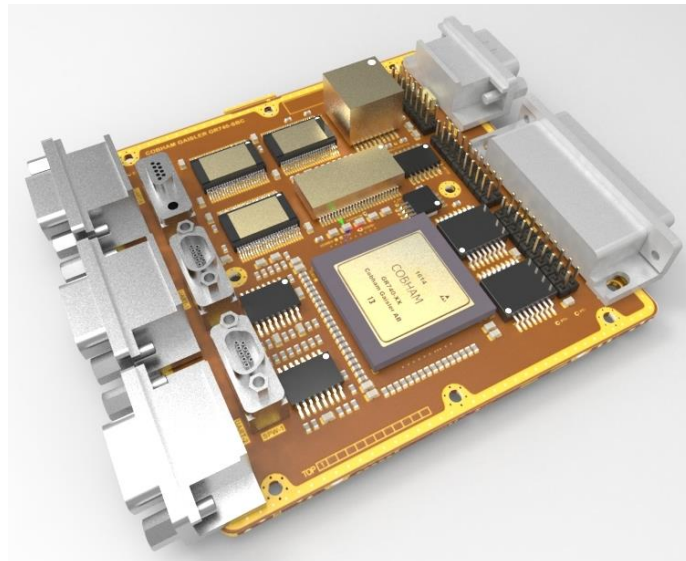


**Figure 17-11: The GR716 Computer Board**

#### 17.4.2.4 Comparison and conclusions

A summary of the pros and cons of the examples presented above can be found in Table 17-4.

	MASCOT	GomSpace Z7000	GR716
<b>Reliability/ Availability</b>	✓	TDA on going to define	✓ (expected)
<b>Interface to comms</b>	Modification to add CAN at least	✓	✓ (activity targets GomX5)
<b>Interface to PDU</b>	✓ (RS-422 can be used)	✓	✓
<b>Interface to payload</b>	Modification to add extra SpW channel	Modification to add SpW channels	✗ (Limited number of SpW ports)
<b>Discrete interfaces</b>	8+8 TTL DIO, 16 Analog In	75 LVDS pairs or 150 DIO	ADC/DAC/GPIO
<b>Maturity</b>	✓	CubeSat heritage only	Under development
<b>Radiation performance</b>	✓	TDA on going to define	✓ (expected)
<b>Physical</b>	5 W, 1 kg	2.3 W, 100 g, 60 x 40 x 6.5 mm <sup>3</sup>	5W, 1.3 kg, 100 x 100 x 15 mm <sup>3</sup>

**Table 17-4: Probe B2 DHS examples comparison**

From the above it becomes clear that although a definitive solution is not proposed here, the probe B2 OBC should be feasible within the following envelope (used at system level for the sizing):

Estimated budgets for the DHS of probe B2	
Unit Size	120 x 120 x 50 mm
Mass	1 kg
Power Consumption	5 W

**Table 17-5: Probe B2 DHS budgets**

**It should be noted that for further reduction, mainly in size, the probe B2 DHS subsystem could be integrated with the PDU.**

## 17.5 Technology Needs

Technology Needs						
*	Equipment Name & Text Reference	Technology	Supplier (Country)	TRL	Funded by	Additional Information
	OSCAR		Airbus	9		
	Next Generation OBC		RUAG Sweden	6		
	IPAC		Thales	5		
	Remote Interface Unit		Airbus DS	9		
	MASCOT Single-Board Computer		Cobham Gaisler	6		Modifications would be required for the mission as described above
	GomSpace Z7000		GomSpace	3		Parallel activity is running to assess radiation performance and to identify potential hardening requirements/techniques
	GR716 computer board		Cobham Gaisler	3		

\* Tick if technology is baselined

This Page Intentionally Blank

## 18 THERMAL

### 18.1 Requirements and Design Drivers

#### 18.1.1 TCS Requirements

The objective of the Thermal Control Subsystem (TCS) is to guarantee that all units, equipment, parts and components remain within their design temperature ranges and that spatial and temporal temperature gradients are not exceeded during the complete mission lifetime. This applies to S/C A and probe B2 stacked together and also for the S/C A and probe B2 when separated from each other. The probe B1 thermal control is not addressed here as it is under JAXA's responsibility.

Table 18-1 summarises the requirements applicable to the TCS in the frame of the Comet Interceptor (CI) study.

Thermal Subsystem Requirements		
Req. ID	Statement	Parent ID
THE-010	The TCS shall maintain all satellite subsystems within their operating range while in operation and within their survival temperature range during all other mission times.	
THE-020	The TCS shall minimise the use of active thermal control techniques.	
THE-030	The TCS shall ensure the probes B1 and B2 do not exceed the TBD temperature range up until deployment.	
THE-040	The TCS shall maintain the propellant tank and feed lines temperatures in the following range for the whole duration of the mission: [TBD].	
THE-050	The TCS shall minimise the necessary amount of heating power for the cold cases.	

**Table 18-1: TCS Requirements**

Table 18-2 and Table 18-3 present the Op. and Non-Op. Design Temperature Limits for the S/C A and probe B2. Unit temperature limits will have to be confirmed in the next steps. Some of them are based on assumptions, experience of the thermal team and previous studies.

AOGNC units	Temp. non-op min (°C)	Temp. op min (°C)	Temp. op max (°C)	Temp. non-op max (°C)
DPU (Data Processing Unit)	-65	-60	35	40
IMU (Northrop Grumman LN200 Core #1&2 (2-off))	-59	-54	71	76
NAVCAM OH 1 (NAVCAM Optical Head #1&2 (2-off))	-65	-60	35	40
STR OH 1 (STR Optical Head #1&2 (2-off))	-40	-60	35	40
SUN LENS (SUN LENS Bison 64 #1 to 6 (6-off))	-45	-40	80	85
RW_RSI_4_215 (Rockwell Collins RSI 4- #215 to 218 (4-off))	-40	-20	70	75

<b>Instrument units</b>	Temp. non-op min (°C)	Temp. op min (°C)	Temp. op max (°C)	Temp. non-op max (°C)
CoCa_CSU (Camera Support)	-25	-20	25	35
CoCa_ELU (Electronics Unit)	-20	-20	60	70
DFP_DISC (Dust Impact Sensor and Counter)	-50	-40	70	80
DFP_E_Box (Electronic Box)	-25	-20	40	50
DFP_SCIENA ENA sensor	-50	-40	65	70
DFP_SCIENA Ion sensor	-50	-40	65	70
MIRMISS_TIRI (Thermal InfraRed Imager)	-40	-30	60	70
DFP_LEES_1 ( Low Energy Electron Spectrometer 1)	-50	-40	50	60
CoCa_PEU (Proximity Electronics Unit)	-20	-20	60	70
CoCa_Rad (Radiator)	-60	-50	-30	60
DFP_COMPLIMENT (COMetary Plasma Light Instrument probe #1)	-190	-190	100	110
MANiac_ELU (Electronics Unit)	-30	-20	40	50
MANiac_NDG (Neutral Density Gauge)	-30	-20	40	50
MANiac_SHU (Sensor Head Unit)	-30	-20	40	50
MIRMISS_MIR_1 (Mid-InfraRed Sensor 1&2 (2-off))	-40	-30	60	70
MIRMISS_NIR (Near InfraRed Sensor)	-40	-30	60	70
MIRMISS_Rad (Radiator)	-60	-50	60	70
DFP_COMPLIMENT (COMetary Plasma Light Instrument boom 1)	-190	-190	100	110
DFP_COM_FGM (COMPLIMENT+FGM+boom_2)	-80	-70	60	70
<b>COM units</b>	Temp. non-op min (°C)	Temp. op min (°C)	Temp. op max (°C)	Temp. non-op max (°C)
X-Band DSTRASP #1&2 (2-off)	-40	-20	65	70
X-Band HGA	-155	-150	150	150
X-Band LGA #1&2 (2-off)	-155	-150	150	150
X-Band RFDN	-40	-30	60	70
X-Band TWT #1&2 (2-off)	-40	-20	60	70
X-Band TWTA EPC #1&2 (2-off)	-30	-20	60	70
ISL GOMx Electronics #1&2 (2-off)	-40	-30	85	95
ISL GOMx Antenna Patch #1 to 6 (6-off)	-40	-30	85	95
<b>CPROP units</b>	Temp. non-op min (°C)	Temp. op min (°C)	Temp. op max (°C)	Temp. non-op max (°C)
Fill Drain Valves	0	0	50	50
Latch Valves	0	0	50	50
Pipes	0	0	50	50

Pressure Transducer #1	0	0	50	50
Propellant Filter	0	0	50	50
Test Ports	0	0	50	50
Tank CPROP #1&2 (2-off)	-48	-48	200	200
5N Thruster #1 to 8 (8-off)	-48	-48	200	200
<b>DH units</b>	Temp. non-op min (°C)	Temp. op min (°C)	Temp. op max (°C)	Temp. non-op max (°C)
OBC (Onboard Computer)	-40	-30	60	75
RIU (Remote Interface Unit)	-40	-30	60	75
<b>EPROP units</b>	Temp. non-op min (°C)	Temp. op min (°C)	Temp. op max (°C)	Temp. non-op max (°C)
PPU (Power Processing Unit)	-45	-25	70	70
Thruster PPS1350	-48	-48	200	200
BPRU	-30	20	50	50
FU	-45	-40	70	70
Miscellaneous	-30	-30	50	50
PRE Card	-40	-20	70	70
XFC	-15	-15	95	95
Propellant Tank #1&2 (2-off)	-20	-20	50	50
<b>MEC units</b>	Temp. non-op min (°C)	Temp. op min (°C)	Temp. op max (°C)	Temp. non-op max (°C)
APM_HDRM_APME (Antenna Pointing Mechanisms + Driver and HDRM)	-45	-45	145	145
SA1 HDRM #1 to 4 (4-off)	-120	-120	120	120
SA2 HDRM #1 to 4 (4-off)	-120	-120	120	120
SA drive electronics	-50	-50	40	40
SADM #1&2 (2-off)	-120	-120	120	120
Clamp Band Ejection System	-40	-40	145	145
<b>PWR units</b>	Temp. non-op min (°C)	Temp. op min (°C)	Temp. op max (°C)	Temp. non-op max (°C)
Solar Array #1&2 (2-off)	-150	-150	150	150
Battery	-10	10	30	45
PCDU	-40	-20	60	60

**Table 18-2: S/C A: Op. and Non-Op. Design Temperature Limits<sup>31</sup>**

<sup>31</sup> Note that these refer to the equipment for the baseline sizing case equipment

	Temp. non-op min (°C)	Temp. op min (°C)	Temp. op max (°C)	Temp. non-op max (°C)
<b>AOGNC units</b>				
RW (Astrofein RW250)	-30	-20	50	60
<b>INS units</b>				
DFP DISC (Dust Impact Sensor and Counter)	-50	-40	60	70
DFP E-Box	-30	-20	40	50
EnVisS (Entire Visible Sky)	-40	-30	40	50
OPIC (Optical Imager for Comets)	-40	-30	70	75
DFP FGM #1&2 (2-off)	-100	-100	60	70
DFP FGM boom	-100	-100	60	70
<b>COM units</b>				
ISL Toroidal LGA	-150	-150	150	150
ISL Electronics	-40	-30	85	95
ISL Active Antenna FE	-40	-30	85	95
<b>DH units</b>				
OBC (Onboard Computer)	-40	-30	60	75
<b>MEC units</b>				
Clamp band Ejection System	-40	-40	145	150
<b>PWR units</b>				
Battery	-10	10	30	45
PDU	-40	-20	60	60

**Table 18-3: Probe B2: Op. and Non-Op. Design Temperature Limits<sup>31</sup>**

### 18.1.2 TCS Design Drivers

The design of the CI Thermal Control Subsystem (TCS) is driven by several factors. Generic design drivers for the TCS are limiting thermal requirements, dissipation and different operational modes. Furthermore, the attitude in space is an important contributor. Other drivers are the dimensions of the spacecraft and its overall shape. Specific thermal design drivers for the CI study are the distance to the Sun, potential fly-bys at celestial bodies other than the target object and the proximity operation at the target body.

For the CI study, the attitude of the spacecraft is relevant with regard to the Sun for power generation, the Earth for communication and the target body for the actual science and mission objectives. Especially with regard to the fact that, in principle, the target body could appear at any time and from any direction. The TCS cannot be sized to cope with any orientation towards the Sun without increasing significantly the TCS complexity and potentially also its mass. Restrictions are mainly caused by the direct impact of solar heat flux on the radiator surfaces. Oversizing the radiators for conditions with prolonged exposure to solar heat flux will directly have a negative impact on heater

power demand and subsequently the power subsystem. As such, constraints were set at system level to ease the design (see Section 7.1).

Different operational modes impact the TCS of CI, especially with regard to dissipation during electric propulsion thrust phases or communication phases. The relevant subsystems are physically separated. Thus their dissipation has to be treated with individual radiators or has to be combined in larger radiators. Larger radiators require means of heat distribution via doublers and/or heat pipes. Furthermore, during the science operation different subsystems of the spacecraft operate for a prolonged period of time requiring yet another distribution or rejection of the dissipated heat.

The distance to the target body was addressed during the previous study. Even at the closest encounter of S/C A at a distance to the target of 1000 km, only an extremely large target would have a thermally relevant impact on the spacecraft.

In the CI study, the shape of the spacecraft is well defined. This impacts the TCS as the locating of tanks and internal electrical boxes is driven by the load bearing structure and in consequence has to be reflected by the location of the radiators. The location of scientific instruments, solar arrays, high gain antenna, inter-satellite-link antennae, and thrusters usually further restrict the available real estate for radiators. Paints or insulating foils are easier to foresee at this stage of a study and are less impacted by the overall shape of the spacecraft.

The distance to the Sun is extremely relevant in any deep space mission for both the hot and the cold cases. The main external heat source for the spacecraft is the direct solar illumination. Assuming that the interception could take place at the closest or farthest distance from the Sun the radiator sizing is performed at the closest proximity with the highest expected dissipation. By contrast, the heater power sizing takes place at the farthest distance from the Sun with the lowest expected dissipation. Apart from radiator and heater power sizing, the distance to the Sun also impacts the overall surface temperature of the spacecraft and hence the selection of the appropriate materials. The impact of the space environment will be further elaborated in Section 18.2.

## 18.2 Environment

The thermally relevant environment is governed by the distance between the spacecraft and the Sun. Table 18-4 shows the solar heat flux between 0.9 and 1.25 Astronomical Units (AU). At the minimum expected distance of 0.9 AU, the solar heat flux is as high as  $1680 \text{ W/m}^2$  corresponding to 1.23 times the solar constant at 1 AU ( $1361 \text{ W/m}^2$ ). At the maximum distance of 1.25 AU, the solar flux is as low as  $871 \text{ W/m}^2$ , corresponding to 0.64 times the solar constant at 1 AU.

	Average Earth Sun distance	Earth at perihelion (January)	Earth at aphelion (July)	Possible closest approach to the Sun	Possible furthest distance from the Sun
Distance (AU) from the Sun	1	0.983	1.016	0.9	1.25
Sun flux density ( $\text{W/m}^2$ )	1361	1408	1318	1680	871

**Table 18-4: Received solar flux vs distance from the Sun**

Figure 18-1 shows that the heat flux received from the target body is negligible if compared to the received heat flux received from the Sun. The left graph of the figure shows the infrared-red (IR) heat flux and the right graph shows the albedo heat flux. For the computation it was assumed that the comet has an emissivity of 1 and an albedo of 0.06. The closest distance between comet and spacecraft was assumed to be 1000 km. The different lines are derived assuming target bodies with a spherical shape and diameters of 10 km, 50 km, 100 km and 200 km. Even in the unrealistic case of a 200 km target body the maximum IR heat flux would be less than 6  $\text{W/m}^2$  and albedo heat flux would be less than 0.4  $\text{W/m}^2$ .

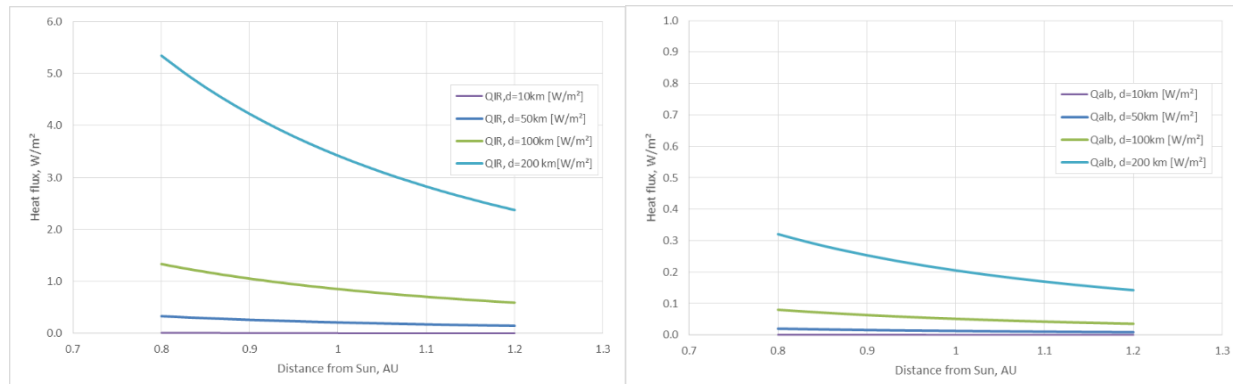


**Figure 18-1: Left) Received IR heat flux, Right) received albedo heat flux; with distance from the Sun for an assumed target body with  $\text{eps} = 1$ , albedo = 0.06 and diameters of 10 km, 50 km, 100 km and 200 km at a closest distance to the target body of 1000 km.**

For the thermal control calculations, albedo/IR flux will be assumed as negligible.

## 18.3 Spacecraft Attitude

### 18.3.1 S/C A

As illustrated in Figure 18-2, S/C A is equipped with 2 deployable solar arrays in +/-Y walls. Once the solar panels are deployed, +Y and -Y walls remain always aligned with the Sun, receiving almost no solar flux, which makes them an ideal place to accommodate radiators. The probes B1 and B2 are attached on +Z side. The chemical and electrical thrusters are accommodated on -Z wall and the remote-sensing

instrument are pointing towards the opposite direction (+Z). As illustrated on the right side of Figure 18-2, it is assumed +X (the generic payload face) never points towards the Sun up to +/-45°, which covers also the comet fly-by.

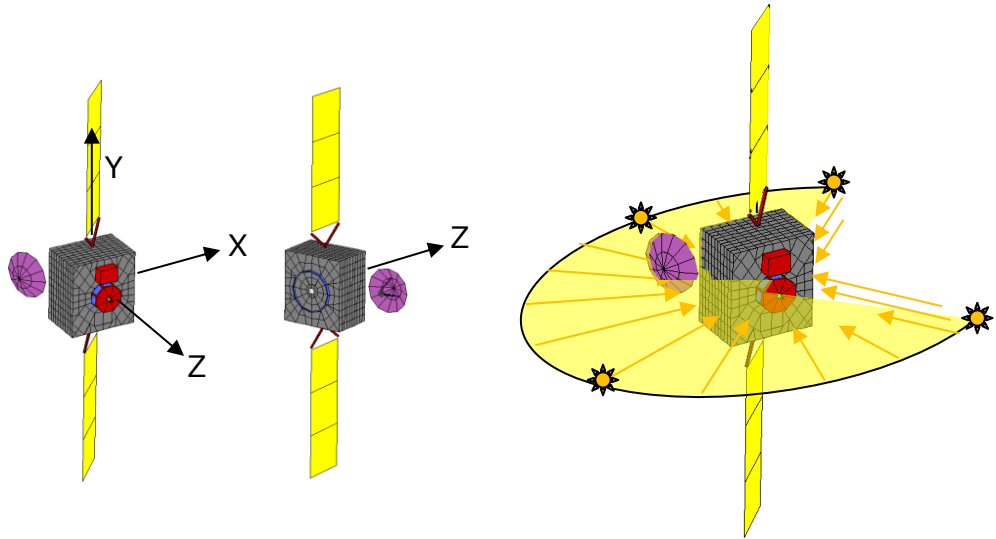


**Figure 18-2: S/C A accommodation and attitude**

### 18.3.2 Probe B2

When it is released from S/C A, the probe B2 is spinning (at least 5 rpm), which is sufficient to homogenise the Sun flux on all the lateral sides ( $\pm X$  and  $\pm Y$ ). +Z is pointed towards the comet (before approach, i.e. along the ram direction) and it is assumed +Z never points towards the Sun up to +/-45°.

## 18.4 Unit Modes and Dissipations

### 18.4.1 S/C A

Table 18-5 below presents S/C A unit dissipations depending on the mode. Note that dissipations are per individual unit.

The LAU mode is assumed to be completely passive.

AOGNC	LAU	SUN	SAFE	STBY	COM	EPTH	SCI
DPU (Data Processing Unit)	0	<b>3.6</b>	<b>3.6</b>	<b>3.6</b>	<b>3.6</b>	<b>3.6</b>	<b>3.6</b>
IMU (Northrop Grumman LN200 Core #1&2 (2-off))	0	<b>6.0</b>	<b>6.0</b>	<b>6.0</b>	<b>6.0</b>	<b>6.0</b>	<b>6.0</b>
NAVCAM OH 1 (NAVCAM Optical Head #1&2 (2-off))	0	0	0	0	0	<b>0.04</b>	<b>0.4</b>
STR OH 1 (STR Optical Head #1&2 (2-off))	0	0	<b>0.4</b>	<b>0.4</b>	<b>0.4</b>	<b>0.4</b>	<b>0.4</b>
RW_RSI_4_215 (Rockwell Collins RSI 4- #215 to 218 (4-off))	0	<b>0.8</b>	<b>2.0</b>	<b>2.0</b>	<b>2.0</b>	0	<b>11.1</b>
INS	LAU	SUN	SAFE	STBY	COM	EPTH	SCI
CoCa_CSU (Camera Support) + ELU (Electronics Unit)	0	0	0	0	0	0	<b>14.4</b>

	LAU	SUN	SAFE	STBY	COM	EPTH	SCI
+ PEU (Proximity Electronics Unit)							
CoCa FPA / Rad (Focal Plane Assembly + Radiator)	0	0	0	0	0	0	<b>0.5</b>
DFP E-Box (Electronic Box)	0	0	0	0	0	0	<b>20.2</b>
+ DISC (Dust Impact Sensor and Counter)							
+ SCIENA ENA sensor & Ion sensor							
+ LEES_1 ( Low Energy Electron Spectrometer 1)							
+ COMPLIMENT (COMetary Plasma Light Instrument probe #1 + FGM + booms)							
MIRMISS_TIRI (Thermal InfraRed Imager)	0	0	0	0	0	0	<b>9</b>
+ MIR (Mid-InfraRed Sensors 1 & 2)							
MANiac_ELU (Electronics Unit)	0	0	0	0	0	0	<b>21.6</b>
+ SHU (Sensor Head Unit)							
MANiac_NDG (Neutral Density Gauge)	0	0	0	0	0	0	<b>3.6</b>
<b>COM</b>	<b>LAU</b>	<b>SUN</b>	<b>SAFE</b>	<b>STBY</b>	<b>COM</b>	<b>EPTH</b>	<b>SCI</b>
X-Band DSTRASP #1&2 (2-off)	0	<b>24.0</b>	<b>24.0</b>	<b>16.0</b>	<b>24.0</b>	<b>16.0</b>	<b>16.0</b>
X-Band TWT #1 (TWT #2 is assumed off)	0	<b>28.3</b>	<b>15.5</b>	0	<b>51.5</b>	0	0
X-Band TWTA EPC #1 (EPC #2 is assumed off)	0	<b>9.0</b>	<b>9.0</b>	0	<b>9.0</b>	0	0
GOMx Electronics #1&2 (2-off)	0	0	0	0	0	0	<b>4.1</b>
GOMx Antenna Patch #1 to 6 (6-off)	0	0	0	0	0	0	<b>3.6</b>
<b>CPROP</b>	<b>LAU</b>	<b>SUN</b>	<b>SAFE</b>	<b>STBY</b>	<b>COM</b>	<b>EPTH</b>	<b>SCI</b>
Latch Valves	0	<b>1.5</b>	0	0	0	<b>0.003</b>	0
Pressure Transducer #1	0	<b>0.2</b>	<b>0.2</b>	<b>0.2</b>	<b>0.2</b>	<b>0.2</b>	<b>0.2</b>
5N Thrusters (cat bed heaters not accounted here)	0	0	0	0	0	0	0
<b>DH</b>	<b>LAU</b>	<b>SUN</b>	<b>SAFE</b>	<b>STBY</b>	<b>COM</b>	<b>EPTH</b>	<b>SCI</b>
OBC (Onboard Computer)	0	<b>23.0</b>	<b>23.0</b>	<b>23.0</b>	<b>23.0</b>	<b>23.0</b>	<b>23.0</b>
RIU (Remote Interface Unit)	0	<b>30.0</b>	<b>30.0</b>	<b>30.0</b>	<b>30.0</b>	<b>30.0</b>	<b>30.0</b>
<b>EPROP</b>	<b>LAU</b>	<b>SUN</b>	<b>SAFE</b>	<b>STBY</b>	<b>COM</b>	<b>EPTH</b>	<b>SCI</b>
PPU (Power Processing Unit)	0	0	0	0	0	<b>80.2</b>	0
<b>MEC</b>	<b>LAU</b>	<b>SUN</b>	<b>SAFE</b>	<b>STBY</b>	<b>COM</b>	<b>EPTH</b>	<b>SCI</b>
APM_HDRM_APME (Antenna Pointing Mechanisms + Driver and HDRM)	0	0	0	0	<b>18.0</b>	0	0
SA drive electronics	0	<b>3.0</b>	<b>5.0</b>	<b>1.0</b>	<b>5.0</b>	<b>5.0</b>	<b>5.0</b>
SADM #1&2 (2-off)	0	<b>2.0</b>	<b>2.4</b>	<b>1.0</b>	<b>15</b>	<b>2.4</b>	<b>15</b>
<b>PWR</b>	<b>LAU</b>	<b>SUN</b>	<b>SAFE</b>	<b>STBY</b>	<b>COM</b>	<b>EPTH</b>	<b>SCI</b>
Battery	0	0	0	0	0	0	0
PCDU	0	<b>30.0</b>	<b>30.0</b>	<b>30.0</b>	<b>30.0</b>	<b>30.0</b>	<b>30.0</b>

**Table 18-5: S/C A units dissipation (W) vs modes**

Note that some units have a constant dissipation throughout the mission, which tends to make their thermal control easy. On the other hand,

- TWT and EPC have peak dissipations during COM, SAFE and SUN modes
- PPU has a peak dissipation during EPTH, and is off the rest of the mission,
- Instruments units are only on during SCI mode, and off the rest of the time,
- RW have peak dissipation during SCI, and low dissipation the rest of the time.

It could be advantageous in future phases to combine these units' accommodation and thermal control, so as to share their heat with thermal spreaders or heat pipes, and save heating power when some of them are off.

#### 18.4.2 Probe B2

Table 18-6 below presents probe B2 unit dissipations depending on the mode. Note that dissipations are per individual unit.

Only two modes are considered: either B2 stowed (i.e. before release from S/C A) or operating after release (with constant power consumption). LAU mode is assumed to be completely passive.

AOGNC	B2 stowed	B2 operating
RW Astrofein RW250	0	4.5
<b>INS</b>	<b>B2 stowed</b>	<b>B2 operating</b>
B2 DFP Dust Impact Sensor and Counter	0	0
B2 DFP E-Box	0	5.2
B2 Entire Visible Sky	0	2.4
B2 Optical Imager for Comets	0	0
B2 DFP FGM #1	0	0.5
B2 DFP FGM #2	0	0.5
B2 DFP FGM boom	0	0
<b>COM</b>	<b>B2 stowed</b>	<b>B2 operating</b>
ISL Toroidal LGA	0	0
B2 GOMx Electronics	0	3.8
B2 GOMx Active Antenna FE	0	0
<b>DH</b>	<b>B2 stowed</b>	<b>B2 operating</b>
OBC (B2 Onboard Computer)	0	3.4
<b>MEC</b>	<b>B2 stowed</b>	<b>B2 operating</b>
Clamp_Band (B2 Clamp Band Ejection System)	0	0
<b>PWR</b>	<b>B2 stowed</b>	<b>B2 operating</b>
Bat_1 (B2 Battery #1)	0	0.1
PDU (B2 PDU)	0	4.1

Table 18-6: Probe B2 units dissipation (W) vs modes<sup>32</sup>

<sup>32</sup> Note that the power values here are lower than the final baseline. The values above suggest a peak consumption of 24.5 W, to be compared with a total dissipation of 46.6 W (average, incl. 20% system margin) or 60.7 W (peak, incl. 20% system margin). Nonetheless, the general design principle still applies and this misalignment is not expected to affect the feasibility. If higher dissipations are to be expected,

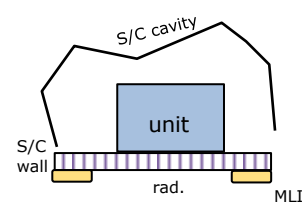
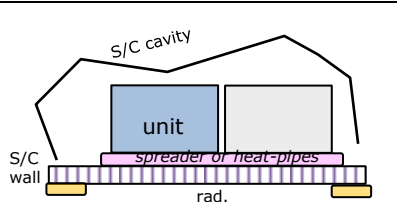
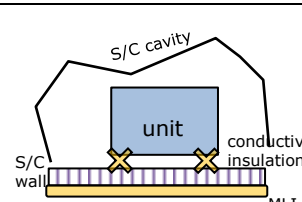
## 18.5 Baseline Thermal Design

### 18.5.1 Thermal Control Design Approach

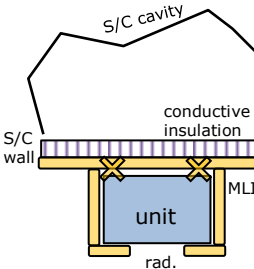
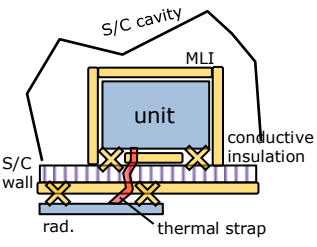
The Thermal Control Subsystem (TCS) is designed to keep all units and equipment within their allowable temperature ranges, during all phases of the mission, minimising heater power and mass. TCS baseline design relies on passive and robust concepts, using well-proven techniques and hardware, e.g. Single-Layer Insulation (SLI), Multi-Layer Insulation (MLI) or temperature sensors and heaters; the latter being the only active hardware in the TCS of this mission.

To facilitate the thermal interface between the units and the spacecraft, 5 categories have been defined:

### 18.5.2 Unit Thermal Categories (thermal control and interface)

Category	Definition	Scheme
<b>Cat 1</b>	Collectively conductively controlled with dedicated radiator	
<b>Cat 2</b>	Collectively conductively controlled with shared radiator ( <i>alu. spreader or heat-pipes</i> )	
<b>Cat 3</b>	Collectively radiatively controlled (and decoupled conductively)	

this could be managed by larger radiators. Note that the radiator sizing currently only considers a steady power dissipation, rather than potential duty cycling of units as is the System baseline (see Section 7.4.5). However both of these effects could lead to an increased heater power required for survival while B2 is not powered.

<b>Cat 4</b>	Individually and independently controlled, insulated from the S/C	
<b>Cat 5</b>	Insulated from the S/C, controlled with S/C provided cold finger	

**Table 18-7: Unit thermal categories (for TCS and thermal interface)**

Most of the dissipating electronic units will fall into category 1 or 2. Units which have advantage to share their heat with other units (TWT + EPC prime and redundant units, PPU, certain instrument units) would be specifically in category 2.

Low dissipating units (e.g. the battery) that can take advantage of the warm radiative environment of the spacecraft cavity will preferably go into category 3.

All external units and appendages, which have either a passive thermal control or a very specific temperature range would enter into category 4 (e.g. most of the instrument sensing units).

For some instruments, there may be some exception where the thermal control requires a remote radiator (with a thermal strap) the location of which would depend on the spacecraft design. In that exceptional case, a category 5 is preferable and the thermal control of the instrument cold finger is given to the Spacecraft Prime.

### 18.5.3 S/C A Thermal Architecture Principles

#### 18.5.3.1 +Y and -Y walls (“North” and “South”) used for radiators

The thermal control design of the CI S/C A is based on a robust and passive concept, with only thermal technologies which have already been flown in previous mission.

The +Y and -Y walls are kept parallel to the ecliptic plane and are not impinged by direct sun flux. Only solar arrays and yoke reflect a reduced part of the received sun flux and emit infrared flux, but this remains limited and predictable. Thus +Y and -Y walls offer the most favourable place to radiate dissipation from instrument and platform units. Several external coatings can be used such as:

- Silver Teflon SSM, which offer a high emissivity and a very low solar absorptivity,
- White paint (e.g MAP PCBE or Z93), which has a slightly higher emissivity but a low-to-medium absorptivity, which has little impact on the radiator performance as it remains in the shadow.

As written above, most of the dissipative units are mounted on heat-pipes to spread their heat along the radiators and to share the heat with other units. This helps limiting heating power when some units are off.

Only instrument units or modules requiring specific low temperature and/or stability (e.g CoCa, MIRMISS) will have their individual radiator, located on + or -Y wall, parallel to the spacecraft wall but insulated from the structure.

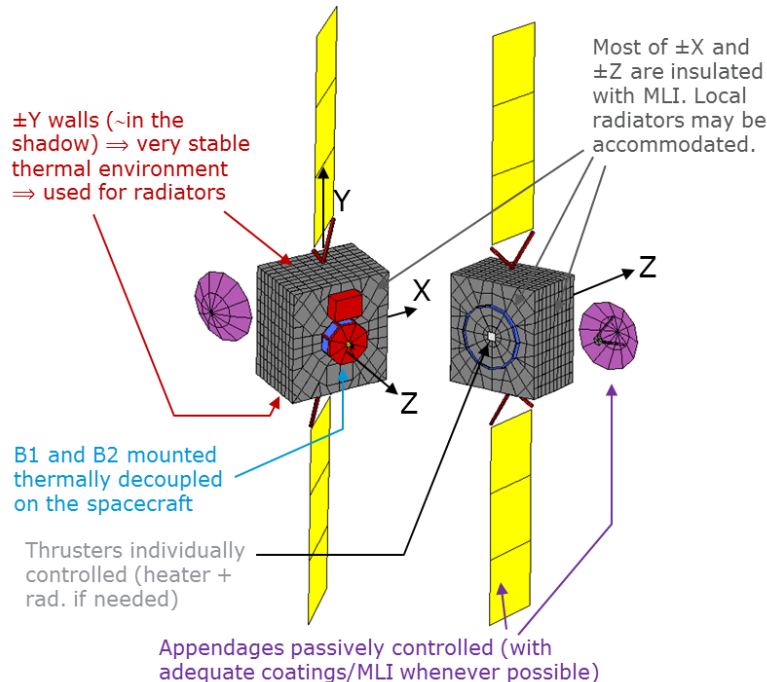


**Figure 18-3: Comet Interceptor external thermal model**

#### 18.5.3.2 Other walls (“Lateral” walls)

The lateral walls (+/-X, +/-Z) are wrapped with MLI, to insulate the spacecraft both from cold space and from the Sun flux. Although it is not the preferred solution for thermal aspects, the external layer can be made of electrically black kapton (e.g. 160XC). At the closest distance from the Sun, the external MLI film may reach a temperature between +150 and +190°C, depending on its direct field of view with Space, which is compatible with polyimide typical temperature limit. To ensure the required insulation, MLI is made out of 15 to 20 layers. For the internal layers, several types of MLI can be used, such as:

- Embossed polyimide VDA coated layers (and no spacer),
- Polyimide VDA coated layers (flat) with a combination of high temperature spacers (between first layers) and medium temperature spacers (between the innermost layers) (such type requires less layers than the previous one, for an equivalent efficiency).

For the units, subsystems or instruments which need to be mounted on the lateral walls, a local radiator may be needed. If possible, +X wall will be preferred, as it is less exposed to the Sun (no Sun illumination occurs above  $\pm 45^\circ$ ). Due to the potential long exposure

to Sun flux along the mission, white paint is not adequate for the lateral wall's radiator and Silver Teflon SSM or rigid OSR tiles are to be considered.

### 18.5.3.3 Internal cavities

Most of the units and sub-systems are accommodated inside the spacecraft. For all the units belonging to thermal categories 1, 2 or 3, radiative exchanges inside the spacecraft cavities will be maximised with high emissive coatings, such as black paint. This contributes to sharing the heat between units and contributes to make the internal cavities a mild radiative environment for low dissipative or passive components (e.g. battery, RF communication components, harness). Internal walls are also highly emissive (either using black paint or letting directly CFRP without any coating, in case of CFRP panel is used). Units with a more stringent thermal requirement are equipped with heating lines (e.g. battery).

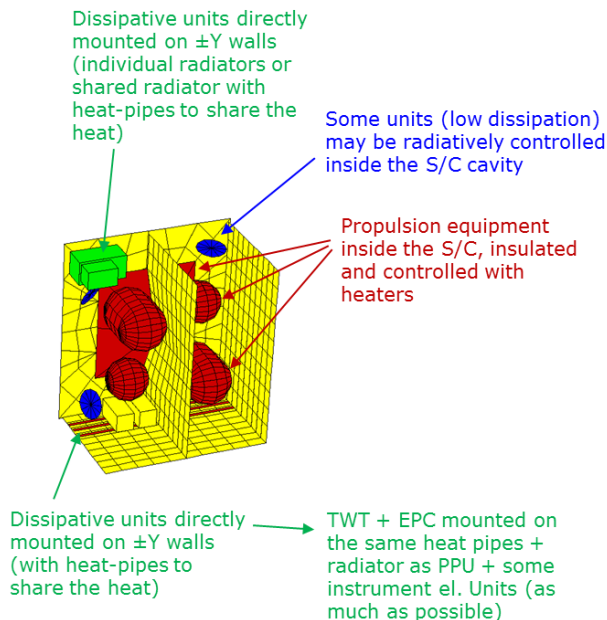


**Figure 18-4: Comet Interceptor internal thermal model (partial view)**

### 18.5.3.4 Propulsion subsystem

The internal propulsion units (tanks, control valves, pressure sensors...etc) and pipes benefit from this mild internal environment. But as the minimum temperature shall not go below  $0^{\circ}\text{C}$ , they are radiatively and conductively insulated from the structure and have with their own thermal control. Propellant tanks (both chemical and electrical) are conductively decoupled from the spacecraft structure using thermal washers and are individually insulated with MLI (as illustrated in Figure 18-4). Most of the propulsion subsystem equipment is wrapped inside an MLI tent (also visible in red, in Figure 18-4). Individual heating lines are installed close to the sensitive components and around the fluid pipes up to the thrusters to ensure their temperature requirement is always met. The external parts of the propulsion system (electrical thruster and chemical thrusters) are conductively and radiatively decoupled from the spacecraft to limit heat leakage when they are passive or excessive heat input into the spacecraft when they are operated.

### 18.5.3.5 High Gain Antenna (HGA)

The High Gain Antenna (HGA) thermal control can be fully passive. Its front side is white painted to avoid exceeding the maximum design temperature under direct Sun illumination at 0.9AU from the Sun. Its backside is insulated with MLI in order to reduce the radiative coupling with the spacecraft.

### 18.5.3.6 Low Gain Antennas (LGA) and ISL Antenna patches

The LGA and the ISL antenna patches may be sun illuminated during the mission. The protruding part is also white painted and the baseplate is conductively decoupled from the spacecraft

### 18.5.3.7 Active thermal control (heating lines)

Software controlled temperature sensors are used to monitor units and equipment temperature, as well as to control the switch on/off for the heaters.

## 18.5.4 Probe B2 Thermal Control

The B2 probe thermal control is based on a set of radiators directly mounted on the unit. This means one of the (lateral) sides of each unit is equipped with SSM adhesive tape and is located directly in view to cold space, as illustrated in Figure 18-5. Only the needed area is used as a radiator, all the rest of the probe surface is insulated with MLI, including the bottom baseplate and the top part, with the exceptions of the clamping mechanism (baseplate) and the antenna on the top part. Due to its complex shape, it is most likely that the RW will not allow the accommodation of a radiator directly implemented on its housing. A thermal strap is then used to connect the RW to a radiator made of a simple aluminium plate with SSM tape.

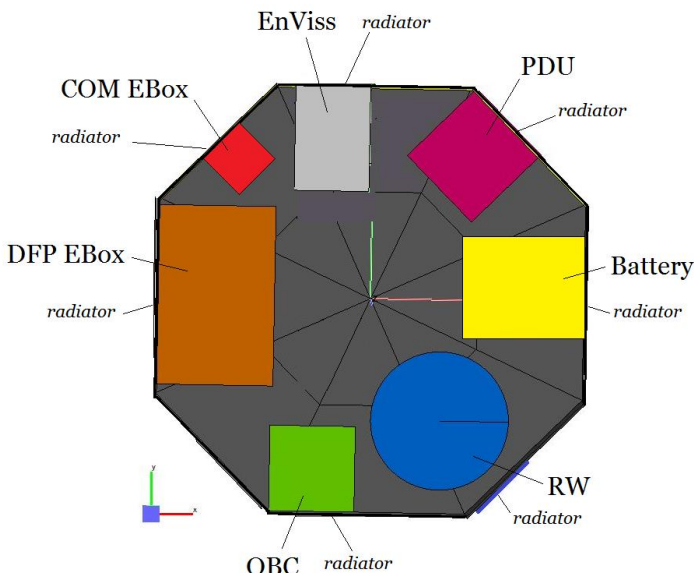


**Figure 18-5: Probe B2 thermal model internal view (partial view)**

While the probe B2 is still attached to S/C A, all the units are off and compensation heaters keep them above the non-operating minimum temperature limit.

## 18.6 Thermal Control Features

The unit temperature control is achieved through the use and the selection of flight-proven materials used on numerous spacecraft. The key features of the thermal control are presented below:

- SSM or white painted radiators reject internal heat dissipation toward Space
- Dedicated radiators are provided for the CoCa and MIRMISS optical head, which require low and stable temperature during imaging
- Heat pipes are implemented on the S/C A +/-Y panels to spread the highly dissipating units (e.g. PPU, TWT) thermal dissipation and share the heat between units.
- A high emissivity finish is used inside the spacecraft when required to maximise the radiative heat transfer to the radiators
- Thermal straps may be used to connect the reaction wheels and some payload units needing a dedicated radiator
- Multi-Layer Insulation (MLI) is used to minimise heat flow from non-radiating areas and to minimise the thermal distortions
- “Cold” coatings on LVA ring external part (Clear Sulphuric Anodisation)
- White paint is used on SADM panel flange, LGA and ISL antenna patches
- Heaters and thermal blankets on the propulsion system prevent propellant from freezing and help controlling propellant temperature
- Software controlled heaters are implemented. Appropriate redundancy is included for all heaters and thermistors to prevent single point failure in the thermal control function
- Low conductive stand-offs for the appendages and external payload units minimise heat transfer to the spacecraft main body.

## 18.7 Radiator and Heater Power Sizing

### 18.7.1 S/C A

Table 18-8 below provides the type of thermal category for each unit and their needed radiator surface.

#### 18.7.1.1 Radiators area

Wall	Units	Unit thermal category	Radiator individual surface (m <sup>2</sup> )	Overall surface (m <sup>2</sup> )
+X	DPU	Cat. 1	0.0128	0.0365
	NAVCAM OH 1	Cat. 1 or 3	0.0142	
	NAVCAM OH 1	Cat. 1 or 3	0.0142	
	STR OH 1	Cat. 4	0.0012	
	STR OH 1	Cat. 4	0.0012	
	MANiac NDG	Cat. 4	0.0119	

Wall	Units	Unit thermal category	Radiator individual surface (m <sup>2</sup> )	Overall surface (m <sup>2</sup> )
	ISL Ant. Patch	Cat. 4	0.0067	
-X	ISL Ant. Patch	Cat. 4	0.0234	
+Y	RW #1	Cat. 1	0.0301	0.4061
	RW #2	Cat. 1	0.0301	
	RW #3	Cat. 1	0.0301	
	RW #4	Cat. 1	0.0301	
	CoCa ELU	Cat. 3	0.0627	
	DFP El. Box	Cat. 3	0.0711	
	MIRMIS TIRI	Cat. 3	0.0244	
	CoCa FPA rad.	Cat. 4	0.0053	
	MANiac SHU	Cat. 3	0.0762	
	APM	Cat. 1	0.0187	
-Y	SADM +Y	Cat. 1	0.0202	0.5712
	ISL Ant. Patch	Cat. 4	0.0072	
	IMU #1	Cat. 2		
	IMU #2	Cat. 2		
	X-Band DSTRASP #1	Cat. 2		
	X-Band DSTRASP #2	Cat. 2		
	X-Band TWT #1	Cat. 2		
	X-Band TWT #2	Cat. 2		
	X-Band EPC #1	Cat. 2		
	X-Band EPC #2	Cat. 2		
	ISL Elec #1	Cat. 2		
	ISL Elec #2	Cat. 2		
	OBC	Cat. 2		
	RIU	Cat. 2		
+Z	PPU	Cat. 2		0.5640
	SADE	Cat. 2		
	SADM -Y	Cat. 1	0.0202	
	ISL Ant. Patch	Cat. 4	0.0072	
	ISL Ant. Patch	Cat. 4	0.0084	
-Z	ISL Ant. Patch	Cat. 4	0.0067	0.0084

**Table 18-8: S/C A unit thermal categories and radiator area**

### 18.7.1.2 Heating power

Table 18-9 provides the individual (or collective) needed heating power, assumed to be average and steady state. It is generally recommended to have 2 times the average value as installed heating power. LAU mode and SUN mode are assumed to be short enough

to account on the initial warm temperature and spacecraft thermal inertia to have all unit temperatures remaining within their required temperature range.

Wall	Units	Power in SAFE (W)	Power in STBY (W)	Power in COM (Y)	Power in EPTH (W)	Power in SCI (W)
+X	DPU	-	-	-	-	-
	NAVCAM OH 1	0.1	0.1	0.1	0.1	0
	NAVCAM OH 1	0.1	0.1	0.1	0.1	0
	STR OH 1	-	-	-	-	-
	STR OH 1	-	-	-	-	-
	MANiac NDG	1.9	1.9	1.9	1.9	0
	ISL Ant. Patch	0.9	0.9	0.9	0.9	0
-X	ISL Ant. Patch	1.1	1.1	1.1	1.1	0
+Y	RW #1	1.8	1.8	1.8	3.8	0
	RW #2	1.8	1.8	1.8	3.8	0
	RW #3	1.8	1.8	1.8	3.8	0
	RW #4	1.8	1.8	1.8	3.8	0
	CoCa ELU	10.1	10.1	10.1	10.1	0
	DFP El. Box	11.5	11.5	11.5	11.5	0
	MIRMISS TIRI	3.1	3.1	3.1	3.1	0
	CoCa FPA rad.	0.5	0.5	0.5	0.5	0
	MANiac SHU	11.4	11.4	11.4	11.4	0
	APM	2.2	2.2	0	2.2	2.2
	SADM +Y	-	-	-	-	-
	ISL Ant. Patch	0.9	0.9	0.9	0.9	0
-Y	IMU #1	8.7 (on heat pipes)	24.1 (on heat pipes)	0	0	24.1 (on heat pipes)
	IMU #2					
	X-Band DSTRASP #1					
	X-Band DSTRASP #2					
	PPU					
	X-Band TWT #1					
	X-Band TWT #2					
	SADE	0	0	0.9	0	0
	X-Band EPC #1	0	3.6	0	3.6	3.6
	X-Band EPC #2					
	ISL Elec #1	2.0	2.0	2.0	2.0	0
	ISL Elec #2					
	OBC	-	-	-	-	-
	RIU	-	-	-	-	-

Wall	Units	Power in SAFE (W)	Power in STBY (W)	Power in COM (Y)	Power in EPTH (W)	Power in SCI (W)
	ISL Ant. Patch	0.9	0.9	0.9	0.9	0
+Z	ISL Ant. Patch	0.9	0.9	0.9	0.9	0
-Z	ISL Ant. Patch	0.9	0.9	0.9	0.9	0
Prop.	Pipes	5.0	5.0	5.0	5.0	5.0
	CPS Thrusters	5.0	5.0	5.0	5.0	5.0
	Valves, PT...	1.1	1.1	1.1	1.1	1.1
	Propellant tanks (2)	6.0	6.0	6.0	6.0	6.0
	Elec. Prop tanks (2)	6.0	6.0	6.0	6.0	6.0
	Elec. Thruster	10.0	10.0	10.0	0.0	10.0
<b>TOTAL</b>		<b>97 W</b>	<b>117 W</b>	<b>87 W</b>	<b>89 W</b>	<b>63 W</b>

**Table 18-9: S/C A unit heating power vs mode**

### 18.7.2 Probe B2

Table 18-10 provides the unit needed radiator surface and their individual needed heating power, assumed to be as average and steady state. As soon as probe B2 is switched on, heating power is not needed anymore.

Units	Radiator individual surface (m <sup>2</sup> )	Heating power when OFF (W)	Heating power when ON (W)
RW	0.0281	3.5	0
DFP DISC	-	0	0
DFP EBox	0.0322	4.0	0
EnVisS	0.0172	1.8	0
OPIC	-	0	0
DFP FGM 1	0.0018	0	0
DFP FGM 2	0.0012	0	0
LGA	-	0	0
ISL Elec.	0.0174	1.1	0
ISL Active Antenna	-	0	0
OBC	0.0151	1.6	0
Battery	0.0048	0.9	0
PDU	0.0182	1.9	0
<b>TOTAL</b>	<b>0.1360 m<sup>2</sup></b>	<b>14.7 W</b>	<b>0</b>

**Table 18-10: Probe B2 unit radiator area and heating power**

## 18.8 List of Equipment

The means to thermally control a spacecraft can be classified as passive and active. Passive methods reach from the selection of adequate optical surface properties via paints, to the application of isolation materials such as multilayer foils. Thermal design is mainly based on passive pieces of equipment. The sole active components baselined in the CI thermal design are electric heaters used to maintain units and equipment above their operating and non-operating minimum temperature. Table 18-11 summarises the selected thermal hardware for the S/C A.

Equipment	Description	Application
<b>Passive thermal hardware</b>		
Thermal fillers	<ul style="list-style-type: none"> <li>- Material used to fill interstitial microscopic cavities caused by surface roughness.</li> <li>- Increase the heat transfer between units and structure.</li> <li>- Made of soft material with a high thermal conductivity.</li> </ul>	<ul style="list-style-type: none"> <li>- Used between high dissipating units and the spacecraft.</li> <li>- The use of a graphite interface filler (Sigraflex) is foreseen.</li> </ul>
Thermal washers	<ul style="list-style-type: none"> <li>- Thermally decouple adjacent surfaces.</li> <li>- Can be made of low conductive metals or composite materials.</li> </ul>	<ul style="list-style-type: none"> <li>- Used between pieces of equipment and the structure if thermal insulation is required (e.g. tanks).</li> <li>- The use of a nylon fibre filled composite (Vetronite) is foreseen.</li> </ul>
Paints	<ul style="list-style-type: none"> <li>- Used to change the optical surface properties of units.</li> <li>- Can be made of a multitude of chemical matrixes and often require a primer before they can be applied.</li> </ul>	<ul style="list-style-type: none"> <li>- Used to change the optical surface properties of the structure or a piece of equipment.</li> <li>- Black paint (Aeroglaze Z306), e.g. applied on the outside of electronic boxes.</li> </ul>
Second Surface Mirror (SSM)	<ul style="list-style-type: none"> <li>- Coating with high emissivity and low absorptivity is applied to dedicated radiator surfaces.</li> </ul>	<ul style="list-style-type: none"> <li>- Currently foreseen for radiators on +Z and -Y/+Y panels.</li> </ul>
Single-Layer-Insulation (SLI)	<ul style="list-style-type: none"> <li>- Single foil attached to a piece of equipment to alter the optical properties and provide insulation with respect to thermal radiation.</li> </ul>	<ul style="list-style-type: none"> <li>- Used on the tanks to radiatively decouple them from the internal spacecraft environment.</li> </ul>
Multi-Layer-Insulation (MLI)	<ul style="list-style-type: none"> <li>- Made up of a stack of foils; used to thermally decouple a unit from its environment (internal or external to a spacecraft).</li> </ul>	<ul style="list-style-type: none"> <li>- MLI with black Kapton as external layer is currently foreseen for all external panels.</li> <li>- MLI with Vapour Deposited Aluminium (VDA) coating is used on the central cylinder to decouple the tanks from their environment.</li> </ul>

Equipment	Description	Application
Thermal straps	<ul style="list-style-type: none"> <li>- Parts that conductively connect heat sources and heat sinks.</li> <li>- Usually made of highly conductive material (e.g. copper, aluminium or graphite), have a relatively large cross sectional area and bear no structural loads.</li> </ul>	Thermal straps are used to improve the conductive link from Power Board, Data Handling Board and Comm. Boards to the surrounding radiators.
Thermistors	<ul style="list-style-type: none"> <li>- Measurement devices to monitor the temperature of a piece of equipment.</li> </ul>	<ul style="list-style-type: none"> <li>- Two thermistors per piece of equipment are foreseen, i.e. one nominal and one redundant thermistor.</li> <li>- Thermistors for the propellant tank and feed lines are foreseen.</li> </ul>
Heat pipes	<ul style="list-style-type: none"> <li>- High heat transfer from heat source to heat sink. Different working fluids depending on temperature range.</li> </ul>	<ul style="list-style-type: none"> <li>- Used between high dissipating units (e.g. PPU, PCDU, TWT, RW) and the spacecraft structure to increase the heat transfer.</li> </ul>
Doublers	<ul style="list-style-type: none"> <li>- Aluminium plate (with high thermal conductivity), to increase and spread the heat transfer between units and structure.</li> </ul>	<ul style="list-style-type: none"> <li>- Used between high dissipating units and the spacecraft.</li> </ul>
<b>Active thermal hardware</b>		
Heaters	<ul style="list-style-type: none"> <li>- Active devices to locally heat up pieces of equipment.</li> <li>- Predominantly, foil heaters are used, where a copper resistor is embedded in a Kapton substrate.</li> </ul>	<ul style="list-style-type: none"> <li>- Heaters are foreseen for pieces of equipment that require additional heat during cold phases. Always in pairs of nominal and redundant.</li> <li>- Heaters for the propellant tank and feed lines included.</li> </ul>

**Table 18-11: Description of S/C A baseline thermal hardware**

### 18.8.1 TCS Mass Budget

The TCS mass budget is shown in Table 18-12. The total sub-system mass is 23.72 kg, including 20% design maturity margin.

Thermal Hardware	Comments	Density [kg/m <sup>2</sup> ]	Area [m <sup>2</sup> ]	Mass [kg]	Mass (incl. margin) [kg]
Paints	Mass includes primer and paint.	0.15	13.3	2.0	2.4
MLI/SLI	Mass includes MLI, stand-offs and grounding straps.	0.4	12.5	5.0	6.0
Thermal fillers	Sigraflex thermal filler sheet (thickness = 0.2 mm)	0.2	1.25	0.25	0.3
SSM	SSM tape and adhesive; mass	0.2	1.0	0.2	0.24

Thermal Hardware	Comments	Density [kg/m <sup>2</sup> ]	Area [m <sup>2</sup> ]	Mass [kg]	Mass (incl. margin) [kg]
	excludes baffles and radiator structure.				
Radiator (aluminium)	For Instruments individual specific thermal control	6.875	0.145	1.0	1.2
Heat pipes	At least two per unit/equipment.	0.33	3 HP	1.0	1.2
Thermistors	PT1000, NTC 15 kOhm or NTC 10 kOhm as required / supported by data handling. Mass includes harness.	0.005	100	0.5	0.6
Thermal straps	High conductivity thermal straps.	0.1	5	0.5	0.6
Thermal washers	Vetronite washers.	0.0005	100	0.05	0.06
Heaters	Kapton foil heaters, harness included in mass	0.010	50	0.5	0.6
<b>TCS Total Mass</b>					<b>11.0 kg</b>
<b>TCS Total Mass</b>					<b>13.2 kg</b>

**Table 18-12: S/C A TCS Mass budget (with margins)**

Thermal Hardware	Comments	Density [kg/m <sup>2</sup> ]	Area [m <sup>2</sup> ]	Mass [kg]	Mass (incl. margin) [kg]
Paints	Mass includes primer and paint.	0.15	1.0	0.15	0.18
MLI/SLI	Mass includes MLI, stand-offs and grounding straps.	0.3	2.0	0.60	0.72
Thermal fillers	Sigraflex thermal filler sheet (thickness = 0.2 mm)	0.2	0.25	0.05	0.06
SSM	SSM tape and adhesive; mass excludes baffles and radiator structure.	0.2	0.15	0.03	0.036
Radiator (aluminium)	For Instruments individual specific thermal control	6.875	0.01	0.07	0.084
Thermistors	PT1000, NTC 15 kOhm or NTC 10 kOhm as required / supported by data handling. Mass includes harness.	0.005	20	0.2	0.24
Thermal straps	High conductivity thermal straps.	0.1	1	0.1	0.12

Thermal Hardware	Comments	Density [kg/m <sup>2</sup> ]	Area [m <sup>2</sup> ]	Mass [kg]	Mass (incl. margin) [kg]
Heaters	Kapton foil heaters, harness included in mass	0.010	10	0.1	0.12
<b>TCS Total Mass</b>			<b>1.3 kg</b>	<b>1.56 kg</b>	

**Table 18-13: Probe B2 TCS Mass budget (with margins)**

## 18.9 Technology Needs

None.

## 19 GROUND SEGMENT & OPERATIONS

### 19.1 Requirements and Design Drivers

The main design drivers for Ground Segment and Operations that have been identified during the CDF study are:

- Need to maintain a very light operational approach. The main items contributing to the operational simplicity will be detailed later in this section.
- Differing operational scenarios during the different Transfer, Encounter and Post-Encounter Phases: Comet Interceptor-Sun-Earth visibility angles, and maximum Earth distance. The operational orbit selected results in varying ground visibility periods and communications data rates.
- Consolidation will occur during L2 Waiting Phase (selection of target comet) – affecting power, thermal and communications strategy and therefore the operations.
- Probes to be treated as payloads: with the addition of the Inter Satellite Link to enable data transfer.
- Comet fly-by is a single opportunity, this implies that the transfer operations shall be such that the S/C A and probes reach the target in a timely manner and must remain functional during the fly-by.

### 19.2 Baseline Design Assumptions

#### 19.2.1 Ground Segment Overview

The overall ground segment architecture in Figure 19-1 reflects a lean approach architecture of a typical interplanetary scientific mission, the main components being:

- The Ground Stations, mainly belonging to the ESA network;
- The Mission Operations Centre (MOC, located in ESOC, Darmstadt), in charge of all mission operations planning, execution, monitoring and control;
- The planning of science operations and co-ordination of the scientific input will be the responsibility of PI teams or provided by ESAC, Madrid.

In addition, due to the special nature of the ESA-JAXA cooperation in the mission:

- The JAXA B1 Mission Operations Centre.

#### Ground Stations:

It is assumed that all communications to ground will be using the X-band, for both TT&C and Science downlink. The ESTRACK 35m stations will be used to provide LEOP support, with addition of First Acquisition Aid antenna (TBC) and short duration support from 15m stations (TBC). If necessary, Augmented Network could be used to complement the ESTRACK Network. Although utilization of non-ESA elements (e.g. other tracking networks, interface with other control centres, etc.) can be a source of significant development cost and effort during operations, it is thought that the JAXA interfaces experience from Bepi-Colombo could be re-used as far as possible. It is assumed that no ESTRACK ground station modification will be required to support the

Comet Interceptor mission. From LEOP until end of L2 transfer phase, the booking and scheduling of the ESTRACK will need to be in close collaboration with other flying missions, in particular with the ARIEL mission.

### **Mission Operations Centre:**

There is a single Comet Interceptor Mission Operations Centre (MOC) at ESOC. Which main responsibilities, among others, are:

- Spacecraft monitoring and control, mission planning for deferred operations, including execution of all platform activities and the commanding of the payload schedules
- S/C A orbit and attitude determination and control (B1 by JAXA, not required for B2)
- Perform all communications from the Ground Stations using Spacecraft A as relay. After release of the probes, operations will be limited to reception of data via ISL
- Plan observations in a commissioning-like approach in coordination with the Science Operations team or PIs
- Mission data distribution.

### **Science Operations Planning:**

Due to the cost requirement of the Comet Interceptor mission, the current assumption is that the interfaces for mission planning shall be kept to the essential with the minimum number of entities involved, as those are key factors in containing the development and operations cost. Given the one-shot nature of the science objectives a need for regular coordination of the payloads is assumed not present.

There is a direct MOC/PIs interfaces for planning products (i.e. not via SOC), there is currently no effort costed for instruments planning coordination. The Science operations team member (provided by ESAC) in charge of the Instruments planning coordination will be functionally reporting to MOC Spacecraft Operations Manager (SOM).

It is assumed that the Science archive is not located at the MOC; it can be in ESAC, by accessing the data from MOC.

ECCS Packet Utilization Standard (PUS-C) services required for the Instruments on-board operations will be specified in the Comet Interceptor OIRD, TBW.

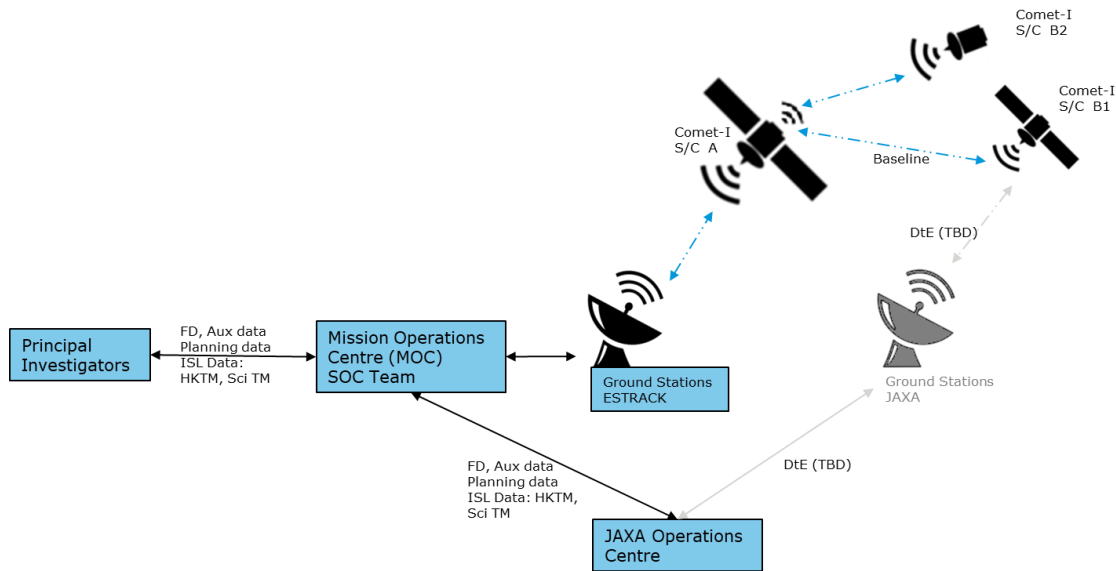


**Figure 19-1 : Proposed Comet Interceptor Ground Segment Architecture**

## 19.3 Mission Phases - Operational Considerations and Assumptions

### 19.3.1 Development Phase

In order to contain the cost within this mission envelope it is assumed that no activity from MOC before L-3years (2025) and the ground segment development will start at L-2yrs. Ground Segment preparation covers all nominal activities related to ground operations systems development and validation.

It is expected that other Science missions, more than one or two, will be in their operational phase such that basic services can be largely shared, if not taken over by other missions, for example: no effort quoted for SPACONs for the complete duration of the Comet Interceptor mission.

The MOC assumes that the Mission Analysis support to Comet Interceptor, during all mission phases, will be covered by the Project.

There will be a high re-usage and sharing of ESOC infrastructure, ESOC resources and manpower where possible with flying missions or missions in development, e.g. ARIEL.

It is assumed that the Spacecraft units and Ground Segment are fully compliant with the latest standards: ECSS (PUS-C and Operability Standard), CCSDS and with mission specific documents: OIRD, SGICD TBW.

### 19.3.2 Launch and Early Orbit Phase (LEOP)

Comet Interceptor will be launched in dual-launch configuration with ARIEL. Like ARIEL, it is assumed that Comet Interceptor has a short LEOP phase of no more than 2 days.

The LEOP operations include all activities up to and including completion of the critical S/C operations to achieve a nominal and stable S/C mode, including launch and launch

vehicle separation, autonomous post-separation sequence, critical deployment of solar arrays and appendages, the initial attitude and control acquisition and execution of TCM#1 (like ARIEL, between L+24 hours and L+48 hours).

The launch will be in dual-launch configuration with ARIEL. Hence, operations coordination with ARIEL encourage the possibility to share the LEOP resources and manpower where possible.

Regarding the Ground Station, it is assumed a quasi-continuous ground coverage during this phase, 15m and 35 m from ESTRACK Network. In case of ESTRACK unavailability, Augmented Network can be used to complement the ground passes. Visibility analysis to be performed in coordination with ARIEL.

The probes and payloads will be off during this phase.

### **Multiple Spacecraft per Aperture**

During the study, the possibility to use the antenna with Multiple Spacecraft per Aperture (MSPA, RD[65]), to receive inputs from two separate spacecraft in parallel at a single ground station, was discussed but found feasible for non-critical phases only. To achieve the TCM#1 burn the MOC needs to have sufficient range and range rate tracking data to establish the injection orbit parameters and allow calculation of the TCM parameters. To do the tracking accurately, the ground station needs to provide a two way signal i.e. uplink and downlink. This then becomes the main driver to not use MSPA during these early LEOP phases of the mission. In addition, the usage of MSPA also introduces some "degradation" in the support capability provided by the ground stations because the redundancy against a possible failure will be reduced.

The usage of MSPA could be envisaged for phases after LEOP, e.g. L2 Waiting Phase. This requires a relative spacecraft separation analysis.

### **Comet Interceptor and ARIEL dual launch specific operations**

The MOC has extensive experience on dual launch LEOP operations. Belonging to a single mission, the Cluster launches were in pairs while Swarm was a single triple launch. Belonging to different missions, but part of the same Family of Missions (Astronomy and Fundamental Physics), was the case of the dual-launch of Herschel and Planck. ARIEL and Comet Interceptor will be a dual launch for two missions belonging to two different families of Missions, Astronomy and Fundamental Physics and Solar System and Exploration Mission, respectively.

The commonalities of dual-launch experience at the MOC are shared Project and Industry support, shared Software and Sim support, shared Mission Control Room, Flight Operations Director and Spacecraft Operations Manager (except for Herschel and Planck), the Flight Control Teams were separated for all the missions examples provided.

As a summary, the dual launch operations MOC experiences are:

- Cluster II (2x2 satellite launch), Swarm (3 satellite launch) examples of multiple launch belonging to the same mission, for which they shared all the above mentioned resources with the exception of the Flight Control Team

- Herschel and Planck, two detached missions with shared Project/Industry support belonging to the same family of mission Astronomy and Fundamental Physics Mission Division.

The sharing of the above cited resources to be followed by ARIEL and Comet Interceptor Science missions will be discussed with ESA D/SCI in the next phases.

### **19.3.3 Commissioning/Transfer Phase**

This phase starts after TCM#1 and includes spacecraft commissioning with the completion of any remaining appendage (HGA) deployment, electrical propulsion functional checks and EP in-flight validation. The duration of the commissioning phase is ~2/3 months after launch.

The spacecraft operations will be conducted by loading activities and dumping the data, possibly using the MSPA if two spacecraft are sharing the same position on the sky TBC.

Regarding the Ground Station it is assumed a 8h/5 days per week of ground coverage during this phase with extended coverage around the TCMs, 35 m from ESTRACK Network. In case of ESTRACK unavailability, the Augmented Network can be used to complement the ground passes. Visibility analysis to be performed in coordination with ARIEL.

The probes and Payloads first light-on may occur during this phase, if required.

### **19.3.4 L2 Waiting Phase**

The duration of this phase is variable and will be run in a quasi-passive operations approach. It starts after the end of the Commissioning/Transfer phase.

During this phase, the operations will be limited to the minimum required:

- Once per week ground stations passes with Ranging/Doppler, ideally during working hours
- Station Keeping Manoeuvre execution every month and WoL TBC every other month
- Platform checkouts and limited payload checkouts.

It is assumed that there are no requirements calling for short ground reaction/response time and there is no need for on-call support.

The effort is highly dependant on a spacecraft design that will enable infrequent ground intervention, low operations activities and preservation of knowledge.

8 hours per week of ground coverage are assumed during this phase, 35 m from ESTRACK Network.

The probes and payloads operations are limited to seldom checks, for example twice per year.

### **19.3.5 Interplanetary Transfer Phase**

The duration of this phase is variable and starts after L2 waiting phase and ends two months before the comet fly-by.

Interplanetary flight generally requires particular effort concerning navigation. The use of electric propulsion is of no dramatic complexity if it is reduced to a mere activation/deactivation of the thrust without particular constraints. It is of significant complexity in case the utilization of electric propulsion is subject to severe and articulated constraints like for BepiColombo (e.g. thrusting is incompatible with communications). This can be avoided/mitigated at the level of spacecraft design if a proper system-level trade-off is done. It is assumed that for Comet Interceptor a system-level trade-off will be performed to mitigate the constraints of electric propulsion operations and communication windows. If the spacecraft design does not allow parallel EP thrust and ground communications it is recommended to enable a low data rate to guarantee that the EP remains operational after the interruption for ground communication.

The use of gravity assists manoeuvres (GAMs) is of no particular complexity but it creates a certain increase in the workload, keeping in mind that Earth GAMs are simpler than other planets. There is an additional operational overhead effort for the cruise phase that is proportional to the number of gravity assists.

The combination of electric propulsion with GAMs increases complexity, and therefore cost, of mission operations and in particular of navigation. If the Comet Interceptor interplanetary transfer shall include a Lunar fly-by this will entail additional operational effort that will be included in the manpower work during this phase.

It is assumed that in this phase there are requirements calling for short ground reaction/response time and there will be a need for on-call support to ensure reaching the target within designed timeline, based on a missed thrust and navigation analysis.

The Ground Station coverage will be increased to 8hours twice per week of the 35 m from ESTRACK Network.

The probes and payloads checks shall be limited to the minimum.

### **19.3.6 Approach Phase**

The approach phase has an estimated duration of two months, with the start of the bulk of the activities with a ramp-up of the operations teams.

The type of operations to be conducted in proximity of the target object are a major cost discriminator. Non-bound orbits like “triangular orbits”, bound orbits or lander delivery are currently not considered types of proximity operations for Comet Interceptor.

It is assumed that for most of the comet encounter considered, there is no EP firing at approach phase which may impose additional attitude constraints, e.g. limitations on ground comms windows versus acquiring of navigation images while performing thrust arcs shall be kept to the minimum.

The Ground Station coverage will be increased and four weeks before encounter there will be a dedicated navigation campaign with reduced periods of Delta-DOR to enable relative navigation. An average of 8 hours per day of the 35 m from ESTRACK Network is assumed during this phase.

The probes and payloads operations will consist of preparation for the probes release, e.g. battery charge, load of the operations on-board, calibration of the units, etc.

From the preparation of the probes for release until the comet fly-by, it will be beneficial to have the collocation of the instrument planning coordinator at ESOC, enabling an efficient coordination and collaboration between the science operations and the mission operations activities.

### **19.3.7 Probes Release Phase**

This phase starts around 2 days before the Comet fly-by.

As per release timeline in Figure 7-16, the spacecraft A performs the first TCM to release probe B1, then after release of probe B1 the S/C A will perform a second TCM to release probe B2. Finally, S/C A will perform the third manoeuvre to achieve the fly-by position. The operations will be loaded into S/C A at the time of the first TCM manoeuvre and ground will monitor the execution of the sequence to ensure there is not high divergence of the operations and manoeuvres sequences. If there is any divergence the sequence will be updated accordingly and with realistic ground turnaround times as suggested in Figure 7-16. It is assumed that the accuracy for probes delivery prior to the encounter is compliant with the ground around time specified.

It is assumed that the MOC performs the S/C A attitude manoeuvres, while any probe B1 attitude manoeuvres will be under JAXA responsibility and pre-loaded before release (or commanded directly from JAXA G/S), and probe B2 will not require such manoeuvres.

It is assumed that the on-board autonomy is in place to perform the nominal and contingency operations. The current assumption is that the only possible ground intervention for this activity would be to enable/disable parts of pre-programmed activities based on an existing contingency procedure and timeline agreed compliant with realistic ground response times. This approach has already been used for similar activities in the past although with less events in the chain.

Extended Ground Station coverage of the 35 m from ESTRACK Network is assumed during this phase.

The probes and payloads operations will consist of pre-programmed Science operations and Inter-Satellite Link operations, as described below.

Also in this phase, it will be beneficial to have the collocation of the instrument planning coordinator at ESOC.

#### **Inter-Satellite Link (ISL) operations**

The ISL operations start after the probes release and end at post fly-by with the completion of the Science data transfer from the probes to S/C A.

The Inter-Satellite Link operations are assumed not stringent on the operational commanding, and the satellites will remain in the ISL FoV to avoid additional attitude limitations.

Although the ISL supports both TM and TC transmission, it is assumed that no TC will be required by the probes after release.

Probe B1 operations are assumed to be relayed via S/C A and delivered from JAXA to MOC for uplink prior to the deployment of B1. There shall be no further uplink from S/C A to B1 after the release of B1.

The minimum PUS-C services required for implementation in the probes On-Board Software will be listed in the Comet Interceptor OIRD.

### **19.3.8 Comet Fly-By Phase**

The Comet Fly-By phase will last a few hours.

Ground communications could be used to monitor the fly-by but no short ground reaction times should be required outside the existing flight operations procedures, designed timelines and available communication data links. It is assumed that S/C A will store the probes B1 and B2 data prior and during the fly-by in a pre-programmed manner.

There will be extended Ground Station coverage of the 35 m ESTRACK Network.

The probes and payloads pre-programmed science operations and ISL Link operations, as described in Section 19.3.7.

It is assumed that the instrument planning coordinator is still at ESOC during this phase.

### **19.3.9 Post-Encounter Phases**

The duration of this phase is, at this stage, variable and it will depend on the Earth distance evolution after comet fly-by. This phase starts after the comet fly-by and ends with the completion of the data downlink from S/C A.

After the encounter, it is assumed that operations will be limited to downlink the science data and wheel off-loading activities (TBC). No additional operations are assumed, e.g. electrical propulsion operations, stringent attitude manoeuvres or critical operations that will require on-call support. It is assumed that recovery of spacecraft anomalies will occur the following working day.

Frequent ESA ground station passes with tracking data will ensure that the data is retrieved before end of mission is declared. The ground station booking will be synchronized with the ground visibility analysis (when available), and the ESA flying missions in the same region of the sky which will be using the ESTRACK Network; in the backup scenario example, the encounter will occur at 30 deg Sun/Earth/Comet which may overlap with missions operating in Mars/Jupiter.

10 hours per day of ESTRACK 35m Network is assumed during this phase.

The probes and Payloads are assumed to be off after Comet Fly-by. Or alternatively, if the probes have survived the fly-by and remain within the ILS range, probes operations will be limited to ISL operations, as described in Section 19.3.7.

### **19.3.10 Decommissioning and Disposal Phase**

This phase was not studied in detail during the CDF Study and the details are subject to iteration during the next phases of the mission.

The duration of this phase is assumed to be 7 days, and it starts after the completion of the S/C A science data dump to Ground.

The operations activities will be limited to the spacecraft passivation and disposal compliant with the Space Debris Mitigation Verification Guidelines as per the Space Debris Mitigation Policy.

The probes and payloads are inoperative and off during this phase.

The Ground Station coverage will be 5 hours/5 days of 35 m ESTRACK Network.

## **19.4 Space and Ground Segment – Operational Considerations and Assumptions**

### **19.4.1 Space Segment**

Compatibility of the space segment with existing ground segment infrastructure and mission operations concepts is a prerequisite for cost containment on the operations side.

In particular, the following aspects shall be considered:

- Compatibility of the Tracking, Telemetry and Commanding (TT&C) subsystem with ECSS and CCSDS standards RD[67] to RD[70] and as per COMMS section 16.1.
- The avionics and payloads compatibility with ECSS packet telemetry and telecommand standards and in general with ESA mission control system, currently SCOS 2000 and EGS-CC based in the future. It is assumed that experience of JAXA Payload operations from Bepi MMO could be re-used as far as possible.
- Services of on-board data handling compatible with ESA mission operations concept: in general PUS-C RD[70], in particular mission timeline (PUS Service 11), use of TC files uplink and – ideally- downlink file transfer (CCSDS File Delivery Protocol CFDP RD[66] or already ESA implemented protocols), prioritization of data downlink, flexible storage mechanism, use of Services 12 and 19, implementation of On-board Control Procedures (OBCP), etc.
- In the Attitude Orbit and Control Subsystem (AOCS) and avionics, the aspects to consider during the study and design phases of Comet Interceptor are as follows:
  - Simple GNC avoiding unnecessary complexity (e.g. avoid vector delta-V modes if not strictly needed)
  - Implementation and commanding of standard guidance function
  - Standard thruster modulators
  - Standard wheel control functions
  - Simple thruster mounting with force free attitude control capability
  - Use of well-proven units (Reaction Control System, Inertial Measurement Unit, Reaction Wheels, Star Tracker)
  - Implementation of accurate accelerometers in general de-risks manoeuvres
  - Symmetrical S/C layout

- Clean definition of attitude constraints, aiming at minimum restrictions in manoeuvrability
- Adequate system mode management logic
- Simple Failure Detection Isolation and Recovery (FDIR) concept
- Articulated antennae add complexity and operations overhead. Proper System level trade-off between benefits and cost shall be considered.
- Ideally, export controlled items should be avoided, but it understood to be unavoidable for some Instruments in Comet Interceptor.

In general, re-use of platforms (at least for what concerns avionics, Tracking Telemetry and Commanding, Reaction Control System) is a significant cost saving measure as demonstrated by Rosetta, Mars Express and Venus Express.

#### **19.4.2 Ground Segment**

As concerns the ground segment the following elements shall be considered as having significant influence on the overheads:

- Utilisation of non-ESA elements (e.g. other tracking networks, interface with other control centres, etc.): having to interface elements outside ESA can be a source of significant development costs and efforts during operations.

It is assumed that Bepi MMO Control Centre interfaces experience for JAXA Payload operations can be re-used as far as possible. The usage of other tracking networks, currently not foreseen, will imply additional testing and validation of those ground stations.

- Size of the scientific community: the larger the number of instruments and teams to interface, the more development is required; Operations costs are less affected by this aspect.
- Degree of re-use: The mission control system will be based on the latest available developed system within the Solar System and Exploration missions family. Specific system modifications will be developed as required. Assumed costs are based on estimates from previously developed control systems, sized for Comet Interceptor.
- In operations the mission planning process is the most effort-demanding process together with navigation. Having a lean mission planning process, with interfaces kept to the minimum essential, and the minimum number of entities involved are key factors in containing the development and operations overheads. Where feasible instruments operations planning should be integrated directly with the overall mission planning process upon direct inputs from the science community.

It is assumed that the Comet Interceptor science operations will be a one-shot event therefore well defined in advance and unlikely to change much, for which the supporting ground segment architecture proposed is shown in Figure 19-1. The science operations and the ground segment architecture will be discussed with ESA D/SCI in the next phases.

- Mission profile allowing the main part of the operations to be performed during normal working time, possibly with very repetitive pattern, is adequate for containing operations costs. Critical operations, near real time operations, short

response times should be avoided to the extent possible. Critical operations extended in time (e.g. ExoMars aerobraking, Rosetta comet characterization, Rosetta end of mission) are very effort demanding.

It may be envisaged to operate during normal working time through the L2 waiting and the post-encounter phases. The critical operations implying near real time and short response times are assumed short and to occur from the approach until beginning of the encounter phases – the concept of operations during the encounter, implying short ground response times, will need to be evaluated.

This Page Intentionally Blank

## 20 PROGRAMMATICS

*Note: due to the dynamic environment of the mission development, elements of the chapter below differ from the details included in the RFI and other ITT documents. The chapter below represents the assumptions at the time of this CDF study (end 2019). This is particularly true for the schedule presented below, which is expected to not reflect the most up-to-date developments.*

### 20.1 Requirements and Design Drivers

The main objective of AIV/programmatics within the Comet-Interceptor study is to validate that the mission is feasible to be launched together with ARIEL given the key dates proposed by the customer, to identify potential bottlenecks for the schedule, to evaluate options for the model philosophy and to assess the schedule.

The main requirements and design drivers for the Comet Interceptor project from a programmatic point of view are:

SubSystem Requirements		
Req. ID	Statement	Parent ID
Prog-010	Launch in 2028 (Q4/2028)	
Prog-020	Launch as co-passenger to ARIEL (with DLS)	
Prog-030	One main S/C (S/C A, ESA) plus two probes (B2 (ESA) and B1 (JAXA)) carried as payloads	
Prog-040	All Comet Interceptor equipment shall be TRL 6 by Mission Selection (Q1 2020)	
Prog-050	All payload and platform units at least TRL 7 by Mission Adoption (Q4 2022)	
Prog-060	Maximum spacecraft development duration of 4 years	
Prog-070	Maximum Cost at Completion (CaC) of 150 M€	

### 20.2 Assumptions and Trade-Offs

Assumptions	
1	Review durations nominal: 30 days
2	ITT 6 months at start of Phase A/B1 and covering from Phase A to Phase D/E1
3	No dedicated ITT issued for the implementation phase (B2/C/D)
4	Payloads Readiness Review just prior to Mission Adoption
5	Phases B2/C/D pending Mission Adoption
6	ESA contingency before acceptance review: 6 months
7	Launch campaign duration: 3 months

- A set of target key dates and milestones for Comet-I had been provided at the beginning of the Comet-I CDF study, they are listed in Table 20-6.

- The procurement approach shall be similar to CHEOPS, i.e. different than the typical phasing for Science M- or L-class missions (this difference in approach is already reflected in the provided key dates in Table 20-6).

## 20.3 Technology Requirements

The Technology Readiness Levels (TRL) present a systematic measure supporting the assessments of the maturity of a technology of interest and enabling a consistent comparison in terms of development status between different technologies.

The TRL definitions are shown in Table 20-1:

TRL	ISO Definition	Associated Model
1	Basic principles observed and reported	Not applicable
2	Technology concept and/or application formulated	Not applicable
3	Analytical and experimental critical function and/or characteristic proof-of concept	Mathematical models, supported e.g. by sample tests
4	Component and/or breadboard validation in laboratory environment	Breadboard
5	Component and/or breadboard critical function verification in a relevant environment	Scaled EM for the critical functions
6	Model demonstrating the critical functions of the element in a relevant environment	Full scale EM, representative for critical functions
7	Model demonstrating the element performance for the operational environment	QM
8	Actual system completed and “flight qualified” through test and demonstration	FM acceptance tested, integrated in the final system
9	Actual system completed and accepted for flight (“flight qualified”)	FM, flight proven

**Table 20-1: TRL scale**

Generally, only technology sufficiently advanced (TRL6 or higher) at the start the Implementation Phase shall be used. The reasoning for this is to guarantee that any technology used is sufficiently mature so that required design adaptations to Comet Interceptor can be done within the nominal project phases (Phase B2, C and D). For Comet Interceptor, it is required that “all payload and platform units are at least TRL 7 by Mission Adoption (Q4 2022)” (Prog-050).

The product tree, as established at the end of the study, is shown in Table 20-2 (S/C A) and Table 20-3 (S/C B2). It identifies for each subsystem the associated equipment, sometimes components, and their TRL.

Min of Value	Product	TRL
SC_A (Spacecraft A)		
AOGNC		
A_DPU (A DTU Data Processing Unit)	✓	9
A_IMU_LN200_1 (A IMU Northrop Grumman LN200 Core #1)	✓	9
A_IMU_LN200_2 (A IMU Northrop Grumman LN200 Core #2)	✓	9
A_NAVCAM_OH_1 (A DTU NAVCAM Optical Head #1)	✓	9
A_NAVCAM_OH_2 (A DTU NAVCAM Optical Head #2)	✓	9
A_STR_OH_1 (A DTU STR Optical Head #1)	✓	9
A_STR_OH_2 (A DTU STR Optical Head #2)	✓	9
A_SUN_LENS_Bison64_1 (A SUN LENS Bison 64 #1)	✓	8
A_SUN_LENS_Bison64_2 (A SUN LENS Bison 64 #2)	✓	8
A_SUN_LENS_Bison64_3 (A SUN LENS Bison 64 #3)	✓	8
A_SUN_LENS_Bison64_4 (A SUN LENS Bison 64 #4)	✓	8
A_SUN_LENS_Bison64_5 (A SUN LENS Bison 64 #5)	✓	8
A_SUN_LENS_Bison64_6 (A SUN LENS Bison 64 #6)	✓	8
RW_RSI_4_215 (A RW Rockwell Collins RSI 4-215)	✓	9
RW_RSI_4_216 (A RW Rockwell Collins RSI 4- #216)	✓	9
RW_RSI_4_217 (A RW Rockwell Collins RSI 4- #217)	✓	9
RW_RSI_4_218 (A RW Rockwell Collins RSI 4- #218)	✓	9
COM		
XDST_1 (X-Band DSTRASP #1)	✓	9
XDST_2 (X-Band DSTRASP #2)	✓	9
XHGA (X-Band HGA)	✓	9
XLGA_1 (X-Band LGA #1)	✓	9
XLGA_2 (X-Band LGA #2)	✓	9
XRFDN (X-Band RFDN)	✓	9
XTWT_1 (X-Band TWT #1)	✓	9
XTWT_2 (X-Band TWT #2)	✓	9
XTWTA_EPC_1 (X-Band TWTA EPC #1)	✓	9
XTWTA_EPC_2 (X-Band TWTA EPC #2)	✓	9
A_ISL_GOMx_board_1 (A GOMx Electronics #1)	!	5
A_ISL_GOMx_board_2 (A GOMx Electronics #2)	!	5
A_ISL_GOMx_Patch_1 (A GOMx Antenna Patch #1)	!	6
A_ISL_GOMx_Patch_2 (A GOMx Antenna Patch #2)	!	6
A_ISL_GOMx_Patch_3 (A GOMx Antenna Patch #3)	!	6
A_ISL_GOMx_Patch_4 (A GOMx Antenna Patch #4)	!	6
A_ISL_GOMx_Patch_5 (A GOMx Antenna Patch #5)	!	6
A_ISL_GOMx_Patch_6 (A GOMx Antenna Patch #6)	!	6
DH		
A_OBC (A Onboard Computer)	!	6
A_RIU (A Remote Interface Unit)	✓	9
PWR		
A_Bat (A Battery)	✓	7
A_PCDU (A PCDU)	✓	7
A_SA (A SolarArray)	✓	7
A_SA_2 (A SolarArray #2)	✓	7

.../...

Min of Value	Product	TRL
<b>SC_A (Spacecraft A)</b>		
CPROP		
A_Lat_Val_1 (A Latch Valves)	✓	9
A_Lat_Val_2 (A Latch Valves)	✓	9
A_Pass_Valve (A Passivation_Valve)	✓	9
A_Pipes (A Pipes)	✓	9
A_Press_Trans_1_1 (A Pressure Transducer #1)	✓	9
A_Press_Trans_1_2 (A Pressure Transducer #1)	✓	9
A_Press_Trans_1_3 (A Pressure Transducer #1)	✓	9
A_Prop_Filt (A Propellant Filter)	✓	9
A_Fil_Dr_Val_1 (A Fill Drain Valve)	✓	9
A_Fil_Dr_Val_2 (A Fill Drain Valve)	✓	9
A_Test_Port_1 (A Test_Ports)	✓	9
A_Test_Port_2 (A Test_Ports)	✓	9
A_Tk_CPROP_1 (A Tank CPROP #1)	✓	9
A_Tk_CPROP_2 (A Tank CPROP #2)	✓	9
A_Thr_5N_1 (A Thruster_MONARC 5N #1)	✓	9
A_Thr_5N_2 (A Thruster_MONARC 5N #2)	✓	9
A_Thr_5N_3 (A Thruster_MONARC 5N #3)	✓	9
A_Thr_5N_4 (A Thruster_MONARC 5N #4)	✓	9
A_Thr_5N_5 (A Thruster_MONARC 5N #5)	✓	9
A_Thr_5N_6 (A Thruster_MONARC 5N #6)	✓	9
A_Thr_5N_7 (A Thruster_MONARC 5N #7)	✓	9
A_Thr_5N_8 (A Thruster_MONARC 5N #8)	✓	9
EPROP		
A_PPU (A Power Processing Unit)	✓	8
A_Thruster_PPS1350 (A Thruster PPS1350)	✓	8
A_BPRU (A BPRU)	✓	8
A_FU (A FU)	✓	8
A_Miscellaneous (A Miscellaneous)	✗	0
A_PRE_Card (A PRE Card)	✓	8
A_XFC (A XFC)	✓	8
A_Prop_Tank_1 (A Propellant Tank #1)	✓	9
A_Prop_Tank_2 (A Propellant Tank #2)	✓	9

.../...

Min of Value	Product	TRL
SC_A (Spacecraft A)		
MEC		
A_APM_HDRM_APME (A Antenna Pointing Mechanisms Subsystem with Driver and HDRM)	✓	8
A_SA1_HDRM_1 (A SA1 HDRM #1)	✓	8
A_SA1_HDRM_2 (A SA1 HDRM #2)	✓	8
A_SA1_HDRM_3 (A SA1 HDRM #3)	✓	8
A_SA1_HDRM_4 (A SA1 HDRM #4)	✓	8
A_SA2_HDRM_1 (A SA2 HDRM #1)	✓	8
A_SA2_HDRM_2 (A SA2 HDRM #2)	✓	8
A_SA2_HDRM_3 (A SA2 HDRM #3)	✓	8
A_SA2_HDRM_4 (A SA2 HDRM #4)	✓	8
A_SADM_1 (A SADM #1)	✓	8
A_SADM_2 (A SADM #2)	✓	8
A_SADEV (A SA drive electronics)	!	6
A_Clamp_Band (A Clamp Band Ejection System)	✓	8
STR		
A_Misc_STR (A Miscellaneous STR)	✗	0
A_RCS_Structure (A RCS Suport)	✓	7
A_SecondarySTR (A Secondary Structure)	✓	7
A_Inserts (A Inserts)	✗	0
A_ShearW (A ShearWebs)	✓	7
A_SA_yoke_1 (A Solar Array Yoke #1)	✓	7
A_SA_yoke_2 (A Solar Array Yoke #2)	✓	7
A_Baseplate (Baseplate)	✓	7
A_ExtPanels_1 (A Closure Panels #1)	✓	7
A_ShieldingPanels_1 (A ShieldingPanels #1)	!	5
A_PL_Panel (Payload Support Panel)	✓	7
TC		
A_TC_FILLER (A TC Thermal Filler)	✓	9
A_TC_HEATER (A TC Heater)	✓	9
A_TC_MLI (A TC Multi Layer Insulation)	✓	9
A_TC_PAINT (A TC Paint)	✓	9
A_TC_RAD (A TC Radiator Panel)	✓	9
A_TC_SO (A TC Stand Offs)	✓	9
A_TC_STRAP (A TC Thermal Strap)	✓	9
A_TC_T_SENS (A TC Temperature Sensor)	✓	9
A_TC_HP (A TC Heat Pipes)	✓	9

Min of Value	Product
	TRL
SC_A (Spacecraft A)	
INS	
A_CoCa_CSU (A CoCa Camera Support)	!
A_CoCa_ELU (A CoCa Electronics Unit)	!
A_DFP_DISC (A DFP Dust Impact Sensor and Counter)	!
A_DFP_E_Box (A DFP E-Box)	!
A_DFP_SCIENA_ENA (A DFP Solar wind and Cometary Ions and Energetic Neutral Atoms-ENA sensor)	!
A_DFP_SCIENA_Ion (A DFP Solar wind and Cometary Ions and Energetic Neutral Atoms-Ion sensor)	!
A_MIRMISS_TIRI (A MIRMISS Thermal InfraRed Imager)	!
A_DFP_LEES_1 (A DFP Low Energy Electron Spectrometer 1)	!
A_CoCa_PEU (A CoCa Proximity Electronics Unit)	!
A_CoCa_Rad (A CoCa Radiator)	X 0
A_DFP_COMPLIMENT_p_1 (A DFP COMetary Plasma Light Instrument probe #1)	!
A_MANiac_ELU (A MANiac Electronics Unit)	!
A_MANiac_NDG (A MANiac Neutral Density Gauge)	!
A_MANiac_SHU (A MANiac Sensor Head Unit)	!
A_MIRMISS_MIR_1 (A MIRMISS Mid-InfraRed Sensor 1)	!
A_MIRMISS_MIR_2 (A MIRMISS Mid-InfraRed Sensor 2)	!
A_MIRMISS_NIR (A MIRMISS Near InfraRed Sensor)	!
A_MIRMISS_Rad (A MIRMISS Radiator)	X 0
A_DFP_COMPLIMENT_boom_1 (A DFP COMetary Plasma Light Instrument boom 1)	!
A_DFP_COM_FGM_boom_2 (A DFP COMPLIMENT+FGM+boom_2)	!
A_MANiac_Harn (A MANiac Harness)	X 0
A_MANiac_Mec (A MANiac Rotating Mechanisms)	X 0
A_CoCa_Harn (A CoCa Harness)	X 0
A_CoCa_MLI (A CoCa Thermal Insulation)	X 0

**Table 20-2: Overview TRL's for S/C A (note that units highlighted with an orange “!” require special development effort as TRL<7)**

Min of Value	Product	TRL
SC_B2 (Spacecraft B2)		
AOGNC		
RW_RW250 (RW Astrofein RW250)	✓	9
COM		
ISL_T_LGA (ISL_ToroidalLGA)	✓	8
B2_ISL_GOMx_board (B2 GOMx Electronics)	!	5
B2_ISL_GOMx_ActiveFE (B2 GOMx Active Antenna FE)	!	6
DH		
B2_OBC (B2 Onboard Computer)	!	6
INS		
B2_DFP_DISC (B2 DFP Dust Impact Sensor and Counter)	!	5
B2_DFP_E_Box (B2 DFP E-Box)	!	5
B2_EnVisS (B2 Entire Visible Sky)	!	4
B2_OPIC (B2 Optical Imager for Comets)	!	4
B2_DFP_FGM_1 (B2 DFP FGM #1)	!	6
B2_DFP_FGM_2 (B2 DFP FGM #2)	!	6
B2_DFP_FGM_boom (B2 DFP FGM boom)	!	4
MEC		
B2_Clamp_Band (B2 Clamp Band Ejection System)	✓	8
PWR		
B2_PDU (B2 PDU)	✗	0
B2_Bat_1 (B2 Battery #1)	✗	0
STR		
B2_Baseplate (Baseplate B2)	✗	0
B2_MLI_Tent_1 (MLI Tent B2 #1)	✓	7
B2_Bumper (B2 bumper)	!	6
B2_COM_SupportSTR (COM_SupportSTR)	✓	7
B2_IF_Ring (IF Ring B2)	✓	7
TC		
B2_TC_FILLER (B2 TC Thermal Filler)	✓	9
B2_TC_HEATER (B2 TC Heater)	✓	9
B2_TC_MLI (B2 TC Multi Layer Insulation)	✓	9
B2_TC_PAINT (B2 TC Paint)	✓	9
B2_TC_RAD (B2 TC Radiator Panel)	✓	9
B2_TC_SO (B2 TC Stand Offs)	✓	9
B2_TC_STRAP (B2 TC Thermal Strap)	✓	9
B2_TC_T_SENS (B2 TC Temperature Sensor)	✓	9

**Table 20-3: Overview TRL's for probe B2 (note that units highlighted with an orange “!” require special development effort as TRL<7)**

For more information and details on the corresponding subsystem equipment, its development status and required development needs, please refer to the relevant subsections in this report. The following list gives an overview (except instruments) of equipment below TRL 7:

Min of Value	Product	TRL
SC_A (Spacecraft A)		
COM		
A_ISL_GOMx_board_1 (A GOMx Electronics #1)	!	5
A_ISL_GOMx_Patch_1 (A GOMx Antenna Patch #1)	!	6
DH		
A_OBC (A Onboard Computer)	!	6
MEC		
A_SADE (A SA drive electronics)	!	6
STR		
A_ShieldingPanels_1 (A ShieldingPanels #1)	!	5

**Table 20-4: Equipment of the S/C (w/o instruments) identified below TRL7**

Notes:

- The Shields (shieldPanels): even if the technology is basic (based on aluminium plate), it seems necessary to consider a development phase to validate the protection performances.

## 20.4 Model Philosophy

A PFM approach is warranted due to the technological maturity of a large number of subsystems. It is supported by dedicated engineering and development models.

In taking into account the programmatic, technical and cost constraints the following models are considered.

### 20.4.1 Equipment / Sub-System Level:

MTD/MD: Mass/thermal dummies for use at system level SM (satellite).

EM/EQM: Engineering/Qualification models for equipment qualification and use in satellite Flatsat.

PFM/FM: Protoplayment or Flight Models for integration in satellite PFM.

### 20.4.2 System Level:

**SQM (Structural Qualification Model):** The main objectives of the SQM are:

- To confirm the design concept
- To qualify at an early stage the structure of the satellite
- To correlate analytical model with the results of the tests (sine, acoustic)
- To assess more precisely the loads for the instruments/equipment (risk mitigation action)

The structure of the SQM (S/C A) will be refurbished to become the Flight Model. (For this to be in principle feasible, compatibility of the PFM with regard to the experienced mechanical test levels (i.e. to avoid over-stressing the structure) on the SM has to be proven).

This approach allows to mitigate risks (schedule, technical), to reduce cost (refurbishment).

*A thermal model in early phase ((S)TM) is not considered as essential as the thermal environment doesn't present any specific constraint and the Analytical Thermal and Thermal Simulation models are mature enough to have good confidence on the analysis. At PFM level, the outcomes of the TVAC test will be used to correlate the thermal model. The surface of the radiators must be adjustable on the PFM following the final thermal analysis.*

**Flatsat (EFM, AVM, SVF):** Electrical and functional representative model for software development, functional verification and FDIR development and validation.

**PFM:** Proto-flight Model to complete qualification and acceptance to confirm readiness for flight.

**RF suitcase:** For ground station compatibility testing.

In addition, spacecraft, payloads and subsystem **simulators** might be needed to validate functions on the Flatsat setup and with the MOC and SOC. They may also support failure investigations at later stage.

## 20.5 Model Test Matrix

The subsequent table provides an overview about the main satellite tests per model.

Model	SQM				EFM/AVM				PFM			
	S/C A	B1	B2	CI	S/CA	B1	B2	CI	S/C A	B1	B2	CI
Level	S/C A	B1	B2	CI	S/CA	B1	B2	CI	S/C A	B1	B2	CI
(Contr contractor)	= Contr	JAXA	TBD	Contr	Contr	JAXA	TBD	Contr	Contr	JAXA	TBD	Contr
General												
Alignment	X a)			X a)					X	X	X	X
Functional					X	X	X	X	X	X	X	X
Performances						X			X	X	X	X (TBC)
Mission / Ground Segment Compatibility Test					X			X a)	X			X
Polarity / End to End Test					X a)			X a)	X			X (TBC)
Mechanical Interfaces (Fit Check)	X b1) d)			X c)					X d)			X
Electrical Interfaces					X b2)			X c)				X
Mechanical												
Physical properties		X f)	X f)	X					X i)	X	X i)	X
Static Loads	X e)	X e)	X e) Q						e)	e) PQ	e) PQ	

Model	SQM				EFM/AVM				PFM			
	S/C A	B1	B2	CI	S/CA	B1	B2	CI	S/C A	B1	B2	CI
Level	S/C A	B1	B2	CI	S/CA	B1	B2	CI	S/C A	B1	B2	CI
(Contr contractor) =	Contr	JAXA	TBD	Contr	Contr	JAXA	TBD	Contr	Contr	JAXA	TBD	Contr
Q				X Q								
Acoustic				X Q								X PQ
Random vibration		X f) g)	X f) g)						X g)	X g)(TBC)		
Sinusoidal vibration		X f)	X f)	X Q					X	X	X	X PQ
Shock probe B1 or B2 separation				X								X
Launcher Separation (drop test / shock test)				X h)								X h)
Micro-vibration susceptibility												
Mechanisms				X f)								X
Structural integrity												
Proof pressure												X
Pressure cycling												
Design burst pressure												
Leak												X
Thermal												
Thermal vacuum									X j) PQ	X	X j) PQ	X j) PQ
Thermal balance									X j) PQ	X	X j) PQ	X j) PQ
Electrical / RF												
Conducted EMC test					X a)	X a)	X a)	X a)	X	X	X	X
Radiated EMC and RF/auto Compatibility Test									X	X	X	X
ESD					X k)	X k)	X k)	X k)				

- a) stand alone and/or In preparation of activity to be performed on PFM
- b1) with scientific instruments and PF equipment (STM or dummy)
- b2) with scientific instruments and PF equipment (EM or simulator)
- c) with B1 and B2 (EM or simulator)
- d) with launcher
- e) could be done on structure only or at element level instead; at S/C level it could be done as quasi-static sine vibration test;
- f) TBC depending representativity of the model
- g) Random/Acoustics to assess
- h) depends on launch vehicle; on SQM this could be a separation/shock test, on PFM rather only a separation test with a Qualif level expected at SQM level and Acceptance expected at PFM level
- i) TBC depending AOCS requirements
- j) TBC depending Thermal criticality and Programmatic constraints, but a TVAC test mandatory at PFM level
- k) TBC depending ESD criticality (Vs instruments specificities)
- Q Qualification
- PQ Proto Qualification (Qualification Level / Acceptance Duration)
- TBC To Be Confirmed

**Table 20-5: Model test matrix**

The probes B1 and B2, the payloads and instruments have to be available for flight acceptance tests together with the S/C A PFM. This is reflected in the schedule and in the corresponding delivery dates.

## 20.6 Ground Support Equipment

One set of assembly, integration and testing MGSE will be sufficient since SQM and PFM campaigns are well decoupled from each other.

Two sets of EGSE (TBC) should be envisaged to allow parallel activities to be executed on the satellite Flatsat model and the PFM satellite.

## 20.7 Development Approach

Most proposed subsystems have a relatively high TRL so that they can be further developed or delta developed within the nominal project phases (TRL 6 or higher at PDR). Only a limited number of technology predevelopments are needed in this mission (§ 20.3 Technology Requirements).

Specifically, the following areas could require predevelopment:

- ISL (Electronics (TRL5), Antenna Patch)
- Shield (panel, tanks (TRL 5))

## 20.8 Schedule

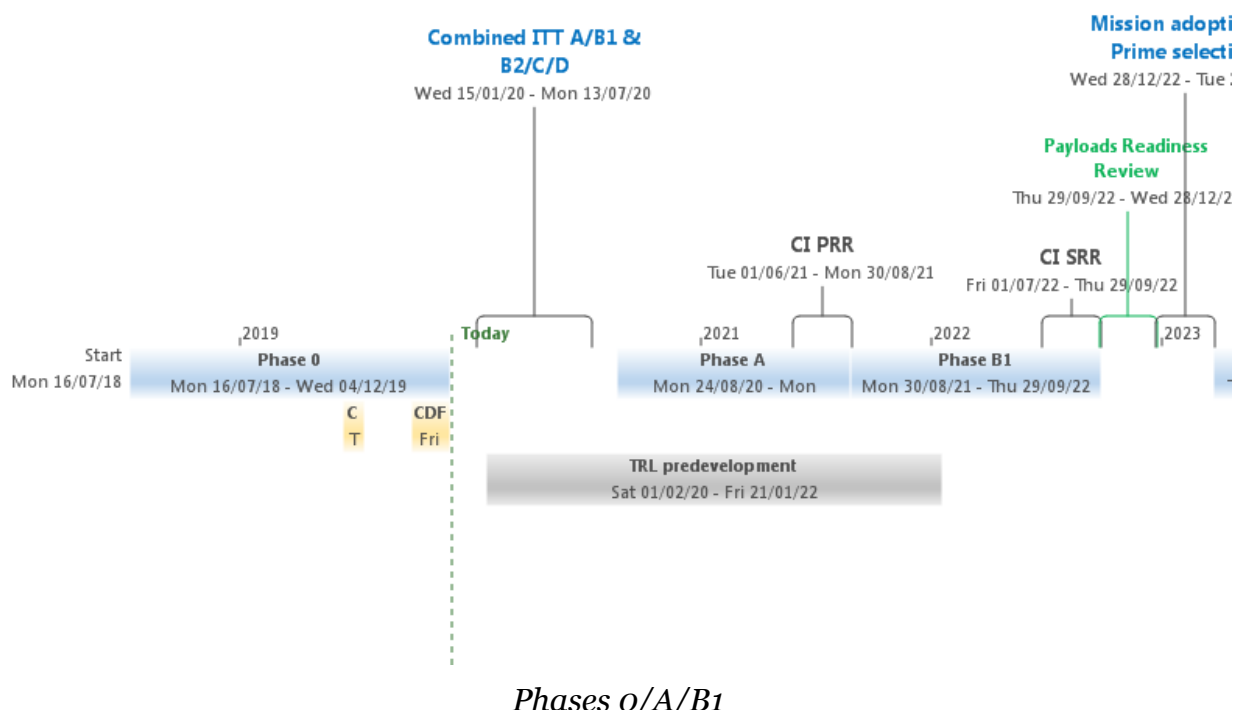
The schedule has been set up to be compatible with the fast development approach for Comet-I. This means that the typical durations and decision milestones for Science missions have to be modified (similar durations and phasing have been realised in CHEOPS) in order to meet the stipulated key dates.

	Milestone	Input to Comet-I study	Output from study	Comet-I
		Target dates	Dates achievable	
Comet-I	ITT issued	Apr 2020	Apr 2020	
	Phase A/B KO	Sep 2020	Sep 2020	
	PRR	Sep 2021	Sep 2021	
	SRR	Sep 2022	Oct 2022	
	Adoption	Nov 2022	Dec 2022/Jan2023	
	Prime selection	Dec 2022	Q1/2023	
	PDR	Q1/2023	Q4/2023	
	CDR	Q2/2024	Q3/2024	
	STM delivery	May 2024	--	
	Q/FAR	Q4/2027	Q4/2027	
Comet-I payloads and instruments	Launch	Q4/2028	Q4/2028	
	pPRR		Payload/Instruments reviews has been placed 6 months before Mission Reviews (assumption).	
	pSRR			
	pPDR			
	pCDR		This needs to be assessed by	

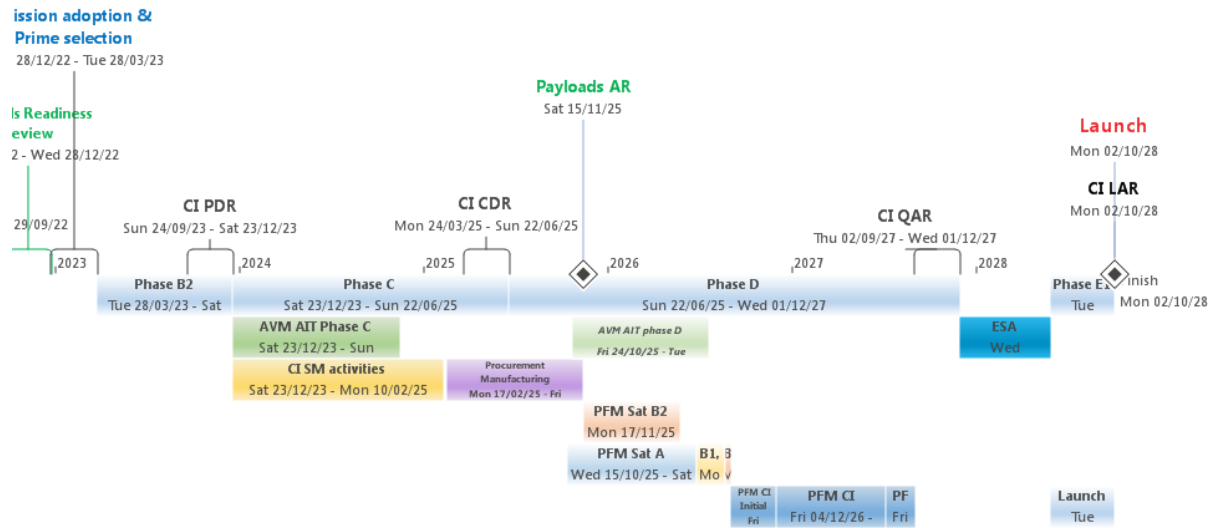
Milestone	Input to Comet-I study	Output from study	Comet-I
pQ/AR		the Payload team taking into account on going activities and schedule	
	pQ/AR	Nov 2025	
	Delivery for integration into Comet-I PFM	<b>Q4/2025</b>	

**Table 20-6: Overview key milestones (listed if given as input, and resulting feasible dates are extracted from the baseline schedule)<sup>33</sup>**

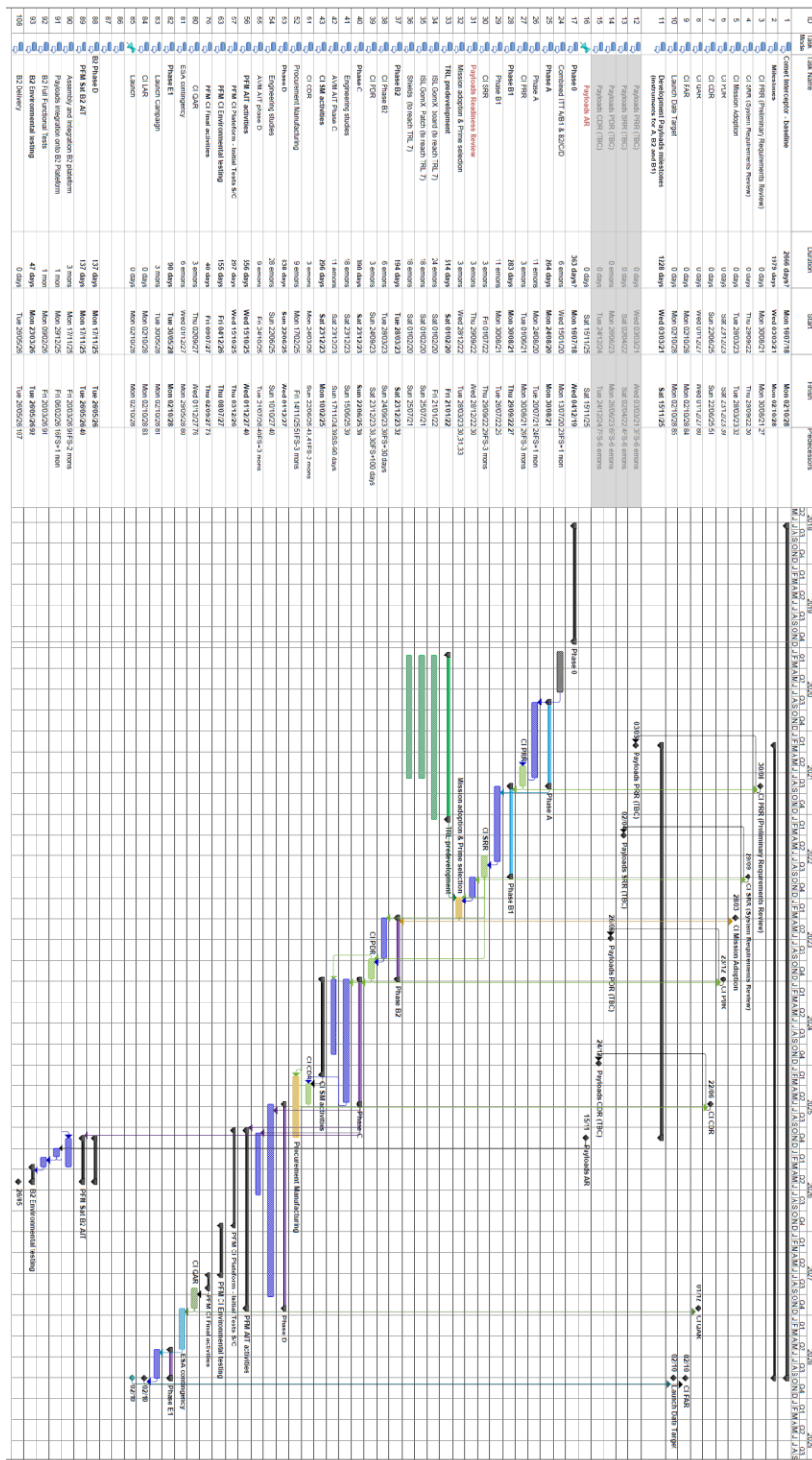
Figure 20-1 shows the overall timeline and baseline schedule for Comet-I.



<sup>33</sup> As noted in the disclaimer at the start of this chapter, the schedule presented here is based on the assumptions used during the CDF study (end 2019). It therefore does not reflect the most up-to-date schedule presented in the other ITT documents.



Phases B2/C/D/E1



The duration of the phases of the project is summarized below:

Phase	Duration	
<b>Phase A</b>	11 months + CI PRR : 12 months	<b>A/B1</b>
<b>Phase B1</b>	11 months + CI SRR : 13 months	25 months
<b>Phase B2</b>	6 months + CI PDR: 9 months	<b>B2/C/D</b>
<b>Phase C</b>	18 months + CI CDR: 18 months	56 months
<b>Phase D</b>	26 months + CI QAR: 29 months	

**Table 20-7: Phase durations<sup>35</sup>**

A Payload Readiness Review is planned after Mission SRR to confirm/assess the maturity of the payloads (TRL7 expected).

The conclusion of the Mission SRR and Payloads Readiness Review will be inputs for the Mission Adoption to authorise the continuation of the phases B2/C/D.

## 20.9 Instruments and Payloads

The payload/instrument schedule was not assessed during the study. Assumptions were taken for the payload/instruments reviews (6 months prior the Mission reviews). The payload/instrumentation schedule should be evaluated as part of this new overall schedule, keeping in mind that the delivery date has been set so that the S/C is ready for launch in Q4 / 2028.

- The instruments and the probe B1 (JAXA) need to be delivered Q4 2025 for integration on probe B2 and on S/C A.
- Once the probe B2 will be fully integrated and tested, it will be delivered to the S/C A for integration and tests (mid 2026).
- Depending on the complexity of this integration and required testing with the S/C A, the delivery date may be adapted, as it depends on the exact sequencing of the assembly and integration activities for B1, B2, PL instruments, and the S/C A, and it subsequently also depends on the corresponding environmental testing.

The durations of the phases are credible and the overall schedule is achievable. However, the contingency is limited to 6 months (for a project of 8 years 2020-2028).

The date of the launch is driven by ARIEL.

## 20.10 Summary and Recommendations

From the programmatic point of view, the TRL 7 requirement by the end of phase B1 is a major criteria to consolidate the overall schedule. The current CDF design does not show a major risk for this topic. However, some parts of the instruments/payload have a

---

<sup>35</sup> As above, the presented schedule does not reflect the most up-to-date schedule used in the other ITT documents.

low TRL level (4). A dedicated review (Payload readiness review) is proposed just prior to the Adoption Review to assess the progress performed.

The schedule was defined taking into account experience from previous projects and also the nature of the project (Fast Mission). The duration of the phases is credible and the overall schedule is achievable but also challenging (only 6 months of contingency on a 8 years project).

The delivery date of the instruments/payloads at the end of 2025 is also a key milestone for this project.

## 21 TECHNICAL RISK

### 21.1 Reliability and Fault Management Requirements

The following reliability and fault management requirements are proposed for the Comet Interceptor mission.

ID	Requirement
RISK-005	<p>The operational availability of the science products during the science phase shall be greater than 99,5% (TBC) over the specified science period.</p> <p><i>Remark: the operational availability is the result of the anomaly-reliability ( how many events are leading to an interruption of the performance and the duration to recover from the anomaly and to return to the specified performance; the 'anomaly reliability' has to be defined in conjunction with the loss-reliability [REQ-010]; specific 'maintainability/ maintenance' requirements are not needed because in the worst case all anomalies during the short and time-critical constellation deployment and encounter might lead to a critical loss of performance</i></p>
RISK-010	<p>The overall reliability of the S/C A shall be <math>\geq 85\%</math> at end of life. (<math>100\% - 85\% = 15\%</math> 'loss unreliability' -&gt; loss of mission*)</p> <p><i>Remark:</i>  <i>* here is meant 'loss of mission' due to technical and operational failure/ error related to S/Cs A and failure/ error which might propagate and could lead to failure of S/C A from the probes B1 and B2; it is not meant 'loss of mission' due to specific environmental conditions around the mission target, like dust impact</i>  <i>** if it is seen from viewpoint of mission objectives suitable loss-reliability targets for the probes B2 and B1 could be defined</i></p>
Overall remark:	<i>it has to be emphasised, that the usual anomaly-reliability (anomalies can be usually compensated with adequate contingency procedures) will contribute remarkably to the 'loss unreliability' especially for B1 and B2 due to the time-criticality of the mission operation short before and during the flyby</i>
RISK-020	The lifetime of S/C A shall be compatible with the 5 years (nominal) mission lifetime.
RISK-030	Single-point failures with a severity of catastrophic or critical (as defined in ECSS-Q-ST-30C/40C) shall be eliminated or prevented by design.
RISK-040	Single-point failures (other than catastrophic or critical) shall be avoided in the design of the units. Retention of single-point failures in the design shall be declared and justified and it is subject to formal approval by ESA.
RISK-050	Retention in the design of single-point failures of any severity rating is subject to formal approval by ESA on a case-by-case basis with a detailed retention rationale.
RISK-060	A failure of one component (unit level) shall not cause failure of, or damage to, another component or subsystem.
RISK-070	The failure of an instrument shall not lead to a safe mode.
RISK-080	Any hazardous situation, which will not cause immediate loss of but may develop into the loss of the S/C A or instrument, shall be prevented by design or protected against.

ID	Requirement
RISK-090	The design shall allow the identification of on-board failures and their autonomous recovery (e.g. by switching to a redundant functional path). Where this can be accomplished without risk to spacecraft and instrument safety, such recovery shall enable the continuity of the mission timeline and performance, in particular during the comet fly-by phase.
RISK-100	Where redundancy is employed, the design shall allow operation and verification of the redundant item/function, independent of nominal use.
RISK-110	The design and operation of vehicle shall be compliant with applicable Space Debris Requirements (e.g. ESA/ADMIN/IPOL Space Debris Mitigation for Agency Projects).
RISK-120	The vehicle design shall be compliant with applicable safety related launch requirements (e.g. CSG Safety Regulations).

\*see applicable mission success criteria's in Table 21-2

\*\* depending on the responsible launch authority and/ or launch operator

### **Table 21-1: Reliability and Fault Management Requirements**

The above preliminary requirements stem from previous similar scientific missions of the European Space Agency.

## **21.2 Risk Management Process and Scope of Risk Assessment**

Risk management is an organised, systematic decision making process that efficiently identifies, analyses, plans, tracks, controls, communicates, and documents risk in order to increase the likelihood of achieving the project/ study goals. The procedure comprises four fundamental steps:

- **Step 1:** Definition of the risk management policy which includes the project success criteria, the severity & likelihood categorisations, and the actions to be taken on risks
- **Step 2:** Identification and assessment of risks in terms of likelihood and severity
- **Step 3:** Decision and action (risk acceptance or implementation of mitigating actions for the risk reduction)
- **Step 4:** Monitoring, communication and documentation and risk acceptance.

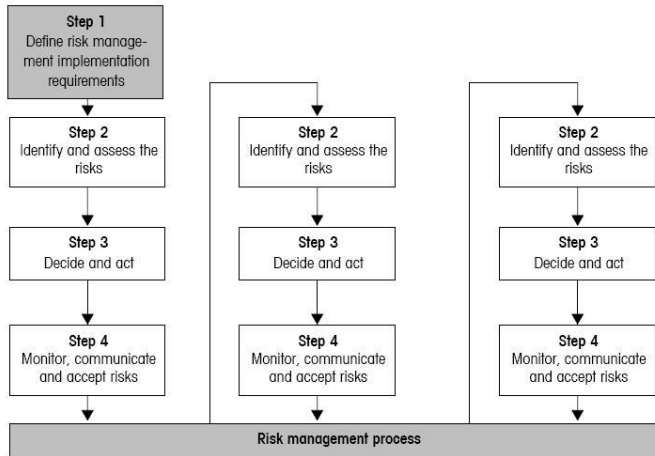


**Figure 21-1: ECSS-M-ST-80C, 2008 Risk Management Process**

The Comet Interceptor CDF-Study is a pre-phase A feasibility assessment and results of all 4 steps have to be seen as preliminary. The full documentation of the Risk assessment is pre-mature at this stage of the project.

The basis for the preliminary risk assessment is the kick-off documentation/presentation of the study. Changes in the kick-off baseline which are caused by identified risks were already seen as mitigation measures in terms of Risk Reduction.

The preliminary risk assessment for COMET Interceptor study is considering risks for the following mission elements:

- Dispenser
- Main spacecraft (S/C A) - incl. payload and platform
- B<sub>2</sub> probe
- B<sub>1</sub> probe in terms of its integration on S/C A and its operation in space only
- Ground segment

Excluding: ...

- B<sub>1</sub> probe in terms of design and manufacturing (design under JAXA responsibility)

During the following pre-project, project and mission phases:

- Study – A/B<sub>2</sub> (design maturity in pre-project phase)
- Development phase – A/B<sub>2</sub> (technological maturity in pre-project phase)
- Mission realisation – A/B<sub>2</sub> (project phase)
- Launch preparation and launch (project/ mission phase) A/B<sub>1</sub>/B<sub>2</sub>
- Mission deployment (LEOP, IOT) – A/B<sub>1</sub>/B<sub>2</sub>
- Parking period around L<sub>2</sub> including leaving the parking orbit A/B<sub>1</sub>/B<sub>2</sub>
- Interplanetary trajectory to mission target including A/B<sub>1</sub>/B<sub>2</sub>
- Deployment before close encounter A/B<sub>1</sub>/B<sub>2</sub>
- Science phase of mission A(/B<sub>1</sub>)/B<sub>2</sub>

- Data transfer from S/C A to Earth.

### 21.2.1 Approach for Risk Identification and Risk Reduction (steps 2 and 3)

The assessment of the specific risks presented in section 21.5 is based on the overall approach for the hazard description visualised hereafter.

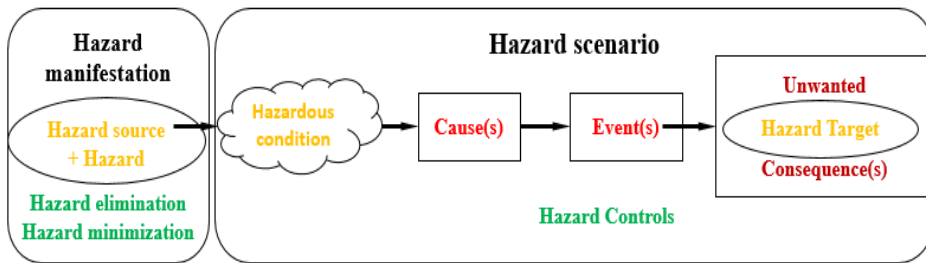


**Figure 21-2: Risk identification and risk reduction**

The assessment starts with the definition of the ‘Hazard Source’, the ‘Hazard’ and the ‘Hazard Target’.

In the next step the ‘primary Hazardous Condition’ which is inherent connected to the Hazard Source, the Hazard and the Hazard Target is identified including the expected ‘Unwanted Consequences’.

Finally the ‘Cause’ (e.g. the failure modes) which is triggering the ‘Event’ originating the Unwanted Consequence is recognised. The occurrence of the Cause, its transition to an Event (or Event Chain) and the realisation of the Unwanted Consequence is often influenced by circumstances summarised as ‘secondary Hazardous Conditions’.

Based on this information the likelihood of the occurrence of the Unwanted Consequences can be judged as a point estimate which applies in general to the ‘worst case’ severity category.

In case the risk is not acceptable in terms of the used risk index, (see section 21.3.3) risk reductions via mitigation measures have to be defined to bring the risk into an acceptable area of the risk index. Such mitigation measures like hazard elimination, hazard minimization and hazard controls are beyond the baseline. They have to be considered in a delta study or in the project/ mission phase.

An initial risk for one Hazard Target can be connected or lead to a new(^)/ additional(+) risks for another Hazard Targets as a consequence of its reduction e.g. the mitigation of dependability risks (e.g. increase of the redundancy) can lead to an impact on other Hazard Targets like programmatic (e.g. possible overrun of the mass budget) and/or cost and/ or schedule. Such risk propagation is visualised hereafter.

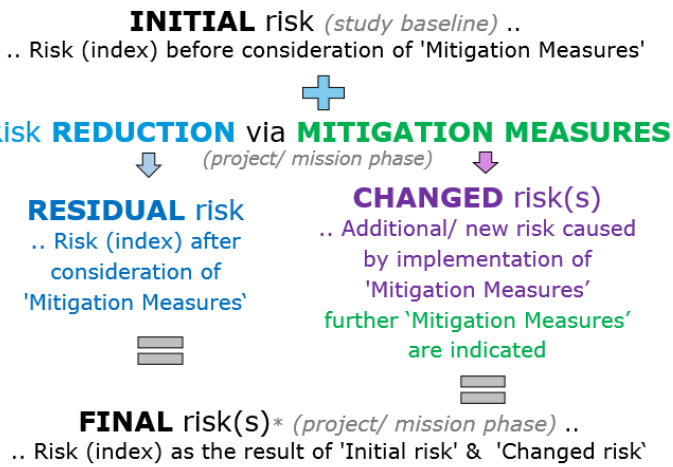


**Figure 21-3: Risk propagation**

The terms used in context of the risk identification are defined as follow:

Hazard Target [HT]	An item/ entity/ person which could get affected by the mishap like performance (science, services, ...)/safety (harm, damage)/ cost/ schedule (see section 21.3.1)
Hazard Source [HS] <sup>3</sup>	An item/ entity of the CDF study and/ or space mission
Hazard <sup>1</sup> [H]	Existing or potential property/ state <sup>2</sup> of a Hazard Source that can result in a mishap for the Hazard Target
Hazardous Condition <sup>2</sup> [HC]	Hazardous conditions are levels/ borders capacities or situation/ circumstances which can initiate or influencing a 'Hazard scenario' and can be associated with <ul style="list-style-type: none"> <li>- primary Hazardous Condition [HCp]</li> <li># intrinsic property (physical, chemical or biological capacity)</li> <li># functional/ physical state of a 'Hazard source' but also</li> <li>- secondary Hazardous Conditions [HCs] related to</li> <li>* technology, design, manufacturing, organisation and other conditions</li> </ul>
Hazard Scenario	The combination of 'Cause(s)' and 'Event(s)', which results into a specific Unwanted Consequence considering as well secondary Hazardous Conditions
Cause [C]	Root Cause which is the origin of a Hazard Scenario
(final) Event [E]	Final physically event or functional/organisational/commercial/... status/ event which is directly leading to the Unwanted Consequence under the given Hazardous Conditions
Event Chain (events)	Several intermediate events might occur between the Cause and the final Event
Unwanted Condition [UC]	Is a/are potential result(s) of a Hazard Scenario which specified the negative effect for the Hazard TARGET[HT] in the frame of the CDF study the Unwanted Conditions has to be specified based on the Study/ Mission Success Criteria's (see section 21.3.2)

Hazard Manifestation	The Hazard Source with its potential Hazards and Hazardous Conditions becomes part of the study baseline/ future mission
Hazard Elimination <sup>4</sup>	The Hazard will be fully eliminated mostly by elimination of the Hazard Source
Hazard Minimisation <sup>4</sup>	The Unwanted Consequences (Severity category) will be downgraded mostly via changes in the primary Hazardous Condition
Hazard Control <sup>4, 5</sup>	Engineering or administrate measurements

Remarks:

- 1/3 Hazards are NOT events (neither accidents nor incidents) but potential threats to the Hazard Target;
- 2 Property or state which can be associated with the design, manufacturing, operation, organisation, application or environment, an intrinsic property of an item/ entity, e.g. unstable isotopes/ radiation, Hardware/ sharp edges, a functional/physical state of an item/ entity e.g. Medium/ high pressure in a vessel; Hardware/ high temperature of a surface, ...
- 3 Prerequisite(s) for the occurrence of 'Hazard scenarios' with their negative effects ('Unwanted Consequences') on 'Hazard Target(s)
- 4 Basic strategies/ Mitigation Measures for the Risk Reduction
- 5 e.g. - Design selection (failure tolerance, ..)
  - Design to minimum risk (Safety margins/factors)
  - Automatic safety device, design to contain,
  - Warning device, crew escape/ safe haven,
  - Dedicated procedures, regulations, standard's, programmes, ...

## 21.3 Risk Management Policy

### 21.3.1 Hazard Targets

The CDF risk management policy for Comet Interceptor study aims at handling risks which may cause serious programmatic/ cost/ schedule\*\*\*/ technological, performance (science return [or] services) \*\*\*/ technical and safety/ protection\* impact on the future project/ mission.

- \* 'Safety' related to the human life and health has a higher priority and importance than 'Safety' related to property and environment. To have a clear split between both safety aspects in the report the term
  - 'safety' is used exclusively for risks related to human life and health on ground and in space
  - 'protection' is used exclusively for risks related to equipment, property, and planetary environments (terrestrial, space and specific solar objects)

\*\* 'Performance' is standing for e.g. 'science' incl. 'technological tests' or 'services' (e.g. telecommunication, navigation , cargo)

\*\*\* The Hazard Target 'Schedule' could have two aspects:

- Cost related (c+sh): each delay might lead to a project extension, shift of launch preparation and the launch, which is usually linked to a cost increase but this does not mean that the mission can not be performed at a later date/ launch opportunity from launch/launcher-viewpoint
- Mission related (m+sh): schedule-constraints like launch window or Earth-orbit escape window has to be considered depending on several mission conditions, like mission destination, Earth-orbit before escaping to e.g. the interplanetary trajectory and the trajectory itself

### 21.3.2 Success Criteria

The success criteria with respect to the program, science, technical, safety/ protection safety, schedule, and cost objectives are presented in Table 21-2:

Risk Domain (Hazard Targets)	Success Criteria
<b>Study &amp; Mission Program</b> (Programmatic)	<p><b>STU1:</b> The mission accomplishes all of the key science goals (characterization [morphology, composition, plasma environment] of a Long Period Comet (LPC)).</p> <ul style="list-style-type: none"> <li>- Determine the bulk composition of the nucleus' surface</li> <li>- Investigate activity in a fresh comet.</li> <li>- Assess the molecular composition of the coma and the isotopic composition.</li> <li><i>-... and more science objectives as defined in the mission objectives</i></li> <li>- Assess how plasma and dust interact in various regions of the coma.</li> </ul> <p><b>MIS1:</b> The mission shall comprise of a main spacecraft - S/C A - and two probes - B2+B1 - that allow parking the main spacecraft in a Halo orbit around the SEL2 point after launch. After the identification of a suitable mission target (see STU1) the departure from parking position shall be initiated for fly-by/ encounter with the target comet, whereby the probes deployment shall take place shortly before encounter</p>
<b>Programmatic (Cost)</b>	<p><b>PR-C1:</b> CaC for ESA <math>\leq</math> 150M€ (2019EC) -&gt; F Class Mission</p> <p><b>PR-C2:</b> The mission design shall follow a “design-to-cost” for all its elements under ESA responsibility</p> <p><b>PR-C3:</b> The mission and system design should make use as far as possible of technologies from suppliers from ESA Member or Cooperating States.</p> <p><i>Remark: Use of equipment subject to US export control regulations shall be agreed on a case-by case basis with the Agency.</i></p>
<b>Programmatic (Schedule)</b>	<p><b>PR-S1:</b> All architecture elements are available and their FRR successful for the launch (NLT 2028)</p> <p><b>PR-S2:</b> The contributions from international partners (e.g. B1 from JAXA) are available at the relevant milestones of the development schedule</p> <p><b>PR-S3:</b> TRL <math>\geq</math> 6 by Q1 2020 and TRL <math>\geq</math> 7 for all components at the time of mission adoption (est. 2022)</p> <p><b>PR-S4:</b> Low development risk during Phase B2/C/D</p> <p><i>Remark: * ISO scale 2016</i></p>
<b>Performance (Science)</b>  <b>Technical</b>	<p><b>PER1:</b> S/C A to perform interplanetary transfer to target and to guarantee complete transfer to Earth of mission data after encounter</p> <p><b>PER2:</b> Probe B2 shall contribute to STU1 and shall transfer data to S/C A</p> <p><b>TEC1:</b> S/C A operates successfully over the designated mission lifetime of 5 years*</p> <p><b>TEC2:</b> A reliability of <math>&gt;85\%</math> at the end of mission/ program **</p>

Risk Domain (Hazard Targets)	Success Criteria
	<i>Remark:</i> * optional extension up to 7 years ** see remarks under [REQ-010]
<u>Safety / Protection</u>	<b>SAF1:</b> Catastrophic hazard (2 Failure/Error Tolerance), critical hazard (1Failure/Error Tolerance) incl. undesired human activities (human related error/failure) <b>SAF2:</b> No SPF can lead to catastrophic hazards; no performance degradation leading to SPF, and no failure propagation [ECSS-Q-ST-40C] <b>SAF3:</b> Mission shall be compliant with applicable ‘Launch Requirements’ (e.g. <i>CSG Safety Regulations</i> ) [ECSS-Q-ST-40C] <b>PRT1:</b> Mission shall be compliant with ESA policy for Space Debris Mitigation ESA/ADMIN/IPOL(2014)2 [ECSS-U-AS-10C]
<u>Design</u>	<b>DES1:</b> Ariane 6.2 (dual launch with ARIEL mission) <b>DES2a:</b> S/C A+B1+B2: 650kg; Probe B1: 30kg; Probe B2: 40kg <b>DES2b:</b> Probes deployment according MIS1

Reference: overall CDF study requirements/ ECSS-Q-ST-40C

**Table 21-2: Success Criteria**

### 21.3.3 Severity and Likelihood Categorisations

For the Comet Interceptor CDF-study a preliminary assessment of the risks for all hazard targets like cost(c), programmatic(pr) in terms of e.g. schedule(sh), technological readiness (tr), performance(dp)\*/ technical(dt) and safety(s)/ protection(p) is performed as described in chap. 21.2.

\* in the frame of this study ‘Performance’ is standing for ‘science’ .. see [PERn & TECn]

The severity of the risk scenarios are classified (based on the study baseline) according to their hazard target of impact. The consequential severity category of the risks scenarios is defined according to the worst case potential effect with respect to programmatic and science / performance objectives, technical and safety/ protection objectives, schedule objectives and/or cost objectives (see Table 21-2).

In addition, identified risks that may jeopardise and/or compromise the Comet Interceptor mission will be ranked in terms of likelihood of occurrence and severity of unwanted consequence (shortened as ‘severity of consequence’) as well for the study baseline as under consideration of possible mitigation actions.

The scoring scheme with respect to the severity of consequence on a scale of 1 to 5 is established in Table 21-3, and the likelihood of occurrence is normalised on a scale of A

to E in Table 21-4 and based on recommendations given for the risk assessment in ECSS-M-ST-8OC.

<b>Severity Score</b>	<b>Dependability Performance</b> (Science return/ Service - dp) & <b>Technical</b> (Dependability – dt)	<b>Safety &amp; Protection</b> (s/p)	<b>Schedule</b> (pr/ sh) incl. technological readiness (pr/ tr)	<b>Cost</b> (pr/ c)
Catastrophic 5	<u>Performance:</u> * Failure leading to the impossibility of fulfilling the mission's performance *  <u>Technical:</u> <u>failure propagation:</u> * from lower subsystem level to highest system level * from S/A to probes/ mission level * leading to loss of safety-related barriers  <u>Remark:</u> * might also cover 'loss of S/C' what, however, can be tailored to 'critical'	<u>Safety:</u> * Loss of life, life- threatening or permanently disabling injury or occupational illness; * Loss of an interfacing manned flight system  <u>Protection:</u> * Loss of interfacing higher system (e.g. third part property) * Severe detrimental environmental effects * Loss of launch site facilities.	Delay results in project cancellation For the project the 'Schedule' is also mission related because of the defined launch window (...??.. weeks) and escape windows (...??.. week) defined by the mission destiny	Cost increase result in project cancellation
Critical 4	<u>Performance:</u> * Failure resulting in a major reduction (70- 90%) in overall performance according mission objective *  <u>Technical:</u> * Major damage to flight systems	<u>Safety:</u> * Temporarily disabling but not life- threatening injury, or temporary occupational illness;  <u>Protection:</u> * Major detrimental environmental effects. * Major damage to or ground facilities. * Major damage to public or private property	Critical launch delay (24-48 months)	Critical increase in estimated cost (20 -50%)
Major 3	<u>Performance:</u> * Failure resulting in a major reduction (30- 70%) in overall performance  <u>Technical:</u> * Major degradation of the flight system	<u>Safety:</u> * Minor injury, minor disability, minor occupational illness.  <u>Protection:</u> * Minor system or environmental damage	Major launch delay (6-24 months)	Major increase in estimated cost (10 -20%)
Significant 2	<u>Performance:</u> * Failure resulting in a substantial reduction (10-30%) in overall performance  <u>Technical:</u> * Minor degradation of system (e.g.: system is still able to control the consequences)	<u>Safety:</u> * Impact less than consequences defined for severity level '3- Major'	Significant launch delay (3-6 months)	Significant increase in estimated cost (5 – 10%)
Minimum 1	<u>Performance:</u> * No/minimal consequences (0 - 10%) in overall performance  <u>Technical:</u> * No/ minimal consequences	<u>Safety:</u> * No/minimal consequences <u>Space Debris Mitigation:</u> casualty risk <10E-4	No/ minimal consequences (1-3 month delay)	No/ minimal consequences (<5%)
No			Initial risk fully	Initial risk fully

Severity Score	Dependability Performance (Science return/ Service - dp) & Technical (Dependability - dt)	Safety & Protection (s/p)	Schedule (pr/ sh) incl. technological readiness (pr/ tr)	Cost (pr/ c)
O	Initial risk fully eliminated	Initial risk fully eliminated	eliminated	eliminated

\* *'mission'* stands for a '.. set of tasks, duties ..' ECSS-S-ST-00-01C; para. 2.3.139

\*\* *'system'* stands for a '..set of interrelated or interacting high level functions

**Table 21-3: Severity Categorisation**

Score	Likelihood	Definition
E	Maximum	Certain to occur, will occur once or more times per project.
D	High	Will occur <b>frequently</b> , about 1 in 10 projects
C	Medium	Will occur <b>sometimes</b> , about 1 in 100 projects
B	Low	Will occur <b>seldom</b> , about 1 in 1000 projects
A	Minimum	Will <b>almost never</b> occur, 1 in 10000 projects

**Table 21-4: Likelihood Categorisation**

#### 21.3.4 Risk Index & Acceptance Policy

The risk index is the combination of the likelihood of occurrence of the consequences and the severity of consequences of a given risk item.

Risk ratings of low risk (green), medium risk (yellow), high risk (red), and very high risk (dark red) were assigned based on the criteria 'Severity' and 'Likelihood' of the risk index scheme (see Table 21-5 and Table 21-6).

The level of criticality of a risk item is denoted by the analysis of the adapted risk index. By policy very high risks are not acceptable and must be reduced (see Table 21-7).

Severity	5A-s	5B-s	5C-s	5D	5E
	5A-p	5B-p	5C-p		
4	4A	4B	4C	4D	4E
3	3A	3B	3C	3D	3E
2	2A	2B	2C	2D	2E
1	1A	1B	1C	1D	1E
	A	B	C	D	E
					Likelihood

**Table 21-5: Initial/ final Risk Index**

Severity	5A-s	5B-s	5C-s	5D	5E
5	5A-p	5B-p	5C-p		
4	4A	4B	4C	4D	4E
3	3A	3B	3C	3D	3E
2	2A	2B	2C	2D	2E
1	1A	1B	1C	1D	1E
	A	B	C	D	E
					Likelihood

**Table 21-6: Adjusted Risk Index**

Risk Index (applicable for generic risk index)*	Risk Magnitude	Proposed Actions (during assessment phase)
5C-s, 5D-s, 5E-s	Very High Risk (harm related)	Unacceptable risk: implement mitigation actions (either likelihood reduction or severity reduction through new baseline) with responsible party.
3E, 4D, 4E, 5C-p, 5D-p, 5E-p	High Risk (protection related)	
2E 3D 4C 5A-s, 5B-p	Medium Risk	Acceptable risk for study however, unacceptable for project: therefore implement further reduction action(s) with responsible party/ project partners
1D, 1E, 2C, 2D, 3B, 3C, 4A, 4B, 5A-p,	Low Risk	Acceptable risk: Monitor and control. Optional reduction.
1A, 1B, 1C, 2A, 2B 3A,	Low Risk	Acceptable risk

*\* the colour code defines as well the acceptable risk level*
**Table 21-7: Proposed Mitigation Actions (project phase)**

## 21.4 Risk Drivers

The following generic risk drivers have been considered in the identification of specific risk items:

- New technologies (TRL)
- Design challenges (configuration, mass, volume, power, lifetime, mission/ performance operation, communication, ...)

- Major mission events, (launch/ escape windows)
- Functional and dependability issues (performance + technical, reliability in terms of loss of S/C (e.g. single point failures – SPF), reliability in terms of anomalies including aspects of science effectiveness [or] service availability)
- Safety and environmental & property factors (protection)
- Programmatic factors (e.g. cost, project delays)

## 21.5 Top Risk Log (preliminary)

Top risk items have been preliminary identified at the mission (ESA) levels. Please refer to Annex A Table A-1 for a complete list of preliminary identified major risks and their corresponding suggested mitigating actions.

The risk index results reflecting the initial risk assessment\* are summarised in Annex A Table A-1 (column risk index (initial)) and reflecting the final assessment in Annex A Table A-1 (risk index (final)) considering mitigation measures as described.

The risks are sorted and marked\* according the study/ mission timeline\*\*:

- **Study (S)**
- Mission **Design + realisation (D)**
- **Launch (preparation), LEOP, IOT incl. S/C deployment after launch (L)**
- **Overall Project Management/ PA/ Engineering incl. design + realisation incl. launch till IOT (OM)**
- **Cruise/ Mission deployment + operation(C)**
- **Mission performance (M)**
- **Overarching Risks (OA) \*\*\***
- Sustainability Risks, like **Space Debris (SD) + Planetary Protection (PP)**
- **Interfacing Risks (I) and Other risks (O)**
- **Overall Cost (OC) + Overall Schedule (OS)**
- **Other risks (O)**

\* the underlined abbreviations are used in Tab 1.5-1 / -1a & 2a/b/c as the beginning initials of the Risk no.

\*\* appearance of ‘root cause’ and ‘events’ (chap. 1.2.1) in the study/ mission timeline

\*\*\* ‘Meta risks’- are pointing to overall study success criteria’s and resulting from several technical/ technological, safety, schedule and cost risks

The risk numbering (1st column of Annex A Table A-1 & -Table 21-8, Table 21-9, Table 21-10) is associated to the study internal risk allocation and does not give a ranking according their importance or any other numerical order.

### **IMPORTANT remark:**

*Safety/ protection, reliability and availability related risks are mentioned in the paragraph above in the second step of the risk management process, and in the risk log hereafter e.g. at the end of ‘Mission Design’ related risks and the beginning of ‘Mission Performance’ related risks.*

- However, this does not mean that these risks are of lower importance. It is because safety, reliability and availability are often affected by and interacting with several other risks scenarios via randomised & systematic failure/ errors (lifetime, launch/space/operation environment, TRL, design fluffs, ... ) or contribution to overall mass, power budget, cost and schedule risks (e.g. via redundancies, safety factors and margins, S/C modes, implementation and verification of related mitigation measures...).

Therefore, the risk assessment in terms of safety, reliability and availability has to consider the outcome of the assessment of several other risk scenarios and is therefore not placed at the beginning of the Risk Log.

**The identified major risks for the Comet Interceptor mission are equally distributed over the various developments, project and deployment/mission phases starting with the study performance (see Annex A Figure A-1). From the view point of mission elements (S/C A and the probes B1 and B2) most of the major risks are applicable to all elements or are interfacing risks between the mission elements.**

Initial Assessment					
Severity	A	B	C	D	Likelihood
5					
4			OMI, SCIIb/c-B2	OCI, DIII6, OA1a/b, SI, IFI, DXX, MD1a, D1b, D1c, MIXc, DIII2b-A	
3				LIII, LIV, MIV-B2, MVII, DIII2a	MIXc, MD1b
2					DIVa
1					
0 (no)					
	A	B	C	D	E

Reference	Risk index (Initial)	Risk scenario	
		HERITAGED from pre-study	
OCI	4D	Cost budget overrun	
DIII6	4D	Exceeding mass budget	
OAla/b	4D	'loss of- reliability exceeded	
SI	4D	Study maturity	
DIII7-B2	3D	Redundancy concept	
DIVa	2E	no/ low TRL	
LIII	3D	number of mission elements & PL instrum.	
OMI	4C	inter-agency cooperation	
IFI	4D	dual launch (second priority mission)	
DXX	4D	uncertainties - baseline launch vehicle A6.2	
LIV	3D	failure of ground station equipment	
MDIa	4D	safe mode during L2 transfer	
DIb	4D	availability* of a target comet	
MDIb	3D	navigation precision	
Dlc	4D	time critical deployment & operations.	
SCIib/c-B2	4C	separation of B2 from A fails	
MIXc	4D	Dust impact & inertia/ kinetic	
MIV-B2	3D	B2 boom instability deployment & dust	
MVII	3D	propulsion caused plumes	
MIXc	3E	(dust) contamination of instruments	
DIII2a	4G	communications between A and B1/2	
DIII2b-A	4D	data transmission to Earth after fly-by	

**Table 21-8: Top Risk Index – Initial assessment**

Table 21-9 considers the risk mitigation measures discussed during the study and documented in the Risk-Log (Annex A, Table A-1). However, these mitigation measures have to be considered and implemented in the development/ project and mission phase of the Comet Interceptor.

Severity	Final Assessment				
	A	B	C	D	E
5					
4			OAla/b, DXX, Dlb, Dlc	OCI ???, DIII6 ???	
3			SI, LIII, OMI, IFI, LIV, SCIIb/c-B2, MIXc, MIV-B2, MVII, MIXc, DIII2a, DIII2b-	MDla, MDlb	
2				DIVa	
1					
0 (no)					
					Likelihood

Reference	Risk index (initial)	Risk scenario	Risk index (final)
		HERITAGED from pre-study	
OCI	4D	Cost budget overrun	???
DIII6	4D	Exceeding mass budget	???
OAla/b	4D	'loss of'- reliability exceeded	4C
SI	4D	Study maturity	3C
DIII7-B2	3D	Redundancy concept	3D
DIVa	2E	no/ low TRL	2D
LIII	3D	number of mission elements & PL instrum.	3D
OMI	4C	inter-agency cooperation	3C
IFI	4D	dual launch (second priority mission)	3C
DXX	4D	uncertainties - baseline launch vehicle A6.2	4C
LIV	4D	failure of ground station equipment	3C
MDla	4D	safe mode during L2 transfer	3D
Dlb	4D	availability* of a target comet	4C
MDlb	3D	navigation precision	3C
Dlc	4D	time critical deployment & operations.	4C
SCIIb/c-B2	4C	separation of B2 from A fails	3C
MIXc	4D	Dust impact & inertia/ kinetic	3C
MIV-B2	3D	B2 boom instability deployment & dust	3C
MVII	3D	propulsion caused plumes	3C
MIXc	4E	(dust) contamination of instruments	3C
DIII2a	4D	communications between A and B1/2	3C
DIII2b-A	4D	data transmission to Earth after fly-by	3C

Table 21-9: Top Risk Index – Final assessment

Because of the explorer character of the mission and the inherent risks related to the mission target (dust and particle environment) the risk index could be adjusted in terms of an acceptance of a higher risk level.

Severity	Adjusted Assessment <i>(as already done in the pre-study)</i>				
	A	B	C	D	E
5					
4			OAIa/b, DXX, DIB, DIC	OCI ???, DIII6 ???	
3			SI, LIII, OMI, IFI, LIV, SCIIB/c-B2, MIXc, MIV-B2, MVII, MIXc, DIII2a, DIII2b-	MDIA, MDIB	
2				DIVa	
1					
0 (no)					
					Likelihood

Reference	Risk index (Initial)	Risk scenario		Risk index (final)	Risk index (adjust.)
		HERITAGED from pre-study			
OCI	4D	Cost budget overrun		???	???
DIII6	4D	Exceeding mass budget		???	???
OAIa/b	4D	'loss of- reliability exceeded		4C	4C
SI	4D	Study maturity		3C	3C
DIII7-B2	3D	Redundancy concept		3D	3D
DIVa	2E	no/ low TRL		2D	2D
LIII	3D	number of mission elements & PL instrum.		3D	3D
OMI	4C	inter-agency cooperation		3C	3C
IFI	4D	dual launch (second priority mission)		3C	3C
DXX	4D	uncertainties - baseline launch vehicle A6.2		4C	4C
LIV	3D	failure of ground station equipment		3C	3C
MDIA	4D	safe mode during L2 transfer		3D	3D
DIB	4D	availability* of a target comet		4C	4C
MDIB	3D	navigation precision		3C	3C
DIC	4D	time critical deployment & operations.		4C	4C
SCIIB/c-B2	4C	separation of B2 from A fails		3C	3C
MIXc	4D	Dust impact & inertia/ kinetic		3C	3C
MIV-B2	3D	B2 boom instability deployment & dust		3C	3C
MVII	3D	propulsion caused plumes		3C	3C
MIXc	4E	(dust) contamination of instruments		3C	3C
DIII2a	4C	communications between A and B1/2		3C	3C
DIII2b-A	4D	data transmission to Earth after fly-by		3C	3C

Table 21-10: Top Risk Index – Adjusted assessment

The 'adjusted risk assessment' shows from technical/ technological viewpoint an acceptable risk level. However, further system / mission adjustment or an adjustment of the mission objectives has still to be done' regarding cost and mass.

### 21.5.1 Risk Log General Conclusions

- Very high risks and high risks are typical of a phase A project. Areas with lack of definition or little previous experience pose a priori more risk to the mission and therefore are the ones with more risk reduction potential
- Experience shows that all risk items with a critical risk index (red, orange area) must be analysed and proposals for risk treatment actions elaborated
- In the end, ideally all risk items should achieve a level of justifiable acceptance
- The risk management process should be further developed during the project definition phase in order to refine the risk identification/analysis and provide evidence that all the risks have been effectively controlled.

### 21.6 Risk Log Specific Conclusions and Recommendations

The scientific objectives of the Comet Interceptor mission:

- The mission accomplishes all of the key science goals (characterization [morphology, composition, plasma environment] of a LPC)
- Determine the bulk composition of the nucleus' surface
- Investigate activity in a fresh comet
- Assess the molecular composition of the coma and the isotopic composition *and more science objectives as defined in the mission objectives*
- Assess how plasma and dust interact in various regions of the coma.

This requires high precision instruments design and operation over a relatively long lifetime under deep space/ close-to-comet environment conditions (galactic radiation, solar flares, high kinetic dust/ particle environment around comet nucleus during encounter). Such an ambitious mission contains naturally a risk potential (see Annex A, Figure A-1 and Annex A, Table A-1).

However this mission can build up and benefit from comprehensive practical ESA-internal experiences for such type of scientific-missions (e.g. Rosetta/ Philae). Therefore most of these initially identified technical and performance risks justified as 'very high' and 'high' could be mitigated (see Table 21-9) sufficiently in the frame of the study.

Nevertheless, the Comet Interceptor study covers a very complex mission with many mission elements and phases where no comprehensive ESA-internal experiences are available. Naturally many risks are identified (see Annex A, Figure A-1 and Annex A, Table A-1). Any of this initially identified risks justified as unacceptable could be mitigated (see Annex A, Figure A-1 and Annex A, Table A-1). In this process of the risk assessment it was considered that for deep space explorer missions in general and in particular for a mission to investigate the core of a comet with its inherent challenges related to radiation and dust particles the acceptable risk level should be adjusted (Table 21-10).

The specific risk drivers for the Comet Interceptor CDF study are:

- Low cost approach (limited financial resources <150Mill Euro) .. **OCI**
- Dual launch in terms of schedule limits and mass restriction (secondary mission) .. **IFI, DIII6**
- Uncertainty about the possible mission target and its reachability .. **DI6**
- Space environment around mission target (dust + flyby (high relative speed)) .. **MIXc**
- Fly-by results into extreme time-critical scenario .. **DIc**
- Several mission elements (A/B1/B2), 2 probes (ESA&JAXA), 5 years mission life time, galactic radiation and COTS technology in deep space .. **OAA/b.1/3** and **MIXa/b**
- No redundancy considered for the mission critical components of the probe (B2) .. **(DIII7-B2)**

Other major risk like the navigation precision before the close encounter which is depending on the distance to the comet nucleus (**MDIb**) and the transmission of the science data first after the exposure of S/C A to the harsh environment close to the comet nucleus in terms of dust impacts will also have an impact on the drivers.

The mitigation measures available at the time of the CDF study are not seen as effective enough to achieve fully the study objectives, and with this an acceptable risk level in terms of mass budget (**DIII6**) and cost limitation (**OCI**).

For all other risks, mitigation measures could be identified which allow the reduction of the baseline risk during the development, project and mission phase to an acceptable level.

Although during the study a final solution for all design aspects was not found (**SI**) it has to be emphasised that several trade-offs for e.g. the power system, the communication system and the S/Cs configuration could be identified and analysed. This will give a sufficient base for a successful completion of the mission/system baseline within 2020.

The TRL risk should not be seen as 'major risk', because the development related risk seems to be relatively low for the Comet Interceptor mission. None of the PL and PF components have actually a TRL lower than 4!.

The 'Risk assessment' shows from technical/technological viewpoint an acceptable risk level. However, further system / mission adjustment or an adjustment of the mission objectives has to be done e.g. for cost and mass targets.

Nevertheless, the unique scientific objectives - to investigate a never-before-close-to-Sun-comet, to give a better understanding of the origin and development of our solar system - should justify a review of the financial frame of the mission and the increase of the possible mission mass to make this mission possible.

## 22 SOFTWARE

### 22.1 Requirements and Design Drivers

SubSystem Requirements		
Req. ID	Statement	Parent ID
SW-010	The S/C A SW shall handle the communication with satellite units, instruments and probes (B1 and B2) before and after separation.	
SW-020	The operations of the S/C A shall rely upon a set of Telemetry and Telecommand Packet Utilisation Standard (PUS) services, as defined in GS&Ops chapter allowing the full range of operations for any mode.	
SW-030	The S/C A SW shall collect science data coming from all instruments and from the probes (B1 and B2) via the Inter Satellite Link (ISL).	
SW-040	The S/C A SW shall provide means to transfer to ground the collected science data in a flexible and configurable manner supporting retransmission of corrupted packets.	
SW-050	The S/C A SW shall be designed for maximum autonomy of operations based on scheduled operations configurable by ground.	
SW-060	The S/C A SW shall ensure that any commands generated by different on-board concurrent sources (e.g. Software, MTL, OBCP, FDIR) shall not result in any conflict leading to permanent units or instruments failures.	
SW-070	Safety of the satellite shall be intrinsically ensured by SW design, i.e. no operational intervention shall be required to guarantee its survivability.	
SW-080	The FDIR functions shall detect, isolate and recover single failures in order to minimise instruments mission data outage without compromising the safety of the satellite / instruments	
SW-090	The FDIR shall include functions to detect software malfunctions, using e.g. watchdog timers to detect SW lockout situations at SW functional level and at the level of HW/SW interfaces.	
SW-100	The SW shall be capable to perform maintenance activities in an autonomous way based on planned timelines and generate corresponding reports.	

## 22.2 Assumptions and Trade-Offs

Assumptions	
1	The S/C A payloads communicate with OBC via SpaceWire link
2	The S/C A payloads are equivalent to PUS terminals
3	On S/C A, Science Mass Memory Unit is used to store science data and it supports routing of SpW packets. It can be a physically self-standing unit or integrated as part of the OBC.
4	Inter Satellite Link communication between S/C A and probes B1/B2 will be based on the CubeSat Space Protocol (CSP)
5	A direct link between Science Mass Memory and TC&TM board is available to downlink science data packets to ground.

## 22.3 Baseline Design

### 22.3.1 S/C A General Architecture

A block diagram of the baseline design is shown in following figure.

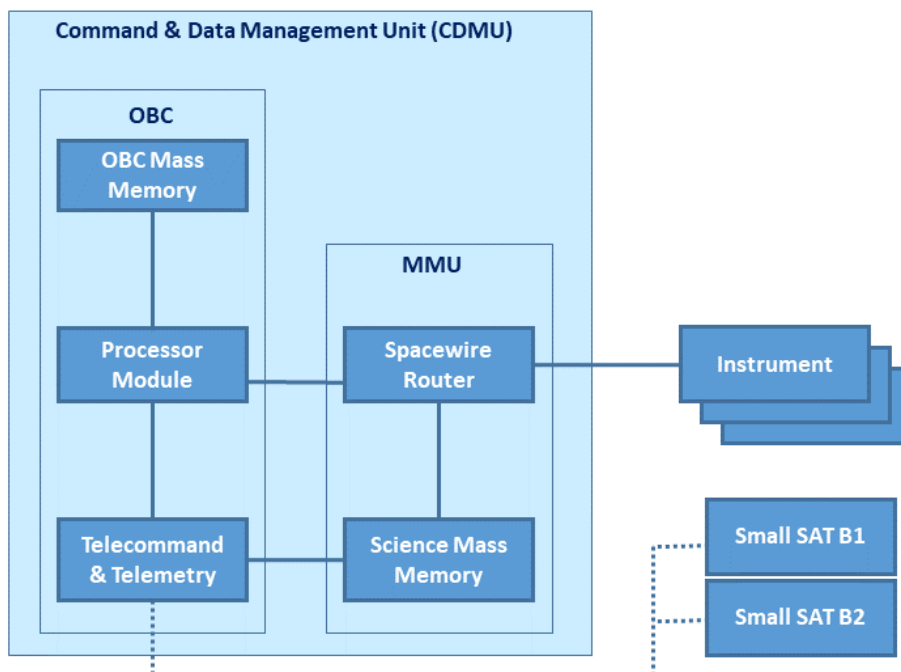


**Figure 22-1: Design overview**

On S/C A, the Command & Data Management Unit (CDMU) is composed of:

- On Board Computer (OBC):
  - Internal mass memory: it can store the HK TMs generated and the configuration of the SW, e.g. MTL and OBCPs
  - Processor Module: it executes the SW image supporting GNC, AOCS, Thermal Control, FDIR, Units Management, etc. etc.

**Telecommand and Telemetry:** the board is in charge to receive TC via X-Band and to forward them on the Processor Module (PM). It downloads TMs to ground, over X-Band for science and not science. Additionally the board handles the S-Band ISL connection to probes.

- Mass Memory Unit:
  - SpaceWire Router: it forwards and exchanges SpaceWire packets between Processor Module, Mass Memory and Instruments based on SpaceWire logical address
  - Science Mass Memory: it contains recorded science TM organized in files & directories. On-Board Software (OBSW) running on the PM manages the file system organization. It supports downlink at file level.
- Instruments: all instruments on S/C A are communicating via SpaceWire link and they are implementing a basic set of PUS services.
- Probes (B1 and B2): the probes are connected to the TM/TC module via umbilical before separation. After releasing, the Inter Satellite Link (ISL) supports the communication. In both cases, the data exchange is based on the CubeSat Space Protocol.

In order to guarantee the maximum autonomy to spacecraft operations, the OBSW running on S/C A shall support different sources of telecommands both generated on-board and received from ground, implementing different PUS services. The TC originated on-board will be uplinked by Ground using file transfer (PUS 13), stored in the OBC Mass Memory, and activated by direct TC, time or events. Routine Science Operations will be conducted principally via Mission Time Line (MTL) and limited On Board Control Procedure (OBCP) usage. The following sources of TC will be considered:

- MTL (PUS 11): TC stored in the mission time-line, emitted by OBSW at a pre-programmed time. The MTL will be the main tool to operate the spacecraft and the instruments allowing the execution of commands at a precise moment in time. The OBSW could support two MTLs, one for nominal mode and one for safe mode.
- TC File: a sequence of TC stored in file, emitted by OBSW while executing the TC file. The commands will be executed one after the other with a configurable delay between them.
- OBCP (PUS 18): TC part of on-board control procedure, emitted by OBSW while executing the OBCP. The procedures are “small” programs interpreted on-board by the OBSW and they support simple control flow via if/then/else/loop statements. The OBCP can access TM data stored in data pool, and, as result of the process, they can issue TCs. The OBCPs can be uploaded without modifying the OBSW image and they are typically used by ground to automate on-board operations.
- Event Actions (PUS 19): TC emitted by OBSW following an event (PUS 5). These TCs are part of the FDIR mechanism based on the combined use of Monitoring Service (PUS 12), Event Service (PUS 5) and Action service (PUS 19).
- Ground: direct commands emitted by Ground, routed to instruments or probe or directly processed by OBSW.

### 22.3.2 Probes Communication

Before separation of the probes B1 and B2, the ground team shall be able to control their internal status and execute maintenance routine operations. Therefore, an interface towards ground shall be implemented. In order to maximise the interoperability of the ground with respect to all the three satellites, the utilisation of PUS standard protocol is envisaged.

Nevertheless, the usage of already available protocol has to be considered in the trade-off, especially if the technology to be adopted in B1 and B2 is based on CubeSat heritage. CubeSat internal and external communication is carried out in most cases with the CubeSat Space Protocol (CSP). The library released under LGPL licence is available and it supports different operating systems, e.g. FreeRTOS, Linux.

Combination of PUS and CSP can be considered and implemented in the S/C A OBSW. The SW running on S/C A will present a dedicated PUS service (mission specific) to ground in order to interact with the B1 and B2 probes. Once a command is received, the OBSW will convert it to the corresponding CSP command and then forward it to the corresponding terminal OBSW that will process the command (on the B1 or B2 probe). Telemetry will be handled in the same way.

Thus, the S/C A OBSW converts PUS packets to/from CSP over umbilical or ISL. To be noted: no command to B1/B2 is foreseen once the probes have been released. The OBSW will manage B1 and B2 as other instruments / units, remotely via ISL once separated only for data acquisition.

The SW conversion mechanism is depicted in Figure 22-2:

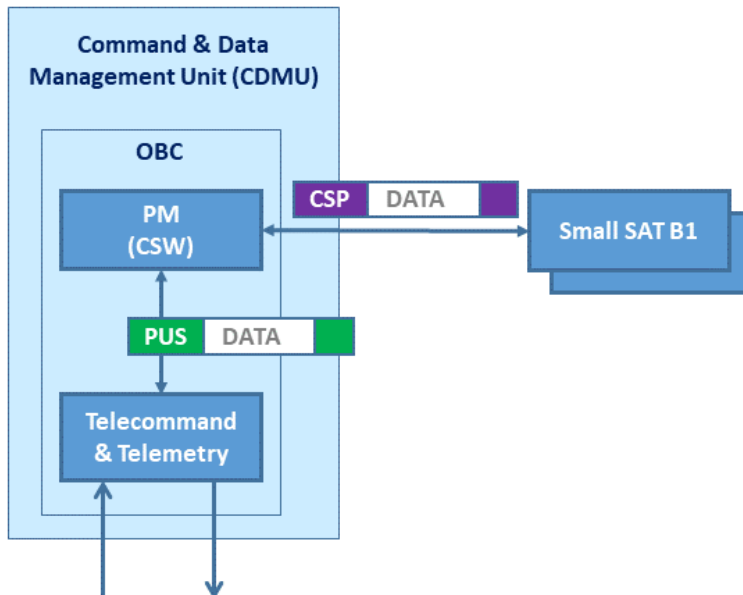


**Figure 22-2: Protocol conversion for ISL communication**

This solution presents the following advantages:

- Reuse of standard protocol with COTS components

- Less implementation effort on probes B1 & B2
- Transparent from Ground (PUS I/F)
- B2 commands can be used in MTL, OBCP and TC list for autonomous operations (e.g. maintenance).

### 22.3.3 Probe B2 Functional Modes

Considering the functionality of B2, the corresponding OBSW can be designed in a reduced and simplified way. A first overview of the main B2 SW operational modes is depicted in Figure 22-3:

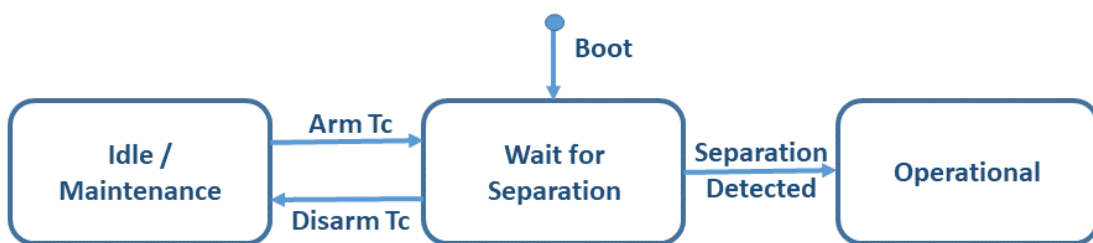


**Figure 22-3: Probe B2 OBSW operational modes**

For safety reasons, the SW boots directly in “Wait for Separation” mode. In this mode the SW is checking continuously for the separation strap signal. Once activated, the SW will transit to “Operational” mode. At every SW reboot, even after separation, the operational mode will be immediately recovered.

In operational mode, the SW executes the predefined science sequence. The sequence will activate, at predefined delta time, the B2 instruments and it will start collecting science data and forwarding them to S/C A via ISL as no data storing is foreseen on the B2 satellite.

Before the S/C A releases the probes, ground can command the B2 to move to “Maintenance” mode. In this mode, execution of Built-In Test (BIT) can be triggered to verify the B2 health status; at the end of the test sequence, the SW generates a report to be downlinked to ground. Furthermore, in this mode, memory patch and dump are allowed as well as parameters or operational sequence configuration. The mode is entered / exited via disarm / arm TCs sent by ground. Optionally, the B2 OBCP can implement a low-level communication interface between ground and B2 units for troubleshooting purposes (e.g. through this interface, ground can communicate directly with the units, for problem investigation and specific tests).

In all the three main modes, the B2 SW shall continuously acquire internal data and provide cyclical House Keeping TM (HK) sent to S/C A via umbilical (before release) or ISL link (after separation).

### 22.3.4 Science Data Telemetry Storage and Downlink

The storing and downlink of science data telemetry will rely on the mass memory capability of S/C A and it will be implemented via SpaceWire logical address routing and forwarding. The SW will mainly handle the acquisition of data coming from the probes

or internal instruments and it will manage the organization of data in the mass memory. The storing process is shown in Figure 22-4:

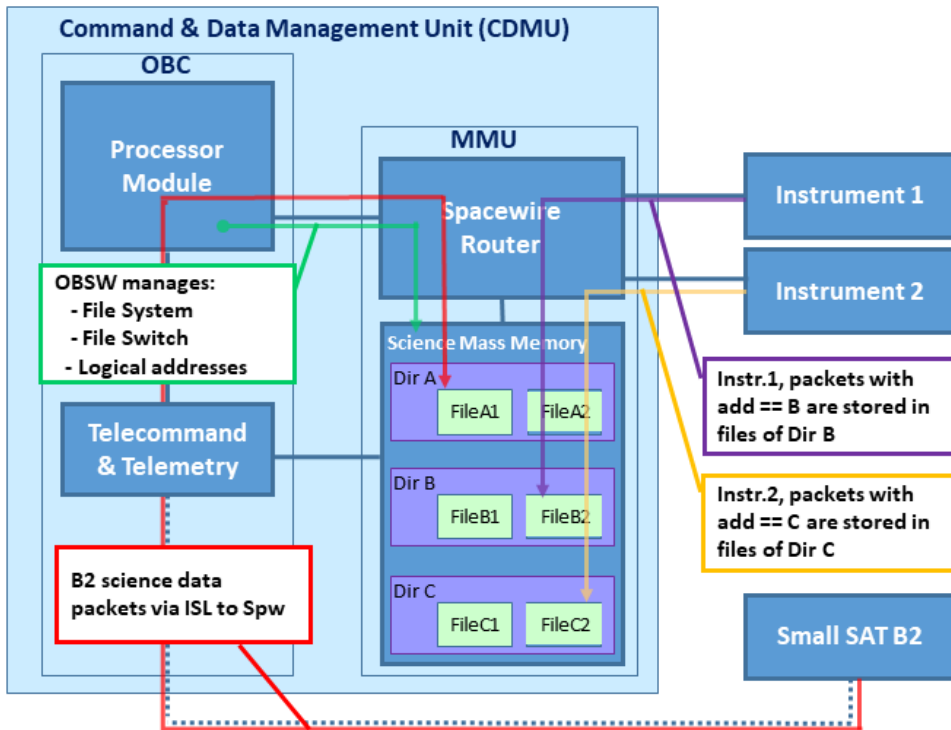


**Figure 22-4: Science TM acquisition and storing**

The OBSW running in the S/C A PM collects science data generated by probe B2 in CSP format, it converts/envelops them in PUS packets and it forwards over SpaceWire to the MMU SpaceWire Router. Science data produced by S/C A instruments (already in SpaceWire format) are sent directly to the router.

Each science data stream is identified by the SpaceWire destination logical address in the associated SpaceWire packets. According to the address, the router sends received SpaceWire packets to the science MMU. Each stream, i.e. SpaceWire Logical Address (LA), is associated to a directory in the Science MMU. The Science MMU or OGSW automatically creates files in directories: the files can be closed when maximum size is reached, by a timeout or by OGSW commands. The File management service (PUS 23) is used to handle the files and directories operations.

Once all the science data is stored and the operational phase is finished, the downlink phase can start. The downlink to ground is performed by the MMU connected directly to the Telecommand & Telemetry Board of the S/C A OBC. In order to implement a flexible and configurable download capability, the OGSW will handle three downlink attributes for each directory created in the MMU as follows:

- Downlink RF band: the attribute identifies which band the science data has to be used in the downlink process (the baseline is to use only X-band, but the field is included for potential future use e.g. additional Ka-band)

- Downlink Eligibility: boolean field used by ground to select if download or not the directory
- Downlink Priority: numerical attribute used by ground to prioritize the downlink of files between different directories.

The downlink of files within the same directory will be executed on file creation order; the first file created will be downlinked first. The OBSW / MMU will implement a specific protocol for Files downlink, supporting:

- File segmentation: each file will be split in segments to fit the maximum size of science TM packet and it will be reconstructed on ground.
- Retransmission: in order to support lossless reception, ground can ask retransmission of corrupted packets sending NACK commands to OBSW.
- File flushing: file on-board will be deleted only when confirmed by ground that all segments have been successfully downlinked.

## 22.4 Options

According to the data handling unit identified, if the OBC provides multi-core processor module, a Time and Space Partition (TSP) architecture can be considered for the OBSW implementation on S/C A.

The TSP allows running multiple separated OBSW images on the same processor module. Specific applications can be segregated and executed in stand-alone execution environment, allowing cooperation of different criticality SW categories on the same OBC. This could be considered particularly useful for narrowing safety/mission critical functions perimeter, decreasing the verification and validation effort.

Furthermore parallel design and development can be carried out, running specific SW instances for specific functionality, e.g. dedicated images for AOCS, I/O handling, data handling and TC/TM processing, etc.

This Page Intentionally Blank

## **23 COST**

Due to the confidential nature of the information contained within the cost chapter, this information is not included in this version of the report.

This Page Intentionally Blank

## 24 SCANNING MIRROR AND PERISCOPE OPTION

### 24.1 Introduction

As discussed in the introduction, two delta-sessions were organised at the end of the Comet Interceptor 2 Study to investigate a significant further system option: namely that of using a scanning mirror to rotate the FoV of some optical payloads on S/C A, rather than rotating the entire S/C. The intention was to determine if advantages in terms of shielding (only one permanent ram face to oncoming cometary dust) and reduced slew needs (and therefore potentially smaller reaction wheels) would offset any potential disadvantages. Also, the navigation and inter-satellite link aspects of both options were to be comparatively assessed.

Note that several previous missions to comets have already used rotating mirrors and periscopes, e.g. Giotto, Stardust, Contour, etc.

### 24.2 Definitions

Note that in the subsections to follow, it is important to distinguish between:

- the scanning mirror (which can rotate and point the instrument(s) to the comet during the flyby)<sup>36</sup>
- the periscope (to protect the instrument(s) and/or the scanning mirror from the incoming dust at the beginning of the flyby), as in Figure 24-1.

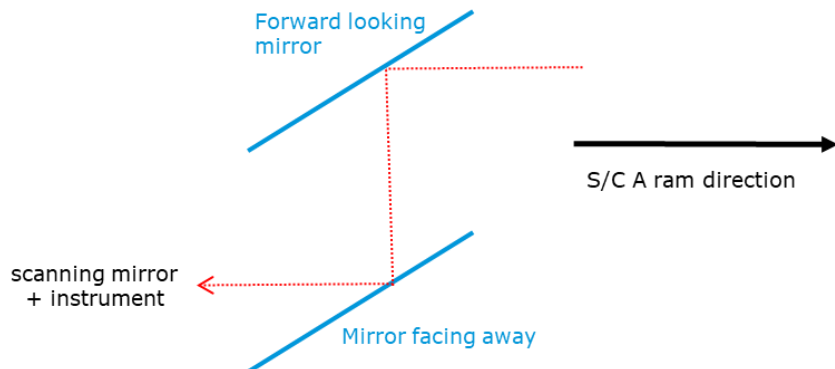


**Figure 24-1: Periscope concept overview (scanning mirror not shown)**

### 24.3 Requirements and Design Drivers

The mission and system requirements are as defined in the Systems chapter (see Section 7.1) for the nominal study baseline. Note that changes to the subsystem requirements are defined in the subsections that follow.

### 24.4 Assumptions and Trade-Offs

The main system-level assumptions are as defined in the Systems chapter (see Section 7.2), with the following additions:

<sup>36</sup> Note that the scanning mirror is referred to as the “rotating mirror” in some later documents.

Assumptions	
...	...
9	The S/C A maintains a fixed attitude with respect to the S/C A-comet relative velocity vector during the fly-by (i.e. no slewing to “face” the comet).
10	The CoCa instrument shall be able to track the comet via a scanning mirror system. This system uses a rotating mirror to “slew” (/scan) the CoCa FoV relative to the S/C A body-fixed axes during the flyby.
11	The MIRMISS instrument may use a similar scanning mechanism to track the comet, which was assessed in the options below (see Section 24.7.4). Otherwise, MIRMISS shall be fixed, which would reduce the science output of the instrument. In this case, MIRMISS is fixed-oriented towards the comet at closest approach, as this is assumed to be the most valuable science period for the instrument.  <i>Note that, as discussed in the Mechanisms section 24.7.4, it was originally discussed whether MIRMISS and CoCa could be oriented onto the same scanning mirror. It was later noted that this would not be desirable, as MIRMISS/TIRI needs to periodically (TBD mins every TBD hours) orient towards a blackbody calibration source. This would reduce the amount of science time available for CoCa. Given the large scanning mirror required to accommodate both payloads together and/or the use of a dichroic beam splitter (with high feasibility/development risk), it was decided that MIRMISS would not be accommodated onto the same scanning mirror as CoCa. Indeed, given the mass constraints, it was decided that only CoCa would be provided with the scanning mirror.<sup>37</sup></i>
12	The impacts of including the NAVCAM via the scanning mirror should also be assessed (but not baseline).
13	If S/C A is not slewing during the flyby, then structural shielding against cometary dust impacts is assumed to only be needed for the ram face of S/C A. Note, S/C A may indeed be knocked off-axis during the flyby by large dust particle impacts. During such periods of off-axis pointing, it is possible that dust impacts the sides of the S/C. These durations are expected to be somewhat small (e.g. 1 min, see the AOCS chapter 24.8.2) and the probability of further large particle impacts very low; however a more detailed analysis of this assumption is required in later phases.
14	It is envisaged to place a “periscope” at one extreme of the range of movement of the scanning mirror. This periscope would pass the incoming external light through two additional mirrors before entering the scanning mirror system. The nominal direction for viewing the comet up until closest approach is close to the ram direction. As such, the first mirror may see a significant oncoming dust field before the closest approach. The use of a periscope would ensure that the mirrors in the scanning mirror system do not receive any impacts during this phase, and so are “fresh” at the start of their rotation during the closest approach.
15	The solar array size was considered to be held constant from the nominal (slewing) baseline, in order to avoid a further mass penalty. This limited the available solar array to 6 m <sup>2</sup> .
16	It was assumed that no solar array drive mechanism (SADM) is used, i.e. the solar

<sup>37</sup> Note that the MIRMISS/NIR sensor does not need to view the calibration source, and could be considered in later work to also look through the scanning mirror / periscope.

### Assumptions

- panels are fixed. The solar array orientation would thus need to be compatible with providing maximum power during the electric propulsion thrusting during the transfer<sup>38</sup>, and a fixed orientation (for minimal projected area to the oncoming dust flow) during the flyby.
- 17 No flip-over manoeuvre is assumed required for nominal fly-by.  
 18 No need for high S/C agility as slewing during flyby is removed.  
 19 The designs of the probes B1 and B2 are unaffected by the change to a scanning mirror solution, and as such their designs are the same as for the baseline (slewing) case. Note however that some impacts on the inter-satellite link relative geometries are to be expected, as discussed further below.

**Table 24-1: System Level Assumptions for Scanning Mirror and Periscope Option**

Further subsystem-level assumptions are discussed in the individual subsystem sections to follow.

At System level, the major trade-off that was performed was regarding the power availability (and impacts thereof) during the fly-by. This tried to assess the power available across the possible flyby geometries (as discussed for the nominal baseline in chapter 7.2), considering the fixed solar array size of 6m<sup>2</sup> and removal of the SADM.

Two extremes are considered here, for the range of possible solar offset angles between 45 deg and 135 deg from the relative velocity vector, as shown in Figure 24-2.

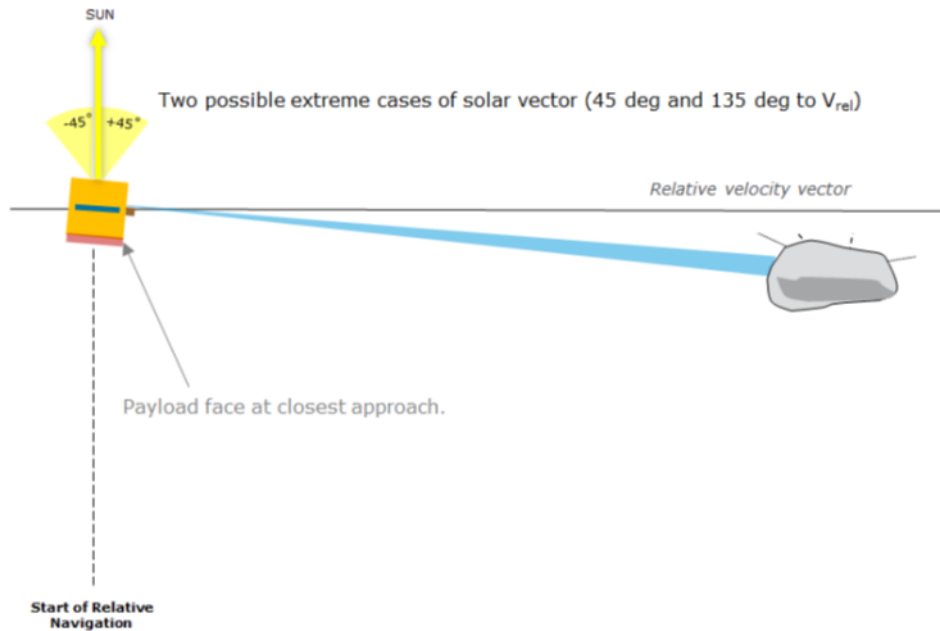


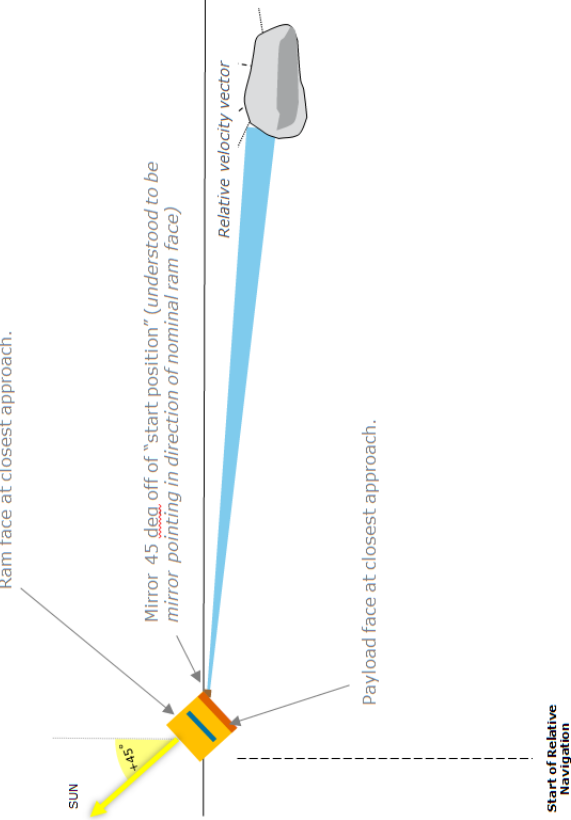
**Figure 24-2: Recall of relative flyby geometry and solar offset angle range**

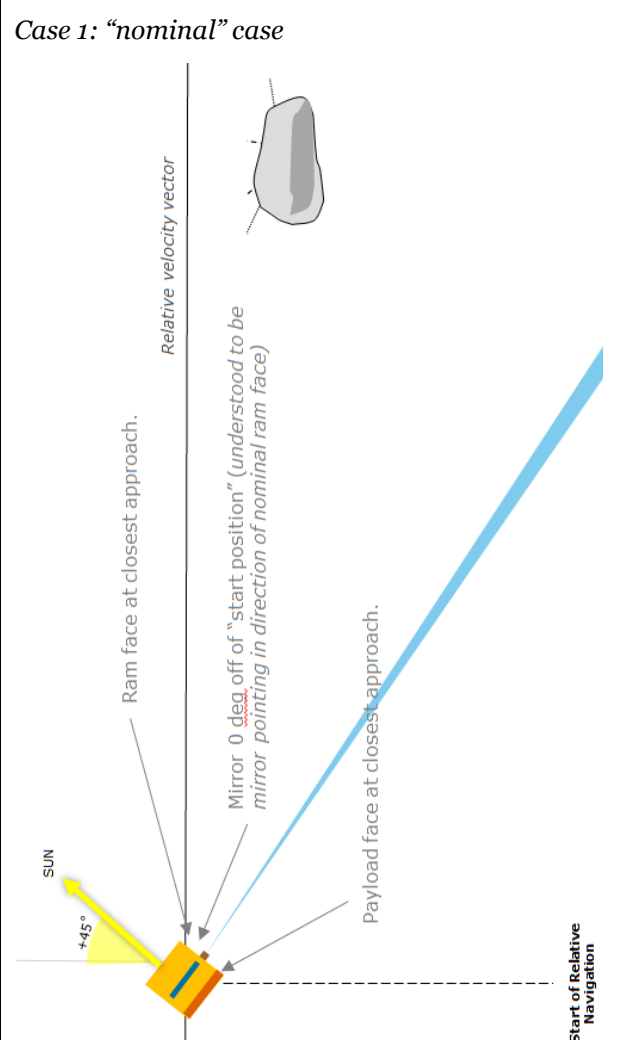
Initial analysis suggested that for these extreme cases, the power available would be insufficient to provide the full science operations as foreseen for the baseline (slewing) option. As such, the following mitigations were foreseen:

<sup>38</sup> The implications of this would need further assessment from mission analysis.

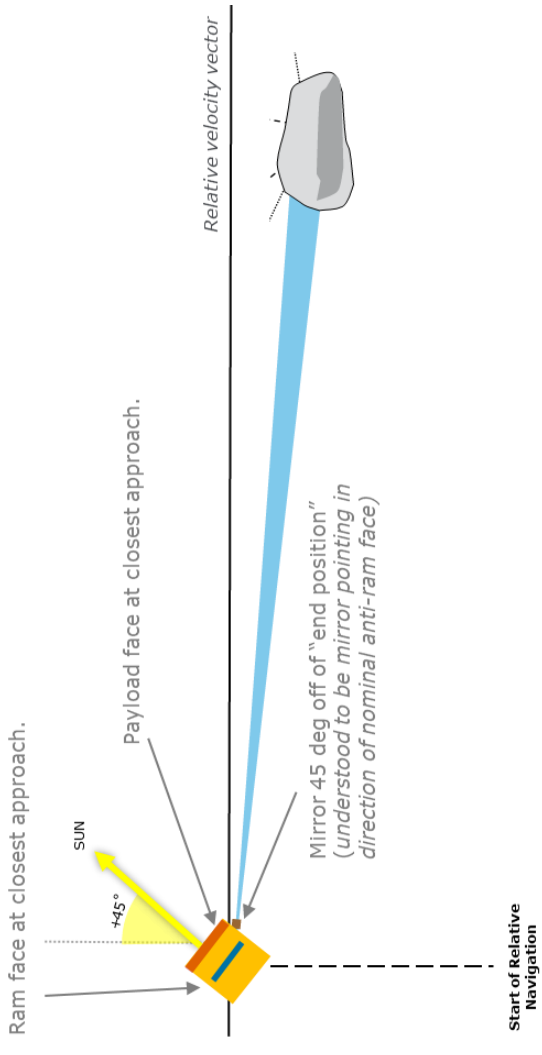
- 1) Improved power modelling of the payloads during the flyby (considering appropriate duty cycles and/or operational profiles).
- 2) Increase the solar array size.
- 3) Change the initial S/C A orientation during the fly-by to ensure a zero deg offset to the Sun.

It was eventually determined that by improving the power modelling of the science modes (as in Option 1), the power available became sufficient to provide the nominal science operations as desired (see Section 24.5.3). Nonetheless, an overview of the impacts of Option 3 is presented in Table 24-2 for completeness.

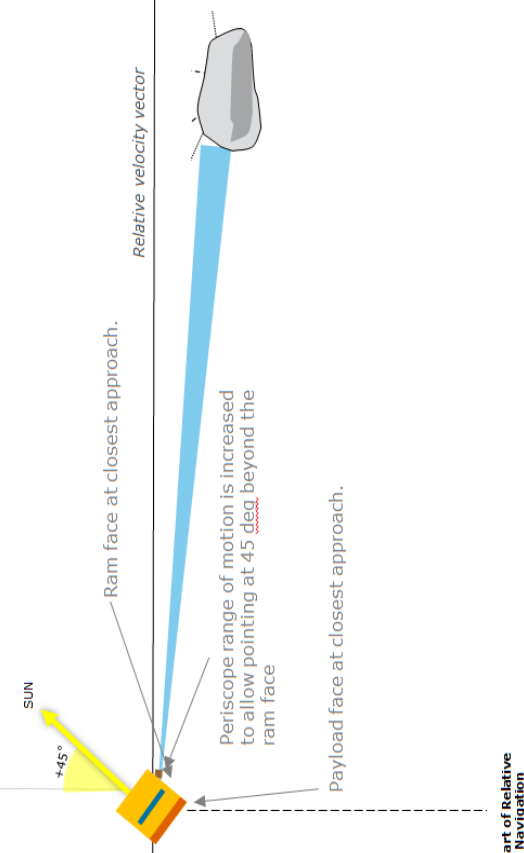
Approach case	Geometry options	Drawbacks
S/C A oriented to have zero offset to Solar angle of 135 deg (w.r.t. the relative velocity vector)		<ol style="list-style-type: none"> <li>1. Not possible to use periscope, which would be nominally pointed in the ram direction, for most of approach.</li> <li>2. Power would still need to be either throttled or battery-assisted for closest approach stages, where solar offset angle is again 45deg (due to payload face + oncoming dust protection pointing constraints).</li> <li>3. Payload mirror would not be able to see comet after flyby (unless either the scanning mirror range of motion goes beyond 180 deg, or the S/C is held at 45 deg solar offset angle – which would limit power).</li> <li>4. Payload face would need non-negligible dust shielding due to exposure to oncoming dust during approach.</li> <li>5. Possible ISL link performance issues.</li> </ol>

<p>S/C A oriented to have zero offset to Solar angle of 45 deg (w.r.t. the relative velocity vector)</p>	<p><i>Case 1: "nominal" case</i></p> 	<p>1. NAVCAM + payloads cannot see the comet (assuming range of motion of scanning mirror is 180 deg).</p>
--	--	--

*Case 2: "flipped" orientation*



1. Direct Sun exposure on payload face.
2. Solar cells would have to be included on both sides of array.
3. "Anti-ram" face would need non-negligible dust shielding.
4. Not possible to use periscope, which would be nominally pointing in the ram direction, for most of approach.
5. ISL link not possible.

<p><i>Case 3: extended scanning mirror range of motion</i></p> 	<ol style="list-style-type: none"> <li>1. Not possible to use periscope, which would be nominally pointing in the ram direction, for most of the approach.</li> <li>2. Power would still need to be either throttled or battery-assisted for closest approach stages, where solar offset angle is again 45deg (due to payload face + oncoming dust protection pointing constraints).</li> <li>3. Extended range of mirror motion required (up to 225 deg)</li> <li>4. Anti-payload face (-X) would need non-negligible dust shielding.</li> <li>5. Possible ISL link performance issues</li> </ol>
--	--

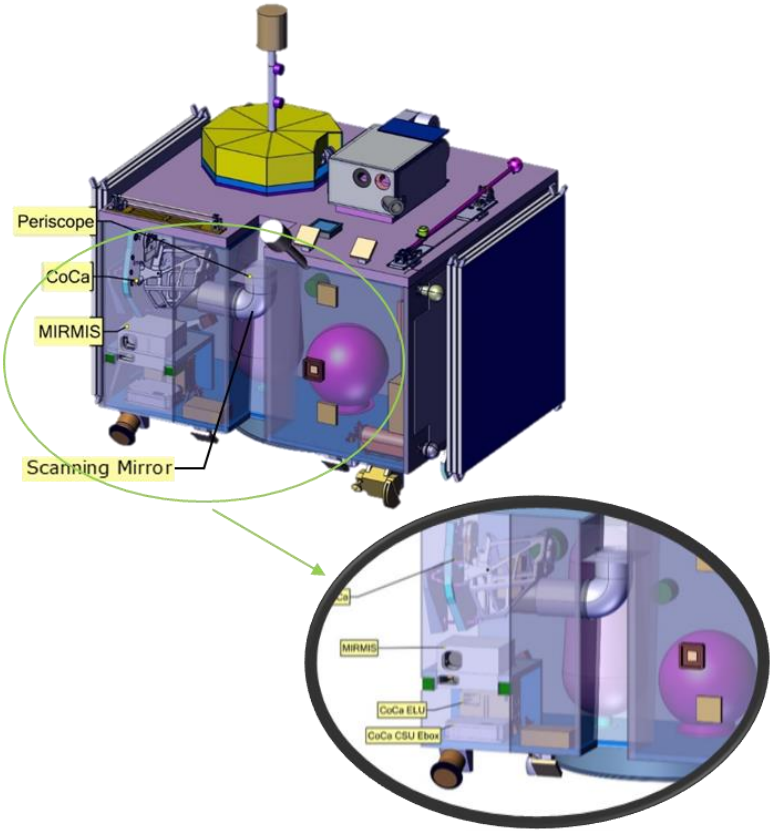
**Table 24-2: Flyby Geometry Options (versus power availability + system impacts)**

## 24.5 Baseline Design

The system decomposition of the Scanning Mirror plus Periscope Comet Interceptor system option follows the classical decomposition into space segment, ground segment and launch segment, and is comparable to the decomposition followed for the baseline (slewing) case.

### 24.5.1 Design Summary

Table 24-3 shows the main characteristics of S/C A for the scanning mirror design option.

Main S/C (S/C A, ESA) – System baseline summary						
Configuration stowed						
Mass	<table> <tr> <td>Dry Mass (w/ margin)</td><td>604 kg</td></tr> <tr> <td>Wet Mass</td><td>738 kg (incl. probes B1 and B2)</td></tr> </table>		Dry Mass (w/ margin)	604 kg	Wet Mass	738 kg (incl. probes B1 and B2)
Dry Mass (w/ margin)	604 kg					
Wet Mass	738 kg (incl. probes B1 and B2)					
Dimensions	<table> <tr> <td>Stowed</td><td>1,974 mm x 2,073 mm x 1,976 mm</td></tr> <tr> <td>Deployed</td><td>9,768 mm x 2,999 mm x 2,484 mm</td></tr> </table>		Stowed	1,974 mm x 2,073 mm x 1,976 mm	Deployed	9,768 mm x 2,999 mm x 2,484 mm
Stowed	1,974 mm x 2,073 mm x 1,976 mm					
Deployed	9,768 mm x 2,999 mm x 2,484 mm					
Instruments	CoCa, DFP, MANiac (no rotation mechanism) and MIRMISS					
AOCS	6x Sun sensors (SS) 2x Star trackers (STR) 2x Inertial Measurement Unit (IMU) 2x Navcam 4x 4 Nms / 0.095 Nm Reaction Wheels (RW)					
Communications	1x 0.9 m diameter steerable X-band High Gain Antenna (HGA) 2x X-band Low Gain Antenna (LGA) 2 x X-band Deep Space Transponder (DST) 2x S-band Inter-Satellite Link (ISL) transceivers 2x S-band ISL Low Gain Antenna (LGA)					
Data Handling	1x On-Board Computer (OBC) 1x Remote Interface Unit (RIU)					
Power	2x 3 m <sup>2</sup> solar arrays 1x Power Conversion and Distribution Unit (PCDU): MPPT for 28V non-regulated bus 1x 512 Wh Secondary Battery					

Chemical Propulsion	Monopropellant (Hydrazine) blow-down system 4(+4)x 5N thrusters 2x 33 L Hydrazine tank (usable)
Electrical Propulsion	1x PPS-1350 Hall effect thruster 2x 32 L Xenon tank (usable)
Thermal	Radiators, SLI and MLI, heat pipes, paints, heaters and thermistors
Structures	Aluminium skin and honeycomb core central shear, side, baseplate and top panels  Varying thicknesses of Al and honeycomb depending on the panel's shielding necessity.. Primary micrometeoroid shielding on 1 panel.
Mechanisms	1x Launcher-separation mechanism 1x B1 linear-separation mechanism 1x B2 linear-separation mechanism 1x 2 degrees of freedom Antenna Pointing Mechanism (APM) 8x Solar panel Hold Down and Release Mechanism (HDRM) 1x Scanning Mirror Assembly (Mirror, Baffle, Drive, Bearings, Ebox) 1x Periscope

**Table 24-3: S/C A summary – scanning mirror and periscope option**

The designs for B1 and B2 are as reported in the baseline (slewing) chapters.

#### 24.5.2 Mass Budget

The mass budget for S/C A is presented in Table 24-4. As per the assumptions above, the mass budgets of the probes B1 and B2 were assumed not to have changed for this alternative configuration option.

As per the baseline (slewing) design option, additional propellant tank shielding was considered for protecting from high impact velocity of dust particles. Note that if the S/C only has one constant ram face, this could potentially be reduced in later design phases by assuming extra shielding in one direction only.

	Mass (kg)
AOGNC	15.19
COM	32.64
CPROP	22.44
DH	19.43
EPROP	38.56
INS	36.47
MEC	34.91
PWR	57.93
STR	134.48
TC	12.96
Tank Shielding	3.84
Dry Mass SC_B1	30.00
Dry Mass SC_B2	40.47
Harness	5%
	23.97

<b>Dry Mass</b>	<b>503.27</b>	
System Margin	20%	100.65
<b>Dry Mass incl. System Margin</b>		<b>603.92</b>
CPROP Fuel Mass		44.70
CPROP Fuel Margin	2%	0.89
CPROP Pressurant Mass		0.80
CPROP Pressurant Margin	2%	0.02
EPROP Fuel Mass		85.92
EPROP Fuel Mass Margin	2%	1.72
<b>Total Wet Mass</b>	<b>737.97</b>	

**Table 24-4: Mass budget for the scanning mirror option**

A reduction of approximately 58.5 kg was achieved with regards to the baseline (slew) case for the scanning mirror configuration. This is mostly due to the following aspects:

- The option does not include a SADM, as discussed in the System assumptions (Table 24-1). This requires further confirmation from Mission Analysis regarding the transfer trajectories and the power required for the electric propulsion.
- The lower S/C agility requirements led to 4 x 4Nms / 0.095 Nm wheels being considered instead of 4 x 4 Nms / 0.215 Nm wheels (ca. 11kg mass reduction).
- Due to the simplified fly-by geometry, 2 x ISL patch antennae are considered instead of 6 (ca. 1.2kg mass reduction).
- Only 1 out of the 3 structural panels are assumed to require dust shielding (ca. 40kg mass reduction), as discussed in Table 24-1.

A dichroic beam splitter mass (1.2 kg incl. margin) is accounted for in the budget, although its implementation is not currently baselined due to development risk and questions regarding it's feasibility for the given instruments (see Section 24.7.5 and Assumption #11 in Table 24-1 above).

Note that as discussed in the Systems chapter for the baseline (slew) case, the actual mass to be considered for B2 should be **35 kg** (see Systems Chapter 7.4.3). For consistency, the wet mass calculations of both the baseline (slew) case and the scanning mirror option consider the B2 mass of 40.5 kg, as in the table above.

### 24.5.3 Equipment List

The equipment list for S/C A is presented in Table 24-6 below. For probes B2 and B1, no changes are assumed compared to the baseline (slew) case.

	Qty	Mass (kg)	Mass Margin (%)	Mass incl. Margin (kg)
SC_A (Spacecraft A)				
<b>AOGNC</b>		14.462	5	15.185
A_DPU (A DTU Data Processing Unit)	1	0.560	5	0.588
A_IMU_LN200_1 (A IMU Northrop Grumman LN200 Core #1)	1	0.750	5	0.788
A_IMU_LN200_2 (A IMU Northrop Grumman LN200 Core #2)	1	0.750	5	0.788
A_NAVCAM_OH_1 (A DTU NAVCAM Optical Head #1)	2	0.752	5	0.790
A_STR_OH_1 (A DTU STR Optical Head #1)	2	0.700	5	0.735
A_SUN_LENS_Bison64_1 (A SUN LENS Bison 64 #1)	6	0.150	5	0.158
RW_RW250 (RW Astrofein RW250)	4	10.800	5	11.340
<b>COM</b>		29.370	10.97725	32.641
XDST_1 (X-Band DSTRASP #1)	2	7.200	5	7.560
XHGA (X-Band HGA)	1	6.050	10	6.655
XLGA_1 (X-Band LGA #1)	2	0.600	5	0.630
XRFDN (X-Band RFDN)	1	10.000	20	12.000
XTWT_1 (X-Band TWT #1)	2	1.600	5	1.680
XTWTA_EPC_1 (X-Band TWTA EPC #1)	2	2.800	5	2.940
A_ISL_GOMx_board_1 (A GOMx Electronics #1)	2	0.820	5	0.861
A_ISL_GOMx_Patch_1 (A GOMx Antenna Patch #1)	2	0.300	5	0.315
<b>CPROP</b>		20.940	7.148997	22.437
A_Lat_Val_1 (A Latch Valves)	2	1.100	5	1.155
A_Pass_Valve (A Passivation_Valve)	1	0.070	5	0.074
A_Pipes (A Pipes)	1	3.000	20	3.600
A_Press_Trans_1_1 (A Pressure Transducer #1)	3	0.660	5	0.693
A_Prop_Filt (A Propellant Filter)	1	0.110	5	0.116
A_Fil_Dr_Val_1 (A Fill Drain Valve)	2	0.140	5	0.147
A_Test_Port_1 (A Test_Ports)	2	0.140	5	0.147
A_Tk_CPROP_1 (A Tank CPROP #1)	2	11.800	5	12.390
A_Thr_5N_1 (A Thruster_MONARC 5N #1)	8	3.920	5	4.116
<b>DH</b>		18.500	5	19.425
A_OBC (A Onboard Computer)	1	6.500	5	6.825
A_RIU (A Remote Interface Unit)	1	12.000	5	12.600
<b>EPROP</b>		36.725	5	38.561
A_PPU (A Power Processing Unit)	1	10.660	5	11.193
A_Thruster_PPS1350 (A Thruster PPS1350)	1	4.350	5	4.568

A_BPRU (A BPRU)	1	2.750	5	2.888
A_FU (A FU)	1	0.675	5	0.709
A_Miscellaneous (A Miscellaneous)	1	3.500	5	3.675
A_PRE_Card (A PRE Card)	1	1.270	5	1.334
A_XFC (A XFC)	1	0.820	5	0.861
A_Prop_Tank_1 (A Propellant Tank #1)	2	12.700	5	13.335
<b>INS</b>		30.440	19.80608	36.468
A_CoCa_CSU (A CoCa Camera Support)	1	6.850	20	8.220
A_CoCa_ELU (A CoCa Electronics Unit)	1	2.100	20	2.520
A_DFP_DISC (A DFP Dust Impact Sensor and Counter)	1	0.350	20	0.420
A_DFP_E_Box (A DFP E-Box)	1	4.940	20	5.928
A_MIRMISS_TIRI (A MIRMISS Thermal InfraRed Imager)	1	5.600	20	6.720
A_DFP_SCIENA_ENA (A DFP Solar wind and Cometary Ions and Energetic Neutral Atoms-ENA sensor)	1	0.900	20	1.080
A_DFP_SCIENA_Ion (A DFP Solar wind and Cometary Ions and Energetic Neutral Atoms-Ion sensor)	1	0.000	0	0.000
A_DFP_LEES_1 (A DFP Low Energy Electron Spectrometer 1)	1	0.800	20	0.960
A_CoCa_PEU (A CoCa Proximity Electronics Unit)	1	0.850	20	1.020
A_CoCa_Rad (A CoCa Radiator)	1	0.200	5	0.210
A_DFP_COMPLIMENT_p_1 (A DFP COMetary Plasma Light Instrument probe #1)	1	0.000	0	0.000
A_MANiac_ELU (A MANiac Electronics Unit)	1	3.500	20	4.200
A_MANiac_NDG (A MANiac Neutral Density Gauge)	1	0.200	20	0.240
A_MANiac_SHU (A MANiac Sensor Head Unit)	1	0.900	20	1.080
A_MIRMISS_MIR_1 (A MIRMISS Mid-InfraRed Sensor 1)	2	0.000	0	0.000
A_MIRMISS_NIR (A MIRMISS Near InfraRed Sensor)	1	0.000	0	0.000
A_MIRMISS_Rad (A MIRMISS Radiator)	1	0.200	5	0.210
A_DFP_COMPLIMENT_boom_1 (A DFP COMetary Plasma Light Instrument boom 1)	1	0.300	20	0.360
A_DFP_COM_FGM_boom_2 (COMPLIMENT+FGM+boom_2)	1	1.700	20	2.040
A_MANiac_Harn (A MANiac Harness)	1	0.350	20	0.420
A_CoCa_Harn (A CoCa Harness)	1	0.350	20	0.420
A_CoCa_MLI (A CoCa Thermal Insulation)	1	0.350	20	0.420
<b>MEC</b>		31.440	7.411576	34.913
A_APM_HDRM_APME (A Antenna Pointing Mechanisms Subsystem with Driver and HDRM)	1	13.100	5	13.755
A_SA1_HDRM_1 (A SA1 HDRM #1)	8	4.000	10	4.400
A_Clamp_Band (A Clamp Band Ejection System)	1	3.000	5	3.150
Scanning mirror assembly (Mirror + Baffle + Drive mechanism + Bearings)	1	4.170	20	5.004
Electronics box for scanning mirror mechanism	1	4.170	20	5.004
Periscope	1	2.000	20	2.400

Dichroic beam combiner + mirror assembly	1	1.000	20	1.200
<b>PWR</b>		<b>52.660</b>	<b>10</b>	<b>57.926</b>
A_SA (A SolarArray)	2	29.260	10	32.186
A_Bat (A Battery)	1	4.900	10	5.390
A_PCDU (A PCDU)	1	18.500	10	20.350
<b>STR</b>		<b>112.066</b>	<b>20</b>	<b>134.479</b>
A_Misc_STR (A Miscellaneous STR)	1	5.000	20	6.000
A_RCS_Structure (A RCS Suport)	1	0.770	20	0.924
A_SecondarySTR (A Secondary Structure)	1	10.000	20	12.000
A_Inserts (A Inserts)	1	4.000	20	4.800
A_ShearW (A ShearWebs)	1	3.810	20	4.572
A_SA_yoke_1 (A Solar Array Yoke #1)	2	2.000	20	2.400
A_Baseplate (Baseplate)	1	28.880	20	34.656
A_ExtPanels_1 (A Closure Panels #1)	1	34.606	20	41.527
A_ShieldingPanels_1 (A ShieldingPanels #1)	1	20.000	20	24.000
A_PL_Panel (Payload Support Panel)	1	3.000	20	3.600
<b>SYE</b>		<b>3.200</b>	<b>20</b>	<b>3.840</b>
A_tank_shields (A_tank_shields)	4	3.200	20	3.840
<b>TC</b>		<b>10.800</b>	<b>20</b>	<b>12.960</b>
A_TC_FILLER (A TC Thermal Filler)	1	0.250	20	0.300
A_TC_HEATER (A TC Heater)	1	0.500	20	0.600
A_TC_MLI (A TC Multi Layer Insulation)	1	5.000	20	6.000
A_TC_PAINT (A TC Paint)	1	2.000	20	2.400
A_TC_RAD (A TC Radiator Panel)	1	1.000	20	1.200
A_TC_SO (A TC Stand Offs)	1	0.050	20	0.060
A_TC_STRAP (A TC Thermal Strap)	1	0.500	20	0.600
A_TC_T_SENS (A TC Temperature Sensor)	1	0.500	20	0.600
A_TC_HP (A TC Heat Pipes)	1	1.000	20	1.200

**Table 24-5: S/C A equipment list: scanning mirror option**

#### 24.5.4 Power Budget

Similarly to the mass budget, the power budget for the scanning mirror option was assessed only for S/C A, as no changes are assumed for B1 or B2.

The power budget for S/C A is shown in Table 24-6. As for the baseline (slew) option, a 20% system margin was added to each mode's total power, except for the EPTH mode. In this specific mode, the Electric Propulsion PPU power is subtracted from the total power, as the thruster is physically not able to sustain a 20% increase in power.

A	LAU	SUN	SAFE	STBY	COM	EPTH	SCI
Total	0.0	266.4	304.6	259.9	401.3	1039.0	379.4
Survival heater B1	0.0	20.0	20.0	20.0	20.0	20.0	0.0
Survival heater B2	0.0	20.0	20.0	20.0	20.0	20.0	0.0
Scan Mirror Mech.	0.0	0.0	0.0	0.0	0.0	0.0	7.0

Losses PCDU	3%	0.0	9.2	10.3	9.0	13.2	32.4	11.6
Losses Harness	3%	0.0	9.2	10.3	9.0	13.2	32.4	11.6
Losses LCLs	1%	0.0	3.1	3.4	3.0	4.4	10.8	3.9
<b>Total w/ losses</b>	<b>0.0</b>	<b>327.8</b>	<b>368.7</b>	<b>320.9</b>	<b>472.2</b>	<b>1154.5</b>	<b>413.5</b>	
						<b>352.9</b>		
System Margin	20%	0.0	65.6	73.7	64.2	94.4	70.6	82.7
<b>incl. Margin</b>	<b>0.0</b>	<b>393.4</b>	<b>442.4</b>	<b>385.1</b>	<b>566.6</b>	<b>1225.1</b>	<b>496.2</b>	

**Table 24-6: Power Budget: scanning mirror option<sup>39</sup>**

At unit level, the power budget breakdown per mode for S/C A is presented in Table 7-35, before losses and system margin. The breakdown for B2 is not presented, as it was not subject to change compared to the baseline (slew) option.

Power Budget	P_mean							
	LAU	SUN	SAFE	STBY	COM	EPTH	SCI	
<b>SC_A (Spacecraft A)</b>	0.00	266.4	304.6	259.9	401.3	1039.0	379.4	
<b>AOGNC</b>	0.00	12.00	12.00	12.00	36.30	16.30	49.00	
A_DPU (A DTU Data Processing Unit)	0.00	0.00	0.00	0.00	3.60	3.60	3.60	
A_IMU_LN200_1 (LN200 Core #1)	0.00	6.00	6.00	6.00	0.00	6.00	6.00	
A_IMU_LN200_2 (LN200 Core #2)	0.00	6.00	6.00	6.00	0.00	6.00	6.00	
A_NAVCAM_OH_1 (Optical Head #1)	0.00	0.00	0.00	0.00	0.00	0.00	0.35	
A_NAVCAM_OH_2 (Optical Head #2)	0.00	0.00	0.00	0.00	0.00	0.00	0.35	
A_STR_OH_1 (A DTU STR Optical Head #1)	0.00	0.00	0.00	0.00	0.35	0.35	0.35	
A_STR_OH_2 (A DTU STR Optical Head #2)	0.00	0.00	0.00	0.00	0.35	0.35	0.35	
A_SUN_LENS_Bison64_1 (Bison 64 #1)	0.00	0.00	0.00	0.00	0.00	0.00	0.00	
A_SUN_LENS_Bison64_2 (Bison 64 #2)	0.00	0.00	0.00	0.00	0.00	0.00	0.00	
A_SUN_LENS_Bison64_3 (Bison 64 #3)	0.00	0.00	0.00	0.00	0.00	0.00	0.00	
A_SUN_LENS_Bison64_4 (Bison 64 #4)	0.00	0.00	0.00	0.00	0.00	0.00	0.00	
A_SUN_LENS_Bison64_5 (Bison 64 #5)	0.00	0.00	0.00	0.00	0.00	0.00	0.00	
A_SUN_LENS_Bison64_6 (Bison 64 #6)	0.00	0.00	0.00	0.00	0.00	0.00	0.00	
A_RW_RW250 (RW Astrofein RW250) #1	0.00	0.00	0.00	0.00	8.00	0.00	8.00	
A_RW_RW250 (RW Astrofein RW250) #2	0.00	0.00	0.00	0.00	8.00	0.00	8.00	
<b>COM</b>	0.00	113.69	87.92	32.00	160.07	32.00	111.07	
A_ISL_GOMx_board_1 (Electronics #1)	0.00	0.00	0.00	0.00	0.00	0.00	4.08	
A_ISL_GOMx_board_2 (Electronics #2)	0.00	0.00	0.00	0.00	0.00	0.00	4.08	
A_ISL_GOMx_Patch_1 (Antenna Patch #1)	0.00	0.00	0.00	0.00	0.00	0.00	5.78	
A_ISL_GOMx_Patch_2 (Antenna Patch #2)	0.00	0.00	0.00	0.00	0.00	0.00	5.78	
XDST_1 (X-Band DSTRASP #1)	0.00	24.00	24.00	16.00	24.00	16.00	24.00	
XDST_2 (X-Band DSTRASP #2)	0.00	24.00	24.00	16.00	24.00	16.00	24.00	

<sup>39</sup> As described in the text, the system margin of 70.6 W for the EPTH mode is calculated as 20% of the total power excluding the EP thruster, which is the 352.9 W shown.

XHGA (X-Band HGA)	0.00	0.00	0.00	0.00	0.00	0.00	0.00
XLGA_1 (X-Band LGA #1)	0.00	0.00	0.00	0.00	0.00	0.00	0.00
XLGA_2 (X-Band LGA #2)	0.00	0.00	0.00	0.00	0.00	0.00	0.00
XRFDN (X-Band RFDN)	0.00	0.00	0.00	0.00	0.00	0.00	0.00
XTWT_1 (X-Band TWT #1)	0.00	28.34	15.46	0.00	51.53	0.00	17.18
XTWT_2 (X-Band TWT #2)	0.00	28.34	15.46	0.00	51.53	0.00	17.18
XTWTA_EPC_1 (X-Band TWTA EPC #1)	0.00	4.50	4.50	0.00	4.50	0.00	4.50
XTWTA_EPC_2 (X-Band TWTA EPC #2)	0.00	4.50	4.50	0.00	4.50	0.00	4.50
<b>CPROP</b>	0.00	57.71	25.61	17.90	17.90	17.07	0.65
A_Thr_5N_1 (A Thruster_MONARC 5N #1)	0.00	5.35	2.75	2.12	2.12	2.05	0.00
A_Thr_5N_2 (A Thruster_MONARC 5N #2)	0.00	5.35	2.75	2.12	2.12	2.05	0.00
A_Thr_5N_3 (A Thruster_MONARC 5N #3)	0.00	5.35	2.75	2.12	2.12	2.05	0.00
A_Thr_5N_4 (A Thruster_MONARC 5N #4)	0.00	5.35	2.75	2.12	2.12	2.05	0.00
A_Thr_5N_5 (A Thruster_MONARC 5N #5)	0.00	5.35	2.75	2.12	2.12	2.05	0.00
A_Thr_5N_6 (A Thruster_MONARC 5N #6)	0.00	5.35	2.75	2.12	2.12	2.05	0.00
A_Thr_5N_7 (A Thruster_MONARC 5N #7)	0.00	5.35	2.75	2.12	2.12	2.05	0.00
A_Thr_5N_8 (A Thruster_MONARC 5N #8)	0.00	5.35	2.75	2.12	2.12	2.05	0.00
A_Tk_CPROP_1 (A Tank CPROP #1)	0.00	0.00	0.00	0.00	0.00	0.00	0.00
A_Tk_CPROP_2 (A Tank CPROP #2)	0.00	0.00	0.00	0.00	0.00	0.00	0.00
A_Fil_Dr_Val_1 (A Fill Drain Valve)	0.00	0.00	0.00	0.00	0.00	0.00	0.00
A_Fil_Dr_Val_2 (A Fill Drain Valve)	0.00	0.00	0.00	0.00	0.00	0.00	0.00
A_Lat_Val_1 (A Latch Valves)	0.00	7.13	1.50	0.15	0.15	0.00	0.00
A_Lat_Val_2 (A Latch Valves)	0.00	7.13	1.50	0.15	0.15	0.00	0.00
A_Press_Trans_1_1 (A Pressure Transducer #1)	0.00	0.22	0.22	0.22	0.22	0.22	0.22
A_Press_Trans_1_2 (A Pressure Transducer #1)	0.00	0.22	0.22	0.22	0.22	0.22	0.22
A_Press_Trans_1_3 (A Pressure Transducer #1)	0.00	0.22	0.22	0.22	0.22	0.22	0.22
<b>DH</b>	0.00	53.00	53.00	53.00	53.00	53.00	53.00
A_OBC (A Onboard Computer)	0.00	23.00	23.00	23.00	23.00	23.00	23.00
A_RIU (A Remote Interface Unit)	0.00	30.00	30.00	30.00	30.00	30.00	30.00
<b>INS</b>	0.00	0.00	0.00	0.00	0.00	0.00	68.76
A_CoCa_CSU (A CoCa Camera Support)	0.00	0.00	0.00	0.00	0.00	0.00	14.40
A_CoCa_ELU (A CoCa Electronics Unit)	0.00	0.00	0.00	0.00	0.00	0.00	0.00
A_CoCa_PEU (A CoCa Proximity Electronics Unit)	0.00	0.00	0.00	0.00	0.00	0.00	0.00
A_CoCa_Rad (A CoCa Radiator)	0.00	0.00	0.00	0.00	0.00	0.00	0.00
A_DFP_COM_FGM_boom_2 (A DFP COMPLIMENT+FGM+boom_2)	0.00	0.00	0.00	0.00	0.00	0.00	0.00
A_DFP_COMPLIMENT_boom_1 (A DFP COMetary Plasma Light Instrument boom 1)	0.00	0.00	0.00	0.00	0.00	0.00	0.00
A_DFP_COMPLIMENT_p_1 (A DFP COMetary Plasma Light Instrument probe #1)	0.00	0.00	0.00	0.00	0.00	0.00	0.00
A_DFP_DISC (Dust Impact Sensor and Counter)	0.00	0.00	0.00	0.00	0.00	0.00	0.00
A_DFP_E_Box (A DFP E-Box)	0.00	0.00	0.00	0.00	0.00	0.00	20.16
A_DFP_LEES_1 (Low Energy Electron Spectrometer 1)	0.00	0.00	0.00	0.00	0.00	0.00	0.00

A_DFP SCIENA_ENA (Solar wind and Cometary Ions and Energetic Neutral Atoms-ENA sensor)	0.00	0.00	0.00	0.00	0.00	0.00	0.00
A_DFP SCIENA_Ion (Solar wind and Cometary Ions and Energetic Neutral Atoms-Ion sensor)	0.00	0.00	0.00	0.00	0.00	0.00	0.00
A_MANiac_ELU (A MANiac Electronics Unit)	0.00	0.00	0.00	0.00	0.00	0.00	0.00
A_MANiac_NDG (Neutral Density Gauge)	0.00	0.00	0.00	0.00	0.00	0.00	3.60
A_MANiac_SHU (A MANiac Sensor Head Unit)	0.00	0.00	0.00	0.00	0.00	0.00	21.60
A_MIRMISS_MIR_1 (Mid-InfraRed Sensor 1)	0.00	0.00	0.00	0.00	0.00	0.00	0.00
A_MIRMISS_MIR_2 (Mid-InfraRed Sensor 2)	0.00	0.00	0.00	0.00	0.00	0.00	0.00
A_MIRMISS_NIR (Near InfraRed Sensor)	0.00	0.00	0.00	0.00	0.00	0.00	0.00
A_MIRMISS_Rad (A MIRMISS Radiator)	0.00	0.00	0.00	0.00	0.00	0.00	0.00
A_MIRMISS_TIRI (Thermal InfraRed Imager)	0.00	0.00	0.00	0.00	0.00	0.00	9.00
<b>MEC</b>	0.00	0.00	0.00	0.00	18.00	0.00	6.00
A_APM_HDRM_APME (A Antenna Pointing Mechanisms Subsystem with Driver and HDRM)	0.00	0.00	0.00	0.00	18.00	0.00	6.00
A_Clamp_Band (A Clamp Band Ejection System)	0.00	0.00	0.00	0.00	0.00	0.00	0.00
A_SA1_HDRM_1 (A SA1 HDRM #1)	0.00	0.00	0.00	0.00	0.00	0.00	0.00
A_SA1_HDRM_2 (A SA1 HDRM #2)	0.00	0.00	0.00	0.00	0.00	0.00	0.00
A_SA1_HDRM_3 (A SA1 HDRM #3)	0.00	0.00	0.00	0.00	0.00	0.00	0.00
A_SA1_HDRM_4 (A SA1 HDRM #4)	0.00	0.00	0.00	0.00	0.00	0.00	0.00
A_SA2_HDRM_1 (A SA2 HDRM #1)	0.00	0.00	0.00	0.00	0.00	0.00	0.00
A_SA2_HDRM_2 (A SA2 HDRM #2)	0.00	0.00	0.00	0.00	0.00	0.00	0.00
A_SA2_HDRM_3 (A SA2 HDRM #3)	0.00	0.00	0.00	0.00	0.00	0.00	0.00
A_SA2_HDRM_4 (A SA2 HDRM #4)	0.00	0.00	0.00	0.00	0.00	0.00	0.00
<b>PWR</b>	0.00	30.00	30.00	30.00	30.00	30.00	30.00
A_PCDU (A PCDU)	0.00	30.00	30.00	30.00	30.00	30.00	30.00
<b>STR</b>	0.00	0.00	0.00	0.00	0.00	0.00	0.00
A_Misc_STR (A Miscellaneous STR)	0.00	0.00	0.00	0.00	0.00	0.00	0.00
<b>TC</b>	0.00	0.00	96.03	115.00	86.02	89.01	60.95
A_TC_FILLER (A TC Thermal Filler)	0.00	0.00	0.00	0.00	0.00	0.00	0.00
A_TC_HEATER (A TC Heater)	0.00	0.00	96.03	115.00	86.02	89.01	60.95
A_TC_HP (A TC Heat Pipes)	0.00	0.00	0.00	0.00	0.00	0.00	0.00
A_TC_MLI (A TC Multi Layer Insulation)	0.00	0.00	0.00	0.00	0.00	0.00	0.00
A_TC_PAINT (A TC Paint)	0.00	0.00	0.00	0.00	0.00	0.00	0.00
A_TC_RAD (A TC Radiator Panel)	0.00	0.00	0.00	0.00	0.00	0.00	0.00
A_TC_SO (A TC Stand Offs)	0.00	0.00	0.00	0.00	0.00	0.00	0.00
A_TC_STRAP (A TC Thermal Strap)	0.00	0.00	0.00	0.00	0.00	0.00	0.00
A_TC_T_SENS (A TC Temperature Sensor)	0.00	0.00	0.00	0.00	0.00	0.00	0.00
<b>EPROP</b>	0.00	0.00	0.00	0.00	0.00	801.59	0.00
A_BPRU (A BPRU)	0.00	0.00	0.00	0.00	0.00	0.00	0.00
A_FU (A FU)	0.00	0.00	0.00	0.00	0.00	0.00	0.00
A_Miscellaneous (A Miscellaneous)	0.00	0.00	0.00	0.00	0.00	0.00	0.00
A_PPU (A Power Processing Unit)	0.00	0.00	0.00	0.00	0.00	801.59	0.00

A_PRE_Card (A PRE Card)	0.00	0.00	0.00	0.00	0.00	0.00	0.00
A_Prop_Tank_1 (A Propellant Tank #1)	0.00	0.00	0.00	0.00	0.00	0.00	0.00
A_Prop_Tank_2 (A Propellant Tank #2)	0.00	0.00	0.00	0.00	0.00	0.00	0.00
A_Thruster_PPS1350 (A Thruster PPS1350)	0.00	0.00	0.00	0.00	0.00	0.00	0.00
A_XFC (A XFC)	0.00	0.00	0.00	0.00	0.00	0.00	0.00

**Table 24-7: Unit Level S/C A Mean Power budgets (per mode)**

It is important to note that although a reduction was achieved across all phases (most notably the COM and SCI phases), due to the fact that a SADM is not included in this option, off-pointing of the solar arrays can still occur due to the possible encounter geometries (as discussed in Section 24.4). As such, an analysis was undertaken to confirm that the system could provide enough power under the extreme solar array offsets of +/- 45 deg.

The peak power mode to be considered, apart from the electric propulsion thrusting, is the case whereby the probes are still attached to S/C A (thus requiring survival heater power), plus both the full payload suite and communications to Earth are ON. This may be the case during regular TT&C contacts during the flyby (up to e.g. 2 months before the closest approach). These ground contacts have been assumed to last for 8 hours per 24 hour period. During the intervening 16 h, constant payload and probe survival heating are required.

The budgets for these peak cases can be found in Table 24-8 (showing both survival heaters ON, i.e. the probes attached, and OFF, i.e. after probe separation).

A	SCI + COM @ 100% duty cycle (heaters OFF)	SCI + COM @ 100% duty cycle (heaters ON)
Total	460.1	460.1
Survival heater B1	0.0	20.0
Survival heater B2	0.0	20.0
Scan Mirror Mech.	7.0	7.0
Losses PCDU	3%	14.0
Losses Harness	3%	14.0
Losses LCLs	1%	4.7
<b>Total w/ losses</b>	<b>499.8</b>	<b>542.6</b>
System Margin	20%	108.5
<b>Total incl. Margin</b>	<b>599.8</b>	<b>651.2</b>

**Table 24-8: Peak flyby power cases: SCI + COMMS (+ probe heating)**

Two assessments are made with these fly-by peak powers in mind.

The first (simplified) assessment focusses on assessing if the solar arrays could provide the necessary power for these generic modes, assuming the worst-case 45 deg off-pointing. This is shown in Table 24-9.

	Probe Heaters OFF	Probe Heaters ON	
Solar cell performance at 1 AU	231.18	231.18	w/m <sup>2</sup>
Sizing heliocentric distance	1.25	1.25	[AU]
Solar cell performance at sizing distance	147.96	147.96	w/m <sup>2</sup>
Solar Array Area	6	6	m <sup>2</sup>
Power available (1.25 AU)	887.7	887.7	W
SA off-pointing	45	45	deg
SA efficiency with off-pointing	0.71	0.71	
Power available (1.25 AU, with off-pointing)	627.7	627.7	W
Power Required SCI + COM (100%)	599.8	651.2	W
Time to sustain SCI + COM (100%) daily	8	8	h
Energy required to sustain Power deficit	N/A	187.7	Wh
Min. Energy available (from LEOP sizing case)	335.3	335.3	Wh
Power Required SCI only	416.2	467.5	W
Available power for battery charging	211.5	160.2	W
Time to recharge (energy only, no losses or battery limitations taken into account)	N/A	1.17	h

**Table 24-9: Peak flyby power cases: solar array + battery capacity assessment<sup>40</sup>**

As shown in Table 24-9, the power available in the worst-case at 1.25 AU is 627.7 W. As such, only the case for payload + TT&C (but without the probe survival heating) can be supported solely by the solar array. However it is clear that the current battery design (sized for LEOP) is sufficient to provide the necessary energy shortfall to cover these peaks, and for the 8 hour ground contacts could be recharged in approximately 1.17 h after the ground contact.

It was additionally noted that the above considerations assumed payload usage at far distances from the comet. As such, it was decided to perform a more consolidated assessment of the flyby timeline in order to determine if the system could provide nominal operations without using the battery. The analysis again considered a worst-case of a 45 deg solar offset angle and a 1.25 AU heliocentric distance.

The following timeline for is assumed for the flyby, split into three phases:

<sup>40</sup> Note that these calculations consider additional margin, as the 7 W required by the scanning mirror will likely not be required during the period when the smallssats are still attached to S/C A.

- - 2 months (start of Relative Nav) to -42 hours (Release of B1)
- - 42 hours (Release of B1) to -42 hours (Release of B2)
- - 42 hours (Release of B2) to -0 hours (closest approach)

The proposed timeline is based on more realistic assumptions for the duty cycling of the payloads, in particular that they are not likely to be ON for long periods before the final ~hours (and some small checkouts before).

Table 24-10 presents the outcome of the analysis for the three phases. Note that the red line indicates the power available to the system from the solar array, while the green line indicates the power required (as step function values only, and not scaled with time).

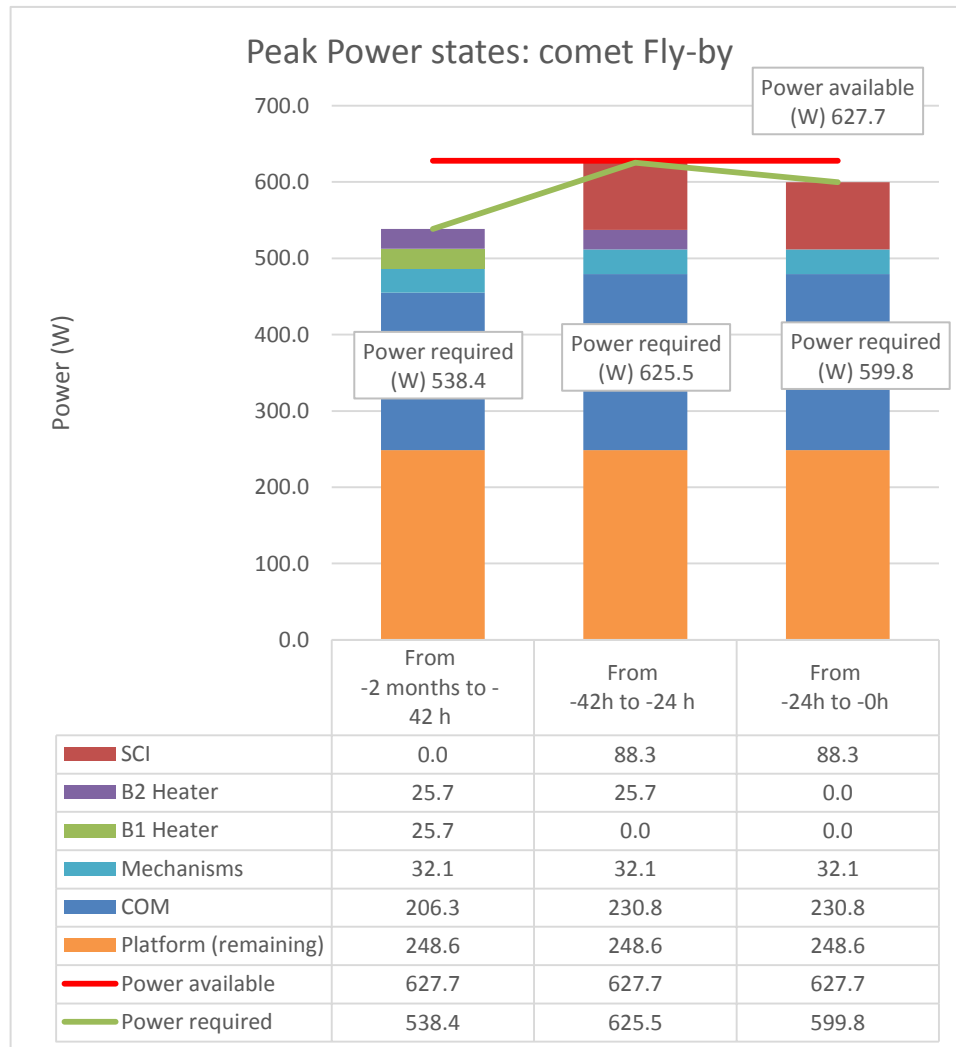


**Table 24-10: Comet Interceptor Science Peak Power Budget breakdown and Power System capability assessment**

As can be seen, the power available is (sometimes marginally) higher than the power demand during all three phases. This demonstrates that, as such, holding the solar array size of 6 m<sup>2</sup> from the baseline (slew) case is considered to be sufficient for the scanning mirror option.

#### 24.5.5 Data Budget

The data budget was assumed to be identical as for the baseline (slew) case. However it is noted that, due to the likely fixed orientation of MIRMISS, it would generate less overall data as for the baseline (slew) case (as it will have a reduced visibility time of the comet).

#### 24.5.6 ΔV Budget

The Delta-V budget was not subject to changes when compared to the baseline option, only the propellant values changed.

### 24.6 Configuration

The inclusion of the scanning mirror plus periscope necessitates some changes to the S/C A configuration.

Wherever possible, it was assumed that the S/C A design from the baseline (slew) case would be re-used with minimal modification. A further dedicated assessment for the scanning mirror option may also wish to address a more optimised configuration.

Starting from the baseline (slew) case, it was clear that the addition of the scanning mirror (and periscope) would require:

- a relocation of the CoCa and MIRMISS instruments need to be relocated.
- the creation of a free FoV for the full rotation range of the scanning mirror
- the addition of the periscope towards the nominal ram (+Z) face

Figure 24-3 shows the location of the CoCa and MIRMISS instruments.

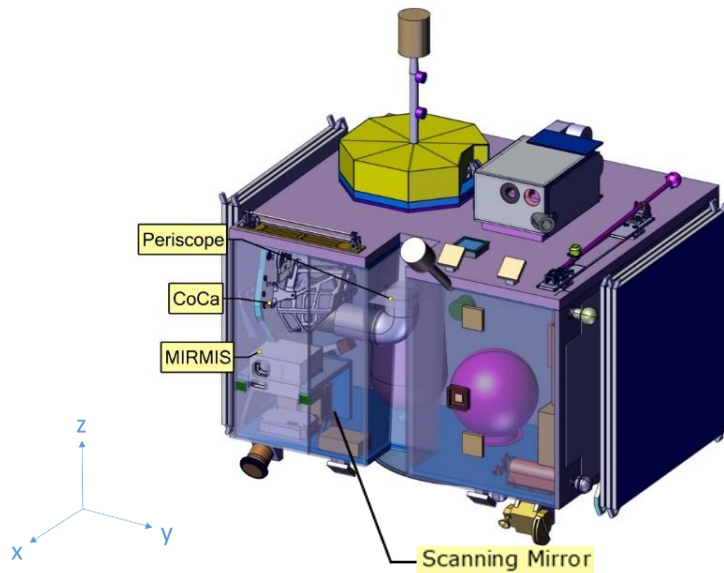


**Figure 24-3: Optional configuration showing scanning mirror option<sup>41</sup>**

<sup>41</sup> Note that the periscope is here only represented by a simple box. For an example of the periscope design, see Section 24.7.6.

As seen in the image, the aperture of the CoCa instrument is looking through a scanning mirror. This can rotate around the +/- Y axis (the axis of the solar arrays) in order to provide a 180 deg (TBC) range of observability for CoCa. Due to this rotation, some area of the +X panel (and smaller areas of the +/-Z panels) needs to be removed, as shown in Figure 24-4.

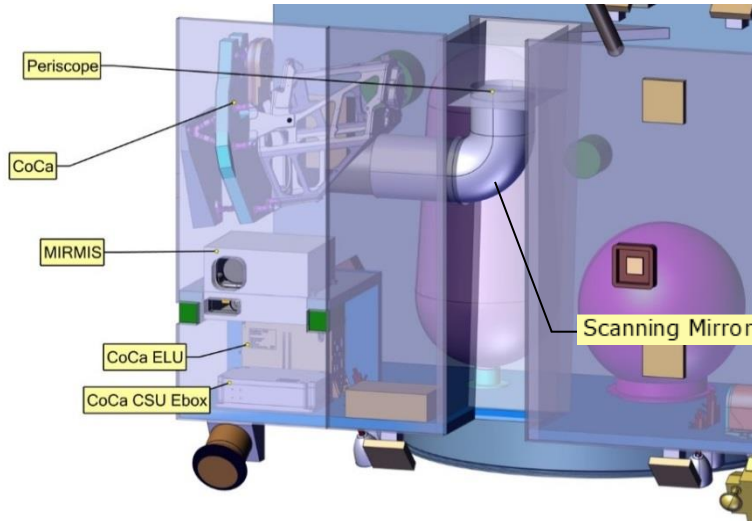


**Figure 24-4: Configuration showing +X modified panel<sup>42</sup>**

Note that the periscope opening to the external space requires (by virtue of design) an opening adjacent to the axis of the scanning mirror FoV. Figure 24-5 provides an indication of these potential locations on the +Z (ram) face. A more detailed assessment is required to determine the best location for the periscope opening, and the impact on units which may need to be moved to accommodate it. An example of such a periscope is provided in Figure 24-11.

<sup>42</sup> See footnote #41.

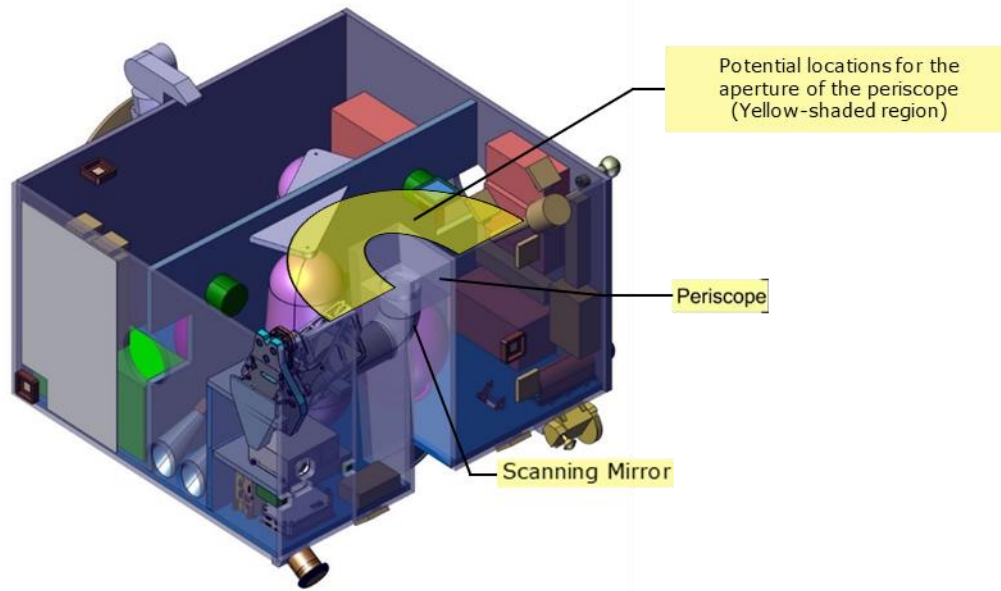


**Figure 24-5: Configuration showing potential locations for the periscope opening<sup>43</sup>**

## 24.7 Mechanisms

### 24.7.1 Requirements and Design Drivers

The inclusion of the scanning mirror (plus periscope) induces the following additional requirements for the mechanisms:

Subsystem Requirements		
Req. ID	Statement	Parent ID
MEC-800	The scanning mirror mechanism shall sustain the launch environment.	
MEC-810	The scanning mirror shall maintain adequate thermo-mechanical stability to the optical instruments.	
MEC-820	The scanning mirror shall provide a maximum rotational rate of 4 deg/s (TBC).	
MEC-830	The scanning mirror shall guarantee an angular repeatability better than 0.01 deg (TBC) across the range of 180 deg.	
MEC-840	The scanning mirror shall provide one-axis rotation.	
MEC-850	The scanning mirror/periscope system shall (TBC) protect the optical instruments from the particle flux across the field of view.	

Note that, for the current design, the requirements for the SADM can be removed from the baseline (slew) case requirements.

<sup>43</sup> See footnote #41.

## 24.7.2 Assumptions

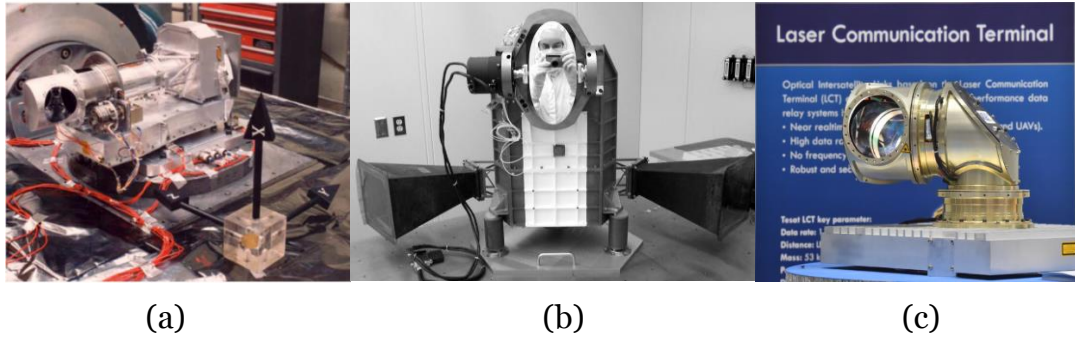
Assumptions	
1	As indicated in the System assumptions, the scanning mirror (plus periscope) shall be included for CoCa, with a design goal (assessed below) to also include MIRMISS. The implications of including also the NAVCAM should be assessed.
2	1 axis gimbal, angular pointing range of +/-90deg (TBC) [as specified in requirements above]
3	Maximum rotational rate required is 4deg/s (TBC) [as specified in requirements above]
4	Angular repeatability: 0.01 deg (TBC) [as specified in requirements above]

## 24.7.3 Trade-Offs Overview

A technical trade-off was performed for a number of potential solutions. In particular, the following elements were assessed:

- Brushless motor (pros: velocity driven, smooth, agile, reactive, possible direct drive; cons: closed loop controller mandatory, more complex driver, encoder, expensive) vs. Stepper motor (pros: position can be held unpowered, simpler electronics, potentially driven in open-loop; cons: in principle less accurate angular resolution, potential backlash in gear train, high gear ratio)
- Gear reduction vs direct drive: hollow shaft construction possible but might be much heavier given the large diameter (~140mm). 1 stage spur gear reduction appears preferable (cons: backlash, lubrication), likely with the need for an embedded anti-backlash feature.
- Commanding driver electronics: Standard stepper motor driver electronics (1 for both scanning mechanisms)
- Bearing assembly and architecture (bearing + housing + brackets)
- Potentiometer vs encoder: the required angular resolution and accuracy likely calls for a fine accurate angular sensor (encoder) and closed loop control strategy
- Launch lock device yes/no: a launch lock device is foreseen, in the form of a pin puller.
- One single scanning mirror enveloping both instruments (CoCa and MIRMISS) vs. dedicated scanning mirror for each mechanism: due to the size of the mirrors needed for the shared option, a dedicated system is preferred for each, with a common building blocks (i.e. the same electronics building blocks as well as mechanisms building blocks (motor, sensors, bearings...))
- Dichroic beam combiner yes/no: it enables using a single periscope of reduced envelope.

Among the explored heritage, Stardust, Contour, Giotto and EDRS were taken into account, as shown in Figure 24-6.



(a)

(b)

(c)

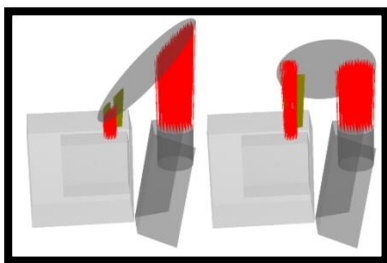
**Figure 24-6: Heritage examples: (a) Stardust; (b) Contour; (c) EDRS LCT**

#### 24.7.4 Scanning Mirror Design

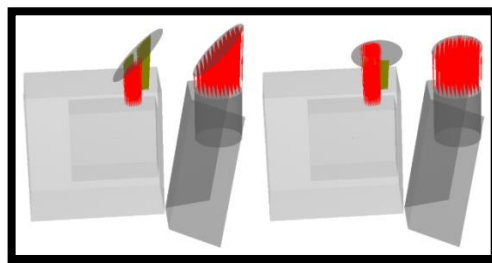
There is a system goal that both MIRMIS and CoCa should look in the same direction, and as such be able to track the comet via a scanning mirror(s). Due to the payload configurations, the optical apertures cannot be positioned adjacent to each other; a minimum 50mm separation between the envelopes at the closest point is considered, as illustrated in Figure 24-7.

To accommodate both instruments via one scanning mirror, an elliptical mirror with a clear aperture of semi-minor axis 187mm and semi-major axis 264.5mm would be required (see Figure 24-7a). This is considered very challenging, suggesting that a solution involving two separate mirrors would be preferable.

If the instruments are to be considered separately, two mirrors with clear apertures of semi-minor axis 74mm and semi-major axis 104.7mm can be used (see Figure 24-7b). Of course, this configuration would require the payloads to be positioned away from each other, to avoid obstructing the other's field of view.



(a)



(b)

**Figure 24-7: Scanning mirror accommodation with respect to instruments:**  
**(a) common mirror; (b) separate mirrors**

The scanning mirror designs for the individual scanning mirrors for CoCa and MIRMIS is shown in Figure 24-8.<sup>44</sup>

<sup>44</sup> Note that only a scanning mirror for CoCa is included the final option baseline.

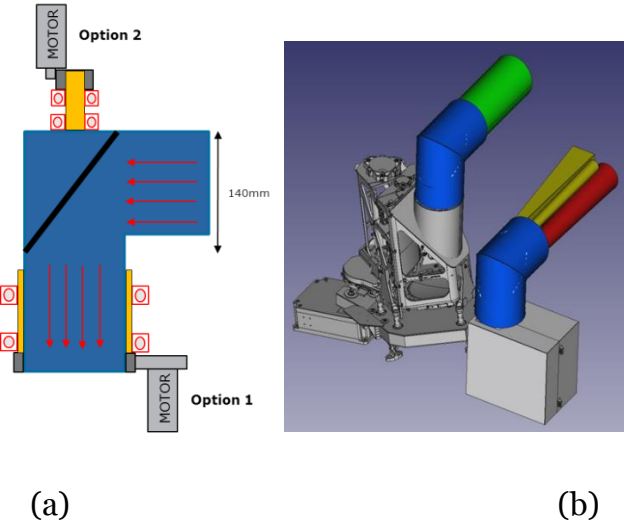


**Figure 24-8: (a) Scanning mirror concept with 2 motor arrangements options; (b) individual scanning mirrors accommodation concept**

#### 24.7.5 Dichroic Beam Splitter

The use of a beam splitter could allow the use of one mirror for both instruments of reduced size, via a scheme as shown in Figure 24-9. The dichroic beam splitter can theoretically be used to combine apertures, by splitting the incoming light by wavelength towards the separate apertures of CoCa and MIRMISS. As such, the two instruments could be positioned much closer and this will reduce the mirror size.

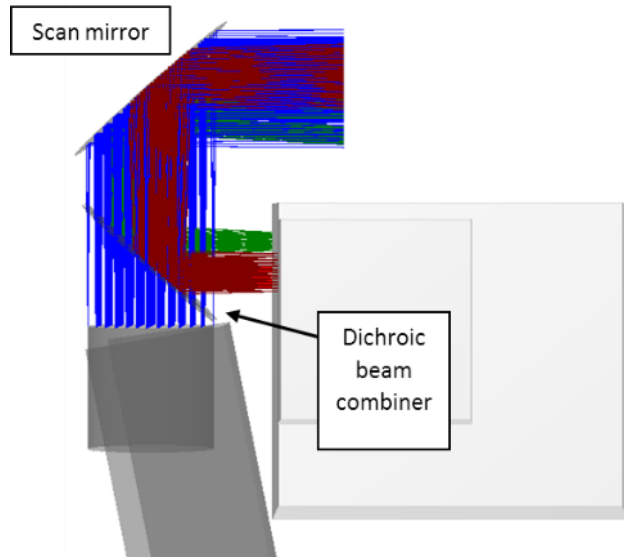


**Figure 24-9: Scanning mirror with dichroic beam combiner**

Such dichroic coatings have high reflectance in a first waveband and high transmission in a second, allowing the two wavebands to be combined with high throughput. The combination of CoCa and MIRMISS is thus theoretically possible, as shown in Figure 24-10, with some loss of throughput where the wavebands overlap. Unfortunately, this

strategy cannot however be used to combine the aperture of the CoCa instrument with that of the navigation camera, as both systems use the same waveband.

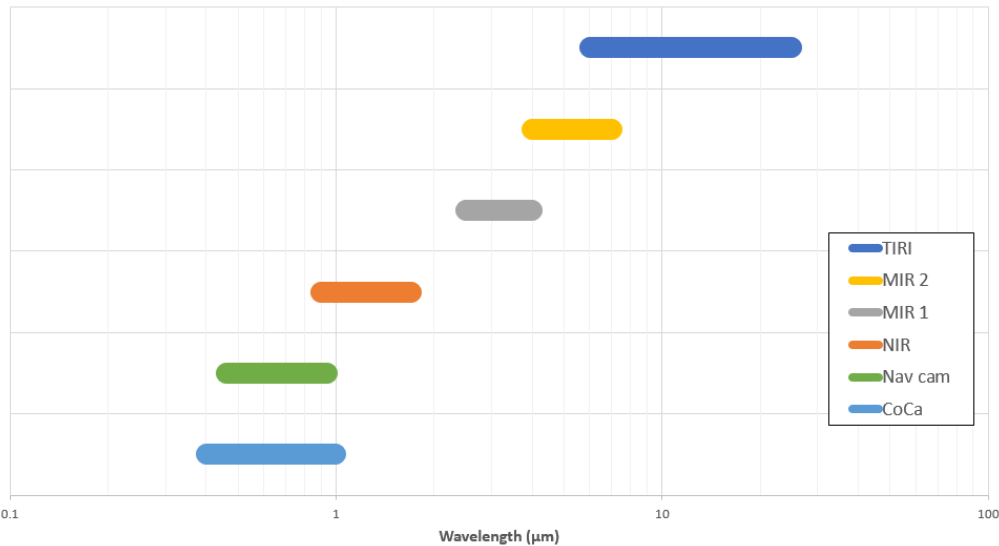


**Figure 24-10: Wavebands of the Comet Interceptor instruments and NAVCAM**

Development of a dichroic coating to achieve the aim of combining CoCa and MIRMISS is a challenging task. This would require various system trade-offs, starting with proving the technical feasibility of such a coating, as high transmission/reflection is unlikely to be achieved across the entirety of the wide wavebands, especially considering the limited material choices available in practice.

#### 24.7.6 Periscope Design

In order to mitigate the risk that the incoming flux of dust particles may damage the performance of the optical instruments during the flyby, a protective static periscope has also been considered. This would be placed in order to be in front of the scanning mirror for the earlier phases of the flyby (when the mirror is exposed to incoming dust flux for a long duration in the ram direction). The principle could be as shown in Figure 24-11. The (rotating) mirror within the scanning mirror system would then be isolated from the oncoming dust environment.

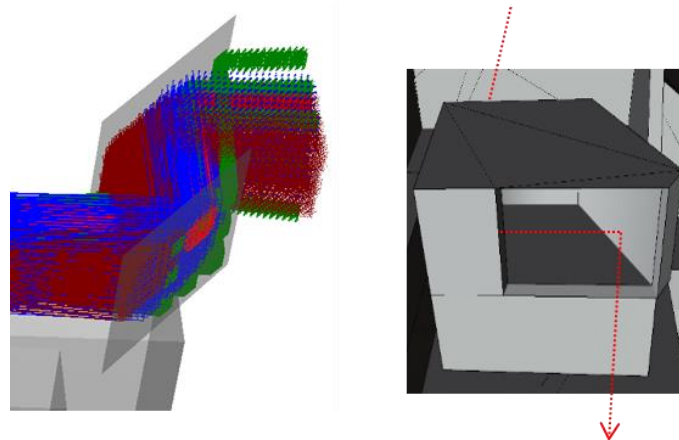


**Figure 24-11: Protective periscope concept**

Towards the closest approach, the scanning mirror would then start to rotate, and no longer view the comet through the (fixed) periscope. As such, the optical payloads would be able to view the comet with a relatively undamaged (from dust) mirror.

Note that the periscope would have some negative impact on the effective observation performance of the instruments across the scientific window (as a shadow angle needs to be accounted for, across which the visibility of the comet is partial or impeded). This is seen by comparing Figure 24-12 (at the start of the flyby) with the obscuring/distorting effects caused by rotations towards the edge of the periscope (as in Figure 24-13).

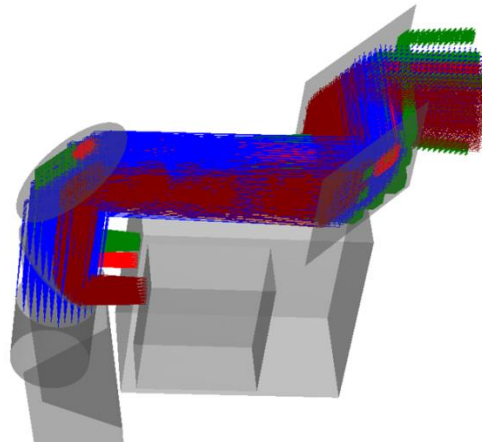


**Figure 24-12: Scanning mirror with periscope: at start of fly-by**

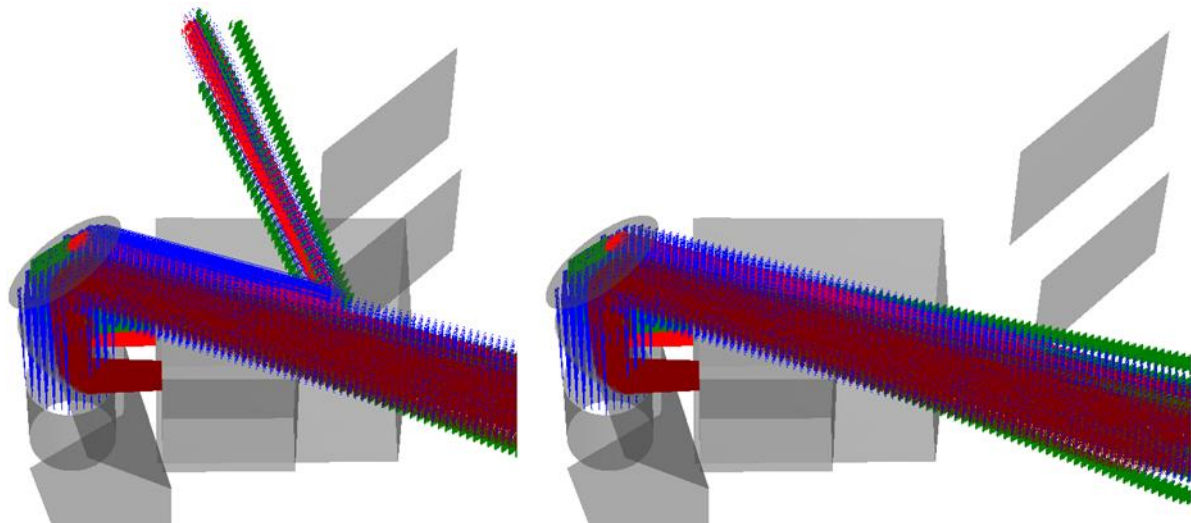


**Figure 24-13: Scanning mirror with periscope: temporary shadow angles (at edge of periscope) after some rotation. The images (left, right) show the reduction in obscuration of intermediate field angles by increasing the scanning mirror to periscope mirror separation**

The periscope is considered to have a short development effort.

#### 24.7.7 List of Equipment

The sizing assumptions for the scanning mirror (per individual unit) are as reported in Table 24-11. This is based on the separate mirror for each instrument concept.

Note that at system level, only one scanning mirror (for CoCa) has been budgeted.

Unit name	Quantity	Mass kg	Maturity level	Margin	Total mass including margin kg
Geared actuator assembly	1	2.1	Bespoke development based on existing technologies	10	2.3
Angular sensor (encoder)	1	0.3	Fully developed	5	0.32
Bearings and periscope strut	1	2	Bespoke development based on existing technologies	20	2.4
Electronic drive unit	1	4.2	Bespoke development based on existing technologies	20	5
SUBSYSTEM TOTAL					10.0*

**Table 24-11: Equipment list – mechanisms scanning mirror per individual unit**

In addition, the masses for the options (dichroic beam splitter and protective periscope) are budgeted are as estimated in Table 24-12.

Note that the mass budget at system level includes one of each of these units (periscope plus dichroic beam splitter), even though the dichroic beam splitter is not formally included in the option baseline.

Unit name	Quantity	Mass kg	Maturity level	Margin	Total mass including margin kg
Dichroic beam splitter	1	1	To be developed	20	1.2
Protective periscope	1	2	To be developed	20	2.4
SUBSYSTEM TOTAL					3.6*

**Table 24-12: Equipment list – mechanism options (periscope + dichroic beam splitter)**

The power of the electronic drive unit for the scanning mirror has been estimated to be 30W peak.

## 24.8 AOCS

If the CoCa payload contains its own comet-tracking mechanism (e.g. the scanning mirror concept outlined above), the AOCS design could be slightly simplified. The periscope design removes the need to slew the S/C and permits continuous alignment of a single face toward the incoming dust during the fly-by. This section highlights potential impacts to the AOCS of this design option.

### 24.8.1 Star Tracker Layout

Limiting the dust impacts to one face increases the scope of feasible orientations for the star trackers' boresights. The boresights can now point anywhere in the -Z hemisphere, rather than being restricted to a half-plane as is the case in the baseline (slewing) design. It also allows them to be placed on the +X or -X faces, which was not previously possible due to dust impacts on those faces. This creates more freedom for the configuration.

The baseline design has the star trackers buried inside the structure on the Y face with cut-outs for the baffles, which is not optimal from an AIT or structural design viewpoint. Furthermore the optical heads may see some of the RCS or EP plumes given that their current boresights are just ~45 deg away from the plume centerlines or possibly less (TBC).

The optimal star tracker location with the alternate payload design would most likely be on the +X (anti-Sun) face pointing halfway between +X and Y.

## 24.8.2 Actuator Sizing

With the alternative fly-by concept the reaction wheel sizing becomes driven entirely by dust impacts rather than the fly-by slew.

The angular momentum induced by small particles can be mitigated using very small wheels (e.g. Astrofein RW90 [0.35 Nms] would be sufficient). However, mitigation of a single large particle impact (up to 100 mg) still requires significant momentum capacity; ~2 Nms per wheel assuming isotropic 4 wheel configuration. Given the availability gap of 2 Nms wheel sizes on the market, the alternative S/C design would also converge toward a 4 Nms wheel.

The advantage of the alternative design is that no torque is required for tracking the comet at the same time as recovering from a large dust particle impact. Therefore, a lower torque wheel (e.g. Astrofein RW250) compared to the baseline would be suitable for achieving similar recovery times.

The primary actuator trade off for the alternative design is summarised below:

Primary attitude actuator	4 x 0.35 Nms / 0.015 Nm wheels	4 x 4 Nms / 0.095 Nm wheels (recommended new baseline)	4 x 4 Nms / 0.215 Nm wheels (previous baseline)	2 x 4 x 5 N RCS
Cost beyond 5N RCS (needed anyway for momentum dump)	Low	Medium	Medium	0
Additional assembly mass beyond 5N RCS	3.6 kg	10 kg	21.6 kg	0
Assembly power average	14 W + RCS for large impact recoveries	24 W (~200 W during large impact recoveries)	24 W (~200 W during large impact recoveries)	72 W when firing
Additional volume beyond 5N RCS	3 300 cm <sup>3</sup>	14 300 cm <sup>3</sup>	48 000 cm <sup>3</sup>	0
Science impact during fly-by	Potential plume disturbances to mass spectrometer during recovery from single large particle impacts	EMC noise	EMC noise	Potential plume disturbances to mass spectrometer due to regular pulsing (at closest approach 1 pulse / minute) & single large particle impact recoveries
Recovery from 100 mg impact at 70 km/s	7 sec Using RCS	58 sec Robust to 1 100mg impact only	25 sec Robust to 1 100 mg impact only	7 sec
Total att. control prop. (mostly to compensate 1cm+1deg EP misalign)	10.2 kg + 100% = 20.4 kg	10.2 kg + 100% = 20.4 kg	10.2 kg + 100% = 20.4 kg	10.6 kg + 100% = 21.2 kg

**Table 24-13: Primary actuator trade-off without the need to slew S/C during fly-by**

With the updated wheel selection (option 2 from Table 24-13), an 11.6 kg mass reduction (relative to the baseline) is realized due to the lower torque requirements.

Note that if the dimension of the dust shield face could be halved, this would reduce the maximum dust-particle-induced momentum and thus the required wheel size to ~1 Nms, which would allow embarkation of e.g. the MSCI MicroWheel 1000, for example. This would lead to a further mass saving of 4.2 kg.

## 24.9 GNC

Given the inclusion of the scanning mirror for CoCa, for navigation purposes the scanning mirror rotation ('in-plane' fast rotation) can be decoupled from the S/C roll ('out-of-plane' error).

A possibility to avoid full closed-loop control with the scanning mirror, is to provide an attitude profile update for the nucleus tracking based on NAVCAM images taken until approximately 1h before the closest approach. Thereafter the scanning mirror would be controlled in open-loop based on this latest on-board profile update.

As can be seen in Figure 13-12 (see GNC chapter) even if there are no OPNAV updates of the attitude profile after that point (1 hour before closest approach), the nucleus remains in the FoV of the NAVCAM and CoCa. The on-board accuracy at that time is 7 times better than at the cut-off time of the divert delta-V (B-plane error ~20 km). Therefore, the pointing error during the science phase would be smaller than the FoV of CoCa.

The feasibility of the strategy shall be confirmed by more detailed analysis of the on-board image processing performances.

This strategy can still provide NAVCAM-based updates until the last ~200 seconds when the nucleus is outside the FoV of the body-fixed NAVCAM (as seen in Figure 24-14)<sup>45</sup>.

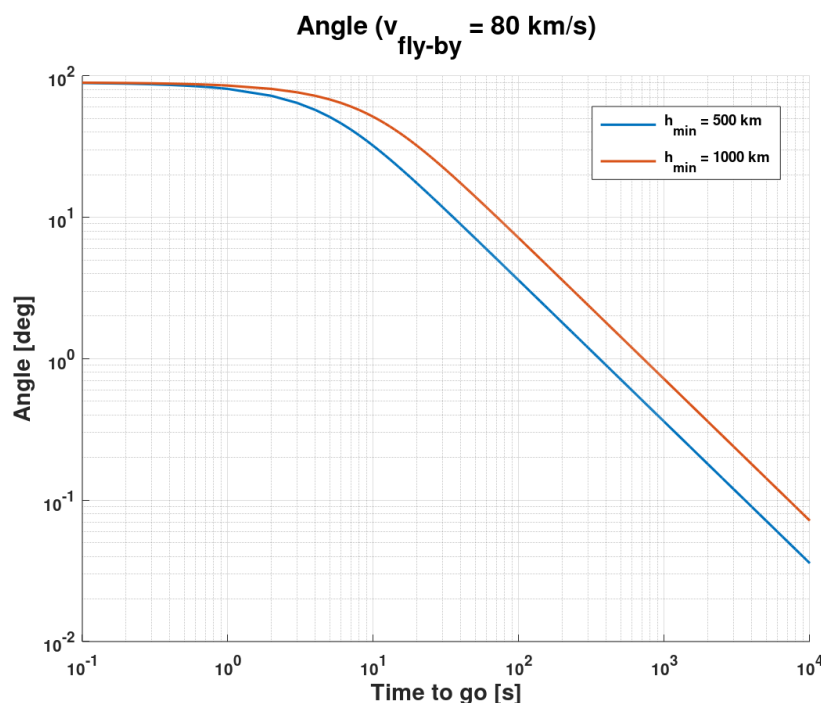


**Figure 24-14: Angle between the LOS to the nucleus and the ram velocity**

Further discussion on the possible GNC strategies is provided in the GNC chapter 13.2.2.2.

<sup>45</sup> Noting the FoV of the NAVCAM, as for the baseline (slew) case of 9 x 7 deg half-angle.

## 24.10 Telecommunications

The possibility to change the S/C architecture to include a scanning mirror and a periscope for the payloads would bring improvements for the communications design.

### 24.10.1 Benefits on S/C A

The presence of a scanning mirror on S/C A allows continuous contact with Earth throughout the entire encounter phase (due to a constant orientation of S/C A). In fact, the loss of contact described in the baseline scenario (section 16.3) is expected during the slew manoeuvre, based on the following assumptions (repeated here for convenience):

- The APM is assumed not able to cope with the maximum slew rate of 4 deg/s
- The slew is performed without APM steering, to avoid the CoG change due to the HGA movement.

### 24.10.2 Benefits for the ISL

For what concerns the ISL, the assumed updated encounter geometry is reported in Figure 24-15.

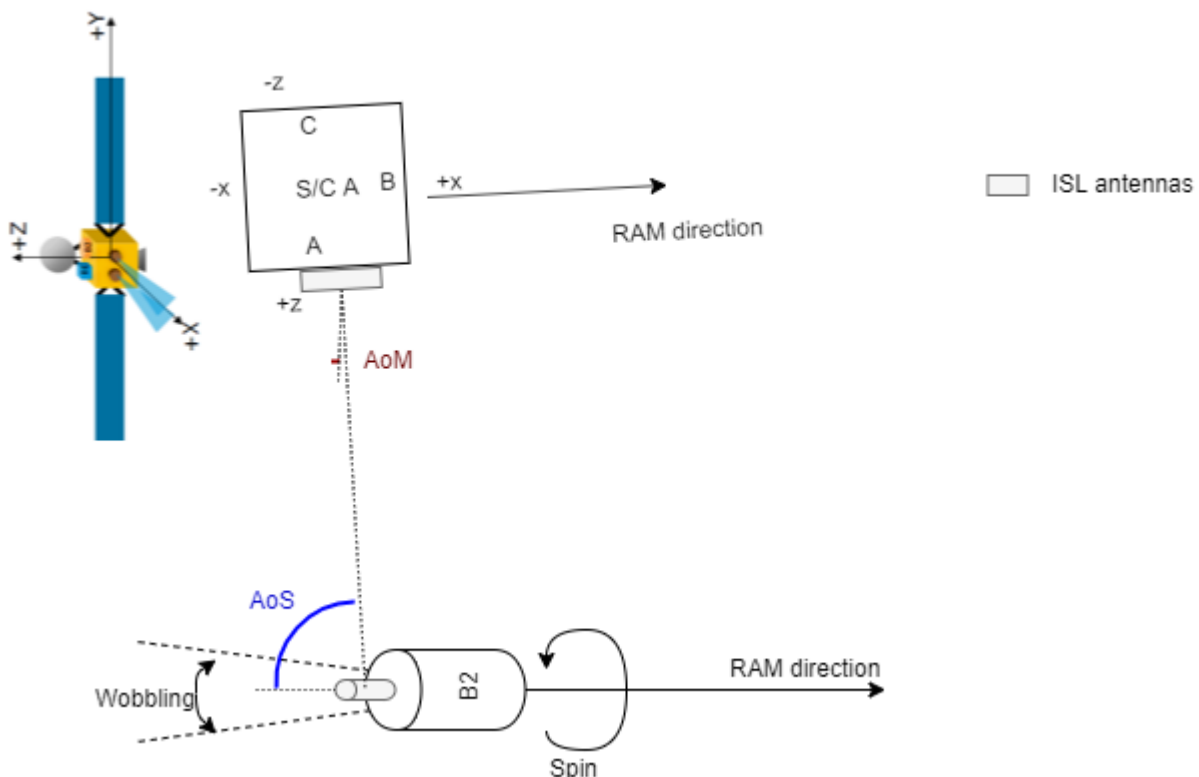


**Figure 24-15: Link geometry during the encounter. No slew is performed by S/C A at the comet encounter. B1 is not shown since its attitude is under JAXA responsibility and not consolidated in the study; however, B1 can be imagined travelling in a region between S/C A and probe B2 with a similar ram direction**

In this new scenario, the requirement COM-ISL-110 for the baseline (slew) case is not applicable anymore. This simplifies the design of the S/C A, therefore, the following elements can be removed from the subsystem:

- LGA-PreEncounter-Prim and LGA-PreEncounter-Backup
- LGA-PostEncounter-Prim and LGA-PostEncounter-Backup
- Transc. 3 Primary and Transc. 3 backup.

This reduces the mass of the subsystem on S/C A by around 0.83 kg and reduces the power consumption by 7.3 W. The design of the probes ISL subsystems remains unchanged.

The new architecture for S/C A is also simpler and cheaper.

The performance of the ISL in the updated reference geometry for the scanning mirror option is reported in the following figures.

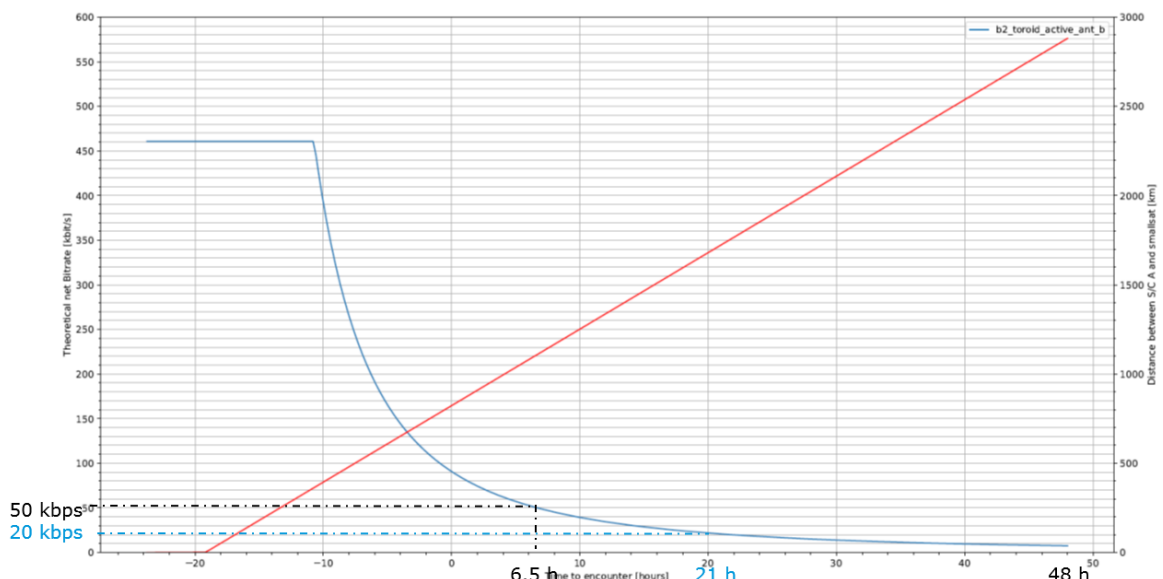


**Figure 24-16: ISL theoretical performance for the link B2 to S/C A in the reference geometry for the scanning mirror option. Red line is relative distance with the axis on the right**

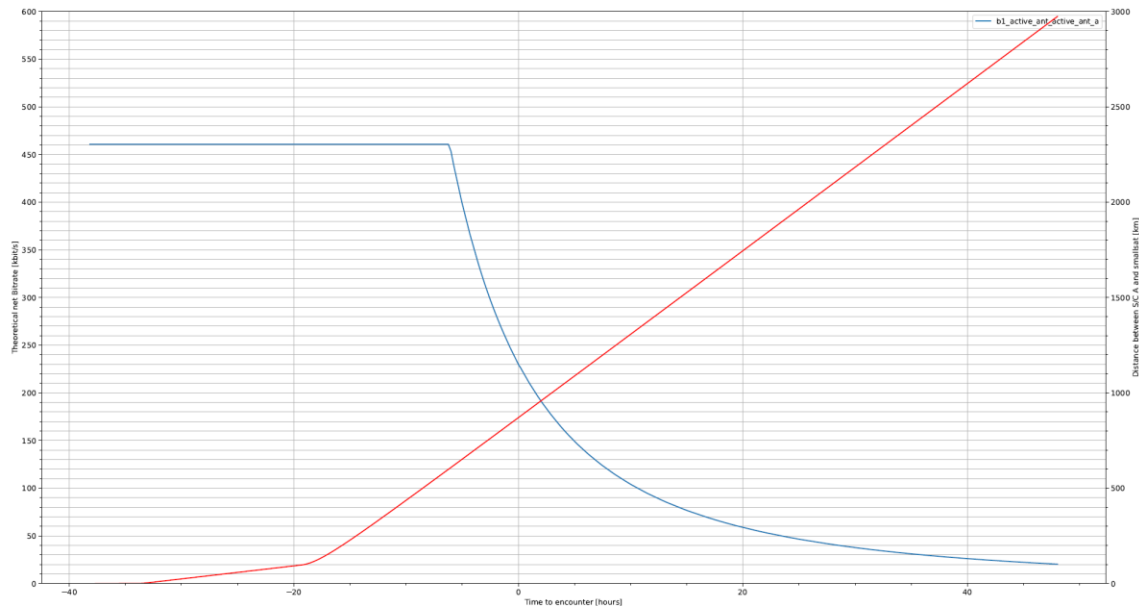


**Figure 24-17: ISL theoretical performance for the link B1 to S/C A in the reference geometry for the scanning mirror option. Red line is relative distance with the axis on the right. Assumed B1 pointing ISL antenna +/- 5 deg towards A**

Comparing Figure 24-16 with Figure 16-9 and Figure 24-17 with Figure 16-11 the ISL performs better for the no-slew flyby option. For the link B2 to S/C A, at encounter, the data rate is 90 kbps instead of 60 kbps without the need to switch between different antennas on S/C A; the same applies for the link B1 to A, 230 kbps is theoretically possible instead of 160 kbps. This means that more science data can be transmitted over the ISL.

One open point regarding this solution is the link performance shortly after the release. The reference geometry shall be updated to include the S/C attitudes prior to the encounter with the foreseen release strategy; this is in order to double-check that just one ISL antenna pair on one face of S/C A is enough to cover also this early post-separation phase.

## 24.11 System Conclusion

The two additional post-IFP delta-sessions of the Comet Interceptor study were used to assess the concept of a scanning mirror (and periscope) for the CoCa instrument and to evaluate, at system subsystems, the impact of such a design option. The main aspects have been addressed above. In addition, Table 24-14 provides some conclusions at System level regarding both concepts (the baseline slewing case, and the scanning mirror option).

Criteria	Nominal baseline (slewing S/C)	Scanning mirror option
System mass	655 kg dry mass, 796 kg wet mass	603 kg dry mass, 738 kg wet mass -> ca. 58 kg saving in wet mass (incl. system margin) <b>Note:</b> this reduction assumes

<b>Criteria</b>	<b>Nominal baseline (slewing S/C)</b>	<b>Scanning mirror option</b>
		removing the SADM, but this has not been confirmed within the Study by mission analysis.
TRL and delta development effort	<ul style="list-style-type: none"> <li>1. Technology development activity for delta qualification for the SADM (e.g. angular step).</li> <li>2. MANIAC rotation mechanism to be developed.</li> </ul>	<p>Development needed for:</p> <ul style="list-style-type: none"> <li>1. Scanning mirror rotation mechanism (TBC based on heritage).</li> <li>2. Electronic box for the scanning mirror (considered not critical).</li> <li>3. Dichroic beam splitter (currently not baselined).</li> </ul>
Cost	<ul style="list-style-type: none"> <li>1. Delta qualification for the SADM Development.</li> </ul>	<ul style="list-style-type: none"> <li>1. Similar to the SADM delta-qualification for the Electronic Box for the rotating mirror.</li> <li>2. Mirror and periscope implies extra cost, but potential savings from the SADM cost.</li> <li>3. Simplification of ISL with potential cost savings.</li> <li>4. Additional AIT/AIV effort due to integration of the scanning mirror plus periscope.</li> </ul>
Risk/robustness of the solution	<ul style="list-style-type: none"> <li>1. End-of-life usage (at high rates) for the SADM.</li> <li>2. Solution relying on an agile S/C with critical manoeuvres required towards the end of the mission lifetime.</li> <li>3. Risk of degraded CoCa and MIRMISS images before the closest approach.</li> </ul>	<ul style="list-style-type: none"> <li>1. End-of-life usage of the scanning mirror. This could have a high risk of jeopardising part or all of the science acquisition from CoCa (i.e. a potential single point of failure).</li> <li>2. In addition, the mission will likely wish to test the scanning mirror before the flyby. In the event that the NAVCAM is also using the scanning mirror, this has the risk that – should the mirror become stuck in a non-nominal position – the wrong face would thereafter need to be pointed towards the comet during the bulk of the flyby, to allow the NAVCAM to see the oncoming comet. This would risk exposing a non-shielded S/C face to the oncoming dust flux.            (...or else reduce the NAVCAM viewing time towards the comet, having potential impacts on the navigation performance).</li> <li>Note however that this is not currently the baseline option.</li> <li>3. Simplification of ISL.</li> <li>4. Only one S/C A face requires to be</li> </ul>

Criteria	Nominal baseline (slewing S/C)	Scanning mirror option
		<p>shielded against the cometary dust environment (compared to three faces for the baseline case).</p> <p>5. The TT&amp;C link to Earth can likely be maintained during the closest approach.</p>
Payload and STR performance	<p>1. RCS, EP plume impingement on the Star Trackers still a potential concern.</p> <p>2. RCS plume impingement on the instruments still a potential concern.</p>	<p>1. The fixed pointing of MIRMISS would lead to a reduction in science time.</p> <p>2. If a dichroic beam splitter is used, the different payload needs might lead to a trade-off for specific measurement bands (i.e. reduction in the measurement of specific wavelengths).</p> <p>3. Slight improvement of the DISC payload performance.</p> <p>4. The probes data rates can be higher.</p>

**Table 24-14: Baseline (slew S/C) vs. Scanning Mirror and Periscope Option**

## 24.12 Technology Needs

All considered technology needs for the scanning mirror option refer to the Mechanisms design:

Technology Needs						
*	Equipment Name & Text Reference	Technology	Supplier (Country)	TRL	Funded by	Additional Information
*	Scanning mirror mechanism	Bespoke development based on some existing heritage	TBD	3	TBD	Fine pointing, flux protection
*	Scanning mirror drive unit	Bespoke development based on some existing heritage	TBD	3	TBD	Fast precise commanding in closed loop
	Dichroic beam combiner	New development based on existing technologies	TBD	3	TBD	Engineering and selection of suitable material optical coatings
*	Protective periscope	New development based on existing technologies				Short development effort

\* Tick if technology is baselined

## 25 CONCLUSIONS

### 25.1 Summary

This Comet Interceptor study was undertaken in order to consolidate and further the work of the previous Comet Interceptor CDF study. While some important open issues still could not be closed during the second study (discussed further below), no technical showstoppers were yet identified for the mission. Nonetheless, it is clear that the mission remains challenging within the programmatic constraints (particularly regarding launch mass and cost). Furthermore, the risks posed by the cometary dust environment will require particular focus in the coming phases.

### 25.2 Study Compliance Matrix

All study objectives of Comet Interceptor 2 were achieved:

Objective	Achieved [Y/N]
Continue and develop further the Comet Interceptor mission, concluding on the mission feasibility, taking into account science and programmatic requirements	Y
Consolidate the mission architecture including mission analysis and operational concepts	Y
Elaborate the conceptual design of the S/C A (main S/C) and B2 (ESA probe) following a “design-to-cost” approach and using as much as possible existing technology and/or platforms with the aim of confirming feasibility of the concept	Y
Consolidate the definition of the schedule and programmatic approach, remaining compatible with the ARIEL mission schedule (dual launch scenario)	Y
Consolidate the mission cost assessment with a target of 150 M€ (total mission cost)	Y
Provide inputs to the RFI/ITT packages for the industrial procurements	Y

**Table 25-1: Study objectives summary**

### 25.3 Major Findings

The major findings of the study are as follows:

- The probabilities of reaching a suitable LPC were re-assessed. After factoring in realistic detection and mission constraints, the probability analysis showed a **probability of 81%** of finding a reachable LPC within the current constraints.

- In addition, several **backup targets** were identified of suitable scientific merit, in the case that a reachable LPC is not found. The latest decision to depart to a backup should be taken by latest 3 years after launch.
- Given the large payload, high transfer delta-V and two probes to be carried, the **system mass remains challenging**. The Study baseline resulted in an estimated total wet mass of 796 kg (compared to the 650 kg target mass).
- The cometary dust environment poses a significant technical risk, and drives the AOCS design and structural shielding required. The high relative impact velocities (up to 70 km/s) leads to **particles on the order of 10 mg and 100 mg posing significant risks** (either of science loss, or catastrophic failure).
- The current expected probability of encountering such particles is 98.9% and 9.9% (for the 10 mg and 100 mg particles, at 1000 km flyby distance) for S/C A, and 48.0% and 4.8% (for the 10 mg and 100 mg particles, at 100 km flyby distance) for probe B2. As such, S/C A is designed to survive impacts from particles up to 100 mg, but still has a **residual 7.1% risk of the penetration of a critical unit during the fly-by**. It is anticipated that this can be lowered further with careful unit placement and additional localised shielding. The B2 probe is only resilient against impacts from 10 mg particles. A more detailed look at the dust environment and shielding conditions needs to be performed in order to reach the most optimal design.
- An Inter-Satellite Link concept seems available to downlink all the necessary data from the B1 and B2 probes to S/C A, before their closest approach at the comet.
- The **downlink time** for all the science data **can greatly exceed 6 months**, in the case of a worst-case comet-to-Earth distance of 2.25 AU. In this case, compression of the science data would need to be considered. The total science data volume to be downloaded will have to be adjusted on a case-by-case basis depending on the selected target and associated geometry for data download.
- Proposals to **reduce the mission cost** may include e.g. removal of the electric propulsion. Removing the electric propulsion would lower the chances of reaching a suitable LPC to 40-56% (depending on the CP system used, but note also these values would still necessitate a system wet mass increase outside the currently foreseen allocation).
- The **GNC for relative navigation at the comet seems challenging** with the current available technologies, leading to a trade-off between desired miss-distance and delta-V for the divert manoeuvres. Various solutions were proposed to avoid pointing loss of the optical instruments during the fly-by, however these would need further assessment in the coming phases.
- The long post-flyby downlink time could be reduced via an increase in the X-band transmitting power (or addition of a Ka-band system). Increasing the X-band transmitting power from 65 W to 100 W could reduce the time to downlink the science data from e.g. ~400 days to 220 days (at 2 AU distance). For a system designed for electric propulsion, such power may be available. Similarly, investigating the possibility to use the 64 m G/S at Usuda (JAXA) would allow downlink rates ca. 3 times higher than for the ESTRACK range. Greater science data compression may be another means to reduce the long downlink times.

- The mission **development timeline appears to be compatible with the ARIEL schedule** for a launch in 2028; nonetheless it will be challenging, particularly for the payloads.

## 25.4 Areas for Further Investigation

The main open issues are:

- A concept involving a **scanning mirror for the CoCa instrument** has been addressed in the final stages of the Study and was found advantageous at system level, as it seems to allow simplifying the S/C A design. This option is discussed in more detail in Chapter 24, Scanning Mirror and Periscope Option and should be addressed further in later work.<sup>46</sup>
- In addition, only a simple assessment could be performed for the system option of removing the electric propulsion system, to reduce the mission cost. A detailed assessment should be performed in later work.
- There remain significant open issues in the **modelling of the cometary dust environment**, particularly for large particles. As these large particles are the ones most impacting mission risk, dedicated work is recommended on closing these uncertainties as soon as possible.
- For the baselined system option including the electric propulsion, the use of an EP thruster gimbal to save AOCS propellant mass (to correct for misalignments) should be traded against the mass due to misalignment. However the mass savings (ca. 12 kg for the gimbal compared to ca. 26 kg for the AOCS propellant) may not be sufficient to justify the additional cost.
- The probe B2 power architecture baselined a case that used only a primary battery as power source, in order to limit the mass, cost and complexity. The power experts highlighted at the end of the Study potential new developments that could alleviate some of these concerns, however their impact could not be assessed within the available time. These should be re-assessed, to determine if they can increase the available science time and robustness with a reasonable system-level impact.
- The placement of the FGM instrument on the probe B2 poses challenges, due to its need to be placed on the anti-ram face, which also houses the ISL antenna. An initial assessment showed that the FGM interferes with the gain pattern of the ISL antenna. A solution was proposed to place the ISL antenna on top of the FGM boom, however the full impacts of this and a concrete design proposal could not be made in the time available.

<sup>46</sup> Note that the scanning mirror is referred to as the “rotating mirror” in some later documents.

This Page Intentionally Blank

## 26 REFERENCES

### 26.1.1.1 Chapter 5 Mission Analysis References

- RD[1] ESA-ARIEL-ESOC-MIS-RP-001, MAS Working Paper No. 612, Ariel Consolidated Report on Mission Analysis, Issue 1, Rev. 0, April 2019.
- RD[2] Comet Interceptor Proposal
- RD[3] The Evolution of Long-Period Comets, Paul Wiegert and Scott Tremaine, Icarus 137, 84–121 (1999)
- RD[4] The orbit and size-frequency distribution of long period comets observed by Pan-STARRS1, Boe et al., Icarus 333 (2019) 252–272

### 26.1.1.2 Chapter 6 Environment References

- RD[5] ECSS-E-ST-10-04C, Space Environment
- RD[6] Rodionov et al, An advanced physical model of cometary activity, Planetary and Space Science 50 (2002) 983 – 1024
- RD[7] Müller et al, An Engineering Model of the Dust Environment of the Inner Coma of Comet P/Wirtanen, Part 1, RO-ESC-TA-5501 Issue 1, October 1998
- RD[8] Müller et al, An Engineering Model of the Dust Environment of the Inner Coma of Comet P/Wirtanen, Part 2, RO-ESC-TA-5501 Issue 1, May 1999
- RD[9] Müller et al, Engineering Coma Model for Churyumov-Gerasimenko, RO-ESC-TN-5556, Draft 0.3 October 17, 2010
- RD[10] Colin Snodgrass and Matt Taylor, cometary flux tabulated model (personal communication)
- RD[11] Fulle et al. Evolution Of The Dust Size Distribution Of Comet 67P/Churyumov–Gerasimenko From 2.2 au To Perihelion. The Astrophysical Journal, 821(1), 14., 2016
- RD[12] Merouane et al., Evolution of the physical properties of dust and cometary dust activity from 67P/Churyumov–Gerasimenko measured in situ by Rosetta /COSIMA. Monthly Notices of the Royal Astronomical Society, 469(Suppl\_2), S459-S474, 2017
- RD[13] McDonnell et al, Giotto's Dust Impact Detection System (DIDSY) and Particulate Impact Analyzer (PIA): Interim assessment of the dust distribution and properties within the coma. International Organization, 1986
- RD[14] Landgraf et al, Prediction of the in-situ dust measurements of the stardust mission to comet 81P/Wild 2, Planetary and Space Science 47 (1999)
- RD[15] Grün, E., H. A. Zook, H. Fechtig, and R. H. Giese, Collisional Balance of the Meteoritic Complex, Icarus, 62, 244-272, 1985.
- RD[16] A. Miller, “ESABASE2/Debris Release 10.0Technical Description”, <https://esabase2.net/wp-content/uploads/2019/01/ESABASE2-Debris-Technical-Description.pdf>, 2019

### **26.1.1.3 Chapter 7 Systems References**

- RD[17] Concurrent Design Facility Studies Standard Margin Philosophy Description, Technical Note, ESA-TECSYE-RS-006510, 14/08/2017

### **26.1.1.4 Chapter 9 Structures References**

- RD[18] Ariane 6 User Manual, Arianespace, issue 1 rev. 0, March 2018
- RD[19] Schaefer F. K., Ryan S., Lambert M., Putzar R. (2008): Ballistic limit equation for equipment placed behind satellite structure walls. International Journal of Impact Engineering 35, 1784 – 1791.

### **26.1.1.5 Chapter 10 Chemical Propulsion References**

- RD[20] *Northrop Grumman D358*, data sheet,  
<https://www.northropgrumman.com/Capabilities/DiaphragmTanks/Documents/DS358.pdf>
- RD[21] *Moog Isp, Thruster line datasheet*,  
[https://www.moog.com/content/dam/moog/literature/Space\\_Defense/spaceliterature/propulsion/Moog-MonopropellantThrusters-Datasheet.pdf](https://www.moog.com/content/dam/moog/literature/Space_Defense/spaceliterature/propulsion/Moog-MonopropellantThrusters-Datasheet.pdf)
- RD[22] *Pyrovalves, Fill, Drain and Vent valves, Latch Valves, Flow Control Valves*, brochure, S. Cortés Borgmeyer, <http://www.space-propulsion.com/spacecraft-propulsion/valves/latch-valve.html>

### **26.1.1.6 Chapter 11 Electric Propulsion References**

- RD[23] The SMART-1 Electric Propulsion Subsystem In Flight Experience, AIAA-2004-3435, C.R. Koppel et al.,  
<https://sci.esa.int/documents/34677/36590/1567255180622-AIAA2004-3435-koppel-smarto9.pdf>

### **26.1.1.7 Chapter 12 Mechanisms References**

- RD[24] Definition file, Vega Programme PLA1194 / VG-DF-16V2-C-002-CASA issue01, 14-07-2014
- RD[25] Vampire Adapter System, Definition File Vampire 937/ P-1241114-RSE issue 02, 2018-09-17, RUAG Space AB
- RD[26] Vampire Adapter System, Definition File Vampire 1194/ P-1236153-RSE issue 03, 2018-06-20, RUAG Space AB
- RD[27] Ariane5 users manual issue 05 Rev 01, July 2011  
The Huygens probe system design, paper from K. C. Clausen 1, H. Hassan 1, M. Verdant , P. Couzin, G. Huttin, M. Brisson, C. Sollazzo and J.-P. Lebreton
- RD[28] Huygens separation mechanism / 1995 ESASP\_374 paper from Dr. Udo R. Herlach, P. Tatalias, B. Schmid & D. Musset / Oerlikon Contravec AG Space, Schaffhauserstrasse 580, 8052 Zurich Switzerland
- RD[29] Exomars Main Separation Assembly Design Report / EXM-OM-DRP-RSSZ-0001, issue 04, 09-10-2012

- RD[30] BEAGLE 2 SUEM Design and Development Summary, Reference: INS/BGL2/DDR/094, Issue 01, Novembre 2002
  - RD[31] EXOMARS HGA-A , Design & mechanism description and analyses, Ref. 865555 & EXM-OM-DJF-MDA-0050, Issue 4, 2013-10-18
  - RD[32] Exomars High Gain TTC Antenna Overview, Paper from D. Dubruel, PY Renaud, C. Dreyer, JP Langevin, T. Tralman, JF Durocher-de-Grandpré, S. Larouche, M. Lanuti, P. Noschese, M. Cova, A. Winton, E. Saenz, P. de Maagt
  - RD[33] Testing of Bepicolombo antenna pointing mechanism, paper from Pablo Campo, Aingeru Barrio, Fernando Martin
  - RD[34] Solar-Orbiter-high-antenna-subsistem , Sener Internet link : <http://www.aerospace.sener/products/solar-orbiter-high-antenna-subsistem>
  - RD[35] Antenna Pointing Mechanisms for solar orbiter high and medium gain antennas, paper from Jorge Vázquez, Iñaki Pinto, Iker Gabiola, I. Ibargoyen, Fernando Martin.
  - RD[36] Mechanisms of the Rosetta high gain antenna, paper from Carlos Pereira HTS AG Wallisellen, Switzerland
  - RD[37] Rosetta's high gain antenna, ESA internet link : <http://sci.esa.int/rosetta/25234-rosetta-s-high-gain-antenna/>
  - RD[38] IPC Technology Harmonisation Advisory Group. European Space Technology Harmonisation Technical Dossier. Solar Array Drive Mechanisms / issue 3 revision 2 - 24/11/2014 / ESA/IPC/THAG(2014)03
  - RD[39] KONGSBERG Adaptive Rotational Mechanism Assembly (KARMA-4), Internet link : <http://esmats.eu/noordwijk/stuff/karma4.pdf>
  - RD[40] The Damper Spring Unit of the Sentinel 1 Solar Array, paper from Frans Doejaaren and Marcel Ellenbroek, Dutch Space BV, Leiden, The Netherlands. Internet link : <http://esmats.eu/amspapers/pastpapers/pdfs/2012/doejaaren.pdf>
  - RD[41] [https://www.ruag.com/sites/default/files/2016-11/PAS\\_381S\\_Separation\\_System.indd](https://www.ruag.com/sites/default/files/2016-11/PAS_381S_Separation_System.indd)
  - RD[42] <http://www.planetarysystemscorp.com/web/wp-content/uploads/2015/09/2000785F-MkII-MLB-User-Manual.pdf>
- 26.1.1.8 Chapter 16 Telecommunications References**
- RD[43] ECSS-E-ST-50C Rev. 2, *Radio Frequency and Modulation*, 4 October 2011, complemented with CCSDS 131.2-B.1, *Flexible advanced coding and modulation scheme for high rate telemetry applications*, March 2012.
  - RD[44] ECSS-E-50-04C, *Telecommand protocols synchronization and channel coding*, 31 July 2008 complemented with CCSDS 231.B-3, *TC synchronization and channel coding*, September 2017.
  - RD[45] ECSS-E-50-01C, *Telemetry synchronization and channel coding*, 31 July 2008.

RD[46] ECSS-E-50-02C, *Ranging and Doppler Tracking*, 31 July 2007, complemented with CCSDS 4.1.4-B-2, *Pseudo-Noise (PN) Ranging Systems*.

RD[47] Space frequency coordination group (SFCG), resolutions and recommendations available at [www.sfcgonline.org](http://www.sfcgonline.org).

### 26.1.1.9 Chapter 17 Data Handling References

RD[48] AS250-OSCAR-MU-DA0024626-V-ASTR: AS250 OSCAR user manual  
23/02/2011

RD[49] OSCAR-ADSE-UM-1000189340: OSCAR MK3 user manual, 4/12/2018

RD[50] <http://www.dsi-as.de/en/product/payload-data-handling-unit,10.htm>

RD[51] RUAG Space Sweden: Next Generation On Board Computer Datasheet, 2017.  
[https://www.ruag.com/sites/default/files/media\\_document/2017-12/Next%20Generation%20On%20Board%20Computer.pdf](https://www.ruag.com/sites/default/files/media_document/2017-12/Next%20Generation%20On%20Board%20Computer.pdf)

RD[52] P-ASIC-NOT-1125417-RSE: CREOLE ASIC User's Manual

RD[53] IPAC On Board Computer, TAS-ESA bilateral meeting, 9 May 2019

RD[54] Airbus Defence & Space: Remote Interface Unit AS250 Datasheet, 2015.  
<https://spaceequipment.airbusdefenceandspace.com/avionics/platform-interface-units/riu>

RD[55] Aeroflex Gaisler : MASCOT On-board Computer based on SpaceWire Links.  
International SpaceWire Conference, 2013.  
<https://core.ac.uk/download/pdf/16455539.pdf>

RD[56] <https://gomspace.com/shop/subsystems/command-and-data-handling/nanomind-z7000.aspx>

RD[57] Cobham Gaisler : Flight Software Workshop Presentation, 2017.  
<http://flightsoftware.jhuapl.edu/files/2017/Day-3/02-Hellstrom-Cobham-HiRel.pdf>

RD[58] [Radiation characterization of MicroSemi ProASIC3 flash FPGA family, Christian Poivey et al, 2010 IEEE Radiation Effects Data Workshop \(REDW\)](#)

RD[59] [Radiation-Tolerant ProASIC3 Low Power Spaceflight Flash FPGAs with Flash\\*Freeze Technology, Revision 5, \(\[https://www.microsemi.com/document-portal/doc\\\_download/131374-radiation-tolerant-proasic3-fpgas-radiation-effects-report\]\(https://www.microsemi.com/document-portal/doc\_download/131374-radiation-tolerant-proasic3-fpgas-radiation-effects-report\)\)](#)

RD[60] [Single-Event Upsets Characterization of the 28nm Artix-7-based Programmable Logic of Xilinx Zynq-7000 FPGA, University of Piraeus, 1 July 2019](#)

RD[61] [Single-Event Upsets Characterization of the 28nm Kintex-7-based Programmable Logic of Xilinx Zynq-7000 FPGA, University of Piraeus, 1 July 2019](#)

RD[62] [Single-Event Characterization of the 28 nm Xilinx Kintex-7 Field-Programmable Gate Array under Heavy Ion Irradiation, Davis S. Lee et al, 2014 IEEE Radiation Effects Data Workshop \(REDW\)](#)

- RD[63] [Multi-Cell Upsets Within the Xilinx Series-7 FPGAs, Michael Whirtlin et al, SANDIA report SAND2014-0974C 498923](#)
- RD[64] [Analyzing the Impact of Radiation-Induced Failures in Programmable SoCs, Lucas Antunes Tambara et al, IEEE Transactions on Nuclear Science \( Volume: 63 , Issue: 4 , Aug. 2016 \)](#)

#### **26.1.1.10 Chapter 19 GS&OPS References**

- RD[65] ARIEL Multiple Spacecraft per Aperture (MSPA), Memo, ESA-OPD-MO-0004, K. Symonds, 13/06/2019
- RD[66] CCSDS 727.0-B-4, CCSDS File Delivery Protocol, Blue book, January 2007
- RD[67] CCSDS 133.0-B-1, Space Packet Protocol, Cor 2. Sep 2012
- RD[68] ECSS-E-ST-50C, Communications, 31 July 2008
- RD[69] ECSS-E-70-11C, Space Segment Operability, 31 July 2008
- RD[70] ECSS-E-70-41C Telemetry and Telecommand Packet Utilization, 15 April 2016

#### **26.1.1.11 Chapter 20 Programmatics References**

- RD[71] ECSS-E-ST-10-02C - Verification
- RD[72] ECSS-E-ST-10-03C - Testing
- RD[73] ECSS-E-AS-11C Dated 1- October 2014, Adoption Notice of ISO 16290, Space Systems – Definition of TRL and their Criteria of Assessment Supplemented by ECSS-E-HB-11A TRL Guidelines, dated 01-03-2017

#### **26.1.1.12 Chapter 21 Technical Risk References**

- RD[74] Space Project Management, Risk Management, ECSS-M-ST-80C, 31 July 2008.

#### **26.1.1.13 Chapter 23 Cost References**

- RD[75] TEC-SYC Cost Risk Procedure, TEC-SYC/5/2010/PRO/HJ, February 2010
- RD[76] ESA Cost Engineering Charter of Services, Issue 4, TEC-SYC/12/2009/GRE/HJ
- RD[77] “Guidelines for the use of TRLs in ESA programmes”, ECSS-E-HB-11A dated 01-03-2017

This Page Intentionally Blank

## 27 ACRONYMS

Acronym	Definition
ADS	Airbus Defence and Space
AES	Advanced Encryption Standard
AIT	Assembly, Integration and Testing
AIV	Assembly, Integration, Validation
AIV/T	Assembly, Integration and Verification/Testing
AKE	Absolute Knowledge Error
AOCS	Attitude and Orbit Control System
AoM	Angle offset from Main S/C
AoS	Angle offset from Probe
APE	Absolute Performance Error
APM	Antenna Pointing Mechanism
APSoC	All Programmable System on Chip
ARIEL	Atmospheric Remote-sensing Infrared Exoplanet Large-survey
ASIC	Application Specific Integrated Circuit
ATB	Avionics Test Bench
AU	Astronomical Unit
AVM	Avionics Model
BCH	Bose–Chaudhuri–Hocquenghem code
BCR	Battery Charge regulator
BDR	Battery Discharge Regulator
BIT	Built In Test
BLD	Bi Level Discrete
BLE	Ballistic Limit Equation
BoL	Beginning of Life
BP	Bundle Protocol
BPRU	Bang bang Pressure Regulator Unit
CA	Closest Approach
CaC	Cost at Completion
CAN	Controller Area Network

<b>Acronym</b>	<b>Definition</b>
CBOD	Clamp Band Opening Device
CCSDS	Consultative Committee for Space Data Systems
CDF	Concurrent Design Facility
CDR	Critical Design Review
CER	Cost Estimation Relationship
CI	Comet Interceptor
CIL	Critical Items List
CLA	Coupled Load Analysis
CLCW	Command Link Control Word
CMA	Cost Model Accuracy
CoCa	Comet Camera
CoG	Centre of Gravity
COMPLIMENT	COMetary Plasma Light InstrUMENT
COTS	Commercial Off The Shelf
CP	Chemical Propulsion
CPDU	Command Pulse Distribution Unit
CPS	Chemical Propulsion System
CSP	CubeSat Space Protocol
CSS	Coarse Sun Sensor
CSU	Camera Support Unit
CTP	Science Core Technology Programme
DAPU	Dust Analyser Processing Unit
DDOR	Delta Differential One-way Ranging
DFP	Dust Field Plasma suite
DH	Data Handling
DLS	Dual Launch System
DMM	Design Maturity Margin
DNC	Dynamically New Comet
DOA	Degree of Adequacy of the cost model
DoD	Depth of Discharge
DoF	Degree of Freedom

<b>Acronym</b>	<b>Definition</b>
DPTD	Discovery, Preparation and Technology Development
DPU	Data Processing Unit
DSM	Deep Space Manoeuvre
DST	Deep Space Transponder
E(Q)M	Engineering (Qualification) Module
ECSS	European Cooperation for Space Standardisation (Standards)
EDAC	Error Detection and Correction
EEPROM	Electrically Erasable Programmable Read Only Memory
EGA	Earth Gravity Assist
EGOS-CC	European Ground Operations System Common Core
ELU	Electronic Unit
EM	Engineering Model
EMC	Electro Magnetic Compatibility
ENA	Energetic Neutral Atoms
EnVisS	Entire Visible Sky
EoL	End of Life
EP	Electric Propulsion
EPC	Electric Power Conditioning
EPE	External Project Events
EQM	Engineering and Qualification Model
ESA	European Space Agency
ESOC	European Space Operations Centre
ESTRACK	ESA Tracking Network
FD	Flight Dynamics
FDIR	Failure Detection Isolation & Recovery
FE	Finite Element
FEM	Finite Element Model
FGM	Flux Gate Magnetometer
FM	Flight Model
FoV	Field of View
FPGA	Field Programmable Gate Array

<b>Acronym</b>	<b>Definition</b>
FSS	Fine Sun Sensor
FU	Filter Unit
G/S	Ground Station
GAM	Gravity Assist Manoeuvres
GCR	Galactic Cosmic Rays
GEO	Geostationary Earth Orbit
GNC	Guidance, Navigation, and Control
GSTP	General Support Technology Programme
GTO	Geostationary Transfer Orbit
HDRM	Hold Down and Release Mechanism
HET	Hall Effect Thruster
HGA	High Gain Antenna
HK	House Keeping
HKP	Housekeeping
HKTM	Housekeeping Telemetry
HPC	High Power Command
HSSL	High Speed Serial Link
I/F	Interface
I/O	Input / Output
I <sub>2</sub> C	Inter-IC
IC	Integrated Circuit
ICA	Ion Composition Analyser
ICD	Interface Control Document
IMU	Inertial Measurement Unit
IO	Input/Output
IoD	In-orbit Demonstration
IOT	In Orbit Test
IP	Image Processing
IPAC	Integrated Processing, Data Handling and AOCS controller
IQM	Inherent Quality of the cost Model
IR	Infra Red

<b>Acronym</b>	<b>Definition</b>
ISL	Inter-Satellite Link
ITT	Invitation To Tender
ITU	International Telecommunication Union
JAXA	Japan Aerospace Exploration Agency
KBO	Kepler Belt Objects
LA	Logical Address
LCL	Latched Current Limiter
LEES	Low Energy Electron Spectrometer
LEO	Low Earth Orbit
LEOP	Launch and Early Operation Phase
LET	Linear Energy Transfer
LGA	Lunar Gravity Assist
LLC	Low Level Command
LM	Launch Mode
LoS	Line of Sight
LPC	Long Period Comet
LPSS	Launcher Payload Separation System
LSST	Large Synoptic Survey Telescope
LV	Launch Vehicle
MAIT	Manufacturing Assembling Integrating Testing
MANiaC	Mass Analyzer for Neutrals in a Coma
MC	Main S/C
MEOP	Maximum Expected Operational Pressure
MGA	Medium Gain Antenna
MGM	Magneto Meter
MIRMIS	Multispectral Infra Red Molecular and Ice Sensor
MLI	Multi layered Insulation
MMH	Monomethylhydrazine (fuel) - CH <sub>3</sub> (NH)NH <sub>2</sub>
MMU	Mass Memory Unit
MOC	Mission Operations Centre
MPPT	Maximum Power Point Tracker (Tracking)

<b>Acronym</b>	<b>Definition</b>
MSPA	Multiple Spacecraft per Aperture
MTL	Mission Time Line
MTQ	Magneto Torquer
NAC	Narrow Angle Camera
NACK	Negative Acknowledge
NIR	Near Infra Red
NOM	Nominal Mode
NSM	Non Structural Mass
NTO	Nitrogen tetroxide (oxidizer) - N <sub>2</sub> O <sub>4</sub>
OBC	On-board Computer
OBCP	On Board Control Procedure
OBSW	On Board Software
OBT	On-board Time
OPIC	Optical Periscope Imager for Comets
PCDU	Power Conditioning and Distribution Unit
PDT	Payload Data Transmitter
PDU	Power Distribution Unit
PF/ PL	Platform/ Payload
PFM	Protoflight Model
PI	Principal Investigator
PLM	Payload Module
PM	Processing Module
POE	Project Owned Events
PPU	Power Processing Unit
PRE	Pressure Regulation Electronics
PROM	Programmable Read Only Memory
PSS	Propulsion Subsystem
PT	Pressure Transducer
PUS	Packet Utilization Standard
QIV	Quality of the Input Values
QM	Qualification Model

<b>Acronym</b>	<b>Definition</b>
QSL	Quasi Static Load
RCS	Reaction Control System
REQ	Requirement
RFI	Request for Information
RHCP	Right Hand Circular Polarization
RIU	Remote Interface Unit
R-LCL	Retriggerable Latch Current Limiter
RNG	Ranging
RSA	Relay Status Acquisition
rSM	Robust Structural Model
RU	Reconfiguration Unit
RW	Reaction Wheels
S/C	Spacecraft
SA	Solar Array
SADM	Solar Array Drive Mechanisms
SAR	Solar Array Regulator
SC	SpaceCraft
SCI	Science Mode
SCIENA	Solar winds and Cometary Ions and Energetic Neutral Atoms Instrument
SCI-FM	Mission Studies Office at ESA's Directorate of Science
SCoC	System Controller on Chip
SCOS	Spacecraft Operating System
SDRAM	Synchronous Dynamic Random Access Memory
SEE	Single Event Effect
SEL	Sun Earth Lagrange Point
SEL2	Sun-Earth Libration Point 2
SGM	SafeGuard Memory
SK	Station Keeping
SLI	Single Layer Insulation
SM	Structural Model
SoC	State of Charge

<b>Acronym</b>	<b>Definition</b>
SoC	System on Chip
SOI	Sphere of Influence
SPC	Science Programme Committee
SPF	Single Point Failure
SPI	Serial Peripheral Interface
SpW	SpaceWire
SRAM	Static Random Access Memory
SSM	Second Surface Mirror
SSM	Simplified Structural Model
SSMM	Solid State Mass Memory
SSTO	Self-Stabilised Terminator Orbit
STM	Structural Thermal Model
STR	Star Tracker
SVF	Software Verification Facility
SVM	Service Module
TAS	Thales Alenia Space
TBC	To Be Confirmed
TC	Telecommands
TCM	Trajectory Correction Manoeuvre
TCS	Thermal Control Sub-system
TGO	Trace Gas Orbiter
TID	Total Ionising Dose
TIDL	Total Ionizing Dose Level
TIDS	Total Ionizing Dose Sensitivity
TIRI	Thermal Infra Red Imager
TM	Telemetry
TM/TC	Telemetry and Telecommand
TNID	Total Non-ionising Dose
TOA	Time of Arrival
TRA	Technology Readiness Assessment
TRL	Technology Readiness Level

Acronym	Definition
TSP	Time Space Partitioning
TT&C	Telemetry Tracking & Command
TWTA	Travelling Wave Tube Amplifier
UART	Universal Asynchronous Receiver Transmitter
UHF	Ultra High Frequency
VDA	Vapour Deposited Aluminium
WAC	Wide Angle Camera
WoL	Wheel Off-Loading
Xe	Xenon
XFC	Xenon Flow Controller
$\Delta t$	Transfer Time
$\Delta v$	Delta-V or velocity increment

This Page Intentionally Blank

## Annex A – Risk Log

The identified major risk for the Comet Interceptor mission are equally distributed over the various developments, project and deployment/ mission phases starting with the study performance (see Fig A-1). Regarding the mission elements (S/C A and smallsats (B1, B2)) most of the major risks are applicable to all elements or are interfacing risks between the mission elements.

HERITAGED from pre-study																			
WORST case approach in terms of 'Severity' & 'Likelihood'	Study		Development need		Project phase		Deployment & Mission												
	 concurrent design facility				A - D		Launch preparation (dual) Launch defined by ARIEL		LEOP/ IOT		Cruise to L2 A+B1+B2		Parking/ Searching peri cruise to target comet A+B1+B2		deployment before encounter A/ B1/ B2		encounter+ observation period A/ B1/ B2		period after encounter A
All 'A', 'B2' incl. Meta-risks	Study maturity	S1	open/ partly closed study items: - communication concept (see also D1b) - power concept (e.g. single or combination of rechargeable/ non-rechargeable batteries)	S1	interface alignment between ESA (A/ B2) and JAXA (B1)	OM1	S/C integration + launch preparation	LIV	If failure of ground station equipment	LIV	Reliability (loss of mission due to system & mission failure/ error)	O1a/b,1	Reliability (loss of mission/ perf. degrad. due to space environment next to comet)	O1a/b,2	Reliability (loss of mission/ data due to system & mission failure/ error) perf. degrad. of 'A'	O1a/b,3			
	3D → RM → 3C DIII6+DIVa	4C → RM → 3C OM1-B1	3D → RM → 3C OM1-B1	4C → RM → 4C OM1-B1	4D → RM → 3C	4D → RM → 4C	4D → RM → 4C	MIXa/b+	4D → RM → 4C	4E → RM → 4C	DIC+DIII2a+MIXc+MIVII+DIII7-B2	4D → RM → 4C MIXa/b+DIII2b-A	4D → RM → 4C MIXa/b+DIII2b-A	MIXab					
	mass budget	DIII6	Cost budget	OC1	new launcher	DXX					space environment - radiation high energetic particles due to galactic radiation (+ solar activities)								
	5E → RM → ?? DIII-A+DIII-B2+DIII-B1+DIII6	4D → RM → ??			4D → RM → 4C					4D → RM → 4C									
	TRL status ( $\geq 5$ at mission adoption)	DIVa			dual launch (ARIEL as prime mission)	IFI	safe mode is entered during L2 transfer	MIDa	availability of target comet	DIB	extreme time-critical operation/performance for/ after release of B1/B2	SCIIb/c-B2+DIII2a	DIC	space environ. - dust (loss of A/ B1/ B2 of the S/C)	MIXc				
	2E → RM → 2D DIVa-A+DIVa-B1				4D → RM → 3C DIII6		4D → RM → 3D	4D → RM → 4C			4D → RM → 4C	4D → RM → 3C	4D → RM → 3C						
'B2' CubeSat ESA	mass budget	DIII-B2									wobbling boom	MIV-B2		n/a no service after encounter expected					
	contributing to DIII6	DIII-B2									3D → RM → 3C								
	mass budget	DIII-									separation + detumbling	B2	no redundancy	DIII7-B2					
	contributing to DIII6										4C → RM → 3C	SCIIb/c-B2		n/a no service after encounter expected					
'A' Mother S/C ESA	mass budget	DIII-A									inaccurate & instable orientation between A+B1/ A+B2	DIII2	plums from B2/ B1 effecting science results	MVII					
	contributing to DIII6	DIII-A									3D → RM → 3C	3D → RM → 3C	3D → RM → 3C	DIII2b-A					
	no/ low TRL	DIVa,			A (min. - almost never)	B (low - seldom)	C (medium - sometimes)	D (high - frequently)	E (max. - certain)	MDI	navigation precision for encounter	3D → RM → 3C							
	contributing to DIVa	DIVa,																	
'B1' CubeSat JAXA	mass budget	DIII-B1		Project schedule	OM1-B1									n/a no service after encounter expected					
	Remark: based on experiences the final mass	DIII-B1																	
	TRL status unknown development not under ESA control	DIVa-B1												n/a no service after encounter expected					

Remark: The Risk Index (RI) after consideration of Risk Mitigation measures (-> RM -> [RI]) does not consider herein the adjustment of the RI (see chap. 21.3.4/ Tab. 21-7)

**Figure A- 1: Risk Summary (major risk)**

All the identified major risks summarised in the above figure are further explained in detail in Table 21-9.

Meta-RISks (risks which are building up on other risk, e.g. which might	Reference	Risk index (Initial)	Risk scenario <small>HERITAGED from pre-study</small>	Cause/ Events	Mitigating Action 1	Mitigating Action 2	Mitigating Action 3	Risk index (final)
	RISK-CI-11 new: OCI	<b>4D</b>	Cost budget overrun results in project cancellation.	Cost at completion (CaC) for ESA <150M (e.c. 2019) yet current CDF estimates are higher.	Limit design to minimum required to complete mission.	Maximize re-use of available technologies.	Discard technology solutions which do not comply with TRL requirements and are thus not compatible in terms of schedule and cost.	???
	RISK-CI-03 new: DIII6	<b>4D</b>	Exceeding mass budget with impact on mission feasibility. A+B1+B2: 100kg over 650kg B2: 4kg over 30kg B1: marginal at budget	Shared A6 L2 launch mass constraints, ARIEL mass increase, launch vehicle uncertainties in launch capability.	Insert sufficient equipment and system mass margins according to maturity levels as per CDF policy.	De-scoping of mission objectives.	Dedicated A6 launch to L2 (impact on cost).	???
OC - 'Cost budget' overrun OS - 'Schedule delay'	OAla/b	<b>4D</b>	'loss of'- reliability of 85%* exceeded	<ul style="list-style-type: none"> <li>- galactic radiation and solar flare over a life time (up to 7a) <i>but also to be considered:</i></li> <li>- several space crafts (A+B2+B1) incl. failure propagation between S/Cs; (random/ systematically failure/ errors)</li> <li>- extreme time-critical constellation deployment (24 ..36h) and mission operation (30min) (anomaly reliability = loss reliability)</li> <li>- deep space conditions for CubeSat technology</li> </ul> <p><i>Remark: * contribution of dust impact (app. 6.6% during encounter not included in the 85%) dominated by destructive impact at propulsion tanks, battery and OBC.. see MIXc</i></p>			<i>see contributing risks below</i>	<b>4C</b>
DIII6 - 'mass budget' overrun OAI.1/3 ab - Reliability (loss of mission/ partly loss of mission/ number of anomalies)	SI	<b>4D</b>	Study maturity a non-sufficient study maturity would result in to high uncertainties in terms of e.g. mass budget, risk identification and finally schedule assumptions and cost estimation	<p>E.g.</p> <ul style="list-style-type: none"> <li>- commu. concept e.g. antenna sizing/ power to reach already critical data rate</li> <li>- power concept in terms of rechargeable+SA/ non- rechargeable batteries</li> <li>- S/C configuration not fully closed (e.g. star tracker)</li> </ul> <p><i>However, several trade off options were</i></p>	settlement of dedicated working groups to solve open design and operation items	delta study	increase of cost and schedule margins or adoption of mission objectives	<b>3C</b>

Risk Assessment is using Worst Case (WC) approach!

Meta-RISKS (risks which are building up on other risk, e.g. which might be)		Reference	Risk index (Initial)	Risk scenario HERITAGED from pre-study	Cause/ Events	Mitigating Action 1	Mitigating Action 2	Mitigating Action 3	Risk index (final)
OC - 'Cost budget' overrun OS - Schedule delay	DIII7-B2		3D	Redundancy concept  because of the assigned limited mass budget no redundancies could be considered in the B2 design  Remark: the extreme short mission operation phase would most probably also not allow to use redundancies efficiently	limited mass budget is leading to design limitations	preferred use of high-reliable components	re-discussion of the assigned mass budget  Remark: most probably not useful because of the mass budget overrun - see DII6)		3D
DII6 - 'mass budget' overrun	DIVa		2E	no/ low TRL  no TRL: PF: for all PF components TRLs could be assigned PL: MIR-MIS-RAD,  low TRL: PF: all PF components are indicated with TRL> 4 PL: CoCa (4), DFP E-box(4), MIRMIS-MIR(4), DFP-COM_FGM-boom(4), EnVisS(4), Optima(4) all other components are indicated with TRL≥ 4	'at the age' technology/ missing information	initiating/ acceleration of development program (e.g. CTP, GSTP)	non-European procurement		2D
OAI.1 and - Reliability (loss of mission/ partly loss of mission/ number of anomalies)	LIII		3D	relatively high number of mission elements (A/B1/B2) and PL instruments might lead to schedule delay	organisational, technical and technological interface issues	intensive alignment with project partners	use organisational experiences from former joint projects		3D
	RISK-CI-07 new: OMI		4C	Delays or technical challenges in the e.g. inter-agency/ international cooperation elements of Comet-I impact on the development cost and schedule of the mission.  Launch delay due to B1 delivery (not under ESA control)	[1] International cooperation mission with certain external risks which are not under ESA's full control. [2] International contributions up to TBD M EUR may be needed to realize project.	Establish a close cooperation with partner agency with regular progress meetings.	Create a trusting and open environment enabling improved communication flow and quicker problem notification.	Adequate funding of dedicated ESA interface team with partner agency.	3C
	RISK-CI-02 new: IFI		4D	dual launch (second priority mission) If there is a delay in the mission design/development/testing then the Comet-I mission is delayed resulting in a delay of ARIEL (prime) mission due to coupling of two missions.	Redefinition of mission objectives leading to changes in design, failures or non-compliances during AIT/V, low TRL of Comet-I instruments.	Insert sufficient margins in schedule	Correct enforcement of the TRL ≥ 6 by Q1 2020 and TRL ≥ 7 by mission adoption in 2022	A standard dual launch would decouple AIT/V campaigns of missions	3C

**Remark:** The risk potential due to No/low TRLs (DIVa) is mentioned herein in a generic way. The TRL risk should not be seen as 'major risk', because the development relate risk seems to be relatively low for the COMET interceptor mission. **Non of the PL and PF componets have a TRL lower than 4!!!.**

Risk Assessment is using Worst Case (WC) approach!

Risk Assessment is using Worst Case (WC) approach!											
Meta-RISKS (risks which are building up on other risk, e.g. which might)			Reference	Risk index (Initial)	Risk scenario HERITAGED from pre-study		Cause/ Events	Mitigating Action 1	Mitigating Action 2	Mitigating Action 3	Risk index (final)
OC - 'Cost budget' overrun OS - 'Schedule delay'	DLI6 - 'mass budget' overrun OS - 'loss of mission/ partly loss of mission/ anomalies'	SI - study maturity	MIXc	4D	Dust impact & inertia/ kinetic is effecting the space craft (A+B1+B2) operation in terms of science results and stability of communication and loss of mission elements (A and/or B1 and/or B2)						
					Impact: 6.6% (WC) loss probability Inertia/ kinetic: Particle mass A 1000km 10mg 12% 100mg 1.4% (WC) B2 100km 5.8% 0.7% (WC) 200km 2.8% 0.3% 400km 1.4% 0.2%		Dust inertia impacting S/C position or space craft penetration (kinetic)	optimisation of distance to target comet (limitation of dust density)	adequate AOCS requirements (S/C stability)	adequate shielding	3C
					Remark: the loss of mission due to dust impacts OAI.2 a/b is not seen as part of the overall budgeted for the loss-reliability (see						
OC - 'Cost budget' overrun OS - 'Schedule delay'	DLI6 - 'mass budget' overrun OS - 'loss of mission/ partly loss of mission/ anomalies'	SI - study maturity	MIV-B2	3D	the boom (magnetometer) instability might be a specific source of S/C instability leading to performance degradation	wobbling of the boom during deployment or S/C vibration due to dust impact at boom		structural analysis (deployment related)	design optimisation (adequate length and cross section, e.g. streamlined)		3C
					the propulsion caused plumes might effect the science performance of the mission element	the propulsion caused plumes is leading to a falsification of measurement results	careful planning of PL configuration & S/C operation		careful planning of configuration of mission elements during observation phase		3C
'Cost budget' overrun OS - 'Schedule delay'	DLI6 - 'mass budget' overrun OS - 'loss of mission/ partly loss of mission/ anomalies'	SI - study maturity	RISK-CI-09  new: MIXc	3E	If (dust) contamination is present then optical instrument units are degraded resulting in loss of scientific return.	Near comet environment, and/or debris generated during spacecraft separations.	Implement optical instrument protection covers against potential debris generated during separation events.		Further study comet dust environment and its impact on optical instruments in order to plan for a safe distance fly-by.		3C
'Cost budget' overrun OS - 'Schedule delay'	DLI6 - 'mass budget' overrun OS - 'loss of mission/ partly loss of mission/ anomalies'	SI - study maturity	RISK-CI-10  new: DIII2a	4C 3D	If there is a loss or degradation of communications between the mother craft and the small spacecraft's during comet close approach then the data rate decreases resulting in considerable loss of science return	Equipment failure, misalignment of spacecraft's, near comet environment.	Fully redundant equipment for communications and omnidirectional transmission from small S/Cs.  Consider other reliability or pointing requirements for small spacecraft's.	Prioritize data transmissions to ensure return of high priority science data.	optimisation of antenna configuration (S/C A) and constellation configuration during encounter		3C
'Cost budget' overrun OS - 'Schedule delay'	DLI3 a/b - Reliability (loss of mission/ partly loss of mission/ number of anomalies)	SI - study maturity	DIII2b-A	4D	critical loss of mission data transmission to Earth after comet fly-by in the 'after encounter'-period of 180d	mostly driven by dust impacts and SEE (galac. Radiation, solar flare) disabling functionalities and mission conditions critical for the data transmission to Earth (e.g. HW/ SW failure/ error) might leading to the loss of critical science	- failure tolerant design - high reliable components - intensive reliability analysis	intensive (lifetime) testing of cortical communication components	analysis of possible contingency possibilities and its consideration in the design and procedures, e.g. increase of 'after encounter'-period -> 540d		3C

Table A- 1: Risk Log (major risks)